Arthritis & Rheumatology

An Official Journal of the American College of Rheumatology
www.arthritisrheum.org and wileyonlinelibrary.com

Cover design: Todd Machen

This journal is printed on acid-free paper.

Arthritis & Rheumatology
An Official Journal of the American College of Rheumatology
www.arthritisrheum.org and wileyonlinelibrary.com

VOLUME 70 APRIL 2018 NO. 4

Cover image: The figure on the cover is a confocal microscopy image of chikungunya virus–infected BHK-21 cells. The image (original magnification × 600) was taken at 16 hours post-infection. Host cell nuclei were stained with DAPI (red), and localization of chikungunya virus capsid protein (green) was determined by indirect immunofluorescence using capsid-specific antibodies. This issue of *Arthritis & Rheumatology* features reports on synovial fluid analysis in patients with chikungunya virus–associated arthritis (Chang et al, pages 585–593) and on the frequency of chronic joint pain after infection with chikungunya virus (Chang et al, pages 578–584), a review of chikungunya virus–associated arthritis (Zaid et al, pages 484–495), and an editorial on the potential scientific and epidemiologic implications of the appearance of the chikungunya virus in the Americas (Miner and Lenschow, pages 477–479). Image courtesy of Adam Taylor, PhD, Institute for Glycomics, Griffith University, Southport, Queensland, Australia.

ACR ANNOUNCEMENTS

AMERICAN COLLEGE OF RHEUMATOLOGY
2200 Lake Boulevard NE, Atlanta, Georgia 30319-5312
www.rheumatology.org

ACR Meetings

Annual Meetings
October 19–24, 2018, Chicago
November 8–13, 2019, Atlanta

State-of-the-Art Clinical Symposium
April 13–15, 2018, Chicago

For additional information, contact the ACR office.

Nominations for ACR Awards of Distinction and Masters Due May 15

The ACR has many Awards of Distinction, including the Presidential Gold Medal. Members who wish to nominate a colleague or mentor for an Award of Distinction must complete the online form at www.rheumatology.org. The nomination process includes a letter of nomination, 2 additional letters of recommendation, and a copy of the nominee's curriculum vitae. Recognition as a Master of the American College of Rheumatology is one of the highest honors the ACR bestows. The designation of Master is conferred on ACR members age 65 or older who have made outstanding contributions to the field of rheumatology through scholarly achievements and/or service to their patients, students, and the profession. To nominate someone for a Master designation, members must complete the online nomination form at www.rheumatology.org and include a letter of nomination, 2 supporting letters from voting members of the ACR, and the nominee's curriculum vitae. Nominees for ACR Master must have reached the age of 65 before October 1, 2018.

ACR Invites Nominations for Volunteer Positions

The ACR encourages all members to participate in forming policy and conducting activities by assuming positions of leadership in the organization. Positions are available in all areas of the work of the American College of Rheumatology and the Rheumatology Research Foundation. Please visit www.rheumatology.org for information about nominating yourself or a colleague for a volunteer position with the College. The deadline for volunteer nominations is June 1, 2018. Letters of recommendation are not required but are preferred.

Education Programs

Eleventh International Congress on Autoimmunity. May 16–20, 2018, Lisbon, Portugal. The International Congress on Autoimmunity encompasses the most up-to-date clinical and basic research findings on more than 80 autoimmune diseases, with courses and lectures by some of the world's most distinguished experts. The official language will be English. Registration fees are €720 (through May 8) and €820 (May 9–onsite) for full participants, and €430 (through May 8 and €480 (May 9–onsite) for trainees (students/fellows/residents) and nurses. Optional courses and functions are available for additional fees. For additional information, e-mail reg_autoimmunity18@kenes.com, phone +41 22 908 0488, or visit the web site http://autoimmunity.kenes.com/2018.

4th Annual Conference of the Emirates Society for Rheumatology. October 10–12, 2018, Dubai, UAE. Conference sessions will cover recent updates in the management of specific rheumatic diseases. An accredited musculoskeletal ultrasound course will be offered, and there will be meet-the-expert sessions and workshops, as well as educational activities for nurses and patients in addition to the numerous sessions geared toward physicians. The deadline for submission of abstracts is July 31, 2018. The official language will be English. The registration fee is $200 through July 3, 2018, and $300 thereafter. For additional information, e-mail infomed@infomedweb.com or Nathalie@infomedweb.com.

Clinical Connections

Effects of HLA–B27 on Gut Microbiota in Experimental Spondyloarthritis Implicate an Ecological Model of Dysbiosis

Gill et al, *Arthritis Rheumatol* 2018;70:555–565.

CORRESPONDENCE
Robert A. Colbert, MD, PhD: colbertr@mail.nih.gov

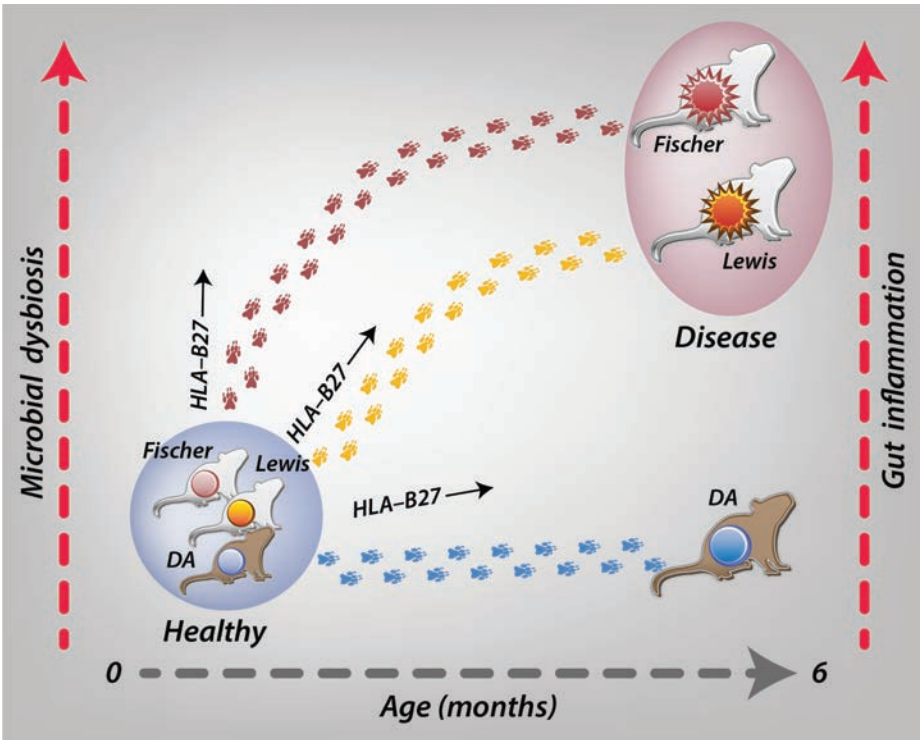

KEY POINTS

- HLA–B27–associated dysbiosis differs with genetic background and environment in experimental murine SpA.
- In susceptible genetic backgrounds, HLA–B27–induced immune dysregulation is strikingly similar and involves tumor necrosis factor, interferon-γ, and Th17 cytokines.
- Although dysbiotic microbes in HLA–B27–transgenic Lewis and Fischer rats are different, they are associated with similar metabolic functions.
- The impact of HLA–B27 on gut microbes in rats implicates an ecological model of dysbiosis in SpA.

SUMMARY

Gut microbes play an important role in nutrient production, immune regulation, and protection against certain disease-causing bacteria. However, gut microbes are also implicated in the development of spondyloarthritis (SpA). HLA–B27, a major genetic risk factor for SpA, causes gut microbial dysbiosis and inflammation when expressed in some rat strains, such as Lewis and Fischer, but has a minimal effect in dark agouti (DA) rats. Lewis and Fischer rats also differ in the temporal development and severity of inflammation, which may also be affected by environment. Gill and colleagues found that in Lewis and Fischer rats expressing HLA–B27, dramatically different patterns of microbial dysbiosis are seen, despite remarkably similar immune and inflammatory changes in the gastrointestinal tract. While the microbes differ taxonomically, there are important overlaps in their predicted metabolic effects. Since different rat strains may be considered to be comparable to different individuals in a human population, the findings of this study emphasize the importance of evaluating microbial communities and their functions to better understand how gut microbiota influence the pathogenesis of SpA.

Increased Expression and Modulated Regulatory Activity of Coinhibitory Receptors PD-1, TIGIT, and TIM-3 in Lymphocytes From Patients With Systemic Sclerosis

Fleury et al, *Arthritis Rheumatol* 2018;70:566–577.

CORRESPONDENCE
Hans Dooms, PhD: hdooms@bu.edu

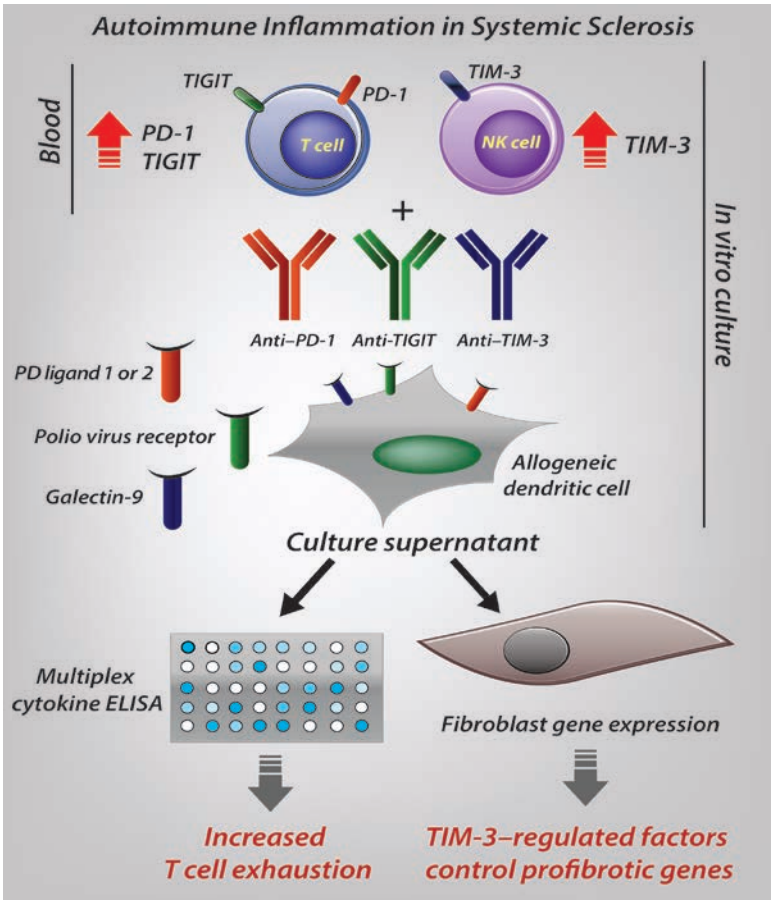

SUMMARY

Coinhibitory receptors (co-IRs) are important regulators of immune responses that are up-regulated during chronic immune activation and inflammation. The co-IRs programmed cell death 1 (PD-1), T cell immunoglobulin and ITIM domain (TIGIT), and T cell immunoglobulin and mucin domain 3 (TIM-3) suppress immune responses by decreasing lymphocyte proliferation and cytokine production. Long-term engagement of these receptors leads to functional exhaustion of lymphocytes, and reversal of this process by antibody blockade is being used for immunotherapy of cancer. Fleury and colleagues found that circulating T and natural killer (NK) cells from systemic sclerosis (SSc) patients express higher levels of co-IRs. PD-1 and TIGIT were increased on various T cell subsets, while NK cells expressed more TIM-3. Blocking co-IRs during in vitro stimulation of lymphocytes from SSc patients resulted in modulated cytokine production. PD-1 was more effective in controlling cytokines than TIGIT or TIM-3 in cells from SSc patients, while TIGIT and TIM-3 activity could not be differentiated from PD-1 in healthy controls. Overall, these data indicate that lymphocytes in the blood of SSc patients are in a state of exacerbated exhaustion. Moreover, the investigators demonstrated that TIM-3 controls soluble factors produced by immune cells that modulate profibrotic gene expression in fibroblasts.

KEY POINTS

- The immune coinhibitory receptors PD-1, TIGIT, and TIM-3 are up-regulated in circulating lymphocyte subsets from SSc patients.
- The increased presence of PD-1+TIGIT+ double-positive T cells and the weaker activity of TIGIT and TIM-3 in SSc patients versus healthy controls indicate that lymphocytes from patients are more functionally exhausted.
- TIM-3 controls the production of soluble factors in immune cells that affect gene expression of SSc fibroblasts.

In this Issue

Highlights from this issue of *A&R* | By Lara C. Pullen, PhD

Large Study of Chikungunya Arthritis Suggests Possible Pathophysiology

In this issue, 2 articles by Chang et al describe observations from one of the largest studies of patients infected with chikungunya virus. The research in the first article by Chang et al (p. 578) is the first to show the frequency of chikungunya virus–related arthritis in the Americas (Colombia) at a 20-month follow-up. The majority (485) of the 500 patients in the study had serologically confirmed chikungunya virus. The patients were predominantly women with an education level of high school or lower, and the majority were of Mestizo ethnicity. Their arthritis tended to affect the small joints such as the wrists, ankles, and fingers.

p. 578

The initial virus symptoms in the cohort lasted approximately 4 days and were significant enough that 16% of the participants reported missing a median of 4 days of school or work. Moreover, one-quarter of the individuals experienced chronic joint pain at 20 months post-infection. When the investigators performed a multivariable analysis, they found the following predictors of persistent joint pain: college graduate status, initial symptoms of headache or knee pain, missed work, normal activities affected, ≥4 days of initial symptoms, and ≥4 weeks of initial joint pain. These results suggest that there is a high frequency of chronic disease and thus reinforce the need to develop prevention and treatment methods.

To that end, in the second study Chang and colleagues (p. 585) hypothesized that persistent, active chikungunya virus was responsible for the chronic arthritis and joint pain. To investigate this hypothesis, they more closely examined 38 participants who had serologically confirmed chikungunya arthritis a median of 22 months after infection. The patients were predominantly female and African Colombian or white Colombian, with moderate disease activity. Initial symptoms included joint pain, swelling, stiffness, and fever. Their most commonly affected joints were the knees, elbows, wrists, fingers, and toes.

p. 585

The researchers tested synovial fluid using quantitative reverse transcription–polymerase chain reaction but were unable to find viral RNA in the synovial fluid. They were also unable to detect viral proteins on mass spectrometry and unable to culture the virus. When the investigators compared patients with controls, they found that both groups had similar plasma concentrations of cytokines and chemokines. The findings allow for the possibility that low levels of the virus persist in the synovial tissue even though it is undetectable in the synovial fluid. The results are also consistent with the possibility that chikungunya may induce arthritis via host autoimmunity. If this proves to be the case, then immunomodulating agents may be an effective treatment for chikungunya arthritis.

Marginal Jawbone Loss May Predict Onset of Rheumatoid Arthritis

Multiple studies have examined the relationship between rheumatoid arthritis (RA) and periodontitis, but results have been contradictory. In this issue, Kindstedt et al (p. 508) report the findings from their investigation into whether periodontitis, as characterized by jawbone loss, precedes the onset of RA symptoms. The researchers also analyzed the plasma levels of a cytokine that is crucial for bone resorption (RANKL) as well as the presence of anti–citrullinated peptide antibodies (ACPAs). The investigators compared these measures in presymptomatic individuals with those in matched referent controls.

p. 508

These are the first findings to indicate that a more severe loss of tooth-supporting bone precedes the onset of RA symptoms. Specifically, they report that in nonsmokers, and only nonsmokers, marginal jawbone loss preceded the clinical onset of RA symptoms. In these patients, increasing levels of bone loss were associated with a higher risk of subsequent development of RA. Although the association was statistically significant, it was modest.

In addition, the investigators found that marginal jawbone loss was significantly greater in RANKL-positive presymptomatic subjects when compared with RANKL-negative presymptomatic patients. However, the marginal jawbone loss was highest in presymptomatic patients who were positive for both ACPAs and RANKL.

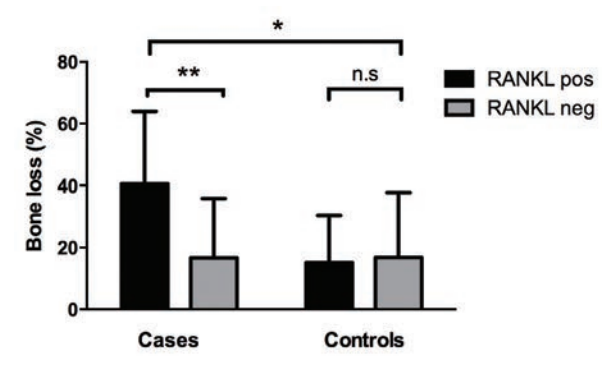

Figure 1. Bone loss in RANKL-positive presymptomatic subjects (cases) and controls and RANKL-negative cases and controls. Bars show the mean ± SD. NS = not significant. * = $P < 0.05$; ** = $P < 0.01$.

Relationship Between Antibody Responses and Rheumatoid Arthritis

Researchers agree that the generation of autoantibodies to citrullinated and noncitrullinated proteins/peptides is a key feature in the pathophysiology of rheumatoid arthritis (RA). However, the location and mechanism of generation of these antibodies remain a mystery. In this issue, Demoruelle et al (p. 516) report on their investigation of individual antibody responses to citrullinated and noncitrullinated peptides/proteins in the sputum, and the association of these responses with neutrophil extracellular traps (NETs) in subjects at risk of developing RA.

p. 516

The researchers first examined at-risk subjects and measured antibody responses to the multiple citrullinated proteins/peptides. They found that antibodies citrullinated fibrinogen, apolipoprotein E, and fibronectin were highly prevalent in at-risk individuals. In addition, the most citrulline-specific antibodies in the sputum of at-risk subjects were directed against fibrinogen, vimentin, and peptides of fibrinogen A and apolipoprotein A1. Moreover, sputum antibody reactivity to particular citrullinated and noncitrullinated proteins/peptides appears to be specific for RA. The authors suggest that these proteins may represent the earliest antigen targets of antibodies generated in the lungs of these subjects.

When the researchers looked more closely at the patterns of autoantibody positivity in at-risk subjects and those with RA, they found that the patterns differed. In addition, at-risk subjects had sputum NET levels that significantly correlated with several citrullinated and some noncitrullinated antibody reactivities. The authors concluded that the association between these proteins/peptides and NETs may be a key feature of early RA-related autoimmunity in the lung. Their results also support the hypothesis that the lung plays a role in early RA-related autoimmunity.

Autoantibodies Associated With Polyarticular Juvenile Idiopathic Arthritis

DEK was originally identified as a nuclear protein, and it is important in the modulation of global chromatin structure. However, DEK has proinflammatory characteristics, as it is a secreted chemotactic factor that is also essential to neutrophil extracellular trap formation. There is also a growing realization that DEK is an autoantigen associated with juvenile idiopathic arthritis (JIA), specifically the oligoarticular subtype. This is because DEK and DEK autoantibodies are found in abundance in the inflamed synovium of patients with JIA. In this issue, Mor-Vaknin et al (p. 594) sought to characterize the nature of DEK autoantibodies in the sera of patients with JIA.

p. 594

The investigators report that DEK autoantibody levels were significantly higher in patients with polyarticular JIA than in those with oligoarticular JIA. Specifically, patients with polyarticular JIA who had more disease flares after cessation of anti–tumor necrosis factor therapy were more likely to exhibit elevated levels of DEK autoantibodies. When the researchers performed immunoblotting, they found that the C-terminal 25–amino acid fragment of DEK was the most immunogenic domain of the DEK molecule in these patients. The authors concluded that DEK autoantibodies may contribute to JIA pathogenesis and thus may be important in the management of JIA.

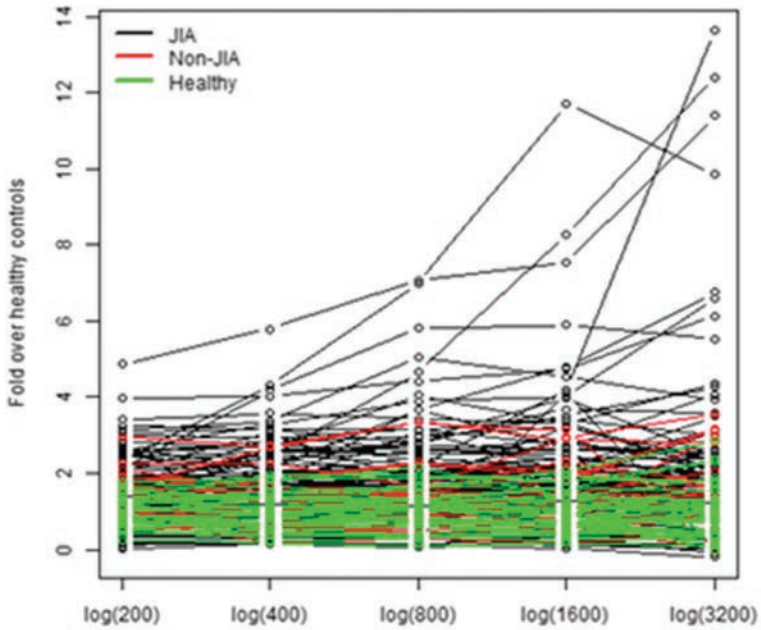

Table: P values by dilution

	D200	D400	D800	D1600	D3200
JIA > Healthy	0.01	0.001	0.002	0.007	0.01
JIA > Non-JIA	0.1	0.01	0.01	0.04	0.12
Healthy < Non-JIA	0.41	0.50	0.56	0.43	0.40

Figure 1. High levels of DEK autoantibodies in patients with JIA. Serum samples from patients with JIA (n = 33), patients with other rheumatic diseases (n = 13), or healthy controls (n = 11) were serially diluted as indicated and tested for anti-DEK antibody levels by enzyme-linked immunosorbent assay (ELISA). Lines represent individual samples. Samples were compared to those from 5 normal healthy controls. Results shown are the average of 2–8 independent ELISAs.

ARTHRITIS & RHEUMATOLOGY
Vol. 70, No. 4, April 2018, pp 477–479
DOI 10.1002/art.40421

Arthritis & Rheumatology
An Official Journal of the American College of Rheumatology
www.arthritisrheum.org and wileyonlinelibrary.com

EDITORIAL

Lessons Learned From Chikungunya in the Americas

Jonathan J. Miner and Deborah J. Lenschow

In 2013, chikungunya virus arrived in the Western Hemisphere, spreading like wildfire across the islands of the Caribbean, Mexico, Central America, and South America, resulting in ~3 million infections (1). Similar to historical outbreaks in the Eastern Hemisphere, chikungunya virus spread quickly in a population without preexisting immunity. The chikungunya virus outbreak also created new challenges for rheumatologists, who were suddenly encountering a disease entity with which there was little familiarity. Included among these challenges was identifying the factors that predispose patients to the development of chronic arthritis, understanding the pathogenesis driving persistent arthritis, and determining treatments that would be efficacious and safe in patients with chikungunya arthritis. In this issue of *Arthritis & Rheumatology*, two new studies and a review address some new discoveries from the chikungunya virus epidemic in the Americas and discuss lessons learned from prior outbreaks of chikungunya arthritis in the Eastern Hemisphere (2–4).

Upon infection with chikungunya virus, ~90% of patients develop acute symptoms, which can include fever, inflammatory arthritis with morning stiffness, and severe pain throughout the first week after infection (5). Some patients also develop a rash and conjunctivitis during the acute phase of the illness. Severe cases can even cause viral encephalitis and occasionally death in neonates (6). Also of concern, especially to the rheumatologist, is the fact that many patients infected with chikungunya virus develop arthralgias and arthritis, which can persist for up to 3 years (7). The mechanisms underlying persistent chikungunya arthritis remain a mystery and are an area of active scientific investigation.

Jonathan J. Miner, MD, PhD, Deborah J. Lenschow, MD, PhD: Washington University School of Medicine, St. Louis, Missouri.

Address correspondence to Jonathan J. Miner, MD, PhD, or Deborah J. Lenschow, MD, PhD, Departments of Medicine, Molecular Microbiology, and Pathology and Immunology, Washington University School of Medicine, 660 South Euclid Avenue, Box 8045, St. Louis, MO 63110. E-mail: jonathan.miner@wustl.edu or dlenschow@wustl.edu.

Submitted for publication January 12, 2018; accepted January 16, 2018.

Alphaviruses are enveloped, single-stranded positive sense RNA viruses belonging to the *Togaviridae* family (5). Alphaviruses can be divided into New World alphaviruses that typically cause encephalitis (e.g., Western equine encephalitis virus) and Old World alphaviruses that cause viral arthritis (e.g., chikungunya virus and Ross River virus). Like some other arthritogenic alphaviruses, chikungunya virus is spread by *Aedes* mosquitos, and in particular *A aegypti,* which is found primarily in tropical and subtropical climates.

Numerous epidemiologic studies were published in the wake of the 2006 chikungunya virus epidemic on Réunion Island, where approximately one-third of the island's population was infected (6,8–11). Those studies defined the frequency of acute and chronic manifestations of disease in the Eastern Hemisphere. However, less was known about epidemiologic outcomes of the chikungunya virus outbreak in the Americas. In one of their studies published in this issue of *Arthritis & Rheumatology*, Chang et al (2) set out to determine the frequency of chronic joint pain after chikungunya virus infection in a Colombian cohort. The authors enrolled 485 serologically confirmed cases and clinically reevaluated the patients 20 months after infection. As noted in our study of a small cohort of chikungunya virus–infected American travelers to Haiti (12), the most commonly affected joints in the patients included the small joints of the distal extremities. At the 20-month follow-up the authors found that arthralgias were persistent in ~25% of the patients. They also identified some interesting correlates of persistent joint pain, including college graduate status, headache at onset of infection, and ≥4 weeks of initial pain, among others.

There are several major implications of this study by Chang et al (2). First, the presence of persistent joint inflammation strongly suggests that the chikungunya virus strain that spread to the Americas caused a chronic arthritis disease phenotype similar to what was described in prior outbreaks in the Eastern Hemisphere. The authors also raised important limitations of the study. For example, Mayaro virus is an arthritogenic Old World

alphavirus that is found in the Amazon and causes inflammatory arthritis with morning stiffness, similar to chikungunya arthritis. Anti–Mayaro virus and anti–chikungunya virus antibodies may cross-react (13), thereby confounding diagnostic testing. Thus, although Mayaro virus was not known to be spreading in this region of Colombia at the time of the study, the presence of confounding Mayaro virus infections could not be completely excluded. Another intriguing question, which was not addressed in this epidemiologic study, is why chikungunya virus tends to preferentially infect distal joints. Notably, a recent study by Prow et al showed that mice infected with chikungunya virus have more severe disease, more robust viral replication, and impaired antiviral type I interferon (IFN) response when the mice are housed at lower temperatures (14). Since distal joints are slightly cooler than proximal joints, temperature-dependent antiviral immunity could be a possible explanation of why chikungunya virus preferentially affects small joints in the distal extremities (3).

Mechanisms of persistent chikungunya arthritis are not well understood, although it is known that there are some intriguing similarities in the immunologic phenotypes of peripheral blood mononuclear cells from patients with rheumatoid arthritis and those with chikungunya arthritis (12). Several hypotheses have been proposed, including the persistence of a low level of replicating virus in the joints, the induction of autoimmunity, and the persistence of viral RNA in the synovium that can act as a pathogen-associated molecular pattern (PAMP) to activate pattern-recognition receptors and trigger chronic inflammation. In a second study by Chang et al (3), the authors looked for evidence of viral persistence in patient synovial fluid 22 months after infection. The results were negative; the authors were unable to culture replicating virus from the synovial fluid and found no evidence of chikungunya viral RNA or proteins in the synovial fluid by several different techniques, including quantitative reverse transcriptase–polymerase chain reaction and mass spectrometry.

A major implication of that study by Chang et al (3) was that persistent chikungunya arthritis may result from induction of autoimmunity rather than low-level viral persistence. Similar to prior studies (5,12), the authors found no association between the presence of anti–cyclic citrullinated peptide autoantibodies or rheumatoid factor antibodies and persistent disease. However, one prior study had identified chikungunya virus RNA and protein in perivascular synovial macrophages in a patient 18 months after infection (15). Viral antigen also persisted in macrophages of nonhuman primates several months after infection (16). Thus, although chikungunya virus RNA was not detected in synovial fluid from patients, the persistence of viral RNA and/or viral antigen in affected joints cannot be excluded without synovial biopsies. Indeed, the absence of viral antigen in synovial fluid does not exclude the possibility that viral RNA in synovial macrophages or other cell types within the joint may be contributing to chronic disease. As a hypothetical example, defective viral genomes, which may have the capacity to replicate and produce PAMPs without generating viral antigen, may be able to activate the type I IFN response locally and cause chronic joint pain. Chang et al did not evaluate IFN-stimulated genes, which would be expected to be up-regulated in the presence of PAMPs. Finally, it is important to underscore that viral RNA testing, as with any testing, has a limit of detection, making very low levels of PAMP difficult to detect.

Nevertheless, the negative findings in this second study by Chang et al (3) are consistent with the authors' hypothesis that persistent immunologic activation, rather than persistent virus, may explain the persistence of chronic joint pain in patients with chikungunya arthritis. The absence of infectious virus is likely to minimize the risk associated with immunomodulatory therapies (e.g., abatacept, tofacitinib, and fingolimod), which remain to be tested in humans but have shown some efficacy in mouse models of chikungunya arthritis (12,17).

Despite promising therapeutic studies in mouse models of chikungunya virus pathogenesis, it is important to underscore that the efficacy and risks of immunosuppressive therapies during the acute phase of infection remain unknown. Since some patients have died of encephalitis during chikungunya virus outbreaks (10), and immunosuppression might confer added risk of severe infection, the use of immunosuppressive therapies for chikungunya arthritis should be considered with caution. This point is also underscored in the third article on chikungunya arthritis, by Zaid et al (4), published in this issue of *Arthritis & Rheumatology*. The authors review the clinical manifestations and epidemiology of chikungunya arthritis as well as the current body of evidence for therapies for chikungunya arthritis (4). Whereas nonsteroidal antiinflammatory drugs have shown some efficacy in treating pain associated with acute and chronic chikungunya arthritis, the authors correctly emphasize the fact that efficacy of disease-modifying antirheumatic drug (DMARD) therapies in chikungunya arthritis has not been clearly established. Small studies have suggested that there may be a role for certain DMARDs in the treatment of chronic chikungunya arthritis (18); however, carefully blinded, randomized controlled trials are necessary to draw firm conclusions about therapeutic interventions. Since chronic joint pain eventually resolves spontaneously,

therapeutic interventions should be stopped periodically to assess for resolution of symptoms.

Patients infected with chikungunya virus develop long-lived immunity. Therefore, many of the people affected by the recent chikungunya virus epidemic in the Americas have developed protective immunity against chikungunya virus. Nevertheless, other chikungunya virus strains that are spread by *Aedes albopictus* might still have the potential to cause outbreaks in previously unaffected parts of the continental US. For example, a very large outbreak on Réunion Island in the Indian Ocean in 2006 was associated with a mutation in the chikungunya virus genome, which led to enhanced replication and transmission in *A albopictus* mosquitos (19), a species that is found in more temperate climates, including parts of Europe and the continental US. Understanding the relationship between viral genetics and the capacity of chikungunya virus to spread in specific mosquito vectors is important, since this has implications for the potential of specific chikungunya virus strains to spread to particular geographic locations. Indeed, the distribution of these specific mosquito vectors correlates with prior chikungunya virus epidemics and has also predicted future outbreaks. The particular strain of chikungunya virus that spread to the Americas in 2013 lacked the *A albopictus*–adapted mutation, which may have limited the spread of chikungunya virus to regions where *A aegyptii* mosquitoes are prevalent, including the islands of the Caribbean, the US Gulf Coast, Mexico, Central America, and South America.

This implies that potential remains for other chikungunya virus strains to eventually spread in the continental US in a population without preexisting immunity against arthritogenic alphaviruses. Furthermore, chikungunya virus–related alphaviruses, including Mayaro virus, which is endemic in South America, also have the potential to emerge and cause outbreaks. A combined effort of basic, translational, and clinical research will prepare future generations for new epidemics, whether it be a re-emergence of chikungunya virus, or the emergence of other arthritogenic alphaviruses.

AUTHOR CONTRIBUTIONS

Dr. Miner drafted the initial version of the article. Drs. Miner and Lenschow revised the editorial critically for important intellectual content and approved the final version to be published.

REFERENCES

1. Yactayo S, Staples JE, Millot V, Cibrelus L, Ramon-Pardo P. Epidemiology of Chikungunya in the Americas. J Infect Dis 2016; 214 Suppl 5:S441–s5.
2. Chang AY, Encinales L, Porras A, Pacheco N, Reid SP, Martins KA, et al. Frequency of chronic joint pain following chikungunya virus infection: a Colombian cohort study. Arthritis Rheumatol 2018;70:578–84.
3. Chang AY, Martins KA, Encinales L, Reid SP, Acuña M, Encinales C, et al. Chikungunya arthritis mechanisms in the Americas: a cross-sectional analysis of chikungunya arthritis patients twenty-two months after infection demonstrating no detectable viral persistence in synovial fluid. Arthritis Rheumatol 2018;70:585–93.
4. Zaid A, Gérardin P, Taylor A, Mostafavi H, Malvy D, Mahalingam S. Chikungunya arthritis: implications of acute and chronic inflammation mechanisms on disease management [review]. Arthritis Rheumatol 2018;70:484–95.
5. Burt FJ, Chen W, Miner JJ, Lenschow DJ, Merits A, Schnettler E, et al. Chikungunya virus: an update on the biology and pathogenesis of this emerging pathogen. Lancet Infect Dis 2017;17:e107–17.
6. Gerardin P, Samperiz S, Ramful D, Boumahni B, Bintner M, Alessandri JL, et al. Neurocognitive outcome of children exposed to perinatal mother-to-child Chikungunya virus infection: the CHIMERE cohort study on Reunion Island. PLoS Negl Trop Dis 2014;8:e2996.
7. Rodriguez-Morales AJ, Cardona-Ospina JA, Fernanda Urbano-Garzón S, Sebastian Hurtado-Zapata J. Prevalence of post-chikungunya infection chronic inflammatory arthritis: a systematic review and meta-analysis. Arthritis Care Res (Hoboken) 2016;68:1849–58.
8. Sissoko D, Malvy D, Ezzedine K, Renault P, Moscetti F, Ledrans M, et al. Post-epidemic Chikungunya disease on Reunion Island: course of rheumatic manifestations and associated factors over a 15-month period. PLoS Negl Trop Dis 2009;3:e389.
9. Javelle E, Ribera A, Degasne I, Gauzere BA, Marimoutou C, Simon F. Specific management of post-chikungunya rheumatic disorders: a retrospective study of 159 cases in Reunion Island from 2006–2012. PLoS Negl Trop Dis 2015;9:e0003603.
10. Gerardin P, Couderc T, Bintner M, Tournebize P, Renouil M, Lemant J, et al. Chikungunya virus-associated encephalitis: a cohort study on La Réunion Island, 2005–2009. Neurology 2016;86: 94–102.
11. Bouquillard E, Fianu A, Bangil M, Charlette N, Ribera A, Michault A, et al. Rheumatic manifestations associated with Chikungunya virus infection: a study of 307 patients with 32-month follow-up (RHUMATOCHIK study). Joint Bone Spine 2017. E-pub ahead of print.
12. Miner JJ, Aw-Yeang HX, Fox JM, Taffner S, Malkova ON, Oh ST, et al. Chikungunya viral arthritis in the United States: a mimic of seronegative rheumatoid arthritis. Arthritis Rheumatol 2015;67:1214–20.
13. Fox JM, Long F, Edeling MA, Lin H, van Duijl-Richter MK, Fong RH, et al. Broadly neutralizing alphavirus antibodies bind an epitope on E2 and inhibit entry and egress. Cell 2015;163:1095–107.
14. Prow NA, Tang B, Gardner J, Le TT, Taylor A, Poo YS, et al. Lower temperatures reduce type I interferon activity and promote alphaviral arthritis. PLoS Pathog 2017;13:e1006788.
15. Hoarau JJ, Jaffar Bandjee MC, Krejbich Trotot P, Das T, Li-Pat-Yuen G, Dassa B, et al. Persistent chronic inflammation and infection by Chikungunya arthritogenic alphavirus in spite of a robust host immune response. J Immunol 2010;184:5914–27.
16. Labadie K, Larcher T, Joubert C, Mannioui A, Delache B, Brochard P, et al. Chikungunya disease in nonhuman primates involves long-term viral persistence in macrophages. J Clin Invest 2010;120:894–906.
17. Teo TH, Chan YH, Lee WW, Lum FM, Amrun SN, Her Z, et al. Fingolimod treatment abrogates chikungunya virus-induced arthralgia. Sci Transl Med 2017;9:eaal1333.
18. Ravindran V, Alias G. Efficacy of combination DMARD therapy vs. hydroxychloroquine monotherapy in chronic persistent chikungunya arthritis: a 24-week randomized controlled open label study. Clin Rheumatol 2017;36:1335–40.
19. Tsetsarkin KA, Vanlandingham DL, McGee CE, Higgs S. A single mutation in chikungunya virus affects vector specificity and epidemic potential. PLoS Pathog 2007;3:e201.

ARTHRITIS & RHEUMATOLOGY
Vol. 70, No. 4, April 2018, pp 480–483
DOI 10.1002/art.40436

EDITORIAL

Marginal Jawbone Loss Is Associated With the Onset of Rheumatoid Arthritis and Is Related to the Plasma Level of RANKL

Paola de Pablo

Periodontitis is arguably the most prevalent chronic inflammatory disease in humans and affects >45% of US adults ages 30 years and older (1,2). The defining feature of periodontitis is chronic inflammation of the tooth-supporting tissue, leading to the progressive, irreversible destruction of periodontal ligament and alveolar bone that results in the formation of periodontal pockets and eventually tooth loss if it is not treated. Host susceptibility is clearly of primary importance, and tobacco smoking is a strong environmental risk factor (2). Periodontitis results from an inappropriate inflammatory response to oral microbiota, possibly exacerbated by the presence of some specific disease–associated bacterial species (3). Some of the bacterial species harbored in periodontal pockets, including *Porphyromonas gingivalis* and *Aggregatibacter actinomycetemcomitans,* have been implicated in the pathogenesis of rheumatoid arthritis (RA).

An increasing number of clinical studies have investigated the association between periodontitis/tooth loss and RA (4). Published studies vary widely with respect to the design, setting, and methods used to ascertain associations between periodontitis and RA. The majority of studies are relatively small case–control studies. Control subjects often were recruited from among the study center staff (e.g., university/hospital staff) or patients attending dental clinics, which raises concerns regarding the validity of the study. Some studies have used self-reported markers of periodontitis, which frequently lack validity. In cohort studies in particular, the assessment of periodontitis typically has not been performed robustly, and there is a lack of consistent criteria used to define a "case" of periodontitis. Periodontitis can be assessed clinically by measuring the periodontal probing depth and attachment levels at various sites of the dentition or by measuring radiographic alveolar bone loss. Definitions of periodontitis in clinical research are based on either of these measures or combinations thereof and vary widely between studies.

Overall results from clinical and epidemiologic studies have suggested that periodontitis and tooth loss are more prevalent in patients with RA (4,5). However, the strength and temporality of the association are uncertain. A recent larger and more robust case–control study demonstrated that periodontitis, as defined based on periodontal examination, was significantly more frequent in anti–citrullinated protein antibody (ACPA)–positive patients with RA compared with control patients with osteoarthritis (odds ratio [OR] 1.59, 95% confidence interval [95% CI] 1.01–2.49). Periodontitis was also associated with significantly higher RA-related antibody levels, disease activity, and radiographic damage (6).

The association between periodontitis and RA may be very important from both a clinical and a public health perspective, because there are several processes through which chronic periodontitis may be part of a causal pathway in the pathogenesis of RA (4). Given the high prevalence of periodontitis, a large proportion of RA incidence and/or morbidity could be attributable to periodontitis if causality was confirmed. Importantly, chronic periodontitis would represent a modifiable risk factor for RA (4), because effective treatments for chronic periodontitis are available (7,8).

Although previous studies have shown an association between the prevalence of both periodontitis and RA, there are no robust data for the association between periodontitis and the incidence of RA. The results of 2 large cohort studies have been published; however, these are marred by the lack of valid clinical assessments of periodontal status in these cohorts. Arkema et al did not observe an association between a self-reported history of periodontal surgery and RA incidence among women in the Nurses' Health Study (9). However, a history of periodontal surgery is a poor proxy for chronic periodontitis,

Dr. de Pablo's work was supported by the National Institute for Health Research

Paola de Pablo, MD, MPH, PhD: University of Birmingham, Queen Elizabeth Hospital, Birmingham, UK.

Address correspondence to Paola de Pablo, MD, MPH, PhD, Institute of Inflammation & Ageing, College of Medical & Dental Sciences, University of Birmingham, Queen Elizabeth Hospital, Birmingham B15 2WB, UK. E-mail: p.depablo@bham.ac.uk.

Submitted for publication January 25, 2018; accepted in revised form January 28, 2018.

likely leading to substantial attenuation of any association. In particular, a history of periodontal surgery is a proxy for a history of periodontitis, not a proxy for current exposure to periodontal inflammation and/or pathogens thought to underpin any causal association between periodontitis and RA. If periodontitis was indeed a causal risk factor for RA, successful periodontal surgery would be expected to reduce RA risk to a level comparable to that in healthy individuals. In addition, the validity of self-reported periodontal surgery itself may also be a concern.

Another large population-based study including nearly 10,000 individuals and 433 incident RA cases followed up for more than 20 years did not show an association between periodontitis and RA incidence (10). However, the dental examination in the First National Health and Nutrition Examination Survey cohort did not include periodontal probing, and the case definition of RA was based on self-report (which is notoriously inaccurate) in 90% of cases.

In contrast, 2 recent very large case–control studies in Taiwan showed an association between periodontitis and the incidence of RA (4,11,12). However, information on smoking, a major confounder in this association, was lacking, and the case definitions of periodontitis and RA were based on administrative data, which raises concerns with regard to the validity. Interestingly, a recent study of 72 treatment-naive patients with arthralgia demonstrated that having periodontitis was associated with disease progression to RA (92% versus 55% of those without periodontitis; $P = 0.04$) and a greater risk for future methotrexate treatment upon the diagnosis of RA (hazard ratio 2.68, 95% CI 1.11–6.50) (13).

In this issue of *Arthritis & Rheumatology*, Kindstedt et al present data suggesting that periodontitis precedes the onset of RA (14). In this case–control study nested in a population-based survey of cohorts in the Medical Biobank of Northern Sweden, radiographs were retrieved from dental offices before the occurrence of symptoms of RA in 45 presymptomatic subjects and 45 controls matched for age, sex, and smoking status who were selected at random. In 31 of the 45 case–control pairs, both the case and control had undergone radiographic examination before the onset of symptoms as well as repeated radiographic examinations after the diagnosis of RA, allowing longitudinal evaluation of bone loss. The case definition of the exposure was based on marginal jawbone loss, which is the hallmark of periodontitis. Compared with matched controls, individuals with presymptomatic RA had a significantly lower number of teeth and increased bone loss, which was more pronounced in those who were positive for both ACPA and RANKL. After stratification for smoking, an age-adjusted model confirmed a modest positive association in 13 matched pairs of never smokers (hazard ratio 1.03, 95% CI 1.01–1.05). Interestingly, bone loss continued after RA was diagnosed, was higher in cases compared with matched controls, and was more marked in ACPA-positive presymptomatic subjects, suggesting that periodontitis was not treated.

The results of the study by Kindstedt et al are consistent with previous data showing higher titers of antibodies to both citrullinated and uncitrullinated peptides in subjects without RA who had periodontitis, particularly those who were never smokers (15). Tolerance breakdown in nonsmokers with periodontitis may be initiated with uncitrullinated peptides, with spreading to citrullinated epitopes as the autoimmune response evolves into presymptomatic RA. Indeed, antibodies against arginine-containing peptides from RA autoantigens were present in a population-based sample of 386 individuals with presymptomatic RA. The presence of these antibodies pre-dated the presence of corresponding antibodies against citrullinated peptides, which appeared closer to onset of symptoms (16). Other studies have also shown the presence of antibodies to native and citrullinated autoantigens in RA, with antibodies against native RA33 being associated with early disease and low structural damage, whereas antibodies targeting citrullinated RA33 were associated with disease duration and erosive disease (17).

Taken together, these results challenge the notion of citrullination being the inciting event underlying loss of tolerance in RA and suggest that there are 2 stages in the development of ACPAs: a first stage in which antibodies against arginine peptides appear, followed by a second stage in which antibodies against citrullinated peptides develop. Although we can only speculate, it is possible that periodontitis contributed to the increased autoantibody seropositivity observed in previous studies (15–18). However, periodontitis is a very common disease, and evidence of citrullination of proteins occurring in periodontal tissue in individuals with periodontitis (19–22) suggests that RA-related inflammation may indeed occur initially in the periodontal pocket.

In support of the notion that a periodontal lesion is a site for the initiation of RA-related autoimmunity, several periodontal pathogens have now been implicated in RA, with citrullination of proteins being the possible link between periodontitis, the generation of RA-related antibodies, and RA development.

At least one periodontal pathogen, *Porphyromonas gingivalis*, possesses a bacterial peptidylarginine deiminase (PAD; hereinafter referred to as PPAD) (23–26) that is responsible for citrullination of bacterial or host proteins, generating neoantigens that could break tolerance, leading to the generation of ACPAs in RA (27). Antibodies to

P gingivalis (as a measure of exposure to *P gingivalis*) have been associated with the presence of RA-related autoantibodies (rheumatoid factor and/or ACPA) in individuals at increased risk of disease but who have not yet developed RA symptoms (28), and higher levels of IgG anti–arginine gingipain type B (anti-RgpB) were also observed in presymptomatic subjects compared with controls without RA and decreased following the diagnosis of RA in a Northern European cohort (29). In contrast, no association was observed between anti-RgpB and presymptomatic RA in a Southern European sample (30). However, these studies did not assess periodontal status.

Overall, reports correlating *P gingivalis* antibodies with the pathogenesis of RA have been equivocal, mostly due to the heterogeneity of the assays used to quantify antibody responses to *P gingivalis* (e.g., antibodies against purified *P gingivalis*–specific RgpB protein versus antibodies against *P gingivalis* cell lysates).

PPAD is also autocitrullinated, and there is an increased antibody response to PPAD in RA, due to reactions with autocitrullinated epitopes on the PPAD molecule (31). Therefore, PPAD is a candidate for inducing an antibody response to citrullinated proteins in RA via autocitrullination, citrullination by human PAD enzymes, or citrullination of other bacterial and/or human proteins (32).

Recent data suggest that another periodontal pathogen, *A actinomycetemcomitans*, is also capable of protein citrullination, including citrullinated autoantigens targeted by autoantibodies in RA. *A actinomycetemcomitans* triggers citrullination through a pore-forming toxin, leukotoxin A (LtxA), that allows extracellular calcium to flow into the cells, where there is amplified citrullination or hypercitrullination of intracellular proteins in neutrophils (22), which is dependent on both bacterial and host components. This phenomenon (LtxA-mediated hypercitrullination) was not observed in other cell types (peripheral blood mononuclear cells or macrophages) treated with LtxA, suggesting a major role for neutrophils as the primary source of citrullinated proteins induced by LtxA, which is intracellular and independent of NETosis.

Antibodies against *A actinomycetemcomitans* were detected in 21% of RA patients compared with 3% of controls, and antibodies against LtxA were also more common in RA patients compared with controls (43% versus 11%) and were associated with citrullinated intracellular proteins (but not citrullinated extracellular proteins) and RA autoantibodies. Interestingly, the association between RA autoantibodies and the shared epitope was restricted to those who had evidence of exposure to LtxA (22), suggesting that *A actinomycetemcomitans* may play a role in the development of autoantibodies in individuals with a genetic predisposition to develop RA. Other pathogens in the oral/periodontal microbiome have been implicated in ACPA seropositivity and RA (33) and their role merits further research.

Further epidemiologic and mechanistic studies on the emergence of autoantibodies that are conducted in large samples of individuals with periodontitis who are at risk of RA are warranted, as well as studies to explore the causal involvement of periodontitis and periodontal pathogens, including interventions to control periodontitis, in the earliest phases before the development of RA.

If periodontitis is indeed a risk factor for RA, intervention trials would be critical to explore this relationship. A few small studies have suggested that anti-infective periodontal treatment might reduce disease activity in patients with established RA (34); however, these studies are very challenging, and no pivotal studies have been conducted to investigate this. Another question is whether treatment of periodontitis in persons at risk for RA (i.e., during the preclinical phases) can delay or prevent the onset of RA. Although this is an intriguing concept, such trials may not be feasible at this time given the relatively low incidence of RA and the need for very long follow-up periods. Nevertheless, the recommendation to seek and maintain good oral and periodontal health, just as the recommendation to seek good general health and avoid smoking, should not await the results of such trials.

AUTHOR CONTRIBUTIONS

Dr. de Pablo drafted the article, revised it critically for important intellectual content, approved the final version to be published, and takes responsibility for the integrity of the data and the accuracy of the data analysis.

REFERENCES

1. Eke PI, Dye BA, Wei L, Slade GD, Thornton-Evans GO, Borgnakke WS, et al. Update on prevalence of periodontitis in adults in the United States: NHANES 2009 to 2012. J Periodontol 2015;86:611–22.
2. Van Dyke TE, Sheilesh D. Risk factors for periodontitis. J Int Acad Periodontol 2005;7:3–7.
3. Wade WG. The oral microbiome in health and disease. Pharmacol Res 2013;69:137–43.
4. De Pablo P, Chapple IL, Buckley CD, Dietrich T. Periodontitis in systemic rheumatic diseases. Nat Rev Rheumatol 2009;5:218–24.
5. Kaur S, White S, Bartold PM. Periodontal disease and rheumatoid arthritis: a systematic review. J Dent Res 2013;92:399–408.
6. Mikuls TR, Payne JB, Yu F, Thiele GM, Reynolds RJ, Cannon GW, et al. Periodontitis and Porphyromonas gingivalis in patients with rheumatoid arthritis. Arthritis Rheumatol 2014;66:1090–100.
7. Van der Weijden GA, Timmerman MF. A systematic review on the clinical efficacy of subgingival debridement in the treatment of chronic periodontitis. J Clin Periodontol 2002;29 Suppl 3:55–71; discussion 90–1.
8. Heitz-Mayfield LJ, Trombelli L, Heitz F, Needleman I, Moles D. A systematic review of the effect of surgical debridement vs non-

surgical debridement for the treatment of chronic periodontitis. J Clin Periodontol 2002;29 Suppl 3:92–102; discussion 60–2.
9. Arkema EV, Karlson EW, Costenbader KH. A prospective study of periodontal disease and risk of rheumatoid arthritis. J Rheumatol 2010;37:1800–4.
10. Demmer RT, Molitor JA, Jacobs DR Jr, Michalowicz BS. Periodontal disease, tooth loss and incident rheumatoid arthritis: results from the First National Health and Nutrition Examination Survey and its epidemiological follow-up study. J Clin Periodontol 2011;38:998–1006.
11. Chen HH, Huang N, Chen YM, Chen TJ, Chou P, Lee YL, et al. Association between a history of periodontitis and the risk of rheumatoid arthritis: a nationwide, population-based, case-control study. Ann Rheum Dis 2013;72:1206–11.
12. Chou YY, Lai KL, Chen DY, Lin CH, Chen HH. Rheumatoid arthritis risk associated with periodontitis exposure: a nationwide, population-based cohort study. PLoS One 2015;10:e0139693.
13. Hashimoto M, Yamazaki T, Hamaguchi M, Morimoto T, Yamori M, Asai K, et al. Periodontitis and Porphyromonas gingivalis in preclinical stage of arthritis patients. PLoS One 2015;10:e0122121.
14. Kindstedt E, Johansson L, Palmqvist P, Koskinen Holm C, Kokkonen H, Johansson I, et al. Association between marginal jawbone loss and onset of rheumatoid arthritis and relationship to plasma levels of RANKL. Arthritis Rheumatol doi: http://onlinelibrary.wiley.com/doi/10.1002/art.40394/abstract. E-pub ahead of print.
15. De Pablo P, Dietrich T, Chapple IL, Milward M, Chowdhury M, Charles PJ, et al. The autoantibody repertoire in periodontitis: a role in the induction of autoimmunity to citrullinated proteins in rheumatoid arthritis? Ann Rheum Dis 2014;73:580–6.
16. Brink M, Hansson M, Ronnelid J, Klareskog L, Rantapaa Dahlqvist S. The autoantibody repertoire in periodontitis: a role in the induction of autoimmunity to citrullinated proteins in rheumatoid arthritis? Antibodies against uncitrullinated peptides seem to occur prior to the antibodies to the corresponding citrullinated peptides. Ann Rheum Dis 2014;73:e46.
17. Konig MF, Giles JT, Nigrovic PA, Andrade F. Antibodies to native and citrullinated RA33 (hnRNP A2/B1) challenge citrullination as the inciting principle underlying loss of tolerance in rheumatoid arthritis. Ann Rheum Dis 2016;75:2022–8.
18. De Pablo P, Dietrich T, Chapple IL, Milward M, Buckley CD, Venables PJ. Response to: 'The autoantibody repertoire in periodontitis: a role in the induction of autoimmunity to citrullinated proteins in rheumatoid arthritis? Antibodies against uncitrullinated peptides seem to occur prior to the antibodies to the corresponding citrullinated peptides' by Brink et al [letter]. Ann Rheum Dis 2014;73:e47.
19. Nesse W, Westra J, van der Wal JE, Abbas F, Nicholas AP, Vissink A, et al. The periodontium of periodontitis patients contains citrullinated proteins which may play a role in ACPA (anti-citrullinated protein antibody) formation. J Clin Periodontol 2012; 39:599–607.
20. Harvey GP, Fitzsimmons TR, Dhamarpatni AA, Marchant C, Haynes DR, Bartold PM. Expression of peptidylarginine deiminase-2 and -4, citrullinated proteins and anti-citrullinated protein antibodies in human gingiva. J Periodontal Res 2013;48:252–61.
21. Laugisch O, Wong A, Sroka A, Kantyka T, Koziel J, Neuhaus K, et al. Citrullination in the periodontium: a possible link between periodontitis and rheumatoid arthritis. Clin Oral Investig 2016; 20:675–83.
22. Konig MF, Abusleme L, Reinholdt J, Palmer RJ, Teles RP, Sampson K, et al. Aggregatibacter actinomycetemcomitans-induced hypercitrullination links periodontal infection to autoimmunity in rheumatoid arthritis. Sci Transl Med 2016;8:369ra176.
23. Travis J, Pike R, Imamura T, Potempa J. Porphyromonas gingivalis proteinases as virulence factors in the development of periodontitis. J Periodontal Res 1997;32:120–5.
24. McGraw WT, Potempa J, Farley D, Travis J. Purification, characterization, and sequence analysis of a potential virulence factor from Porphyromonas gingivalis, peptidylarginine deiminase. Infect Immun 1999;67:3248–56.
25. Rosenstein ED, Greenwald RA, Kushner LJ, Weissmann G. Hypothesis: the humoral immune response to oral bacteria provides a stimulus for the development of rheumatoid arthritis. Inflammation 2004;28:311–8.
26. Shirai H, Blundell TL, Mizuguchi K. A novel superfamily of enzymes that catalyze the modification of guanidino groups. Trends Biochem Sci 2001;26:465–8.
27. Wegner N, Wait R, Sroka A, Eick S, Nguyen KA, Lundberg K, et al. Peptidylarginine deiminase from Porphyromonas gingivalis citrullinates human fibrinogen and α-enolase: implications for autoimmunity in rheumatoid arthritis. Arthritis Rheum 2010;62:2662–72.
28. Mikuls TR, Thiele GM, Deane KD, Payne JB, O'Dell JR, Yu F, et al. Porphyromonas gingivalis and disease-related autoantibodies in individuals at increased risk of rheumatoid arthritis. Arthritis Rheum 2012;64:3522–30.
29. Johansson L, Sherina N, Kharlamova N, Potempa B, Larsson B, Israelsson L, et al. Concentration of antibodies against Porphyromonas gingivalis is increased before the onset of symptoms of rheumatoid arthritis. Arthritis Res Ther 2016;18:201.
30. Fisher BA, Cartwright AJ, Quirke AM, de Pablo P, Romaguera D, Panico S, et al. Smoking, Porphyromonas gingivalis and the immune response to citrullinated autoantigens before the clinical onset of rheumatoid arthritis in a Southern European nested case-control study. BMC Musculoskelet Disord 2015;16:331.
31. Quirke AM, Lugli EB, Wegner N, Hamilton BC, Charles P, Chowdhury M, et al. Heightened immune response to autocitrullinated Porphyromonas gingivalis peptidylarginine deiminase: a potential mechanism for breaching immunologic tolerance in rheumatoid arthritis. Ann Rheum Dis 2014;73:263–9.
32. Quirke AM, Lundberg K, Potempa J, Mikuls TR, Venables PJ. PPAD remains a credible candidate for inducing autoimmunity in rheumatoid arthritis: comment on the article by Konig et al. Ann Rheum Dis 2015;74:e7.
33. Scher JU, Ubeda C, Equinda M, Khanin R, Buischi Y, Viale A, et al. Periodontal disease and the oral microbiota in new-onset rheumatoid arthritis. Arthritis Rheum 2012;64:3083–94.
34. Kaur S, Bright R, Proudman SM, Bartold PM. Does periodontal treatment influence clinical and biochemical measures for rheumatoid arthritis? A systematic review and meta-analysis. Semin Arthritis Rheum 2014;44:113–22.

ARTHRITIS & RHEUMATOLOGY
Vol. 70, No. 4, April 2018, pp 484–495
DOI 10.1002/art.40403

REVIEW

Chikungunya Arthritis

Implications of Acute and Chronic Inflammation Mechanisms on Disease Management

Ali Zaid,[1] Patrick Gérardin,[2] Adam Taylor,[1] Helen Mostafavi,[1] Denis Malvy,[3] and Suresh Mahalingam[1]

In the past decade, arboviruses—arthropod-borne viruses—have been the focus of public health institutions worldwide following a spate of devastating outbreaks. Chikungunya virus, an arbovirus that belongs to the alphavirus genus, is a reemerging arthritogenic virus that has caused explosive outbreaks since 2006, notably on Réunion Island, and more recently in the Caribbean, South America, India, and Southeast Asia. The severity of arthritic disease caused by chikungunya virus has prompted public health authorities in affected countries to develop specific guidelines to tackle this pathogen. Chikungunya virus disease manifests first as an acute stage of severe joint inflammation and febrile illness, which later progresses to a chronic stage, during which patients may experience debilitating and persisting articular pain for extended periods. This review aims to provide a broad perspective on current knowledge of chikungunya virus pathogenesis by identifying key clinical and experimental studies that have contributed to our understanding of chikungunya virus to date. In addition, the review explores the practical aspects of treatment and management of both acute and chronic chikungunya virus based on clinical experience during chikungunya virus outbreaks. Finally, recent findings on potential therapeutic solutions—from antiviral agents to immunomodulators—are reviewed to provide both viral immunologists and clinical rheumatologists with a balanced perspective on the nature of a reemerging arboviral disease of significant public health concern, and insight into future therapeutic approaches to better address the treatment and management of chikungunya virus.

Introduction

Arthropod-borne viral infections have recently dominated the headlines following a spate of significant outbreaks around the world. Mosquito-borne viruses such as chikungunya virus have sparked the attention of global health organizations and led to robust public health interventions. Outbreaks of chikungunya virus had been reported in Africa, Asia, and the Indian and Pacific Oceans since the mid-2000s; a small number of cases have also been reported within Europe (1,2). In 2013 the chikungunya virus epidemic reached the Americas and it is now spreading through South America, with >1 million cases reported (3–5). In the US, travel-associated cases have been reported in 37 states (1) within the mainland US (as of January 2017), with cases of local transmission also reported in Florida (2). Of more pressing concern, India (3) and most Southeast Asian countries have been subjected to unabated epidemics that have proven difficult to control. Propitious climate, facilitated by seasonal monsoons and urban areas where mosquito vector control is lacking, along with a reservoir of naive populations, are major contributing factors to the risk posed by locally acquired chikungunya virus infections in developing countries (4). While developed economies that have experienced significant numbers of traveler-imported cases are

Dr. Mahalingam is recipient of a Australian National Health and Medical Research Council Senior Research Fellowship (grant 1059167).

[1]Ali Zaid, PhD, Adam Taylor, PhD, Helen Mostafavi, BSc, Suresh Mahalingam, PhD: Griffith University, Gold Coast, Queensland, Australia; [2]Patrick Gérardin, MD, PhD: INSERM CIC1410, Centre Hospitalier Universitaire de la Réunion, Saint Pierre, Réunion, France, and CNRS 9192, INSERM U1187, Université de la Réunion, Sainte Clotilde, Réunion, France; [3]Denis Malvy, MD, PhD: Department of Tropical Medicine and Clinical International Health, University Hospital Center and INSERM 1219, University of Bordeaux, Bordeaux, France.

Address correspondence to Suresh Mahalingam, PhD, Emerging Viruses and Inflammation Research Group, Institute for Glycomics, Griffith University, Gold Coast Campus, Queensland 4222, Australia. E-mail: s.mahalingam@griffith.edu.au.

Submitted for publication August 3, 2017; accepted in revised form December 18, 2017.

somewhat equipped to manage the chikungunya virus disease burden, less economically developed regions of the world—in particular densely populated urban areas—where epidemics have become most resilient have seen their public health systems overwhelmed by the disease (3,5).

Chikungunya virus symptoms include a range of acute manifestations, among which fever, severe joint and muscle pain, headache, and rashes are prominent. However, there is mounting concern over the persistence of long-lasting manifestations associated with debilitating effects of the disease and the deterioration of overall health and quality of life (6–9). Among these, chronic arthralgia/arthritis (joint pain/joint stiffness plus joint swelling, respectively), musculoskeletal injury, and fatigue—and, to a lesser extent, neurocognitive and sensorineural manifestations—have been shown to contribute significantly to the economic burden of the disease (10,11). Although vaccines have reached human trials (12,13) and a range of potential antiviral compounds have undergone preclinical evaluation (14,15), no licensed vaccines or antiviral therapies are available. Both acute and chronic disease manifestations are of significant concern, and there are currently no specific, approved drugs to treat either form of the disease. Chronic chikungunya virus poses important questions with regard to public health policy and interventions. Should efforts be directed at managing the early stages of the disease, to limit the consequences on population productivity and lessen the burden of a "patient rush" on often-under equipped hospitals, or should more attention be focused on limiting the development of chronic disease, associated with persistent rheumatic disease and a risk of long-term impact on population health?

In this review, we address the key pathophysiologic mechanisms that drive acute and chronic chikungunya arthritis, arguably the most incapacitating phenotype among long-lasting chikungunya virus disease manifestations, based on recent animal experimental disease models and epidemiologic studies. We explore the latest findings in therapeutic development aimed at both limiting viral spread and at immune and inflammatory mechanisms, and address the implications of such findings in current and future clinical care of chikungunya virus patients.

Chikungunya virus is recognized as an emerging biphasic disease, described as an acute infection followed by persistent symptoms. Hence, experts have defined 3 successive clinical stages, taking into account known difficulties in practical management. In symptomatic, infected individuals, the first stage encompasses an acute incapacitating febrile viremic phase together with residual symptoms. The 2 final stages are characterized by persistent manifestations: a post-acute stage (from 21 days after the onset of infection to the end of the third month) and a chronic stage (beyond 3 months). Schematically, the disease progresses to resolution without sequelae either spontaneously or after treatment, or to a persistence of articular and general symptoms, or to aggravation due to an inflammatory or degenerative process.

Acute and post-acute stages of chikungunya virus (≤3 months after the onset of infection)

After a silent incubation of 4–7 days, the acute stage of chikungunya virus disease can be divided into 2 distinct phases, the viremic phase (5–10 days) and the post-viremic phase (6–21 days) (16–18). In the most common manifestations, the viremic phase is marked by unusually high-grade fever (>39°C) with abrupt onset, accompanied by severe incapacitating oligo- or polyarthralgia/arthritis (<4 or ≥4 joints, respectively, with debilitating and sudden injury), myalgia, headache, backache, and cutaneous rash, whereas the post-viremic phase is characterized by apyrexia (no fever), polyarthralgia/arthritis, and to a lesser extent, myalgia, pruritus, fatigue, and lymphadenopathies and anorexia, though the latter are less common (18). Joint pain is most often symmetric and additive and affects the large and smaller articulations of both the arms (most commonly the wrists, followed by the phalanges, shoulders, and elbows) and the legs (most commonly the ankles, followed by the knees, feet, and hips). Atypical locations include vertebral, temporomandibular, or sternoclavicular articulations (17). Stiffness and swelling, indicative of synovitis, are observed in the ankles, phalanges, wrists, and toes, but very exceptionally in larger joints (17). After infection, IgM antibody isotype appears within days of the onset of symptoms, and neutralizing anti–chikungunya virus IgG typically appears by the second week (19).

Acute chikungunya virus infection (<21 days after the onset of infection) is consistently associated with a strong host antiviral type I interferon (IFN) response. RNA sequencing (RNASeq) analysis of acute chikungunya virus infection in a mouse model revealed that approximately half of all genes up-regulated after infection are IFN-stimulated genes (ISGs) (20,21). IFNα is detected early in infection, reaching levels of 700 pg/ml in the plasma of chikungunya virus–infected patients, coinciding with the onset of disease symptoms (16,22). During the acute stage, patient viremia has been shown to directly correlate with production of cytokines such as IFNα and interleukin-6 (IL-6) (20,22). Although this correlation is lacking in other studies, it is broadly accepted that all patients experiencing acute chikungunya virus infection

produce high levels of IFNα (20). This is also observed in animal models of acute chikungunya virus disease (21,23–25). Indeed, chikungunya virus infection is generally fatal in mice deficient in type I IFN responses, while arthritogenic manifestations are exacerbated in IFNα/β-deficient mice infected with chikungunya virus (24–26). Furthermore, downstream effectors of IFN induction such as ISGs play key roles in inhibiting chikungunya virus infection (21), and a strong IFN response is associated with a milder course of disease in mice infected with alphaviruses (24,25,27). The ability of alphaviruses to develop mechanisms to inhibit host IFN induction and signaling (28) also highlights the importance of this early innate immune response in controlling infection (29).

In addition to a potent type I IFN response, the acute stage of chikungunya virus infection (<21 days after the onset of infection) is associated with elevated patient plasma levels of multiple soluble factors, including proinflammatory cytokines and chemokines (CCL2, macrophage migration inhibitory factor, CCL4, CXCL10, IL-6, IL-8, and IL-16), antiinflammatory cytokines (IL-1 receptor A, IL-10, and IL-13), growth factors (granulocyte colony-stimulating factor [G-CSF], granulocyte–macrophage colony-stimulating factor [GM-CSF], vascular endothelial growth factor, and stem cell growth factor β) and other mediators (IFNγ, IL-4, IL-7, and CXCL9) (20–22,30–33). This results in intense monocyte trafficking to the infected tissues (33), along with strong activation of both CD8+ T and natural killer (NK) cells to assist in clearing the virus (20,34). The post-acute stage of chikungunya virus (from the fourth week to the third month after the onset of infection) is characterized by very polymorphous manifestations prolonging the initial inflammatory symptoms (acute arthritis) by diverse rheumatic disorders, including periarticular involvement, slowly regressive enthesitis, tenosynovitis, and bursitis, together with nonrheumatic and systemic symptoms (18). This stage is marked by persistence of IL-6 and GM-CSF secretions and production of IL-17 in the most affected patients, or by eotaxin and hepatocyte growth factor in those who have fully recovered (20).

Chronic stage of chikungunya virus (>3 months after the onset of infection)

While 50–60% of patients with acute chikungunya virus recover fully or with mild-to-moderate sequelae, in some the disease evolves to a chronic stage that can last up to several years (18,35). Beyond the post-acute stage, chronic chikungunya virus is thus characterized by the persistence of arthritic conditions associated with long-term sequelae, such as fatigue and depression, stemming from prior rheumatic conditions, although not a prerequisite, or in the wake of an authentic arthritogenic alphaviral infection. Chronic chikungunya virus is associated with high levels of circulating IL-6 and IL-12 (22,31,36). IL-6 is specifically expressed in the affected joints and could stimulate the release of RANKL while inhibiting the action of its decoy receptor osteoprotegerin released by osteoblasts, resulting in osteoclastogenesis and severe bone loss, as has been shown in mice (37–40). Indeed, while bone loss is not a defining feature in patients with chronic chikungunya arthritis, recent studies appear to implicate IL-6 as a possible biomarker of chronic chikungunya virus (41,42).

In addition to soluble host factors responsible for regulating antiviral responses, CD4+ T cells have been shown to be a major driver of arthritic disease during chikungunya virus infection in mouse models (43,44) and in the follow-up of patients with chronic chikungunya arthritis (45). Moreover, impaired NK cell function was shown to be associated with chronic arthritis in infected patients (46). Importantly, Treg cells, a subset of CD4+ T cells, may play a role in moderating excessive chikungunya virus–induced immune responses. Treg cells compete with naive T cells to interact with antigen-presenting dendritic cells. Treg cells interacting with dendritic cells were shown to cause mature dendritic cells to down-regulate costimulatory signaling, curtailing the expansion of chikungunya virus–specific CD4+ T cells, thus effectively reducing chikungunya virus–induced joint swelling in mice (47). B cells and neutralizing antibodies, especially the IgG3 subclass, are also critical for chikungunya virus clearance (19,48). The immaturity of cellular and humoral immunity may, if only partly, explain the rarity of chronic arthralgia in children younger than 3 years of age.

The role of myeloid cells is less clear in the chronic stage of human chikungunya virus infection, where they may be involved in the clearance of infected cell debris which, when acting as a source of pathogen-associated molecular patterns, may trigger or drive chronic chikungunya virus (49). Monocytes and macrophages recruited to the sites of inflammation during chikungunya virus infection dominate the cellular infiltrates (23,33). However, in studies using mice deficient in the chemokine receptor CCR2, the monocyte/macrophage infiltrate was replaced by a severe neutrophil infiltrate, exacerbating chikungunya virus–induced inflammation and cartilage damage (50). Thus, although recruited CCR2+ monocyte/macrophages contribute to inflammation, they may also be needed to prevent excessive pathology or promote resolution of disease following chikungunya virus infection.

Interestingly, a recent RNA Seq analysis of chikungunya virus–infected mouse tissues demonstrated good concordance with the expression of genes reported to be up-regulated in chikungunya virus patients (21). Most

genes were associated with inflammation, indicating consistent proinflammatory gene expression in both mouse and non-human primate models and chikungunya virus–infected patients. This suggests that chronic chikungunya virus may represent an extension of acute disease rather than an activation of, or progression to, new inflammatory immunopathologies. Antiinflammatory treatments that effectively target acute chikungunya virus may thus also have utility in treating chronic chikungunya virus (21). Prominent in the RNA Seq analysis of chikungunya virus infection in mice was the serine protease granzyme A (21). Granzyme A was found to play a proinflammatory role in chikungunya virus in mice and was also found in the sera of chikungunya virus–infected non-human primates and in symptomatic chikungunya virus–infected patients. The mouse granzyme A inhibitor, Serpinb6b, significantly reduced foot swelling in chikungunya virus–infected mice, indicating that granzyme A may be a potential therapeutic candidate (21). Granzyme A was also recently shown to be important in a mouse model of rheumatoid arthritis (RA) (51), an example of the significant overlap between chikungunya arthritis and RA (43,45).

Chronic chikungunya arthritis and implications for therapy

Risk factors for the development of chronic chikungunya arthralgia/arthritis. Although most patients recover from acute chikungunya virus infection within days or weeks, instances of persistent post–chikungunya virus rheumatic disease—chronic and incapacitating joint morbidities—have been reported in a recent systematic review (35), and in up to 40% of patients on average in a recent meta-analysis (52). This often painful, incapacitating chronic chikungunya virus disease—of a primarily rheumatic nature, though as noted above, prior rheumatic conditions are not a prerequisite—can persist for years in some patients and is highly detrimental to their health and quality of life (6–10,36,52–63). Although there have been numerous studies focusing on acute chikungunya virus infection and potential treatments, the mechanisms that cause chikungunya virus to progress to a chronic stage are still poorly understood.

One hypothesis is that comorbidities such as preexisting joint disease (e.g., osteoarthritis or RA), metabolic syndrome features (e.g., hypertension, obesity, or diabetes mellitus), or both prior to chikungunya virus infection may exacerbate chikungunya virus–induced arthritis or increase patient susceptibility to developing chronic chikungunya virus polyarthritis (54,58,59). In the population-based TELECHIK study, preexisting rheumatic disorders and metabolic syndrome were both associated with long-lasting rheumatic pain in an unadjusted analysis (10,58). However, a separate study from Réunion Island showed that only 2.8% of the hospital-based patients who had chronic chikungunya virus had preexisting joint disease (59). Given such discrepancies across studies, any link between preexisting joint disease and an increased risk of developing chikungunya arthritis remains unproven (35,53,57,62,63). Risk factors for the development of chronic chikungunya arthralgia include an age of >45 years (54,58), severe (9,54,58) or long-lasting (9,60) acute chikungunya virus, a high viral load (>10^9/ml) during the viremic phase (36), and an intense chikungunya virus immune response in the post-viremic phase (58).

The case for viral persistence. In most viral arthritides, arthritic disease is associated with the presence or persistence of replicating virus and/or viral debris in joint tissues (64). A substantial body of evidence supports the view that the same underlying mechanism is responsible for alphaviral arthritides, including chikungunya arthritis. Poo et al reported detection of significant levels of chikungunya virus RNA in the feet of wild-type C57BL/6 mice up to 100 days after infection (65), which is consistent with studies in non-human primate models (23,66), and to date, a single clinical observation (36). Chikungunya virus proteins and continued virus-specific T cell responses were also detected throughout the chronic stage of disease in C57BL/6 mice (65) and in rhesus macaques (66). Importantly, the latter model showed that the intensity of the T cell response was age dependent, as evidenced by diminished T cell infiltrates and a more pronounced persistence of chikungunya virus in the tissues of aged monkeys (66), consistent with human pathology (54,58). Interestingly, the hierarchy of the T cell response in humans follows a shift from CD4 to CD8, which may be indicative of a role of aging in chikungunya virus immunopathology (67).

Although persistent chikungunya virus RNA has been detected in chronic disease (with double-stranded RNA by itself known to be arthritogenic [68]), investigators have been unable to isolate infectious virus from tissue or sera in mouse models and human studies (36,65). Human studies have shown high levels of chikungunya virus–specific IgM up to 180 days in patients with no preexisting musculoskeletal disease prior to infection (36,53), and even a case of severe destructive arthritis that exhibited chikungunya virus–specific IgM over 24 months (55). These findings suggest that the persistence of viral antigens could be a contributing factor to the development of chronic chikungunya arthritis, but the underlying molecular mechanisms are still unknown, and a statistical association between persistent chikungunya virus–specific IgM and chronic arthralgia has not yet been established (53). Immunohistochemical analysis revealed the presence of

chikungunya virus antigen in muscle satellite cells and perivascular macrophages in muscle and synovial tissue in patients with chronic chikungunya virus (36,69). This suggests that infection of muscle satellite cells—myogenic precursor cells responsible for postnatal muscle growth and repair—could be an underlying cause of the persistence of chikungunya virus in muscle tissues (69,70).

Clinical care of chikungunya virus patients: lessons learned from a decade of outbreaks

Current treatment of patients with acute and post-acute chikungunya virus (≤3 months after the onset of infection). The management of acute chikungunya virus involves both supportive care and physical measures, and the physician's role is important. Given the potential for corticosteroids to exacerbate viral arthritides (71), treatment with nonsteroidal antiinflammatory drugs (NSAIDs) remains a key disease management approach (72). However, to date there is no effective antiviral treatment licensed for clearing the virus. In the acute stage of chikungunya virus (≤3 weeks after the onset of infection), the therapeutic aims are first to alleviate fever and pain and then to prevent short-term (i.e., organ dysfunction due to chikungunya virus or of iatrogenic origin), post-acute, and chronic complications. In the post-acute stage (≥4 weeks after the onset of infection), the therapeutic strategy is based on a patient-centered approach, with the objectives of relieving pain and inflammation, preventing stiffness, loss of muscle tone, and loss of physical fitness, and limiting the consequences of the inflammatory process (18). At this stage, treatment primarily consists of analgesics and NSAIDs, though it must be noted that NSAID treatment depends on the clinical presentation, since no NSAID class has demonstrated a clear benefit or effectiveness for post–chikungunya virus symptoms. NSAIDs are prescribed at full dose (within critical tolerance), and their effectiveness is reassessed (with regard to dose and schedule) during the first week or within the first 10 days. If well tolerated, NSAID treatment can be extended up to several weeks before gradual weaning.

For fever and pain alleviation, acetaminophen is relied on as a first-line medication (level 1). The risk of acute hepatitis is increased in the case of severe pain (which often requires supratherapeutic doses), underlying comorbidities (alcohol use, liver diseases, or malnutrition), or drug interactions (unwanted self-medication). When acetaminophen fails, second-line treatment consists of adding weak opioids (level 2), for instance, codeine combined with acetaminophen (adult regimen contraindicated during breastfeeding), adding codeine to acetaminophen (restricted to patients age >12 years), or adding tramadol to acetaminophen (adult formulation, or pediatric formulation for children >3 years) (18). When second-line treatment fails, morphine (level 3) (extended or immediate action) can be used on a case-by-case basis, usually in the hospital, under strict monitoring and after assessment of the risk/benefit ratio due to possible side effects (respiratory, neurologic, digestive, and urinary) (18).

Corticosteroids are generally strongly discouraged, given the lack of a clear benefit in the course of severe arthritis, since it has been suggested that they may cause a rebound of arthritis or tenosynovitis (18). Notwithstanding their inherent risk, the use of corticosteroids may, in our experience, be warranted when strictly limited to highly inflammatory polyarticular injury associated with tenosynovitis or severe synovitis or when NSAID treatment has failed. Generally, a 10 mg/day course of prednisone for 5 days (with immediate de-escalation within 10 days) was found to be sufficient in moderate NSAID-refractory cases (18). As a general rule, the total duration of corticosteroid treatment must be <4 weeks, and must be followed by a switch to an NSAID to avoid deleterious clinical rebound and/or drug-induced dependence. Of note, other agents such as chloroquine have been shown to be ineffective in relieving acute pain (73) with inconclusive results regarding efficacy in relieving post-acute pain as a suboptimal cotreatment with acetaminophen (74). In the case of disease-modifying antirheumatic drugs (DMARDs), which are further discussed below, current consensus suggests no formal indication to initiate DMARD therapy before the last phase of the post-acute stage (8 weeks after the onset of infection), even with a specific antirheumatic agent such as methotrexate (MTX). Other DMARDs, such as hydroxychloroquine (HCQ), have not been shown to be effective in the treatment of post-acute chikungunya virus (75).

Systemic, cardiac, hepatic, renal, and metabolic comorbidities should be monitored closely, since some may be exacerbated by chikungunya virus or increase the severity and duration of chikungunya virus–specific arthralgia (18). Together with nonspecific routine measures used in arthritis when pain persists beyond the third week, therapeutic strategies often focus on pain management. This usually combines level 1 and level 2 analgesics with, in some cases, antineuropathic drugs (nefopam, antiepileptic, or antidepressant pain relievers) if necessary (DN4 score for neuropathic pain of ≥4) (76). As outlined above, corticosteroid treatment, either topical or via infiltration (intraarticular or intracapsular administration), should be used only for local involvement, including tenosynovitis, bursitis, capsulitis, and carpal tunnel syndrome, or synovitis that does not respond to oral treatment.

Gaps and perspectives in the treatment of acute and post-acute chikungunya virus. The intensity or duration of pain during the acute phase has been correlated with high viral loads, providing clues that viral clearance should be hastened. Ribavirin and IFNα have shown synergistic antiviral activity against chikungunya virus in vitro; however, neither of these are recommended for daily use due to the risk of side effects (77). Favipiravir (T-705), a viral RNA polymerase inhibitor licensed in Japan for the treatment of influenza, was also found to inhibit chikungunya virus replication in vitro (78) and could become the focus of studies assessing its usefulness in treating chikungunya virus. Suramin, a licensed drug for sleeping sickness, has also shown in vitro antiviral activity through multiple mechanisms and was effective against mutant chikungunya virus strains resistant to ribavirin or favipiravir (79). Curcumin, a turmeric-derived compound used as a food additive and in herbal medicine, and its derivatives exhibit similar antiviral properties through inhibition of virus cell binding in in vitro studies (80). Finally, the short peptides pimozide and 5-tetradecyloxy-2-furoic acid were found to exhibit high synergistic antiviral activity in studies using a genome-wide loss-of-function screen (81), which further reinforces the usefulness of such a broad genome-wide scale approach in chikungunya virus disease studies. Despite significant advances in the development of chikungunya virus antiviral agents and substantial mechanistic evidence of in vitro efficacy, neither of these compounds has yet been evaluated in humans infected with chikungunya virus.

Current treatment of patients with chronic chikungunya virus (>3 months after the onset of infection). The therapeutic approach to chronic chikungunya virus requires a rheumatologist and a pain specialist, as for chronic inflammatory diseases (18). It focuses on the phenotype displayed by the individual patient, including the presence or absence of inflammatory symptoms (i.e., at least 1 joint with chronic arthritis), the number of joints involved, and the level of clinical inflammatory activity (e.g., joint destruction or extraarticular involvement). Practically, 2 distinct evolving patterns of persistent chikungunya virus rheumatic disorders can be distinguished. The large majority of patients who still have pain beyond 3 months after acute infection present with varied musculoskeletal injury, primarily tendinopathies. These patients should experience substantial improvements with prolonged administration of NSAIDs (with strictly limited use of corticosteroids) in combination with local complementary therapies. In contrast, ~5% of patients will experience conditions that fulfill the criteria for chronic inflammatory diseases, primarily potentially destructive arthritis and synovitis. Little is known about the immune (or viral) mechanisms underlying the progressive form of the disease, the development of arthritis, or predictors of this outcome.

Morphologic assessment, designed to evaluate for fulfillment of current criteria for RA and spondyloarthritis (SpA), and laboratory tests are generally performed to confirm the diagnosis and screen for evidence of inflammatory or destructive mechanisms. Incidentally, RA is the most common post–chikungunya virus chronic inflammatory disease, followed by peripheral SpA. Alternatively, nondestructive arthritis that does not meet the criteria for RA or SpA is referred to as undifferentiated polyarthritis, and may be indicated after alternative causes (such as connectivitis or lupus-like syndrome) have been ruled out. Once the type of persistent chronic chikungunya virus condition has been identified, individualized treatment is proposed based on the diagnosis, functional prognosis, and the patient's condition. Treatments aim to preserve functional outcome in order to reduce psychosocial impact and improve health-related quality of life. Ideally, treatment should begin within the first month of the chronic stage (after >10 weeks of post-acute stage).

DMARDs. Chronic chikungunya arthritis shares several characteristics with RA, such as persistent debilitating arthralgia and exacerbated inflammatory response (31,36,43,45,72). Because of these parallels, chloroquine, HCQ, and DMARDs such as MTX and sulfasalazine have been evaluated in some peri-epidemic clinical trials of treatments for chronic chikungunya arthritis (74,82–85). When compared with HCQ alone, treatment with DMARDs, either alone or in combination with HCQ and corticosteroids, has resulted in reductions in joint pain, disability, and impaired activity in cohort studies of patients with chronic chikungunya arthritis (84,85). In contrast, a cohort study showed that almost all patients had progression of disease-induced bone erosion and joint space narrowing upon follow-up despite treatment with HCQ or DMARDs, and a 2-year follow-up study involving 625 patients showed that treatment of chronic chikungunya arthritis with sulfasalazine and MTX was effective (82,86). Given the conflicting outcomes of those studies, it remains unclear whether specific DMARDs are effective in treating chronic chikungunya arthritis (85).

Experts have reached a consensus, however, that MTX should be recommended as first-line treatment (18). Though the efficacy of HCQ and other DMARDs has not been established per se using randomized controlled trials, these treatments should be considered on a case-by-case basis, either as a complement to or as an alternative to MTX (18,63,84). DMARDs must be monitored for effectiveness (using the Disease Activity Score in 28 joints) and tolerance and should be stopped after a durable remission of several months has been achieved. The specialist may

then refer to national guidelines to choose the second-line drug (combination or replacement treatments or biologic agents). However, in most cases, DMARD treatment may be assessed and stopped for patients whose disease remains in remission after a complete response has been sustained for several months (up to 2 years). Physical therapy includes rest limitation, maintenance of articular amplitude and muscular tone, and lymphatic drainage (manual, using compression stockings, or using pressotherapy) (18). Its benefit depends on the extent and the intensity of joint involvement and the disease impact in terms of autonomy and quality of life. When considering second-line treatment for patients with chronic post–chikungunya inflammatory diseases that fail to respond to first-line treatment, a multidisciplinary, case-by-case approach is advised. This may include enrollment in clinical trials assessing treatments that are recommended in national/international guidelines. One option would involve a regimen switch to combination therapy with alternative DMARDs or a biologic agent, either alone or in combination with other DMARDs.

Gaps and perspectives in the treatment of chronic chikungunya virus. Chronic pain has been linked to chikungunya virus persistence in synovial macrophages as well as to IL-6 and IL-12 secretion. To the best of our knowledge, anti–IL-6 (tocilizumab), anti–IL-12/IL-23p40 (ustekinumab), and anti-CD20 (rituximab) monoclonal antibodies (mAb) have not been tested empirically in chronic chikungunya virus, whereas anti–tumor necrosis factor (etanercept) therapy has been shown to exacerbate tissue damage in a mouse model of alphaviral arthritis (87). While several approaches (biologic, prophylactic, and palliative) are being explored and characterized to manage acute and chronic chikungunya virus, the development and testing of such therapeutic solutions should be done in close consultation with rheumatologists.

Therapeutic strategies that target monocyte chemotactic proteins or CCR2, such as bindarit, which was shown to ameliorate chikungunya virus–induced arthritis and bone loss in a mouse model (88,89), might be considered promising for further evaluation in the treatment of alphaviral arthritides. Of note, treatment of RA patients with CCR2 blockers was unsuccessful (90). Interestingly, pentosan polysulfate (PPS), a glycosaminoglycan currently approved in the US for the treatment of interstitial cystitis, has undergone promising clinical trials for the treatment of noninfectious arthritis and has been shown to maintain levels of cartilage proteoglycans in experimental animal models of arthritis (91,92). In chikungunya virus–infected mice, PPS treatment decreased the level of joint swelling and reduced levels of the soluble factors CCL2, IL-6, IL-9, and G-CSF during acute inflammation (93). Although the exact mechanism of action of PPS is unclear, treatment was associated with an early increase in antiinflammatory IL-10 levels, suggesting an indirect mechanism by which inflammation is dampened (93). As part of the Australian Government Department of Health Therapeutic Goods Administration Special Access Scheme, PPS, currently in phase II clinical trials, has now been successfully used to treat 5 patients with Ross River virus–induced arthralgia that had failed to respond to current standard treatment. Ross River virus is an Australian arthritogenic alphavirus that causes viral polyarthritis with clinical manifestations (severe, incapacitating joint pain) similar to those seen in chikungunya arthritis.

More recently, targeting CD4+ T cells with clinically approved T cell–suppressive drugs, including the sphingosine 1-phosphate receptor agonist fingolimod (also known as FTY720), successfully reduced chikungunya virus–induced disease in mice by blocking lymphoid egress and subsequent migration of CD4+ T cells into the joints (94). Although the US Food and Drug Administration (FDA) approved fingolimod as a treatment for multiple sclerosis in 2010, there are currently no clinical trials to assess efficacy in chikungunya arthritis.

Neutralizing antibodies and prophylactic treatment. A number of studies have sought to characterize the neutralizing capacity of chikungunya virus–specific antibodies, the epitopes responsible for neutralization, and the mechanism of viral inhibition (95–102). Robustly neutralizing mAb to chikungunya virus bind the E2 envelope glycoprotein with conserved epitopes identified on the A and B domain. Antibodies block multiple steps in the viral life cycle, including entry and egress, by crosslinking adjacent E2 spikes of the E2 glycoprotein or impeding fusion. Importantly, these broadly neutralizing ultrapotent mAb protect against infection by multiple alphaviruses, including chikungunya virus (95–97).

Neutralizing antibodies have been tested in mouse models as treatment for persistent chikungunya virus infection. The effect of a neutralizing anti–chikungunya virus mAb on RAG-$1^{-/-}$ mice (devoid of B and T cells) with persistent chikungunya virus infection was to enable effective clearance of infectious virus in quadriceps muscle tissue and sera, although without reducing chikungunya virus RNA load in joint tissue (103). In a separate study by Poo et al, chikungunya virus viremia became undetectable in persistently infected RAG-$1^{-/-}$ and B cell–deficient μMT mice beginning 10 days and 30 days, respectively, after administration of polyclonal anti–chikungunya virus antiserum (65). However, viremia recovered to levels similar to those observed prior to administration of the antibody, indicating that effective clearance of chikungunya virus may require robust and long-lasting B and T cell responses (65).

Further, another study showed that a highly conserved amino acid on the E2 glycoprotein promoted chikungunya virus persistence in mouse joints and impaired neutralization by antibodies targeting the E2 domain. Mutation of this conserved region allowed viral clearance and enhanced neutralization, providing the structural basis for the mechanism by which chikungunya virus evades B cell–mediated clearance in chronic joint infection (98). Finally, rhesus macaques with chikungunya virus infection treated with SVIR001, a recombinant human IgG1 mAb that recognizes the E2 glycoprotein of chikungunya virus, showed more robust viral clearance and less severe joint inflammation compared with isotype-treated controls (99). In addition, SVIR001 reduced viral

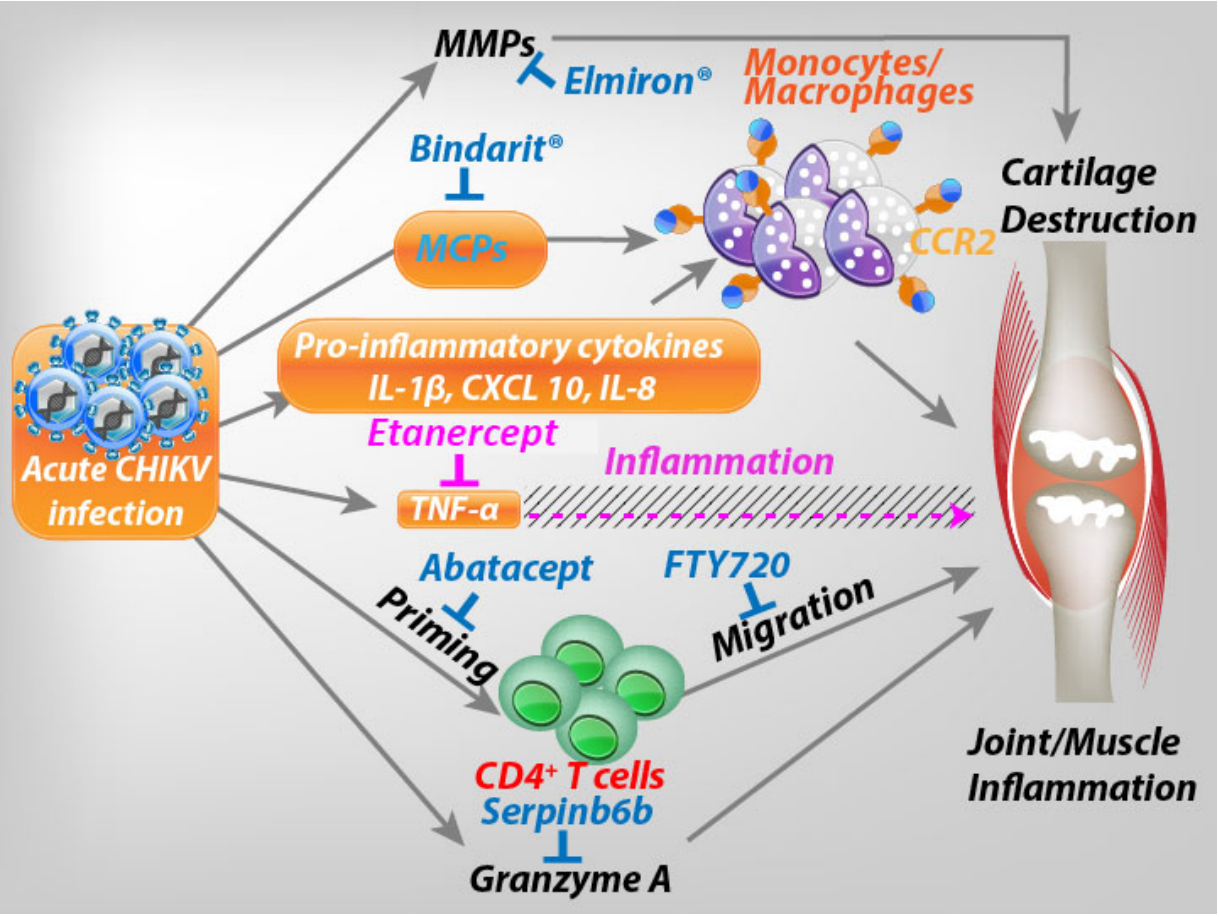

Figure 1. Schematic overview of the mechanisms of tissue inflammation leading to alphaviral arthritis. Based on experimental models of alphavirus infection, key cytokine-dependent inflammatory pathways have been identified and targeted to explore therapeutic avenues. Principally, monocyte chemotactic proteins (MCPs) such as CCL2 and CCL3, which drive monocytic infiltration into joint and muscle tissue in alphaviral inflammation (50,89) (e.g., chikungunya virus [CHIKV] infection), can be targeted using MCP inhibitors such as bindarit, while potent proinflammatory cytokines and chemokines such as interleukin-1 (IL-1), CXCL10, and IL-8 are also the focus of current studies. Scavenging soluble MCPs such as CCL2 restrict CCR2-dependent monocyte/macrophage infiltration, which is required for chikungunya arthritis (87,88). Pentosan polysulfate (Elmiron) has been shown to limit chikungunya virus–induced arthritis and cartilage damage by significantly reducing tissue expression of matrix metalloproteinases (MMPs) that drive cartilage damage in alphaviral infection (92) and in experimental models of cartilage damage (91). RNA sequencing analysis of chikungunya virus–infected tissue in mice has shown a prominent role of granzyme A in driving arthritic inflammation, and the use of the mouse granzyme A inhibitor Serpinb6b was found to dampen tissue inflammation and swelling in chikungunya virus–infected mice (21). In addition to targeting innate inflammatory mechanisms, modulating adaptive immunity has been shown to reduce tissue infiltration, either by inhibiting priming of CD4+ T cells using abatacept (105) or by blocking egress of CD4+ T cells from the lymph nodes to the joints (93) using FTY720 (fingolimod). The role of tumor necrosis factor (TNF) in alphavirus inflammation, despite its prominent expression in the tissues of infected mice and humans, appears to rely on a more complex mechanism. Inhibition of TNF using etanercept in a mouse model of alphaviral arthritis was shown to significantly exacerbate inflammatory disease and cellular infiltration (86), thereby reinforcing the need for a cautious approach when considering biologic therapies for the treatment of alphaviral diseases such as chikungunya virus.

burden at the site of infection, as well as at distant sites, but also diminished the number of activated innate immune cells and levels of proinflammatory cytokines and chemokines (99). Therefore, more studies are needed to examine the utility of neutralizing antibodies as a therapeutic approach to persistent chikungunya virus infection, and to confirm the efficacy of these approaches in humans.

In contrast, studies have shown that prophylactic treatment with chikungunya virus–specific mAb prevents joint inflammation in chikungunya virus–infected wild-type mice and can protect against fatal chikungunya virus infection in AG129, RAG-2$^{-/-}$, and IFNAR-1$^{-/-}$ mice (98–103). Administration of chikungunya virus–specific mAb to RAG-1$^{-/-}$ mice prior to infection resulted in drastically reduced viremia and chikungunya virus RNA levels in ankle joints of animals with persistent chikungunya virus infection (103). Passive immunization with chikungunya virus IgG in IFNα/βR$^{-/-}$ mice also prevented mortality from chikungunya virus infection (102). However, these studies only examined the effect of using mAb as prophylaxis for acute chikungunya virus infection. Thus, our understanding of the prophylactic use of mAb in chronic chikungunya arthritis is still incomplete, and more studies are needed. Nevertheless, prophylactic treatment could be effective for individuals at increased risk of chikungunya virus infection in critical settings, such as mother-to-child transmission (104) or hospitalized individuals with life-threatening acute disease (105).

Combined therapy with biologic agents. A recent study by Miner et al sought to target both humoral and adaptive arms of the immune response by using abatacept, a drug approved in 2005 by the FDA for the treatment of RA, in combination with an anti–chikungunya virus neutralizing antibody, and assessed their ability to decrease acute joint swelling in chikungunya virus–infected mice (106). Abatacept, a human IgG fusion protein paired with a CTLA-4 extracellular domain motif, prevents antigen-presenting cells from delivering costimulatory signals to T cells. In the study by Miner et al, abatacept reduced T cell accumulation in the joints of infected mice and, in combination with an anti–chikungunya virus neutralizing antibody, abolished signs of inflammatory disease and markedly reduced levels of chemokines, proinflammatory cytokines, and infiltrating leukocytes (106). Notwithstanding the promising preclinical outcomes and innovative approaches, these candidate therapies, along with the other examples cited earlier in this review (summarized in Figure 1), warrant further evaluation in the treatment of chikungunya virus–induced joint pathologies in a clinical setting, keeping in mind the potential risk of immunosuppression when targeting host response mechanisms.

Conclusions

Chikungunya virus, a previously neglected tropical arthritogenic alphaviral infection, has gained global significance in the last decade after a series of devastating outbreaks, exposing the severe public health and economic burdens as well as the significant risk of acquired disabilities incurred by international travelers. The clinical and immunopathologic phenotype of this chronic inflammatory rheumatic disease is reminiscent of RA, and studies in animal models of alphaviral infections have helped to elucidate previously unknown mechanisms of disease and brought to light novel therapeutic approaches. Based on its newly recognized public health importance and its strong potential for reemergence, chikungunya arthritis should be the focus of further experimental forays to develop novel therapeutic approaches and should also gain further attention from rheumatologists worldwide.

ACKNOWLEDGMENT

We would like to thank Dr. Michael Rolph for proofreading this review.

AUTHOR CONTRIBUTIONS

All authors drafted the article, revised it critically for important intellectual content, and approved the final version to be published.

REFERENCES

1. Centers for Disease Control and Prevention. Chikungunya virus: 2016 final data for the United States. URL: https://www.cdc.gov/chikungunya/geo/united-states-2016.html.
2. Kuehn BM. Chikungunya virus transmission found in the United States: US health authorities brace for wider spread. JAMA 2014;312:776–7.
3. Seyler T, Hutin Y, Ramanchandran V, Ramakrishnan R, Manickam P, Murhekar M. Estimating the burden of disease and the economic cost attributable to chikungunya, Andhra Pradesh, India, 2005–2006. Trans R Soc Trop Med Hyg 2010;104:133–8.
4. Gould EA, Higgs S. Impact of climate change and other factors on emerging arbovirus diseases. Trans R Soc Trop Med Hyg 2009;103:109–21.
5. Rodríguez-Barraquer I, Solomon SS, Kuganantham P, Srikrishnan AK, Vasudevan CK, Iqbal SH, et al. The hidden burden of dengue and chikungunya in Chennai, India. PLoS Negl Trop Dis 2015;9:e0003906.
6. Soumahoro MK, Gérardin P, Boelle PY, Perrau J, Fianu A, Pouchot J, et al. Impact of chikungunya virus infection on health status and quality of life: a retrospective cohort study. PLoS One 2009;4:e7800.
7. Marimoutou C, Vivier E, Oliver M, Boutin JP, Simon F. Morbidity and impaired quality of life 30 months after chikungunya infection: comparative cohort of infected and uninfected French military policemen in Reunion Island. Medicine (Baltimore) 2012;91:212–9.
8. Marimoutou C, Ferraro J, Javelle E, Deparis X, Simon F. Chikungunya infection: self-reported rheumatic morbidity and

impaired quality of life persist 6 years later. Clin Microbiol Infect 2015;21:688–93.
9. Couturier E, Guillemin F, Mura M, Léon L, Virion JM, Letort MJ, et al. Impaired quality of life after chikungunya virus infection: a 2-year follow-up study. Rheumatology (Oxford) 2012;51: 1315–22.
10. Gérardin P, Fianu A, Malvy D, Mussard C, Boussaïd K, Rollot O, et al. Perceived morbidity and community burden after a chikungunya outbreak: the TELECHIK survey, a population-based cohort study. BMC Med 2011;9:5.
11. Soumahoro MK, Boelle PY, Gaüzere BA, Atsou K, Pelat C, Lambert B, et al. The chikungunya epidemic on La Réunion Island in 2005–2006: a cost-of-illness study. PLoS Negl Trop Dis 2011;5:e1197.
12. Goo L, Dowd KA, Lin TY, Mascola JR, Graham BS, Ledgerwood JE, et al. A virus-like particle vaccine elicits broad neutralizing antibody responses in humans to all chikungunya virus genotypes. J Infect Dis 2016;214:1487–91.
13. Ramsauer K, Schwameis M, Firbas C, Müllner M, Putnak RJ, Thomas SJ, et al. Immunogenicity, safety, and tolerability of a recombinant measles-virus-based chikungunya vaccine: a randomised, double-blind, placebo-controlled, active-comparator, first-in-man trial. Lancet Infect Dis 2015;15:519–27.
14. Abdelnabi R, Neyts J, Delang L. Antiviral strategies against chikungunya virus. Methods Mol Biol 2016;1426:243–53.
15. Abdelnabi R, Neyts J, Delang L. Chikungunya virus infections: time to act, time to treat. Curr Opin Virol 2017;24:25–30.
16. Borgherini G, Poubeau P, Staikowsky F, Lory M, Le Moullec N, Becquart JP, et al. Outbreak of chikungunya on Reunion Island: early clinical and laboratory features in 157 adult patients. Clin Infect Dis 2007;44:1401–7.
17. Staikowsky F, Talarmin F, Grivard P, Souab A, Schuffenecker I, Le Roux K, et al. Prospective study of chikungunya virus acute infection in the Island of La Réunion during the 2005–2006 outbreak. PLoS One 2009;4:e7603.
18. Simon F, Javelle E, Cabie A, Bouquillard E, Troisgros O, Gentile G, et al. French guidelines for the management of chikungunya (acute and persistent presentations): November 2014. Med Mal Infect 2015;45:243–63.
19. Kam YW, Simarmata D, Chow A, Her Z, Teng TS, Ong EK, et al. Early appearance of neutralizing immunoglobulin G3 antibodies is associated with chikungunya virus clearance and long-term clinical protection. J Infect Dis 2012;205:1147–54.
20. Wauquier N, Becquart P, Nkoghe D, Padilla C, Ndjoyi-Mbiguino A, Leroy EM. The acute phase of chikungunya virus infection in humans is associated with strong innate immunity and T CD8 cell activation. J Infect Dis 2011;204:115–23.
21. Wilson JA, Prow NA, Schroder WA, Ellis JJ, Cumming HE, Gearing LJ, et al. RNA-Seq analysis of chikungunya virus infection and identification of granzyme A as a major promoter of arthritic inflammation. PLoS Pathog 2017;13:e1006155.
22. Chow A, Her Z, Ong EK, Chen JM, Dimatatac F, Kwek DJ, et al. Persistent arthralgia induced by chikungunya virus infection is associated with interleukin-6 and granulocyte macrophage colony-stimulating factor. J Infect Dis 2011;203:149–57.
23. Labadie K, Larcher T, Joubert C, Mannioui A, Delache B, Brochard P, et al. Chikungunya disease in nonhuman primates involves long-term viral persistence in macrophages. J Clin Invest 2010;120:894–906.
24. Couderc T, Chrétien F, Schilte C, Disson O, Brigitte M, Guivel-Benhassine F, et al. A mouse model for chikungunya: young age and inefficient type-I interferon signaling are risk factors for severe disease. PLoS Pathog 2008;4:e29.
25. Gardner CL, Burke CW, Higgs ST, Klimstra WB, Ryman KD. Interferon-α/β deficiency greatly exacerbates arthritogenic disease in mice infected with wild-type chikungunya virus but not with the cell culture-adapted live-attenuated 181/25 vaccine candidate. Virology 2012;425:103–12.
26. Rudd PA, Wilson J, Gardner J, Larcher T, Babarit C, Le TT, et al. Interferon response factors 3 and 7 protect against chikungunya virus hemorrhagic fever and shock. J Virol 2012;86:9888–98.
27. Poddar S, Hyde JL, Gorman MJ, Farzan M, Diamond MS. The interferon-stimulated gene IFITM3 restricts infection and pathogenesis of arthritogenic and encephalitic alphaviruses. J Virol 2016;90:8780–94.
28. Fros JJ, Pijlman GP. Alphavirus infection: host cell shut-off and inhibition of antiviral responses. Viruses 2016;8:E166.
29. Breakwell L, Dosenovic P, Karlsson Hedestam GB, D'Amato M, Liljeström P, Fazakerley J, et al. Semliki Forest virus nonstructural protein 2 is involved in suppression of the type I interferon response. J Virol 2007;81:8677–84.
30. Kelvin AA, Banner D, Silvi G, Moro ML, Spataro N, Gaibani P, et al. Inflammatory cytokine expression is associated with chikungunya virus resolution and symptom severity. PLoS Negl Trop Dis 2011;5:e1279.
31. Chaaitanya IK, Muruganandam N, Sundaram SG, Kawalekar O, Sugunan AP, Manimunda SP, et al. Role of pro-inflammatory cytokines and chemokines in chronic arthropathy in CHIKV infection. Viral Immunol 2011;24:265–71.
32. Teng TS, Kam YW, Lee B, Hapuarachchi HC, Wimal A, Ng LC, et al. A systematic meta-analysis of immune signatures in patients with acute chikungunya virus infection. J Infect Dis 2015; 211:1925–35.
33. Her Z, Malleret B, Chan M, Ong EK, Wong SC, Kwek DJ, et al. Active infection of human blood monocytes by chikungunya virus triggers an innate immune response. J Immunol 2010;184:5903–13.
34. Thanapati S, Das R, Tripathy AS. Phenotypic and functional analyses of NK and NKT-like populations during the early stages of chikungunya infection. Front Microbiol 2015; 6:895.
35. Van Aalst M, Nelen CM, Goorhuis A, Stijnis C, Grobusch MP. Long-term sequelae of chikungunya virus disease: a systematic review. Travel Med Infect Dis 2017;15:8–22.
36. Hoarau JJ, Jaffar-Bandjee MC, Krejbich Trotot P, Das T, Li-Pat-Yuen G, Dassa B, et al. Persistent chronic inflammation and infection by chikungunya arthritogenic alphavirus in spite of a robust host immune response. J Immunol 2010;184: 5914–27.
37. Kwan Tat S, Padrines M, Théoleyre S, Heymann D, Fortun Y. IL-6, RANKL, TNF-α/IL-1: interrelations in bone resorption pathophysiology. Cytokine Growth Factor Rev 2004;15:49–60.
38. Noret M, Herrero L, Rulli N, Rolph M, Smith PN, Li RW, et al. Interleukin 6, RANKL, and osteoprotegerin expression by chikungunya virus-infected human osteoblasts. J Infect Dis 2012;206: 455–7.
39. Chen W, Foo SS, Rulli NE, Taylor A, Sheng KC, Herrero LJ, et al. Arthritogenic alphaviral infection perturbs osteoblast function and triggers pathologic bone loss. Proc Natl Acad Sci U S A 2014;111:6040–5.
40. Fonseca JE, Santos MJ, Canhão H, Choy E. Interleukin-6 as a key player in systemic inflammation and joint destruction. Autoimmun Rev 2009;8:538–42.
41. Rodríguez-Morales AJ, Hoyos-Guapacha KL, Vargas-Zapata SL, Meneses-Quintero OM, Gutiérrez-Segura JC. Would be IL-6 a missing link between chronic inflammatory rheumatism and depression after chikungunya infection? Rheumatol Int 2017; 37:1149–51.
42. Sepúlveda-Delgado J, Vera-Lastra OL, Trujillo-Murillo K, Canseco-Ávila LM, Sánchez-González RA, Gómez-Cruz O, et al. Inflammatory biomarkers, disease activity index, and self-reported disability may be predictors of chronic arthritis after chikungunya infection: brief report. Clin Rheumatol 2017;36: 695–9.
43. Nakaya HI, Gardner J, Poo YS, Major L, Pulendran B, Suhrbier A. Gene profiling of chikungunya virus arthritis in a mouse model

reveals significant overlap with rheumatoid arthritis. Arthritis Rheum 2012;64:3553–63.
44. Gasque P, Jaffar-Bandjee MC. Blunting CHIKV infection by keeping T cells in check. Sci Transl Med 2017;9:eaam6567.
45. Miner JJ, Aw Yeang HX, Fox JM, Taffner S, Malkova ON, Oh ST, et al. Chikungunya viral arthritis in the United States: a mimic of seronegative rheumatoid arthritis. Arthritis Rheumatol 2015;67:1214–20.
46. Thanapati S, Ganu M, Giri P, Kulkarni S, Sharma M, Babar P, et al. Impaired NK cell functionality and increased TNF-α production as biomarkers of chronic chikungunya arthritis and rheumatoid arthritis. Hum Immunol 2017;78:370–4.
47. Lee WW, Teo TH, Her Z, Lum FM, Kam YW, Haase D, et al. Expanding regulatory T cells alleviates chikungunya virus-induced pathology in mice. J Virol 2015;89:7893–904.
48. Lum FM, Teo TH, Lee WW, Kam YW, Renia L, Ng LF. An essential role of antibodies in the control of chikungunya virus infection. J Immunol 2013;190:6295–302.
49. McCarthy MK, Morrison TE. Persistent RNA virus infections: do PAMPS drive chronic disease? Curr Opin Virol 2017;23:8–15.
50. Poo YS, Nakaya H, Gardner J, Larcher T, Schroder WA, Le TT, et al. CCR2 deficiency promotes exacerbated chronic erosive neutrophil-dominated chikungunya virus arthritis. J Virol 2014; 88:6862–72.
51. Santiago L, Menaa C, Arias M, Martin P, Jaime-Sánchez P, Metkar S, et al. Granzyme A contributes to inflammatory arthritis in mice through stimulation of osteoclastogenesis. Arthritis Rheumatol 2017;69:320–34.
52. Rodríguez-Morales AJ, Cardona-Ospina JA, Fernanda Urbano-Garzón S, Sebastian Hurtado-Zapata J. Prevalence of post-chikungunya infection chronic inflammatory arthritis: a systematic review and meta-analysis. Arthritis Care Res (Hoboken) 2016; 68:1849–58.
53. Borgherini G, Poubeau P, Jossaume A, Gouix A, Cotte L, Michault A, et al. Persistent arthralgia associated with chikungunya virus: a study of 88 adult patients on Reunion Island. Clin Infect Dis 2008;47:469–75.
54. Sissoko D, Malvy D, Ezzedine K, Renault P, Moscetti F, Ledrans M, et al. Post-epidemic Chikungunya disease on Reunion Island: course of rheumatic manifestations and associated factors over a 15-month period. PLoS Negl Trop Dis 2009;3:e389.
55. Malvy D, Ezzedine K, Mamani-Matsuda M, Autran B, Tolou H, Receveur MC, et al. Destructive arthritis in a patient with chikungunya virus infection with persistent specific IgM antibodies. BMC Infect Dis 2009;9:200.
56. Larrieu S, Pouderoux N, Pistone T, Filleul L, Receveur MC, Sissoko D, et al. Factors associated with persistence of arthralgia among chikungunya virus-infected travellers: report of 42 French cases. J Clin Virol 2010;47:85–8.
57. Manimunda SP, Vijayachari P, Uppoor R, Sugunan AP, Singh SS, Rai SK, et al. Clinical progression of chikungunya fever during acute and chronic arthritic stages and the changes in joint morphology as revealed by imaging. Trans R Soc Trop Med Hyg 2010;104:392–9.
58. Gérardin P, Fianu A, Michault A, Mussard C, Boussaïd K, Rollot O, et al. Predictors of chikungunya rheumatism: a prognostic survey ancillary to the TELECHIK cohort study. Arthritis Res Ther 2013;15:R9.
59. Schilte C, Staikowsky F, Staikovsky F, Couderc T, Madec Y, Carpentier F, et al. Chikungunya virus-associated long-term arthralgia: a 36-month prospective longitudinal study. PLoS Negl Trop Dis 2013;7:e2137.
60. Yaseen HM, Simon F, Deparis X, Marimoutou C. Identification of initial severity determinants to predict arthritis after chikungunya infection in a cohort of French gendarmes. BMC Musculoskelet Disord 2014;15:249.
61. Rahim AA, Thekkekara RJ, Bina T, Paul BJ. Disability with persistent pain following an epidemic of chikungunya in rural South India. J Rheumatol 2016;43:440–4.
62. Javelle E, Ribéra A, Degasne I, Gaüzere BA, Marimoutou C, Simon F. Specific management of post-chikungunya rheumatic disorders: a retrospective study of 159 cases in Reunion Island from 2006–2012. PLoS Negl Trop Dis 2015;9:e0003603.
63. Bouquillard E, Fianu A, Bangil M, Charlette N, Ribéra A, Michault A, et al. Rheumatic manifestations associated with chikungunya virus infection: a study of 307 patients with 32-month follow-up (RHUMATOCHIK study). Joint Bone Spine 2017. E-pub ahead of print.
64. Suhrbier A, Mahalingam S. The immunobiology of viral arthritides. Pharmacol Ther 2009;124:301–8.
65. Poo YS, Rudd PA, Gardner J, Wilson JA, Larcher T, Colle MA, et al. Multiple immune factors are involved in controlling acute and chronic chikungunya virus infection. PLoS Negl Trop Dis 2014;8:e3354.
66. Messaoudi I, Vomaske J, Totonchy T, Kreklywich CN, Haberthur K, Springgay L, et al. Chikungunya virus infection results in higher and persistent viral replication in aged rhesus macaques due to defects in anti-viral immunity. PLoS Negl Trop Dis 2013;7:e2343.
67. Hoarau JJ, Gay F, Pellé O, Samri A, Jaffar-Bandjee MC, Gasque P, et al. Identical strength of the T cell responses against E2, nsP1 and capsid CHIKV proteins in recovered and chronic patients after the epidemics of 2005–2006 in La Reunion Island. PLoS One 2013;8: e84695.
68. Narendra SC, Chalise JP, Höök N, Magnusson M. Dendritic cells activated by double-stranded RNA induce arthritis via autocrine type I IFN signaling. J Leukoc Biol 2014;95:661–6.
69. Ozden S, Huerre M, Riviere JP, Coffey LL, Afonso PV, Mouly V, et al. Human muscle satellite cells as targets of chikungunya virus infection. PLoS One 2007;2:e527.
70. Motohashi N, Asakura A. Muscle satellite cell heterogeneity and self-renewal. Front Cell Dev Biol 2014;2:1.
71. Mylonas AD, Harley D, Purdie DM, Pandeya N, Vecchio PC, Farmer JF, et al. Corticosteroid therapy in an alphaviral arthritis. J Clin Rheumatol 2004;10:326–30.
72. Suhrbier A, Jaffar-Bandjee MC, Gasque P. Arthritogenic alphaviruses: an overview. Nat Rev Rheumatol 2012;8:420–9.
73. De Lamballerie X, Boisson V, Reynier JC, Enault S, Charrel RN, Flahault A, et al. On chikungunya acute infection and chloroquine treatment. Vector Borne Zoonotic Dis 2008;8:837–9.
74. Chopra A, Saluja M, Venugopalan A. Effectiveness of chloroquine and inflammatory cytokine response in patients with early persistent musculoskeletal pain and arthritis following chikungunya virus infection. Arthritis Rheumatol 2014;66:319–26.
75. Padmakumar B, Jayan JB, Menon RM, Krishnankutty B, Payippallil R, Nisha RS. Comparative evaluation of four therapeutic regimes in chikungunya arthritis: a prospective randomized parallel-group study. Indian J Rheumatol 2009;4:94–101.
76. Bouhassira D, Attal N, Alchaar H, Boureau F, Brochet B, Bruxelle J, et al. Comparison of pain syndromes associated with nervous or somatic lesions and development of a new neuropathic pain diagnostic questionnaire (DN4). Pain 2005;114:29–36.
77. Gallegos KM, Drusano GL, D'Argenio DZ, Brown AN. Chikungunya virus: in vitro response to combination therapy with ribavirin and interferon alfa 2a. J Infect Dis 2016;214:1192–7.
78. Delang L, Segura Guerrero N, Tas A, Quérat G, Pastorino B, Froeyen M, et al. Mutations in the chikungunya virus non-structural proteins cause resistance to favipiravir (T-705), a broad-spectrum antiviral. J Antimicrob Chemother 2014;69:2770–84.
79. Albulescu IC, van Hoolwerff M, Wolters LA, Bottaro E, Nastruzzi C, Yang SC, et al. Suramin inhibits chikungunya virus replication through multiple mechanisms. Antiviral Res 2015;121: 39–46.
80. Mounce BC, Cesaro T, Carrau L, Vallet T, Vignuzzi M. Curcumin inhibits Zika and chikungunya virus infection by inhibiting cell binding. Antiviral Res 2017;142:148–57.
81. Karlas A, Berre S, Couderc T, Varjak M, Braun P, Meyer M, et al. A human genome-wide loss-of-function screen identifies effective chikungunya antiviral drugs. Nat Commun 2016;7:11320.

82. Bouquillard E, Combe B. A report of 21 cases of rheumatoid arthritis following chikungunya fever. a mean follow-up of two years. Joint Bone Spine 2009;76:654–7.
83. Mathew AJ, Goyal V, George E, Thekkemuriyil DV, Jayakumar B, Chopra A, et al. Rheumatic-musculoskeletal pain and disorders in a naïve group of individuals 15 months following a chikungunya viral epidemic in south India: a population based observational study. Int J Clin Pract 2011;65:1306–12.
84. Ravindran V, Alias G. Efficacy of combination DMARD therapy vs. hydroxychloroquine monotherapy in chronic persistent chikungunya arthritis: a 24-week randomized controlled open label study. Clin Rheumatol 2017;36:1335–40.
85. Martí-Carvajal A, Ramon-Pardo P, Javelle E, Simon F, Aldighieri S, Horvath H, et al. Interventions for treating patients with chikungunya virus infection-related rheumatic and musculoskeletal disorders: a systematic review. PLoS One 2017;12:e0179028.
86. Ganu MA, Ganu AS. Post-chikungunya chronic arthritis: our experience with DMARDs over two year follow up. J Assoc Physicians India 2011;59:83–6.
87. Zaid A, Rulli NE, Rolph MS, Suhrbier A, Mahalingam S. Disease exacerbation by etanercept in a mouse model of alphaviral arthritis and myositis. Arthritis Rheum 2011;63:488–91.
88. Chen W, Foo SS, Taylor A, Lulla A, Merits A, Hueston L, et al. Bindarit, an inhibitor of monocyte chemotactic protein synthesis, protects against bone loss induced by chikungunya virus infection. J Virol 2015;89:581–93.
89. Rulli NE, Rolph MS, Srikiatkhachorn A, Anantapreecha S, Guglielmotti A, Mahalingam S. Protection from arthritis and myositis in a mouse model of acute chikungunya virus disease by bindarit, an inhibitor of monocyte chemotactic protein-1 synthesis. J Infect Dis 2011;204:1026–30.
90. Vergunst CE, Gerlag DM, Lopatinskaya L, Klareskog L, Smith MD, van den Bosch F, et al. Modulation of CCR2 in rheumatoid arthritis: a double-blind, randomized, placebo-controlled clinical trial. Arthritis Rheum 2008;58:1931–9.
91. Parsons CL, Mulholland SG. Successful therapy of interstitial cystitis with pentosanpolysulfate. J Urol 1987;138:513–6.
92. Kumagai K, Shirabe S, Miyata N, Murata M, Yamauchi A, Kataoka Y, et al. Sodium pentosan polysulfate resulted in cartilage improvement in knee osteoarthritis: an open clinical trial. BMC Clin Pharmacol 2010;10:7.
93. Herrero LJ, Foo SS, Sheng KC, Chen W, Forwood MR, Bucala R, et al. Pentosan polysulfate: a novel glycosaminoglycan-like molecule for effective treatment of alphavirus-induced cartilage destruction and inflammatory disease. J Virol 2015;89:8063–76.
94. Teo TH, Chan YH, Lee WW, Lum FM, Amrun SN, Her Z, et al. Fingolimod treatment abrogates chikungunya virus-induced arthralgia. Sci Transl Med 2017;9:eaal1333.
95. Long F, Fong RH, Austin SK, Chen Z, Klose T, Fokine A, et al. Cryo-EM structures elucidate neutralizing mechanisms of anti-chikungunya human monoclonal antibodies with therapeutic activity. Proc Natl Acad Sci U S A 2015;112:13898–903.
96. Fox JM, Long F, Edeling MA, Lin H, van Duijl-Richter MK, Fong RH, et al. Broadly neutralizing alphavirus antibodies bind an epitope on E2 and inhibit entry and egress. Cell 2015;163:1095–107.
97. Smith SA, Silva LA, Fox JM, Flyak AI, Kose N, Sapparapu G, et al. Isolation and characterization of broad and ultrapotent human monoclonal antibodies with therapeutic activity against chikungunya virus. Cell Host Microbe 2015;18:86–95.
98. Hawman DW, Fox JM, Ashbrook AW, May NA, Schroeder KM, Torres RM, et al. Pathogenic chikungunya virus evades B cell responses to establish persistence. Cell Rep 2016;16:1326–38.
99. Broeckel R, Fox JM, Haese N, Kreklywich CN, Sukulpovi-Petty S, Legasse A, et al. Therapeutic administration of a recombinant human monoclonal antibody reduces the severity of chikungunya virus disease in rhesus macaques. PLoS Negl Trop Dis 2017;11:e0005637.
100. Pal P, Dowd KA, Brien JD, Edeling MA, Gorlatov S, Johnson S, et al. Development of a highly protective combination monoclonal antibody therapy against chikungunya virus. PLoS Pathog 2013;9:e1003312.
101. Fric J, Bertin-Maghit S, Wang CI, Nardin A, Warter L. Use of human monoclonal antibodies to treat chikungunya virus infection. J Infect Dis 2013;207:319–22.
102. Couderc T, Khandoudi N, Grandadam M, Visse C, Gangneux N, Bagot S, et al. Prophylaxis and therapy for chikungunya virus infection. J Infect Dis 2009;200:516–23.
103. Hawman DW, Stoermer KA, Montgomery SA, Pal P, Oko L, Diamond MS, et al. Chronic joint disease caused by persistent chikungunya virus infection is controlled by the adaptive immune response. J Virol 2013;87:13878–88.
104. Gérardin P, Barau G, Michault A, Bintner M, Randrianaivo H, Choker G, et al. Multidisciplinary prospective study of mother-to-child chikungunya virus infections on the island of La Réunion. PLoS Med 2008;5:e60.
105. Lémant J, Boisson V, Winer A, Thibault L, André H, Tixier F, et al. Serious acute chikungunya virus infection requiring intensive care during the Reunion Island outbreak in 2005–2006. Crit Care Med 2008;36:2536–41.
106. Miner JJ, Cook LE, Hong JP, Smith AM, Richner JM, Shimak RM, et al. Therapy with CTLA4-Ig and an antiviral monoclonal antibody controls chikungunya virus arthritis. Sci Transl Med 2017;9:eaah3438.

ARTHRITIS & RHEUMATOLOGY
Vol. 70, No. 4, April 2018, pp 496–507
DOI 10.1002/art.40396

REVIEW

Abnormal B Cell Development in Systemic Lupus Erythematosus

What the Genetics Tell Us

Sarah Karrar and Deborah S. Cunninghame Graham

Introduction

Systemic lupus erythematosus (SLE) is an autoimmune disease characterized by B cell dysfunction, production of autoantibodies directed toward cellular and nuclear components, and multiorgan damage caused by immune complex deposition and inflammation within affected tissues (1). It largely affects women of childbearing age (the third and fourth decades of life) and is associated with significant morbidity and mortality.

In healthy individuals, B cells with autoreactive receptors are selected out during B cell maturation, starting at the initial stages of B cell receptor (BCR) development in the bone marrow and continuing through to the fine tuning that occurs in activated mature B cells in secondary lymphoid tissue. Studies in lupus patients as well as mouse models indicate that these processes are altered in SLE.

The etiology of the disease is complex and its phenotype is highly heterogeneous, but genetic susceptibility is thought to contribute as much as 60% of disease risk (2). Although rare monogenic causes do exist, heredity in SLE is complex, with multiple common variants contributing to disease, with patients having to achieve a certain "genetic threshold" for disease risk. This genetic risk, in combination with environmental factors (exposure to ultraviolet sunlight, smoking, and infections including Epstein-Barr virus have all been implicated), leads to development of the disease (1). In this review, we summarize some of the B cell anomalies in SLE and incorporate evidence from studies in humans and mouse models, together with data from genetic association studies, to explain the mechanisms behind B cell dysregulation in SLE.

The B cell phenotype in SLE

The crucial role of B cells in SLE pathogenesis is well recognized, from producing autoantibodies to abnormal regulation of immune responses (3,4). Various abnormalities have been noted in SLE B cells. First, there is an imbalance of B cell subtype numbers, with an increase in class-switched memory B cells relative to naive B cells (3). Second, B cells from SLE patients have exaggerated BCR responses, with receptor crosslinking leading to increased calcium influx and tyrosine phosphorylation of downstream signaling molecules (3). Increased memory B cell numbers confer significant disease risk as these have a lower activation threshold, allowing autoreactive B cells to thrive with minimal antigen contact, while enhanced receptor activation contributes to the steady-state active phenotype seen in SLE (3,5).

B cells contribute to disease mainly by producing autoantibodies targeting nuclear components including DNA (anti–double-stranded DNA [anti-dsDNA]), RNP particles (anti-Ro, anti-La, and anti-Sm), histones, and nonhistone chromatin proteins. These are present in >90% of patients and contribute to disease progression via immune complex formation (6). Titers of these autoantibodies (especially anti-dsDNA) correlate positively with increased disease activity, and serial measurements are used to monitor patients for disease flares (6). There is also evidence that autoantibodies cross-react with cellular components other

Dr. Karrar's work was supported by the Medical Research Council (Clinical Research Fellowship grant MR/N021118/1). Dr. Cunninghame Graham's work was supported by Arthritis Research UK (grant 20265).

Sarah Karrar, MBBS, BSc, Deborah S. Cunninghame Graham, BSc, PhD: King's College London, London, UK.

Address correspondence to Deborah S. Cunninghame Graham, BSc, PhD, Department of Medical and Molecular Genetics, Divisions of Genetics and Molecular Medicine and King's College London School of Medicine, Guy's Hospital, Great Maze Pond, London SE1 9RT, UK. E-mail: deborah.cunninghame-graham@kcl.ac.uk.

Submitted for publication July 14, 2017; accepted in revised form November 29, 2017.

than nuclear targets (7). For example, anti-dsDNA antibodies bind to major glycosaminoglycan components in the glomerular basement membrane, suggesting a possible direct role in nephritis (7). In mouse models, transfer of autoantibodies from diseased to unaffected animals leads to development of typical immune complex–mediated nephritis (8). Moreover, in MRL/*lpr* mice (which develop lupus-like disease spontaneously), disease severity can be attenuated and mortality reduced by ~50% if antibody secretion is blocked, providing robust evidence that autoantibodies are more than spectators in disease etiology (9).

A recent explosion in genome-wide association studies (GWAS) has identified >80 potential risk loci across multiple immunopathologic pathways (10). In this review, we discuss how genetic variants affect the development of B cells, allowing them to overcome several checkpoints to break self tolerance, and how they contribute to the abnormal active phenotype observed in SLE. We examine how these genes alter both early developmental pathways in the bone marrow and late maturation processes to cause B cell dysregulation.

Central tolerance checkpoint of B cell development in the bone marrow in SLE

Normal B cell development starts in the bone marrow, where the first round of negative selection of

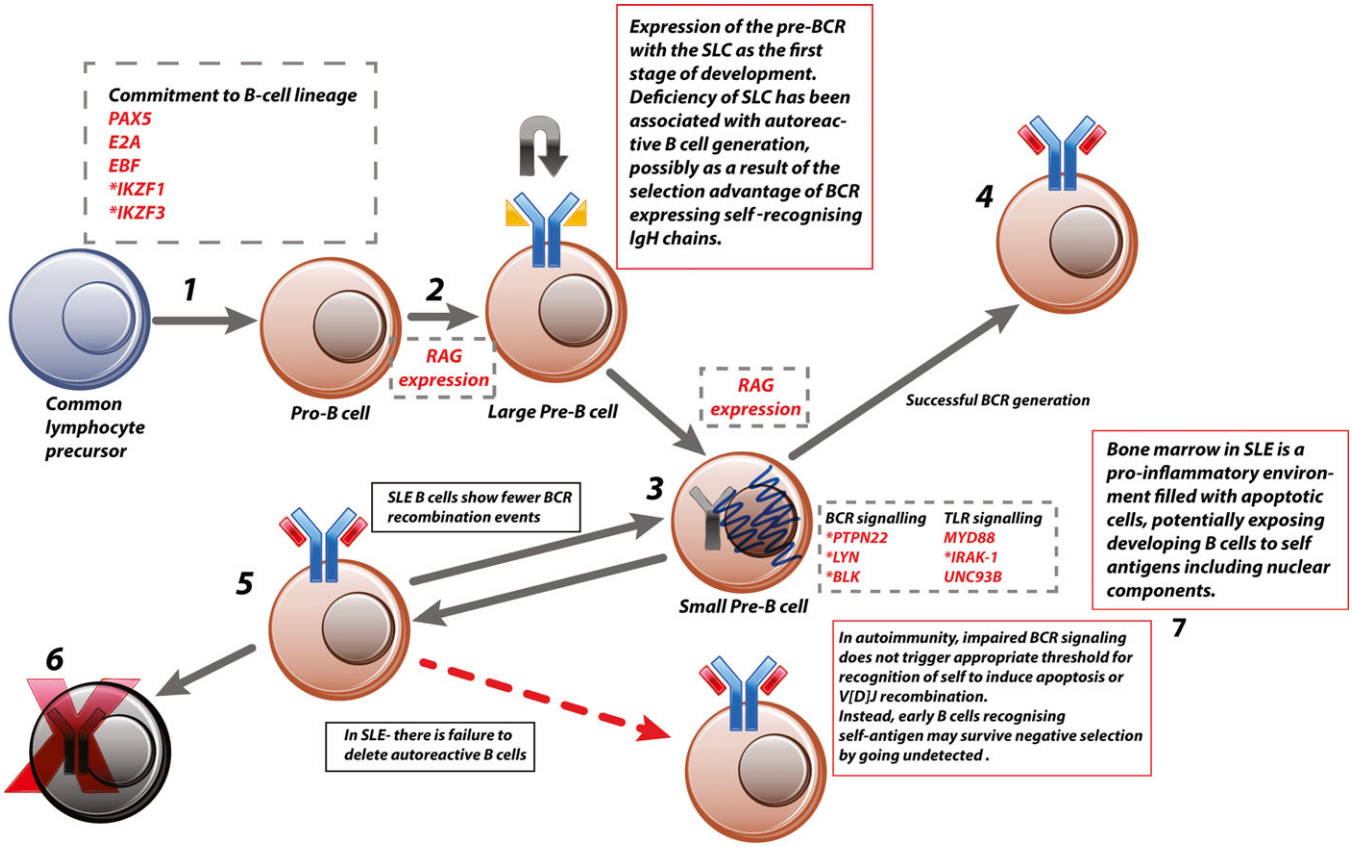

Figure 1. Central tolerance. **1,** Common lymphocyte precursor commits to B cell lineage via expression of B cell–specific transcription factors (e.g., early B cell factor [EBF]), which initiates IgH rearrangement. **2,** Expression of the generated IgH component of the pre–B cell receptor (pre-BCR) is combined with the surrogate light chain (SLC). **3,** Successful signaling through the pre-BCR leads to a short burst of proliferation and internalization of the pre-BCR and commences a second wave of recombination, this time in the light-chain gene. **4,** The generated BCR is then assessed for self-recognition. Those cells that have generated non–self-recognizing BCRs with functioning signaling switch off recombination-activating gene (RAG) expression and become immature B cells. **5,** Because V[D]J recombination is a stochastic process, a proportion of pre–B cells will generate autoreactive BCRs. This is detected by excess BCR signaling due to high-affinity binding within the bone marrow or abundance of antigen. This leads to continued V[D]J recombination until acceptable BCR is generated or all possible recombination has been exhausted. **6,** Failure to generate a non–self-recognizing BCR leads to apoptosis. **7,** In autoimmune disease this process is impaired, potentially by reduced signaling through the developing BCR, which fails to trigger the threshold for apoptosis. Genes or proteins involved at each stage are shown in dashed boxes. * = genes identified as risk-associated loci in systemic lupus erythematosus (SLE). TLR = Toll-like receptor; MyD88 = myeloid differentiation factor 88; IRAK-1 = interleukin-1 receptor–associated kinase 1; Unc-93B = Unc-93 homolog B.

Table 1. Summary of loci identified in genome-wide association studies and their role in B cell development*

Gene	Role in B cell development	Effect of risk variant	Mechanism of contribution to disease	B cell phenotype
Early B cell development and central tolerance				
IKZF1	Transcription factor helps regulate transition of multipotent progenitor cells to pro–B cells and pre–B cells	Regulates *IKZF1* expression, possibly increasing expression; also affects expression of C1qB and several IFN response genes (11)	Unknown	Knockout mice show developmental block in early B cell differentiation (13)
IKZF3†	Transcription factor helps regulate transition of pro–B cells and pre–B cells; also important in differentiation of plasma cells and development of B cell memory	Unknown	Unknown	Block in early B cell differentiation at the pre–B cell stage (13); knockout mice lack B cell immunologic memory and develop SLE-like disease (48)
B cell maturation in lymphoid tissue and peripheral tolerance				
ETS1	Transcription factor regulating B cell development in the GC	Down-regulation of expression (25)	Risk allele increased binding of pSTAT-1, leading to reduced expression (25)	Transgenic knockout mice show inability to induce B cell anergy in autoreactive cells (25)
UBE2L3	Ubiquitin-conjugating enzyme E2, which modulates NF-κB activity	Increased expression in B cells (26)	Increases NF-κB activation via LUBAC-mediated ubiquitination of IκBα (26)	Higher numbers of plasmablasts and plasma cells; basal active state in unstimulated B cells; modulated response to stimulatory signals such as TNF (26)
MHCII	Antigen-presenting molecules expressed on activated B cells	Variants in HLA–DRB1, DQA1, and DQA2 have all been reported; effect of risk variants unknown	Potentially enhanced presentation of autoantibodies in disease	HLA–DRB1*03:01 variant associated with anti-La and anti-Ro (71)
CD80	Costimulatory molecule expressed on activated B cells and promotes T cell activation via engagement with CD28 on T cell membrane	Unknown	Unknown	CD80 is known to be overexpressed in B cells from SLE patients (72)
BCR and pre-BCR signaling molecules affecting both central and peripheral tolerance				
PTPN22	Pre-BCR and BCR signaling molecule	Loss of function of *PTPN22* due to missense mutation (28,29)	Altered central tolerance with no clonal deletion of autoreactive B cells (28,29); peripheral B cells show enhanced activation via CD40 (28,29)	Subjects with the risk variant have impaired BCR signaling, more autoreactive B cells (28,29); active peripheral B cells (28,29)

Table 1. *(Cont'd)*

Gene	Role in B cell development	Effect of risk variant	Mechanism of contribution to disease	B cell phenotype
BLK	Src family kinase important in pre-BCR signaling	Down-regulation of Blk expression (33); splice variant which is prone to inactivation and degradation (34)	Potentially reduced pre-BCR signaling and failure of central tolerance (33)	Blk-knockout mice develop autoimmune disease similar to SLE and increase in B-1a cells; humans with the risk phenotype also showed increased levels of anti-dsDNA (even healthy individuals) (33,34)
CSK	Src family kinase important in BCR signaling	Increased expression of Csk (30)	Increased Lyp phosphorylation and augmented BCR signaling (30)	Active mature B cell phenotype (30)
LYN	Src family kinase important in pre-BCR signaling	Unknown	Unknown; variant is protective against severe disease (31)	SLE patients demonstrate reduced expression; knockout mice develop lupus-like disease with aberrant BCR signaling (31)
TLR7	Toll-like receptor	Increased TLR-7 expression (11); increased IFN response genes (11)	Possible enhanced IFN signaling (11); possible altered handling of nuclear material, increasing risk of anti-DNA antibodies (40)	Patients with the variant are at increased risk of nephritis and more likely to have anti-dsDNA antibodies (40)
Memory cells and long-lived plasma cells				
OX40L	Membrane-bound protein on memory B cells; member of TNFSF important in GC T cell–B cell interaction	Unknown	May augment memory B cell and T cell stimulation, leading to more active B cell phenotype (46)	Possible active memory B cell phenotype; OX40L levels correlate with disease activity and more severe disease (46)
BACH2	Transcription factor which regulates GCs; B cell differentiation into memory B cells and class-switching; role in central tolerance checkpoint and pre-BCR signaling (47)	Unknown	Unknown	Knockout mice have reduced B cell numbers and reduced numbers of memory B cells (47)
PRDM1	Encodes for BLIMP-1, a transcription factor important for plasma cell differentiation; negatively regulated by ETS-1; repressor of IFNγ gene expression	Reduced expression in DCs (55); no effect in B cells (55); unknown effect in plasma cells	Possible active DC phenotype promoting B cell stimulation and differentiation (55)	Conditional DC-knockout female mice develop SLE and increased numbers of GC B cells (55)
BANK1	Scaffolding protein involved in BCR signaling	Splice variant (49,50)	Variant forms larger and more widespread scaffold, potentially augmenting BCR signaling (49,50)	Altered BCR- and CD40-mediated signaling, expansion of memory B cell numbers (49,50)

* Where possible, the effect of the risk variant is included along with the way it potentially contributes to the B cell phenotype in systemic lupus erythematosus (SLE). IFN = interferon; GC = germinal center; LUBAC = linear ubiquitin chain assembly complex; TNF = tumor necrosis factor; BCR = B cell receptor; anti-dsDNA = anti–double-stranded DNA; TLR-7 = Toll-like receptor 7; TNFSF = TNF ligand superfamily; BLIMP-1 = B lymphocyte–induced maturation protein 1; DCs = dendritic cells.
† Also has crucial role in long-lived plasma cell development.

autoreactive B cells (termed central tolerance) occurs. This process is summarized in Figure 1. Many potential abnormalities in central tolerance have been implicated in SLE, including failure of adequate negative selection of autoreactive B cells and inadequate receptor editing (steps 6 and 3, respectively, in Figure 1), both of which are critical steps in maintaining tolerance to self (11).

The molecular mechanisms by which SLE autoreactive B cells evade central tolerance have yet to be fully elucidated. There are some clues, however, from various genetic studies (12). Patients with single-gene mutations resulting in primary immunodeficiencies frequently develop a wide range of autoimmune diseases in addition to increased susceptibility to infections (12). Their mutations teach us that central tolerance is largely dependent on adequate BCR signaling in the bone marrow (12) (steps 2 and 3 in Figure 1). In X-linked agammaglobulinemia, a defect in the gene for Bruton's tyrosine kinase (needed for downstream BCR signaling) results in increased frequency of autoreactive B cells (12). One possible mechanism is that binding to self antigen does not induce a strong enough response in BCR signaling to trigger clonal deletion (12). Conversely, deficiency in Wiscott-Aldrich syndrome protein (WASP; a negative regulator of BCR signaling) results in more stringent central control mechanisms, with WASP-knockout mice showing a much lower proportion of autoreactive B cells being released from the bone marrow. Their mature B cells also show abnormal peripheral tolerance and hyperactive phenotype, possibly driven by T cell abnormalities (12).

Outside of single-gene mutations, GWAS have expanded our knowledge of the molecular basis of B cell developmental anomalies in SLE (13,14). These GWAS have identified several SLE susceptibility loci near genes known to be important for early B cell development and BCR signaling (see Table 1 for summary). Variants affecting BCR signaling are discussed in more detail later in this review (13,14).

In early B cell development, several stages have been described which are associated with distinct genetic and molecular events. Two of these genes have been identified as risk loci and are discussed in the next section.

SLE risk loci and their role in the commitment to B cell lineage, common lymphoid progenitors, B lymphocyte precursors, pro–B cells, and pre–B cells

Commitment of the multipotent progenitor cells in the bone marrow to lymphocyte development depends on the expression of several transcription factors, including Ikaros (encoded by *IKZF1*) and Aiolos (encoded by *IKZF3*), among others (13,15) (step 1 in Figure 1). Ikaros in particular is known to be crucial for early commitment to B cell lineage. Its exact role in the early multipotent progenitor cells is unknown, although we know that mice deficient in Ikaros fail to develop any common lymphocyte precursors, with arrest of B cell development before lineage commitment to the B cell–biased lymphoid progenitor (16). Low expression of Ikaros allows generation of some B cells, but overall numbers remain low and differentiation is impaired at all stages (16).

The pre–B cell stage is characterized by the expression of the pre-BCR, and successful signaling through the pre-BCR arrests recombination of the IgH chain and the initiation of expression of the Ig light chains of the final BCR (17) (step 2 in Figure 1). Ikaros and its closely related family member Aiolos are both induced on engagement of the pre-BCR and help terminate signaling through the pre-BCR (steps 2 and 3 in Figure 1), promote exit from the cell cycle, and allow rearrangement of the Ig light-chain genes. Ikaros also induces expression of recombination-activating gene 1 (RAG-1) and RAG-2 and is required for IgH V_H gene recombination, allowing the pro–B cell to progress to the large pre–B cell stage (18).

Both the Ikaros and Aiolos variants (single-nucleotide polymorphism [SNP] rs4917014, which lies within the 3′-untranslated region [3′-UTR] of the *IKZF1* gene [encoding Ikaros] [$P = 2.7 \times 10^{-23}$], and SNP rs2941509, which lies within the 5′-UTR of the *IKZF3* gene [encoding Aiolos] [$P = 3.198 \times 10^{-6}$]) have been associated with increased transcription of their respective genes in whole blood (13,15) (Table 1). In models of overexpression in pre–B cell lines, increases in Ikaros and/or Aiolos induce termination of IgH recombination and stop signaling through pre-BCRs. However, high levels of expression are required to induce this process; therefore, it is plausible that both of these variants are promoting early transition to the small pre–B cell and may be contributing to the inadequate receptor editing observed in SLE (11,16,19).

Humans with germline mutations in *IKZF1* have an early block in common lymphocyte precursor development, with reduced pro–B cell numbers and normal pre–B cell numbers (20). Approximately half of the reported patients also developed autoimmune disease, including 1 who had SLE, suggesting that dysfunction and abnormalities of early B cell development can result in both immunodeficiency and autoimmunity (20).

Checkpoint at B cell maturation in the lymphoid tissue, from immature B cell to plasma cell and peripheral tolerance

Many abnormalities in peripheral tolerance have been identified in SLE, from problems with somatic

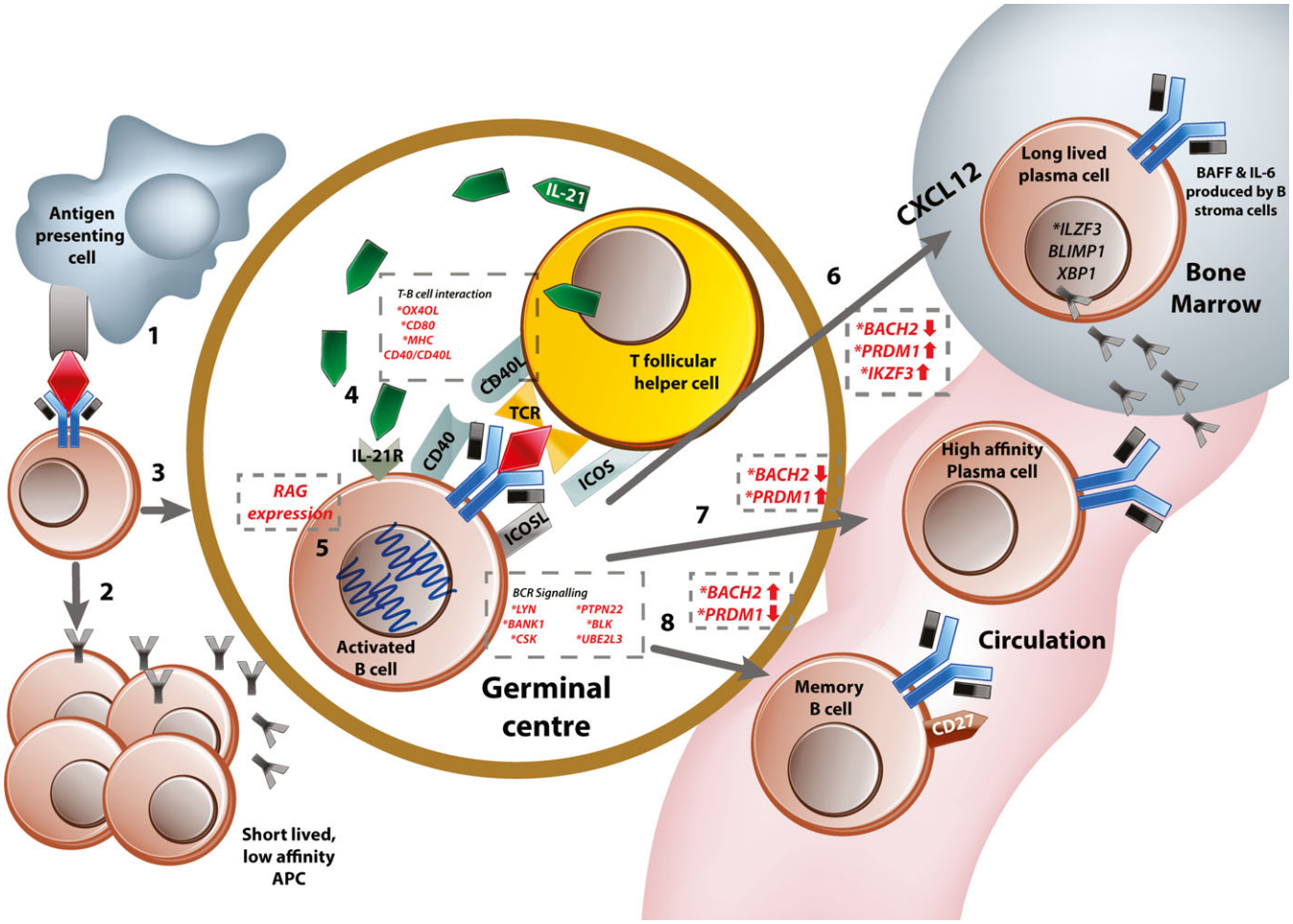

Figure 2. Peripheral tolerance. **1,** Naive B cells in the marginal zone encounter their relevant antigen as presented by resident antigen-presenting cells (APCs). **2,** Some activated B cells remain outside the germinal center and become short-lived low-affinity antibody-producing cells. **3,** Activated B cells migrate to the germinal center (under influence of CXCL12 produced by bone marrow stromal cells), **4,** where they interact with follicular helper T cells whose T cell receptors (TCRs) recognize self antigen. This also involves bidirectional signaling through multiple costimulatory molecules and the B cell receptor (BCR). **5,** At this stage, most B cells undergo a round of somatic hypermutation to achieve affinity maturation. This requires expression of the *RAG* genes. Following this, activated B cells can differentiate into 3 potential cell types. **6,** Long-lived plasma cells are selected from the pool of B cells with the highest affinity receptors. They up-regulate expression of CXCR4 and migrate toward their niche (usually in the bone marrow), where they reside and continue to produce background antibody. **7,** Some activated cells terminally differentiate into high-affinity plasma cells, which are responsible for the "second wave" of high-affinity antibody after antigen exposure. **8,** B cells with low-affinity BCRs are preferentially selected to become memory B cells. Genes or proteins involved at each of the regulatory stages are shown in dashed boxes. * = genes identified as risk-associated loci in systemic lupus erythematosus (SLE). IL-21 = interleukin-21; MHC = major histocompatibility complex; IL-21R = IL-21 receptor; RAG = recombination-activating gene; ICOS = inducible costimulator; BANK-1 = B cell scaffold protein with ankyrin repeats 1; UBE2L3 = ubiquitin-conjugating enzyme E2 L3; BLIMP-1 = B lymphocyte–induced maturation protein 1; XBP-1 = X-box binding protein 1.

hypermutation to memory B cell dysfunction (see Figure 2 for summary). First, SLE patients show aberrant and raised RAG expression in peripheral B cells (step 6 in Figure 2), raising the possibility that some autoreactive B cells arise as a result of mutation of a "healthy" BCR into one that recognizes self antigen (21). This hypothesis is supported by analysis of genetic variation in the Ig produced by autoimmune mice, showing that point mutations can render a previously self-tolerant BCR autoreactive (22). These data have been replicated in the analysis of anti-dsDNA antibodies from humans with SLE (23). Second, autoantibodies in SLE often evolve over the duration of the disease, recognizing different epitopes of their respective antigens and frequently achieving a higher affinity (23,24). The raised levels of interleukin-6 (IL-6) seen in the disease may contribute to this, as IL-6 is a known up-regulator of RAG gene expression (25).

The other major player in this process of secondary maturation and in the maintenance of tolerance is the T cell–B cell interaction (step 5 in Figure 2). This is

supported by evidence from single-gene immunodeficiency disorders, mouse models, and GWAS (12,14,26). Patients with single-gene mutations in CD40, CD40L, and major histocompatibility complex (MHC) class II develop a significant proportion of autoreactive B cells, including those with receptors recognizing nuclear components (including antinuclear antibodies [ANAs]) (26). This is despite their having normal central tolerance processes in the bone marrow (12,26). In the *Sle1* murine model, disease risk is inherited via a region on chromosome 1, carrying polymorphisms in genes encoding multiple receptors needed for T cell–B cell interactions (including *Slam*, *Ly108*, *Cd84*, *Cracc*, and *Ly9*) (27). In the germinal centers (GCs) of these mice, transient short-term contact between B cells and T cells allows rare autoreactive B cells and T cells to "sample" many different cells in the GC, increasing chances of interaction for positive costimulation (27). Shorter contact times between immune cells are also known to alter their function (e.g., poorer Treg cell ability to induce tolerance in target cells due to shorter contact times) (28). It is possible that shorter T cell–B cell contact in the GC may lead to chronic, low-grade activation, allowing autoreactive B cells to survive due to background low-quality contact, without receiving adequate signals to become anergic.

Patients and mice with deficiencies in CD40, CD40L, and MHC class II who have poor T cell–B cell interaction overcome lack of B cell stimulation by up-regulating BAFF, a stimulatory cytokine that promotes B cell survival and proliferation (26). This has important consequences for B cell activation and murine models in which mice that overexpress BAFF develop lupus-like disease with ANAs and anti-dsDNA (29). These findings suggest that in the absence of specific and controlled BCR activation, more generic signals (such as BAFF) promote indiscriminate B cell activation and survival of self antigens recognizing B cells and normal foreign antigens recognizing cells equally (29). Variants in loci near or within *OX40L*/*TNFSF4,* MHC class II, and *CD80* have all been implicated as associated with risk of SLE in various GWAS (13,14,30,31) (Table 1).

The SLE-associated variant rs6590330 in the promoter of the gene *ETS1* results in down-regulation of expression of the transcription factor ETS-1 in whole blood from humans (30). Studies in transgenic mice that are both deficient in Ets-1 and express an autoreactive BCR indicate that while central tolerance is maintained, deficiency in Ets-1 results in impaired anergic responses (32). B cells from Ets-$1^{-/-}$ mice produced autoantibodies despite receiving appropriate "anergy" signals and continued to secrete them even in the absence of interaction with cognate antigen (32). Some features of B cell anergy (such as reduced BCR-mediated tyrosine phosphorylation and Ca^{2+} influx) could be induced in deficient cells after stimulation with high-affinity antigen; however, this could not switch off autoantibody production (32).

The *UBE2L3* gene (which codes for ubiquitin-conjugating enzyme E2, also known as UBCH7) on chromosome 22 contains a risk variant (associated SNP rs140490, $P = 7.5 \times 10^{-8}$) within its promoter that leads to increased expression and protein levels in B cells (but not in other immune cells such as T cells) (31). UBCH7 drives NF-κB activation through increased linear ubiquitin chain assembly complex–mediated ubiquitination and subsequent proteasomal degradation of IκBα, an inhibitor of NF-κB (31). Raised basal levels of NF-κB led to steady-state activation and augmented responses to stimulatory signals (31). This resulted in higher numbers of both plasmablasts and plasma cells and modulated response to stimulatory signals such as CD40 and tumor necrosis factor (TNF) (Table 1 and step 5 in Figure 2) in carriers of the risk variant (31).

Variants affecting B cell signaling molecules affect both peripheral and central tolerance mechanisms

Variants affecting B cell and pre–B cell signaling affect both central and peripheral tolerance, and many genes involved in both BCR and pre-BCR signaling have been identified from GWAS (13,14). These variants contribute to the generation of autoreactive B cells and the activated phenotype identified in peripheral B cells in SLE (13,14) (Table 1). Variants resulting in impaired BCR signaling are thought to contribute to autoimmunity in a mechanism analogous to that noted in the monogenic immunodeficiencies discussed above, in which inadequate pre-BCR signaling leads to failure in reaching the threshold for clonal deletion or BCR rearrangement (12,33). Variants contributing to increased BCR-mediated signaling may promote the peripheral active B cell phenotype characteristic of SLE (34,35). Risk variants identified in SLE include PTPN22, Blk, Csk, and Lyn (13,14,36) (step 3 in Figure 1 and step 4 in Figure 2).

The risk allele (SNP rs476601, $P = 3.4 \times 10^{-12}$) for *PTPN22*, which encodes the tyrosine kinase Lyp, is associated with impaired BCR signaling and is thought to contribute to autoreactive B cell survival through various mechanisms (14) (Table 1). This risk variant is associated with faulty central tolerance and failure to remove autoreactive B cells in the bone marrow (33). In addition, peripheral B cells carrying this risk allele up-regulated many genes involved in B cell activation, including those involved in BCR, CD40, and Toll-like receptor (TLR) signaling as well as cytokine receptors (e.g., IL-21 receptor [IL-21R] and IL-4R) (34). Moreover, these B

cells show increased surface expression of CD40 as well as enhanced responses to CD40 engagement, potentially contributing to the active peripheral phenotype (34). Up-regulation of these proactivation genes is thought to be a mechanism by which B cells overcome the deficit in Lyp function caused by the risk variant (34).

Blk, a Src family tyrosine kinase, is normally up-regulated at the pre–B cell stage and is important in the transduction of pre-BCR signaling (37). Blk phosphorylates the Ig α- and β-subunits of the BCR and is known to bind the phosphatidylinositol lipase C-γ230, forming a complex with the B cell adaptor protein ankyrin repeats (encoded by the *BANK1* gene and, interestingly, also a susceptibility locus for SLE) during BCR signaling (38). The disease-associated SNPs for Blk (rs922483 and rs1382568) both result in the down-regulation of Blk expression and potential failure of adequate pre-BCR signaling (36,39) (Table 1). A third and rarer coding variant of Blk associated with SLE that results in an alanine-for-threonine substitution in its SH3 domain leads to hypophosphorylation, inactivation, and rapid degradation of the protein (40). This variant also demonstrates impaired binding to B cell scaffold protein with ankyrin repeats 1 (BANK-1) scaffolding, which is important in signal transduction (40).

$Blk^{-/-}$ mice develop autoimmune disease, with anti-dsDNA autoantibodies and immune complex–mediated glomerulonephritis, together with an increase in the proportion of B-1 cells (a low-affinity IgM-producing subtype of B cells in mice) (41). Expansion of this subtype of B cells in other murine models of lupus is well documented and is thought to be important, particularly in driving nephritis (41). In a mechanism similar to that of the Lyp variant, this may contribute to autoimmunity by impairing central tolerance mechanisms. However, abnormalities in peripheral BCR signaling have also been described, with low baseline BCR activity at rest but enhanced responses on activation, heightened ability to stimulate T cells, and increased numbers of isotype-switched memory B cells (42).

CSK, located on chromosome 15, carries a risk variant (SNP rs34933034) that up-regulates expression of Csk, a Src family tyrosine kinase important in the BCR signaling cascade (35). B cells from those carrying the risk allele show increased levels of Csk expression and increased subsequent phosphorylation of Lyp, augmented BCR responses, and activation of mature B cells (35).

Lyn, another member of the Src kinase family, has also been associated with SLE (36,43). Initial GWAS identified rs57829816 in the 5′ region ($P = 5.4 \times 10^{-9}$) and rs2667978 in the 3′ region ($P = 5.1 \times 10^{-8}$) in women of European ancestry, with both variants being protective. Further transancestral case–control studies identified a third variant in American women of European ancestry, rs6983130 in the 5′-UTR of the gene ($P = 0.000111$) (36). This variant was also protective and was associated with less severe disease within cases (36). No association between any Lyn variants and disease has been identified in populations of African or Asian ancestry, nor has there been any association with changes in protein or transcript levels (36,43,44). However, data from SLE patients have shown them to have lower levels of Lyn compared to healthy controls, implying that lower levels may be associated with disease (45,46). In addition, studies in B cell lines show that Lyn is required for inhibitory signals in response to weak BCR crosslinking (47). $Lyn^{-/-}$ mice are susceptible to an inducible immune complex–mediated nephritis as well as to antibody-induced arthritis (47).

Patients deficient in IL-1R–associated kinase 4, myeloid differentiation factor 88, and Unc-93 homolog B (signaling molecules in the TLR pathway) also have high levels of autoreactive B cells, suggesting that impaired signaling via these pathways results in survival of autoreactive BCRs, possibly by failing to pass the signaling threshold for clonal deletion in the bone marrow (12) (step 3 in Figure 1). These patients also demonstrated impaired receptor editing and had defects in peripheral tolerance (48). SNP rs3853839 in the 3′-UTR of TLR-7 ($P = 2 \times 10^{-9}$) has been associated with SLE in several GWAS (14). This variant is associated with increased transcript levels and amplified signaling, resulting in an enhanced interferon (IFN) signature (14). A study in Danish patients with SLE found that variants in TLRs 7–9 were associated with certain disease phenotypes and specific serologic markers (49). For example, some TLR-7 variants were associated with nephritis and anti-dsDNA antibodies (49).

Checkpoint at the level of memory cells and long-lived plasma cells in SLE

Although abnormalities in both central and peripheral tolerance are pivotal to pathology, memory B cells and long-lived plasma cells contribute substantially to disease propagation (50). One of the most striking B cell findings in SLE is the high prevalence of mature, antigen-experienced class-switched memory cells (3). The effect of having a relatively large proportion of these cells is multifold. First, these cells are primed for action and have a lower activation threshold compared to naive B cells. Second, they exhibit resistance to regulatory and inhibitory signals (3). In addition, SLE patients have a unique group of memory B cells in the periphery which lack CD27 expression (a hallmark of memory B cell phenotype), the numbers of which correlate with increased disease activity, renal involvement, and higher serum levels of autoantibodies (51).

The endurance of autoreactive long-lived plasma cells and their resistance to treatments such as B cell depletion and chemotherapy demonstrate the importance of this plasma cell subtype in disease persistence. In lupus-prone mice, long-lived plasma cells develop early and continue to expand throughout their lifetime (50). Murine models indicate a prominent role for these long-lived plasma cells in autoimmunity; for example, antibodies derived from long-lived plasma cells were found in diseased kidneys of NZB/NZW mice (8). In addition, these long-lived plasma cells are thought to be responsible for the production of anti-RNA antibodies, which explains why the titers of these antibodies are not altered with B cell depletion therapy (52,53).

Development and survival of long-lived plasma cells and memory cells is complex and depends on a functioning GC (54). Within the GC, there is stringent selection of cells with high-affinity receptors to become long-lived plasma cells, while memory B cells undergo a less rigorous selection process (Figure 2) (54). Memory B cells do acquire increased affinity over time, and some studies suggest that they may re-enter the follicle and undergo further maturation. While long-lived plasma cells reside in "niches" usually within the bone marrow, memory B cells are found circulating in the periphery and dwelling in secondary lymphoid tissue (54).

Various GWAS in SLE have identified an association with the gene encoding the protein OX40L/TNF ligand superfamily member 4 (55) (Table 1 and step 5 in Figure 2). This gene codes for a membrane-bound protein expressed on the surface of memory B cells, with its unique receptor OX40 primarily expressed on CD4+ Th cells. The OX40L–OX40 interaction results in bidirectional signaling in both the B cell and T cell involved, activation in both cells, and augmentation of the immune response (55). Although the effect of the identified variant on OX40L expression has not been fully identified, we know that both OX40L and OX40 are found at higher levels in patients with SLE, particularly those with more active disease and with a more severe disease phenotype (as indicated by the presence of nephritis) (55). These findings suggest that these proteins contribute to the increased number and more active phenotype of memory B cells in SLE.

GWAS data sets also show disease association with many of the genes associated with the development of immunologic memory including *BACH2*, *PRDM1*, and *IKZF3* (13,14,56) (Table 1 and steps 6–8 in Figure 2). The exact effect of the risk variant in each of these genes on function is not yet known, but these associations hint that the proteins may contribute to the dysregulation of the developmental pathways in memory and long-lived plasma cells. Of particular interest, we know that mice lacking Aiolos fail to develop immunologic memory although they have normal initial responses to antigen exposure and are at increased risk of developing B cell lymphoma (57). Aiolos$^{-/-}$ mice also develop a lupus-like disease in old age, with typical autoantibodies and immune complex deposition (57). This autoimmune phenotype comes about as a result of a B cell defect with retention of both relatively normal T cells and innate immune system (57).

Two polymorphisms in *BANK1* have been identified as associated with risk (13,14,40,58) (Table 1). Both impair BCR and CD40 signaling and are associated with an expansion of memory B cells in vivo (58) (step 4 in Figure 2). *BANK1* encodes a scaffolding protein that acts during BCR signaling by promoting phosphorylation of Src tyrosine kinases such as Lyn through enabling protein–protein interactions between them and inositol 1,4,5-trisphosphate receptor (59). One of the risk polymorphisms (rs10516487) is associated with alternative splicing which results in a protein that forms larger and more widespread scaffolds within the cytoplasm (59). The effect of the other risk variant (rs17266594) on BANK-1 expression is currently unknown.

Extrinsic factors

Failure of tolerance in SLE is due in large part to the intrinsic defects discussed above, but it is important to note that B cells develop in an abnormal milieu in lupus patients compared to healthy controls. Analysis of bone marrow aspirates from patients with SLE demonstrates some interesting findings (60). First, there were more apoptotic cells within lupus bone marrow, potentially exposing developing pre–B cells to more nuclear self antigens and propagating the development of autoreactive BCRs (60). Second, there were increased numbers of CD4+ T cells, macrophages, and plasma cells, creating a proinflammatory environment (60). These inflammatory cells produced significant amounts of IFN (a high level of the cytokine in the bone marrow was associated with increased disease activity), which has profound effects on B cell development (61). An abundance of IFN in bone marrow leads to arrested development at the early stages and expansion at the transitional B cell stage (61). Similarly, the lymphoid tissue in SLE is also altered (62). The GCs are areas with a high proportion of cells undergoing proliferation and apoptosis. Under normal circumstances, apoptotic cells are rapidly cleared, but in SLE there are well-known defects in this process (for extensive review, see ref. 63) potentially leading to persistence of apoptotic material including nuclear components and perpetuating the antigen-driven B cell response (62).

Although epigenetic annotation of risk variants identifies the B cell as the main cell of interest for the disease, risk variants affecting many aspects of the immune system from innate to adaptive have been described (14,64–66). Many of the risk loci associated with SLE discussed in this review also affect genes with multilineage functions. For example, the *IKZF1* variant has also been shown to affect expression of complement components and several IFN response genes, while Lyp is required for T cell receptor signaling (14,67).

Another good example of this is the variant affecting *PRDM1*, which encodes for B lymphocyte–induced maturation protein 1 (BLIMP-1), a transcription factor crucial for plasma cell differentiation. The effect of the risk variant rs548324, however, is demonstrable in dendritic cells (DCs), which show a reduction in expression as a result of the variant, a reduction not replicated in B cells (68). BLIMP-1 knockout in DCs is associated with an increase in IL-6 secretion as well as increased numbers of follicular T cells and GC B cells, with female mice developing SLE-like disease (68). Therefore, while the ultimate phenotypic outcome of a specific variant may be B cell dysfunction, the actual molecular abnormality may not be B cell specific.

Summary

Although the immunologic abnormalities in SLE are complex, numerous, and not fully understood, B cells have a central role in the development of the disease, from driving immune complex production to secretion of proinflammatory cytokines. Since SLE is an archetypal complex disease, the genetic association data reflect that complexity, with many variants, affecting several areas of the immune system (13,14).

The advent of GWAS has identified many potential abnormal pathways relevant to the breaking of self tolerance in SLE (summarized in Table 1). The data emphasize the central role of B cells, with a significant proportion of identified genes affecting B cell function and epigenetic annotation reinforcing this (13,14,65,66). GWAS have also helped to explain clinical variability between individuals—it is easy to see how each patient is likely to have a different combination of risk variants resulting in a pattern of immune dysfunction unique to that individual. We can already see how variants in TLR genes can help predict disease and serologic markers, or how variants in the gene for Lyn can protect against hematologic involvement (36,49).

Traditionally, B cell–targeted therapy has mostly been focused on depletion of numbers (e.g., through targeting CD20-mediated depletion through rituximab), but with our growing understanding, less crude approaches are being investigated. For example, Aiolos depletion therapy with the CC-220 molecule results in down-regulation of genes mediating B cell differentiation, reduces proliferation, and inhibits antibody secretion in B cells from SLE patients (69). Emerging therapy such as epratuzumab (a monoclonal antibody to CD22) has been shown to block B cell differentiation and activation directly through selective inhibition of BLIMP-1 (encoded by *PRDM1*), demonstrating how data from GWAS can inform future drug therapy (70).

Although the results from GWAS confirm the complexity of SLE pathogenesis and show that different intrinsic B cell abnormalities are likely to drive disease in each individual case, the principles underlying the loss of central tolerance (deficient BCR signaling) and peripheral tolerance (dysregulated T cell–B cell interaction) are universal. Genetic information helps us to personalize therapy, whereby relevant molecules can be targeted through understanding the exact pathways involved in an individual's disease.

AUTHOR CONTRIBUTIONS

Drs. Karrar and Cunninghame Graham drafted the article, revised it critically for important intellectual content, and approved the final version to be published.

REFERENCES

1. Kaul A, Gordon C, Crow MK, Touma Z, Urowitz MB, van Vollenhoven R, et al. Systemic lupus erythematosus. Nat Rev Dis Prim 2016;2:16039.
2. Deafen D, Escalante A, Weinrib L, Horwitz D, Bachman B, Roy-Burman P, et al. A revised estimate of twin concordance in systemic lupus erythematosus. Arthritis Rheum 1992;35:311–8.
3. Iwata S, Tanaka Y. B-cell subsets, signaling and their roles in secretion of autoantibodies. Lupus 2016;25:850–6.
4. Lund FE. Cytokine-producing B lymphocytes-key regulators of immunity. Curr Opin Immunol 2008;20:332–8.
5. Grammer AC, Fischer R, Lee O, Zhang X, Lipsky PE. Flow cytometric assessment of the signaling status of human B lymphocytes from normal and autoimmune individuals. Arthritis Res Ther 2004; 6:28–38.
6. Fritzler MJ. Clinical relevance of autoantibodies in systemic rheumatic diseases. Mol Biol Rep 1996;23:133–45.
7. Van Bavel CC, van der Vlag J, Berden JH. Glomerular binding of anti-dsDNA autoantibodies: the dispute resolved? Kidney Int 2007;71:600–1.
8. Cheng Q, Mumtaz IM, Khodadadi L, Radbruch A, Hoyer BF, Hiepe F. Autoantibodies from long-lived "memory" plasma cells of NZB/W mice drive immune complex nephritis. Ann Rheum Dis 2013;72:2011–7.
9. Chan OT, Hannum LG, Haberman AM, Madaio MP, Shlomchik MJ. A novel mouse with B cells but lacking serum antibody reveals an antibody-independent role for B cells in murine lupus. J Exp Med 1999;189:1639–48.
10. Chen L, Morris DL, Vyse TJ. Genetic advances in systemic lupus erythematosus. Curr Opin Rheumatol 2017;29:423–33.
11. Kil LP, Hendriks RW. Aberrant B cell selection and activation in systemic lupus erythematosus. Int Rev Immunol 2013;32:445–70.

12. Meffre E. The establishment of early B cell tolerance in humans: lessons from primary immunodeficiency diseases. Ann N Y Acad Sci 2011;1246:1–10.
13. Morris DL, Sheng Y, Zhang Y, Wang YF, Zhu Z, Tombleson P, et al. Genome-wide association meta-analysis in Chinese and European individuals identifies ten new loci associated with systemic lupus erythematosus. Nat Genet 2016;48:940–6.
14. Teruel M, Alarcon-Riquelme ME. The genetic basis of systemic lupus erythematosus: what are the risk factors and what have we learned? J Autoimmun 2016;74:161–75.
15. Westra HJ, Peters MJ, Esko T, Yaghootkar H, Schurmann C, Kettunen J, et al. Systematic identification of trans eQTLs as putative drivers of known disease associations. Nat Genet 2013; 45:1238–43.
16. Schwickert TA, Tagoh H, Gültekin S, Dakic A, Axelsson E, Minnich M, et al. Stage-specific control of early B cell development by the transcription factor Ikaros. Nat Immunol 2014;15:283–93.
17. Melchers F, Karasuyama H, Haasner D, Bauer S, Kudo A, Sakaguchi N, et al. The surrogate light chain in B-cell development. Immunol Today 1993;14:60–8.
18. Reynaud D, Demarco IA, Reddy KL, Schjerven H, Bertolino E, Chen Z, et al. Regulation of B cell fate commitment and immunoglobulin heavy-chain gene rearrangements by Ikaros. Nat Immunol 2008;9:927–36.
19. Ma S, Pathak S, Trinh L, Lu R. Interferon regulatory factors 4 and 8 induce the expression of Ikaros and Aiolos to down-regulate pre-B-cell receptor and promote cell-cycle withdrawal in pre-B-cell development. Blood 2008;111:1396–403.
20. Hoshino A, Okada S, Yoshida K, Nishida N, Okuno Y, Ueno H, et al. Abnormal hematopoiesis and autoimmunity in human subjects with germline IKZF1 mutations. J Allergy Clin Immunol 2017;140:223–31.
21. Girschick HJ, Grammer AC, Nanki T, Vazquez E, Lipsky PE. Expression of recombination activating genes 1 and 2 in peripheral B cells of patients with systemic lupus erythematosus. Arthritis Rheum 2002;46:1255–63.
22. Shlomchik M, Mascelli M, Shan H, Radic MZ, Pisetsky D, Marshak-Rothstein A, et al. Anti-DNA antibodies from autoimmune mice arise by clonal expansion and somatic mutation. J Exp Med 1990;171:265–92.
23. Zhang J, Jacobi A. Pathogenic autoantibodies in systemic lupus erythematosus are derived from both self-reactive and non-self–reactive B cells. Mol Med 2008;14:1.
24. Arbuckle MR, McClain MT, Rubertone MV, Scofield RH, Dennis GJ, James JA, et al. Development of autoantibodies before the clinical onset of systemic lupus erythematosus. N Engl J Med 2003;349:1526–33.
25. Hillion S, Garaud S, Devauchelle V, Bordron A, Berthou C, Youinou P, et al. Interleukin-6 is responsible for aberrant B-cell receptor-mediated regulation of RAG expression in systemic lupus erythematosus. Immunology 2007;122:371–80.
26. Hervé M, Isnardi I, Ng Y, Bussel JB, Ochs HD, Cunningham-Rundles C, et al. CD40 ligand and MHC class II expression are essential for human peripheral B cell tolerance. J Exp Med 2007;204:1583–93.
27. Sinai P, Dozmorov I, Song R, Schwartzberg P, Wakeland E, Wulfing C. T/B-cell interactions are more transient in response to weak stimuli in SLE-prone mice. Eur J Immunol 2014;44:3522–31.
28. Davis DM. Mechanisms and functions for the duration of intercellular contacts made by lymphocytes. Nat Rev Immunol 2009;9:543–55.
29. Lesley R, Xu Y, Kalled SL, Hess DM, Schwab SR, Shu HB, et al. Reduced competitiveness of autoantigen-engaged B cells due to increased dependence on BAFF. Immunity 2004;20:441–53.
30. Lu X, Zoller EE, Weirauch MT, Wu Z, Namjou B, Williams AH, et al. Lupus risk variant increases pSTAT1 binding and decreases ETS1 expression. Am J Hum Genet 2015;96:731–9.
31. Lewis MJ, Vyse S, Shields AM, Boeltz S, Gordon PA, Spector TD, et al. UBE2L3 polymorphism amplifies NF-κB activation and promotes plasma cell development, linking linear ubiquitination to multiple autoimmune diseases. Am J Hum Genet 2015;96:221–34.
32. Russell L, John S, Cullen J, Luo W, Shlomchik MJ, Garret-Sinha LA. Requirement for transcription factor Ets1 in B cell tolerance to self-antigens. J Immunol 2015;195:3574–83.
33. Arechiga AF, Habib T, He Y, Zhang X, Zhang ZY, Funk A, et al. Cutting edge: the PTPN22 allelic variant associated with autoimmunity impairs B cell signaling. J Immunol 2009;182:3343–7.
34. Menard L, Saadoun D, Isnardi I, Ng YS, Meyers G, Massad C, et al. The PTPN22 allele encoding an R620W variant interferes with the removal of developing autoreactive B cells in humans. J Clin Invest 2011;121:3635–44.
35. Manjarrez-Orduño N, Marasco E, Chung SA, Katz MS, Kiridly JF, Simpfendorfer KR, et al. CSK regulatory polymorphism is associated with systemic lupus erythematosus and influences B-cell signaling and activation. Nat Genet 2012;44:1227–30.
36. Lu R, Vidal GS, Kelly JA, Delgado-Vega AM, Howard XK, Macwana SR, et al. Genetic associations of LYN with systemic lupus erythematosus. Genes Immun 2009;10:397–403.
37. Geier JK, Schlissel MS. Pre-BCR signals and the control of Ig gene rearrangements. Semin Immunol 2006;18:31–9.
38. Akerblad P, Sigvardsson M. Early B cell factor is an activator of the B lymphoid kinase promoter in early B cell development. J Immunol 1999;163:5453–61.
39. Pamuk ON, Gurkan H, Pamuk GE, Tozkir H, Duymaz J, Yazar M. BLK pathway-associated rs13277113 GA genotype is more frequent in SLE patients and associated with low gene expression and increased flares. Clin Rheumatol 2016:1–7.
40. Díaz-Barreiro A, Bernal-Quirós M, Georg I, Marañón C, Alarcón-Riquelme M, Castillejo-López C. The SLE variant Ala71Thr of BLK severely decreases protein abundance and binding to BANK1 through impairment of the SH3 domain function. Genes Immun 2016;17:128–38.
41. Wu YY, Georg I, Díaz-Barreiro A, Varela N, Lauwerys B, Kumar R, et al. Concordance of increased B1 cell subset and lupus phenotypes in mouse and human dependent on BLK expression levels. J Immunol 2016;8:583–92.
42. Simpfendorfer KR, Armstead BE, Shih A, Li W, Curran M, Manjarrez-Orduño N, et al. Autoimmune disease–associated haplotypes of BLK exhibit lowered thresholds for B cell activation and expansion of Ig class-switched B cells. Arthritis Rheumatol 2015;67:2866–76.
43. Harley JB, Alarcón-Riquelme ME, Criswell LA, Jacob CO, Kimberly RP, Moser KL, et al. Genome-wide association scan in women with systemic lupus erythematosus identifies susceptibility variants in ITGAM, PXK, KIAA1542 and other loci. Nat Genet 2008;40:204–10.
44. Lonsdale J, Thomas J, Salvatore M, Phillips R, Lo E, Shad S, et al. The Genotype-Tissue Expression (GTEx) project. Nat Genet 2013;45:580–5.
45. Liossis SN, Solomou EE, Sikakis PP. Lyn deficiency in B cells from patients with systemic lupus erythematosus: comment on the article by Flores-Borja et al [letter]. Arthritis Rheum 2006;54: 2036–7.
46. Flores-Borja F, Kabouridis PS, Jury EC, Isenberg DA, Mageed RA. Decreased Lyn expression and translocation to lipid raft signaling domains in B lymphocytes from patients with systemic lupus erythematosus. Arthritis Rheum 2005;52:3955–65.
47. Mkaddem SB, Murua A, Flament H, Titeca-Beauport D, Bounaix C, Danelli L, et al. Lyn and Fyn function as molecular switches that control immunoreceptors to direct homeostasis or inflammation. Nat Commun 2017;8:246.
48. Isnardi I, Ng YS, Srdanovic I, Motaghedi R, Rudchenko S, von Bernuth H, et al. IRAK-4- and MyD88-dependent pathways are essential for the removal of developing autoreactive B cells in humans. Immunity 2008;29:746–57.
49. Enevold C, Nielsen CH, Jacobsen RS, Hermansen ML, Molbo D, Avlund K, et al. Single nucleotide polymorphisms in genes encoding toll-like receptors 7, 8 and 9 in Danish patients with systemic lupus erythematosus. Mol Biol Rep 2014;41:5755–63.

50. Taddeo A, Khodadadi L, Voigt C, Mumtaz IM, Cheng Q, Moser K, et al. Long-lived plasma cells are early and constantly generated in New Zealand Black/New Zealand white F1 mice and their therapeutic depletion requires a combined targeting of autoreactive plasma cells and their precursors. Arthritis Res Ther 2011;17.
51. Jacobi AM, Reiter K, Mackay M, Aranow C, Hiepe F, Radbruch A, et al. Activated memory B cell subsets correlate with disease activity in systemic lupus erythematosus: delineation by expression of CD27, IgD, and CD95. Arthritis Rheum 2008;58:1762–73.
52. Liu Z, Zou Y, Davidson A. Plasma cells in systemic lupus erythematosus: the long and short of it all. Eur J Immunol 2011;41:588–91.
53. Grammer AC, Lipsky PE. B cell abnormalities in systemic lupus erythematosus. Arthritis Res Ther 2003;5 Suppl 4:S22–7.
54. Phan TG, Tangye SG. Memory B cells: total recall. Curr Opin Immunol 2017;45:132–40.
55. Manku H, Graham DS, Vyse TJ. Association of the co-stimulator OX40L with systemic lupus erythematosus. J Mol Med 2009;87: 229–34.
56. Igarashi K, Kurosaki T, Roychoudhuri R. BACH transcription factors in innate and adaptive immunity. Nat Rev Immunol 2017;17:437–50.
57. Cortés M, Georgopoulos K. Aiolos is required for the generation of high affinity bone marrow plasma cells responsible for long-term immunity. J Exp Med 2004;199:209–19.
58. Dam EM, Habib T, Chen J, Funk A, Glukhova V, Davis-Pickett M, et al. The BANK1 SLE-risk variants are associated with alterations in peripheral B cell signaling and development in humans. Clin Immunol 2016;173:171–80.
59. Kozyrev SV, Bernal-Quirós M, Alarcón-Riquelme ME, Castillejo-López C. The dual effect of the lupus-associated polymorphism rs10516487 on BANK1 gene expression and protein localization. Genes Immun 2012;13:129–38.
60. Park J, Moon S, Lee J, Park J, Lee D, Jung K, et al. Bone marrow analysis of immune cells and apoptosis in patients with systemic lupus erythematosus. Lupus 2014;23:975–85.
61. Palanichamy A, Bauer JW, Yalavarthi S, Meednu N, Barnard J, Owen T, et al. Neutrophil mediated IFN activation in the bone marrow alters B cell development in human and murine SLE. J Immunol 2014;192:906–18.
62. Woods M, Zou YR, Davidson A. Defects in germinal center selection in SLE. Front Immunol 2015;6:1–7.
63. Muñoz LE, Lauber K, Schiller M, Manfredi AA, Herrmann M. The role of defective clearance of apoptotic cells in systemic autoimmunity. Nat Rev Rheumatol 2010;6:280–9.
64. Rhodes B, Vyse TJ. The genetics of SLE: an update in the light of genome-wide association studies. Rheumatology (Oxford) 2008;47:1603–11.
65. Trynka G, Sandor C, Han B, Xu H, Stranger BE, Liu XS, et al. Chromatin marks identify critical cell types for fine mapping complex trait variants. Nat Genet 2013;45:124–30.
66. Farh KK, Marson A, Zhu J, Kleinewietfeld M, Housley WJ, Beik S, et al. Genetic and epigenetic fine mapping of causal autoimmune disease variants. Nature 2014;518:337–43.
67. Jofra T, di Fonte R, Hutchinson TE, Dastmalchi F, Galvani G, Battaglia M, et al. Protein tyrosine phosphatase PTPN22 has dual roles in promoting pathogen versus homeostatic-driven CD8 T-cell responses. Immunol Cell Biol 2017;95:121–8.
68. Jang SH, Chen H, Gregersen PK, Diamond B, Kim SJ. Kruppel-like factor4 regulates PRDM1 expression through binding to an autoimmune risk allele. JCI Insight 2017;2:e89569.
69. Nakayama Y, Kosek J, Capone L, Hur EM, Schafer PH, Ringheim GE. Aiolos overexpression in systemic lupus erythematosus B cell subtypes and BAFF-induced memory B cell differentiation are reduced by CC-220 modulation of cereblon activity. J Immunol 2017;199:2388–407.
70. Giltiay NV, Shu GL, Shock A, Clark EA. Targeting CD22 with the monoclonal antibody epratuzumab modulates human B-cell maturation and cytokine production in response to Toll-like receptor 7 (TLR7) and B-cell receptor (BCR) signaling. Arthritis Res Ther 2017;19:91.
71. Morris DL, Fernando MM, Taylor KE, Chung SA, Nititham J, Alarcon-Riquelme ME, et al. MHC associations with clinical and autoantibody manifestations in European SLE. Genes Immun 2014;15:210–7.
72. Folzenlogen D, Hofer MF, Leung DY, Freed JH, Newell MK. Analysis of CD80 and CD86 expression on peripheral blood B lymphocytes reveals increased expression of CD86 in lupus patients. Clin Immunol Immunopathol 1997;83:199–204.

ARTHRITIS & RHEUMATOLOGY
Vol. 70, No. 4, April 2018, pp 508–515
DOI 10.1002/art.40394

Association Between Marginal Jawbone Loss and Onset of Rheumatoid Arthritis and Relationship to Plasma Levels of RANKL

Elin Kindstedt, Linda Johansson, Py Palmqvist, Cecilia Koskinen Holm, Heidi Kokkonen, Ingegerd Johansson, Solbritt Rantapää Dahlqvist, and Pernilla Lundberg

Objective. **To investigate whether periodontitis, characterized by marginal jawbone loss, precedes the onset of symptoms of rheumatoid arthritis (RA), and to analyze plasma levels of RANKL (a cytokine that is crucial for bone resorption) and anti–citrullinated peptide antibodies (ACPAs) in presymptomatic individuals compared with matched referent controls.**

Methods. **Marginal jawbone loss was measured on dental radiographs of the premolar/molar regions in the jaws in 176 subjects, 93 of whom subsequently developed RA. Among these participating subjects, 46 had documented radiographs predating symptom onset, and 45 cases could be matched to controls, according to sex, age, and smoking status. Plasma RANKL concentrations were analyzed using enzyme-linked immunosorbent assay. A receiver operating characteristic curve was used to define the cutoff value for RANKL positivity.**

Results. **Bone loss was significantly greater in presymptomatic subjects classified as never smokers compared with that in controls, and increasing levels of bone loss were associated with a higher risk of the subsequent development of RA (hazard ratio 1.03, 95% confidence interval 1.01–1.05). No association between jawbone loss and RA was observed in smokers. A significantly greater extent of marginal jawbone loss was detected in RANKL-positive presymptomatic subjects, and even more pronounced jawbone loss was observed in those who were positive for both RANKL and ACPA.**

Conclusion. **Marginal jawbone loss preceded the clinical onset of RA symptoms, but this was observed only in nonsmokers. Moreover, marginal jawbone loss was significantly greater in RANKL-positive presymptomatic subjects compared with RANKL-negative presymptomatic subjects and was highest in presymptomatic subjects positive for both ACPA and RANKL.**

Periodontitis and rheumatoid arthritis (RA) are both characterized by chronic inflammation at soft tissue sites, leading to a loss of adjacent bone (1–5). In periodontitis, tooth-related bacteria evoke gingival inflammation, which in disease-susceptible individuals may cause a loss of jawbone (5–7). Patients with progressive periodontitis have elevated serum levels of C-reactive protein (5,8), a finding that supports the hypothesis that periodontal inflammation causes a systemic load in these patients. The mechanisms of induction of RA remain unclear, but autoantibodies and increased concentrations of proinflammatory and antiinflammatory cytokines are known to predate the onset of disease symptoms (9,10). Despite their different etiologies, periodontitis and RA share a number of similarities concerning host-mediated pathogenesis, genetics (e.g., manifest as an association with HLA antigens), and environmental risk factors such as smoking (1–3,6,7,11). Both diseases lead to significant morbidity; in periodontitis, this ultimately leads to tooth loss and loss of masticatory function, while in RA, there is a loss of joint function and mobility (11).

Supported by King Gustaf V's 80-Year Fund (grant to Dr. Rantapää Dahlqvist), the Swedish Rheumatism Association (grant 386341 to Drs. Rantapää Dahlqvist and Lundberg), the Swedish Research Council (grant K2013-52X-20307-07-3 to Dr. Rantapää Dahlqvist), the Swedish Dental Society (grant 396172401 to Drs. Kindstedt and Lundberg), and the Västerbotten County Council (ALF grants 9961802 and VLL-645361 to Drs. Rantapää Dahlqvist and Lundberg, TUA grant 327691 to Dr. Lundberg, and Spjutspets grant 356091 to Dr. Lundberg).

Elin Kindstedt, PhD, DDS, Linda Johansson, Py Palmqvist, PhD, DDS, Cecilia Koskinen Holm, PhD, DDS, Heidi Kokkonen, PhD, Ingegerd Johansson, DDS, PhD, Solbritt Rantapää Dahlqvist, PhD, MD, Pernilla Lundberg, PhD, DDS: Umeå University, Umeå, Sweden.

Drs. Rantapää Dahlqvist and Lundberg contributed equally to this work.

Address correspondence to Solbritt Rantapää Dahlqvist, PhD, MD, Department of Clinical Medicine and Public Health/Rheumatology, Umeå University, SE-901 87 Umeå, Sweden (e-mail: solbritt.rantapaa.dahlqvist@umu.se); or to Pernilla Lundberg, PhD, DDS, Department of Odontology/Molecular Periodontology, Umeå University, SE-901 87 Umeå, Sweden (e-mail: Pernilla.lundberg@umu.se).

Submitted for publication June 7, 2017; accepted in revised form November 22, 2017.

The majority of epidemiologic studies have shown that periodontitis and RA are associated (12–19), and that treatment of periodontitis in patients with RA reduces joint symptoms (20), but it is not known how these diseases may be related (11,21). A number of mechanisms, including infectious, inflammatory, and genetic traits, have been proposed (11,21), but prospective studies on the association between periodontitis and RA are sparse.

Enhanced local bone loss is commonly seen in the vicinity of the inflammatory process in diseases such as RA and periodontitis (22,23). During balanced physiologic remodeling, osteoblasts form as much bone as the osteoclasts have resorbed, thereby keeping the bone mass constant. In states of unbalanced bone remodeling, such as periodontitis and RA, bone turnover is characterized by increased formation and activity of osteoclasts and by reduced stimulation of bone formation by osteoblasts, leading to bone loss (6,22,23).

Mature bone-resorbing osteoclasts are formed by fusion of mononuclear progenitor cells derived from myeloid hematopoietic stem cells. The specific cytokine driving osteoclast differentiation is RANKL, which activates the receptor RANK expressed by osteoclast progenitors. RANKL is produced as a membrane-bound or secreted ligand by osteoblasts, fibroblasts, or activated T cells and B cells (23). The production of RANKL by various cell types is controlled by systemic and local stimuli, including hormones, inflammation mediators, and bacterial products (6,22,23). Moreover, in RA, anti–citrullinated peptide antibodies (ACPAs), e.g., against citrullinated vimentin, have been directly linked to osteoclast differentiation and bone resorption in patients with RA, as shown both in vivo and in vitro (24). Recently, elevated RANKL levels were shown to be associated with ACPA positivity in patients with early untreated RA, with bone destruction (25), and with radiologic progression after 2 years in patients with early RA (26).

The involvement of the RANKL system is well established in the pathogenesis of diseases of bone metabolism, including periodontitis, RA, postmenopausal osteoporosis, and bone malignancies such as multiple myeloma (23,27). The RANKL level is increased in the serum of affected individuals, and antibodies directed toward RANKL form part of the treatment regimen in all of these conditions except periodontitis (27–31).

Thus, the hypothesis of a link between periodontitis and the development of RA has long been debated, but prospective studies are lacking. The aim of the current study was to assess whether periodontitis, displayed as marginal jawbone loss, precedes the onset of symptoms of RA, and whether plasma RANKL levels are related to jawbone loss in subjects in whom RA subsequently develops.

PATIENTS AND METHODS

Study participants. The present case–control study was nested in a population-based survey of cohorts within the Medical Biobank of Northern Sweden (www.biobank.umu.se/biobank/nshds/). Study cases with a registered date of symptom onset were identified by coanalyzing the register of the Medical Biobank cohorts with the register of patients attending the Department of Rheumatology at University Hospital, Umeå, and fulfilling the American College of Rheumatology 1987 classification criteria for RA (32).

RA was diagnosed (including in individuals who had symptoms for <12 months) at the Early Arthritis Clinic at Norrlands University Hospital, Umeå, Sweden, by a senior rheumatologist who carefully monitored the patient-reported date of onset of RA-related symptoms. The time points preceding onset of symptoms are referred to as the "presymptomatic time." The earliest date for joint symptoms was thus defined as the date of symptom onset. The dental radiographs selected for the hazard estimates were obtained well before the identified date of symptom onset (1–7 years preceding symptom onset, as described below). However, no information on joint symptoms was available from the dental records at the time when dental radiographic analyses were performed.

In total, 232 individuals for whom information was available prior to the onset of RA symptoms (referred to as presymptomatic individuals) and 194 matched controls were identified from the register of the Medical Biobank and were alive at the time of this study. Both cases and control subjects were invited, by mail, to participate in the study and were asked to answer a questionnaire on self-assessed dental status, smoking habits, and contact information for their dental clinic. Responses to the questionnaire were obtained from 149 cases (64.2%) and 143 controls (73.7%). Dental radiographs of the premolar/molar regions of the jaw could be obtained from the providers of dental care in 176 of the subjects (Table 1). Among these identified subjects, 93 were subsequently diagnosed as having RA, and 83 were used as population-based controls.

Of the 93 subjects with presymptomatic RA, 46 had radiographs available before the onset of RA symptoms. Radiographs for the remaining 47 subjects were available only from the same year as symptom onset (n = 2) or later after RA symptom onset. Thus, 46 subjects for whom radiographs were available prior to becoming symptomatic for RA formed the group to which a referent control group, matched for sex, age (±3 years), and smoking status (never, past, or current smoker), was selected at random, without any replacements. Due to the very low prevalence of current smokers among the potential controls, the final study group comprised 45 cases and 45 matched controls (Table 2). In several of these cases and controls, repeated radiographic examinations were also performed after the onset of RA symptoms. In 31 of the 45 case–control pairs, both the case and the matched referent control had undergone a radiographic examination before the onset of symptoms, as well as repeated radiographic examinations for longitudinal evaluation of bone loss after becoming symptomatic and being diagnosed as having RA.

Assessment of bone loss. Bone loss was assessed on bitewing radiographs of the premolar/molar sections of the jaws. Radiographs were obtained from dental offices after the participants had granted their permission. Two films were available per section, ranging from the mesial surface of the first premolar to the distal surface of the second molar. Third molars positioned as a

Table 1. Characteristics of the 176 subjects who consented to participate, according to study group*

Characteristic	Controls (n = 83)	Presymptomatic subjects (n = 93)
% men/% women	26.5/73.5	25.8/74.2
Age, mean (95% CI) years	55.5 (54.6–56.5)	56.8 (55.9–57.7)
Birth year, mean (min–max)	1946 (1933–1967)	1945 (1930–1968)
No. of radiographic evaluations, mean (min–max)	7.9 (1–26)	7.5 (1–26)†
Smoking status at time of radiographic evaluation		
Never smoker, %	33.4	26.7
Previous smoker, %	60.8	68.6
Current smoker, %	5.8	4.8
Dental care provider		
Public dental clinic, %	31.2	26.3
Private office, %	30.3	31.9
Combination of public and private, %	38.5	41.8
Anti–CCP-2 positivity, no./no. evaluated (%)	3/83 (3.6)	39/93 (41.9)‡
RF positivity, no./no. evaluated (%)	1/47 (2.1)	37/92 (40.2)§
HLA SE, no./no. evaluated (%)	–	61/92 (66.3)

* Radiographs of the premolar/molar regions in the jaws of 93 presymptomatic subjects (n = 694 visits) and 83 control subjects in whom rheumatoid arthritis (RA) did not develop (n = 659 visits) were obtained and evaluated for missing teeth and teeth with or without bone loss. 95% CI = 95% confidence interval; min = minimum; max = maximum; anti–CCP-2 = anti–cyclic citrullinated peptide 2; RF = rheumatoid factor; SE = shared epitope.
† Mean 6.4 (min–max 0–18) and 4.5 (min–max 0–16) number of radiographic evaluations before and after RA diagnosis, respectively.
‡ The frequency of positivity at the time of RA diagnosis was 74.7%.
§ The frequency of positivity at the time of RA diagnosis was 78.6%.

second molar were regarded as second molars. Other types of radiographs, such as apical and panoramic images, were occasionally used to confirm the assessments.

For the presymptomatic individuals (cases), radiographs obtained 1–7 years (mean 3.8 years, 95% confidence interval [95% CI] 3.2–4.4 years) before the symptoms of RA (referred to as year 0) were selected for evaluation of jawbone loss. Radiographs obtained in age-matched individuals without RA were used as controls.

Bone loss was scored as present (score of 1) or not present (score of 0) for each tooth in the examined sections. The presence of bone loss (score of 1) was scored if a reduction in marginal bone level corresponded to more than two-thirds of the height of the tooth crown of the same tooth. This criterion was based on an attachment loss of 3–4 mm, defined by the American Academy of Periodontology as moderately severe periodontitis (33,34), and an estimate that, on average, two-thirds of the height of the tooth crown corresponds to 3.7 mm. The latter was defined by measurements of the height of the total tooth crown, i.e., the distance from the cement–enamel junction to the crown ridge in premolars. This distance was on average 5.4 mm, meaning that two-thirds of the height of the crown corresponded to 3.7 mm, i.e., 3–4 mm. Bone loss was assessed by 2 dentists (EK and CKH) who had calibrated their evaluations. Interobserver agreement was evaluated for 20 individual radiographic observations, which yielded a kappa value of 0.91.

One of the following characteristics was noted for each tooth: 1) intact, i.e., the tooth could be assessed in its entirety and showed no sign of bone loss exceeding two-thirds of the length of the tooth crown, 2) bone loss, i.e., the tooth displayed bone loss exceeding two-thirds of the length of the tooth crown at any site, and if the marginal bone level was not captured on the bitewing radiographs (because of severe bone loss), it was also scored as bone loss, 3) missing, i.e., the tooth was missing or a retained root tip was present, or 4) not assessable, i.e., the tooth could not be evaluated.

Total bone loss was defined as the sum of the number of teeth with scored bone loss and lost teeth in proportion to the number of teeth assessable for scoring.

Plasma analysis. Plasma samples from the cases (n = 47) were analyzed for the levels of RANKL before the onset of symptoms, including within the same year as symptom onset, with a median time predating the onset of symptoms of 4.0 years (interquartile range 2.0–7.2 years). Plasma samples from the controls (n = 83) were analyzed when radiographs of the jaws were available for these subjects. The radiographic examinations were

Table 2. Characteristics of the final study group*

Characteristic	Controls (n = 45)	Presymptomatic subjects (n = 45)
No. of men/no. of women	9/36	9/36
Age, mean (95% CI) years	55.2 (52.6–57.7)	55.2 (52.7–57.8)
Birth year, mean (min–max)	1945 (1935–1964)	1944 (1930–1961)
Year of radiographic evaluation, mean (min–max)	1999 (1980–2011)	1999 (1991–2007)
Time from radiographic evaluation to event, mean (95% CI) years†	3.8 (3.2–4.4)	14.2 (11.9–16.5)
Smoking status at time of radiographic evaluation, %		
Never smoker	28.9	28.9
Previous smoker	68.9	68.9
Current smoker	2.2	2.2
Dental care provider		
Public dental clinic, %	27.9	30.2
Private office, %	34.9	30.2
Combination of public and private, %	37.2	39.5
Dental status		
No. of intact teeth, mean (95% CI)	9.9 (8.6–11.1)	7.8 (6.5–9.0)‡
Total bone loss, % (95% CI)§	32.9 (24.8–41.0)	46.9 (38.8–55.0)¶

* The final study group included 45 subjects for whom the marginal jawbone level could be evaluated before the onset of rheumatoid arthritis (RA) symptoms (presymptomatic patients) and a control group matched for sex, age, and smoking status. Total bone loss is defined as the sum of the number of teeth with scored bone loss (teeth that could be evaluated and in which bone loss was evident) and lost teeth (teeth that are missing, possibly due to major bone loss) in proportion to the number of teeth accessible for scoring. 95% CI = 95% confidence interval; min = minimum; max = maximum.
† Event refers to RA symptom onset in cases and end of study period in controls.
‡ $P = 0.020$ versus controls, by Student's *t*-test.
§ Mean values were adjusted for sex, age at radiography, year of radiography, smoking status, and dental care provider.
¶ $P = 0.017$ versus controls.

selected at a time point that was as close as possible to the date of plasma sampling. Consequently, for these analyses, we were unable to keep the matched pairs, as previously described.

The plasma concentration of total (free and bound) RANKL was measured using a RANKL human enzyme-linked immunosorbent assay kit (BioVendor) in accordance with the protocol described by the manufacturer. A cutoff value for RANKL positivity was defined using a receiver operating characteristic curve, yielding a cutoff value for positivity of >0.927 nmoles/liter, with a specificity of 97.9%. Positivity for ACPA, rheumatoid factor (RF), and the HLA shared epitope was analyzed as previously described (26).

Statistical analysis. Categorical variables, i.e., sex, smoking status at the time of radiographic evaluation (never or ever smoker [past or current]), and dental care provider (public dental clinic, private office, or a combination of public and private), are presented as numbers or proportions (percent). Differences in distribution between the cases and controls were tested by chi-square test.

For continuous, normally distributed variables (i.e., age, birth year, year of radiographic evaluation), mean values with 95% CIs or minimum–maximum values are presented. Differences in group mean values between presymptomatic subjects and referent controls were tested using Student's *t*-test when values were normally distributed; otherwise, comparisons were performed using nonparametric tests. RANKL concentrations were logarithmically transformed to reach normality. Using the generalized linear model procedure, group mean values for the number of intact teeth and total jawbone loss were standardized for potential confounders, i.e., sex, age at the time of radiographic evaluation, year of radiographic evaluation, smoking status, and dental care provider. In addition, sensitivity analyses with stratification for smoking status, i.e., never smokers and ever smokers, were performed.

Hazard ratios (HRs) (with 95% CIs) for subsequent development of RA according to increasing levels of total jawbone loss were calculated from Cox proportional hazards models, using a time-dependent covariate (age) and adjustment for potential confounders (dental care provider and year of radiographic evaluation). All tests were 2-sided, and *P* values less than 0.05 were considered significant. SPSS version 23.0 was used for the data analyses.

Ethics approval. This study was approved by the Regional Ethical Review Board at Umeå University (Dnr no. 2013/347-31M). Data were collected and analyzed in accordance with the guidelines of the Declaration of Helsinki, including the requirement that written consent be obtained from the participants, and in accordance with the Swedish Personal Data Act.

RESULTS

Study group characteristics. The characteristics of the 176 consenting participants for whom dental records were available are shown in Table 1. The characteristics of the 45 presymptomatic subjects and their matched referent controls are shown in Table 2. The proportions of men and women, never smokers and ever smokers, and dental care providers, as well as the mean age and mean birth year, were similar between the subsample of 90 presymptomatic subjects and matched controls and the total sample of 176 subjects.

Comparison of bone loss in presymptomatic subjects and matched controls. The mean number of intact teeth, i.e., teeth with jawbone loss of less than two-thirds of the tooth crown, was significantly lower in presymptomatic subjects compared with matched controls (mean 7.8 versus 9.9; $P = 0.02$). In addition, the proportion of teeth with jawbone loss in the 45 presymptomatic subjects and their matched controls was significantly higher in those who developed RA symptoms years after the assessment (46.9% versus 32.9%; $P = 0.017$) (Table 2).

Stratification according to smoking status revealed that these differences were seen only in subjects who reported having always been a nonsmoker (Table 3). In presymptomatic subjects who never smoked, the mean

Table 3. Characteristics of the final study groups, stratified according to smoking status*

Characteristic	Controls (n = 45)	Presymptomatic subjects (n = 45)
Never smoker		
No. of women	13	13
Age, mean (95% CI), years	58.0 (52.6–63.4)	57.7 (52.4–63.0)
Birth year, mean (min–max)	1945 (1935–1964)	1942 (1932–1961)
Year of radiographic evaluation, mean (min–max)	2003 (1994–2009)	1999 (1991–2007)
Dental care provider		
Public dental clinic, %	15.4	30.8
Private office, %	46.2	23.1
Combination of public and private, %	38.5	46.2
Dental status†		
No. of intact teeth, mean (95% CI)	10.8 (8.5–13.1)	7.1 (4.8–9.4)‡
Total bone loss, % (95% CI)	26.0 (12.1–39.9)	52.4 (38.5–66.3)§
Ever smoker (past + current)		
No. of men/no. of women	9/23	9/23
Age, mean (95% CI) years	54.0 (51.1, 57.0)	54.3 (51.2, 57.3)
Birth year, mean (min–max)	1945 (1936–1956)	1945 (1930–1961)
Year of radiographic evaluation, mean (min–max)†	1999 (1980–2011)	1999 (1991–2006)
Dental care provider		
Public dental clinic, %	33.3	30.0
Private office, %	30.0	33.3
Combination of public and private, %	36.7	36.7
Dental status†		
No. of intact teeth, mean (95% CI)	9.3 (7.8–13.1)	8.3 (6.7–10.8)
Total bone loss, % (95% CI)	36.8 (26.8–46.7)	43.7 (33.7–53.6)

* Total bone loss is defined as the sum of the number of teeth with scored bone loss (teeth that could be evaluated and in which bone loss was evident) and lost teeth (teeth that are missing, possibly due to major bone loss) in proportion to the number of teeth accessible for scoring. 95% CI = 95% confidence interval; min = minimum; max = maximum.

† Mean values were adjusted for sex, age at radiography, year of radiography, and dental care provider.

‡ $P = 0.039$ versus controls.

§ $P = 0.015$ versus controls.

number of intact teeth was 7.1, compared with a mean of 10.8 intact teeth in the referent controls ($P = 0.039$). The corresponding values for the mean number of teeth with total bone loss were 52.4 in presymptomatic cases and 26.0 in matched referent controls ($P = 0.015$). A numerically similar trend was seen in ever smokers (past and current), but differences between the groups were not statistically significant (Table 3).

Following the univariate tests, Cox regression analyses were performed to compare subjects in whom RA symptoms developed with those in whom RA symptoms did not develop for the levels of jawbone loss, in all case–control sets as well as in each smoking stratum (Table 4). The crude model (including total bone loss in those teeth that were accessible for scoring and age) showed positive associations in nonsmokers (HR 1.026, 95% CI 1.005–1.047, $P = 0.017$). In models additionally adjusted for dental care provider and for year of radiographic evaluation, the HR was not affected, but the 95% CI was wider, and the P value was borderline significant (0.050) (Table 4). No association was seen among ever smokers (Table 4).

Changes in bone loss could be tracked from 4 years before (year –4) up to 6 years after the onset of symptomatic RA in 31 case–referent control sets in which both the presymptomatic subject (case) and the matched referent had radiographs available after the year that the presymptomatic subject developed symptoms of RA (Figure 1). The level of jawbone loss at year –4 was standardized to 0, and any bone level alteration was determined for the year of RA symptom onset (year 0), and 3, 5, and 6 years thereafter. Both the presymptomatic subjects and their matched controls displayed increased bone loss over time, but from 5 years onward, the mean loss increment was significantly higher in the presymptomatic subjects ($P < 0.05$).

Plasma RANKL. In presymptomatic subjects, the median (first quartile, third quartile) RANKL concentration

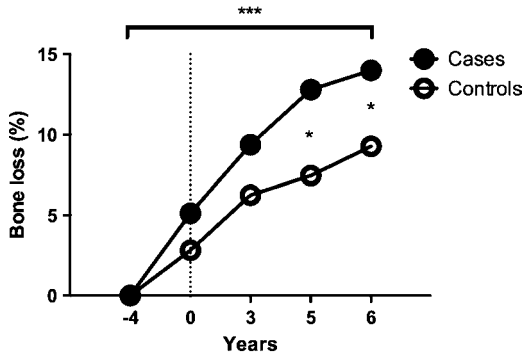

Figure 1. Mean increase in bone loss in presymptomatic subjects (cases) and matched controls over time. The percent bone loss at year –4 was standardized to 0. The year of rheumatoid arthritis (RA) symptom onset was set to year 0. Increased bone loss 3, 5, and 6 years after RA symptom onset is shown. Group differences calculated after the repeated-measures analysis of variance showed a difference between groups. * = $P < 0.05$, cases versus controls; *** = $P < 0.001$.

was 0.355 nmoles/liter (0.176, 0.695), whereas the concentration in controls was 0.305 nmoles/liter (0.146, 0.524), but the difference was not significant. Among presymptomatic subjects, 14.9% had levels above the cutoff compared with 6.1% of controls ($P = 0.098$). RANKL-positive presymptomatic subjects had a significantly greater extent of marginal jawbone loss compared with RANKL-negative presymptomatic subjects ($P = 0.031$) (Figure 2). There was a weak correlation between the RANKL concentration and jawbone loss ($r_s = 0.296$, $P = 0.043$). These measurements were not significantly different in controls, irrespective of RANKL positivity. There was no association between RF positivity and bone loss in the presymptomatic subjects or controls, although ACPA-positive presymptomatic subjects had higher values for bone loss compared with controls (27.3% and 13.9%, respectively; $P < 0.05$). The concentration of RANKL was significantly higher in presymptomatic subjects who were positive for either ACPA

Table 4. Hazard ratios for the subsequent development of rheumatoid arthritis according to increasing total jawbone loss*

	All matched subjects		Ever smoker (past + current)		Never smoker	
Model	HR (95% CI)	P	HR (95% CI)	P	HR (95% CI)	P
Crude	1.006 (0.996–1.016)	0.246	0.998 (0.985–1.011)	0.689	1.026 (1.005–1.047)	0.017
Adjusted	1.006 (0.997–1.015)	0.209	1.004 (0.981–1.018)	0.525	1.025 (1.000–1.050)	0.050

* Hazard ratios (HRs) and 95% confidence intervals (95% CIs) were calculated from Cox proportional hazards models with a time-dependent covariate (age) and adjustment for potential confounders. The crude model included total bone loss as a percent of teeth accessible for evaluation and a time-dependent covariate (age). The adjusted model included total bone loss as a percent of teeth accessible for evaluation, a time-dependent covariate (age), dental care provider, and year of radiographic evaluation.

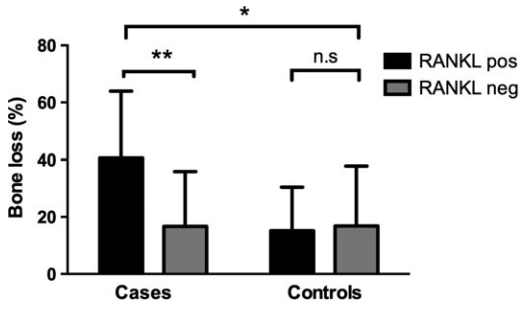

Figure 2. Bone loss in RANKL-positive presymptomatic subjects (cases) and controls and RANKL-negative cases and controls. Bars show the mean ± SD. NS = not significant. * = $P < 0.05$; ** = $P < 0.01$.

or RF ($P < 0.002$ and $P < 0.001$, respectively). In subjects who were positive for both ACPA and RANKL, bone loss was significantly higher compared with that in subjects in the subgroups (mean ± SEM 53.8 ± 6.4% versus 20.4 ± 5.3% in the subgroup positive for ACPA only, 18.8 ± 10.8% in the subgroup positive for RANKL only, and 13.1 ± 3.2% in the subgroup negative for both ACPA and RANKL; $P < 0.016$).

DISCUSSION

The current study is, to our knowledge, the first to show that a more severe loss of tooth supporting bone precedes the onset of RA symptoms. This was particularly evident in nonsmoking presymptomatic subjects. Moreover, this study showed that subjects with presymptomatic RA who were RANKL-positive displayed a significantly higher degree of marginal jawbone loss, particularly those who were ACPA-positive.

Although several cross-sectional studies have shown that patients with RA have a higher prevalence of periodontitis compared with individuals with healthy joints (12–19), several studies have shown contradictory results (35–37). This discrepancy could be due to various reasons, including the use of different disease classifications, cohort sizes, and the notion that treatment of RA could affect periodontal health (13,37,38).

Our finding of increased periodontal jawbone loss before the onset of RA symptoms in patients compared with controls was statistically significant, but the association was modest. This was probably attributable to the low number of individuals for whom radiographs obtained prior to the development of RA symptoms were available. This is a weak point of our study, as was the fact that we were unable to obtain information regarding periodontitis classification and diagnosis and were reliant on the obligate outcome measurement of periodontitis, namely jawbone loss. In a prospective study of periodontal disease and the risk of RA, Arkema et al observed no association between severe periodontitis (as assessed by the history of periodontal surgery and/or tooth loss), and the risk of RA (35). The different results between the Arkema study and our study could be due to the fact that periodontal surgery is performed only in individuals with severe periodontitis, while estimation of marginal bone loss is a more nuanced measure of the severity of periodontal disease. Patients with arthralgia who were diagnosed as having periodontitis had an increased risk of future treatment with methotrexate as a consequence of a diagnosis of RA (39), which is consistent with our findings. Further large prospective controlled epidemiologic studies could possibly strengthen the observation that periodontitis precedes RA.

An association between periodontitis and RA has been considered since the early 1820s.The relationship has been intensively debated during the past 2 decades, and several hypotheses regarding pathogenic links have been proposed (11,21,38). Smoking is a common environmental factor associated with both diseases. Consequently, we were able to see bone loss differences only in nonsmokers, which is consistent with the results of a previous study (18). Genetic factors are driving the host responses in both RA and periodontitis, which could serve as common ground. Periodontitis is primarily an infectious inflammatory condition that progresses to chronic inflammation, thus representing similarities with the inflammatory process in RA (2,40). An imbalance between proinflammatory and antiinflammatory cytokines is evident in both RA and periodontitis. Both conditions are associated with soft tissue and bone destruction involving inflammatory cytokines such as interleukin-1, tumor necrosis factor, and prostaglandin E_2, enzymes such as matrix metalloproteinases, and increased RANKL levels (2,22,23).

In the current study, we observed that marginal jawbone loss was significantly greater in RANKL-positive presymptomatic subjects compared with RANKL-negative presymptomatic subjects. Furthermore, the highest marginal jawbone loss was observed in subjects who were positive for both ACPA and RANKL. The observation that periodontal jawbone loss was more severe in "RA-predisposed" RANKL-positive individuals could indicate that there may be a subgroup of presymptomatic individuals who share a pathologic pathway of imbalanced immunoinflammatory bone remodeling with individuals who have severe periodontitis. In this study, it was not possible to determine whether the source of RANKL was periodontitis, and we cannot rule out the possibility that the relationship between RANKL and increased jawbone loss in presymptomatic individuals was associative or causative, but the observation motivates further larger studies.

The periodontium not only is a reservoir for cytokines that are released into the circulation but also is a habitat for bacteria. In a sensitive host, a dysbiotic gram-negative flora evokes an inflammatory response in the periodontium. The periodontal pathogen *Porphyromonas gingivalis*, which expresses the enzyme peptidylarginine deiminase and has the capacity to citrullinate proteins and generate antibodies (e.g., ACPA), has been suggested as a possible link between periodontal infection and RA (11,41). Another recently discussed microbial species is *Aggregatibacter actinomycetecomitans*, which has hypercitrullinating abilities (42). Periodontitis in patients with RA has been observed, particularly in those who are ACPA-positive and/or RF-positive or have a higher concentration of these antibodies (18,43), although this finding has not been confirmed by other groups of investigators (16). Periodontitis per se has been shown to be related to ACPA (anti–citrullinated α-enolase peptide 1) but also to uncitrullinated peptides of autoantigens in RA (44). We showed that the combination of positivity for both RANKL and ACPA was related to increased marginal jawbone loss. Because ACPAs have been shown to potentiate RANKL-induced osteoclast formation and bone resorption, it is possible that the high jawbone loss that we observed in RANKL-positive presymptomatic subjects was driven by ACPA.

Our study has some limitations. For example, the cases and controls were identified from a population-based survey for cardiovascular disease risk factors. In both cases and controls, blood samples were obtained at certain age points, whereas dental radiography was performed at time points that were completely unrelated to the timing of blood withdrawal, which will result in a reduced number of included individuals with data available for subgroup analyses. Because our findings that increased periodontal jawbone loss preceded symptoms of RA are based on the patient's report on symptom onset to the senior rheumatologist and not to the dentist at the time of the oral examination, we are not able to ascertain that radiography, in all cases, was performed in asymptomatic subjects. To decrease the risk of evaluating jawbone loss in symptomatic individuals, radiographs in the defined presymptomatic subjects were selected 1 year preceding the self-reported date of symptom onset. Another limitation is the lack of information on family history of diseases other than cardiovascular diseases and diabetes.

In conclusion, the key finding of this study indicates that in subjects who subsequently developed RA, more pronounced marginal jawbone loss was associated with preexisting periodontitis. Although this association was statistically significant, the relationship was modest. Moreover, marginal jawbone loss and the plasma RANKL level were related in ACPA-positive presymptomatic subjects. Additional research, with regard to both basic mechanisms as well as clinical studies, are needed to determine whether there is a causative link between periodontitis and RA or whether jawbone loss and RA represent a "2 sides of the same coin" phenomenon.

ACKNOWLEDGMENTS

We would like to acknowledge the staff at the Medical Biobank of Northern Sweden for providing samples from the Medical Biobank. Special thanks to Mrs. Britt-Inger Nordell and Mrs. Sonja Odeblom at Västerbotten County Council for requisition of the dental radiographs and questioners.

AUTHOR CONTRIBUTIONS

All authors were involved in drafting the article or revising it critically for important intellectual content, and all authors approved the final version to be published. Drs. Rantapää Dahlqvist and Lundberg had full access to all of the data in the study and take responsibility for the integrity of the data and the accuracy of the data analysis.

Study conception and design. Rantapää Dahlqvist, Lundberg.

Acquisition of data. Kindstedt, L. Johansson, Palmqvist, Koskinen Holm, Kokkonen, Rantapää Dahlqvist.

Analysis and interpretation of data. Kindstedt, L. Johansson, Koskinen Holm, Kokkonen, I. Johansson, Rantapää Dahlqvist.

REFERENCES

1. Klareskog L, Catrina AI, Paget S. Rheumatoid arthritis. Lancet 2009;373:659–72.
2. McInnes IB, Schett G. The pathogenesis of rheumatoid arthritis. N Engl J Med 2011;365:2205–19.
3. Bascones A, Noronha S, Gomez M, Mota P, Gonzalez Moles MA, Villarroel Dorrego M. Tissue destruction in periodontitis: bacteria or cytokines fault? Quintessence Int 2005;36:299–306.
4. Janssen KM, Vissink A, de Smit MJ, Westra J, Brouwer E. Lessons to be learned from periodontitis. Curr Opin Rheumatol 2013;25: 241–7.
5. Pihlstrom BL, Michalowicz BS, Johnson NW. Periodontal diseases. Lancet 2005;366:1809–20.
6. Yucel-Lindberg T, Bage T. Inflammatory mediators in the pathogenesis of periodontitis. Expert Rev Mol Med 2013;15:e7.
7. Hajishengallis G. Periodontitis: from microbial immune subversion to systemic inflammation. Nat Rev Immunol 2015;15:30–44.
8. Bostrom EA, Kindstedt E, Sulniute R, Palmqvist P, Majster M, Holm CK, et al. Increased eotaxin and MCP-1 levels in serum from individuals with periodontitis and in human gingival fibroblasts exposed to pro-inflammatory cytokines. PloS One 2015;10: e0134608.
9. Rantapää-Dahlqvist S, de Jong BA, Berglin E, Hallmans G, Wadell G, Stenlund H, et al. Antibodies against cyclic citrullinated peptide and IgA rheumatoid factor predict the development of rheumatoid arthritis. Arthritis Rheum 2003;48:2741–9.
10. Kokkonen H, Söderström I, Rocklöv J, Hallmans G, Lejon K, Rantapää Dahlqvist S. Up-regulation of cytokines and chemokines predates the onset of rheumatoid arthritis. Arthritis Rheum 2010;62:383–91.
11. Rutger Persson G. Rheumatoid arthritis and periodontitis–inflammatory and infectious connections: review of the literature. J Oral Microbiol 2012;4.

12. Käßer UR, Gleissner C, Dehne F, Michel A, Willershausen-Zönnchen B, Bolten WW. Risk for periodontal disease in patients with longstanding rheumatoid arthritis. Arthritis Rheum 1997;40: 2248–51.
13. Mercado FB, Marshall RI, Klestov AC, Bartold PM. Relationship between rheumatoid arthritis and periodontitis. J Periodontol 2001;72:779–87.
14. Pischon N, Pischon T, Kroger J, Gulmez E, Kleber BM, Bernimoulin JP, et al. Association among rheumatoid arthritis, oral hygiene, and periodontitis. J Periodontol 2008;79:979–86.
15. Garib BT, Qaradaxi SS. Temporomandibular joint problems and periodontal condition in rheumatoid arthritis patients in relation to their rheumatologic status. J Oral Maxillofac Surg 2011;69: 2971–8.
16. De Smit M, Westra J, Vissink A, Doornbos-van der Meer B, Brouwer E, van Winkelhoff AJ. Periodontitis in established rheumatoid arthritis patients: a cross-sectional clinical, microbiological and serological study. Arthritis Res Ther 2012;14:R222.
17. Scher JU, Ubeda C, Equinda M, Khanin R, Buischi Y, Viale A, et al. Periodontal disease and the oral microbiota in new-onset rheumatoid arthritis. Arthritis Rheum 2012;64:3083–94.
18. Potikuri D, Dannana KC, Kanchinadam S, Agrawal S, Kancharla A, Rajasekhar L, et al. Periodontal disease is significantly higher in non-smoking treatment-naive rheumatoid arthritis patients: results from a case-control study. Ann Rheum Dis 2012;71:1541–4.
19. Joseph R, Rajappan S, Nath SG, Paul BJ. Association between chronic periodontitis and rheumatoid arthritis: a hospital-based case-control study. Rheumatol Int 2013;33:103–9.
20. Ortiz P, Bissada NF, Palomo L, Han YW, Al-Zahrani MS, Panneerselvam A, et al. Periodontal therapy reduces the severity of active rheumatoid arthritis in patients treated with or without tumor necrosis factor inhibitors. J Periodontol 2009;80:535–40.
21. Araujo VM, Melo IM, Lima V. Relationship between periodontitis and rheumatoid arthritis: review of the literature. Mediators Inflamm 2015;2015:259074.
22. Souza PP, Lerner UH. The role of cytokines in inflammatory bone loss. Immunol Invest 2013;42:555–622.
23. Takayanagi H. Osteoimmunology and the effects of the immune system on bone. Nat Rev Rheumatol 2009;5:667–76.
24. Harre U, Georgess D, Bang H, Bozec A, Axmann R, Ossipova E, et al. Induction of osteoclastogenesis and bone loss by human autoantibodies against citrullinated vimentin. J Clin Invest 2012; 122:1791–802.
25. Hensvold AH, Joshua V, Li W, Larkin M, Qureshi F, Israelsson L, et al. Serum RANKL levels associate with anti-citrullinated protein antibodies in early untreated rheumatoid arthritis and are modulated following methotrexate. Arthritis Res Ther 2015; 17:239.
26. Boman A, Kokkonen H, Arlestig L, Berglin E, Rantapaa-Dahlqvist S. Receptor activator of nuclear factor κ-B ligand (RANKL) but not sclerostin or gene polymorphisms is related to joint destruction in early rheumatoid arthritis. Clin Rheumatol 2017;36:1005–12.
27. Anandarajah AP, Schwarz EM. Anti-RANKL therapy for inflammatory bone disorders: mechanisms and potential clinical applications. J Cell Biochem 2006;97:226–32.
28. Yue J, Griffith JF, Xiao F, Shi L, Wang D, Shen J, et al. Repair of bone erosion in rheumatoid arthritis by denosumab: a high-resolution peripheral quantitative computed tomography study. Arthritis Care Res (Hoboken) 2017;69:1156–63.
29. Heymann D. Anti-RANKL therapy for bone tumours: basic, preclinical and clinical evidences. J Bone Oncol 2012;1:2–11.
30. Sims NA, Ng KW. Implications of osteoblast-osteoclast interactions in the management of osteoporosis by antiresorptive agents denosumab and odanacatib. Curr Osteoporos Rep 2014;12: 98–106.
31. Belibasakis GN, Bostanci N. The RANKL-OPG system in clinical periodontology. J Clin Periodontol 2012;39:239–48.
32. Arnett FC, Edworthy SM, Bloch DA, McShane DJ, Fries JF, Cooper NS, et al. The American Rheumatism Association 1987 revised criteria for the classification of rheumatoid arthritis. Arthritis Rheum 1988;31:315–24.
33. Page RC, Eke PI. Case definitions for use in population-based surveillance of periodontitis. J Periodontol 2007;78:1387–99.
34. Eke PI, Page RC, Wei L, Thornton-Evans G, Genco RJ. Update of the case definitions for population-based surveillance of periodontitis. J Periodontol 2012;83:1449–54.
35. Arkema EV, Karlson EW, Costenbader KH. A prospective study of periodontal disease and risk of rheumatoid arthritis. J Rheumatol 2010;37:1800–4.
36. Demmer RT, Molitor JA, Jacobs DR Jr, Michalowicz BS. Periodontal disease, tooth loss and incident rheumatoid arthritis: results from the First National Health and Nutrition Examination Survey and its epidemiological follow-up study. J Clin Periodontol 2011;38:998–1006.
37. Eriksson K, Nise L, Kats A, Luttropp E, Catrina AI, Askling J, et al. Prevalence of periodontitis in patients with established rheumatoid arthritis: a Swedish population based case-control study. PLoS One 2016;11:e0155956.
38. Kobayashi T, Yoshie H. Host responses in the link between periodontitis and rheumatoid arthritis. Curr Oral Health Rep 2015;2:1–8.
39. Hashimoto M, Yamazaki T, Hamaguchi M, Morimoto T, Yamori M, Asai K, et al. Periodontitis and porphyromonas gingivalis in preclinical stage of arthritis patients. PLoS One 2015;10:e0122121.
40. Kornman KS. Mapping the pathogenesis of periodontitis: a new look. J Periodontol 2008;79:1560–8.
41. Rosenstein ED, Greenwald RA, Kushner LJ, Weissmann G. Hypothesis: the humoral immune response to oral bacteria provides a stimulus for the development of rheumatoid arthritis. Inflammation 2004;28:311–8.
42. Konig MF, Abusleme L, Reinholdt J, Palmer RJ, Teles RP, Sampson K, et al. Aggregatibacter actinomycetemcomitans-induced hypercitrullination links periodontal infection to autoimmunity in rheumatoid arthritis. Sci Transl Med 2016;8:369ra176.
43. Dissick A, Redman RS, Jones M, Rangan BV, Reimold A, Griffiths GR, et al. Association of periodontitis with rheumatoid arthritis: a pilot study. J Periodontol 2010;81:223–30.
44. De Pablo P, Dietrich T, Chapple IL, Milward M, Chowdhury M, Charles PJ, et al. The autoantibody repertoire in periodontitis: a role in the induction of autoimmunity to citrullinated proteins in rheumatoid arthritis? Ann Rheum Dis 2014;73:580–6.

ARTHRITIS & RHEUMATOLOGY
Vol. 70, No. 4, April 2018, pp 516–527
DOI 10.1002/art.40401

Antibody Responses to Citrullinated and Noncitrullinated Antigens in the Sputum of Subjects With Rheumatoid Arthritis and Subjects at Risk for Development of Rheumatoid Arthritis

M. Kristen Demoruelle,[1] Emily Bowers,[1] Lauren J. Lahey,[2] Jeremy Sokolove,[3] Monica Purmalek,[4] Nickie L. Seto,[4] Michael H. Weisman,[5] Jill M. Norris,[6] Mariana J. Kaplan,[4] V. Michael Holers,[1] William H. Robinson,[2] and Kevin D. Deane[1]

Objective. **The location and mechanisms involved in the initial generation of autoantibodies to citrullinated and noncitrullinated proteins/peptides during the natural history of rheumatoid arthritis (RA) development is incompletely understood. This study sought to explore individual antibody responses to citrullinated and noncitrullinated proteins/peptides in the sputum and associations with neutrophil extracellular traps (NETs) in subjects at risk for the future development of RA.**

Methods. **Serum and sputum samples were obtained from 41 RA-free subjects who were considered at risk for the development of RA based on familial or serologic risk factors, from 20 subjects classified as having RA, and from 22 healthy control subjects. Samples were evaluated using a bead-based array for IgG reactivity to 29 citrullinated proteins/peptides and 21 noncitrullinated proteins/peptides. Cutoff levels for antibody positivity were established in a separate control group. NET levels in the sputum were measured using sandwich enzyme-linked immunosorbent assays that quantitate DNA–myeloperoxidase and DNA–neutrophil elastase complexes.**

Results. **In at-risk subjects, antibody responses to the citrullinated forms of fibrinogen, apolipoprotein E, and fibronectin were highly prevalent. The most citrulline-specific antibodies in the sputum of at-risk subjects were those to fibrinogen, vimentin, and peptides of fibrinogen A and apolipoprotein A1. Patterns of sputum autoantibody positivity differed between at-risk subjects and subjects with RA. In at-risk subjects, increasing sputum NET levels significantly correlated with several citrullinated and some noncitrullinated antibody reactivities.**

Conclusion. **These findings suggest that sputum antibody reactivity to particular citrullinated and noncitrullinated proteins/peptides is specific for RA and for subjects at risk of RA, and the association of these proteins/peptides with NETs may be a key feature of early RA–related autoimmunity in the lung. These results further support the hypothesis that the lung plays a role in early RA–related autoimmunity.**

Citrullination is the posttranslational modification of peptidylarginine to peptidylcitrulline that is catalyzed through peptidylarginine deiminase (PAD) enzymes (1). Citrullination is a normal physiologic process that can be up-regulated during inflammation (2).

The views expressed herein are solely those of the authors and do not necessarily represent the official views of the NIH.

Supported by the NIH (grants AR-066712, AR-063676, and Intramural Research Program grant ZIA-AR-041199 from the National Institute of Arthritis and Musculoskeletal and Skin Diseases, grants AI-101981 and AI-103023 from the National Institute of Allergy and Infectious Diseases, grant HD-057022 from the Office of Research on Women's Health, and Colorado Clinical and Translational Science award UL1-TR-001082-04), the Rheumatology Research Foundation (Within our Reach and Scientist Development awards), and the Walter S. and Lucienne Driskill Foundation.

[1]M. Kristen Demoruelle, MD, PhD, Emily Bowers, MD, V. Michael Holers, MD, Kevin D. Deane, MD, PhD: University of Colorado Denver, Aurora; [2]Lauren J. Lahey, BS, William H. Robinson, MD, PhD: Stanford University, Stanford, California; [3]Jeremy Sokolove, MD: VA Palo Alto Healthcare System and Stanford University, Stanford, California, and AbbVie Pharmaceuticals, San Francisco, California; [4]Monica Purmalek, BS, Nickie L. Seto, BS, Mariana J. Kaplan, MD: National Institute of Arthritis and Musculoskeletal and Skin Diseases, NIH, Bethesda, Maryland; [5]Michael H. Weisman, MD: Cedars-Sinai Medical Center, Los Angeles, California; [6]Jill M. Norris, PhD: Colorado School of Public Health, Aurora.

Dr. Holers has received consulting fees from Janssen Pharmaceuticals (less than $10,000). Dr. Deane has received consulting fees from Janssen Pharmaceuticals (less than $10,000).

Address correspondence to M. Kristen Demoruelle, MD, PhD, University of Colorado School of Medicine, Division of Rheumatology, 1775 Aurora Court, Mail Stop B-115, Aurora, CO 80045. E-mail: Kristen.Demoruelle@UCDenver.edu.

Submitted for publication May 24, 2017; accepted in revised form December 14, 2017.

In addition, citrullination of certain self antigens has been associated with autoimmune responses that are characterized by antibodies to citrullinated protein/peptide antigens (ACPAs) (3).

Serum ACPAs are strongly associated with rheumatoid arthritis (RA). In RA, ACPA reactivity to a number of different citrullinated protein/peptide antigens has been identified. Antibody reactivity to the native noncitrullinated counterparts of these antigens has also been identified in many RA patients (4–9). Furthermore, serum antibody reactivity to citrullinated and noncitrullinated antigens has been identified prior to the onset of clinically apparent synovitis during a "preclinical" phase of RA development (10–12), and several studies have demonstrated that an increasing number of citrullinated antigens are targeted as individuals transition from a state of preclinical RA to classified RA (13,14). These findings suggest that a key part of RA development is early reactivity to a limited number of citrullinated as well as noncitrullinated antigens, with expansion/epitope spreading over time as inflammatory arthritis and classified RA develop.

As the goals in RA management shift to include the prevention of arthritis (15), it is necessary to further understand the mechanisms underlying the initial development of antibody responses in RA and identify relevant immune targets for prevention. Several lines of evidence suggest that one major site where RA-related antibodies may be initially generated is the lung mucosa (16–19). Relevant to this study, our group has demonstrated through induced sputum testing that ACPAs, as characterized by anti–cyclic citrullinated peptide (anti-CCP) antibodies, are generated in the lung in a portion of subjects with classified RA and individuals with an increased risk of developing RA in the future (17,19). However, individual sputum antibody reactivities to citrullinated and noncitrullinated peptides/proteins have not been characterized in these subjects.

In addition to understanding early autoantibody targets in sputum, it is also important to understand potential mechanisms that could generate these autoantibody responses. One mechanism of particular interest is the formation of neutrophil extracellular traps (NETs). NET formation (termed NETosis) can externalize citrullinated and noncitrullinated proteins that can be taken up by antigen-presenting cells, which could lead to antibody generation (8). NETs can also serve as antigenic targets for RA-related autoantibodies (20,21). Furthermore, our group has identified a strong positive correlation between sputum levels of anti-CCP and NETs in subjects at risk for RA (19), but the individual sputum autoantibodies associated with NETosis have not been previously identified. Therefore, in this study, we sought to explore antibody responses to individual citrullinated and noncitrullinated proteins/peptides as well as associations with NETosis in the sputum of subjects at risk for the development of RA.

SUBJECTS AND METHODS

Study subjects. *Recruitment.* Subjects were recruited from the Studies of the Etiology of RA (SERA) Lung Study, as described in detail elsewhere (17,19). Briefly, the SERA Lung Study was designed to evaluate the natural history of RA through the prospective study of individuals who have an increased risk of developing RA in the future (22). The SERA Lung Study was designed to study biomarkers of autoimmunity in the lung during different phases of RA development, using blood and sputum samples obtained from subjects in the SERA cohort who were considered at risk for RA, as well as subjects classified as having RA and healthy control subjects. For the current study, randomly selected stored samples from subjects who participated in the SERA Lung Study between January 2011 and December 2014 were included.

At-risk subjects. We included 41 subjects without current or prior inflammatory arthritis who were at risk for developing RA based on familial or serologic risk factors. Specifically, we included 30 subjects with a familial risk of RA, defined as having a first-degree relative (FDR) with RA. Four (13%) of 30 FDRs were serum anti-CCP positive (by the anti–CCP-2 and/or anti–CCP-3.1 tests). We also included 11 subjects with a serologic risk of RA, defined as having serum anti-CCP positivity (by the anti–CCP-2 and/or anti–CCP-3.1 tests) in the absence of inflammatory arthritis, as identified through community health fair, clinic, or research-based blood test screenings.

RA subjects. We included 20 subjects with established RA who met classification criteria for RA (23,24) based on medical chart review. All were serum anti-CCP positive (by the anti–CCP-2 and/or anti–CCP-3.1 tests), and 16 (80%) of 20 were currently or previously taking disease-modifying antirheumatic drugs or biologic agents.

Healthy controls. We included 44 healthy control subjects who were recruited through local advertisement and were without RA or inflammatory arthritis, did not have an FDR with RA, and were serum anti-CCP negative (according to the anti–CCP-2 and anti–CCP-3.1 tests). These 44 subjects were randomly split into 2 groups of 22 each. One group was used to establish cutoff levels for antibody positivity (cutoff controls), and the other group was used for comparative analyses (comparator controls).

Study visit. Paired samples of blood and sputum were collected from all subjects at their study visit. Subjects without RA underwent a joint-focused interview and 66–count joint examination to confirm the absence of clinically evident inflammatory arthritis. Standardized questionnaires were used to obtain demographic information and self-reported histories of smoking and chronic lung disease.

Genetic testing. Blood was tested for the presence of alleles containing the shared epitope (SE), using previously described methods (22). The alleles considered to contain the SE were as follows: DRB1*04:01, 04:04, 04:05, 04:08, 04:09, and 04:10, and DR1*01:01 and 01:02.

Sputum collection and processing. Induced sputum was collected using established protocols (17,19). Briefly, subjects underwent a 15-minute inhalation of nebulized hypertonic

saline. To minimize salivary contamination, subjects underwent an oral wash prior to inhalation of saline, and during the sputum collection, subjects were instructed to spit any saliva into a separate container and only use the sputum collection cup when producing a sample from coughing. In addition, sputum samples used in this study had <10 squamous epithelial cells/high-power field as revealed by light microscopy, or <80% squamous epithelial cells on cell differential testing, consistent with the lower airway origin of the sample (25,26).

After collection, the sputum sample underwent weight-based dilution with phosphate buffered saline, followed by mechanical syringe–based homogenization. Samples then underwent centrifugation, and the sputum supernatant was used for all biomarker testing.

Citrullinated and noncitrullinated antibody testing. Serum and sputum were tested for IgG reactivity to 29 individual citrullinated proteins/peptides using a bead-based array (developed in the laboratory of WHR), as described in detail elsewhere (3,9,27). These citrullinated proteins/peptides were selected based on antigens that have been reported in the literature as well as those that have been identified in immune complexes isolated from the synovial tissue of RA patients (28) (see Supplementary Table 1, available on the *Arthritis & Rheumatology* web site at http://onlinelibrary.wiley.com/doi/10.1002/art.40401/abstract). For 21 of the 29 citrullinated proteins/peptides, a noncitrullinated/native equivalent was also tested. Antigens were conjugated to spectrally distinct beads (Bio-Plex) and incubated with the subject's sample for 30 minutes at room temperature. After washing, the beads were incubated with phycoerythrin-conjugated anti-human IgG antibody at room temperature, and then passed through a Luminex 200 detector (Bio-Plex software version 5.0; Bio-Rad) that quantified (in fluorescence intensity) the amount of antibody bound to each bead. All antibody testing was performed in a blinded manner.

We established a positive cutoff level in the sputum and serum for each citrullinated and noncitrullinated protein/peptide antibody whose levels were above the 95th percentile of the 22 cutoff controls (i.e., present in <5%). This definition for autoantibody positivity is recommended in the American College of Rheumatology RA classification criteria (24).

To test the reproducibility of the antigen array for sputum, 10 sputum samples were randomly selected, in a blinded manner, to undergo repeated testing for levels of antibodies to citrullinated antigens, and included samples from subjects with RA, at-risk subjects, and healthy control subjects. The mean ± SD coefficient of variation, which was calculated for each of the 29 antibodies to citrullinated antigens, was 7.2 ± 1.7%.

Anti-CCP testing. Clinical ACPA testing commonly uses commercially available anti-CCP assays, although these assays cannot distinguish individual ACPAs. In this study, serum was tested for anti-CCP using 2 different commercial enzyme-linked immunosorbent assays (ELISAs), the anti–CCP-3.1 ELISA (specific for IgG/IgA; Inova Diagnostics) and the anti–CCP-2 ELISA (specific for IgG; Axis-Shield). Serum positivity was determined on the basis of the manufacturer's recommended cutoff levels (≥20 units for anti–CCP-3.1 and >5 units for anti–CCP-2).

Sputum was also tested for anti-CCP, but this was limited to the anti–CCP-2 assay (targeting IgG). Because the anti–CCP-2 test is an IgG-only assay, it was comparable with the isotype reactivity detected by our antigen array testing. Results of the anti–CCP-2 test, expressed in ELISA units, were calculated using the standard curve provided by the manufacturer, followed by multiplication of the sputum dilution factor. We established a cutoff level for sputum anti–CCP-2 positivity using the same approach used for determining positive/negative levels of serum and sputum citrullinated and noncitrullinated antibodies (i.e., above the 95th percentile of the cutoff controls).

Rheumatoid factor (RF) testing. Sputum was tested for RF isotypes (IgA, IgG, and IgM) using commercial ELISAs (Inova Diagnostics). In accordance with the approach applied to other sputum antibody levels, we established a cutoff level for sputum RF positivity that was above the 95th percentile of the cutoff control group.

NET complex testing. Twenty-four at-risk subjects and 33 healthy controls who had an adequate volume of sputum available underwent NET testing. NETs were quantified in the sputum cell-free supernatant by measuring NET-specific protein/nucleic acid complexes, using a sandwich ELISA that detects DNA–myeloperoxidase (MPO) and DNA–neutrophil elastase (NE) complexes, as previously described (29). Briefly, for DNA–MPO complexes, high-binding 96-well ELISA microplates were incubated overnight at 4°C with mouse anti-human MPO (clone 4A4; AbD, Serotec) in coating buffer from the Cell Death Detection ELISA kit (Roche). After blocking with 1% bovine serum albumin, plates were incubated overnight at 4°C with 10% sputum in blocking buffer and then washed, and anti–DNA-POD (monoclonal anti-DNA antibody from mouse clone MCA-33 conjugated with peroxidase; Roche) was added for 1.5 hours at room temperature. Tetramethylbenzidine substrate (Sigma) was then added, and the absorbance at 450 nm was measured after the addition of Stop reagent (Sigma). Because this assay detects binding of protein complexes and not antibodies, amplification of RF is unlikely.

Similar methods were used for the detection of DNA–NE complexes, with the antibody used to coat plates being rabbit anti-NE (Calbiochem). In addition, after overnight incubation with sputum, plates were incubated for 1 hour at room temperature with mouse anti–double-stranded DNA monoclonal antibody (Millipore), followed by anti-mouse IgG–horseradish peroxidase conjugate (Bio-Rad). To control for plate-to-plate variation, the same healthy control samples were included on every plate, and an optical density (OD) index was calculated based on the average absorbance at 450 nm in the healthy control samples. All samples were run in duplicate.

Statistical analysis. Characteristics of the subjects were compared between groups using the Kruskal-Wallis test for comparisons of age groups, and the chi-square/Fisher's exact test for comparisons of dichotomous variables. Regression models were used to compare associations between sputum antibody positivity (logistic models) and sputum antibody levels (linear models) while accounting for covariates. The median number of positive antibodies in the serum and sputum were compared using nonparametric matched-pairs analyses. Cohen's kappa coefficient was used to compare agreement between sputum and serum antibody positivity. Because antibody levels followed a non-normal distribution, the Kruskal-Wallis test (for comparisons of 3 groups) and Mann-Whitney test (for comparisons of 2 groups) were used to compare antibody levels between groups, and Spearman's corelation coefficient was used to determine correlations between antibody and NET levels. Before comparing the different antibodies and because each antibody had a unique range of reactivity, we normalized the values for each antibody by dividing the antibody level by the median level in the cutoff control group for that particular antibody. In addition, when

comparing ratios of citrullinated antibody levels to noncitrullinated antibody levels, we used these normalized values.

P values less than 0.05 were considered significant, except in analyses that compared each of the 29 individual antibodies. For these analyses, we used Bonferroni correction to account for multiple comparisons, and *P* values less than or equal to 0.002 (0.05 divided by 29 comparisons) were considered significant. All analyses were performed using SPSS software (version 23), and graphs were generated using GraphPad Prism (version 7).

RESULTS

Demographic characteristics. Compared to healthy controls, at-risk subjects and subjects with RA were older and marginally more often male. Furthermore, subjects with RA were more likely to be current smokers (Table 1). Other demographic characteristics were not significantly different between the groups.

Sputum antibody responses to citrullinated proteins/peptides. Overall, sputum from 18 (43.9%) of 41 at-risk subjects and 15 (75.0%) of 20 RA subjects demonstrated ≥1 positive antibody response to 1 of the 29 citrullinated proteins/peptides tested (Table 1). This prevalence was significantly higher in at-risk subjects and RA subjects compared to healthy controls (each $P < 0.01$). In logistic regression analyses adjusted for age, at-risk and RA subjects were more likely to have ≥1 positive finding of sputum antibodies to a citrullinated protein/peptide compared to healthy controls (in at-risk subjects, odds ratio [OR] 21.3, 95% confidence interval [95% CI] 1.8–253.1; in RA subjects, OR 79.1, 95% CI 5.5–1,143.3). In addition, the total number of sputum antibodies to citrullinated proteins/peptides was significantly higher in at-risk subjects and RA subjects compared to healthy controls (see Supplementary Figure 1, available on the *Arthritis & Rheumatology* web site at http://onlinelibrary.wiley.com/doi/10.1002/art.40401/abstract).

Within the group of at-risk subjects, the most prevalent sputum antibody responses to citrullinated proteins/peptides were directed to Cit-fibrinogen (34.1%), Cit–apolipoprotein E (31.7%), Cit-fibronectin (31.7%), Cit–histone 2B (29.3%), and Cit–histone 2A (26.8%) (Table 2; for the full list, see Supplementary Table 2 [http://onlinelibrary.wiley.com/doi/10.1002/art.40401/abstract]). In models accounting for multiple comparisons, anti–Cit-fibrinogen, anti–Cit–apolipoprotein E, and anti–Cit-fibronectin were significantly more prevalent in at-risk subjects compared to healthy controls ($P \leq 0.002$).

Among subjects with RA, the most prevalent sputum antibodies to citrillunated proteins/peptides were directed to Cit–histone 2B (40.0%), Cit-filaggrin$^{48–65\ \text{cyclic}}$ (40.0%), Cit–histone 2A (35.0%), Cit–fibrinogen A$^{616–635\ \text{cyclic}}$ (30.0%), Cit–fibronectin$^{1029–1042}$ (30.0%), and Cit-clusterin$^{231–250\ \text{cyclic}}$ (30.0%) (Table 2 and Supplementary Table 2). Sputum antibodies to Cit–histone 2B and Cit-filaggrin$^{48–65\ \text{cyclic}}$ were significantly more prevalent in RA subjects compared to healthy controls ($P \leq 0.002$). Notably, antibodies to Cit–histone 2B and Cit–histone 2A were among the most prevalent sputum antibody responses both in at-risk subjects and in RA subjects.

Sputum antibody responses to noncitrullinated proteins/peptides. In addition to anticitrullinated antibodies, antibodies to noncitrullinated/native proteins

Table 1. Characteristics of the study subjects

	Cutoff controls (n = 22)	Comparator controls (n = 22)	At-risk subjects (n = 41)*	RA subjects (n = 20)	*P*†
Age, median (range) years	37 (23–65)	31 (22–65)	54 (29–79)	57 (36–75)	<0.01
Female, no. (%)	20 (91)	18 (82)	27 (66)	13 (65)	0.10
Non-Hispanic white, no. (%)	15 (68)	16 (73)	30 (73)	11 (55)	0.66
Ever smoker, no. (%)	5 (23)	6 (27)	14 (34)	10 (50)	0.26
Current smoker, no. (%)	0 (0)	1 (5)	1 (2)	4 (20)	0.02
≥1 shared epitope allele, no. (%)	8 (36)	10 (46)	20 (49)	12 (67)‡	0.29
Chronic lung disease, no. (%)	3 (14)	1 (5)	10 (24)	4 (20)	0.23
Serum anti-CCP+, no. (%)	0 (0)	0 (0)	15 (37)	20 (100)	<0.01
≥1 sputum ACPA+ result, no. (%)§	4 (18)	1 (5)	18 (44)	15 (75)	<0.01
≥1 serum ACPA+ result, no. (%)§	8 (36)	6 (27)	23 (56)	19 (95)	<0.01

* In comparisons of rheumatoid arthritis (RA)–free at-risk subjects who were included based on familial risk factors versus those included based on serologic risk factors, there was no significant difference in any of the characteristics listed, except that the frequency of serum anti–cyclic citrullinated peptide (anti-CCP) positivity was higher in serologic at-risk subjects compared to familial at-risk subjects (100% versus 13%; $P < 0.01$). Notably, there was no difference in the prevalence of ≥1 sputum anti–citrullinated protein antibody (ACPA)–positive result in at-risk subjects stratified by inclusion risk factor (47% of familial at-risk subjects versus 36% of serologic at-risk subjects; $P = 0.73$).

† *P* values for comparison of median age between all groups were determined by Kruskal-Wallis test. *P* values for comparisons of prevalence of or positivity for any of the other characteristics between all groups were determined by chi-square/Fisher's exact test.

‡ Only 18 of the 20 RA subjects had DNA available for shared epitope testing.

§ Positivity for ACPAs was defined as a positive antibody response to 1 of the 29 citrullinated proteins/peptides tested in this study.

Table 2. Most prevalent sputum antibody responses to citrullinated proteins/peptides in at-risk and RA subjects*

	Healthy controls (n = 22)	At-risk subjects (n = 41)	RA subjects (n = 20)	*P* for group comparisons†		
				At-risk subjects vs. healthy controls	RA subjects vs. healthy controls	At-risk subjects vs. RA subjects
Cit-fibrinogen	0 (0)	14 (34)	5 (25)	0.001‡	0.018	0.564
Cit–apolipoprotein E	0 (0)	13 (32)	3 (15)	0.002‡	0.099	0.222
Cit-fibronectin	0 (0)	13 (32)	3 (15)	0.002‡	0.099	0.222
Cit–histone 2B	0 (0)	12 (29)	8 (40)	0.005	0.001‡	0.402
Cit–histone 2A	1 (5)	11 (27)	7 (35)	0.043	0.018	0.511
Cit-filaggrin$^{48–65\ cyclic}$	0 (0)	4 (10)	8 (40)	0.288	0.001‡	0.013
Cit–fibrinogen A$^{616–635\ cyclic}$	0 (0)	5 (12)	6 (30)	0.153	0.007	0.153
Cit-fibronectin$^{1029–1042}$	0 (0)	7 (17)	6 (30)	0.086	0.007	0.247
Cit-clusterin$^{231–250\ cyclic}$	0 (0)	6 (15)	6 (30)	0.083	0.007	0.156

* Values are the number (%) of subjects. RA = rheumatoid arthritis.
† *P* values for comparisons of the prevalence of positivity between 2 groups were determined using chi-square or Fisher's exact test, as appropriate.
‡ Significant difference at $P \leq 0.002$, based on Bonferroni correction for multiple comparisons.

have been identified in the serum of subjects with preclinical or early classified RA (4–9). These findings suggest that early autoimmunity may be characterized by reactivity to native proteins initially, with evolution to citrullinated epitopes over time through epitope spreading. Therefore, it is important to understand antibody reactivity to both citrullinated and noncitrullinated antigens during different phases of RA development.

Overall, we identified ≥1 positive finding for a sputum antibody to a noncitrullinated protein/peptide in 23 (56.1%) of 41 at-risk subjects and 13 (65.0%) of 20 RA subjects. Frequency of sputum positivity for ≥1 antibody to a noncitrullinated antigen was significantly higher both in at-risk subjects and in RA subjects compared to healthy controls (56% and 65%, respectively, versus 14% in healthy controls; each $P < 0.01$).

Comparison of sputum antibody responses to citrullinated and noncitrullinated proteins/peptides. For the 21 antibodies that had a citrullinated and noncitrullinated antigen counterpart, we examined the subjects who demonstrated sputum antibody positivity to citrullinated proteins/peptides and considered a citrullinated:noncitrullinated ratio of >1 to be consistent with specificity for citrullinated antigens. In at-risk subjects with a positive test result for a sputum antibody to any citrullinated protein/peptide, a high prevalence of citrulline-specific antibodies (in ≥75% of subjects) was demonstrated for the proteins fibrinogen and vimentin and the peptides apolipoprotein A1$^{231–248}$, fibrinogen A$^{556–575\ cyclic}$, and fibrinogen A$^{582–599}$ (Table 3).

In RA subjects with a positive test result for a sputum antibody to any citrullinated protein/peptide, a high prevalence of citrulline-specific antibodies (in ≥75% of subjects) was demonstrated for the proteins histone 2A, histone 2B, and vimentin and the peptides histone 2A/a-2$^{1–20}$, fibrinogen A$^{41–60\ cyclic}$, fibrinogen A$^{556–575\ cyclic}$, and fibrinogen A$^{616–635\ cyclic}$. In RA subjects compared to at-risk subjects, there was a nonsignificant trend toward a higher prevalence of citrulline specificity for fibrinogen A$^{616–635\ cyclic}$ and filaggrin$^{48–65\ cyclic}$. In addition, in the

Table 3. Prevalence of higher sputum citrullinated antibody levels relative to noncitrullinated antibody levels in subjects with sputum antibody positivity for each citrullinated protein/peptide*

	At-risk subjects (n = 41)	RA subjects (n = 20)
Citrullinated proteins		
Apolipoprotein A1	1/7 (14)	1/3 (33)
Histone 2A	5/11 (45)	6/7 (86)
Histone 2B	5/12 (42)	6/8 (75)
Fibrinogen	11/14 (79)	3/5 (60)
Vimentin	6/8 (75)	4/4 (100)
Citrullinated peptides		
Apolipoprotein A1$^{231–248}$	3/4 (75)	1/3 (33)
Biglycan$^{247–266\ cyclic}$	2/4 (50)	2/4 (50)
Clusterin$^{231–250\ cyclic}$	2/6 (33)	3/6 (50)
Histone 2A/a-2$^{1–20}$	1/2 (50)	3/3 (100)
Histone 2B/a$^{62–81\ cyclic}$	2/3 (67)	0/2 (0)
Enolase 1A$^{5–21}$	2/8 (25)	2/5 (40)
Fibrinogen A$^{41–60\ cyclic}$	2/3 (67)	3/4 (75)
Fibrinogen A$^{211–230\ cyclic}$	2/4 (50)	1/3 (33)
Fibrinogen A$^{556–575\ cyclic}$	4/5 (80)	3/3 (100)
Fibrinogen A$^{582–599}$	3/4 (75)	0/1 (0)
Fibrinogen A$^{616–635\ cyclic}$	2/5 (40)	6/6 (100)
Fibrinogen B$^{54–72}$	2/5 (40)	1/4 (25)
Fibrinogen B$^{246–267}$	1/5 (20)	1/5 (20)
Filaggrin$^{48–65\ cyclic}$	0/4 (0)	5/8 (63)
Vimentin$^{1–16}$	2/5 (40)	1/4 (25)
Vimentin$^{58–77\ cyclic}$	1/3 (33)	3/5 (60)

* Values are the number of at-risk subjects or rheumatoid arthritis (RA) subjects with a citrullinated:noncitrullinated ratio of >1/total number of subjects with a positive sputum antibody response to that particular protein or peptide (percentage). All citrullinated:noncitrullinated ratios were calculated as the normalized antibody level divided by the median level for that antibody in the cutoff control group. None of the *P* values for between-group differences (calculated by Fisher's exact test) were significant.

1 comparator control subject who had positive findings for sputum antibodies to 2 citrullinated proteins/peptides, both antibody responses demonstrated citrulline specificity with a citrullinated:noncitrullinated ratio of >1.

Comparison of sputum ACPA positivity by antigen array and by anti–CCP-2 ELISA. We found that in all 6 at-risk subjects who were sputum anti–CCP-2 positive and in 11 (92%) of 12 RA subjects who were sputum anti–CCP-2 positive, a positive test result for ≥1 sputum antibody to a citrullinated protein/peptide was also demonstrated on the antigen array. All of these sputum anti–CCP-2–positive at-risk and RA subjects with a positive antibody response to a citrullinated protein/peptide demonstrated citrulline specificity to at least one of those antigens based on a citrullinated:noncitrullinated ratio of >1. In 12 (34%) of the 35 at-risk subjects and 4 (50%) of the 8 RA subjects who were sputum anti–CCP-2 negative, a positive result for ≥1 sputum antibody to a citrullinated protein/peptide was demonstrated on antigen array. Among the 12 anti-CCP-2–negative at-risk subjects and 4 anti–CCP-2–negative RA subjects who had a positive antibody response to a citrullinated protein/peptide, 11 at-risk subjects and all 4 RA subjects demonstrated citrulline specificity to at least one of those antigens.

Sputum antibody positivity in subjects stratified by serum antibody status. In assays of the same 29 citrullinated proteins/peptides that were tested in the sputum, we identified 18 (44%) of 41 at-risk subjects and 19 (95%) of 20 RA subjects who had ≥1 positive finding of an antibody to a citrullinated antigen in the serum. The majority of these serum antibody responses demonstrated citrulline specificity (see Supplementary Table 3, available on the *Arthritis & Rheumatology* web site at http://onlinelibrary.wiley.com/doi/10.1002/art.40401/abstract). Additionally, in at-risk subjects, antibodies to the proteins fibrinogen and vimentin as well as the peptides fibrinogen $A^{582–599}$ and fibrinogen $A^{556–575\ cyclic}$ demonstrated high citrulline specificity both in the sputum and in the serum.

Following these experiments, we stratified at-risk subjects based on serum positivity for antibodies to citrullinated antigens. The rationale for this stratification is that more of the at-risk subjects who had already developed a systemic RA–related autoimmune response could be assumed to be further along the pathway to developing classifiable RA compared to serum antibody–negative individuals, although even among serum ACPA–positive subjects, not all will develop classifiable RA. In these analyses, we tested for reactivity to the 29 citrullinated protein/peptide antigens and found ≥1 positive finding for a sputum antibody in 6 (33.3%) of 18 serum antibody–negative at-risk subjects and 12 (52.2%) of 23 serum antibody–positive at-risk subjects. The prevalence of each sputum anticitrullinated antibody stratified by serum status is listed in Supplementary Table 4 (available on the *Arthritis & Rheumatology* web site at http://onlinelibrary.wiley.com/doi/10.1002/art.40401/abstract).

Within the group of at-risk subjects, there was overall poor agreement with regard to findings of a positive antibody response to citrullinated antigens between the sputum and the serum ($\kappa \leq 0.25$). However, there was higher agreement for Cit–enolase $1A^{5–21}$ ($\kappa = 0.55$), for which 4 (50%) of 8 at-risk subjects who were positive for anti–Cit–enolase $1A^{5–21}$ in the sputum also showed positivity in the serum.

Among the at-risk subjects who were negative for serum antibodies to citrullinated antigens, the most

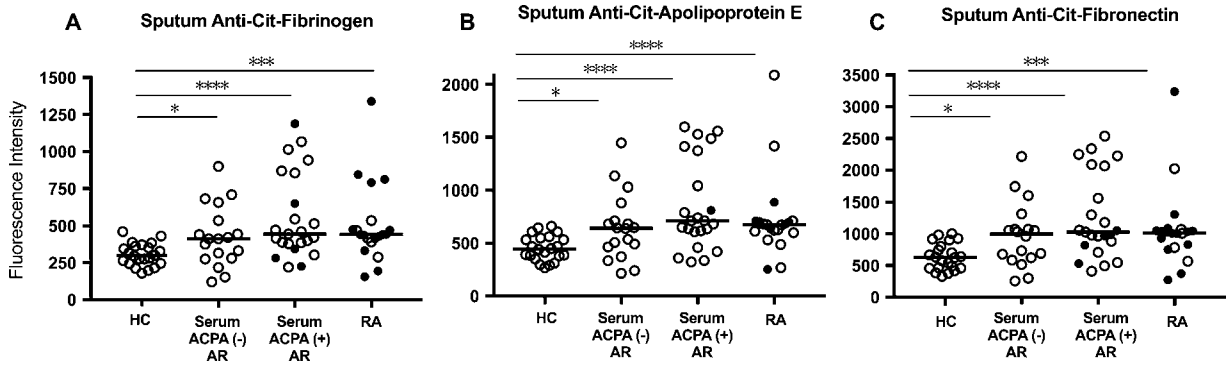

Figure 1. Sputum levels of antibodies to citrullinated proteins by subject group. Levels of sputum anti–Cit-fibrinogen (**A**), anti–Cit–apolipoprotein E (**B**), and anti–Cit-fibronectin (**C**) were compared between comparator healthy controls (HC) (n = 22), serum anti–citrullinated protein antibody (ACPA)–negative at-risk (AR) subjects (n = 18), serum ACPA–positive at-risk subjects (n = 23), and rheumatoid arthritis (RA) subjects (n = 20). An antibody response to a citrullinated protein/peptide antigen was defined as antibody positivity to any of the 29 citrullinated antigens tested in the study. Symbols represent individual subjects; horizontal lines indicate the median. * = $P \leq 0.01$; *** = $P \leq 0.001$; **** = $P \leq 0.0001$, by Mann-Whitney U test.

prevalent sputum antibodies were directed to Cit-fibrinogen (27.8%), Cit–apolipoprotein E (22.2%), and Cit-fibronectin (22.2%). Similarly, among at-risk subjects who were positive for any serum antibody response to a citrullinated protein/peptide, the most prevalent sputum antibodies were to Cit-fibrinogen (39.1%), Cit–apolipoprotein E (39.1%), and Cit-fibronectin (39.1%), but also included Cit–histone 2B (39.1%), Cit–histone 2A (34.8%), Cit–enolase 1A$^{5–21}$ (30.4%), Cit–apolipoprotein E$^{277–296\ \text{cyclic}}$ (30.4%), and Cit-vimentin (30.4%). These rates were all higher compared to the rates in healthy controls (each $P \leq 0.05$), with a significantly higher prevalence of antibodies to Cit-fibrinogen, Cit–apolipoprotein E, Cit-fibronectin, and Cit–histone 2B (each $P \leq 0.002$).

In addition to the prevalence of antibody positivity, the median levels of anti–Cit-fibrinogen, anti–Cit–apolipoprotein E, and anti–Cit-fibronectin in the sputum were each significantly higher in serum antibody–positive at-risk and RA subjects compared to healthy controls (Figures 1A–C).

Sputum NET levels and ACPA positivity in at-risk subjects. Overall, sputum NET levels were higher in at-risk subjects with ≥1 positive antibody response to a citrullinated or noncitrullinated antigen in the sputum (n = 15) compared to sputum antibody–negative healthy controls (n = 27). Specifically, in at-risk subjects with ≥1 positive antibody response to a citrullinated or noncitrullinated antigen, the median OD index for sputum DNA–MPO was 6.3 (interquartile range [IQR] 3.7–8.1) as compared to 3.7 (IQR 3.1–4.4) in healthy controls ($P < 0.01$), and for DNA–NE, the median OD index was 4.9 (IQR 2.6–12.2) as compared to 3.5 (IQR 2.6–5.0) in healthy controls ($P = 0.06$). These differences are consistent with our prior published findings with regard to NET levels in sputum anti-CCP–positive at-risk subjects and healthy control subjects (19).

We also determined correlations between the sputum levels of NET complexes and antibodies to citrullinated and noncitrullinated proteins/peptides, using a conservative approach that identified significant associations only if 2 separate NET assays (those for DNA–MPO and DNA–NE) demonstrated a significant correlation ($P \leq 0.002$) after accounting for multiple comparisons. With this approach, we found a significant positive correlation between sputum NET levels and the majority of antibody responses to citrullinated proteins/peptides (27 [93%] of 29) in the sputum (Table 4 and Figures 2A–D). Furthermore, after adjustment for a history of ever smoking—a factor that has been associated with NETosis (30,31)—sputum NET levels remained significantly associated with 15 of 29 antibodies, including antibodies to Cit-fibrinogen, Cit–apolipoprotein A1$^{231–248}$, and Cit–fibrinogen A$^{582–599}$ (Table 4), all of which also had been demonstrated to have high sputum citrulline specificity in at-risk subjects. The following antigens also demonstrated significant associations between sputum NET levels and the antibody responses to the citrullinated antigen, but not the noncitrullinated antigen, after adjustment for ever smoking: histone 2A/a-2$^{1–20}$, fibrinogen A$^{211–230\ \text{cyclic}}$, fibrinogen B$^{36–52}$, and vimentin$^{58–77\ \text{cyclic}}$.

Of note, a noncitrullinated form of the antigen was not available for testing of the following antigens that showed significant associations between sputum antibodies to citrullinated proteins/peptides and NET levels: apolipoprotein E, apolipoprotein E$^{277–296\ \text{cyclic}}$, histone

Table 4. Correlations between sputum levels of antibodies to citrullinated proteins/peptides and sputum neutrophil extracellular trap levels in at-risk subjects

	DNA–MPO		DNA–NE	
	r	*P*	r	*P*
Citrullinated proteins*				
Apolipoprotein A1	0.86	<0.001	0.66	<0.001
Apolipoprotein E†	0.93	<0.001	0.73	<0.001
Histone 2A	0.80	<0.001	0.69	<0.001
Histone 2B	0.79	<0.001	0.66	<0.001
Fibrinogen†	0.91	<0.001	0.74	<0.001
Fibronectin	0.90	<0.001	0.72	<0.001
Vimentin	0.79	<0.001	0.67	<0.001
Citrullinated peptides*				
Apolipoprotein A1$^{231–248}$†	0.79	<0.001	0.72	<0.001
Apolipoprotein E$^{277–296\ \text{cyclic}}$†	0.89	<0.001	0.80	<0.001
Biglycan$^{247–266\ \text{cyclic}}$	0.76	<0.001	0.66	<0.001
Clusterin$^{221–240\ \text{cyclic}}$	0.81	<0.001	0.65	<0.001
Clusterin$^{231–250\ \text{cyclic}}$	0.74	<0.001	0.67	<0.001
Histone 2A/a-2$^{1–20}$†	0.78	<0.001	0.70	<0.001
Histone 2A/a-2$^{1–20\ \text{cyclic}}$†	0.75	<0.001	0.70	<0.001
Histone 2B/a$^{62–81\ \text{cyclic}}$	0.80	<0.001	0.68	<0.001
Enolase 1A$^{5–21}$†	0.91	<0.001	0.77	<0.001
Fibrinogen A$^{27–43}$†	0.83	<0.001	0.74	<0.001
Fibrinogen A$^{41–60\ \text{cyclic}}$	0.72	<0.001	0.62	0.001
Fibrinogen A$^{211–230\ \text{cyclic}}$†	0.80	<0.001	0.69	<0.001
Fibrinogen A$^{556–575\ \text{cyclic}}$	0.65	<0.001	0.56	0.004
Fibrinogen A$^{582–599}$†	0.81	<0.001	0.71	<0.001
Fibrinogen A$^{616–635\ \text{cyclic}}$†	0.86	<0.001	0.77	<0.001
Fibrinogen B$^{36–52}$†	0.84	<0.001	0.73	<0.001
Fibrinogen B$^{54–72}$†	0.83	<0.001	0.74	<0.001
Fibrinogen B$^{246–267}$	0.78	<0.001	0.72	<0.001
Fibronectin$^{1029–1042}$	0.64	<0.001	0.58	0.003
Filaggrin$^{48–65\ \text{cyclic}}$†	0.81	<0.001	0.71	<0.001
Vimentin$^{1–16}$	0.81	<0.001	0.70	<0.001
Vimentin$^{58–77\ \text{cyclic}}$†	0.84	<0.001	0.76	<0.001

* The following noncitrullinated proteins/peptides were significantly correlated with the levels of DNA–myeloperoxidase (MPO) and DNA–neutrophil elastase (NE) complexes after adjustment for ever smoking: apolipoprotein A1, fibrinogen, histone 2A, apolipoprotein A1$^{231–248}$, enolase 1A$^{5–21}$, fibrinogen A$^{582–599}$, fibrinogen A$^{616–635\ \text{cyclic}}$, fibrinogen B$^{54–72}$, and filaggrin$^{48–65\ \text{cyclic}}$.

† This citrullinated protein/peptide remained significantly correlated with DNA–MPO and DNA–NE levels ($P \leq 0.002$) after adjustment for ever smoking.

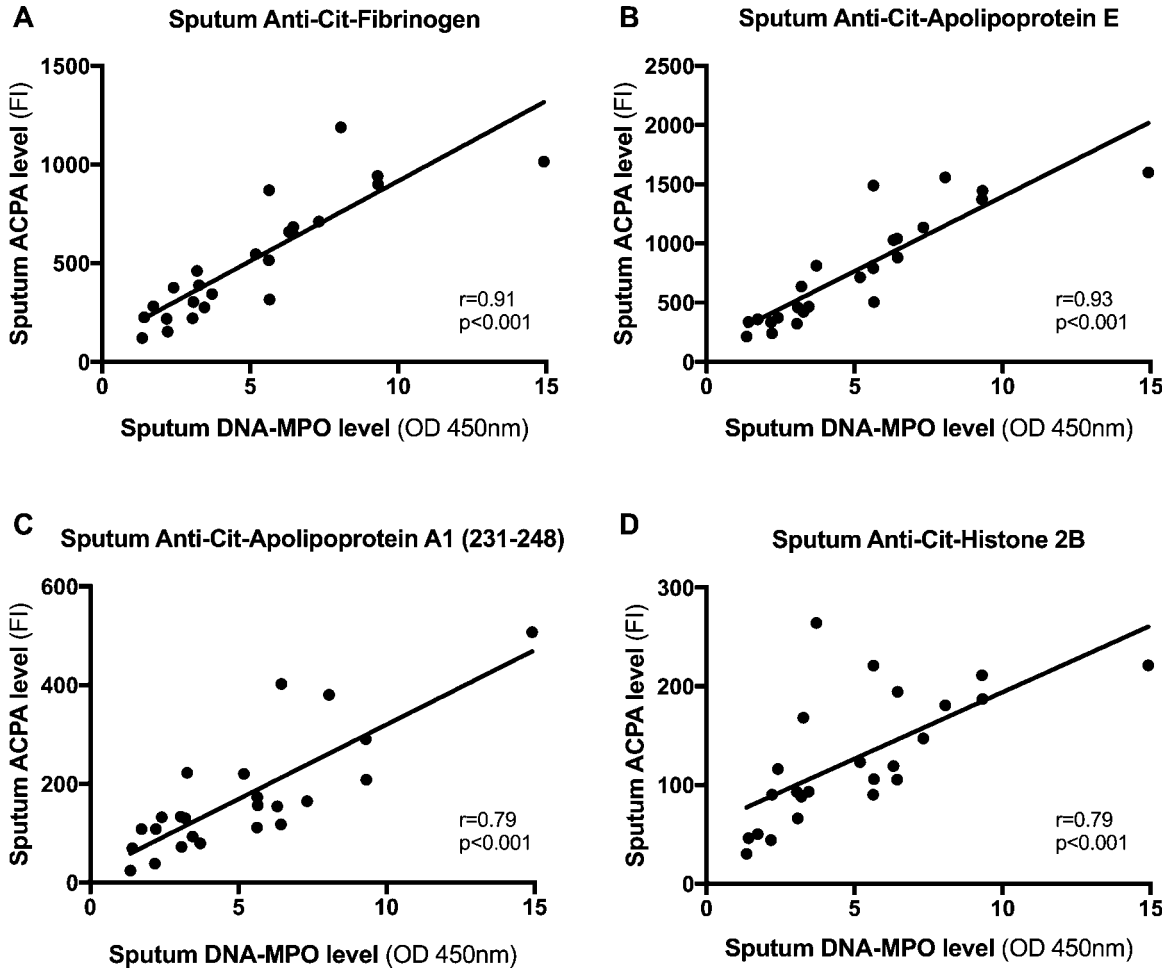

Figure 2. Correlations between sputum anti–citrullinated protein antibody (ACPA) levels and neutrophil extracellular trap (NET) levels in at-risk subjects. Sputum levels of anti–Cit-fibrinogen **(A)**, anti–Cit–apolipoprotein E **(B)**, anti–Cit–apolipoprotein $A1^{231–248}$ **(C)**, and anti–Cit–histone 2B **(D)** in at-risk subjects were analyzed in relation to sputum levels of NETs, as measured with DNA–myeloperoxidase (MPO) complexes. Symbols represent individual subjects. Correlations were calculated using Spearman's correlation coefficients (r values). FI = fluorescence intensity.

2A/a-$2^{1–20\ \text{cyclic}}$, and fibrinogen $A^{27–43}$. Moreover, there was no significant difference in age, sex, race, frequency of SE positivity, or smoking history between the 24 at-risk subjects who underwent NET testing and the 17 who did not (data not shown).

We also examined the 33 healthy controls who underwent sputum NET testing. There was a significant correlation ($P \leq 0.002$) between sputum NET levels and levels of antibodies to the following peptides: Cit-biglycan$^{247–266\ \text{cyclic}}$, Cit-clusterin$^{221–240\ \text{cyclic}}$, Cit-clusterin$^{231–250\ \text{cyclic}}$, Cit–fibrinogen $A^{556–575\ \text{cyclic}}$, Cit–fibrinogen $B^{54–72}$, Cit–fibrinogen $B^{246–267}$, Cit-filaggrin$^{48–65\ \text{cyclic}}$, Cit–histone 2A/a-$2^{1–20}$, and Cit–histone 2B/$a^{62–81\ \text{cyclic}}$.

Correlations of sputum NET levels and RF levels. To determine whether the relationships seen between NET levels and citrullinated/noncitrullinated antibodies were limited to the antibodies discussed above or whether they might involve other autoantibody systems, we evaluated the correlation of sputum NET levels and sputum RF isotypes in the 9 at-risk subjects who were negative for sputum citrullinated and noncitrullinated antibodies. We found a significant correlation between IgA-RF and NET levels in the sputum, using both NET assays (for DNA–MPO, $P < 0.01$; for DNA–NE, $P = 0.04$). However, there was no significant association between NET levels and IgM-RF or IgG-RF (for IgM-RF, $P = 0.24$ on the DNA–MPO assay, $P = 0.61$ on the DNA–NE assay; for IgG-RF, $P = 0.10$ on the DNA–MPO assay, $P = 0.27$ on the DNA–NE assay). These results suggest that there is not a general association between autoantibodies and NETs in the sputum. Of interest, these findings are consistent with those in prior studies that demonstrated a strong association of

IgA-RF with NET formation, whereas IgG-RF was weakly associated, and IgM-RF was not associated, with NET formation (32).

DISCUSSION

Understanding the development of ACPAs is a critical step in understanding the overall etiology and pathogenesis of RA. Our prior work demonstrated the presence of anti-CCP antibodies in the sputum of subjects considered at risk for the development of RA (17,19). In this study, we demonstrate for the first time that a subset of individual antibody responses to citrullinated and noncitrullinated antigens are detectable in the sputum of subjects at risk for RA, including at-risk subjects who are serum antibody negative; these findings are thereby informative of very early RA–related autoantibody development. We also demonstrate that sputum antibodies to both citrullinated and noncitrullinated antigens are significantly more prevalent in at-risk subjects and RA subjects compared to healthy controls. Furthermore, several sputum antibodies were found to be strongly correlated with increasing NET levels in subjects at risk for RA. Taken together, these data suggest that sputum antibody responses to particular citrullinated and noncitrullinated antigens, in association with higher levels of local NETosis in the lung, may be a key feature of early RA–related autoimmunity.

In this study, we found several sputum antibodies of particular interest in subjects at risk for RA. Sputum anti–Cit-fibrinogen, anti–Cit–apolipoprotein E, and anti–Cit-fibronectin antibodies were more prevalent in at-risk subjects, including serum ACPA–negative at-risk subjects, suggesting that these proteins may represent the earliest antigen targets of antibodies generated in the lung in subjects at risk of RA. In particular, anti–Cit-fibrinogen demonstrated high citrulline specificity in the sputum and serum of at-risk subjects. In the lung, protein levels of fibrinogen, apolipoprotein E, and fibronectin are known to be increased in the setting of inflammation and injury (33–35), and lung tissue plasma cells in RA patients have demonstrated production of anti–Cit-fibrinogen antibodies (36). Linking these concepts and considering our prior work demonstrating increased inflammation of the airways in at-risk subjects (16,19), it may be that increased levels of these proteins promote the generation of an autoimmune response in a portion of subjects at risk of developing RA.

In addition to fibrinogen, antibodies directed to vimentin, fibrinogen $A^{582–599}$, and fibrinogen $A^{556–575\ \text{cyclic}}$ also demonstrated citrulline specificity in the sputum and serum of at-risk subjects. In addition, antibodies to Cit–enolase $1A^{5–21}$ uniquely demonstrated agreement between the sputum and the serum in at-risk subjects. Although these findings are cross-sectional, they suggest that these antibody responses may play a role in transitions from localized mucosal to systemic autoimmunity.

An additional sputum antibody of interest is anti–Cit–histone 2B, which was the only sputum antibody to a citrullinated antigen that was significantly more prevalent both in serum antibody–positive at-risk subjects and in serum antibody–positive RA subjects compared to healthy controls. Antibodies directed to Cit–histone 2B also demonstrated higher citrulline specificity in the sputum of RA subjects. Taken together with the findings from murine models demonstrating that NET-associated anti–Cit–histone 2B antibodies were associated with development of arthritis (37), these data suggest that anti–Cit–histone 2B in the sputum may be relevant in the transition from an at-risk status to classified RA.

We also found that the individual sputum antibodies most prevalent in at-risk subjects differed from those most prevalent in subjects with classified RA. While this finding could be related to the effects of RA treatment, it may also reflect epitope spreading or changes in the lung during the evolution of RA-related autoimmunity. Moreover, we found that the number of autoantigens demonstrating high citrulline specificity increased in the sputum from at-risk subjects to RA subjects, and increased to a larger degree in the serum. While epitope spreading is well described in the serum during the preclinical period of RA (13,38), our findings suggest that epitope spreading may also occur in the lung, although longitudinal studies are needed to test this hypothesis.

Recently, our group described a significant correlation between sputum levels of anti-CCP and sputum levels of NET remnants (19). In this study, we expanded on that finding to demonstrate that several sputum antibodies to citrullinated as well as noncitrullinated antigens significantly correlated with sputum NET levels in at-risk subjects. Sputum NETs correlated with antibodies to Cit-histone and Cit-vimentin peptides, but not their noncitrullinated counterparts, and it is of interest that these are 2 citrullinated proteins that have been identified in the protein cargo of NETs induced in the neutrophils of patients with RA (20).

In this study, we could not determine whether immunogenic proteins on NETs triggered local autoantibody generation or whether local autoantibodies triggered the increase in NET levels. However, findings from several recent studies support the hypothesis that NETs could trigger ACPAs, including studies showing that NETs themselves may trigger immune responses associated with autoimmunity (39), that NETs in lupus patients can alter the structure and function of proteins, including

apolipoproteins (40), and that the uptake of NET proteins by antigen-presenting cells is associated with systemic ACPAs (8).

We also identified correlations between sputum NETs and antibodies to citrullinated antigen targets that have not been previously described in NETs. Additional studies are needed, but this finding could be attributed to a unique protein cargo in the NETs generated in at-risk subjects, the release of PAD enzymes from NETs, which can result in citrullination of nearby proteins that could trigger ACPAs (41) or can result in cross-reactivity of ACPAs to several citrullinated antigen targets, as has been demonstrated in RA patients (42–44). It is of note that whereas some ACPAs in patients with RA demonstrate cross-reactivity to multiple citrullinated antigens, others demonstrate nonoverlapping citrullinated antigen binding (43). We also found that multiple anti–citrullinated antigen antibodies and RF-IgA, but not RF-IgM and RF-IgG, were associated with markers of NETosis in the sputum, suggesting that NETs are preferentially associated with certain antibodies. Overall, these findings support the importance of additional studies that could specifically address the possibility of antibody cross-reactivity in the sputum as well as the role of NETs in specific antibody responses.

Furthermore, we identified correlations between sputum NETs and several sputum antibodies to citrullinated and noncitrullinated antigens in healthy controls. Although the sputum antibody levels were significantly lower in healthy controls compared to at-risk subjects or RA subjects, these findings suggest the possibility that even in individuals without a known risk for RA, low levels of antibody responses to citrullinated or noncitrullinated antigens may be associated with mucosal NETosis, perhaps reflecting a role for antibodies to citrullinated or noncitrullinated antigens in the normal regulation of mucosal processes that, in some cases, may become dysregulated, leading to greater mucosal immunity, and ultimately to systemic inflammation and classified RA. Each of these potential mechanisms and hypotheses could improve our understanding of the early phases of ACPA development and should be explored in future studies.

In this study, we also found that at-risk and RA subjects had higher sputum reactivity to noncitrullinated proteins/peptides compared to healthy controls. This finding suggests that broad antibody reactivity to both noncitrullinated and citrullinated antigens occurs in the lungs of these subjects, but that more citrulline-specific reactivity is generated toward certain antigens and is more prevalent in subjects with RA. These findings support the hypothesis that early localized autoimmunity may be directed to native proteins, with evolution to citrullinated epitopes occurring through epitope spreading (4–6,45). However, it is also possible that tolerance to citrullinated proteins is initially broken, and that the autoimmune responses to epitopes intramolecularly spread to native epitopes on the same proteins. Longitudinal studies are needed to understand the temporal relationship between antibodies to citrullinated and noncitrullinated proteins/peptides.

There are several caveats to our study, including its cross-sectional design, which limits inferences regarding the evolution of autoantibody responses over time. In addition, there is the potential for oral-pharyngeal contamination of the sputum, and antibody translocation from the circulation. However, we believe that the novel cross-sectional findings in this study are important to support longitudinal studies. In addition, as described in Subjects and Methods, since we ensured careful collection of the sputum samples to minimize salivary contamination, and since we previously demonstrated the minimal translocation of antibodies from the serum to the sputum (17,19), we believe that the findings herein reflect lung and airway biology. Furthermore, the antigen array that we used was based on proteins known to be relevant in the RA joint, and while there are shared RA-related antigens between the lung and joints (46), it may be that to more deeply understand initial breaks in tolerance related to the lung, the autoimmune response to lung-specific antigens needs to be evaluated. Furthermore, the portion of our at-risk population who were sputum ACPA positive is likely higher than the portion who will go on to develop classified RA. Longitudinal studies will be informative to understand what factors lead to progression from local mucosal to systemic autoimmunity and, ultimately, classified RA.

We also did not test for antibody cross-reactivity in this study. While future studies are needed in this area, we believe our current findings cannot all be explained by cross-reactivity, because some individuals had only 1 positive finding of a sputum antibody to a single citrullinated antigen, and some individuals had sputum antibodies to citrullinated antigens in the absence of positivity for a noncitrullinated antibody. Finally, serum ACPA fine specificities differ between different RA populations (47), and it may be that similar findings could occur in the sputum, supporting the importance of additional sputum studies in other at-risk populations.

In conclusion, we identified several sputum autoantibodies of particular interest in subjects at risk for the future development of RA, including sputum ACPAs with early citrulline specificity and those with strong associations with NETs in the sputum. These findings further support the hypothesis that the lung likely plays an

important role in the development and evolution of RA-related autoimmunity.

AUTHOR CONTRIBUTIONS

All authors were involved in drafting the article or revising it critically for important intellectual content, and all authors approved the final version to be published. Dr. Demoruelle had full access to all of the data in the study and takes responsibility for the integrity of the data and the accuracy of the data analysis.

Study conception and design. Demoruelle, Bowers, Holers, Deane.

Acquisition of data. Demoruelle, Lahey, Sokolove, Purmalek, Seto, Weisman, Norris, Kaplan, Holers, Robinson, Deane.

Analysis and interpretation of data. Demoruelle, Bowers, Kaplan, Holers, Robinson, Deane.

ADDITIONAL DISCLOSURES

Author Sokolove is currently an employee of AbbVie.

REFERENCES

1. Gyorgy B, Toth E, Tarcsa E, Falus A, Buzas EI. Citrullination: a posttranslational modification in health and disease. Int J Biochem Cell Biol 2006;38:1662–77.
2. Baka Z, Gyorgy B, Geher P, Buzas EI, Falus A, Nagy G. Citrullination under physiological and pathological conditions. Joint Bone Spine 2012;79:431–6.
3. Chandra PE, Sokolove J, Hipp BG, Lindstrom TM, Elder JT, Reveille JD, et al. Novel multiplex technology for diagnostic characterization of rheumatoid arthritis. Arthritis Res Ther 2011; 13:R102.
4. Konig MF, Giles JT, Nigrovic PA, Andrade F. Antibodies to native and citrullinated RA33 (hnRNP A2/B1) challenge citrullination as the inciting principle underlying loss of tolerance in rheumatoid arthritis. Ann Rheum Dis 2016;75:2022–8.
5. De Pablo P, Dietrich T, Chapple IL, Milward M, Chowdhury M, Charles PJ, et al. The autoantibody repertoire in periodontitis: a role in the induction of autoimmunity to citrullinated proteins in rheumatoid arthritis? Ann Rheum Dis 2014;73:580–6.
6. Quirke AM, Perry E, Cartwright A, Kelly C, De Soyza A, Eggleton P, et al. Bronchiectasis is a model for chronic bacterial infection inducing autoimmunity in rheumatoid arthritis. Arthritis Rheumatol 2015;67:2335–42.
7. Yoshida M, Tsuji M, Kurosaka D, Kurosaka D, Yasuda J, Ito Y, et al. Autoimmunity to citrullinated type II collagen in rheumatoid arthritis. Mod Rheumatol 2006;16:276–81.
8. Carmona-Rivera C, Carlucci PM, Moore E, Lingampalli N, Uchtenhagen H, James E, et al. Synovial fibroblast-neutrophil interactions promote pathogenic adaptive immunity in rheumatoid arthritis. Sci Immunol 2017;2:eaag3358.
9. Hueber W, Kidd BA, Tomooka BH, Lee BJ, Bruce B, Fries JF, et al. Antigen microarray profiling of autoantibodies in rheumatoid arthritis. Arthritis Rheum 2005;52:2645–55.
10. Demoruelle MK, Parish MC, Derber LA, Kolfenbach JR, Hughes-Austin JM, Weisman MH, et al. Performance of anti–cyclic citrullinated peptide assays differs in subjects at increased risk of rheumatoid arthritis and subjects with established disease. Arthritis Rheum 2013;65:2243–52.
11. Majka DS, Deane KD, Parrish LA, Lazar AA, Baron AE, Walker CW, et al. Duration of preclinical rheumatoid arthritis-related autoantibody positivity increases in subjects with older age at time of disease diagnosis. Ann Rheum Dis 2008;67:801–7.
12. Rantapää-Dahlqvist S, de Jong BA, Berglin E, Hallmans G, Wadell G, Stenlund H, et al. Antibodies against cyclic citrullinated peptide and IgA rheumatoid factor predict the development of rheumatoid arthritis. Arthritis Rheum 2003;48:2741–9.
13. Sokolove J, Bromberg R, Deane KD, Lahey LJ, Derber LA, Chandra PE, et al. Autoantibody epitope spreading in the preclinical phase predicts progression to rheumatoid arthritis. PLoS One 2012;7:e35296.
14. Brink M, Hansson M, Mathsson L, Jakobsson PJ, Holmdahl R, Hallmans G, et al. Multiplex analyses of antibodies against citrullinated peptides in individuals prior to development of rheumatoid arthritis. Arthritis Rheum 2013;65:899–910.
15. Finckh A, Escher M, Liang MH, Bansback N. Preventive treatments for rheumatoid arthritis: issues regarding patient preferences. Curr Rheumatol Rep 2016;18:51.
16. Demoruelle MK, Weisman MH, Simonian PL, Lynch DA, Sachs PB, Pedraza IF, et al. Airways abnormalities and rheumatoid arthritis–related autoantibodies in subjects without arthritis: early injury or initiating site of autoimmunity? Arthritis Rheum 2012; 64:1756–61.
17. Willis VC, Demoruelle MK, Derber LA, Chartier-Logan CJ, Parish MC, Pedraza IF, et al. Sputum autoantibodies in patients with established rheumatoid arthritis and subjects at risk of future clinically apparent disease. Arthritis Rheum 2013;65:2545–54.
18. Reynisdottir G, Karimi R, Joshua V, Olsen H, Hensvold AH, Harju A, et al. Structural changes and antibody enrichment in the lungs are early features of anti–citrullinated protein antibody–positive rheumatoid arthritis. Arthritis Rheumatol 2014;66:31–9.
19. Demoruelle MK, Harrall KK, Ho L, Purmalek MM, Seto NL, Rothfuss HM, et al. Anti–citrullinated protein antibodies are associated with neutrophil extracellular traps in the sputum in relatives of rheumatoid arthritis patients. Arthritis Rheumatol 2017; 69:1165–75.
20. Khandpur R, Carmona-Rivera C, Vivekanandan-Giri A, Gizinski A, Yalavarthi S, Knight JS, et al. NETs are a source of citrullinated autoantigens and stimulate inflammatory responses in rheumatoid arthritis. Sci Transl Med 2013;5:178ra40.
21. Corsiero E, Bombardieri M, Carlotti E, Pratesi F, Robinson W, Migliorini P, et al. Single cell cloning and recombinant monoclonal antibodies generation from RA synovial B cells reveal frequent targeting of citrullinated histones of NETs. Ann Rheum Dis 2016;75:1866–75.
22. Kolfenbach JR, Deane KD, Derber LA, O'Donnell C, Weisman MH, Buckner JH, et al. A prospective approach to investigating the natural history of preclinical rheumatoid arthritis (RA) using first-degree relatives of probands with RA. Arthritis Rheum 2009;61:1735–42.
23. Aletaha D, Neogi T, Silman AJ, Funovits J, Felson DT, Bingham CO III, et al. 2010 rheumatoid arthritis classification criteria: an American College of Rheumatology/European League Against Rheumatism collaborative initiative. Arthritis Rheum 2010;62: 2569–81.
24. Arnett FC, Edworthy SM, Bloch DA, McShane DJ, Fries JF, Cooper NS, et al. The American Rheumatism Association 1987 revised criteria for the classification of rheumatoid arthritis. Arthritis Rheum 1988;31:315–24.
25. In 't Veen JC, de Gouw HW, Smits HH, Sont JK, Hiemstra PS, Sterk PJ, et al. Repeatability of cellular and soluble markers of inflammation in induced sputum from patients with asthma. Eur Respir J 1996;9:2441–7.
26. Gershman NH, Wong HH, Liu JT, Mahlmeister MJ, Fahy JV. Comparison of two methods of collecting induced sputum in asthmatic subjects. Eur Respir J 1996;9:2448–53.
27. Robinson WH, DiGennaro C, Hueber W, Haab BB, Kamachi M, Dean EJ, et al. Autoantigen microarrays for multiplex characterization of autoantibody responses. Nat Med 2002;8:295–301.
28. Monach PA, Hueber W, Kessler B, Tomooka BH, BenBarak M, Simmons BP, et al. A broad screen for targets of immune complexes decorating arthritic joints highlights deposition of

nucleosomes in rheumatoid arthritis. Proc Natl Acad Sci U S A 2009;106:15867–72.
29. Lood C, Blanco LP, Purmalek MM, Carmona-Rivera C, De Ravin SS, Smith CK, et al. Neutrophil extracellular traps enriched in oxidized mitochondrial DNA are interferogenic and contribute to lupus-like disease. Nat Med 2016;22:146–53.
30. Hosseinzadeh A, Thompson PR, Segal BH, Urban CF. Nicotine induces neutrophil extracellular traps. J Leukoc Biol 2016;100: 1105–12.
31. Lee J, Luria A, Rhodes C, Raghu H, Lingampalli N, Sharpe O, et al. Nicotine drives neutrophil extracellular traps formation and accelerates collagen-induced arthritis. Rheumatology (Oxford) 2017;56:644–53.
32. Aleyd E, Al M, Tuk CW, van der Laken CJ, van Egmond M. IgA complexes in plasma and synovial fluid of patients with rheumatoid arthritis induce neutrophil extracellular traps via FcαRI. J Immunol 2016;197:4552–9.
33. Limper AH, Roman J. Fibronectin: a versatile matrix protein with roles in thoracic development, repair and infection. Chest 1992;101:1663–73.
34. Yamashita CM, Fessler MB, Vasanthamohan L, Lac J, Madenspacher J, McCaig L, et al. Apolipoprotein E-deficient mice are susceptible to the development of acute lung injury. Respiration 2014;87:416–27.
35. Haidaris PJ. Induction of fibrinogen biosynthesis and secretion from cultured pulmonary epithelial cells. Blood 1997;89:873–82.
36. Rangel-Moreno J, Hartson L, Navarro C, Gaxiola M, Selman M, Randall TD. Inducible bronchus-associated lymphoid tissue (iBALT) in patients with pulmonary complications of rheumatoid arthritis. J Clin Invest 2006;116:3183–94.
37. Sohn DH, Rhodes C, Onuma K, Zhao X, Sharpe O, Gazitt T, et al. Local joint inflammation and histone citrullination in a murine model of the transition from preclinical autoimmunity to inflammatory arthritis. Arthritis Rheumatol 2015;67:2877–87.
38. Van der Woude D, Rantapaa-Dahlqvist S, Ioan-Facsinay A, Onnekink C, Schwarte CM, Verpoort KN, et al. Epitope spreading of the anti-citrullinated protein antibody response occurs before disease onset and is associated with the disease course of early arthritis. Ann Rheum Dis 2010;69:1554–61.
39. Papadaki G, Kambas K, Choulaki C, Vlachou K, Drakos E, Bertsias G, et al. Neutrophil extracellular traps exacerbate Th1-mediated autoimmune responses in rheumatoid arthritis by promoting DC maturation. Eur J Immunol 2016;46:2542–54.
40. Smith CK, Vivekanandan-Giri A, Tang C, Knight JS, Mathew A, Padilla RL, et al. Neutrophil extracellular trap–derived enzymes oxidize high-density lipoprotein: an additional proatherogenic mechanism in systemic lupus erythematosus. Arthritis Rheumatol 2014;66:2532–44.
41. Spengler J, Lugonja B, Ytterberg AJ, Zubarev RA, Creese AJ, Pearson MJ, et al. Release of active peptidyl arginine deiminases by neutrophils can explain production of extracellular citrullinated autoantigens in rheumatoid arthritis synovial fluid. Arthritis Rheumatol 2015;67:3135–45.
42. Amara K, Steen J, Murray F, Morbach H, Fernandez-Rodriguez BM, Joshua V, et al. Monoclonal IgG antibodies generated from joint-derived B cells of RA patients have a strong bias toward citrullinated autoantigen recognition. J Exp Med 2013;210:445–55.
43. Ioan-Facsinay A, el-Bannoudi H, Scherer HU, van der Woude D, Menard HA, Lora M, et al. Anti-cyclic citrullinated peptide antibodies are a collection of anti-citrullinated protein antibodies and contain overlapping and non-overlapping reactivities. Ann Rheum Dis 2011;70:188–93.
44. Masson-Bessiere C, Sebbag M, Girbal-Neuhauser E, Nogueira L, Vincent C, Senshu T, et al. The major synovial targets of the rheumatoid arthritis-specific antifilaggrin autoantibodies are deiminated forms of the α- and β-chains of fibrin. J Immunol 2001;166: 4177–84.
45. Li S, Yu Y, Yue Y, Liao H, Xie W, Thai J, et al. Autoantibodies from single circulating plasmablasts react with citrullinated antigens and Porphyromonas gingivalis in rheumatoid arthritis. Arthritis Rheumatol 2016;68:614–26.
46. Ytterberg AJ, Joshua V, Reynisdottir G, Tarasova NK, Rutishauser D, Ossipova E, et al. Shared immunological targets in the lungs and joints of patients with rheumatoid arthritis: identification and validation. Ann Rheum Dis 2015;74:1772–7.
47. Too CL, Murad S, Hansson M, Alm LM, Dhaliwal JS, Holmdahl R, et al. Differences in the spectrum of anti–citrullinated protein antibody fine specificities between Malaysian and Swedish patients with rheumatoid arthritis: implications for disease pathogenesis. Arthritis Rheumatol 2017;69:58–69.

ARTHRITIS & RHEUMATOLOGY
Vol. 70, No. 4, April 2018, pp 528–536
DOI 10.1002/art.40408

Hypomethylation of CYP2E1 and DUSP22 Promoters Associated With Disease Activity and Erosive Disease Among Rheumatoid Arthritis Patients

Amanda Mok,[1] Brooke Rhead,[1] Calliope Holingue,[1] Xiaorong Shao,[1] Hong L. Quach,[1] Diana Quach,[1] Elizabeth Sinclair,[2] Jonathan Graf,[2] John Imboden,[2] Thomas Link,[2] Ruby Harrison,[2] Vladimir Chernitskiy,[2] Lisa F. Barcellos,[1] and Lindsey A. Criswell[2]

***Objective*. Epigenetic modifications have previously been associated with rheumatoid arthritis (RA). In this study, we aimed to determine whether differential DNA methylation in peripheral blood cell subpopulations is associated with any of 4 clinical outcomes among RA patients.**

***Methods*. Peripheral blood samples were obtained from 63 patients in the University of California, San Francisco RA cohort (all satisfied the American College of Rheumatology classification criteria; 57 were seropositive for rheumatoid factor and/or anti–cyclic citrullinated protein). Fluorescence-activated cell sorting was used to separate the cells into 4 immune cell subpopulations (CD14+ monocytes, CD19+ B cells, CD4+ naive T cells, and CD4+ memory T cells) per individual, and 229 epigenome-wide DNA methylation profiles were generated using Illumina HumanMethylation450 BeadChips. Differentially methylated positions and regions associated with the Clinical Disease Activity Index score, erosive disease, RA Articular Damage score, Sharp score, medication at time of blood draw, smoking status, and disease duration were identified using robust regression models and empirical Bayes variance estimators.**

***Results*. Differential methylation of CpG sites associated with clinical outcomes was observed in all 4 cell types. Hypomethylated regions in the *CYP2E1* and *DUSP22* gene promoters were associated with active and erosive disease, respectively. Pathway analyses suggested that the biologic mechanisms underlying each clinical outcome are cell type–specific. Evidence of independent effects on DNA methylation from smoking, medication use, and disease duration were also identified.**

***Conclusion*. Methylation signatures specific to RA clinical outcomes may have utility as biomarkers or predictors of exposure, disease progression, and disease severity.**

Rheumatoid arthritis (RA) is the most common systemic autoimmune disease, with a global prevalence of ~1% (1). Although the precise model of pathogenesis is not known, it is thought to involve the activation of both innate and adaptive immune responses as well as the destruction of cartilage and subchondral bone by resident synoviocytes, leading to joint damage and disability. The cause of RA is complex, with contributions from both genetic and nongenetic risk factors.

The strongest genetic risk factors for RA are variants of the *HLA–DRB1* gene. The shared epitope (SE) alleles encoding the QKRRA and QRRRA amino acid sequences at positions 70–74 explain much of the genetic predisposition to RA (2). Recently, a large study demonstrated that the association between the major histocompatibility complex (MHC) and RA is best explained by 5 amino acids: 3 in *HLA–DRB1* and 1 each in *HLA–B* and *HLA–DPB1,* of which 2 are the same as those of the shared epitope (3). Of the 16 resulting *DRB1* haplotypes, valine/lysine/alanine at positions 11/71/74 is the most strongly

Supported by the Rheumatology Research Foundation (Within Our Reach grant and a Health Professional Research preceptorship), the NIH (National Library of Medicine grant T32-LM-012417), the Genentech Foundation, the UCSF-Stanford Arthritis Center of Excellence (supported in part by the Arthritis Foundation), and the Rosalind Russell/Ephraim P. Engleman Rheumatology Research Center at the University of California, San Francisco.

[1]Amanda Mok, MPH, Brooke Rhead, BS, Calliope Holingue, MPH, Xiaorong Shao, MA, Hong L. Quach, BA, Diana Quach, BA, Lisa F. Barcellos, PhD, MPH: University of California, Berkeley; [2]Elizabeth Sinclair, PhD, Jonathan Graf, MD, John Imboden, MD, Thomas Link, MD, PhD, Ruby Harrison, BA, Vladimir Chernitskiy, BA, Lindsey A. Criswell, MD, MPH, DSc: University of California, San Francisco.

Drs. Barcellos and Criswell contributed equally to this work.

Address correspondence to Lindsey A. Criswell, MD, MPH, DSc, University of California, San Francisco, 513 Parnassus Avenue, Room S857, San Francisco, CA 94143. E-mail: lindsey.criswell@ucsf.edu.

Submitted for publication April 21, 2017; accepted in revised form December 20, 2017.

associated with RA, and it corresponds to the *DRB1**04:01 allele (3), a well-documented association (3,4).

DNA methylation is an epigenetic modification that results from the addition of a methyl group to a cytosine DNA base in the context of cytosine–phosphate–guanine dinucleotide (CpG), and has been shown to modulate gene expression as well as determinants of higher-order DNA structure (5,6). Methylation profiles can be maintained across cell division cycles and between generations and may contribute to the "missing heritability" suggested by current genome-wide association study findings (7). In addition, DNA methylation states can be altered by a number of environmental exposures, such as tobacco smoke, air pollutants, paternal and maternal lifestyle factors, and antibiotic use (8). Thus, DNA methylation profiles may link genetic and environmental signals and serve as the intermediate between those risk factors and disease susceptibility.

A growing body of epidemiologic evidence supports an association between RA and DNA methylation. Genome-wide and candidate gene studies in RA patients and healthy controls have demonstrated disease-associated methylation differences in peripheral blood mononuclear cells (PBMCs), purified T cells and B cells, and fibroblast-like synoviocytes (9–12). Interestingly, treatment with methotrexate is able to revert RA-associated global hypomethylation in T cells and monocytes and restore regulatory T cell function through reduction in methylation of the *FOXP3* upstream enhancer (13,14). One proof-of-concept study of DNA methylation at first diagnosis identified 6 CpG sites associated with response to disease-modifying antirheumatic drugs (DMARDs) in patients with early RA (15). However, studies to date have typically been limited to case–control comparisons and have not identified methylation differences specific to RA case subgroups or clinical outcomes.

In this study, we assessed DNA methylation signals associated with 4 RA clinical outcomes, history of smoking, medication use, and disease duration. Such signatures may be useful as biomarkers or predictors of exposure, disease progression, or response to treatment.

PATIENTS AND METHODS

Study participants. Participants included 63 women of European ancestry from the RA cohort at the University of California, San Francisco (UCSF), all of whom met the American College of Rheumatology (ACR) 1987 criteria for RA (Table 1) (16). All participants provided a peripheral blood sample for genotyping, cell sorting, and DNA methylation profiling. The following clinical outcomes were determined for each RA patient: the Clinical Disease Activity Index (CDAI) score, presence of erosive disease, total Rheumatoid Arthritis Articular Damage (RAAD) score, and modified Sharp score for all joints (17,18). The CDAI is a sum of the tender joint count, swollen joint count, patient's global assessment of disease activity, and physician's global assessment of disease activity. It was treated as a dichotomized variable based on the presence of active disease (CDAI score >2.8) or remission (CDAI score ≤2.8), in accordance with the ACR recommendations (19). The European League Against Rheumatism (EULAR) criteria were used to classify erosive disease (20). According to the EULAR classification, erosive disease is defined as cortical breaks in at least 3 separate joints of the hands and feet as observed on radiographs, and this was treated as a binary variable (20). The modified Sharp score is a more detailed measure of radiographic damage, where each hand, wrist, and foot joint is scored for erosions and for joint space narrowing (18). The RAAD score is computed by evaluating 35 large and small joints using a goniometer and scoring them on a 3-point scale, and it may therefore capture aspects of joint failure not reflected on radiography-based scores (21).

Table 1. Characteristics of the study participants at the time of blood draw*

Seropositive, no. (%)	
Anti-CCP or RF	57 (90.5)
Anti-CCP	53 (89.8)
RF	46 (75.4)
Age, mean ± SD	56.4 ± 14.8
Ever smoked, no. (%)	33 (52.4)
Disease duration, mean ± SD years	14.0 ± 10.5
Active disease (CDAI >2.8), no. (%)	45 (76.2)
Erosive disease, no. (%)	39 (63.9)
RAAD score, mean ± SD	10.1 ± 13.0
Sharp score, mean ± SD	47.2 ± 74.0
Current DMARD or anti-TNF therapy, no. (%)	52 (82.5)

* Anti-CCP = anti–cyclic citrullinated peptide; RF = rheumatoid factor; CDAI = Clinical Disease Activity Index; RAAD = Rheumatoid Arthritis Articular Damage; DMARD = disease-modifying antirheumatic drug; anti-TNF = anti–tumor necrosis factor.

Study approval. Written informed consent was obtained from all participants prior to inclusion in this study. Research was conducted in compliance with the Declaration of Helsinki. Institutional Review Board approval was obtained at UCSF, where the study subjects were recruited.

Genotyping and methylation assessment. Single-nucleotide polymorphism (SNP) genotyping and DNA methylation profiling were performed as previously described (22). Briefly, study participants were genotyped using Illumina HumanOmniExpress, HumanOmniExpressExome, or Human660W-Quad microarrays, and principal components analysis was performed using EigenStrat to characterize genetic ancestry and account for any heterogeneity in our study population (23). PBMCs were isolated from whole blood, and the following cell subpopulations were identified by fluorescence-activated cell sorting: monocytes (CD45+CD14+), B cells (CD45+CD14–CD3–CD19+), naive CD4+ T cells (CD45+CD14–CD19–CD3+CD4+CD27+CD45RA+), as well as memory CD4+ T cells (CD45+CD14–CD19–CD3+CD4+CD45RA–). A total of 229 epigenome-wide DNA methylation profiles were generated using the Illumina Infinium HumanMethylation450 BeadChip, and β values (the ratio of methylated probe intensity to total intensities) were reported per CpG site.

Extensive quality control measures were performed, including background signal subtraction, all sample mean

normalization, and beta-mixture quantile normalization (24–26). Samples with low detection rates ($P > 0.05$) in more than 20% of sites were removed from analysis. The following sites were also removed from analysis: CpG sites with low detection rates ($P > 0.05$) in more than 20% of samples, non-CpG "rs" SNP probes, cross-reactive probes, and European-specific polymorphic CpGs (27). In total, we retained 428,232 CpG sites in 229 samples (58 CD14+ monocyte samples, 57 CD19+ B cell samples, 56 CD4+ naive T cell samples, and 58 CD4+ memory T cell samples).

Statistical analysis. Using the Lumi R package (28,29), methylation β values were transformed to M values in order to better approximate the homoscedasticity assumption in most statistical analyses. For each RA clinical outcome, robust linear regression models were fitted to each CpG site to assess for association with methylation, adjusting for age, history of smoking, genetic ancestry, DMARD treatment (methotrexate, hydroxychloroquine, leflunomide), anti–tumor necrosis factor treatment (anti-TNF; adalimumab, certolizumab, or golimumab), and disease duration at the time of blood draw. Regression models were fitted separately for each cell type. A robust empirical Bayes procedure as implemented in the Limma R package was used to shrink CpG-wise variances by pooling the ensemble of all CpG sites, a technique used to improve statistical power and accuracy when the sample size is small (30). Per the regression model, P values were adjusted using the Bonferroni correction for 428,232 tests.

Analysis of differentially methylated regions (DMRs) was performed as implemented in the Bumphunter R package (31). Coefficients from the above regression models were smoothed over genomic distance, generating candidate regions of differentially methylated CpG sites. Statistical significance was assigned to individual regions by calculating an empirical P value derived from 1,000 bootstrapped results. The empirical family-wise error rate was used to control for Type I error. Genomic annotations were obtained from the GRCh37/hg19 UCSC Genome Browser, specifically the RefSeq gene track, CpG island track, and chromatin state segmentation by hidden Markov model tracks for 2 blood tissues (GM12878 and K562) (32).

Pathway analysis was performed using the missMethyl R package in order to determine whether certain biologic pathways are associated with RA clinical outcomes (33). Enrichment for Gene Ontology (GO) terms was performed using genes that contained differentially methylated CpG sites as identified from regression modeling, while taking into account the number of probes per gene. The Benjamini-Hochberg method was used to control the false discovery rate (FDR) (34).

Comparisons of DNA methylation profiles associated with each RA clinical outcome were performed in 2 ways. First, to identify cell type–specific profiles shared among RA clinical outcomes, 16 CpG sets were defined as the differentially methylated CpG sites associated with each RA clinical outcome per cell type, using the following significance thresholds: Bonferroni-adjusted $P < 0.05$, FDR $q < 0.05$, FDR $q < 0.10$, and unadjusted $P < 0.05$. Statistical significance thresholds were varied in order to capture DNA methylation differences that were smaller in magnitude but consistent across multiple RA clinical outcomes or across multiple cell types. Second, to identify DNA methylation profiles shared among RA clinical outcomes regardless of cell type, 4 CpG sets were defined as the differentially methylated CpG sites associated with each RA clinical outcome in any cell type at the same thresholds of statistical significance. The pairwise overlap between CpG sets was computed as a count (total number of CpG sites shared between 2 CpG sets) and as a shared percentage (proportion of CpG sites in one CpG set that were also found in a second CpG set).

RESULTS

Disease activity. Genome-wide analyses comparing cases with active disease (CDAI >2.8; categorized as low/minimal, moderate, and high/severe disease activity) to cases with disease in remission (CDAI ≤2.8) identified 27 CpG sites (14 hypermethylated and 13 hypomethylated) associated with active disease (Bonferroni-adjusted $P < 0.05$), independently of any history of smoking, medication use, and disease duration (Supplementary Figure 1 and Supplementary Table 1, available on the *Arthritis & Rheumatology* web site at http://onlinelibrary.wiley.com/doi/10.1002/art.40408/abstract). We identified 1 statistically significant DMR containing 11 CpG sites on chromosome 10 (Figure 1A). This region is hypomethylated in cases with active disease compared to those with disease in remission in both CD14+ monocytes and naive CD4+ T cells, and it is located in the 5′ region of cytochrome P450 2E1 (*CYP2E1*).

Erosive disease. Genome-wide assessment of differential methylation associated with erosive disease identified 84 CpG sites (10 hypermethylated and 74 hypomethylated; Bonferroni-adjusted $P < 0.05$) that were independent of any history of smoking, medication use, and disease duration (Supplementary Figure 2 and Supplementary Table 2, available at http://onlinelibrary.wiley.com/doi/10.1002/art.40408/abstract). Most of these sites (74%) were identified in CD19+ B cells. DMR analyses identified a hypomethylated region on chromosome 6 containing 10 CpG sites that was associated with erosive disease in all 4 cell types (Figure 1B). This region overlaps with the transcription start site of dual-specificity phosphatase 22 (*DUSP22*).

RAAD score. A dose-dependent association between RAAD scores and methylation levels was identified for 89 CpG sites genome-wide (15 hypermethylated and 74 hypomethylated; Bonferroni-adjusted $P < 0.05$), independently of any history of smoking, medication use, and disease duration (Supplementary Figure 3 and Supplementary Table 3, available at http://onlinelibrary.wiley.com/doi/10.1002/art.40408/abstract). Most of these CpG sites were differentially methylated only in CD14+ monocytes, with 1 CpG (cg06355652) hypomethylated in both CD14+ monocytes and naive CD4+ T cells. DMR analyses did not yield significant associations with RAAD scores.

Modified Sharp score. A total of 168 CpG sites (139 hypermethylated and 29 hypomethylated) demonstrated a dose-dependent association with the modified

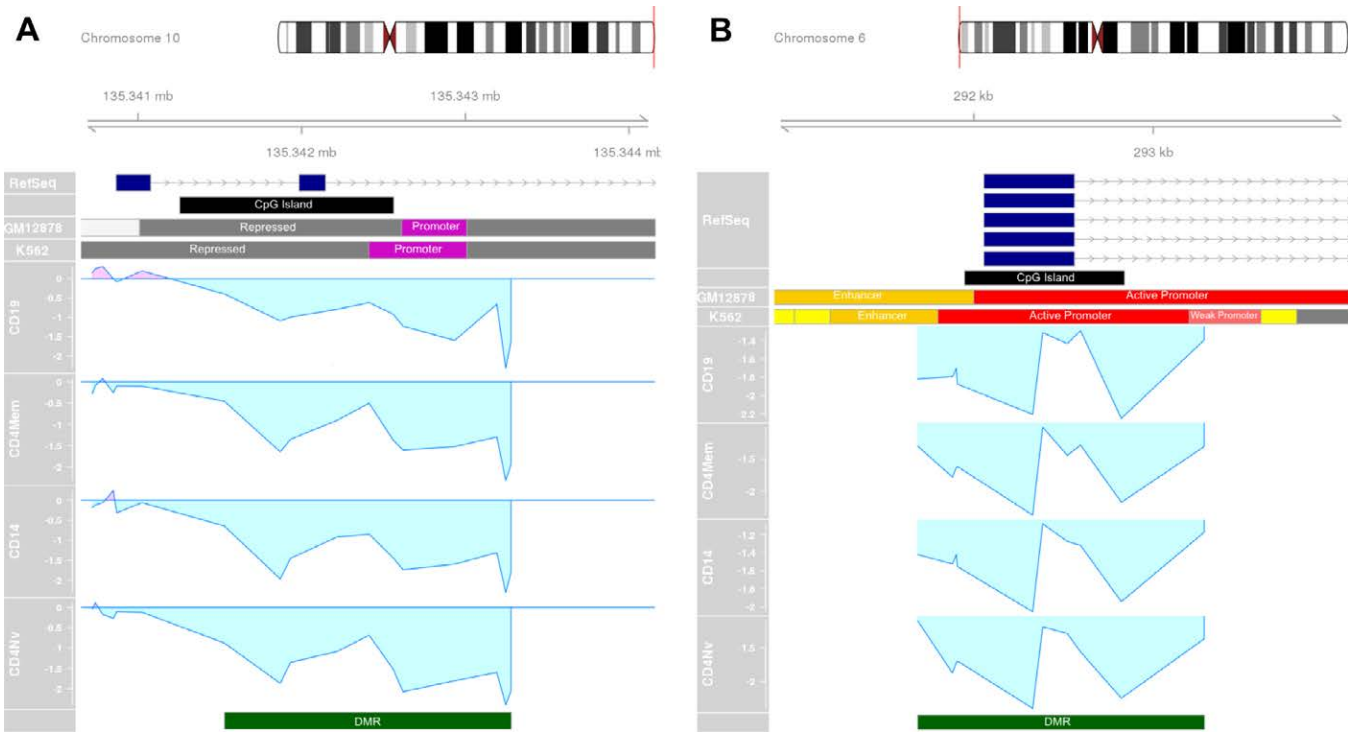

Figure 1. Association between hypomethylation of differentially methylated regions (DMRs) at promoter regions and rheumatoid arthritis clinical outcomes. Methylation differences between active and inactive disease (**A**) or between erosive and nonerosive disease (**B**) are plotted over genomic intervals, with the DMR demarcated in green. Gene positions are denoted in purple and CpG islands in black. Red/pink regions represent promoter regions, orange/yellow regions represent enhancer regions, and gray regions represent polycomb-repressed chromatin in GM12878 and K562 cell types. The DMR on chromosome 10 associated with active disease in CD14+ monocytes and CD4+ naive T cells overlaps with the *CYP2E1* promoter (**A**). The DMR on chromosome 6 associated with erosive disease in all 4 immune cell types overlaps with the *DUSP22* promoter region (**B**).

Sharp score (Bonferroni-adjusted $P < 0.05$), independently of any history of smoking, medication use, and disease duration (Supplementary Figure 4 and Supplementary Table 4, available at http://onlinelibrary.wiley.com/doi/10.1002/art.40408/abstract). Six CpG sites were differentially methylated in the same direction across multiple cell types. No regions of differential methylation were associated with the modified Sharp score after correcting for multiple hypothesis testing.

Comparison of DNA methylation profiles among RA clinical outcomes. In order to identify CpG sites associated with multiple RA clinical outcomes, we performed intersections of CpG sets identified from the previous analyses where each RA clinical outcome was treated separately. Methylation profiles observed in the current study were largely unique to specific RA clinical outcomes and to individual cell types (Figure 2A). The vast majority of CpG sites were associated with only 1 RA clinical outcome and were differentially methylated in only 1 cell type. Varying the statistical significance threshold did not change our findings (Supplementary Figures 5A–C, available at http://onlinelibrary.wiley.com/doi/10.1002/art.40408/abstract). Pooling CpG sites across cell types for an RA outcome also did not reveal any sets of CpG sites that were differentially methylated across multiple RA clinical outcomes (Figure 2B and Supplementary Figure 6, available at http://onlinelibrary.wiley.com/doi/10.1002/art.40408/abstract).

Pathway analyses for RA clinical outcomes. Pathway analysis of differentially methylated genes associated with disease activity identified enrichment of 32 GO terms (FDR $q < 0.05$), as summarized in Supplementary Table 5 (available at http://onlinelibrary.wiley.com/doi/10.1002/art.40408/abstract). Only CpG sites that were differentially methylated in naive CD4+ T cells were enriched for GO terms. The top enriched pathways suggest dysregulation of the innate immune response: positive regulation of interferon-γ (IFNγ) production, negative regulation of natural killer cell–mediated cytotoxicity, and antigen presentation (Table 2).

Pathway analysis of differentially methylated genes associated with the modified Sharp score

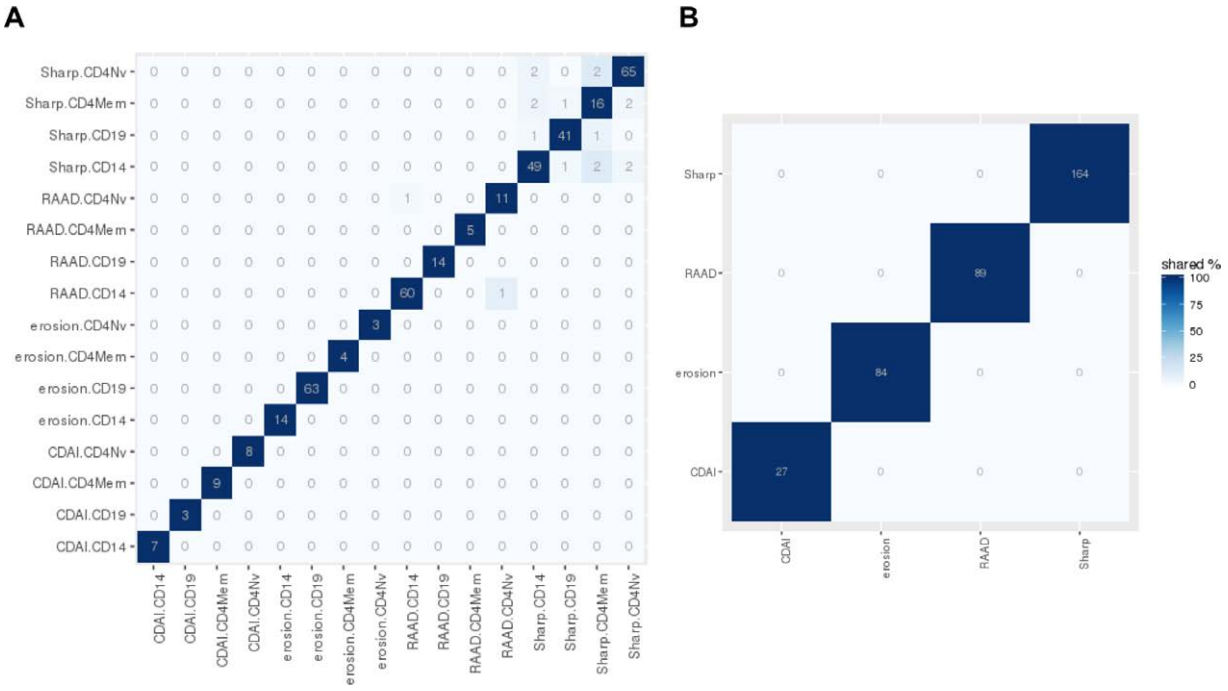

Figure 2. CpG sites associated with rheumatoid arthritis (RA) clinical outcomes are specific to outcome and to cell type. The shared percentage reflects the proportion of CpG sites identified in each row of the CpG set that were also identified in each column of the CpG set using a significance threshold of Bonferroni-adjusted $P < 0.05$. The value in each cell reflects the number of CpG sites in the intersection of row and column CpG sets. Values on the diagonal reflect the total number of differentially methylated sites for that outcome and cell type. **A,** Similarity of RA clinical outcomes by CpG methylation, keeping cell types separate. **B,** Similarity of RA clinical outcomes by CpG methylation, pooling cell types together at a significance threshold of Bonferroni-adjusted $P < 0.05$. The following outcomes were assessed: the modified Sharp score, the Rheumatoid Arthritis Articular Damage (RAAD) score, erosive disease (erosion), and the Clinical Disease Activity Index (CDAI) score. CD4Nv = CD4+ naive T cells; CD4Mem = CD4+ memory T cells. Color figure can be viewed in the online issue, which is available at http://onlinelibrary.wiley.com/doi/10.1002/art.40408/abstract.

identified enrichment of 9 GO terms (FDR q < 0.05), as summarized in Supplementary Table 6 (available at http://onlinelibrary.wiley.com/doi/10.1002/art.40408/abstract). The results suggest that dysregulation of voltage-gated calcium-channel transport and preganglionic parasympathetic fiber development in CD14+ monocytes plays a role in the development of radiographic erosions as measured by the modified Sharp score (Table 2).

History of smoking. Across all regression models, a total of 154 CpG sites (44 hypermethylated and 110 hypomethylated) showed differential methylation associated with any history of smoking (Bonferroni-adjusted $P < 0.05$), independently of all other covariates (Figure 3). The results are summarized in Supplementary Table 7 (available at http://onlinelibrary.wiley.com/doi/10.1002/art.40408/abstract). The association between smoking and

Table 2. Top GO pathways significantly enriched for associations with rheumatoid arthritis clinical outcomes*

GO accession no.	Group/term	*P*	Cell type	No. of genes in group	Differentially methylated genes in group
Active disease					
GO:0032729	Positive regulation of IFNγ production	3.55×10^{-7}	CD4 naive	61	*WNT5A*, *LTA*, *HLA–A*
GO:0045953	Negative regulation of natural killer cell cytotoxicity	7.82×10^{-6}	CD4 naive	10	*HLA–A*, *TAP1*
GO:0002484	Antigen presentation and presentation of endogenous peptide antigen via MHC class I via ER pathway	7.08×10^{-6}	CD4 naive	9	*HLA–A*, *TAP1*
Modified Sharp score					
GO:0034762	Regulation of transmembrane transport	1.81×10^{-5}	CD14	424	*CACNB2*, *KCNJ6*, *ANO1*, *CACNA1H*, *CACNA1G*, *CTTNBP2NL*
GO:0021783	Preganglionic parasympathetic fiber development	1.18×10^{-5}	CD14	16	*NAV2*, *PLXNA4*, *NRP1*

* GO = Gene Ontology; IFNγ = interferon-γ; MHC = major histocompatibility complex; ER = endoplasmic reticulum.

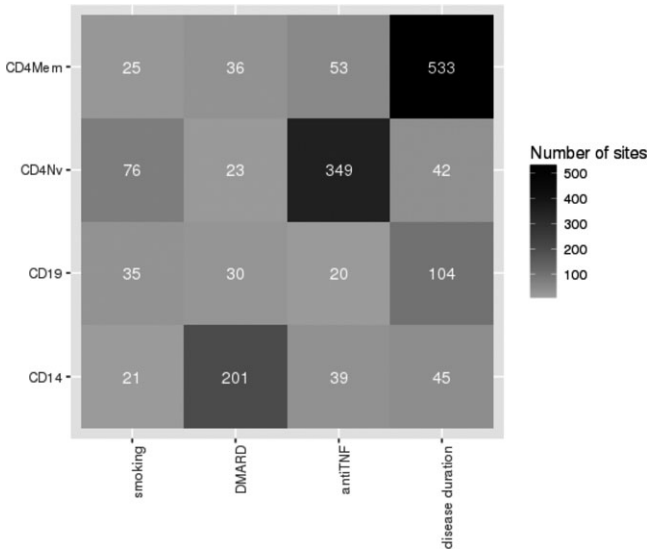

Figure 3. Summary of covariate analyses. Values represent the number of CpG sites whose methylation is associated with that covariate (columns) in that cell type (rows). CpG sites were included if they were significantly differentially methylated in any regression model. Effects of medication and disease duration are cell type–specific. Covariates were any history of smoking, treatment with a disease-modifying antirheumatic drug (DMARD), treatment with an anti–tumor necrosis factor (anti-TNF) agent, and duration of disease. CD4Mem = CD4+ memory T cells; CD4Nv = CD4+ naive T cells.

DNA methylation was observed for all cell types and for all RA clinical outcomes; ~50% of associated CpG sites were present in naive CD4+ T cells. No regions of differential methylation or enrichment for GO terms were significantly associated with smoking.

DMARD treatment. Results from regression modeling demonstrated evidence of association between DMARD treatment and DNA methylation for 285 CpG sites (250 hypermethylated and 35 hypomethylated; Bonferroni-adjusted $P < 0.05$), independently of all other covariates (Figure 3). The results are summarized in Supplementary Table 8 (available at http://onlinelibrary.wiley.com/doi/10.1002/art.40408/abstract). The majority of CpG sites (71%) were identified in the CD14+ monocyte population. Results from regression models for the modified Sharp score had the highest proportion of CpG sites associated with DMARD treatment (38%). No regions of differential methylation or enrichment for GO terms were associated with DMARD treatment.

Anti-TNF treatment. A total of 451 CpG sites (407 hypermethylated and 44 hypomethylated) had methylation differences associated with anti-TNF treatment (Bonferroni-adjusted $P < 0.05$), independently of all other covariates (Figure 3). The results are summarized in Supplementary Table 9 (available at http://onlinelibrary.wiley.com/doi/10.1002/art.40408/abstract). A majority of this signal was identified in naive CD4+ T cells (77%) and was enriched for "homophilic cell adhesion via plasma membrane adhesion molecules" (GO term 0007156; $P = 2.80 \times 10^{-8}$).

Disease duration. Associations between disease duration and DNA methylation were observed for 718 CpG sites (188 hypermethylated and 530 hypomethylated; Bonferroni-adjusted $P < 0.05$), which was independent of all other covariates (Figure 3). The results are summarized in Supplementary Table 10 (available at http://onlinelibrary.wiley.com/doi/10.1002/art.40408/abstract). DNA methylation levels were the most affected in memory CD4+ T cells (74%), which also showed enrichment for "homophilic cell adhesion via plasma membrane adhesion molecules" (GO term 0007156; $P = 1.53 \times 10^{-8}$).

DISCUSSION

In this study of DNA methylation in sorted immune cell types, we identified methylation profiles associated with clinical outcomes of RA. Our findings indicate that the profiles were highly specific for each clinical outcome and for individual cell types. We also found that medication use and disease duration at the time of blood draw were significantly associated with DNA methylation in specific cell types.

We identified a region of 11 hypomethylated CpG sites near the transcription start site of *CYP2E1* associated with active disease, as indicated by the CDAI score. A multivariate hidden Markov model trained on histone modifications observed in chromatin immunoprecipitation sequencing experiments performed on 2 blood samples predicts this region to be a promoter, suggesting that CYP2E1 expression is elevated in the monocytes and naive T cells of patients with active disease (35,36). CYP2E1 is a member of the cytochrome P450 enzyme family and is responsible for the metabolism of exogenous substrates such as nicotine, ethanol, acetaminophen, and aspartame (37). Expression of *CYP2E1* is induced by lipopolysaccharide and interleukin-4 (IL-4) in human astrocytes and hepatocytes and is regulated by the oxidative stress pathway in monocytes, implying some immune function (38,39). Interestingly, alcohol consumption has been linked to impaired priming of CD4+ T cells by dendritic cells and to the production of autoantibodies against CYP2E1 (40,41). While the identified DMR reflects the independent association between active disease and DNA methylation after accounting for any history of smoking and current medication use, we were unable to investigate other environmental or dietary exposures, such as alcohol consumption, that might contribute to the methylation of the *CYP2E1* promoter.

We also identified a region of 10 hypomethylated CpGs near the transcription start site of *DUSP22* that was associated with erosive disease. This region overlaps with an active promoter chromatin state in blood tissues and was differentially methylated in all 4 cell types we examined (36). DUSP22 is a protein phosphatase involved in MAPK signaling, and it appears to lie at the intersection of several immune signaling pathways, including those mediated through the T cell antigen receptor, IL-6 leukemia-inhibiting factor, and the estrogen receptor (42,43). A study of the DUSP22-knockout mouse showed autoimmune tendencies: splenic T cells had stronger responses to anti-CD3 stimulation, serum levels of proinflammatory cytokines and autoantibodies were higher, and symptoms in an experimental autoimmune encephalomyelitis mouse model developed faster and were more severe (44). Hypomethylation observed among RA cases with erosive disease in the current study should lead to increased messenger RNA (mRNA) expression of *DUSP22.* Further studies are needed to confirm the relationship between methylation and expression and to understand the dynamics between mRNA expression and protein levels in order to understand how *DUSP22* might contribute to erosive disease.

Examination of the differentially methylated CpG sites using Gene Ontology identified cellular processes underlying disease activity and severity. Disease activity was related to differential methylation of CpG sites in genes involved in the IFNγ signaling and antigen-presentation pathways; the finding that these effects were observed only in naive CD4+ T cells suggests that this population is biased toward Th1 differentiation. In addition, pathway analysis of the CpG sites associated with the modified Sharp score showed dysregulation of transmembrane transport and preganglionic parasympathetic fiber development in CD14+ monocytes. Previous studies of cardiovascular autonomic nervous system function in RA patients led to the hypothesis that the equilibrium between the opposing effects of the sympathetic and parasympathetic nervous systems has been disrupted (45). Our results support this theory and further highlight the role played by the autonomic nervous system as a modulator of immune function and a possible target for future RA therapies.

Much of the differential methylation observed for RA clinical outcomes was present in CD14+ monocytes and naive CD4+ T cells, which further highlights the role of these immune subpopulations in RA pathogenesis and disease progression. Treatment of normal synovial fibroblasts with an inhibitor of DNA methylation was able to reproduce the hypomethylation and activated phenotype observed in RA synovial fibroblasts (46). A previous study of RA patients reported higher frequencies of CD14+CD16+ circulating monocytes in patients with active disease, and response to drug therapy was correlated with changes in these frequencies (47,48). These circulating monocytes can migrate into the synovial joint, where they can recruit lymphocytes to the inflamed joint and drive the polarization of CD4+ helper T cells (49). Furthermore, activated T cells from the peripheral immune system are able to stimulate the differentiation of monocytes into osteoclasts, thereby contributing to bone damage and production of radiographic lesions (50). Thus, the interactions between monocytes and T cells in both peripheral blood and synovial joints may prove interesting for therapeutics that target disease activity and progression.

RA is a heterogeneous disease with symptom presentations and prognoses that differ between patients. Therefore, it may be important to consider various measures of disease activity and severity in order to identify the different biologic mechanisms that underlie disease heterogeneity. We analyzed 4 RA clinical outcome measures: disease activity as measured by the CDAI score, erosive disease, the RAAD score, and the modified Sharp score. Each of these 4 measures captures different aspects of RA disease progression and is associated with different risk factors and prognoses. By analyzing each measure separately, we were able to investigate the association between RA disease heterogeneity and DNA methylation and to identify profiles specific to each clinical outcome. We found that DNA methylation profiles were highly specific to each clinical outcome measure, suggesting that different biologic processes drive different measures of disease activity and severity. These results can help in the development of new therapies targeted toward specific manifestations and thus aid in the generation of patient-specific treatment plans.

Our previous analysis in the same RA patient population identified predominantly hypomethylated candidate CpG sites in naive and memory CD4+ T cells from the patients as compared to healthy controls (22). Comparison of the results from the current study of clinical phenotypes with the previous RA case–control study did not reveal significant overlap of differential methylation. These findings suggest that DNA methylation changes relevant to disease susceptibility in RA are largely distinct from those that contribute to disease severity and phenotypic expression.

The strengths of our study include the large sample size and selection of female RA cases to minimize confounding by sex. By sorting PBMCs before performing DNA methylation profiling, we were able to avoid major confounding by cell-type heterogeneity and to analyze cell-specific effects for each RA clinical outcome. Using

genome-wide SNP data, we were also able to compute principal components reflecting genetic ancestry, further avoiding potential confounding by population stratification. Our analyses were also able to demonstrate associations between DNA methylation and any history of smoking, medication use, and disease duration at the time of blood draw.

Limitations of our study include its cross-sectional nature, which limited our ability to determine causality or temporality of these DNA methylation differences relative to disease progression. Our RA patient sample consisted only of women of European ancestry, thus restricting the ability to extrapolate our results beyond this population. DNA methylation profiling was performed on microarray chips, and imputation or pyrosequencing must be performed to assess methylation at CpG sites not assayed on the chip. Last, we examined DNA from peripheral blood cells and not from cells in the synovial joint. While circulating immune cells can be recruited into the joint compartment from the periphery, we may not be capturing local biologic processes that drive joint damage.

In summary, we have shown that different measures of RA disease activity and severity are associated with specific DNA methylation profiles and that these methylation differences are also highly cell type–specific. Our results further support the premise that genetic, as well as epigenetic, variations may drive clinical heterogeneity in RA.

AUTHOR CONTRIBUTIONS

All authors were involved in drafting the article or revising it critically for important intellectual content, and all authors approved the final version to be published. Dr. Criswell had full access to all of the data in the study and takes responsibility for the integrity of the data and the accuracy of the data analysis.

Study conception and design. Mok, Rhead, Holingue, Barcellos, Criswell.

Acquisition of data. Shao, H. L. Quach, D. Quach, Sinclair, Graf, Imboden, Link, Harrison, Chernitskiy, Barcellos, Criswell.

Analysis and interpretation of data. Mok, Rhead, Holingue, Barcellos, Criswell.

REFERENCES

1. Symmons DP. Epidemiology of rheumatoid arthritis: determinants of onset, persistence and outcome. Best Pract Res Clin Rheumatol 2002;16:707–22.
2. Gregersen PK, Silver J, Winchester RJ. The shared epitope hypothesis: an approach to understanding the molecular genetics of susceptibility to rheumatoid arthritis. Arthritis Rheum 1987; 30:1205–13.
3. Raychaudhuri S, Sandor C, Stahl EA, Freudenberg J, Lee H, Jia X, et al. Five amino acids in three HLA proteins explain most of the association between MHC and seropositive rheumatoid arthritis. Nat Genet 2012;44:291–6.
4. Mackie SL, Taylor JC, Martin SG, YEAR Consortium, UKRAG Consortium, Wordsworth P, et al. A spectrum of susceptibility to rheumatoid arthritis within HLA-DRB1: stratification by autoantibody status in a large UK population. Genes Immun 2012;13:120–8.
5. Ehrlich M, Lacey M. DNA methylation and differentiation: silencing, upregulation and modulation of gene expression. Epigenomics 2013;5:553–68.
6. Henckel A, Nakabayashi K, Sanz LA, Feil R, Hata K, Arnaud P. Histone methylation is mechanistically linked to DNA methylation at imprinting control regions in mammals. Hum Mol Genet 2009;18:3375–83.
7. Trerotola M, Relli V, Simeone P, Alberti S. Epigenetic inheritance and the missing heritability. Hum Genomics 2015;9:17.
8. Pacchierotti F, Spanò M. Environmental impact on DNA methylation in the germline: state of the art and gaps of knowledge. Biomed Res Int 2015;2015:123484.
9. Liu Y, Aryee MJ, Padyukov L, Fallin MD, Hesselberg E, Runarsson A, et al. Epigenome-wide association data implicate DNA methylation as an intermediary of genetic risk in rheumatoid arthritis. Nat Biotechnol 2013;31:142–7.
10. Nile CJ, Read RC, Akil M, Duff GW, Wilson AG. Methylation status of a single CpG site in the IL6 promoter is related to IL6 messenger RNA levels and rheumatoid arthritis. Arthritis Rheum 2008;58:2686–93.
11. Glossop JR, Emes RD, Nixon NB, Haworth KE, Packham JC, Dawes PT, et al. Genome-wide DNA methylation profiling in rheumatoid arthritis identifies disease-associated methylation changes that are distinct to individual T- and B-lymphocyte populations. Epigenetics 2014;9:1228–37.
12. Nakano K, Whitaker JW, Boyle DL, Wang W, Firestein GS. DNA methylome signature in rheumatoid arthritis. Ann Rheum Dis 2013;72:110–7.
13. De Andres MC, Perez-Pampin E, Calaza M, Santaclara FJ, Ortea I, Gomez-Reino JJ, et al. Assessment of global DNA methylation in peripheral blood cell subpopulations of early rheumatoid arthritis before and after methotrexate. Arthritis Res Ther 2015;17:233.
14. Cribbs AP, Kennedy A, Penn H, Amjadi P, Green P, Read JE, et al. Methotrexate restores regulatory T cell function through demethylation of the FoxP3 upstream enhancer in patients with rheumatoid arthritis. Arthritis Rheumatol 2015;67:1182–92.
15. Glossop JR, Nixon NB, Emes RD, Sim J, Packham JC, Mattey DL, et al. DNA methylation at diagnosis is associated with response to disease-modifying drugs in early rheumatoid arthritis. Epigenomics 2017;9:419–28.
16. Arnett FC, Edworthy SM, Bloch DA, McShane DJ, Fries JF, Cooper NS, et al. The American Rheumatism Association 1987 revised criteria for the classification of rheumatoid arthritis. Arthritis Rheum 1988;31:315–24.
17. Aletaha D, Nell VP, Stamm T, Uffmann M, Pflugbeil S, Machold K, et al. Acute phase reactants add little to composite disease activity indices for rheumatoid arthritis: validation of a clinical activity score. Arthritis Res Ther 2005;7:R796–806.
18. Ory PA. Interpreting radiographic data in rheumatoid arthritis. Ann Rheum Dis 2003;62:597–604.
19. Anderson J, Caplan L, Yazdany J, Robbins ML, Neogi T, Michaud K, et al. Rheumatoid arthritis disease activity measures: American College of Rheumatology recommendations for use in clinical practice. Arthritis Care Res (Hoboken) 2012;64:640–7.
20. Van der Heijde D, van der Helm-van Mil AH, Aletaha D, Bingham CO, Burmester GR, Dougados M, et al. EULAR definition of erosive disease in light of the 2010 ACR/EULAR rheumatoid arthritis classification criteria. Ann Rheum Dis 2013;72:479–81.
21. Zijlstra TR, Bernelot Moens HJ, Bukhari MA. The rheumatoid arthritis articular damage score: first steps in developing a clinical index of long term damage in RA. Ann Rheum Dis 2002;61:20–3.
22. Rhead B, Holingue C, Cole M, Shao X, Quach HL, Quach D, et al. Rheumatoid arthritis naive T cells share hypermethylation sites with synoviocytes. Arthritis Rheumatol 2017;69:550–9.

23. Patterson N, Price AL, Reich D. Population structure and eigenanalysis. PLoS Genet 2006;2:e190.
24. Davis S, Du P, Bilke S, Triche T Jr, Bootwalla M. methylumi: Handle Illumina methylation data. R package version 2140. 2015. URL: http://www.bioconductor.org/packages/release/bioc/html/methylumi.html.
25. Yousefi P, Huen K, Schall RA, Decker A, Elboudwarej E, Quach H, et al. Considerations for normalization of DNA methylation data by Illumina 450K BeadChip assay in population studies. Epigenetics 2013;8:1141–52.
26. Teschendorff AE, Marabita F, Lechner M, Bartlett T, Tegner J, Gomez-Cabrero D, et al. A beta-mixture quantile normalization method for correcting probe design bias in Illumina Infinium 450k DNA methylation data. Bioinformatics 2013;29:189–96.
27. Chen Y, Lemire M, Choufani S, Butcher DT, Grafodatskaya D, Zanke BW, et al. Discovery of cross-reactive probes and polymorphic CpGs in the Illumina Infinium HumanMethylation450 microarray. Epigenetics 2013;8:203–9.
28. Du P, Zhang X, Huang CC, Jafari N, Kibbe WA, Hou L, et al. Comparison of Beta-value and M-value methods for quantifying methylation levels by microarray analysis. BMC Bioinformatics 2010;11:587.
29. Du P, Kibbe WA, Lin SM. lumi: a pipeline for processing Illumina microarray. Bioinformatics 2008;24:1547–8.
30. Ritchie ME, Phipson B, Wu D, Hu Y, Law CW, Shi W, et al. limma powers differential expression analyses for RNA-sequencing and microarray studies. Nucleic Acids Res 2015;43:e47.
31. Jaffe AE, Murakami P, Lee H, Leek JT, Fallin MD, Feinberg AP, et al. Bump hunting to identify differentially methylated regions in epigenetic epidemiology studies. Int J Epidemiol 2012;41:200–9.
32. Ernst J, Kheradpour P, Mikkelsen TS, Shoresh N, Ward LD, Epstein CB, et al. Mapping and analysis of chromatin state dynamics in nine human cell types. Nature 2011;473:43–9.
33. Phipson B, Maksimovic J, Oshlack A. missMethyl: an R package for analysing methylation data from Illumina's HumanMethylation450 platform. Bioinformatics 2016;32:286–8.
34. Benjamini Y, Hochberg Y. Controlling the false discovery rate: a practical and powerful approach to multiple testing. J R Statisitical Soc Ser B 1995;57:289–300.
35. Ernst J, Kellis M. Discovery and characterization of chromatin states for systematic annotation of the human genome. Nat Biotechnol 2010;28:817–25.
36. Consortium RE, Kundaje A, Meuleman W, Ernst J, Bilenky M, Yen A, et al. Integrative analysis of 111 reference human epigenomes. Nature 2015;518:317–30.
37. Lieber CS. Microsomal ethanol-oxidizing system (MEOS): the first 30 years (1968–1998): a review. Alcohol Clin Exp Res 1999; 23:991–1007.
38. Kelicen P, Tindberg N. Lipopolysaccharide induces CYP2E1 in astrocytes through MAP kinase kinase-3 and C/EBP/β and -δ. J Biol Chem 2004;279:15734–42.
39. Jin M, Ande A, Kumar A, Kumar S. Regulation of cytochrome P450 2e1 expression by ethanol: role of oxidative stress-mediated pkc/jnk/sp1 pathway. Cell Death Dis 2013;4:e554.
40. Mandrekar P, Catalano D, Dolganiuc A, Kodys K, Szabo G. Inhibition of myeloid dendritic cell accessory cell function and induction of T cell anergy by alcohol correlates with decreased IL-12 production. J Immunol 2004;173:3398–407.
41. Albano E. Free radical mechanisms in immune reactions associated with alcoholic liver disease. Free Radic Biol Med 2002;32:110–4.
42. Alonso A, Merlo JJ, Na S, Kholod N, Jaroszewski L, Kharitonenkov A, et al. Inhibition of T cell antigen receptor signaling by VHR-related MKPX (VHX), a new dual specificity phosphatase related to VH1 related (VHR). J Biol Chem 2002;277:5524–8.
43. Sekine Y, Ikeda O, Hayakawa Y, Tsuji S, Imoto S, Aoki N, et al. DUSP22/LMW-DSP2 regulates estrogen receptor-α-mediated signaling through dephosphorylation of Ser-118. Oncogene 2007; 26:6038–49.
44. Li JP, Yang CY, Chuang HC, Lan JL, Chen DY, Chen YM, et al. The phosphatase JKAP/DUSP22 inhibits T-cell receptor signalling and autoimmunity by inactivating Lck. Nat Commun 2014;5:3618.
45. Koopman F, Stoof S. Restoring the balance of the autonomic nervous system as an innovative approach to the treatment of rheumatoid arthritis. Mol Med 2011;17:1.
46. Karouzakis E, Gay RE, Michel BA, Gay S, Neidhart M. DNA hypomethylation in rheumatoid arthritis synovial fibroblasts. Arthritis Rheum 2009;60:3613–22.
47. Kawanaka N, Yamamura M, Aita T, Morita Y, Okamoto A, Kawashima M, et al. CD14+, CD16+ blood monocytes and joint inflammation in rheumatoid arthritis. Arthritis Rheum 2002; 46:2578–86.
48. Amoruso A, Sola D, Rossi L, Obeng JA, Fresu LG, Sainaghi PP, et al. Relation among anti-rheumatic drug therapy, $CD14^+CD16^+$ blood monocytes and disease activity markers (DAS28 and US7 scores) in rheumatoid arthritis: a pilot study. Pharmacol Res 2016; 107:308–14.
49. Roberts CA, Dickinson AK, Taams LS. The interplay between monocytes/macrophages and $CD4^+$ T cell subsets in rheumatoid arthritis. Front Immunol 2015;6:1–19.
50. Kotake S, Udagawa N, Hakoda M, Mogi M, Yano K, Tsuda E, et al. Activated human T cells directly induce osteoclastogenesis from human monocytes: possible role of T cells in bone destruction in rheumatoid arthritis patients. Arthritis Rheum 2001;44: 1003–12.

The American College of Rheumatology is Launching an Open Access Journal and Seeking an Editor-in-Chief

DOI 10.1002/art.40510

The American College of Rheumatology is excited to announce that a third official journal of the College is scheduled to be launched in January 2019. This journal will be entirely open access. More details will be coming soon, as will the call for applications for the position of Editor-in-Chief. ACR/ARHP members who have current or past experience on the editorial board of *Arthritis & Rheumatology* or *Arthritis Care & Research* (Associate Editor level or higher) are invited to apply.

23. Patterson N, Price AL, Reich D. Population structure and eigenanalysis. PLoS Genet 2006;2:e190.
24. Davis S, Du P, Bilke S, Triche T Jr, Bootwalla M. methylumi: Handle Illumina methylation data. R package version 2140. 2015. URL: http://www.bioconductor.org/packages/release/bioc/html/methylumi.html.
25. Yousefi P, Huen K, Schall RA, Decker A, Elboudwarej E, Quach H, et al. Considerations for normalization of DNA methylation data by Illumina 450K BeadChip assay in population studies. Epigenetics 2013;8:1141–52.
26. Teschendorff AE, Marabita F, Lechner M, Bartlett T, Tegner J, Gomez-Cabrero D, et al. A beta-mixture quantile normalization method for correcting probe design bias in Illumina Infinium 450k DNA methylation data. Bioinformatics 2013;29:189–96.
27. Chen Y, Lemire M, Choufani S, Butcher DT, Grafodatskaya D, Zanke BW, et al. Discovery of cross-reactive probes and polymorphic CpGs in the Illumina Infinium HumanMethylation450 microarray. Epigenetics 2013;8:203–9.
28. Du P, Zhang X, Huang CC, Jafari N, Kibbe WA, Hou L, et al. Comparison of Beta-value and M-value methods for quantifying methylation levels by microarray analysis. BMC Bioinformatics 2010;11:587.
29. Du P, Kibbe WA, Lin SM. lumi: a pipeline for processing Illumina microarray. Bioinformatics 2008;24:1547–8.
30. Ritchie ME, Phipson B, Wu D, Hu Y, Law CW, Shi W, et al. limma powers differential expression analyses for RNA-sequencing and microarray studies. Nucleic Acids Res 2015;43:e47.
31. Jaffe AE, Murakami P, Lee H, Leek JT, Fallin MD, Feinberg AP, et al. Bump hunting to identify differentially methylated regions in epigenetic epidemiology studies. Int J Epidemiol 2012;41:200–9.
32. Ernst J, Kheradpour P, Mikkelsen TS, Shoresh N, Ward LD, Epstein CB, et al. Mapping and analysis of chromatin state dynamics in nine human cell types. Nature 2011;473:43–9.
33. Phipson B, Maksimovic J, Oshlack A. missMethyl: an R package for analysing methylation data from Illumina's HumanMethylation450 platform. Bioinformatics 2016;32:286–8.
34. Benjamini Y, Hochberg Y. Controlling the false discovery rate: a practical and powerful approach to multiple testing. J R Statisitical Soc Ser B 1995;57:289–300.
35. Ernst J, Kellis M. Discovery and characterization of chromatin states for systematic annotation of the human genome. Nat Biotechnol 2010;28:817–25.
36. Consortium RE, Kundaje A, Meuleman W, Ernst J, Bilenky M, Yen A, et al. Integrative analysis of 111 reference human epigenomes. Nature 2015;518:317–30.
37. Lieber CS. Microsomal ethanol-oxidizing system (MEOS): the first 30 years (1968–1998): a review. Alcohol Clin Exp Res 1999; 23:991–1007.
38. Kelicen P, Tindberg N. Lipopolysaccharide induces CYP2E1 in astrocytes through MAP kinase kinase-3 and C/EBP/β and -δ. J Biol Chem 2004;279:15734–42.
39. Jin M, Ande A, Kumar A, Kumar S. Regulation of cytochrome P450 2e1 expression by ethanol: role of oxidative stress-mediated pkc/jnk/sp1 pathway. Cell Death Dis 2013;4:e554.
40. Mandrekar P, Catalano D, Dolganiuc A, Kodys K, Szabo G. Inhibition of myeloid dendritic cell accessory cell function and induction of T cell anergy by alcohol correlates with decreased IL-12 production. J Immunol 2004;173:3398–407.
41. Albano E. Free radical mechanisms in immune reactions associated with alcoholic liver disease. Free Radic Biol Med 2002;32:110–4.
42. Alonso A, Merlo JJ, Na S, Kholod N, Jaroszewski L, Kharitonenkov A, et al. Inhibition of T cell antigen receptor signaling by VHR-related MKPX (VHX), a new dual specificity phosphatase related to VH1 related (VHR). J Biol Chem 2002;277:5524–8.
43. Sekine Y, Ikeda O, Hayakawa Y, Tsuji S, Imoto S, Aoki N, et al. DUSP22/LMW-DSP2 regulates estrogen receptor-α-mediated signaling through dephosphorylation of Ser-118. Oncogene 2007; 26:6038–49.
44. Li JP, Yang CY, Chuang HC, Lan JL, Chen DY, Chen YM, et al. The phosphatase JKAP/DUSP22 inhibits T-cell receptor signalling and autoimmunity by inactivating Lck. Nat Commun 2014;5:3618.
45. Koopman F, Stoof S. Restoring the balance of the autonomic nervous system as an innovative approach to the treatment of rheumatoid arthritis. Mol Med 2011;17:1.
46. Karouzakis E, Gay RE, Michel BA, Gay S, Neidhart M. DNA hypomethylation in rheumatoid arthritis synovial fibroblasts. Arthritis Rheum 2009;60:3613–22.
47. Kawanaka N, Yamamura M, Aita T, Morita Y, Okamoto A, Kawashima M, et al. CD14+, CD16+ blood monocytes and joint inflammation in rheumatoid arthritis. Arthritis Rheum 2002; 46:2578–86.
48. Amoruso A, Sola D, Rossi L, Obeng JA, Fresu LG, Sainaghi PP, et al. Relation among anti-rheumatic drug therapy, $CD14^+CD16^+$ blood monocytes and disease activity markers (DAS28 and US7 scores) in rheumatoid arthritis: a pilot study. Pharmacol Res 2016; 107:308–14.
49. Roberts CA, Dickinson AK, Taams LS. The interplay between monocytes/macrophages and $CD4^+$ T cell subsets in rheumatoid arthritis. Front Immunol 2015;6:1–19.
50. Kotake S, Udagawa N, Hakoda M, Mogi M, Yano K, Tsuda E, et al. Activated human T cells directly induce osteoclastogenesis from human monocytes: possible role of T cells in bone destruction in rheumatoid arthritis patients. Arthritis Rheum 2001;44: 1003–12.

The American College of Rheumatology is Launching an Open Access Journal and Seeking an Editor-in-Chief

DOI 10.1002/art.40510

The American College of Rheumatology is excited to announce that a third official journal of the College is scheduled to be launched in January 2019. This journal will be entirely open access. More details will be coming soon, as will the call for applications for the position of Editor-in-Chief. ACR/ARHP members who have current or past experience on the editorial board of *Arthritis & Rheumatology* or *Arthritis Care & Research* (Associate Editor level or higher) are invited to apply.

ARTHRITIS & RHEUMATOLOGY
Vol. 70, No. 4, April 2018, pp 537–546
DOI 10.1002/art.40400

Differences in Safety of Nonsteroidal Antiinflammatory Drugs in Patients With Osteoarthritis and Patients With Rheumatoid Arthritis

A Randomized Clinical Trial

Daniel H. Solomon,[1] M. Elaine Husni,[2] Katherine E. Wolski,[2] Lisa M. Wisniewski,[2] Jeffrey S. Borer,[3] David Y. Graham,[4] Peter Libby,[1] A. Michael Lincoff,[2] Thomas F. Lüscher,[5] Venu Menon,[2] Neville D. Yeomans,[6] Qiuqing Wang,[2] Weihang Bao,[7] Manuela F. Berger,[7] and Steven E. Nissen,[2] on behalf of the PRECISION Trial Investigators

Objective. **To determine the relative risks of cardiovascular (CV), gastrointestinal (GI), and renal adverse events during long-term treatment with celecoxib, compared with ibuprofen and naproxen, in patients with osteoarthritis (OA) and patients with rheumatoid arthritis (RA).**

Methods. **A total of 24,081 patients with OA or RA who had a moderate or high risk for CV disease were enrolled internationally into a double-blind randomized controlled trial. Interventions included celecoxib at a dosage of 100–200 mg twice daily, ibuprofen at a dosage of 600–800 mg 3 times daily, or naproxen at a dosage of 375–500 mg twice daily. The main outcomes were the first occurrence of a major adverse CV event, GI event, or renal event, and mortality.**

Results. **In the subgroup of patients with OA, the risk of a major adverse CV event was significantly reduced when celecoxib was compared with ibuprofen (hazard ratio [HR] 0.84, 95% confidence interval [95% CI] 0.72–0.99), but no significant difference was observed when celecoxib was compared with naproxen. In the RA subgroup, comparisons of celecoxib versus ibuprofen and celecoxib versus naproxen for the risk of major adverse CV events revealed HRs of 1.06 (95% CI 0.69–1.63) and 1.22 (95% CI 0.78–1.92), respectively. In the OA subgroup, comparisons of celecoxib versus ibuprofen for the risk of GI events showed an HR of 0.68 (95% CI 0.51–0.91), and a comparison of celecoxib versus naproxen showed an HR of 0.73 (95% CI 0.55–0.98). Duplicate comparisons in patients with RA revealed HRs of 0.48 (95% CI 0.22–1.07) and 0.54 (95% CI 0.24–1.24), respectively. In patients with OA, a comparison of celecoxib versus ibuprofen for the risk of renal events showed an HR of 0.58 (95% CI 0.40–0.82). In patients with**

ClinicalTrials.gov identifier: NCT00346216.

The PRECISION trial and these analyses were funded by Pfizer.

[1]Daniel H. Solomon, MD, MPH, Peter Libby, MD: Brigham and Women's Hospital, Harvard Medical School, Boston, Massachusetts; [2]M. Elaine Husni, MD, MPH, Katherine E. Wolski, MPH, Lisa M. Wisniewski, RN, A. Michael Lincoff, MD, Venu Menon, MD, Qiuqing Wang, MS, Steven E. Nissen, MD: Cleveland Clinic, Cleveland, Ohio; [3]Jeffrey S. Borer, MD: State University of New York, Downstate College of Medicine, Brooklyn, New York; [4]David Y. Graham, MD: Baylor College of Medicine, Veterans Affairs Medical Center, Houston, Texas; [5]Thomas F. Lüscher, MD: Royal Brompton & Harefield Hospitals, London, UK; [6]Neville D. Yeomans, MD: Western Sydney University, Campbelltown, New South Wales, Australia; [7]Weihang Bao, PhD, Manuela F. Berger, MD: Pfizer, New York, New York.

Drs. Solomon and Husni contributed equally to this work.

Dr. Solomon has received research support from Pfizer and royalties for a peer-reviewed chapter titled *NSAIDS: Therapeutic use and variability of response in adults* in UpToDate (2017). Dr. Husni has received consulting fees and/or honoraria from AbbVie, Bristol-Myers Squibb, Amgen, UCB, Regeneron, and Janssen (less than $10,000 each) and research support from Sanofi Genzyme. Dr. Borer has received consulting fees and/or honoraria from Pfizer (more than $10,000). Dr. Graham has received consulting fees from RedHill Biopharma, BioGaia, and Takeda (less than $10,000 each) research support from RedHill Biopharma. Dr. Libby has received research support from Novartis (less than $10,000). Dr. Lincoff has received consulting fees from Novo Nordisk (more than $10,000). Dr. Lüscher has received consulting fees, speaking fees, and/or honoraria from Bayer Health Care (less than $10,000). Dr. Yeomans has received consulting fees and/or honoraria from Pfizer (less than $10,000). Drs. Bao and Berger own stock or stock options in Pfizer.

Address correspondence to M. Elaine Husni, MD, MPH, Department of Rheumatic and Immunologic Diseases, Cleveland Clinic, 9500 Euclid Avenue, Cleveland, OH 44195. E-mail: husnie@ccf.org.

Submitted for publication August 2, 2017; accepted in revised form December 12, 2017.

RA, celecoxib treatment was associated with significantly lower mortality compared with naproxen treatment (HR 0.47, 95% CI 0.25–0.88).

Conclusion. **Treatment with celecoxib at approved dosages conferred a similar or lower risk of CV, GI, and renal adverse events compared with treatment with ibuprofen or naproxen in patients with OA and patients with RA.**

Nonsteroidal antiinflammatory drugs (NSAIDs) are effective for the treatment of joint pain in patients with osteoarthritis (OA) and those with rheumatoid arthritis (RA). In the US alone, health care workers write more than 100 million NSAID prescriptions annually (1), and ~50% of patients with arthritis require daily treatment with some type of analgesic (2,3). Many pharmacologic and nonpharmacologic options exist. NSAIDs represent the most widely used medications because of their established analgesic benefit, but the relative safety across members of this drug class is less certain. Selecting the most appropriate analgesic can challenge treating clinicians because of the variable effectiveness and safety of these agents.

Previous studies underscored the risk of cardiovascular (CV) events associated with selective cyclooxygenase 2 (COX-2) inhibitors, leading to the withdrawal of rofecoxib (4). However, controversy remained regarding the CV-related safety of the selective COX-2 inhibitor, celecoxib (5,6). In 2005, the US Food and Drug Administration (FDA) strengthened the warning for adverse CV events for all non-aspirin NSAIDs. Subsequent studies further questioned the safety of nonselective NSAIDs (7–9). In addition, the relative safety of nonselective NSAIDs associated with the relative gastrointestinal (GI) and renal safety of different NSAIDs remains poorly defined. These issues are critical for patients with OA and patients with RA, who already have a higher risk of adverse CV events compared with the general population and often experience multiple comorbidities (10,11).

Based on these concerns, Pfizer initiated a CV safety trial, the Prospective Randomized Evaluation of Celecoxib Integrated Safety versus Ibuprofen Or Naproxen (PRECISION) trial, in order to provide new, more definitive and useful information for patients, providers, and regulators about the safety of celecoxib and NSAIDs. The PRECISION trial, a global safety study among patients with OA or RA, enrolled >24,000 patients worldwide (12). The recently published results demonstrated the noninferiority of moderate doses of celecoxib compared with moderate doses of ibuprofen and naproxen with respect to CV safety based on an intent-to-treat (ITT) analysis. Furthermore, an on-treatment analysis including follow-up time while being treated with the study drug demonstrated better safety of celecoxib for GI end points compared with ibuprofen and naproxen. For renal end points, celecoxib exhibited increased safety only when compared with ibuprofen (13). However, previously published studies did not uniformly demonstrate an increased risk of adverse CV events in patients with RA receiving selective COX-2 inhibitors (14). Our group conducted analyses in the prespecified OA and RA subgroups to further define the relative CV, GI, and renal safety associated with celecoxib compared with ibuprofen and naproxen in these common types of arthritis.

PATIENTS AND METHODS

Study design and study population. Briefly, the PRECISION trial was a noninferiority trial designed to assess the risk of CV events associated with celecoxib compared with the risk associated with commonly used NSAIDs (e.g., ibuprofen and naproxen). The trial was conducted at 923 centers in the US, Canada, Australia, Brazil, Colombia, Costa Rica, Mexico, Panama, Peru, Philippines, Taiwan, Hong Kong, and Ukraine from October 2006 to April 2016. The Institutional Review Board/Independent Ethics Committee at each study site approved the trial, and all patients provided written informed consent before participating. The trial could not be performed in Europe because of restrictions placed on the prescribing of coxibs by the European Medicines Agency.

Eligible patients included those who were at least 18 years of age and had clinically diagnosed OA or RA for a duration of at least 6 months (15–17) and who required long-term daily therapy with an NSAID. Participants were required to have established CV disease or CV risk factors. These risk factors included a known history of a major adverse CV event, occlusive disease of the coronary and non-coronary arteries, a clinical diagnosis of diabetes, or evidence of CV risk based on concomitant risk factors, including age ≥65 years in women and >55 years in men, hypertension, dyslipidemia, left ventricular hypertrophy, microalbuminuria, urine protein:creatinine ratio of >2, an ankle–brachial index of <0.9, cigarette smoking, a waist-to-hip ratio of ≥0.90, and a family history of premature CV disease. Exclusion criteria included any of the following CV events within 3 months prior to enrollment: major adverse CV event, unstable angina, electrophysiologic evidence of unstable cardiac rhythm, or any major surgery; planned coronary, CV, or peripheral revascularization; New York Heart Association class III or IV heart failure (18) or known left ventricular dysfunction with an ejection fraction of ≤35%; active significant GI, hepatic, renovascular, or coagulation disorder; history of acute joint trauma; allergy or hypersensitivity to celecoxib, ibuprofen, naproxen, or aspirin; poor response to disease-modifying antirheumatic drug or oral corticosteroid treatments; and requirement for treatment with medications excluded during the course of the study. Women were excluded if they were pregnant, might become pregnant, or were lactating. Additional selection criteria are shown in Supplementary Table 1, available on the *Arthritis & Rheumatology* web site at http://onlinelibrary.wiley.com/doi/10.1002/art.40400/abstract). Details of the RA cohort are available in Supplementary Tables 2 and 3.

Table 1. Baseline characteristics of the randomized patients according to treatment*

	Osteoarthritis				Rheumatoid arthritis			
	Total (n = 21,645)	Celecoxib (n = 7,259)	Ibuprofen (n = 7,208)	Naproxen (n = 7,178)	Total (n = 2,436)	Celecoxib (n = 813)	Ibuprofen (n = 832)	Naproxen (n = 791)
Age, mean ± SD years	64 ± 9.3	63 ± 9.4	64 ± 9.3	64 ± 9.3	61 ± 9.9	59 ± 9.5	61 ± 9.9	61 ± 10.2
Female sex	13,661 (63.1)	4,566 (62.9)	4,574 (63.5)	4,521 (63.0)	1,784 (73.2)	609 (74.9)	600 (72.1)	575 (72.7)
BMI, mean ± SD kg/m^2	32.8 ± 7.3	32.8 ± 7.3	32.8 ± 7.4	32.7 ± 7.3	30.9 ± 7.1	31.0 ± 7.4	30.6 ± 6.8	31.0 ± 7.1
Aspirin use	10,161 (46.9)	3,403 (46.9)	3,390 (47.0)	3,368 (46.9)	904 (37.1)	298 (36.7)	322 (38.7)	284 (35.9)
Cardiovascular risk category								
Primary prevention†	16,748 (77.4)	5,600 (77.1)	5,569 (77.3)	5,579 (77.7)	1,852 (76.0)	609 (74.9)	636 (76.4)	607 (76.7)
Secondary prevention‡	4,897 (22.6)	1,659 (22.9)	1,639 (22.7)	1,599 (22.3)	584 (24.0)	204 (25.1)	196 (23.6)	184 (23.3)
History of diabetes	7,717 (36.0)	2,581 (36.0)	2,629 (36.8)	2,507 (35.3)	779 (32.4)	262 (32.5)	256 (31.2)	261 (33.4)
History of hypertension	16,927 (79.0)	5,699 (79.4)	5,665 (79.3)	5,563 (78.3)	1,817 (75.5)	597 (74.1)	638 (77.9)	582 (74.4)
History of dyslipidemia	13,670 (63.8)	4,617 (64.3)	4,526 (63.4)	4,527 (63.7)	1,378 (57.3)	463 (57.4)	476 (58.1)	439 (56.2)
Current smoker	3,917 (18.3)	1,353 (18.9)	1,293 (18.1)	1,271 (17.9)	500 (20.8)	175 (21.7)	167 (20.4)	158 (20.2)
Prior statin use	11,913 (55.0)	4,023 (55.4)	3,939 (54.6)	3,951 (55.0)	1,065 (43.7)	344 (42.3)	368 (44.2)	353 (44.6)
Prior DMARD use	383 (1.8)	113 (1.6)	124 (1.7)	146 (2.0)	1,375 (56.4)	459 (56.5)	460 (55.3)	456 (57.6)
Systolic BP, mean ± SD mm Hg	125 ± 10.5	125 ± 10.4	125 ± 10.4	125 ± 10.6	125 ± 11.0	124 ± 11.2	126 ± 10.7	124 ± 11.2
Diastolic BP, mean ± SD mm Hg	75 ± 8.0	75 ± 8.0	76 ± 8.0	75 ± 8.0	76 ± 7.9	76 ± 8.1	76 ± 7.7	76 ± 7.9
HAQ DI score, mean ± SD	1.09 ± 0.6	1.10 ± 0.6	1.09 ± 0.6	1.08 ± 0.6	1.27 ± 0.7	1.27 ± 0.7	1.27 ± 0.7	1.27 ± 0.7
VAS pain score, mean ± SD mm (0–100 scale)	54.31 ± 23.6	54.18 ± 23.4	54.40 ± 23.4	54.37 ± 23.9	51.93 ± 24.9	52.36 ± 24.9	51.75 ± 24.8	51.68 ± 25.2
Total cholesterol, mean ± SD mg/dl	188.5 ± 43.1	188.6 ± 43.2	188.4 ± 43.5	188.6 ± 42.6	192.3 ± 42.8	193.6 ± 42.2	191.5 ± 42.9	191.8 ± 43.5
LDL cholesterol, mean ± SD mg/dl	106.4 ± 36.9	106.4 ± 36.9	106.3 ± 37.2	106.4 ± 36.7	108.9 ± 36.0	109.9 ± 35.5	108.5 ± 35.8	108.2 ± 36.9
HDL cholesterol, mean ± SD mg/dl	51.2 ± 14.8	51.2 ± 14.8	51.0 ± 14.7	51.4 ± 14.9	53.2 ± 15.9	53.0 ± 15.7	53.1 ± 16.5	53.4 ± 15.4
Triglycerides, median (IQR) mg/dl	134 (97–188)	133 (97–189)	135 (97–189)	134 (97–186)	128 (94–185)	131 (96–190)	125 (92–183)	128 (95–182)
Glycated hemoglobin, median (IQR) %	6.8 (6.2–8.0)	6.9 (6.2–8.0)	6.8 (6.1–8.0)	6.8 (6.1–7.9)	7.0 (6.1–8.3)	7.0 (6.1–8.4)	6.9 (6.0–8.3)	6.9 (6.1–8.1)
Creatinine, mean ± SD mg/dl	0.9 ± 0.2	0.9 ± 0.2	0.9 ± 0.2	0.9 ± 0.2	0.8 ± 0.2	0.8 ± 0.2	0.8 ± 0.2	0.8 ± 0.2

* Except where indicated otherwise, values are the number (%). BMI = body mass index; DMARD = disease-modifying antirheumatic drug; BP = blood pressure; HAQ DI = Health Assessment Questionnaire disability index; VAS = visual analog scale; LDL = low-density lipoprotein; HDL = high-density lipoprotein; IQR = interquartile range.
† Subjects at high risk for cardiovascular disease.
‡ Subjects with previously diagnosed cardiovascular disease at the time of study enrollment.

Study protocol. Patients who met the entry criteria and were willing to provide informed consent were randomized in a double-blind manner to receive celecoxib 100 mg twice daily in patients with OA and up to 200 mg twice daily in patients with RA, ibuprofen 600–800 mg 3 times daily, or naproxen 375–500 mg twice daily with matching placebos (1:1:1 allocation). Dose escalation was allowed at the discretion of the patient and investigator if symptom relief was not adequate. The allocation of patients is illustrated in a CONSORT diagram in Supplementary Figure 1, available on the *Arthritis & Rheumatology* web site at http://onlinelibrary.wiley.com/doi/10.1002/art.40400/abstract. Randomization was stratified according to geographic region, low-dose aspirin use (yes or no), and arthritis type (OA or RA) and implemented using an interactive voice response system. All patients were provided open-label esomeprazole at a dosage of 20–40 mg/day and were allowed to receive aspirin (≤325 mg/day, with 75–100 mg considered to be optimal for protection against CV events and recommended for the prevention of CV events) (see Supplementary Table 4). After randomization and the baseline visit, patients had scheduled visits at months 1, 2, 4, 8, and 12 and every 6 months thereafter until month 42. Study patients were required to complete at least 18 months of follow-up visits. Follow-up visits included clinical assessments and laboratory testing as well as identification of new adverse events or changes in CV, renal, and GI status, and arthritis outcomes.

The primary end point of the parent study was the first occurrence of a composite end point consisting of CV death, nonfatal myocardial infarction, or nonfatal stroke, which is identical to the primary composite end point of the Antiplatelet Trialists Collaboration (APTC). Trial completion required collection of a specific number of primary end points: 580 primary end points for the ITT analysis and 420 end points for the on-treatment analysis (analysis of patients receiving the assigned treatments). Sample size calculations estimated that >20,000 patients would be required to meet these goals. In order to reach the requisite number of end points, >24,000 patients were ultimately enrolled.

In the current analyses, findings in patients with OA and patients with RA were reported separately. The primary outcomes for these 2 subgroups were based on an ITT analysis, with the on-treatment analysis used as a sensitivity analysis. Analyzed outcomes included major adverse CV events (APTC event plus revascularization or hospitalization for transient ischemic attack or unstable angina) plus clinically significant GI, renal, and all-cause mortality events. Clinically significant GI events were defined as gastroduodenal hemorrhage; gastric outlet obstruction; perforation of the gastroduodenum, small bowel, or large bowel; hemorrhage of the large bowel, small bowel, or acute GI hemorrhage of unknown origin; new-onset iron deficiency anemia; or symptomatic gastric or duodenal ulcer. Clinically significant renal events included development of renal insufficiency or renal failure, defined based on development of any of the following: serum creatinine level of ≥2.0 mg/dl and an increase of ≥0.7 mg/dl from baseline; hospitalization for acute renal failure with a doubling of the baseline serum creatinine level or hyperkalemia with a ≥50% increase in the serum creatinine level; or initiation of dialysis. A Clinical Events Committee adjudicated all of the above end points in a blinded manner, using prespecified definitions.

The analgesic efficacy of the treatments was evaluated at baseline and follow-up using the pain score on a visual analog scale (VAS). For the assessment of function, patients completed the Health Assessment Questionnaire disability index (HAQ DI) (19) at baseline, at months 1, 12, 24, 36, and 42, and at the time of premature study drug discontinuation, if applicable. All patients who discontinued the study drug treatment were followed up per protocol through month 42 or to study completion, whichever occurred first.

Statistical analysis. The primary analyses in the PRECISION trial assessed noninferiority for the frequency of adverse CV events during treatment with celecoxib versus treatment with naproxen and ibuprofen. The current analyses focused on the OA and RA subgroups. Noninferiority hypotheses were not tested, and no adjustments were made for multiple comparisons. Furthermore, no adjustment to the value of alpha was made to account for multiple comparisons, because each comparison was assumed to be independent. For comparisons between groups, P values less than 0.05 were considered significant. The P value threshold of <0.10, based on nominal P values, was considered significant for the interaction between

Table 2. Frequency of adjudicated clinical end points in the intent-to-treat population*

	Osteoarthritis				Rheumatoid arthritis			
	Total (n = 21,645)	Celecoxib (n = 7,259)	Ibuprofen (n = 7,208)	Naproxen (n = 7,178)	Total (n = 2,436)	Celecoxib (n = 813)	Ibuprofen (n = 832)	Naproxen (n = 791)
MACE end point	949 (4.38)	294 (4.05)	343 (4.76)	312 (4.35)	118 (4.84)	43 (5.29)	41 (4.93)	34 (4.30)
APTC end point	525 (2.43)	162 (2.23)	190 (2.64)	173 (2.41)	82 (3.37)	26 (3.20)	28 (3.37)	28 (3.54)
Composite serious GI events	292 (1.35)	77 (1.06)	111 (1.54)	104 (1.45)	43 (1.77)	9 (1.11)	19 (2.28)	15 (1.90)
Major clinical GI events	160 (0.74)	50 (0.69)	63 (0.87)	47 (0.65)	23 (0.94)	5 (0.62)	9 (1.08)	9 (1.14)
Anemia of GI origin	143 (0.66)	29 (0.40)	52 (0.72)	62 (0.86)	23 (0.94)	4 (0.49)	12 (1.44)	7 (0.88)
Renal events	192 (0.89)	48 (0.66)	82 (1.14)	62 (0.86)	28 (1.15)	9 (1.11)	10 (1.20)	9 (1.14)
All major safety events	1,507 (6.96)	449 (6.19)	558 (7.74)	500 (6.97)	204 (8.37)	62 (7.63)	71 (8.53)	71 (8.98)
All-cause mortality	374 (1.73)	117 (1.61)	124 (1.72)	133 (1.85)	63 (2.59)	15 (1.85)	18 (2.16)	30 (3.79)

* The major adverse cardiovascular (CV) event (MACE) end point is defined as the first occurrence of CV-related death, nonfatal myocardial infarction (MI), nonfatal stroke, hospitalization for unstable angina, revascularization, or hospitalization for transient ischemic attack. The Antiplatelet Trialists Collaboration (APTC) end point is defined as the first occurrence of CV-related death, nonfatal MI, or nonfatal stroke. All major safety events include MACE, composite serious gastrointestinal (GI) and renal events, and all-cause mortality. Composite serious GI events include gastroduodenal hemorrhage, gastric outlet obstruction, gastroduodenal small or large bowel perforation, small or large bowel hemorrhage, acute GI hemorrhage, symptomatic gastric or duodenal ulcer or anemia (defined as a decrease in the hemoglobin concentration of ≥2 gm/dl or hematocrit ≥10% with no clinical evidence of acute GI bleed and biochemical evidence of iron deficiency). All major safety events include MACE, composite serious GI events, renal events, and all-cause mortality. Values are the number (%).

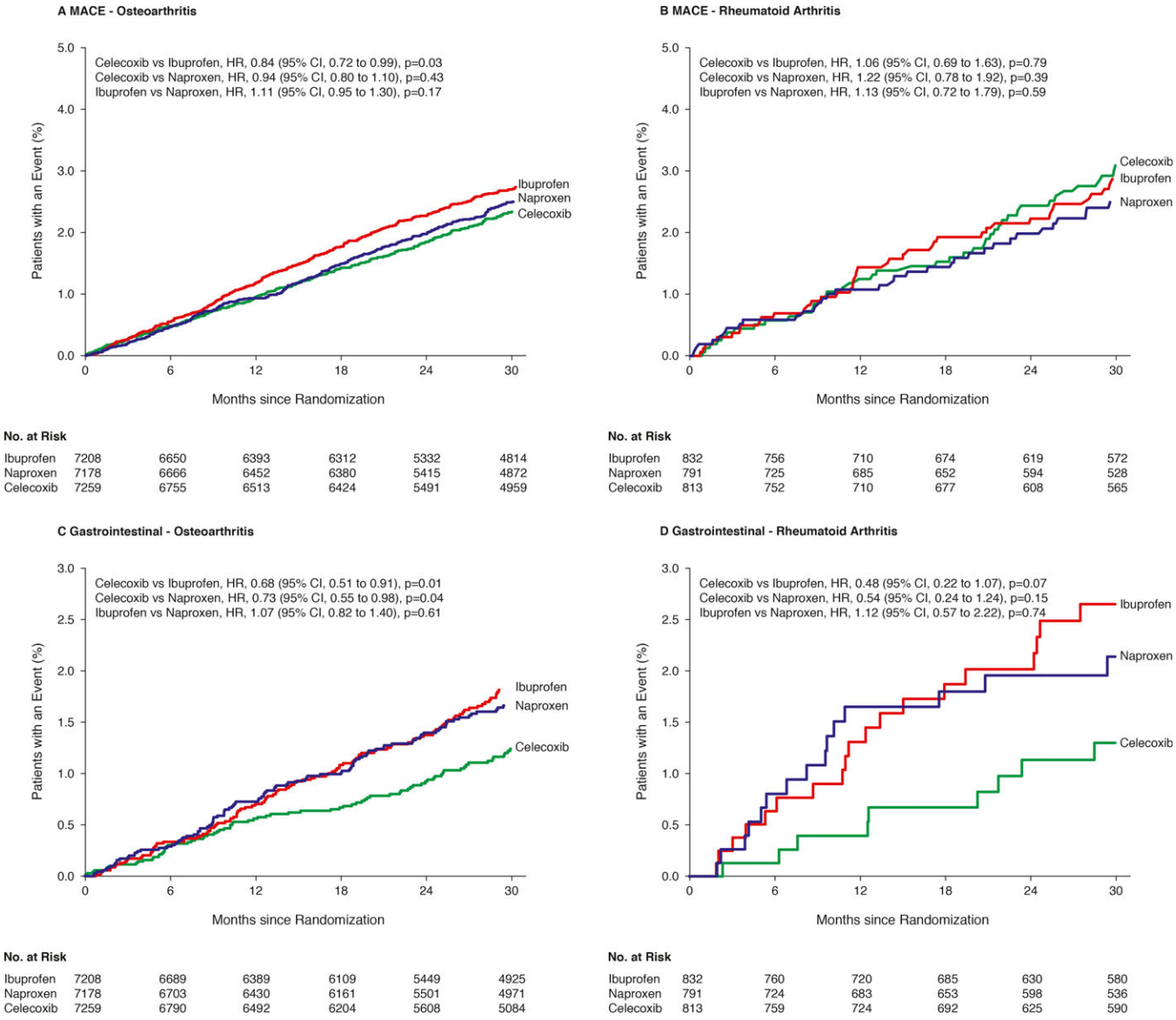

Figure 1. Time-to-event analysis of primary and secondary outcomes in patients with osteoarthritis and patients with rheumatoid arthritis, showing cumulative event rates across the 3 treatment arms. **A** and **B,** Major adverse cardiovascular events (MACEs). **C** and **D,** Gastrointestinal events. **E** and **F,** Renal events. **G** and **H,** All-cause mortality. Hazard ratios (HRs) with 95% confidence intervals (95% CIs) and *P* values were calculated using Cox proportional hazards regression models with adjustment for stratification factors.

type of arthritis (OA/RA) and treatment. Cumulative event curves were constructed for each of the 3 treatment arms, in the OA and RA subgroups separately. Hazard ratios (HRs) and corresponding 95% confidence intervals (95% CIs) comparing treatment groups for the 4 safety outcomes of interest were calculated using Cox proportional hazards regression models, with adjustment for stratification factors (geographic region and low-dose aspirin use). An interaction between treatment group and arthritis type was tested in the Cox models for each drug-to-drug comparison by adding the interaction term to the model. Analyses were censored after 30 months in the ITT population and after 43 months in the on-treatment population. All analyses were performed using SAS version 9.4.

RESULTS

Among the 24,081 patients enrolled in the PRECISION trial, 89.9% (n = 21,645) had OA and 10.1% (n = 2,436) had RA. The mean age of the patients with OA was 64 years, and 63% were female (Table 1). Twenty-three percent of those with OA had experienced a previous CV event; 47% used daily aspirin, and 18% smoked cigarettes. The 3 treatment arms were well balanced among patients with OA. In contrast, patients with RA were slightly younger than those with OA, with a mean age of 61 years,

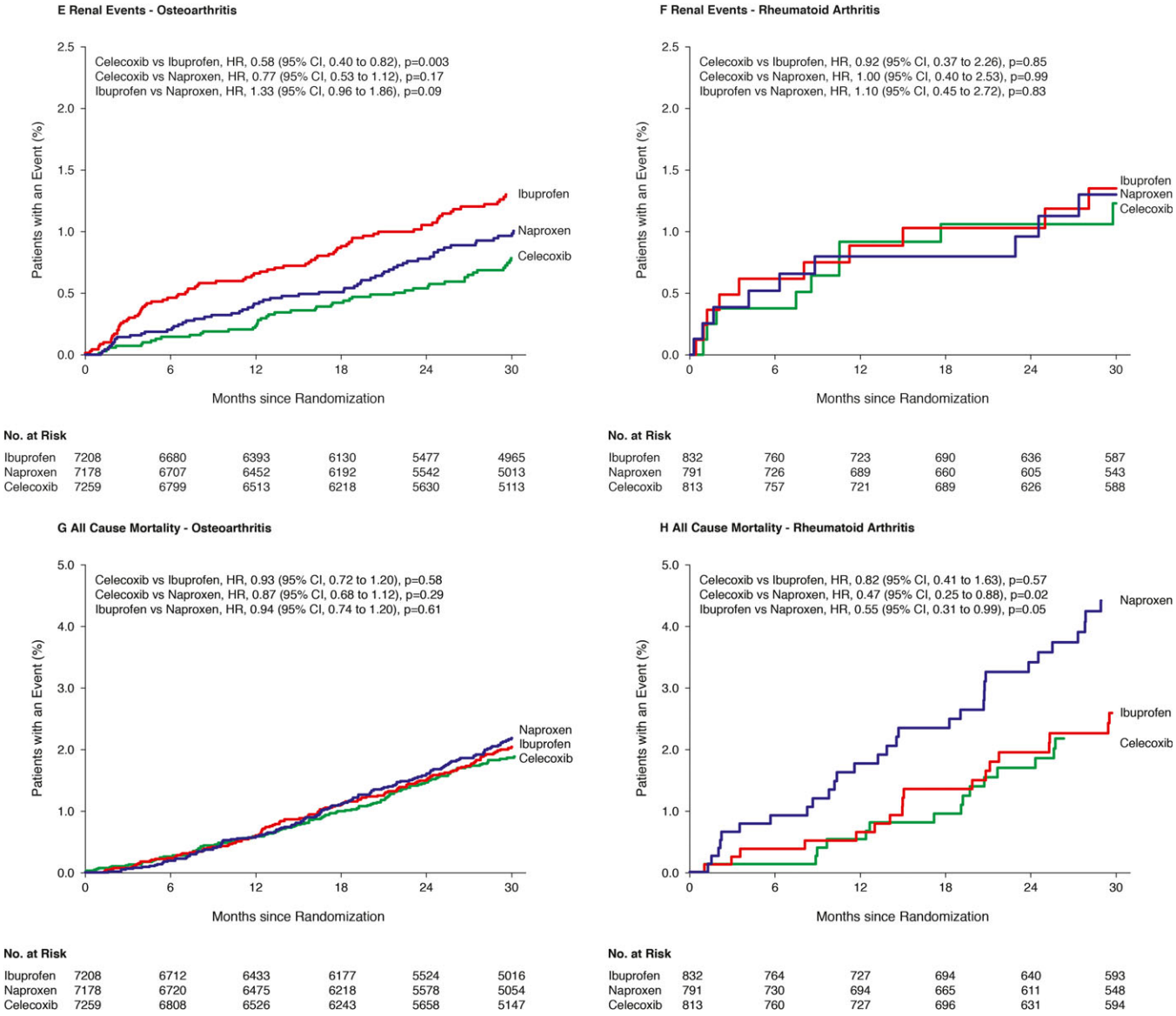

Figure 1. *(cont'd)*

and 73% were female (Table 1). Similar to patients with OA, 24% of those with RA had a previous CV event, but fewer used daily aspirin (37%), and slightly more smoked cigarettes (21%). Allocation of the patients with RA to the 3 treatment arms was well balanced. Use of an increased dosage of the 3 treatments was similar in the RA subgroup, but for regulatory reasons, the protocol did not permit celecoxib up-titration in the OA subgroup, resulting in different proportions of patients using the maximum allowable dosages (see Supplementary Table 5, available on the *Arthritis & Rheumatology* web site at http://onlinelibrary.wiley.com/doi/10.1002/art.40400/abstract). The mean ± SD doses in the OA group were as follows: celecoxib 100 ± 3 mg, naproxen 426 ± 52 mg, and ibuprofen 681 ± 82 mg. In the RA group, the doses were celecoxib 141 ± 42 mg, naproxen 425 ± 52 mg, and ibuprofen 681 ± 82 mg. Among patients with OA, the percentages in whom NSAIDs were up-titrated were as follows: 0.3% of those receiving celecoxib, 55.3% of those receiving naproxen, and 55.3% of those receiving ibuprofen. Among patients with RA, the percentages were 56%, 54.9%, and 56.5%, respectively.

The frequency of adjudicated clinical end points is shown in Table 2. Among patients with OA, 4.4% met the major adverse CV event end point compared with 4.8% of those with RA ($P = 0.30$). The cumulative incidences

for the 3 treatment arms in patients with OA and patients with RA are shown in Figures 1A and B. There were significantly fewer major adverse CV events in the OA subgroup when comparing celecoxib to ibuprofen (HR 0.84, 95% CI 0.72–0.99), but not among the RA group (HR 1.06, 95% CI 0.69–1.63). The treatment-by-arthritis-type (OA versus RA) interaction was not significant ($P = 0.29$). In both the OA group and the RA group, the risk of a major adverse CV event did not differ significantly between those randomized to receive celecoxib and those randomized to receive naproxen.

The frequency of adverse GI events was similar in patients with OA and patients with RA (1.35% versus 1.77%; $P = 0.096$) (Table 2). The frequency of adverse GI events in patients with OA was 1.06% in those randomized to receive celecoxib, 1.54% in those randomized to receive ibuprofen, and 1.45% in those randomized to receive naproxen. A similar pattern was observed in patients with RA, with 1.11% in those randomized to receive celecoxib, 2.28% in those randomized to receive ibuprofen, and 1.90% in those randomized to receive naproxen. The cumulative event curves for adverse GI events are shown in Figures 1C and D. The HRs comparing celecoxib with ibuprofen (0.68, 95% CI 0.51–0.91) and comparing celecoxib with naproxen (0.73, 95% CI 0.55–0.98) demonstrated a significantly reduced risk of an adverse GI event in patients with OA randomized to receive celecoxib. Patients with RA showed a similar pattern of GI risk, with reduced risk comparing celecoxib with ibuprofen (HR 0.48, 95% CI 0.22–1.07) and celecoxib with naproxen (HR 0.54, 95% CI 0.24–1.24), but neither comparison excluded null values. Treatment according to arthritis type interactions did not differ significantly ($P > 0.10$ for both).

The frequency of adverse renal events was 0.89% in patients with OA and 1.15% in patients with RA ($P = 0.20$) (Table 2). The cumulative incidence for OA showed fewer renal events in patients receiving celecoxib (Figure 1E). The risk of renal adverse events in patients with OA was lower in those randomized to celecoxib than that in those randomized to ibuprofen (HR 0.58, 95% CI 0.40–0.82) and was numerically lower but not statistically different between celecoxib and naproxen (HR 0.77, 95% CI 0.53–1.12). The cumulative event curve for RA showed no differences across treatment arms (Figure 1F) and the HRs demonstrated no differences in risk across agents. The interaction between treatment group and arthritis type did not reach statistical significance (HR 0.47, 95% CI 0.25–0.88) (Figure 1H). The interaction between celecoxib versus naproxen and arthritis type met the criteria for statistical significance (P for interaction = 0.07).

The primary analysis was an ITT analysis, but we also performed on-treatment analyses (Figure 2). The results of the on-treatment analysis qualitatively resembled those of the ITT analysis, with most estimates showing somewhat larger differences. An exploratory analysis also assessed a composite end point of all major safety events, including major adverse CV events, serious GI or renal events, and all-cause mortality. The frequency of this end point was higher in patients with RA than in patients with OA (8.37% and 6.96%, respectively; $P = 0.01$) (Table 2). In the OA subgroup, the HRs comparing celecoxib versus ibuprofen (0.80, 95% CI 0.70–0.90) and celecoxib versus naproxen (0.90, 95% CI 0.80–1.03) showed fewer major safety events with celecoxib. The HRs for the RA subgroup did not show any difference in the risk of major safety events between treatment arms. The interactions between treatment group and arthritis type for this end point were not statistically significant ($P > 0.10$ for all comparisons).

Finally, we examined functional status as measured by the HAQ DI and pain score on a VAS (see Supplementary Figure 2). At baseline, patients with OA had higher mean ± SD pain scores on a VAS (54.3 ± 23.6 mm versus 51.9 ± 24.9 mm in patients with RA; $P < 0.001$). The improvements in the pain score in patients with OA were similar across treatment arms. Patients with RA treated with ibuprofen had statistically significantly greater improvement in pain compared with patients with RA treated with celecoxib ($P = 0.02$), but the modest difference had unclear clinical significance. As observed for the pain score, patients with OA had similar changes in HAQ DI scores across treatment arms, but among patients with RA, it was slightly better for those receiving ibuprofen compared with those treated with celecoxib ($P = 0.02$).

DISCUSSION

Arthritis is the most common cause of disability in the US. In 2014, ~15 million arthritis patients requiring treatment with analgesics reported severe joint pain (20). In 2000, more than 100 million NSAID prescriptions were written in the US (21). NSAIDs differentially affect COX isoforms, potentially accounting for the benefits and varying toxicities across agents. The PRECISION trial demonstrated similar CV safety for moderate doses of the selective COX-2 inhibitor celecoxib and the nonselective NSAIDs ibuprofen and naproxen (13). In a set of analyses in prespecified subgroups according to type of arthritis (OA and RA), we observed fewer major adverse CV events in patients with OA treated with celecoxib compared with those treated with ibuprofen. Patients with OA

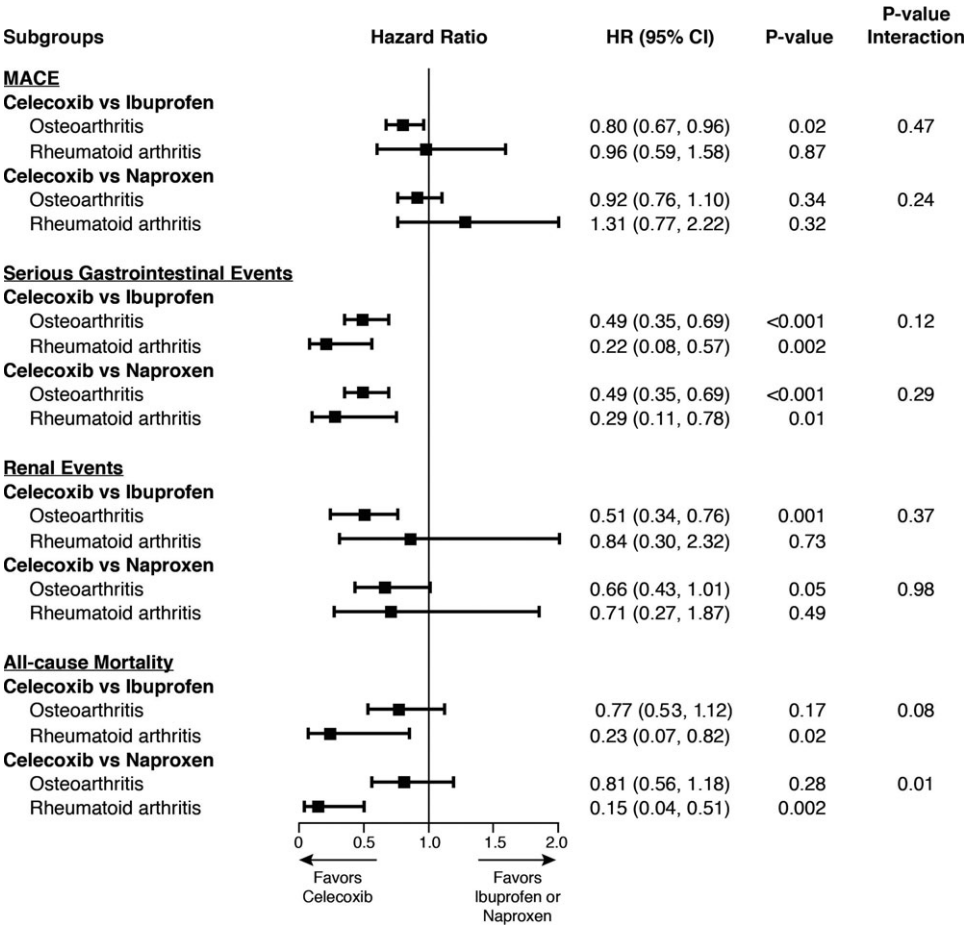

Figure 2. On-treatment sensitivity analysis showing the hazard ratios (HRs) with 95% confidence intervals (95% CIs) for the 4 adjudicated outcomes across the osteoarthritis and rheumatoid arthritis subgroups. MACE = major adverse cardiovascular event.

treated with celecoxib also experienced less GI toxicity than those treated with ibuprofen or naproxen; this was not observed in RA, but the statistical power in that subgroup was limited. Adjudicated renal adverse events were less common in celecoxib-treated compared with ibuprofen-treated patients with OA but not patients with RA.

These subgroup analyses add important and clinically relevant information to our understanding of the safety of selective and nonselective NSAIDs in patients with OA and patients with RA. The findings regarding CV safety in both OA and RA provide reassurance to those being treated with celecoxib and those considering celecoxib treatment. Because RA is associated with a 1.5–2.0 times greater risk of CV events, presumed in part to the chronic systemic inflammatory nature of RA (which may promote plaque instability and major adverse CV events), the safety of different NSAIDs in patients with RA might differ from that in patients with OA (22). The results presented herein suggest a slightly lower CV risk for celecoxib users with OA compared with ibuprofen users with OA; however, a similar CV risk was observed when comparing the different NSAIDs in RA patients. As expected, the frequency of adverse events was higher in patients with RA than in patients with OA. These findings support the efforts underway to refine risk stratification and CV management strategies in RA.

Patients treated with celecoxib also had a reduced risk for other end points. Among patients with OA, the risk of GI adverse events was significantly lower in those treated with celecoxib than in those receiving either ibuprofen or naproxen. This finding is not surprising based on the results of prior meta-analyses (23), but most individual studies have not clearly demonstrated improved GI safety of celecoxib (24). Similar to the frequency of CV events observed in patients with RA, the frequency of GI events in patients with RA in the current study was higher than that in patients with OA (25).

The reduced all-cause mortality among patients with RA treated with celecoxib compared with naproxen was not anticipated. The number of deaths was relatively small in each group: 15 in the celecoxib group (1.85%) and 30 in the naproxen group (3.79%), thus precluding strong conclusions. This reduction resulted from a combination of reduced mortality across various causes (i.e., infection, cancer, respiratory) (see Supplementary Table 6). Further examination of these deaths is underway, but this finding may have resulted from chance. Future studies of cause-specific mortality that includes more events will be helpful; such studies will likely require the use of observational data sets.

The PRECISION trial was conducted as a randomized, double-blind, active drug–controlled trial. Randomization was stratified based on the underlying arthritis diagnosis (OA or RA) and whether patients were receiving aspirin as prophylaxis against CV events. The trial was powered based on the total number of events across all patients and not on the size of each subgroup; therefore, the statistical power for some subgroup analyses does not permit drawing firm conclusions. The ITT population was chosen for the primary analysis, but the on-treatment population showed directionally similar results (see Figure 2), some of which were statistically significant, while others were not. The withdrawal rate during the PRECISION trial was higher than expected but was similar across treatment arms among all patients and also in the OA and RA subgroups (see Supplementary Figure 3). Dosing of the 3 treatments was slightly different in the OA and RA subgroups based on limitations imposed by drug regulators for using celecoxib 100 mg twice daily in the OA subgroup; this issue may have influenced the results. Prior studies have demonstrated an increased risk of adverse effects with celecoxib as well as nonselective NSAIDs at higher dosages (9,26,27).

In conclusion, these subgroup analyses of the PRECISION trial, based on the underlying arthritis diagnosis, yield results that are similar but not identical to those of the overall trial. The OA subgroup randomized to receive celecoxib treatment experienced fewer CV events compared with the subgroup randomized to ibuprofen, but not the subgroup randomized to naproxen. The OA subgroup receiving celecoxib experienced fewer clinically significant adverse GI events than the subgroups receiving ibuprofen or naproxen, with similar trends observed in patients with RA. Renal events were less common in the OA subgroup receiving treatment with celecoxib compared with the subgroup randomized to ibuprofen but not in the subgroup randomized to naproxen, and in RA patients, there were no differences between patients receiving the 3 drugs. These findings give providers, patients, and regulators a greater understanding of the relative safety of different NSAIDs (COX-2–selective and nonselective). Current safety information from the FDA regarding NSAIDs focuses on the risk of CV events and does not differentiate between agents. The results of the PRECISION trial and these subgroup analyses confirm that celecoxib does not increase the risk of CV events. However, celecoxib conferred slight reductions in the risk for several outcomes compared with other commonly used NSAIDs. Regulators and professional organizations might consider whether these data regarding differential safety across NSAIDs warrant new recommendations for the optimal use of the agents studied in the PRECISION trial.

AUTHOR CONTRIBUTIONS

All authors were involved in drafting the article or revising it critically for important intellectual content, and all authors approved the final version to be published. Dr. Solomon had full access to all of the data in the study and takes responsibility for the integrity of the data and the accuracy of the data analysis.

Study conception and design. Solomon, Husni, Wolski, Wisniewski, Borer, Graham, Libby, Lincoff, Lüscher, Menon, Yeomans, Wang, Bao, Berger, Nissen.

Acquisition of data. Solomon, Husni, Wolski, Wang.

Analysis and interpretation of data. Solomon, Husni, Wolski, Wang, Bao, Nissen.

ACKNOWLEDGMENTS

We thank the committees, study centers, and investigators participating in the PRECISION trial.

ROLE OF THE STUDY SPONSOR

Pfizer had no role in the study design or in the collection, analysis, or interpretation of the data, the writing of the manuscript, or the decision to submit the manuscript for publication. Publication of this article was not contingent upon approval by Pfizer.

REFERENCES

1. IMS Health. National Prescription Audit, Oral NSAID Market 2013.
2. Marcum ZA, Perera S, Donohue JM, Boudreau RM, Newman AB, Ruby CM, et al, for the Health, Aging and Body Composition Study. Analgesic use for knee and hip osteoarthritis in community-dwelling elders. Pain Med 2011;12:1628–36.
3. Gibson T, Clark B. Use of simple analgesics in rheumatoid arthritis. Ann Rheum Dis 1985;44:27–9.
4. Bresalier RS, Sandler RS, Quan H, Bolognese JA, Oxenius B, Horgan K, et al, for the Adenomatous Polyp Prevention on Vioxx (APPROVe) Trial Investigators. Cardiovascular events associated with rofecoxib in a colorectal adenoma chemoprevention trial [published erratum appears in N Engl J Med 2006;355:221]. N Engl J Med 2005;352:1092–102.
5. McGettigan P, Henry D. Cardiovascular risk with non-steroidal anti-inflammatory drugs: systematic review of population-based controlled observational studies. PLoS Med 2011;8:e1001098.
6. Solomon SD, Wittes J, Finn PV, Fowler R, Viner J, Bertagnolli MM, et al. Cardiovascular risk of celecoxib in 6 randomized

placebo-controlled trials: the cross trial safety analysis. Circulation 2008;117:2104–13.
7. Kearney PM, Baigent C, Godwin J, Halls H, Emberson JR, Patrono C. Do selective cyclo-oxygenase-2 inhibitors and traditional non-steroidal anti-inflammatory drugs increase the risk of atherothrombosis? Meta-analysis of randomised trials. BMJ 2006;332:1302–8.
8. Trelle S, Reichenbach S, Wandel S, Hildebrand P, Tschannen B, Villiger PM, et al. Cardiovascular safety of non-steroidal anti-inflammatory drugs: network meta-analysis. BMJ 2011;342:c7086.
9. Olsen AM, Fosbøl EL, Lindhardsen J, Folke F, Charlot M, Selmer C, et al. Long-term cardiovascular risk of nonsteroidal anti-inflammatory drug use according to time passed after first-time myocardial infarction: a nationwide cohort study. Circulation 2012;126:1955–63.
10. Solomon DH, Karlson EW, Rimm EB, Cannuscio CC, Mandl LA, Manson JE, et al. Cardiovascular morbidity and mortality in women diagnosed with rheumatoid arthritis. Circulation 2003;107:1303–7.
11. Veronese N, Trevisan C, De Rui M, Bolzetta F, Maggi S, Zambon S, et al. Association of osteoarthritis with increased risk of cardiovascular diseases in the elderly: findings from the Progetto Veneto Anziano study cohort. Arthritis Rheumatol 2016;68:1136–44.
12. Becker MC, Wang TH, Wisniewski L, Wolski K, Libby P, Lüscher TF, et al. Rationale, design, and governance of Prospective Randomized Evaluation of Celecoxib Integrated Safety versus Ibuprofen Or Naproxen (PRECISION), a cardiovascular end point trial of nonsteroidal antiinflammatory agents in patients with arthritis. Am Heart J 2009;157:606–12.
13. Nissen SE, Yeomans ND, Solomon DH, Lüscher TF, Libby P, Husni ME, et al, for the PRECISION Trial Investigators. Cardiovascular safety of celecoxib, naproxen, or ibuprofen for arthritis. N Engl J Med 2016;375:2519–29.
14. Combe B, Swergold G, McLay J, McCarthy T, Zerbini C, Emery P, et al. Cardiovascular safety and gastrointestinal tolerability of etoricoxib vs diclofenac in a randomized controlled clinical trial (the MEDAL study). Rheumatology (Oxford) 2009;48:425–32.
15. Altman R, Alarcón G, Appelrouth D, Bloch D, Borenstein D, Brandt K, et al. The American College of Rheumatology criteria for the classification and reporting of osteoarthritis of the hip. Arthritis Rheum 1991;34:505–14.
16. Altman R, Alarcón G, Appelrouth D, Bloch D, Borenstein D, Brandt K, et al. The American College of Rheumatology criteria for the classification and reporting of osteoarthritis of the hand. Arthritis Rheum 1990;33:1601–10.
17. Altman R, Asch E, Bloch D, Bole G, Borenstein D, Brandt K, et al, for the Diagnostic and Therapeutic Criteria Committee of the American Rheumatism Association. Development of criteria for the classification and reporting of osteoarthritis: classification of osteoarthritis of the knee. Arthritis Rheum 1986;29:1039–49.
18. The Criteria Committee of the New York Heart Association. Nomenclature and criteria for diagnosis of diseases of the heart and great vessels. 9th ed. Boston: Little Brown; 1994. p. 253–6.
19. Fries JF, Spitz P, Kraines RG, Holman HR. Measurement of patient outcome in arthritis. Arthritis Rheum 1980;23:137–45.
20. Barbour KE, Boring M, Helmick CG, Murphy LB, Qin J. Prevalence of severe joint pain among adults with doctor-diagnosed arthritis – United States, 2002–2014. MMWR Morb Mortal Wkly Rep 2016;65:1052–6.
21. Laine L. Approaches to nonsteroidal anti-inflammatory drug use in the high-risk patient. Gastroenterology 2001;120:594–606.
22. Goodson NJ, Brookhart AM, Symmons DP, Silman AJ, Solomon DH. Non-steroidal anti-inflammatory drug use does not appear to be associated with increased cardiovascular mortality in patients with inflammatory polyarthritis: results from a primary care based inception cohort of patients. Ann Rheum Dis 2009;68:367–72.
23. Deeks JJ, Smith LA, Bradley MD. Efficacy, tolerability, and upper gastrointestinal safety of celecoxib for treatment of osteoarthritis and rheumatoid arthritis: systematic review of randomised controlled trials. BMJ 2002;325:619.
24. Silverstein FE, Faich G, Goldstein JL, Simon LS, Pincus T, Whelton A, et al. Gastrointestinal toxicity with celecoxib vs nonsteroidal anti-inflammatory drugs for osteoarthritis and rheumatoid arthritis: the CLASS study: a randomized controlled trial. JAMA 2000; 284:1247–55.
25. Fries JF, Williams CA, Bloch DA, Michel BA. Nonsteroidal anti-inflammatory drug-associated gastropathy: incidence and risk factor models. Am J Med 1991;91:213–22.
26. Strand V. Are COX-2 inhibitors preferable to non-selective non-steroidal anti-inflammatory drugs in patients with risk of cardiovascular events taking low-dose aspirin? Lancet 2007;370:2138–51.
27. Chan FK, Lanas A, Scheiman J, Berger MF, Nguyen H, Goldstein JL. Celecoxib versus omeprazole and diclofenac in patients with osteoarthritis and rheumatoid arthritis (CONDOR): a randomised trial. Lancet 2010;376:173–9.

ARTHRITIS & RHEUMATOLOGY
Vol. 70, No. 4, April 2018, pp 547–554
DOI 10.1002/art.40407

Utilization and Short-Term Outcomes of Primary Total Hip and Knee Arthroplasty in the United States and Canada

An Analysis of New York and Ontario Administrative Data

Peter Cram,[1] Bruce E. Landon,[2] John Matelski,[3] Vicki Ling,[4] Therese A. Stukel,[5] J. Michael Paterson,[4] Rajiv Gandhi,[6] Gillian A. Hawker,[7] and Bheeshma Ravi[7]

Objective. **Total knee arthroplasty (TKA) and total hip arthroplasty (THA) are common and effective surgical procedures. This study sought to compare utilization and short-term outcomes of primary TKA and THA in adjacent regions of Canada and the United States.**

Methods. **The study was designed as a retrospective cohort study of patients who underwent primary TKA or THA, comparing administrative data from New York and Ontario in 2012–2013. Demographic features of the TKA and THA patients, per capita utilization rates, and short-term outcomes were compared between the jurisdictions.**

Results. **A higher percentage of New York hospitals performed TKA compared to Ontario hospitals (75.7% versus 42.1%; $P < 0.001$), and the mean annual procedural volume for TKAs was lower in New York hospitals (mean 179 versus 327 in Ontario hospitals; $P < 0.001$). After direct standardization, utilization was significantly lower in New York compared to Ontario, both for TKA (16.1 TKAs versus 21.4 TKAs per 10,000 population per year; $P < 0.001$) and for THA (10.5 THAs versus 11.5 THAs per 10,000 population per year; $P < 0.001$). For those who underwent TKA, the length of stay in Ontario hospitals was significantly longer (mean 3.7 days versus 3.4 days in New York hospitals; $P < 0.001$). A smaller percentage of New York patients were discharged directly home (46.2% versus 90.9% of Ontario patients; $P < 0.001$), but 30-day and 90-day readmission rates were higher in New York compared to Ontario (30-day rates, 4.6% versus 3.9% [$P < 0.001$]; 90-day rates, 8.4% versus 6.7% [$P < 0.001$]). For the THA cohorts, the results with regard to length of stay, discharge disposition, and readmission rates were similar to those for TKA.**

Conclusion. **Ontario has higher utilization of total joint arthroplasty than New York but has a smaller percentage of hospitals performing these procedures. Patients are more likely to be discharged home and less likely to be readmitted in Ontario. Our results suggest areas where each jurisdiction could improve.**

Primary total knee arthroplasty (TKA) and total hip arthroplasty (THA) are safe and effective treatments

The opinions, results, and conclusions reported herein are those of the authors and are independent from the funding sources. No endorsement by the ICES or the Ontario MOHLTC is intended or should be inferred. Parts of this material are based on data and/or information compiled and provided by the Canadian Institute for Health Information (CIHI). However, the analyses, conclusions, opinions, and statements expressed in the material are those of the authors and not necessarily those of the CIHI.

Supported by the Institute for Clinical Evaluative Sciences, which is funded by an annual grant from the Ontario Ministry of Health and Long-Term Care. Dr. Cram's work was supported by the NIH (National Institute of Arthritis and Musculoskeletal and Skin Diseases grant K24-AR-062133).

[1]Peter Cram, MD, MBA: University of Toronto, Sinai Health System and University Health Network, and Institute for Clinical Evaluative Sciences, Toronto, Ontario, Canada; [2]Bruce E. Landon, MD, MBA: Harvard Medical School, Boston, Massachusetts; [3]John Matelski, MSc: Sinai Health System and University Health Network, Toronto, Ontario, Canada; [4]Vicki Ling, MSc, J. Michael Paterson, MSc: Institute for Clinical Evaluative Sciences, Toronto, Ontario, Canada; [5]Therese A. Stukel, PhD: Institute for Clinical Evaluative Sciences and Institute of Health Policy, Management and Evaluation, University of Toronto, Toronto, Ontario, Canada, and Dartmouth Institute for Health Policy and Clinical Practice, Geisel School of Medicine at Dartmouth, Hanover, New Hampshire; [6]Rajiv Gandhi, MD, MSc: University of Toronto, Toronto, Ontario, Canada; [7]Gillian A. Hawker, MD, MSc, Bheeshma Ravi, MD, PhD: University of Toronto and Canada Institute for Clinical Evaluative Sciences, Toronto, Ontario, Canada.

Address correspondence to Peter Cram, MD, MBA, Division of General Internal Medicine, Toronto General Hospital, Eaton 14th Floor, 200 Elizabeth Street, Toronto, Ontario M5G 2C4, Canada. E-mail: peter.cram@uhn.ca.

Submitted for publication June 21, 2017; accepted in revised form December 20, 2017.

for patients with advanced arthritis (1,2). With an aging population, demand for total joint arthroplasty (TJA [which includes both TKA and THA]) is increasing (3,4).

Unlike emergency procedures such as hip fracture repair or percutaneous coronary intervention for ST-segment elevation myocardial infarction, primary TKA and THA are prototypical "preference sensitive" procedures. Patients and providers have considerable discretion over when and whether to proceed with surgery (5). Payors, both public and private, have considerable interest in restraining the utilization of TJA, given that each surgery costs between $10,000 and $20,000 (6,7). Most publicly funded health care systems (e.g., Canada, England) use some sort of rationing to limit surgical volumes (8), often resulting in wait times of 2–12 months (9). At the same time, government payors face relentless political pressure from patients and physicians to minimize wait times (10). In comparison, the US uses a relatively laissez faire approach to controlling volumes for most procedures, including TJA. There is a general belief that rates of utilization of most procedures, including TJA, are far higher in the US than in other Organization for Economic Cooperation and Development (OECD) countries (11,12), but empirical data are extremely limited (13–15).

We used administrative data on primary TKA and THA patients from New York and Ontario to compare the rates of utilization, hospital procedural volumes, and short-term outcomes (length of stay [LOS], readmission rates, and discharge disposition). We hypothesized that 1) utilization of TJA would be higher in New York compared to Ontario; 2) hospital volumes would be lower in New York; and 3) a greater percentage of Ontario residents would be discharged home after surgery.

PATIENTS AND METHODS

Patient data. *New York.* We used data from the New York State Inpatient Database (SID) obtained as part of the Agency for Healthcare Research and Quality (AHRQ) Healthcare Cost and Utilization Project (16). The SID has been used extensively in prior research (17). Briefly, the SID contains administrative data for all patients in New York admitted to acute care hospitals, excluding small numbers of hospitals operated by the Veterans Administration Health System and certain specialty hospitals such as psychiatric hospitals. Data elements provided by the AHRQ for each admission include patient demographics (age [in years], sex), primary and secondary diagnoses and procedures (coded using International Classification of Diseases, Ninth Revision, Clinical Modification [ICD-9-CM] codes), discharge disposition (e.g., died in hospital, discharged home, post–acute care), a unique patient identifier (used to track patient readmissions over time), and a unique hospital identifier. Comorbid conditions in the SID are captured using algorithms developed by Elixhauser et al (18).

Ontario. We used Ontario Discharge Abstract Data (DAD) obtained through the Institute for Clinical Evaluative Sciences (ICES). These records provide information on all hospitalizations paid for by the Ontario provincial health insurance plan, which pays for virtually all hospital care provided within the province and provides insurance to all legal residents of Ontario (virtually 100% of the population) (19,20). Similar to the SID files, the Ontario DAD provide information regarding patient demographics, primary and secondary diagnoses coded using ICD-10 codes for each hospitalization, discharge disposition, and patient and hospital identifiers. Comorbid conditions were identified using the Quan ICD-10 adaptation of the Elixhauser comorbidity coding scheme (21).

Cohort generation. We identified adults ages ≥18 years who underwent primary TKA or THA between January 1, 2012 and September 30, 2013, identified based on ICD-9-CM codes 81.54 and 81.51 for the New York SID and Canadian Classification of Intervention codes VG53 and VA53 for the Ontario DAD. Data from September 30 to December 31, 2013 were used for ascertainment of 90-day readmission rates only (22). We excluded patients who were assigned codes suggestive of trauma or hip fracture, patients whose procedures were performed on an emergent basis (since primary TKA and THA are typically not urgent), patients with a prior TKA or THA within 90 days of the index procedure (because of concern that the second admission could represent a readmission), and patients who underwent ≥2 TKA or THA procedures during the same hospitalization. Inclusion and exclusion criteria were applied to the New York SID and Ontario data using similar methods.

Outcomes. Our study included 4 complementary outcomes: 1) per capita utilization of TKA and THA; 2) hospital LOS; 3) discharge disposition (home versus other); and 4) all-cause hospital readmission occurring within 30 days and 90 days of discharge. After all primary TKA and THA procedures performed in New York and Ontario during the study period were identified, we calculated the annual utilization rates (per 10,000 population). Estimates from the New York population were obtained from US Census data (available at https://www.health.ny.gov/statistics/vital_statistics/2010/table01.htm). Estimates from the Ontario population were obtained from analogous Canadian census data. We linked the New York data to the American Hospital Association annual survey to ascertain information regarding hospital teaching status and bed size. We linked the Ontario DAD to the Ontario Health Insurance Plan Registered Persons Database for mortality information, and to information from the Ontario Ministry of Health and Long-Term Care.

Statistical analysis. All data analyses were conducted separately for the TKA and THA cohorts using similar methods and approaches. First, we compared patient demographics and key comorbid conditions captured during the inpatient hospitalization for patients who underwent TKA in New York and Ontario. We compared continuous measures using the *t*-test and categorical measures using the chi-square statistic.

Second, using similar bivariate methods, we compared the percentage of hospitals in New York and Ontario performing TKA, the mean and median annual procedural volumes at these hospitals, and the percentage of hospitals performing TKA that were categorized as major teaching hospitals (23). Similar analyses were performed for the THA cohorts.

Third, we calculated annualized primary TKA utilization rates (number of procedures per 10,000 population per year) for New York and Ontario. The numerator for these calculations was the annualized number of TKA procedures performed between January 1, 2012 and September 30, 2013, while the denominator was the population of adults ages ≥18 years. We calculated utilization for the entire adult population (ages ≥18 years), by age-specific population stratum (e.g., age <50 years, 50–59 years, etc.), and by patient sex (men and women), using analogous numerators and denominators. Similar analyses were performed for the THA cohorts.

We calculated standardized TKA and THA utilization rates for New York using direct standardization, with the Ontario population used as the reference; this allows us to compare utilization in New York and Ontario based on the assumption of similar population demographics in terms of age and sex (24). We compared utilization of TKA and THA in New York and Ontario using Poisson regression.

Fourth, we compared unadjusted outcomes in the TKA and THA cohorts in New York and Ontario. In particular, we compared the mean hospital LOS, discharge disposition, and hospital readmission rates within 30 days and 90 days of surgery.

Fifth, we examined adjusted outcomes for each study end point, using generalized linear models. We used 3 statistical models for each end point: model 1, adjusted only for patient demographics; model 2, adjusted for demographics plus hospital procedural volume; and model 3, adjusted for all model 2 factors plus comorbid conditions. Comorbid conditions were included in our models based on clinical plausibility and having a reasonable prevalence in both our New York and Ontario populations; of note, because in-hospital mortality was extremely rare, statistical concerns allowed us to include only 2 comorbid conditions related to mortality in model 3.

This analysis was approved by the Research Ethics Board at ICES. All analyses were performed using either SAS or R statistical software packages.

RESULTS

We identified 40,118 primary TKAs performed in Ontario and 40,831 TKAs performed in New York between January 1, 2012 and September 30, 2013 (Table 1). For THA, our cohorts consisted of 21,513 THAs performed in Ontario and 26,605 in New York (Table 1).

Focusing on TKA, a smaller percentage of procedures in Ontario were performed on patients ages <50 years when compared to those in New York (2.6% versus 5.0%; $P < 0.001$) (Table 1). A smaller percentage of TKAs in Ontario than in New York were performed on women (62.7% versus 65.4%; $P < 0.001$). The prevalence of all comorbid conditions was significantly lower in Ontario when compared to New York. Findings for THA followed a similar pattern (Table 1).

Continuing to focus on TKA (Table 2), a significantly smaller percentage of Ontario hospitals performed TKA when compared to New York hospitals (42.1% versus 75.7%; $P < 0.001$). Alternatively, the mean annual procedural volume for TKAs in Ontario hospitals was significantly higher than that in New York hospitals (mean 327 versus 179; $P < 0.001$). Results focusing on THA were similar (Table 2), with a lower percentage of Ontario hospitals performing the procedure and a higher mean procedural volume for THAs in Ontario.

In analyses using direct standardization, utilization of TKA per 10,000 adults in Ontario was significantly higher (21.4 per 10,000 population per year) as compared to New York (16.1 per 10,000 population per year) ($P < 0.001$) (Table 3). In stratified analyses,

Table 1. Characteristics of the patients who underwent primary TKA or THA in Ontario and New York in 2012–2013*

	TKA			THA		
	Ontario (n = 40,118)	New York (n = 40,831)	*P*	Ontario (n = 21,513)	New York (n = 26,605)	*P*
Demographic feature						
Age						
<50 years	1,058 (2.6)	2,032 (5.0)	<0.001	1,485 (6.9)	2,376 (8.9)	<0.001
50–59 years	7,348 (18.3)	8,493 (20.8)		4,094 (19.0)	6,071 (22.8)	
60–69 years	14,759 (36.8)	14,413 (35.3)		6,747 (31.4)	8,493 (31.5)	
70–79 years	12,418 (31.0)	11,723 (28.7)		6,135 (28.5)	6,491 (24.4)	
80–89 years	4,402 (11.0)	4,057 (9.9)		2,868 (13.3)	3,087 (11.6)	
≥90 years	133 (0.3)	113 (0.3)		184 (0.9)	192 (0.7)	
Female	25,154 (62.7)	26,684 (65.4)	<0.001	11,966 (55.6)	14,493 (56.6)	0.004
Comorbid condition						
Congestive heart failure	320 (0.8)	1,416 (3.5)	<0.001	155 (0.7)	1,114 (4.2)	<0.001
Coronary artery disease	568 (1.4)	2,128 (5.2)	<0.001	322 (1.5)	1,647 (6.2)	<0.001
Hypertension with complications	31 (0.1)	2,112 (5.2)	<0.001	14 (0.1)	1,432 (5.4)	<0.001
Diabetes	6,966 (17.4)	8,790 (21.5)	<0.001	2,538 (11.8)	4,106 (15.4)	<0.001
COPD	1,738 (4.3)	6,611 (16.2)	<0.001	889 (4.1)	3,939 (14.8)	<0.001
Renal failure	279 (0.7)	2,251 (5.5)	<0.001	181 (0.8)	1,572 (5.9)	<0.001

* Values are the number (%) of patients. TKA = total knee arthroplasty; THA = total hip arthroplasty; COPD = chronic obstructive pulmonary disease.

Table 2. Hospital characteristics*

	TKA			THA		
	Ontario (n = 164)	New York (n = 202)	*P*	Ontario (n = 164)	New York (n = 202)	*P*
Hospitals performing procedure, no. (%)	69 (42.1)	153 (75.7)	<0.001	68 (41.5)	155 (76.7)	<0.001
Annual procedural volume						
Mean ± SD	327 ± 222	179 ± 324	<0.001	181 ± 146	120 ± 299	0.011
Median (IQR)	291 (189–428)	93 (30–208)	NA	153 (82–223)	50 (16–127)	NA
Hospital volume (for those performing ≥1 procedure), no. (%)						
<25 procedures	1 (1.5)	34 (22.2)	<0.001†	4 (5.9)	30 (19.4)	<0.001†
25–49 procedures	2 (2.9)	14 (9.2)		4 (5.9)	14 (9.0)	
50–99 procedures	8 (11.6)	14 (9.2)		15 (22.1)	19 (12.3)	
100–199 procedures	9 (13.0)	17 (11.1)		23 (33.8)	12 (7.7)	
200–299 procedures	16 (23.2)	19 (12.4)		12 (17.7)	27 (17.4)	
300–399 procedures	12 (17.4)	30 (19.6)		4 (5.9)	13 (8.4)	
≥400 procedures	21 (30.4)	25 (16.3)		6 (8.8)	40 (25.8)	
Bed number, mean ± SD	214 ± 143	92 ± 52	<0.001	216 ± 143	91 ± 52	<0.001
Major teaching hospital, no. (%)	13 (18.8)	25 (16.7)	0.791	13 (19.1)	25 (16.4)	0.724

* TKA = total knee arthroplasty; THA = total hip arthroplasty; IQR = interquartile range; NA = not applicable.
† *P* for trend.

utilization of TKA in Ontario was significantly higher for all age strata when compared to New York, with the exception of patients ages <50 years (Table 3). Utilization of TKA both by women and by men was significantly higher in Ontario compared to New York. Results focusing on THA also showed higher utilization in Ontario when compared to New York, both in aggregate and for most age strata (Table 3).

In unadjusted analyses focusing on outcomes (Table 4), hospital LOS for TKA was significantly longer in Ontario than in New York (mean 3.7 days versus 3.4 days; $P < 0.001$), while the frequency of in-hospital mortality among those who underwent TKA was significantly higher in Ontario than in New York, although in terms of clinical significance, this difference was small (frequency of in-hospital mortality 0.07% in Ontario versus 0.03% in New York; $P = 0.035$).

A significantly higher percentage of Ontario TKA patients as compared to New York TKA patients were discharged home after surgery (90.9% versus 46.2%; $P < 0.001$). In addition, a lower percentage of Ontario TKA patients compared to New York TKA patients were transferred to another acute-care hospital (0.7% versus 2.8%; $P < 0.001$). Hospital readmission within 30 days of TKA was lower in Ontario than in New York (3.9% versus 4.6%; $P < 0.001$); similarly, readmission within 90 days

Table 3. Per capita numbers and utilization of TKA and THA in Ontario and New York

	Per capita number*						Utilization rate†					
	Ontario			New York			TKA			THA		
	TKA	THA	Population	TKA	THA	Population	Ontario	New York	*P*	Ontario	New York	*P*
Total	40,118	21,513	10,694,170	40,831	26,605	15,053,173	21.44	16.14	<0.001	11.5	10.51	<0.001
Age <50 years	1,058 (2.6)	1,485 (6.9)	5,987,033 (56.0)	2,032 (5.0)	2,376 (8.9)	8,711,634 (57.9)	1.01	1.33	<0.001	1.42	1.60	0.5
Age 50–59 years	7,348 (18.3)	4,094 (19.0)	1,958,582 (18.3)	8,493 (20.8)	6,071 (22.8)	2,657,336 (17.7)	21.44	18.26	<0.001	11.94	13.06	0.864
Age 60–69 years	14,759 (36.8)	6,747 (31.4)	1,392,999 (13.0)	14,413 (35.3)	8,378 (31.5)	1,839,471 (12.2)	60.54	44.77	<0.001	27.68	26.03	<0.001
Age 70–79 years	12,418 (31.0)	6,135 (28.5)	818,017 (7.6)	11,723 (28.7)	6,491 (24.4)	1,062,198 (7.1)	86.75	63.07	<0.001	42.86	34.92	<0.001
Age ≥80 years	4,535 (11.3)	3,052 (14.2)	537,539 (5.0)	4,170 (10.2)	3,289 (12.4)	782,534 (5.2)	48.21	30.45	<0.001	32.44	24.02	<0.001
Men	14,964 (37.3)	9,547 (44.4)	5,193,017 (48.6)	14,147 (34.6)	11,612 (43.6)	7,165,866 (47.6)	16.47	11.28	<0.001	10.51	9.26	<0.001
Women	25,154 (62.7)	11,966 (55.6)	5,501,153 (51.4)	26,684 (65.4)	14,993 (56.4)	7,887,307 (52.4)	26.13	19.33	<0.001	12.43	10.86	<0.001

* Values are the number (%) of total knee arthroplasty (TKA) or total hip arthroplasty (THA) procedures per 10,000 population per year.
† Values are the total utilization rate, directly standardized to match the age and sex of the New York populations to the Ontario populations.

Table 4. Unadjusted outcomes in patients who underwent primary TKA or THA in Ontario and New York*

	TKA			THA		
	Ontario (n = 40,118)	New York (n = 40,831)	*P*	Ontario (n = 21,513)	New York (n = 26,605)	*P*
Length of stay, mean ± SD days	3.72 ± 2.1	3.43 ± 1.8	<0.001	3.91 ± 2.5	3.46 ± 2.4	<0.001
Discharge disposition, no. (%)						
Died in hospital	27 (0.07)	13 (0.03)	0.035	18 (0.1)	16 (0.06)	0.428
Discharged home	36,479 (90.9)	18,865 (46.2)	<0.001	19,054 (88.6)	14,078 (52.9)	<0.001
Transfer to another acute-care hospital	280 (0.7)	1,129 (2.8)	<0.001	272 (1.3)	569 (2.1)	<0.001
Post–acute care	3,312 (8.3)	20,810 (51.0)	<0.001	2,161 (10.1)	11,934 (44.9)	<0.001
Other	20 (0.05)	14 (0.03)	0.363	8 (0.04)	8 (0.03)	0.862
Readmission, no. (%)						
30-day hospital readmission	1,569 (3.9)	1,862 (4.6)	<0.001	1,017 (4.7)	1,134 (4.3)	0.015
90-day hospital readmission	2,666 (6.7)	3,403 (8.4)	<0.001	1,603 (7.5)	2,197 (8.3)	0.001

* TKA = total knee arthroplasty; THA = total hip arthroplasty.

was lower in Ontario as compared to New York (6.7% versus 8.4%; $P < 0.001$). Analyses focusing on patients who underwent THA revealed that the differences between Ontario and New York were similar to those for TKA for most of the outcomes in unadjusted analyses (Table 4).

In adjusted analyses (adjusted for age, sex, hospital procedural volume, and comorbid conditions) focusing on outcomes in patients who underwent TKA (Table 5), the frequency of in-hospital mortality in TKA patients was similar between Ontario and New York in all 3 statistical models. The mean hospital LOS for TKA was significantly longer in Ontario than in New York in all 3 models, whereas both 30-day and 90-day readmission rates in TKA patients from Ontario were significantly lower than those from New York. Adjusted analyses focusing on THA patients demonstrated results similar to those for TKA (Table 6) (the full regression models with coefficients are shown in Supplementary Tables 1–4, available on the *Arthritis & Rheumatology* web site at http://onlinelibrary.wiley.com/doi/10.1002/art.40407/abstract).

DISCUSSION

In this analysis of population-based administrative data, we found that rates of utilization of both TKA and THA were higher in Ontario, Canada as compared to the state of New York. We also found that a smaller percentage of Ontario hospitals performed TJA, and Ontario hospitals had higher surgical volumes compared to New York hospitals. Furthermore, Ontario hospitals appeared to have longer hospital LOS but lower rates of hospital readmissions, and a significantly higher percentage of Ontario residents were discharged home after surgery.

Several of our results warrant elaboration. It is important to consider our TKA and THA utilization data in the context of prior studies of joint arthroplasty utilization. In a prior analysis of US Medicare data (from adults ages ≥65 years), we found primary TKA and THA utilization rates of ~60 procedures and ~25 procedures per 10,000 population per year, respectively, in 2008–2010 (25–27). In the current study, we

Table 5. Adjusted outcomes in patients who underwent total knee arthroplasty in New York and Ontario*

	Model 1†		Model 2‡		Model 3§	
	New York	Ontario	New York	Ontario	New York	Ontario
In-hospital mortality	0.019 (0.008–0.046)	0.035 (0.018–0.066)	0.028 (0.012–0.067)	0.033 (0.016–0.065)	0.025 (0.010–0.062)	0.027 (0.013–0.055)
Hospital LOS	3.454 (3.432–3.476)	3.856 (3.827–3.885)	3.474 (3.451–3.498)	3.815 (3.783–3.847)	3.463 (3.434–3.491)	3.690 (3.656–3.723)
30-day hospital readmission	4.136 (3.903–4.383)	3.353 (3.136–3.584)	4.498 (4.23–4.781)	3.498 (3.256–3.757)	4.411 (4.097–4.749)	3.210 (2.971–3.468)
90-day hospital readmission	8.161 (7.73–8.613)	5.989 (5.702–6.290)	8.359 (8.000–8.732)	6.100 (5.783–6.433)	8.950 (8.380–9.556)	5.727 (5.408–6.065)

* Values are the adjusted proportion experiencing mortality (95% confidence interval), adjusted hospital length of stay (LOS) in days (95% confidence interval), and adjusted percentage experiencing readmission at 30 days and 90 days after initial discharge (95% confidence interval).
† Adjusted for patient age and sex.
‡ Adjusted for model 1 factors plus hospital procedural volume.
§ Adjusted for model 2 factors plus comorbid conditions.

Table 6. Adjusted outcomes in patients who underwent total hip arthroplasty in New York and Ontario*

	Model 1†		Model 2‡		Model 3§	
	New York	Ontario	New York	Ontario	New York	Ontario
In-hospital mortality	0.019 (0.007–0.055)	0.041 (0.018–0.097)	0.025 (0.008–0.074)	0.045 (0.019–0.110)	0.023 (0.007–0.070)	0.040 (0.017–0.097)
Hospital LOS	3.486 (3.447–3.525)	4.161 (4.100–4.221)	3.579 (3.538–3.621)	4.139 (4.072–4.206)	3.565 (3.516–3.613)	4.013 (3.944–4.081)
30-day hospital readmission	4.065 (3.757–4.397)	4.133 (3.784–4.511)	4.472 (4.119–4.854)	4.243 (3.857–4.667)	4.549 (4.137–5.000)	4.006 (3.625–4.424)
90-day hospital readmission	8.161 (7.73–8.613)	6.932 (6.486–7.407)	8.866 (8.377–9.381)	7.064 (6.567–7.595)	8.948 (8.377–9.553)	6.688 (6.196–7.215)

* Values are the adjusted proportion experiencing mortality (95% confidence interval), adjusted hospital length of stay (LOS) in days (95% confidence interval), and adjusted percentage experiencing readmission at 30 days and 90 days after initial discharge (95% confidence interval).
† Adjusted for patient age and sex.
‡ Adjusted for model 1 factors plus hospital procedural volume.
§ Adjusted for model 2 factors plus comorbid conditions.

observed utilization rates in our older populations that were roughly similar to those previously reported.

There are very few studies that have directly compared TKA and THA utilization and outcomes between different countries. Pabinger and colleagues used pooled data obtained from the OECD to examine TJA utilization in ~20 countries. They found that in 2011, TKA utilization ranged between 2 per 10,000 population (in Poland) and 23 per 10,000 population (in the US) (13), and THA utilization ranged between 8 per 10,000 population (in Poland) and 29 per 10,000 population (in Germany). We are aware of only one study that directly compared TKA and THA utilization in the US and Canada. In that study, Ravi et al used 2001–2007 data from the US Nationwide Inpatient Sample and the province of Ontario; the team found that in 2001, rates of utilization of TKA and THA were ~30% and ~10% higher, respectively, in the US when compared to Ontario, but differences had declined by 2007 (15).

Historically, most single-payor health care systems have done relatively well with cost control but have fared poorly with access. The phenomenon of wait lists for elective surgical procedures, including TKA and THA, in Ontario has been well described, as well as the negative impact of wait times on patients' physical function (28,29). In the early part of the 21st century, the Canadian government (including Ontario) faced considerable public pressure to improve health care access and reduce wait times, and specifically to improve access to TJA (30,31). The government responded with an array of new initiatives and policies. We suspect that these efforts might explain our finding that utilization of TJA in Ontario has now surpassed utilization in New York.

While differences in health care system structures and financing might explain the differences in TJA utilization observed in the present study, there are other potential explanations. It is possible that differences in the prevalence of advanced osteoarthritis or obesity could underlie the differences in TJA utilization, but we are unaware of any convincing data supporting this hypothesis (32–34). Another possible explanation for the higher utilization of TJA in Ontario might be that there is a lower threshold for surgery than for medical management in Ontario as compared to New York. Although appropriateness criteria for TJA have been developed (35–37), widespread implementation has been limited by the need for detailed clinical, radiographic, and patient-reported symptom scores. Our reliance on administrative data precluded us from investigating appropriateness in this study, but this is certainly an area for further investigation.

We observed that a substantially smaller percentage of Ontario hospitals offered TJA, and those that offered TJA had significantly higher procedural volumes compared to New York hospitals; this likely reflects differences in the regulatory environment. Ontario—like many single-payor systems with substantial government involvement—relies on centralized planning to determine which hospitals should offer which services (38,39). In the US, hospitals are encouraged to be entrepreneurial, with the idea that competition breeds lower price and higher quality; hospitals are typically able to offer most clinical services with minimal regulatory barriers. Moreover, in the US, TJA is typically thought to be profitable for hospitals (7). Thus, it is not surprising that the percentage of hospitals performing TJA in New York is far higher but the procedural volumes are substantially lower when compared to Ontario.

It is important to address the differences in outcomes that we observed. Patients in Ontario were much more likely to be discharged home and much less likely to be discharged to post–acute care (e.g., inpatient rehabilitation) when compared to patients in New York. Post–acute

care is expensive, and supply in Ontario is extremely limited, making discharge home the preferred option (40). In contrast, post–acute care in the US is typically available and covered by insurance, making it easy for hospitals to discharge patients to rehabilitation. It is noteworthy that even with ~90% of Ontario patients discharged home after TJA, hospital readmission rates were actually lower than in New York. The combination of lower utilization of post–acute care in Ontario and lower readmission rates suggests that there are still significant efficiencies to be gained in the US (41,42).

A number of other findings warrant brief mention. We would be remiss if we did not speak to the differences in comorbidity that we observed. One possible explanation would be that TKA and THA recipients in New York truly have prevalence rates of heart failure, hypertension, and diabetes that are markedly higher than in Ontario; this seems implausible. Rather, we suspect that the well-recognized pressure to "up-code" for purposes of reimbursement and risk adjustment is the major driver of the differences observed (43,44). If differences in comorbidity reflect cross-border differences in coding practices rather than true differences in the prevalence of comorbid conditions, adjustment for such comorbidities could introduce major bias into risk-adjustment models.

It is important to point out limitations in our study. Our analysis was limited to patients in Ontario, Canada and the state of New York; generalizing our findings to the entire country of Canada and the entire US should be done with caution, particularly given the marked differences in health care delivery across Canada's different provinces.

Furthermore, our study relied on hospital administrative data and lacked reliable information on comorbidities, and we were unable to assess data on patient-reported outcomes and long-term follow-up. In addition, we were unable to exclude unicompartmental procedures from our TKA cohort because the granularity of ICD-9 coding is limited, and unicompartmental procedures represent ~10% of knee arthroplasty procedures (45,46). We included unicompartmental procedures in both our New York cohorts and our Ontario cohorts to avoid biasing our results.

Finally, we are unable to comment on the indications for each procedure or their clinical appropriateness (36,47,48). Thus, although utilization in Ontario was greater than that in New York, we are unable to say whether higher TJA utilization represents underuse in New York or overuse in Ontario.

In summary, we found higher utilization of TJA in Ontario than in New York, but evidence of greater efficiency (e.g., higher hospital volumes and lower readmission rates) in Ontario. Taken together, our results hint at opportunities for further improvement in each locale.

AUTHOR CONTRIBUTIONS

All authors were involved in drafting the article or revising it critically for important intellectual content, and all authors approved the final version to be published. Dr. Cram had full access to all of the data in the study and takes responsibility for the integrity of the data and the accuracy of the data analysis.

Study conception and design. Cram, Landon, Matelski, Ling, Paterson, Ravi.

Acquisition of data. Cram, Matelski, Ling, Paterson.

Analysis and interpretation of data. Cram, Landon, Matelski, Ling, Stukel, Paterson, Gandhi, Hawker, Ravi.

REFERENCES

1. Losina E, Walensky RP, Kessler CL, Emrani PS, Reichmann WM, Wright EA, et al. Cost-effectiveness of total knee arthroplasty in the United States: patient risk and hospital volume. Arch Intern Med 2009;169:1113–21; discussion 1121–2.
2. Hawker GA, Badley EM, Croxford R, Coyte PC, Glazier RH, Guan J, et al. A population-based nested case-control study of the costs of hip and knee replacement surgery. Med Care 2009; 47:732–41.
3. Culliford D, Maskell J, Judge A, Cooper C, Prieto-Alhambra D, Arden NK. Future projections of total hip and knee arthroplasty in the UK: results from the UK Clinical Practice Research Datalink. Osteoarthritis Cartilage 2015;23:594–600.
4. Kurtz SM, Ong KL, Lau E, Bozic KJ. Impact of the economic downturn on total joint replacement demand in the United States: updated projections to 2021. J Bone Joint Surg Am 2014; 96:624–30.
5. Lurie JD, Bell JE, Weinstein J. What rate of utilization is appropriate in musculoskeletal care? Clin Orthop Relat Res 2009;467:2506–11.
6. Cram P, Ravi B, Vaughan-Sarrazin MS, Lu X, Li Y, Hawker G. What drives variation in episode-of-care payments for primary TKA? An analysis of Medicare administrative data. Clin Orthop Relat Res 2015;473:3337–47.
7. Cram P, Lu X, Li Y. Bundled payments for elective total knee arthroplasty: an analysis of Medicare administrative data. Geriatr Orthop Surg Rehabil 2015;6:3–10.
8. Jaakkimainen L, Glazier R, Barnsley J, Salkeld E, Lu H, Tu K. Waiting to see the specialist: patient and provider characteristics of wait times from primary to specialty care. BMC Fam Pract 2014;15:16.
9. Canadian Institute for Health Information. Benchmarks for treatment and wait time trending across Canada. URL: http://waittimes.cihi.ca/.
10. Bird C. Wait times increasing for hip and knee replacement. CMAJ 2013;185:E325.
11. Anderson GF, Reinhardt UE, Hussey PS, Petrosyan V. It's the prices, stupid: why the United States is so different from other countries. Health Aff (Millwood) 2003;22:89–105.
12. Spiro T, Lee EO, Emanuel EJ. Price and utilization: why we must target both to curb health care costs. Ann Intern Med 2012; 157:586–90.
13. Pabinger C, Lothaller H, Geissler A. Utilization rates of knee-arthroplasty in OECD countries. Osteoarthritis Cartilage 2015; 23:1664–73.
14. Pabinger C, Geissler A. Utilization rates of hip arthroplasty in OECD countries. Osteoarthritis Cartilage 2014;22:734–41.
15. Ravi B, Croxford R, Reichmann WM, Losina E, Katz JN, Hawker GA. The changing demographics of total joint arthroplasty recipients in the United States and Ontario from 2001 to 2007. Best Pract Res Clin Rheumatol 2012;26:637–47.

16. Agency for Healthcare Research and Quality. HCUP databases. Overview of the State Inpatient Databases (SID). April 2017. URL: http://www.hcup-us.ahrq.gov/sidoverview.jsp.
17. White C. Cutting Medicare hospital prices leads to a spillover reduction in hospital discharges for the nonelderly. Health Serv Res 2014;49:1578–95.
18. Elixhauser A, Steiner C, Harris DR, Coffey RM. Comorbidity measures for use with administrative data. Med Care 1998;36:8–27.
19. Ravi B, Jenkinson R, Austin PC, Croxford R, Wasserstein D, Escott B, et al. Relation between surgeon volume and risk of complications after total hip arthroplasty: propensity score matched cohort study. BMJ 2014;348:g3284.
20. Stukel TA, Fisher ES, Alter DA, Guttmann A, Ko DT, Fung K, et al. Association of hospital spending intensity with mortality and readmission rates in Ontario hospitals. JAMA 2012;307: 1037–45.
21. Quan H, Sundararajan V, Halfon P, Fong A, Burnand B, Luthi JC, et al. Coding algorithms for defining comorbidities in ICD-9-CM and ICD-10 administrative data. Med Care 2005;43:1130–9.
22. Daneshvar P, Forster AJ, Dervin GF. Accuracy of administrative coding in identifying hip and knee primary replacements and revisions. J Eval Clin Pract 2012;18:555–9.
23. Newcombe RG. Interval estimation for the difference between independent proportions: comparison of eleven methods. Stat Med 1998;17:873–90.
24. Ko DT, Tu JV, Samadashvili Z, Guo H, Alter DA, Cantor WJ, et al. Temporal trends in the use of percutaneous coronary intervention and coronary artery bypass surgery in New York State and Ontario. Circulation 2010;121:2635–44.
25. Singh JA, Lu X, Rosenthal GE, Ibrahim S, Cram P. Racial disparities in knee and hip total joint arthroplasty: an 18-year analysis of national Medicare data. Ann Rheum Dis 2014;73: 2107–15.
26. Cram P, Lu X, Kates SL, Singh JA, Li Y, Wolf BR. Total knee arthroplasty volume, utilization, and outcomes among Medicare beneficiaries, 1991–2010. JAMA 2012;308:1227–36.
27. Cram P, Lu X, Kaboli PJ, Vaughan-Sarrazin MS, Cai X, Wolf BR, et al. Clinical characteristics and outcomes of Medicare patients undergoing total hip arthroplasty, 1991–2008. JAMA 2011;305: 1560–7.
28. Davis AM, Agnidis Z, Badley E, Davey JR, Gafni A, Gollish J, et al. Waiting for hip revision surgery: the impact on patient disability. Can J Surg 2008;51:92–6.
29. Hudak PL, Grassau P, Glazier RH, Hawker G, Kreder H, Coyte P, et al. "Not everyone who needs one is going to get one": the influence of medical brokering on patient candidacy for total joint arthroplasty. Med Decis Making 2008;28:773–80.
30. Gaudet MC, Ehrmann Feldman D, Rossignol M, Zukor D, Tanzer M, Gravel C, et al. The wait for total hip replacement in patients with osteoarthritis. Can J Surg 2007;50:101–9.
31. Snider MG, MacDonald SJ, Pototschnik R. Waiting times and patient perspectives for total hip and knee arthroplasty in rural and urban Ontario. Can J Surg 2005;48:355–60.
32. Zhang Y, Jordan JM. Epidemiology of osteoarthritis. Clin Geriatr Med 2010;26:355–69.
33. Wallace IJ, Worthington S, Felson DT, Jurmain RD, Wren KT, Maijanen H, et al. Knee osteoarthritis has doubled in prevalence since the mid-20th century. Proc Natl Acad Sci U S A 2017; 114:9332–6.
34. Birtwhistle R, Morkem R, Peat G, Williamson T, Green ME, Khan S, et al. Prevalence and management of osteoarthritis in primary care: an epidemiologic cohort study from the Canadian Primary Care Sentinel Surveillance Network. CMAJ Open 2015;3:E270–5.
35. Ghomrawi HM, Schackman BR, Mushlin AI. Appropriateness criteria and elective procedures: total joint arthroplasty. N Engl J Med 2012;367:2467–9.
36. Ghomrawi HM, Alexiades M, Pavlov H, Nam D, Endo Y, Mandl LA, et al. Evaluation of two appropriateness criteria for total knee replacement. Arthritis Care Res (Hoboken) 2014;66:1749–53.
37. Quintana JM, Arostegui I, Escobar A, Azkarate J, Goenaga JI, Lafuente I. Prevalence of knee and hip osteoarthritis and the appropriateness of joint replacement in an older population. Arch Intern Med 2008;168:1576–84.
38. Naylor CD. Health care in Canada: incrementalism under fiscal duress. Health Aff (Millwood) 1999;18:9–26.
39. Naylor D, Girard F, Mintz JM, Fraser N, Jenkins T, Power C. Unleashing innovation: excellent healthcare for Canada. Report of the Advisory Panel on Healthcare Innovation. Ottawa: Health Canada; 2015. p. 1–164.
40. Mahomed NN, Davis AM, Hawker G, Badley E, Davey JR, Syed KA, et al. Inpatient compared with home-based rehabilitation following primary unilateral total hip or knee replacement: a randomized controlled trial. J Bone Joint Surg Am 2008;90:1673–80.
41. Whitcomb WF, Lagu T, Krushell RJ, Lehman AP, Greenbaum J, McGirr J, et al. Experience with designing and implementing a bundled payment program for total hip replacement. Jt Comm J Qual Patient Saf 2015;41:406–13.
42. Tsai TC, Joynt KE, Wild RC, Orav EJ, Jha AK. Medicare's Bundled Payment initiative: most hospitals are focused on a few high-volume conditions. Health Aff (Millwood) 2015;34:371–80.
43. Vaughan-Sarrazin MS, Lu X, Cram P. The impact of paradoxical comorbidities on risk-adjusted mortality of Medicare beneficiaries with cardiovascular disease. Medicare Medicaid Res Rev 2011;1:E1–17.
44. Landon BE, Mechanic RE. The paradox of coding: policy concerns raised by risk-based provider contracts. N Engl J Med 2017; 377:1211–3.
45. Liddle AD, Judge A, Pandit H, Murray DW. Adverse outcomes after total and unicompartmental knee replacement in 101,330 matched patients: a study of data from the National Joint Registry for England and Wales. Lancet 2014;384:1437–45.
46. Riddle DL, Jiranek WA, McGlynn FJ. Yearly incidence of unicompartmental knee arthroplasty in the United States. J Arthroplasty 2008;23:408–12.
47. Hawker G, Bohm ER, Conner-Spady B, De Coster C, Dunbar M, Hennigar A, et al. Perspectives of Canadian stakeholders on criteria for appropriateness for total joint arthroplasty in patients with hip and knee osteoarthritis. Arthritis Rheumatol 2015;67:1806–15.
48. Escobar A, Quintana JM, Arostegui I, Azkarate J, Guenaga JI, Arenaza JC, et al. Development of explicit criteria for total knee replacement. Int J Technol Assess Health Care 2003;19:57–70.

ARTHRITIS & RHEUMATOLOGY
Vol. 70, No. 4, April 2018, pp 555–565
DOI 10.1002/art.40405

Effects of HLA–B27 on Gut Microbiota in Experimental Spondyloarthritis Implicate an Ecological Model of Dysbiosis

Tejpal Gill,[1] Mark Asquith,[2] Stephen R. Brooks,[1] James T. Rosenbaum,[3] and Robert A. Colbert[1]

Objective. **To investigate whether HLA–B27–mediated experimental spondyloarthritis (SpA) is associated with a common gut microbial signature, in order to identify potential drivers of pathogenesis.**

Methods. **The effects of HLA–B27 on 3 genetic backgrounds, dark agouti (DA), Lewis, and Fischer, were compared, using wild-type littermates and HLA–B7–transgenic Lewis rats as controls. Cecum and colon tissue specimens or contents were collected from the rats at 2, 3–4, and 6–8 months of age, and histologic analysis was performed to assess inflammation, RNA sequencing was used to determine gene expression differences, and 16S ribosomal RNA gene sequencing was used to determine microbiota differences.**

Results. **Both HLA–B27–transgenic Lewis rats and HLA–B27–transgenic Fischer rats developed gut inflammation, while DA rats were resistant to the effects of HLA–B27, and HLA–B7–transgenic rats were not affected. Immune dysregulation was similar in affected Lewis and Fischer rats and was dominated by activation of interleukin-23 (IL-23)/IL-17, interferon, tumor necrosis factor, and IL-1 cytokines and pathways in the colon and cecum, while DA rats exhibited low-level cytokine dysregulation without inflammation. Gut microbial changes in HLA–B27–transgenic rats were strikingly divergent on the 3 different host genetic backgrounds, including different patterns of dysbiosis in HLA–B27–transgenic Lewis and HLA–B27–transgenic Fischer rat strains, with some overlap. Interestingly, DA rats lacked segmented filamentous bacteria that promote CD4+ Th17 cell development, which may explain their resistance to disease.**

Conclusion. **The effects of HLA–B27 on gut microbiota and dysbiosis in SpA are highly dependent on the host genetic background and/or environment, despite convergence of dysregulated immune pathways. These results implicate an ecological model of dysbiosis, with the effects of multiple microbes contributing to the aberrant immune response, rather than a single or small number of microbes driving pathogenesis.**

Spondyloarthritis (SpA) is an immune-mediated inflammatory disease encompassing several conditions that exhibit overlapping clinical features and genetic predisposition (1,2). Considerable evidence supports a link between gastrointestinal (GI) tract inflammation and the development of SpA (3). Among patients with ankylosing spondylitis (AS), the prototype of SpA, 7% have coexisting inflammatory bowel disease (IBD), and another 60% have subclinical gut inflammation (4). Similarly, arthritis develops in 10–50% of patients with IBD, and AS develops in nearly 10% of patients (5).

Direct evidence showing that gut microbiota is critical for the development of SpA was derived from an animal model. Rats transgenic for HLA–B27, a major genetic risk factor for SpA, and human β_2-microglobulin ($h\beta_2m$), referred to hereafter as HLA–B27–transgenic, develop key features of human SpA when they are housed in a conventional or specific pathogen–free animal facility. In a germ-free environment, however, gut inflammation and joint inflammation are prevented (6,7). Recolonization of the gut with bacteria is sufficient to induce inflammatory gut and joint disease, implicating commensal bacteria in the development of HLA–B27–induced SpA (7). More recently, our group demonstrated that expression of HLA–B27 and $h\beta_2m$, as well as the

Supported by the NIH (National Institute of Arthritis, Musculoskeletal and Skin Diseases Intramural Research Program grant Z01-AR-041184 to Dr. Colbert), the Stan and Madelle Rosenfeld Family Trust, the William and Mary Bauman Foundation, the Spondylitis Association of America, and Research to Prevent Blindness (grants to Dr. Rosenbaum). Dr. Asquith is a Jane Bruckel Scholar of the Spondylitis Association of America.

[1]Tejpal Gill, PhD, Stephen R. Brooks, PhD, Robert A. Colbert, MD, PhD: National Institute of Arthritis, Musculoskeletal and Skin Diseases, NIH, Bethesda, Maryland; [2]Mark Asquith, PhD: Oregon Health and Science University, Portland; [3]James T. Rosenbaum, MD: Legacy Devers Eye Institute and Oregon Health and Science University, Portland.

Drs. Gill and Asquith contributed equally to this work.

Address correspondence to Robert A. Colbert, MD, PhD, Pediatric Translational Research Branch, NIAMS/NIH, 10 Center Drive, Building 10, Room 12N/248B, Bethesda, MD 20892. E-mail: colbertr@mail.nih.gov.

Submitted for publication May 18, 2017; accepted in revised form December 19, 2017.

non–disease-associated HLA–B7 allele, alters gut microbial communities in this animal model, providing compelling evidence that major histocompatibility complex class I proteins can shape the microbiome (8). Alterations in gut microbiota in association with human SpA have also been observed in juvenile-onset disease (9), psoriatic arthritis (10), and AS (11).

The mechanism or mechanisms by which HLA–B27 promotes the development of SpA remain unclear. Despite the central role of HLA–B27 in presenting peptides to cytotoxic CD8+ T lymphocytes, evidence showing that these cells drive disease in rats is lacking, and the SpA phenotype develops normally in *Cd8a*-deficient HLA–B27–transgenic animals (12). In contrast, compelling evidence has implicated CD4+ T cells in the pathogenicity of inflammatory disease (13), as demonstrated by activation of the interleukin-23 (IL-23)/IL-17 axis in both joint and gut inflammation in rats (14) as well as in humans with SpA (15).

Aberrant features of HLA–B27, such as its tendency to misfold and dimerize, which can lead to endoplasmic reticulum stress and expression of aberrant cell surface complexes, have been implicated, and both misfolding and dimerization are linked to activation of the IL-23/IL-17 axis (16). In addition, a growing appreciation for the contribution of endogenous microbiota to many disease states led Rosenbaum and Davey to hypothesize that an HLA–B27–induced change in gut microbiota may be a key intermediary in the development of SpA (17). Recent evidence suggests that innate immune activation and Th17 cell expansion may precede the development of dysbiosis and gut inflammation in HLA–B27–transgenic rats (18). Thus, it is important to understand how HLA–B27 shapes the gut microbiome.

Herein, we observed, quite unexpectedly, considerable differences in HLA–B27–mediated dysbiosis between 3 different rat strains. On the disease-permissive Lewis and Fischer backgrounds, different patterns of gut microbial dysbiosis were associated with common immune dysregulation reflecting activation of the IL-23/IL-17, interferon-γ (IFNγ), tumor necrosis factor (TNF), and IL-1 pathways in the cecum and colon. Our results indicate that the effects of HLA–B27 on gut microbiota diverge with different host genetic background and/or environment, despite similar mechanisms of immune dysregulation and inflammation. These results have important implications for understanding how HLA–B27 may shape the intestinal microbiome and promote disease in the diverse human population.

MATERIALS AND METHODS

Animals. All of the HLA–B27/hβ_2m–transgenic rats used in this study carried the same transgene locus (33-3), which contains genomic HLA–B27 and hβ_2m DNA (19). The 33-3 locus was backcrossed from the original Fischer (F344) strain to the DA background (13) and then subsequently from the DA to the Lewis background for more than 10 generations (20). HLA–B7–transgenic rats homozygous for the 120-4 transgene locus on the Lewis background were used (13) to ensure that expression of heavy chains in these rats was comparable with that in HLA–B27–transgenic rats (20). While the HLA–B27–transgenic DA rats were resistant to disease, the HLA–B27–transgenic Lewis rats developed gut inflammation but not arthritis during the study period. HLA–B27–transgenic Fischer rats also developed gut inflammation and also more frequently developed arthritis (~30%), beginning at ~3 months of age.

In the current study, both male and female transgenic Lewis, Fischer, and DA rats were used, with transgene-negative littermates (wild-type [WT]) used as controls. All rats were bred and housed at the National Institutes of Health (NIH), with the exception of HLA–B27–transgenic and WT Fischer rats, which were bred and housed at Oregon Health & Science University (OHSU). Animals were weaned at 21 days, and cohorts were randomly selected to undergo euthanasia at 2, 3–4, or 6–8 months of age. Fischer rats were housed after weaning according to their genotype, whereas the DA and Lewis rats were co-housed for a short period of time before being separated (according to weight limit requirements per cage). The DA and Lewis rat cohorts selected for euthanasia at 2 months of age were housed singly after weaning. All animals were maintained under specific pathogen–free conditions and fed Purina 5008 rat chow. Experiments were performed following approval by the Institutional Animal Care and Use Committees at the National Institute of Arthritis and Musculoskeletal and Skin Diseases (NIAMS) or OHSU.

Histologic assessment. Hematoxylin and eosin–stained tissue sections from paraffin-embedded ileum, cecum, and colon samples were scored in a blinded manner by 2 independent observers, using an established scoring system (21). Samples with initially discordant scores (scores differing by >1) were rerandomized and rescored to eliminate discrepancies.

Host transcriptome analysis. Tissue samples obtained from the cecum and colon were homogenized in TRIzol reagent (Invitrogen), and RNA was isolated using a standard phenol–chloroform extraction method. All samples used for RNA sequencing had an RNA integrity number of >8. Library preparation for RNA samples was performed according to the Illumina protocol. Single-end sequencing of 50 bases was performed using an Illumina HiSeq 2000 system, and raw reads were mapped to the rat rn5 genome, using TopHat version 2.0.8. Transcript expression levels (in reads per kilobase million [RPKM]) and analysis of variance (ANOVA) were performed using Partek Genomics Suite 6.6. Differentially expressed genes were defined as those with a minimum 2-fold change ($P < 0.05$ and $q < 0.2$), with an RPKM value of >1 for various comparisons. Principal components analysis (PCA) was performed using Partek Genomics Suite 6.6, and Euler diagrams were constructed with eulerr (https://cran.r-project.org/package=eulerr) using RStudio 1.0.136.

Prediction of immune cell types. The Immunological Genome Project (ImmGen) function in ToppGene (22) was used

to predict immune cell types, based on functional annotation of differentially expressed genes. Genes with increased expression (>2-fold; $P < 0.05$, $q < 0.2$) in HLA–B27–transgenic or HLA–B7–transgenic rats compared with WT controls on various backgrounds were used. We used ToppGene, which maps differentially expressed genes to multiple immune cell subtypes identified in ImmGen and then groups them into broader immune cell types. These are represented by multiple lines distinguished by color, with each line representing a *P* value (y-axis) based on the quality of the match to a specific immune cell subtype.

Microbial community analysis. DNA was isolated from the ileum (mucosa), cecum (mucosa and lumen), and colon (lumen), using a Qiagen DNeasy kit. The 16S ribosomal RNA genes were amplified using 515–806 primers as specified by the Earth Microbiome Project (http://www.earthmicrobiome.org/), sequenced on an Illumina MiSeq system (23), and processed in Qiita (www.qiita.ucsd.edu). Data were quality-filtered using QIIME (Quantitative Insights into Microbial Ecology) version 1.9.1, and taxa were identified and assigned to the species level (phylogenetic level 7). We compared the relative frequency of gut microbes in the ileum (mucosa), cecum (mucosa and lumen), and colon (lumen) at the species level (maximum >0.1%; $P < 0.05$, $q < 0.1$) and in the WT controls. Operational taxonomic units classified to the species level were used. To construct Euler diagrams, eulerr (https://cran.r-project.org/package=eulerr) was used in RStudio 1.0.136.

Statistical analysis. For RNA sequencing data, ANOVA was used to compare differences between group means of $\log_2$-transformed RPKM values (offset by 0.1). Using the Partek Genomics Suite, we performed false discovery rate (FDR) analysis to account for multiple tests ($q < 0.2$). For the microbiome analysis, nonparametric Wilcoxon signed rank tests using the FDR approach to correct for multiple comparisons were used to compare relative frequencies ($P < 0.05$, $q < 0.1$). Individual Wilcoxon tests were performed to calculate statistical significance between groups, using JMP version 12.2.0. RPKM counts for individual genes were assessed with 2-tailed *t*-tests, using GraphPad Prism 6.

RESULTS

Variable penetrance and severity of HLA–B27–induced gut inflammation. To determine the role of genetic background on HLA–B27–induced gut inflammation and dysbiosis, we compared the effects of the same transgene locus (33-3) that encodes HLA–B27 and hβ_2m, in DA, Lewis, and Fischer rats (13). HLA–B7/hβ_2m–transgenic rats (120-4 transgene locus) were used as an HLA class I control for the Lewis background. The animals were weaned at 3 weeks of age and then randomized to undergo euthanasia at 2, 3–4, or 6–8 months of age. Samples were collected from the terminal ileum, cecum, and distal colon for histologic analysis, microbiome studies, and gene expression analysis (Figure 1A and also Supplementary Table 1, available on the *Arthritis & Rheumatology* web site at http://onlinelibrary.wiley.com/doi/10.1002/art.40405/abstract).

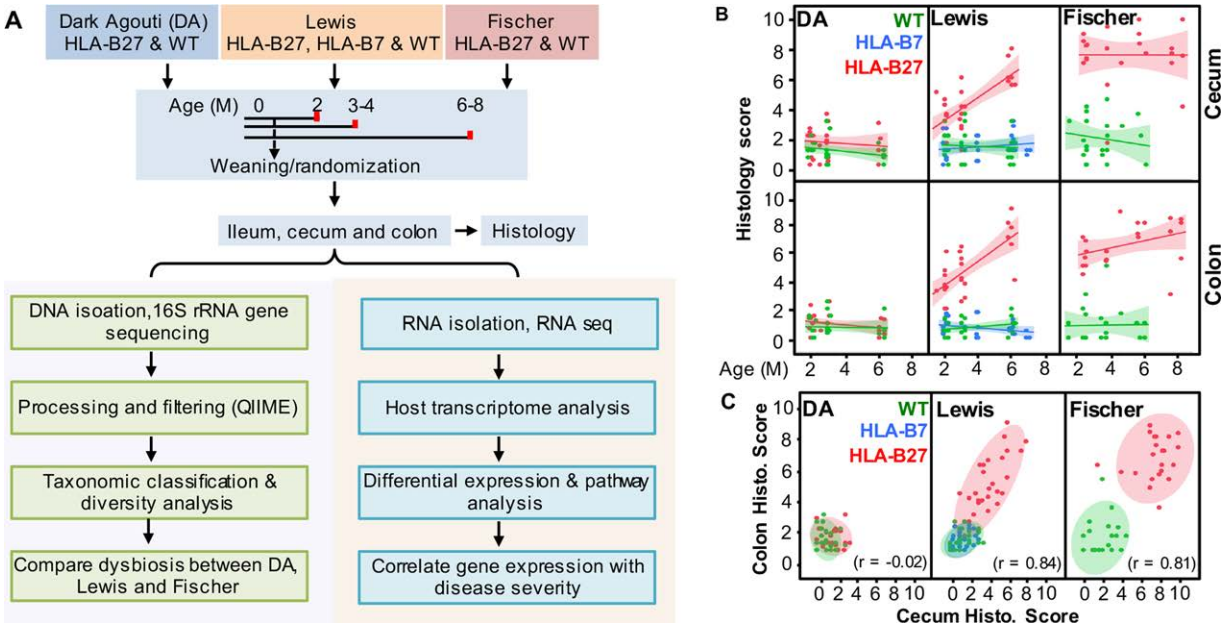

Figure 1. Experimental design and histologic (Histo.) assessment of HLA–B27–associated gut inflammation. **A**, Schematic representation of the experimental design. **B**, Histology scores for the cecum and colon in the rat cohorts, according to age. Each data point represents the mean score for 4–8 tissue sections from an individual rat. Scoring was performed according to an established scoring system (21). The lines were generated by regression analysis, and the shaded areas depict 95% confidence intervals (95% CIs). Rats with scores of >2.5 were considered abnormal. **C**, Correlation between cecum and colon histology scores. Each data point represents the score for an individual rat; shaded areas depict 95% CIs. WT = wild-type; M = months; rRNA = ribosomal RNA; QIIME = Quantitative Insights into Microbial Ecology; seq = sequence.

Histology scores revealed that the presence and severity of gut inflammation are strongly dependent on background. DA rats were resistant to the effects of HLA–B27, while Lewis and Fischer rats developed inflammation in the cecum and colon, which was already apparent at 2 months of age (Figure 1B), while the ileum was spared (results not shown). At age 2–3 months, Fischer rats were affected more severely, although by 6 months of age cecum and colon histology scores were comparable between HLA–B27–transgenic Lewis and Fischer rats. HLA–B7 did not cause GI tract inflammation in Lewis rats, which is consistent with previous observations (13). We did not observe sex differences in gut inflammation between HLA–B27–transgenic Lewis and HLA–B27–transgenic Fischer rats (data not shown). In affected rats, there was a strong correlation between cecum and colon histology scores (Figure 1C), indicating consistent involvement at both sites. Representative images of cecum and colon histology are shown in Supplementary Figure 1 (available on the *Arthritis & Rheumatology* web site at http://onlinelibrary.wiley.com/doi/10.1002/art.40405/abstract).

Similar immune and inflammatory response in Lewis and Fischer rats. To characterize immune dysregulation during gut inflammation, we analyzed differentially expressed genes in cecum and colon tissue. PCA revealed strong clustering of samples from HLA–B27–transgenic Lewis and Fischer rats that exhibited inflammation, separate from Lewis and Fischer WT controls, respectively (Supplementary Figure 2A, available on the *Arthritis & Rheumatology* web site at http://onlinelibrary.wiley.com/doi/10.1002/art.40405/abstract). In contrast, samples from HLA–B7–transgenic Lewis and HLA–B27–transgenic DA rats that had normal histology scores clustered with their respective background controls. There was no clustering of samples according to sex (data not shown).

Next, we identified differentially expressed genes (HLA–B27–transgenic versus WT) in the cecum and colon of DA, Lewis, and Fischer rats (fold change >2 or <−2; $P < 0.05$, $q < 0.2$). Significantly overexpressed genes (Figure 2A) or underexpressed genes (Supplementary Figure 2B) in the cecum and colon were more numerous in Fischer rats, followed by Lewis rats. Disease-resistant DA rats had relatively few differentially expressed genes, which was consistent with the normal histology scores. The vast majority of up-regulated genes on the Lewis (81%) and DA (93%) backgrounds overlapped with Fischer backgrounds, as shown in area-proportional Euler diagrams (Figure 2A). In HLA–B7–transgenic rats, there were 38 and 45 differentially expressed genes in the cecum and colon, respectively, but there was minimal overlap with the effects of HLA–B27 on the DA, Lewis,

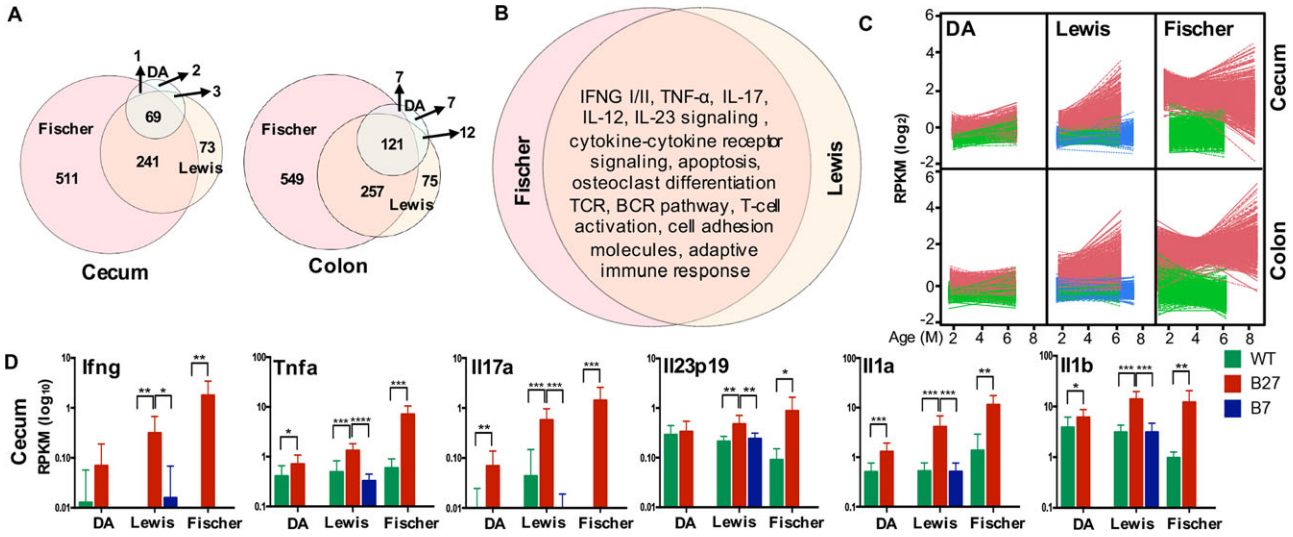

Figure 2. HLA–B27–associated gene expression in DA, Lewis, and Fischer rat cecum and colon. **A**, The numbers of differentially expressed genes (HLA–B27–transgenic versus wild-type [WT]) on DA, Lewis, and Fischer backgrounds in the cecum and colon are shown in Euler diagrams depicting overlaps and the lack of overlaps between backgrounds. Genes were selected based on a fold increase of >2, with $P < 0.05$ and $q < 0.2$. **B**, Differentially expressed genes in the cecum and colon of HLA–B27–transgenic Lewis and Fischer rats were identified by pathway analysis using ToppGene. Results for the cecum and colon were identical. The Euler diagram shows complete overlap of inflammatory pathways between Lewis and Fischer rats ($P < 0.05$). **C**, Temporal expression patterns of transcripts positively correlated ($r > 0.6$) with disease scores in the cecum and colon in DA, Lewis, and Fischer rats are shown. **D**, Expression of the selected individual genes in the cecum in DA, Lewis, and Fischer rats is shown. Individual genes represent key cytokines in the pathways shown in **B**. Shown are $\log_2$-transformed reads per kilobase million (RPKM) values for each gene. Bars show the mean ± SEM (n = 9–16 rats per group). * = $P < 0.05$; ** = $P < 0.01$; *** = $P < 0.001$; **** = $P < 0.0001$. IFNγ = interferon-γ; TNF = tumor necrosis factor; IL-17 = interleukin-17; TCR = T cell receptor; BCR = B cell receptor.

or Fischer backgrounds (results not shown). Pathway analysis of HLA–B27–associated up-regulated genes revealed inflammatory pathways such as IFNγ, TNF, IL-23, IL-17, IL-12, Toll-like receptor, T cell receptor, and B cell receptor–mediated signaling as well as others, while the pathways identified by down-regulated genes revealed a loss of metabolism that included lipids and proteins, biologic oxidation, and digestion and absorption, with a huge overlap between HLA–B27–transgenic Lewis and Fischer rats (Figure 2B and Supplementary Figure 2C, respectively). In addition, the same pathways were identified in the cecum and colon.

To determine whether HLA–B27–associated pathways (Figure 2B) were correlated with disease severity, we independently identified genes that had increased expression and were most strongly correlated ($r > 0.6$) with histology scores in the cecum and colon across all genotypes and backgrounds (Figure 1B). The temporal pattern of expression of positively correlated genes is shown in Figure 2C, and that of negatively correlated genes is shown in Supplementary Figure 2D. As expected, there was an age-dependent increase in expression in HLA–B27–transgenic Lewis rats and consistently high expression in HLA–B27–transgenic Fischer rats, whereas expression levels in HLA–B7–transgenic Lewis rats were not different from those in control rats.

Pathway analysis of the genes positively correlated and those negatively correlated with the severity of inflammation in the cecum as well as the colon revealed considerable overlap with the pathways shown in Figure 2B and Supplementary Figure 2C, respectively. Interestingly, there was low-level up-regulation of a small subset of these genes in HLA–B27–transgenic DA rats (Figure 2C) despite normal histology scores. These differences were most pronounced at 2–3 months of age and were lost in older HLA–B27–transgenic DA rats. Expression of several of the cytokine genes driving these inflammatory pathways in the cecum and colon is shown in Figure 2D and Supplementary Figure 2E, respectively. The relative expression of these genes in HLA–B27–transgenic rats compared with that in their WT controls was consistent with differences in disease penetrance and severity between backgrounds (Figure 1B).

Using differentially expressed genes to predict increases in the number of immune cell types in transgenic compared with WT rats revealed strikingly similar profiles in the cecum and colon and also between HLA–B27–transgenic Lewis and Fischer rats (Supplementary Figure 3, available on the *Arthritis & Rheumatology* web site at http://onlinelibrary.wiley.com/doi/10.1002/art.40405/abstract). These included myeloid cells, α/β and γ/δ T cells, natural killer cells, and lymphoid stromal cells. No immune cell differences were identified in HLA–B7–transgenic rats. Interestingly, despite their lack of a clinical phenotype, the HLA–B27–transgenic DA rats demonstrated signals for several cell types, although they were weaker, particularly for B cells and myeloid cells (Supplementary Figure 3).

Shared HLA–B27–induced inflammatory pathways contrast background-dependent dysbiosis. The striking overlap in dysregulated immune pathways associated with HLA–B27 in the Lewis and Fischer backgrounds suggested that there might be a core group of dysbiotic microbes. To evaluate this possibility, we determined the relative abundance of microbes at the species level in all tissue sites and rat strains. This evaluation revealed 90 microbes that were differentially abundant (HLA class I–transgenic versus WT) in at least 1 tissue location on at least 1 genetic background. Hierarchical clustering of these 90 microbes resulted in distinct groups based on tissue location and genetic background (Supplementary Figure 4, available on the *Arthritis & Rheumatology* web site at http://onlinelibrary.wiley.com/doi/10.1002/art.40405/abstract). We did not observe sex-based differences in dysbiosis (data not shown).

The first hierarchal division in the dendrogram was driven by microbial differences between the large intestine (cecum and colon) and the ileum (Supplementary Figure 4). Unexpectedly, we observed several background-specific differences in the effects of HLA–B27 in the cecum and colon (Figure 3). There were HLA–B27–associated increases in the abundance of *Akkermansia* and *Bacteroides uniformis* in Fischer rats, while these microbes were not significantly different in HLA–B27–transgenic Lewis or DA rats compared with their respective WT controls. There were also HLA–B27–associated increases in *Roseburia* and *Anaerotruncu* and a decrease in *Coprococcus,* which were limited to the Fischer background. In contrast, the frequency of *f_Christenellaceae* was decreased in the cecum mucosa in HLA–B27–transgenic Lewis rats but not in DA or Fischer rats. Furthermore, there were HLA–B27–associated decreases in the abundance of *Mucispirillum schaedleri* and an unknown species of genus, *Mucispirillum*, on the Lewis background, which were not seen in Fischer or DA rats. Lewis rats showed an HLA–B27–associated increase in *Prevotella* at multiple tissue sites (e.g., cecum and colon lumen), but an increase was not observed in HLA–B27–transgenic Fischer rats in the cecum lumen and in DA rats. In addition, there was an HLA–B27–associated increase in the frequency of an unclassified genus of *f_Barnesiellaceae* in cecum and colon fractions in Lewis rats and in cecal mucosa in DA rats but not Fischer rats. In the ileum of Lewis rats, there was an HLA–B27–associated increase in the frequency of

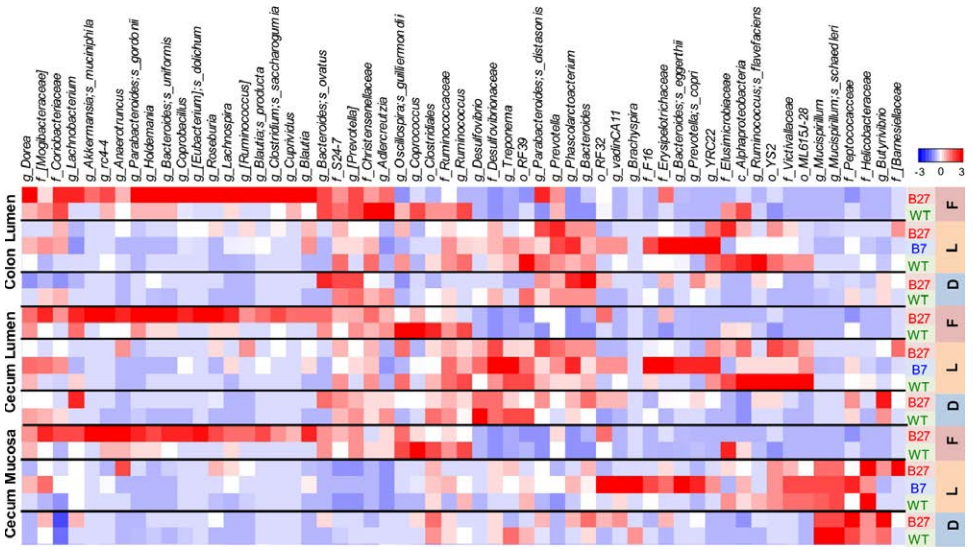

Figure 3. Relative abundance of species-level microbes in cecum and colon samples from DA (D), Lewis (L), and Fischer (F) rats. The heatmap shows unsupervised hierarchical clustering of species-level microbes in HLA–B27/HLA–B7–transgenic rats compared with wild-type (WT) controls on DA, Lewis, and Fischer backgrounds. Samples from the ileum (mucosa), cecum (mucosa and lumen), and colon (lumen) were used. Microbes exhibiting differences in relative abundance, as calculated using a nonparametric Wilcoxon test for paired data ($P < 0.05$, $q < 0.1$) in at least 1 tissue type on at least 1 background, were used to construct the heatmap. Genera with a high relative abundance of ileum fractions are shown in Supplementary Figure 4 (available on the *Arthritis & Rheumatology* web site at http://onlinelibrary.wiley.com/doi/10.1002/art.40405/abstract).

Sutterella that was also observed in other tissue sites in Lewis rats and in the cecum fractions in DA rats, while it was not seen in Fischer rats (see Supplementary Figure 4). Statistically significant differences between these 90 microbes ($q < 0.1$) and an additional 20 microbes ($q < 0.2$ but > 0.1) and their phylogeny are shown in Supplementary Tables 2 and 3, respectively. These additional microbes were included, because many exploratory analyses such as ours use a q value of <0.2 as a selection criterion.

A comparison of differentially abundant (HLA–B27–transgenic versus WT) microbes at the species level in each background and each tissue site, using area-proportional Euler diagrams, is shown in Figure 4. This demonstrated a lack of overlap in HLA–B27–associated differences between Lewis and Fischer backgrounds in the ileum and cecum mucosa and a small overlap in the cecum and colon lumen. Taken together, these results showed that there was a substantial effect of genetic background and/or environment on HLA–B27–associated differences in gut microbiota, although shared microbes were also apparent.

Absence of segmented filamentous bacteria in disease-resistant DA rats. A potentially important difference between backgrounds is the absence of *Candidatus arthromitus* in the DA rats, independent of HLA–B27. *C arthromitus*, more commonly known as segmented

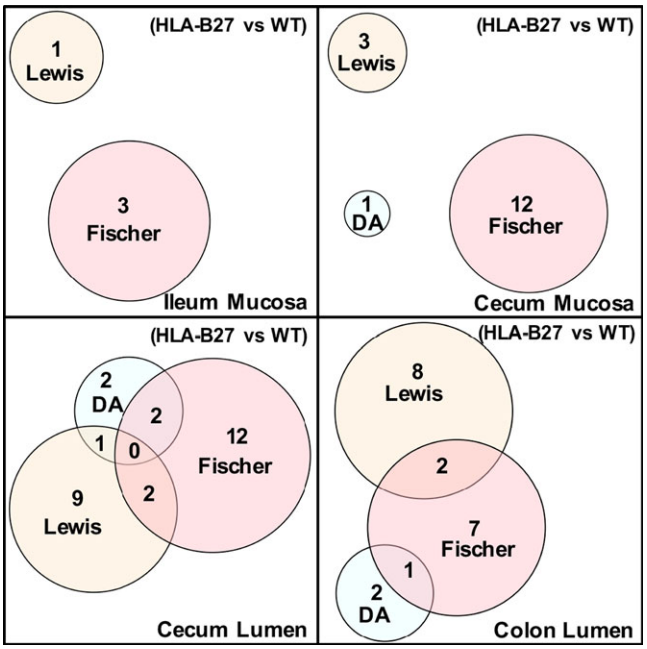

Figure 4. Background-dependent microbial dysbiosis. Area-proportional Euler diagrams show the overlap and the lack of overlap in HLA–B27–associated microbes. Species-level microbes (numbers) that are significantly different between HLA–B27–transgenic and wild-type (WT) controls ($P < 0.05$, $q < 0.1$) on the DA, Lewis, and Fischer backgrounds are shown.

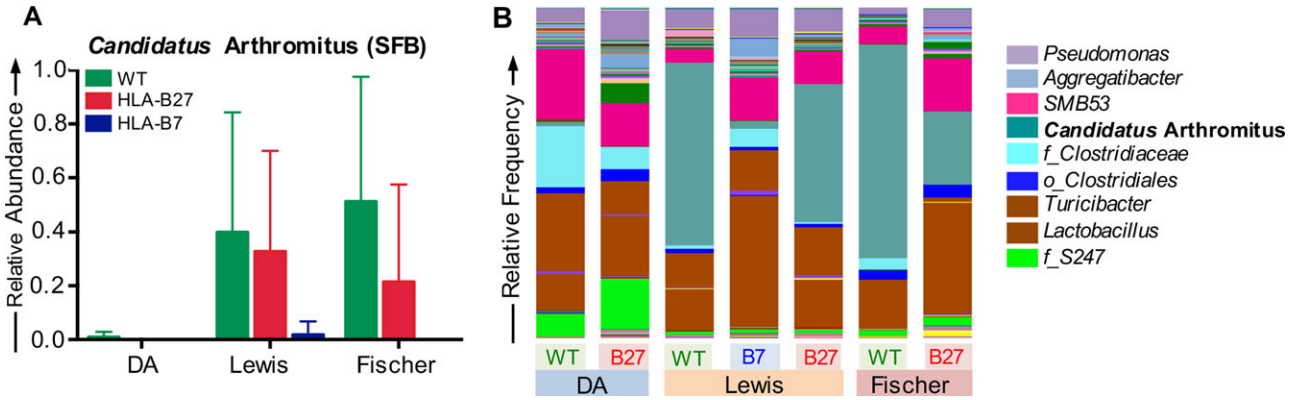

Figure 5. Absence of segmented filamentous bacteria (SFB) in DA rats. **A**, Relative abundance of SFB (*Candidatus arthromitus*) in DA, Lewis, and Fischer rats. Bars show the mean ± SEM (n = 9–31 rats per genotype per background). **B**, Relative frequency of species-level microbes in ileum mucosa in DA, Lewis, and Fischer transgenic and wild-type (WT) rats.

filamentous bacteria (SFB), is a major constituent (although variable) in the ileum of both HLA–B27–transgenic and WT Lewis and Fischer rats (Figure 5A). SFB are known to attach to intestinal epithelial cells and potentiate induction of Th17 cells that play a key role in several inflammatory diseases (24), including colitis (25,26), and thus their absence in DA rats could be responsible for resistance to HLA–B27–mediated disease on this background. It is also worth noting that the frequency of SFB was very low in HLA–B7–transgenic Lewis rats. In DA and HLA–B7–transgenic Lewis rats lacking SFB, 2 major contributors to this niche appeared to be *f_Clostridiaceae* (unknown genera) and *Lactobacillus*, respectively (Figure 5B).

Background-dependent HLA–B27–induced microbial dysbiosis. To further assess the effects of HLA–B27 in disease-permissive backgrounds, we performed PCA based on the differential relative abundance of microbes in Lewis and Fischer rats transgenic for HLA–B27. This comparison revealed major differences between the Lewis and Fischer backgrounds (Figure 6A). However, within each background there was a clear distinction between HLA–B27–transgenic rats and WT controls. The lack of convergence of samples from HLA–B27–transgenic Lewis rats and HLA–B27–transgenic Fischer rats in the PCA suggested that HLA–B27 drives dysbiosis in a background-specific manner. Indeed, when we compared the effects of HLA–B27 on the 2 backgrounds, there was a paucity of core dysbiotic organisms (Figure 6B). To ensure that background-specific effects of HLA–B27 were not attributable to differences in disease severity, we selected samples from HLA–B27–transgenic rats (Lewis and Fischer) with similar histology scores (range 5–8) and reanalyzed them in comparison with their age-matched controls. This revealed slightly altered profiles in each background, but there was no increase in overlap (data not shown), confirming the background-dependence of HLA–B27–associated dysbiosis.

DISCUSSION

Host–microbe interactions play an important role in the development of many immune-mediated inflammatory diseases (27). In SpA, this interaction ranges from the pathogenic gram-negative intracellular bacteria that trigger reactive arthritis in HLA–B27–positive individuals to gut commensal bacteria that are necessary for the development of experimental SpA in HLA–B27–transgenic rats (7) and possibly in humans. Although many additional genes contribute to the risk of SpA in humans, the prominent role of HLA–B27 has fueled the notion that it might promote SpA by altering gut microbiota (17).

In the current study, we hypothesized that comparing gut microbiota in 3 distinct rat strains that differ with regard to disease penetrance and HLA–B27–mediated disease severity would facilitate the identification of common microbial signatures associated with experimental SpA. However, we observed that gut microbial changes associated with HLA–B27 were strikingly different between DA, Lewis, and Fischer rat strains, in which disease penetrance also differs. Therefore, to better understand microbial shifts in the context of inflammation (dysbiosis), we compared disease-susceptible Lewis and Fischer rat strains. This revealed persistent differences in microbiota between the strains, which were not due to differences in disease severity.

To ensure that the lack of overlap was not attributable to the conservative FDR value ($q < 1$), we performed the same analysis using a q value of <0.2 (Supplementary Tables 2 and 3, available on the *Arthritis & Rheumatology* web site at http://onlinelibrary.wiley.

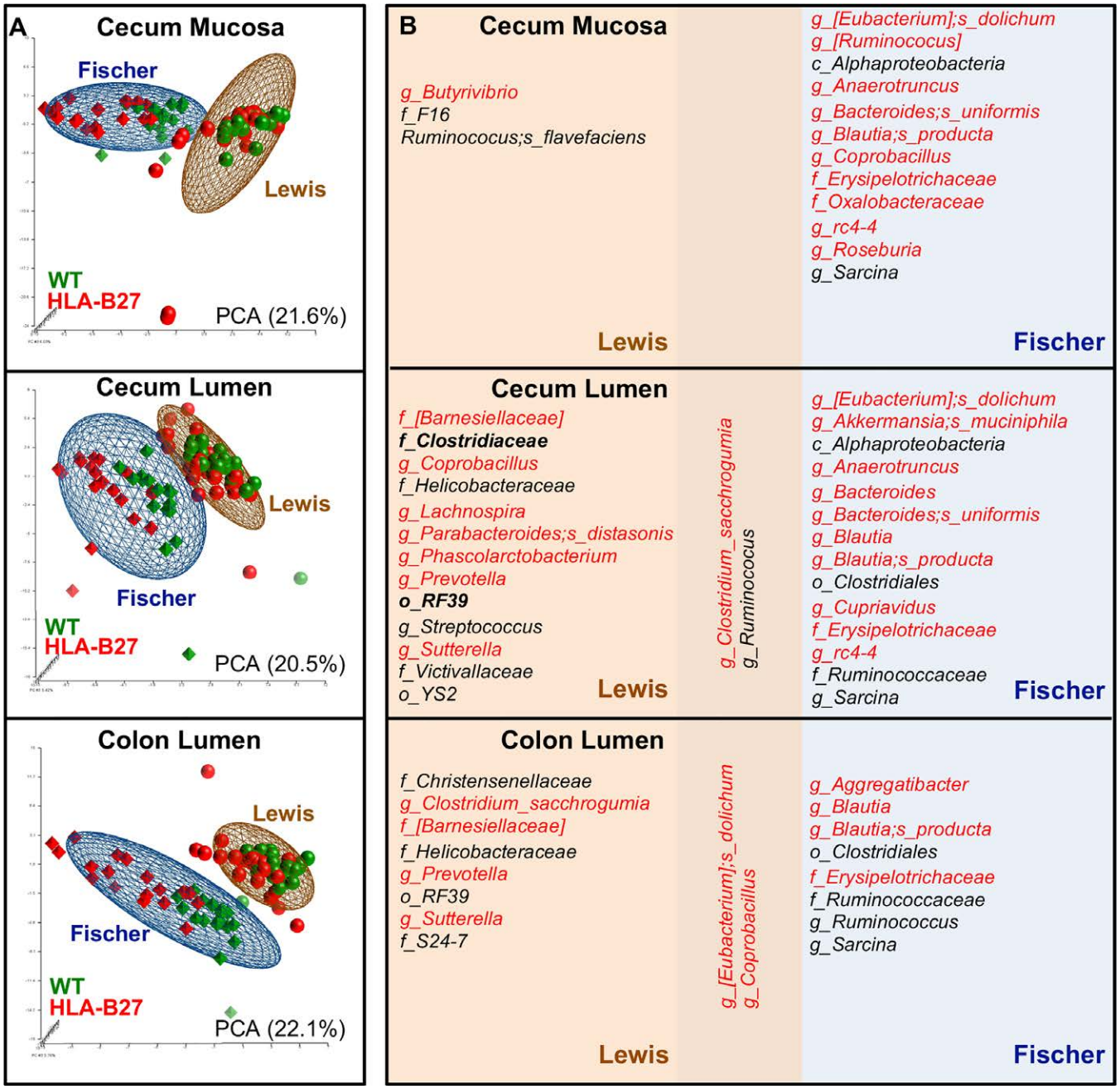

Figure 6. Microbial dysbiosis in Lewis and Fischer rats. **A**, Primary components analysis (PCA) of species-level data for samples obtained from the cecum mucosa, cecum lumen, and colon lumen. Each data point represents the first 3 principal components from the analysis of a single sample obtained from 1 rat. The distribution of samples from Lewis (sphere) and Fischer (tetrahedron) backgrounds are represented by ellipsoids (brown and blue, respectively), with HLA–B27–transgenic and wild-type (WT) genotypes shown as red and green, respectively. **B**, Overlap of HLA–B27–induced dysbiosis on Lewis and Fischer backgrounds. Microbes with increased (red) or decreased (black) relative frequencies in HLA–B27–transgenic rats compared with WT rats are indicated. All of the microbes shown are differentially expressed in HLA–B27–transgenic Lewis and Fischer rats ($P < 0.05$, $q < 0.1$).

com/doi/10.1002/art.40405/abstract). While this resulted in an increased number of overlapping and nonoverlapping microbes, the percentage of overlapping microbes remained unaltered. It should be noted that although WT rats of these 3 backgrounds exhibited considerable overlap of their gut microbiota, the relative abundance of

these microbes differed substantially (for additional information, see Supplementary Figure 5 and Supplementary Table 4). The paucity of shared dysbiotic microbiota associated with HLA–B27 was in striking contrast to the common dysregulated immune pathways in Lewis and Fischer rat strains, characterized by prominent increases in IL-1, IL-23, IL-17, IFNγ, and TNF cytokines and pathways. Taken together, our data indicate that background has a prominent effect on HLA–B27–induced microbial dysbiosis despite common immune dysregulation.

Although arthritis is an important component of SpA, HLA–B27–transgenic Lewis rats infrequently exhibited arthritis prior to 6 months of age at our facility, thus precluding any relevant analysis. On the Fischer background, 32% of the HLA–B27–transgenic rats developed arthritis (mostly older animals). A comparison of the species-level gut microbiota in rats with arthritis and in age-matched HLA–B27–transgenic rats without arthritis did not reveal any significant microbial differences. However, given the relatively small number of rats with arthritis, further studies will be needed before any conclusions can be drawn.

We have implied that the different effects of HLA–B27 on gut microbiota in Lewis and Fischer rats are primarily attributable to genetic background. However, it is important to note that the Fischer rat colony was maintained at OHSU, while all other rats were bred and housed at the NIH. Although all rats were maintained on a diet of the same commercially available rat chow, environmental differences are likely to alter microbial communities between Lewis and Fischer rats. However, an environmental contribution to differences between Lewis and Fischer strains does not alter the fact that dramatically different patterns of dysbiosis occur in the context of common immune dysregulation caused by HLA–B27. We have previously housed Fischer rats at the NIH and observed increased severity of gut inflammation in HLA–B27–transgenic rats at disease onset (based on the stool consistency), similar to what we report here for animals housed in 2 different facilities. This further supports an important role for genetic background in causing differences between Fischer and Lewis HLA–B27–transgenic rats.

Although changes in microbiota composition can cause (or be a response to) an immune stimulus, in reality they may be a combination of both factors and evolve rapidly, making it difficult to establish a temporal relationship (28). Previous work in HLA–B27–transgenic Fischer rats revealed gut inflammation prior to microbial changes (18), but that analysis was limited to select microbiota and thus did not rule out other earlier differences. In the current study, although we initially analyzed cohorts based on age, we eventually grouped together rats of all ages in order to simplify the analyses. However, our initial analysis showed immune dysregulation and microbial dysbiosis at the earliest time point in HLA–B27–transgenic Lewis and Fischer rats (data not shown), thus precluding any conclusions about cause and effect. Nevertheless, the results in DA rats underscore the fact that HLA–B27 can cause immune dysregulation (e.g., low-level increase in *Il1a*, *Il1b*, *Tnf*, and *Il17a* transcripts, with immune cell changes) without progression to a disease phenotype. These changes seen in young HLA–B27–transgenic DA rats were not sustained in older animals. This could be attributable to the lack of SFB in DA rats. SFB are required for Th17 cell development in several rodent strains (24) and thus may be critical in experimental SpA. These bacteria are known to colonize ileal epithelium shortly before weaning and are highly refractory to in vitro culturing (29). It should be noted that HLA–B27–transgenic DA rats have been reported to develop severe gut inflammation and cachexia, which were not seen in WT rats when they were inadvertently exposed to an unknown infectious agent (13). The episode was transient but nevertheless suggests that they are not completely resistant to the effects of HLA–B27.

It is clear from the current study and previous work (8) that HLA–B7 is associated with major shifts in gut microbial composition (Supplementary Table 2, http://onlinelibrary.wiley.com/doi/10.1002/art.40405/abstract). Herein, we document the absence of immune dysregulation in these animals, at the level of both individual cytokines and immune cell signatures, indicating that microbial differences are not sufficient to provoke an inflammatory response (8) and underscoring the unique effects of HLA–B27.

Because the majority of microbes associated with HLA–B27–induced disease differ between the Lewis and Fischer backgrounds, we considered that there might be important functional overlaps. Two prominent examples are HLA–B27–associated increases in *Akkermansia muciniphila* (*p_Verrucomicrobia*) in Fischer and *Prevotella* (*p_Bacteroidetes*) in Lewis strains. While they are phylogenetically diverse, both of these microbes disrupt mucosal homeostasis and have been linked to gut inflammation by disrupting mucosal homeostasis (9,30). *Akkermansia* exacerbates inflammation by degrading the mucous layer overlying gut epithelial cells, thereby weakening the protective barrier (31). *A muciniphila* has been reported to be increased in a subset of patients with juvenile SpA (9) and exacerbated *Salmonella*-induced gut inflammation (31). In contrast, a decrease in the abundance of *A muciniphila* has been linked to obesity in mouse models (32,33).

Our results suggest that mucus degradation by *A muciniphila*, along with dysregulated goblet cell production during inflammation, may be sufficient to bring lumenal bacteria closer to the gut epithelium and promote

inflammation. Similarly, *Prevotella* has been implicated in dysbiosis due to NLRP6 deficiency (34), colitis (30), ankylosing spondylitis (35), and psoriatic arthritis (10). *Prevotella* encodes enzymes (e.g., superoxide reductase and phosphoadenosine phosphosulphate reductase), enabling it to resist host reactive oxygen species and invade epithelial cell crypts, most likely by outcompeting commensal organisms that normally maintain mucosal homeostasis (30). Lipopolysaccharide (LPS) from *A muciniphila* has been shown to be more immunostimulatory than that from *Prevotella* (36), which may also explain the differences in disease severity between Fischer and Lewis backgrounds.

Although we highlighted a surprising lack of common dysbiotic microbes between different backgrounds, there were core similarities between HLA–B27–transgenic Lewis and Fischer rats, particularly in the lumen of the cecum and colon, which may play a role in disease development. This group includes short-chain fatty acid producers such as *Clostridium* and *Coprobacillus*, the relative abundance of which is increased, and *Ruminococcus,* the production of which is decreased (37). Short-chain fatty acids such as butyrate are important because they influence regulatory T cell homeostasis (38). In addition, colonic epithelial cells from germ-free mice exhibit a mitochondrial respiration deficit and enhanced autophagy as a consequence of reduced production of short-chain fatty acids (39). Recent studies have shown an increase in the frequency of the short-chain fatty acid producer *Ruminococcus gnavus* (40) and the medium-chain fatty acid producer *Dialister* (41) in SpA. Because some short-chain fatty acid producers in HLA–B27–transgenic rats are increased while others are decreased, additional studies will be needed to determine the overall impact of these changes. Despite the phylogenetic differences in the HLA–B27–associated Lewis and Fischer microbiota, these nonoverlapping microbes may perturb common metabolic pathways, thus explaining shared immune dysregulation in these animals. Future studies using metagenomic sequencing along with metabolomic analysis will enable further characterization and provide functional relevance to these microbial changes.

Gut microbiota play an important role in the development of the host immune system, which in turn shapes the composition of gut microbiota (42,43). It is clear from observations in animal models that gut microbial communities co-evolve with their host and exhibit strong ecological interactions, varying according to the host genotype, diet, and colonization history (43). Our results demonstrate that the effect of HLA–B27 on gut microbiota in experimental SpA is largely dependent on host genetics and environment. In addition, dysbiotic microbes contributing to HLA–B27–associated inflammation need not be linked taxonomically, but rather, similarities in their metabolic functions and/or gut microenvironment are key drivers of pathogenesis. In addition, HLA–B27–mediated disease in rats might depend on SFB, although this needs to be determined experimentally.

In summary, the results of gene expression analysis and microbial community profiling to characterize the effect of HLA–B27 on 3 different genetic backgrounds provide an unprecedented and comprehensive view of the complexity of microbial dysbiosis associated with common immune dysregulation and gut inflammation in SpA. Although we observed a common immune signature associated with gut inflammation, microbial dysbiosis was surprisingly different. The absolute dependence of this model on gut microbiota, together with the striking differences between host backgrounds, implicate an ecological model of dysbiosis in HLA–B27–induced experimental SpA in which the effects of multiple microbes contribute to the aberrant immune response, rather than a single or small number of microbial genera driving pathogenesis. Given that recombinant inbred animal strains are analogous to unrelated human individuals, our results suggest that characterization of functionally similar dysbiotic microbial communities may be critical to revealing underlying mechanisms of host–microbe interactions contributing to SpA.

ACKNOWLEDGMENTS

We thank Maxime Breban for providing the HLA–B27–transgenic Fischer rats and Joel Taurog for providing the HLA–B7–transgenic Lewis rats. We thank Gustavo Gutierrez-Cruz, Kristina Zaal, and Kalyani Mishra for performing RNA sequencing, imaging, and genotyping, respectively, at the NIAMS core facility. Thanks are due to Rob Knight and Justine Debelius at the University of California, San Diego, for performing microbiome sequencing. We also thank Patrick Stauffer and Paul Montgomery at OHSU, and the NIAMS animal facility for providing assistance with the necropsies. The NIH High Performing Computation system Biowulf cluster (http://hpc.nih.gov) was used for analysis.

AUTHOR CONTRIBUTIONS

All authors were involved in drafting the article or revising it critically for important intellectual content, and all authors approved the final version to be published. Dr. Colbert had full access to all of the data in the study and takes responsibility for the integrity of the data and the accuracy of the data analysis.

Study conception and design. Gill, Asquith, Rosenbaum, Colbert.

Acquisition of data. Gill, Asquith.

Analysis and interpretation of data. Gill, Asquith, Brooks, Rosenbaum, Colbert.

REFERENCES

1. Taurog JD, Chhabra A, Colbert RA. Ankylosing spondylitis and axial spondyloarthritis. N Engl J Med 2016;374:2563–74.

2. Parkes M, Cortes A, van Heel DA, Brown MA. Genetic insights into common pathways and complex relationships among immune-mediated diseases. Nat Rev Genet 2013;14:661–73.
3. De Wilde K, Debusschere K, Beeckman S, Jacques P, Elewaut D. Integrating the pathogenesis of spondyloarthritis: gut and joint united? Curr Opin Rheumatol 2015;27:189–96.
4. Jacques P, Elewaut D. Tumor necrosis factor α–induced proteins: natural brakes on inflammation. Arthritis Rheum 2012;64:3831–4.
5. Helmick CG, Felson DT, Lawrence RC, Gabriel S, Hirsch R, Kwoh CK, et al. Estimates of the prevalence of arthritis and other rheumatic conditions in the United States. Part I. Arthritis Rheum 2008;58:15–25.
6. Taurog JD, Richardson JA, Croft JT, Simmons WA, Zhou M, Fernandez-Sueiro JL, et al. The germfree state prevents development of gut and joint inflammatory disease in HLA-B27 transgenic rats. J Exp Med 1994;180:2359–64.
7. Rath HC, Herfarth HH, Ikeda JS, Grenther WB, Hamm TE Jr, Balish E, et al. Normal luminal bacteria, especially Bacteroides species, mediate chronic colitis, gastritis, and arthritis in HLA-B27/human β2 microglobulin transgenic rats. J Clin Invest 1996;98:945–53.
8. Lin P, Bach M, Asquith M, Lee AY, Akileswaran L, Stauffer P, et al. HLA-B27 and human β2-microglobulin affect the gut microbiota of transgenic rats. PLoS One 2014;9:e105684.
9. Stoll ML, Kumar R, Morrow CD, Lefkowitz EJ, Cui X, Genin A, et al. Altered microbiota associated with abnormal humoral immune responses to commensal organisms in enthesitis-related arthritis. Arthritis Res Ther 2014;16:486.
10. Scher JU, Ubeda C, Artacho A, Attur M, Isaac S, Reddy SM, et al. Decreased bacterial diversity characterizes the altered gut microbiota in patients with psoriatic arthritis, resembling dysbiosis in inflammatory bowel disease. Arthritis Rheumatol 2015;67:128–39.
11. Costello ME, Ciccia F, Willner D, Warrington N, Robinson PC, Gardiner B, et al. Intestinal dysbiosis in ankylosing spondylitis. Arthritis Rheumatol 2015;67:686–91.
12. May E, Dorris ML, Satumtira N, Iqbal I, Rehman MI, Lightfoot E, et al. CD8αβ T cells are not essential to the pathogenesis of arthritis or colitis in HLA-B27 transgenic rats. J Immunol 2003;170:1099–105.
13. Taurog JD, Maika SD, Satumtira N, Dorris ML, McLean IL, Yanagisawa H, et al. Inflammatory disease in HLA-B27 transgenic rats. Immunol Rev 1999;169:209–23.
14. DeLay ML, Turner MJ, Klenk EI, Smith JA, Sowders DP, Colbert RA. HLA–B27 misfolding and the unfolded protein response augment interleukin-23 production and are associated with Th17 activation in transgenic rats. Arthritis Rheum 2009;60:2633–43.
15. Smith JA, Colbert RA. The interleukin-23/interleukin-17 axis in spondyloarthritis pathogenesis: Th17 and beyond [review]. Arthritis Rheumatol 2014;66:231–41.
16. Bowness P. HLA-B27. Annu Rev Immunol 2015;33:29–48.
17. Rosenbaum JT, Davey MP. Time for a gut check: evidence for the hypothesis that HLA–B27 predisposes to ankylosing spondylitis by altering the microbiome. Arthritis Rheum 2011;63:3195–8.
18. Asquith MJ, Stauffer P, Davin S, Mitchell C, Lin P, Rosenbaum JT. Perturbed mucosal immunity and dysbiosis accompany clinical disease in a rat model of spondyloarthritis. Arthritis Rheumatol 2016;68:2151–62.
19. Hammer RE, Maika SD, Richardson JA, Tang JP, Taurog JD. Spontaneous inflammatory disease in transgenic rats expressing HLA-B27 and human β2m: an animal model of HLA-B27-associated human disorders. Cell 1990;63:1099–112.
20. Layh-Schmitt G, Yang EY, Kwon G, Colbert RA. HLA–B27 alters the response to tumor necrosis factor α and promotes osteoclastogenesis in bone marrow monocytes from HLA–B27–transgenic rats. Arthritis Rheum 2013;65:2123–31.
21. Izcue A, Hue S, Buonocore S, Arancibia-Carcamo CV, Ahern PP, Iwakura Y, et al. Interleukin-23 restrains regulatory T cell activity to drive T cell-dependent colitis. Immunity 2008;28:559–70.
22. Heng TS, Painter MW. The Immunological Genome Project: networks of gene expression in immune cells. Nat Immunol 2008;9:1091–4.
23. Caporaso JG, Lauber CL, Walters WA, Berg-Lyons D, Huntley J, Fierer N, et al. Ultra-high-throughput microbial community analysis on the Illumina HiSeq and MiSeq platforms. ISME J 2012;6:1621–4.
24. Atarashi K, Tanoue T, Ando M, Kamada N, Nagano Y, Narushima S, et al. Th17 cell induction by adhesion of microbes to intestinal epithelial cells. Cell 2015;163:367–80.
25. Caselli M, Tosini D, Gafa R, Gasbarrini A, Lanza G. Segmented filamentous bacteria-like organisms in histological slides of ileocecal valves in patients with ulcerative colitis. Am J Gastroenterol 2013;108:860–1.
26. Stepankova R, Powrie F, Kofronova O, Kozakova H, Hudcovic T, Hrncir T, et al. Segmented filamentous bacteria in a defined bacterial cocktail induce intestinal inflammation in SCID mice reconstituted with CD45RBhigh CD4+ T cells. Inflamm Bowel Dis 2007;13:1202–11.
27. Haberman Y, Tickle TL, Dexheimer PJ, Kim MO, Tang D, Karns R, et al. Pediatric Crohn disease patients exhibit specific ileal transcriptome and microbiome signature. J Clin Invest 2014;124:3617–33.
28. Huttenhower C, Kostic AD, Xavier RJ. Inflammatory bowel disease as a model for translating the microbiome. Immunity 2014;40:843–54.
29. Ericsson AC, Hagan CE, Davis DJ, Franklin CL. Segmented filamentous bacteria: commensal microbes with potential effects on research. Comp Med 2014;64:90–8.
30. Scher JU, Sczesnak A, Longman RS, Segata N, Ubeda C, Bielski C, et al. Expansion of intestinal Prevotella copri correlates with enhanced susceptibility to arthritis. Elife 2013;2:e01202.
31. Ganesh BP, Klopfleisch R, Loh G, Blaut M. Commensal Akkermansia muciniphila exacerbates gut inflammation in Salmonella Typhimurium-infected gnotobiotic mice. PLoS One 2013;8:e74963.
32. Everard A, Belzer C, Geurts L, Ouwerkerk JP, Druart C, Bindels LB, et al. Cross-talk between Akkermansia muciniphila and intestinal epithelium controls diet-induced obesity. Proc Natl Acad Sci U S A 2013;110:9066–71.
33. Schneeberger M, Everard A, Gomez-Valades AG, Matamoros S, Ramirez S, Delzenne NM, et al. Akkermansia muciniphila inversely correlates with the onset of inflammation, altered adipose tissue metabolism and metabolic disorders during obesity in mice. Sci Rep 2015;5:16643.
34. Elinav E, Strowig T, Kau AL, Henao-Mejia J, Thaiss CA, Booth CJ, et al. NLRP6 inflammasome regulates colonic microbial ecology and risk for colitis. Cell 2011;145:745–57.
35. Wen C, Zheng Z, Shao T, Liu L, Xie Z, Le Chatelier E, et al. Quantitative metagenomics reveals unique gut microbiome biomarkers in ankylosing spondylitis. Genome Biol 2017;18:142.
36. Vatanen T, Kostic AD, d'Hennezel E, Siljander H, Franzosa EA, Yassour M, et al. Variation in microbiome LPS immunogenicity contributes to autoimmunity in humans. Cell 2016;165:1551.
37. Morrison DJ, Preston T. Formation of short chain fatty acids by the gut microbiota and their impact on human metabolism. Gut Microbes 2016;7:189–200.
38. Thorburn AN, McKenzie CI, Shen S, Stanley D, Macia L, Mason LJ, et al. Evidence that asthma is a developmental origin disease influenced by maternal diet and bacterial metabolites. Nat Commun 2015;6:7320.
39. Donohoe DR, Garge N, Zhang X, Sun W, O'Connell TM, Bunger MK, et al. The microbiome and butyrate regulate energy metabolism and autophagy in the mammalian colon. Cell Metab 2011;13:517–26.
40. Breban M, Tap J, Leboime A, Said-Nahal R, Langella P, Chiocchia G, et al. Faecal microbiota study reveals specific dysbiosis in spondyloarthritis. Ann Rheum Dis 2017;76:1614–22.
41. Tito RY, Cypers H, Joossens M, Varkas G, Van Praet L, Glorieus E, et al. Dialister as a microbial marker of disease activity in spondyloarthritis. Arthritis Rheumatol 2017;69:114–21.
42. Nicholson JK, Holmes E, Kinross J, Burcelin R, Gibson G, Jia W, et al. Host-gut microbiota metabolic interactions. Science 2012;336:1262–7.
43. Dethlefsen L, McFall-Ngai M, Relman DA. An ecological and evolutionary perspective on human-microbe mutualism and disease. Nature 2007;449:811–8.

ARTHRITIS & RHEUMATOLOGY
Vol. 70, No. 4, April 2018, pp 566–577
DOI 10.1002/art.40399

Increased Expression and Modulated Regulatory Activity of Coinhibitory Receptors PD-1, TIGIT, and TIM-3 in Lymphocytes From Patients With Systemic Sclerosis

Michelle Fleury,[1] Anna C. Belkina,[1] Elizabeth A. Proctor,[2] Christopher Zammitti,[1] Robert W. Simms,[1] Douglas A. Lauffenburger,[2] Jennifer E. Snyder-Cappione,[1] Robert Lafyatis,[3] and Hans Dooms[1]

Objective. **Immune dysfunction is an important component of the disease process underlying systemic sclerosis (SSc), but the mechanisms contributing to altered immune cell function in SSc remain poorly defined. This study was undertaken to measure the expression and function of the coinhibitory receptors (co-IRs) programmed cell death 1 (PD-1), T cell immunoglobulin and ITIM domain (TIGIT), T cell immunoglobulin and mucin domain 3 (TIM-3), and lymphocyte activation gene 3 (LAG-3) in lymphocyte subsets from the peripheral blood of patients with SSc.**

Methods. **Co-IR expression levels on subsets of immune cells were analyzed using a 16-color flow cytometry panel. The functional role of co-IRs was determined by measuring cytokine production after in vitro stimulation of SSc and healthy control peripheral blood mononuclear cells (PBMCs) in the presence of co-IR–blocking antibodies. Supernatants from cultures of stimulated PBMCs were added to SSc fibroblasts, and their impact on fibroblast gene expression was measured. Mathematical modeling was used to reveal differences between co-IR functions in SSc patients and healthy controls.**

Results. **Levels of the co-IRs PD-1 and TIGIT were increased, and each was coexpressed, in distinct T cell subsets from SSc patients compared to healthy controls. Levels of TIM-3 were increased in SSc natural killer cells. PD-1, TIGIT, and TIM-3 antibody blockade revealed patient-specific roles of each of these co-IRs in modulating activation-induced T cell cytokine production. In contrast to healthy subjects, blockade of TIGIT and TIM-3, but not PD-1, failed to reverse inhibited cytokine production in SSc patients, indicating that enhanced T cell exhaustion is present in SSc. Finally, cytokines secreted in anti–TIM-3–treated PBMC cultures distinctly changed the gene expression profile in SSc fibroblasts.**

Conclusion. **The altered expression and regulatory capacity of co-IRs in SSc lymphocytes may contribute to disease pathophysiology by modulating the cytokine-mediated cross-talk of immune cells and fibroblasts at sites of inflammation and/or fibrosis.**

Systemic sclerosis (SSc) is an autoimmune connective tissue disorder characterized by external skin thickening that can progress to internal organ fibrosis in the presence of immune abnormalities (1,2). Autoantibodies and lymphopenia are often detected in SSc patients (2). CD8+ T cells and CD4+ Treg cells have been shown to produce increased levels of the profibrotic cytokine interleukin-13 (IL-13) (3,4), while natural killer (NK) cells have been reported to be less cytotoxic and have defects in interferon-γ (IFNγ) production (5). However, while differences in the cytokines produced in SSc may contribute to disease pathophysiology (6), the mechanisms underlying these changes in immune cell cytokine production remain largely unknown.

Supported by the NIH (National Institute of Allergy and Infectious Diseases Research Training in Immunology grant T32-AI-007309 to Ms Fleury and National Institute of Arthritis and Musculoskeletal and Skin Diseases Scleroderma Center of Research Translation grant 1P50-AR-060780 to Dr. Lafyatis). Dr. Dooms' work was supported by funding from the Boston University Department of Medicine (Arthritis Center/Rheumatology Section).

[1]Michelle Fleury, BS, Anna C. Belkina, MD, PhD, Christopher Zammitti, BS, Robert W. Simms, MD, Jennifer E. Snyder-Cappione, PhD, Hans Dooms, PhD: Boston University School of Medicine, Boston, Massachusetts; [2]Elizabeth A. Proctor, PhD, Douglas A. Lauffenburger, PhD: Massachusetts Institute of Technology, Cambridge; [3]Robert Lafyatis, MD: Boston University School of Medicine, Boston, Massachusetts, and University of Pittsburgh, Pittsburgh, Pennsylvania.

Dr. Lafyatis has received consulting fees from Sanofi, Merck, Genentech, Bristol-Myers Squibb, Formation, and UCB (less than $10,000 each) and grant support from Pfizer, Momenta, Regeneron, Corbus, and Prism.

Address correspondence to Hans Dooms, PhD, Boston University School of Medicine, Arthritis Center/Rheumatology Section, 72 East Concord Street, E519, Boston, MA 02118. E-mail: hdooms@bu.edu.

Submitted for publication August 21, 2017; accepted in revised form December 5, 2017.

The function of T cells and NK cells is regulated by coinhibitory receptors (co-IRs) such as programmed cell death 1 (PD-1), lymphocyte activation gene 3 (LAG-3), T cell immunoglobulin and ITIM domain (TIGIT), and T cell immunoglobulin and mucin domain 3 (TIM-3) (7,8). Engagement of these receptors by their ligands limits cytokine production in response to stimulation of the cells by either T cell receptor (TCR) or activating NK cell receptor. Co-IRs thus play critical physiologic roles in limiting tissue damage from excessive immune activation. However, chronically increased expression of multiple co-IRs is a hallmark of immune exhaustion (9), in which immune cells are no longer able to execute effector functions to fight chronic viral infections and cancer (10,11).

In autoimmunity, co-IRs are protective. Antibody blockade or genetic deletion of PD-1, TIM-3, TIGIT, and LAG-3 in mouse models of autoimmune disease, such as models of type 1 diabetes, lupus, and multiple sclerosis, all result in accelerated or exacerbated disease (7). Treatment of cancer patients with co-IR blockade often precipitates autoimmune adverse events (12). As a corollary, reinforcing immune checkpoints in autoimmune disease may have therapeutic benefit. In support of this, one study demonstrated correlation of an exhaustion-like phenotype, marked by an increase in co-IR expression, with fewer flares in lupus patients (10), and the presence of TIM-3+ T cells was associated with milder forms of multiple sclerosis (13). Moreover, in patients with SSc, the PD-1 pathway was recently found to be involved in regulating disease severity (14).

In the present study, we determined the expression of the co-IRs PD-1, TIGIT, TIM-3, and LAG-3 on lymphocyte subsets from the peripheral blood of patients with SSc, and assessed their role in cytokine regulation and fibroblast activation. PD-1, TIM-3, and TIGIT showed increased expression in specific T cell and NK cell subsets from SSc patients. Cytokine production in the presence of co-IR–blocking antibodies against PD-1, TIM-3, and TIGIT revealed significant patient-specific variation in the function of individual co-IRs. In most subjects, however, at least one co-IR was actively suppressing cytokine production, indicative of the presence of exhausted cell populations. Multivariate analysis revealed that TIGIT and TIM-3 were functionally distinct from PD-1 in SSc patients, but not in healthy controls. Finally, changes in the cytokines produced by peripheral blood mononuclear cells (PBMCs) after TIM-3 blockade resulted in altered fibroblast gene expression.

The results of our study thus suggest that increased co-IR expression in SSc lymphocyte subsets contributes to patient-specific activities involved in the modulation of cytokine production. Suppressed and/or excessive production of specific cytokines in the local microenvironment may subsequently promote pathogenic fibrotic or inflammatory responses in connective tissue and vascular cells.

PATIENTS AND METHODS

Patients and healthy controls. All samples and clinical data were collected under a protocol approved by the Institutional Review Board at Boston University. Blood samples obtained from 30 patients with SSc and 21 healthy subjects were collected in EDTA blood collection tubes (BD Vacutainer). Classification of the diagnosis in all patients was made according to the American College of Rheumatology criteria for SSc (1). The patients had not received immunosuppressive therapy for at least 6 months prior to the time of blood collection. Patients and healthy controls were matched according to age.

Sample collection. Blood samples were collected and PBMCs were isolated on the same day. To do this, Lymphoprep (Stem Cell Technologies) was underlaid under the blood, and PBMCs were separated by density-dependent centrifugation. PBMC samples were frozen in 50% RPMI medium (10% fetal bovine serum [FBS], 1% nonessential amino acids, 1% HEPES, 1% penicillin/streptomycin, 1% sodium pyruvate, 0.1% β-mercaptoethanol) with 40% FBS and 10% DMSO, and then stored in liquid nitrogen.

Flow cytometry analysis. PBMCs were thawed, stained, and analyzed in a manner as previously reported (15), using a BD FACSAria SORP with FACSDiva software (BD Biosciences). Expert-guided gating of the cells, utilizing FlowJo version 10 and Cytobank, was performed by 3 independent analysts (MF, ACB, and JES-C). A tSNE dimensionality reduction was performed using a Cytobank platform with the following parameters: input of 500,000 single, live, CD14−/CD19− events; clustering channels (all arcsin-transformed) for CD3, CD4, CD8, CD25, CD127, CD45RO, γδ TCR, CD16, CD56, Vα24, and CD1d-PBS57; total number of iterations 3,000; theta 0.5; perplexity 30.

In vitro stimulation of PBMCs with allogeneic monocyte-derived dendritic cells (DCs). Monocyte-derived DCs were produced after selection of CD14+ cells (Stem Cell Technologies) from PBMCs isolated from a buffy coat, in accordance with the manufacturer's instructions. CD14+ monocytes were cultured for 5 days in 7.5 ng/ml IL-4 (BD Biosciences) and 20 ng/ml granulocyte–macrophage colony-stimulating factor (Miltenyi Biotec). On day 4, 1 ng/ml of *Escherichia coli* lipopolysaccharide (Sigma) was added to the cultures to mature the DCs. Previously frozen PBMCs from patients and healthy controls were thawed and cocultured with allogeneic DCs at a 1:10 ratio of DCs to PBMCs with 5 μg/ml of blocking antibodies, including anti–PD-1 (clone J116; eBioScience), anti-TIGIT (clone MBSA43; eBioScience), anti–TIM-3 (clone F38-2E2; BioLegend), or isotype control (clone P3.6.2.8.1; eBioScience), in the presence of human Fc Block (BD Biosciences). Cultures were kept in an atmosphere of 37°C and 5% CO_2 for 5 days, and supernatants were collected and stored at −80°C.

Multiplex cytokine analysis. Supernatants from in vitro stimulation cultures were analyzed using a 14-plex cytokine bead array kit (Milliplex MAP; Millipore) on a Luminex 100 platform, to determine cytokine concentrations. A human

Th17 Magnetic Bead Panel (Milliplex MAP HTH17MAG-14K-14) was used to detect concentrations of IFNγ, IL-10, IL-13, IL-22, IL-9, IL-33, IL-2, IL-21, IL-4, IL-23, IL-5, IL-6, IL-27, and tumor necrosis factor (TNF). Data were analyzed using Milliplex Analysis software, version 5.1. The standard curve was determined by interpolation from corresponding standards. IL-22 and IL-33 were excluded from these analyses because they were below the limit of detection. Undetectable values were given an arbitrary value of 0. Values were clustered using Gene Cluster version 3.0 and then normalized, mean centered, and clustered by complete linkage, followed by visualization in JavaTree.

Fibroblast cell culture. SSc human dermal fibroblasts were grown to 80% confluence in Dulbecco's modified Eagle's medium with 10% FBS, and 2.5×10^5 cells were serum-starved overnight with medium containing 0.5% FBS. Next, the medium was replaced with 50% supernatant from in vitro–stimulated PBMC cultures and 50% RPMI medium containing 10% FBS. As controls, additional cultures were set up with 10 ng/ml transforming growth factor β1 (TGFβ1; R&D Systems), 30 ng/ml IL-13 (R&D Systems), or no cytokines. Cells were incubated for 24 hours at 37°C, washed with phosphate buffered saline, and lysed with RLT buffer (Qiagen). RNA was collected with an RNeasy Mini kit (Qiagen).

Gene expression analysis. For analyses of gene expression, 100 ng of RNA was added to NanoString polymerase chain reaction tubes, followed by the addition of 20 μl Reporter CodeSet diluted in Buffer CodeSet and 5 μl of Capture ProbeSet reagent (NanoString Technologies). Samples were placed in an MJ Mini thermocycler (Bio-Rad) at 67°C and processed in an nCounter Prep Station (NanoString Technologies). Expression values for each gene were normalized to those for a variety of housekeeping genes, following a previously described method (16). Values were clustered using the Gene Cluster program (version 3.0) and normalized, mean centered, and clustered by complete linkage, followed by visualization in JavaTree.

Mathematical modeling. Partial least squares discriminant analysis (PLSDA) was conducted in MatLab using the PLS Toolbox (Eigenvector Research). Data were normalized along each parameter by Z score before application of the algorithm. Cytokines or genes with non-zero values in fewer than one-half of the subjects were excluded from these analyses. Cross-validation was performed with one-fifth of the relevant data set, and the number of latent variables (LVs) was chosen to minimize cross-validation error. Model confidence was calculated by randomly permuting the response variables 100 times and rebuilding the model to form a distribution of error for random models. We then compared our model to this distribution using the Mann-Whitney U test. The importance of each parameter to the model prediction was quantified using a variable importance in projection (VIP) score. A VIP score of >1 (representing above average contribution) was considered important for model performance and prediction. The LASSO method (Mathworks; Matlab) was applied for variable selection in the gene expression data to determine the minimum gene set necessary for distinguishing treatment groups. K-fold cross-validation was utilized to optimize the set of gene parameters such that the error of the resulting model was minimized.

Statistical analysis. Groups were compared by *t*-tests, which were performed using the R function t.test, with correction for multiple comparisons made using R function p.adjust. The fdr parameter was used for false discovery rate adjustment.

RESULTS

Increased co-IR expression in T and NK cell subsets in SSc PBMCs, as revealed by immunophenotyping. While the expression of co-IRs, as a hallmark of T cell exhaustion, has been associated with disease outcome in several autoimmune diseases, including lupus and type 1 diabetes (10), an extensive comparison of the expression of multiple co-IRs between SSc patients and healthy subjects has not been performed. Therefore, we isolated PBMCs from SSc patients and age-matched healthy controls (Table 1) and stained the cells with a 16-color flow cytometry antibody panel to characterize expression of 4 co-IRs on various immune cell subsets simultaneously (15). Importantly, only patients who were not taking immunosuppressants were selected for our study, to rule out any role of immune-modulating drugs on expression levels.

Table 1. Baseline demographic and clinical features of the SSc patients and healthy controls*

	Healthy controls (n = 19)	SSc patients (n = 28)
Sex, no. male/no. female	8/11	1/27
Age, median (range) years	52 (25–69)	57 (32–68)
Age at onset, median (range) years	NA	46 (24–74)
Disease duration, median (range) years	NA	7.3 years (1 month–42 years)
Race, Hispanic white/black/white	0/1/18	2/0/26
No. with dcSSc/no. with lcSSc	NA	6/22
Modified Rodnan skin thickness score, median (range)	NA	5 (0–36)†
Lungs		
ILD	NA	9
PAH	NA	10

* NA = not applicable; dcSSc = diffuse cutaneous systemic sclerosis; lcSSc = limited cutaneous systemic sclerosis; ILD = interstitital lung disease; PAH = pulmonary arterial hypertension.
† For 7 patients, no score was reported.

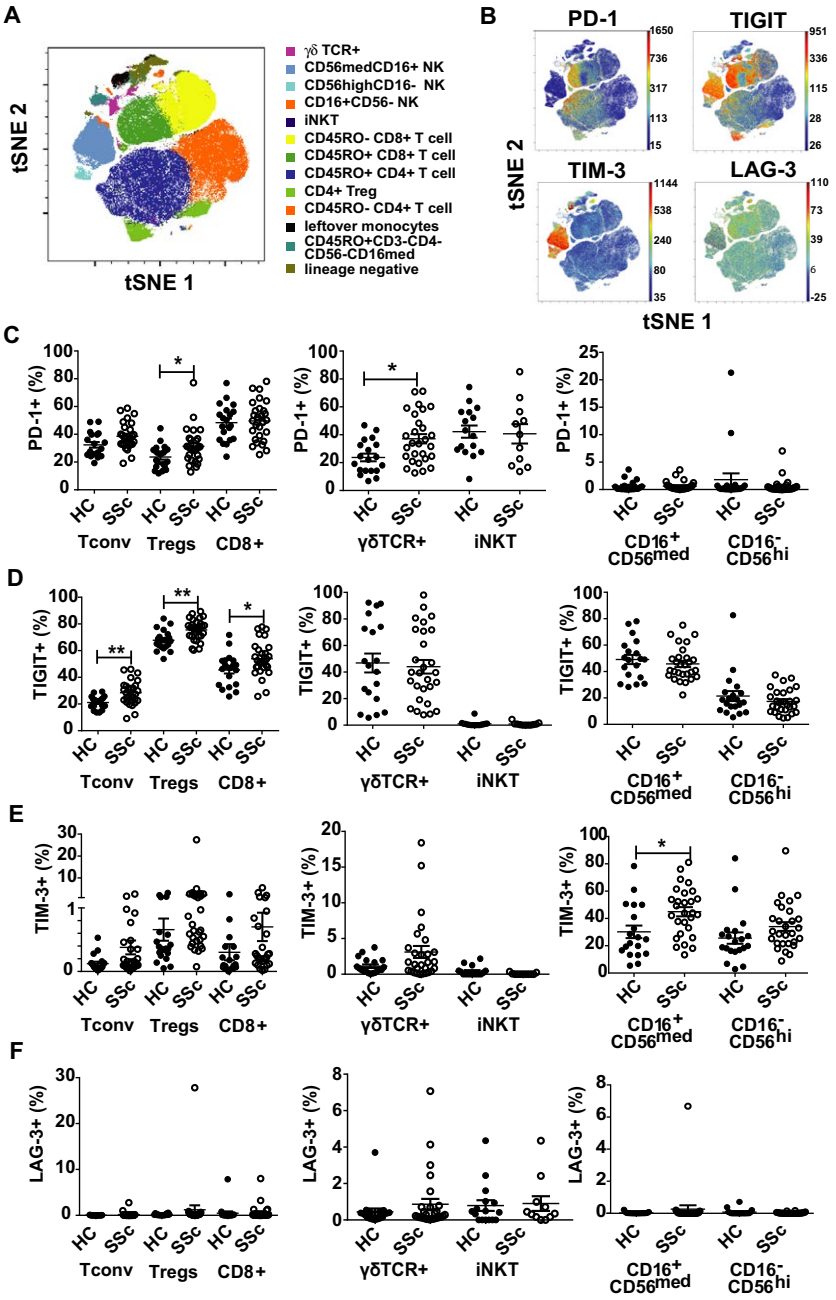

Figure 1. Increased expression of programmed cell death 1 (PD-1), T cell immunoglobulin and ITIM domain (TIGIT), and T cell immunoglobulin and mucin domain 3 (TIM-3) in defined peripheral blood lymphocyte subsets from patients with systemic sclerosis (SSc). Peripheral blood mononuclear cells (PBMCs) were isolated from SSc patients and healthy controls (HC). The PBMCs were stained with a 16-color antibody panel for flow cytometry. **A,** Single, live CD19−CD14− events were gated using flow cytometry data from a representative sample, and tSNE dimension reduction was applied with lineage marker channels used for clustering. Populations were gated manually and events were overlaid on the tSNE map to show positioning of 12 separate subsets of immune cells. **B,** The tSNE plots show the expression of PD-1, TIGIT, TIM-3, and lymphocyte activation gene 3 (LAG-3) on immune cell subsets, mapped as described in **A** (color scale depicts fluorescence intensity as a measure of expression level). **C–E,** Using manual gating, the percentage of PD-1+ cells (**C**), TIGIT+ cells (**D**), TIM-3+ cells (**E**), and LAG-3+ cells (**F**) within CD4+CD25^{low}CD45RO+ conventional T (Tconv) cells, CD4+CD25^{high}CD127^{low}CD45RO+ Treg cells, CD8+CD45RO+ T cells, γδ T cell receptor–positive (TCR+) T cells, invariant natural killer T (iNKT) cells (only shown if >20 events were recorded), CD16+CD56^{medium} NK cells, and CD16−CD56^{high} NK cells was determined. Each symbol represents an individual subject; bars show the mean ± SEM. Differences between groups were determined using the *t*-test with false discovery rate adjustment. * = $P \leq 0.05$; ** = $P \leq 0.01$. Color figure can be viewed in the online issue, which is available at http://onlinelibrary.wiley.com/doi/10.1002/art.40399/abstract.

Twelve distinct immune cell types could be identified in analyses applying an automated viSNE algorithm that blindly clusters cell subsets using fluorescence data (Figure 1A). Expression of the co-IRs PD-1, TIM-3, TIGIT, and LAG-3 showed significant cell-type specificity, with PD-1 mostly expressed in CD45RO+ memory T cells, TIGIT in T cells and NK cells, and TIM-3 predominantly in NK cells (Figure 1B). LAG-3 showed an overall low expression.

To compare co-IR expression on blood lymphocyte subsets between SSc patients and healthy controls, we defined 10 distinct subsets of T and NK cells using a manual gating strategy (further details available upon request from the corresponding author). After exclusion of dead cells as well as CD19+ B cells and CD14+ monocytes, CD3+ T cells were further divided into CD4+CD8− T helper cells, CD4−CD8+ cytotoxic T cells, γδ T cells, and invariant NK T (iNKT) cells. Within the CD4+ T cells, high expression levels of CD25 and low levels of CD127 were used to delineate a population enriched in regulatory T cells, hereinafter referred to as Treg cells (17,18). Since the CD25+CD127^{low} phenotype does not equate 100% to FoxP3+ Treg cells, it is critical to consider that changes in co-IR expression within this population may also represent a small subset of activated effector CD4+ T cells. CD4+ and CD8+ T cell subsets were subdivided into CD45RO+ memory and CD45RO− naive subsets (19). It is important to note that we did not observe any differences in the frequencies of the major T cell types between SSc patients and healthy controls, except for an increase in CD25+CD127− Treg cells in the SSc group. Interestingly, the Treg cell subset showed a reduction in cells with a CD45RO+ effector/memory phenotype in SSc patients (results available upon request from the corresponding author).

For CD4+ conventional T cells, CD4+ Treg cells, and CD8+ T cells, the expression of PD-1, TIGIT, TIM-3, and LAG-3 was determined within the CD45RO+ effector/memory population, since naive T cells typically express low levels of these receptors (representative dot plots of co-IR staining are available upon request from the corresponding author). In SSc patients, the numbers of PD-1–expressing cells within the Treg cell subset and within γδ T cells were significantly increased compared to those from healthy subjects, while no differences in PD-1 expression were observed on CD8+ T cells, iNKT cells, or NK cells (Figure 1C). The difference in PD-1 expression on CD4+ conventional T cells did not reach statistical significance after false discovery rate analysis, but strongly trended toward an increase in SSc patients (P = 0.054) (Figure 1C).

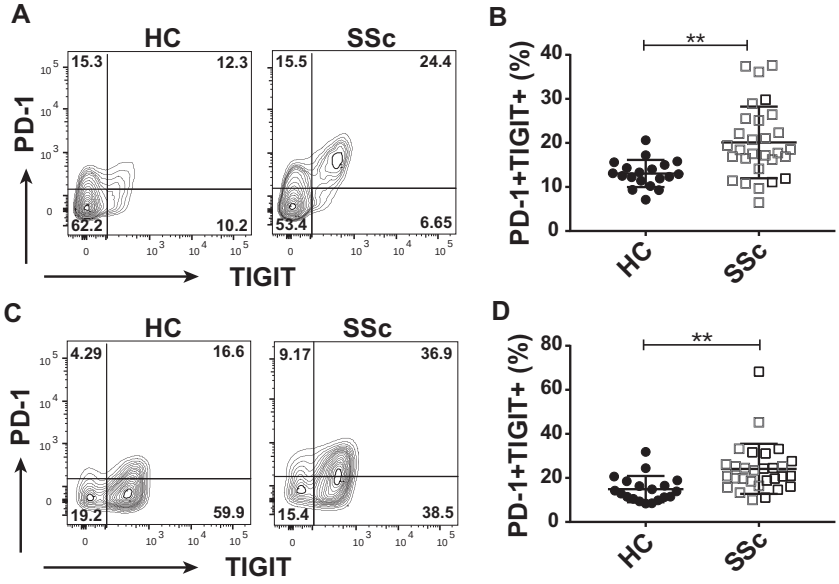

Figure 2. Increased levels of PD-1+TIGIT+ double-positive T cells in SSc patients. Coexpression of PD-1 and TIGIT on lymphocyte subsets was analyzed using manual gating. **A** and **B,** Representative dot plots show the distributions of PD-1+TIGIT+ double-positive cells **(A)** and graphs show the percentages of PD-1+TIGIT+ cells **(B)** among CD4+ conventional T cells from healthy controls and SSc patients. **C** and **D,** Representative dot plots show the distributions of PD-1+TIGIT+ double-positive Treg cells **(C)** and graphs show the percentages of PD-1+TIGIT+ Treg cells **(D)** from healthy controls and SSc patients. In **B** and **D**, each symbol represents an individual subject; bars show the mean ± SEM. ** = $P \leq 0.01$. See Figure 1 for definitions.

TIGIT was enhanced on conventional CD4+ T cells, Treg cells, and CD8+ T cells from SSc patients. However, no enhancement of TIGIT was seen on γδ T cells, iNKT cells, and NK cells from SSc patients, thus showing a somewhat different pattern than PD-1 (Figure 1D).

TIM-3 showed low expression levels on all T cell subsets, confirming the findings from viSNE analysis, and no differences between healthy controls and SSc patients were observed (Figure 1E). As noted above, TIM-3 was strongly present on NK cells and further increased on the CD16+CD56^{medium} cell subset in SSc patients. LAG-3 was minimally present on all analyzed cell subsets, and there were no noteworthy differences between healthy subjects and SSc patients (Figure 1F). Not surprisingly, co-IRs were expressed at lower levels in CD45RO− naive conventional T cells, Treg cells, and CD8+ cells, although some differences in SSc patients compared to healthy controls were still apparent (results available upon request from the corresponding author).

Finally, we performed a separate analysis of patients with high percentages of Treg cells. We determined that the presence of significantly more Treg cells (or CD25+CD127^{low} activated effector cells) in 7 patients could not be attributed to SSc disease type (limited versus diffuse) or the presence or absence of lung and skin involvement (results not shown). Intriguingly, patients with high Treg cell percentages also had

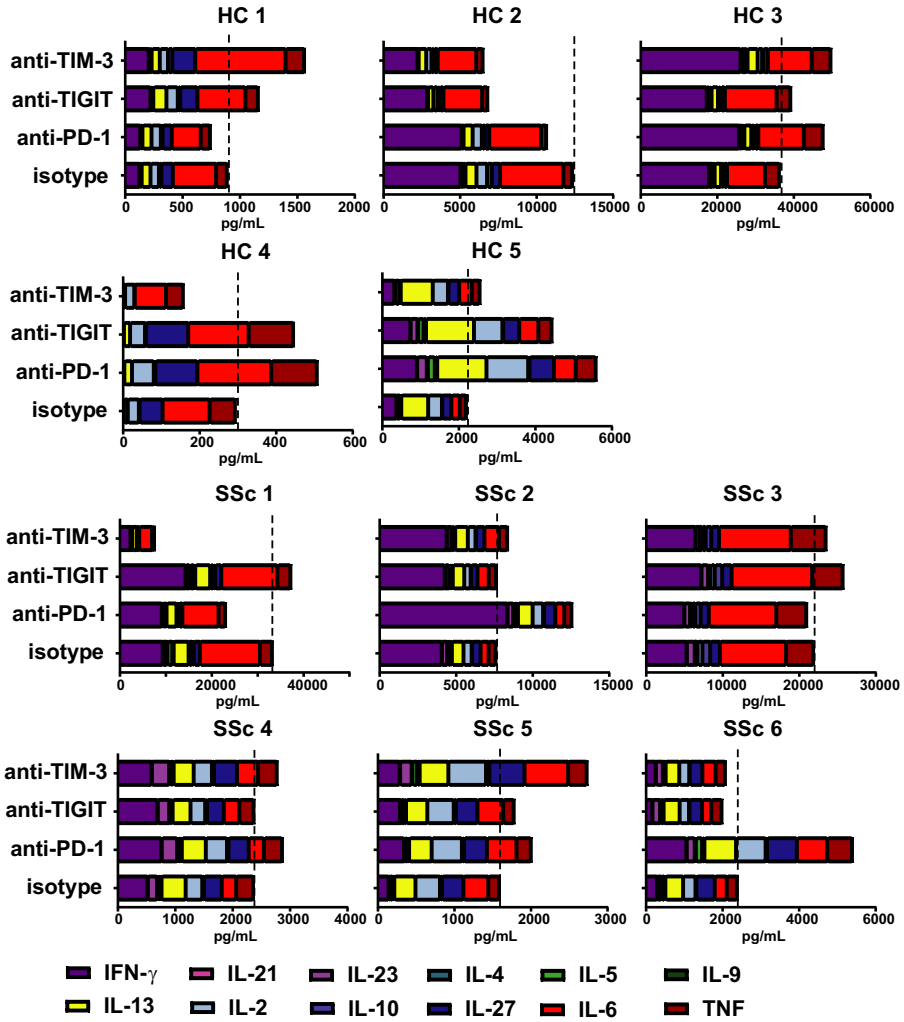

Figure 3. Subject-specific activities of coinhibitory receptors in controlling lymphocyte cytokine production. PBMCs from SSc patients and healthy controls were stimulated with dendritic cells from a healthy donor in the absence or presence of anti–PD-1, anti-TIGIT, or anti–TIM-3 blocking antibodies, and supernatants were analyzed with a 14-cytokine multiplex assay. Bar graphs show the amount (in pg/ml) of each of the indicated cytokines produced by the cells from individual healthy subjects and SSc patients. The broken vertical line indicates the level of total cytokine produced in the isotype control cultures. IFNγ = interferon-γ; IL-21 = interleukin-21; TNF = tumor necrosis factor (see Figure 1 for other definitions).

increased co-IR expression (results available upon request from the corresponding author), potentially suggestive of a more "activated" disease environment in these patients, which could lead to Treg cell expansion and enhanced co-IR expression.

Increased frequency of T lymphocytes coexpressing PD-1 and TIGIT in SSc patients. One hallmark of exhausted T cells is the accumulated expression of multiple co-IRs on the cell surface (9). Comprehensive co-IR signature analysis revealed that CD4+ conventional T cells and Treg cells from SSc patients contained an increased frequency of PD-1+TIGIT+ double-positive cells compared to those from healthy subjects (Figures 2A–D). In NK $CD56^{medium}$ cells, coexpression of TIGIT and TIM-3 showed a trend toward increased presence in SSc patients compared to healthy controls (results not shown). The increased presence of T cells expressing combinations of co-IRs in SSc patients suggests that immune dysfunction and T cell exhaustion were increased in those patients. Perhaps surprisingly, this augmented exhaustion signature, as well as the increased levels of single co-IR–positive cell populations (as described above), did not correlate with disease duration in SSc patients (results not shown). The striking exhaustion phenotype, however, prompted us to investigate the functional role of co-IRs in the activation of T cells from SSc patients.

Patient-specific activity of PD-1, TIGIT, and TIM-3 in controlling T cell cytokine production. To directly test whether co-IRs differentially regulate T cell responses in SSc patients and healthy subjects, we designed an assay using monocyte-derived DCs from a healthy donor as an allogeneic stimulus in a mixed lymphocyte reaction (MLR). This assay requires cognate T cell–DC interactions for T cell activation, thereby facilitating physiologic engagement of co-IRs on the T cells with their ligands on the DCs (20). For this reason, an MLR is often used to test the functionality of novel checkpoint inhibitors for cancer immunotherapy (21–23). By using the same DC donor to stimulate responders, we could eliminate the possibility that differing amounts of inhibitory receptor ligands present on the DCs would be a potential confounding variable. Co-IR–blocking antibodies against PD-1, TIGIT, and TIM-3 were added to the MLR to prevent the binding of ligands to the receptors.

In the first set of experiments, we confirmed that antibody treatment did not affect the viability or ratios of the CD4+ and CD8+ T cell subsets in the MLR cultures (results available upon request from the corresponding author). We next collected supernatants from MLR cultures, and 14 cytokines were measured using a multiplex platform. As expected, the amounts and types of cytokines produced by individual subjects showed significant variability (Figure 3). Nevertheless, 2 distinct profiles could be readily observed: 1) subjects who showed a response dominated by the proinflammatory cytokines IFNγ, IL-6, and TNF (healthy control subjects 1–4 and SSc patients 1–3 in Figure 3), and 2) subjects with a more diverse cytokine response and increased presence of Th2 cytokines (healthy control subject 5 and SSc patients 4–6 in Figure 3).

In most cases, co-IR blockade did not appear to selectively promote the production of specific cytokines, and therefore none of the co-IR–blocking antibody treatments led to dramatic changes in the composition of patient-specific cytokine profiles (Figure 3). In 4 of 5 healthy control subjects and 4 of 6 SSc patients, at least 2 of the co-IR–blocking antibodies increased the total amount of cytokines produced. In both healthy subjects and SSc patients, PD-1 appeared to be the strongest regulator of cytokine secretion (Figure 3 and Figure 4A). The role of TIGIT and TIM-3 was modest in SSc patients, whereas in most healthy subjects, TIGIT and/or TIM-3 were potent secondary regulators of total cytokine secretion (Figure 4A).

Interestingly, there was significant patient-specific variation in the cytokine-regulating activities of co-IRs. This experiment demonstrated that co-IR expression in SSc PBMCs is not exclusively a marker of a dysfunctional immune system, but rather, interactions of co-IRs with their ligands can actively regulate T cell effector functions and thus may play a role in the T cell–dependent pathogenic processes of SSc.

To establish whether co-IR blockade during the MLR cultures differentially affected the cytokine response of immune cells between SSc patients and healthy subjects, the large data set was analyzed using advanced bioinformatics and mathematical modeling. Unsupervised hierarchical clustering of cultures from subjects with various treatments and cytokines resulted in individual donors, rather than treatment groups, clustering together, masking any indication of potential effects of the blocking antibodies on cytokine production (results available upon request from the corresponding author). Therefore, to determine whether the activities of PD-1, TIGIT, and TIM-3 in SSc patients and healthy subjects could be differentiated, we performed PLSDA. The PLSDA method is a mathematical analysis method that uses LVs to determine which parameters contribute to causing the greatest difference between samples. PLSDA is useful when the behaviors of multiple analytes of interest, in this case cytokines, are known to be interdependent and can reveal combinations of cytokines whose fluctuation, as a group, maximally correlates with the anti–co-IR antibody treatments (24,25).

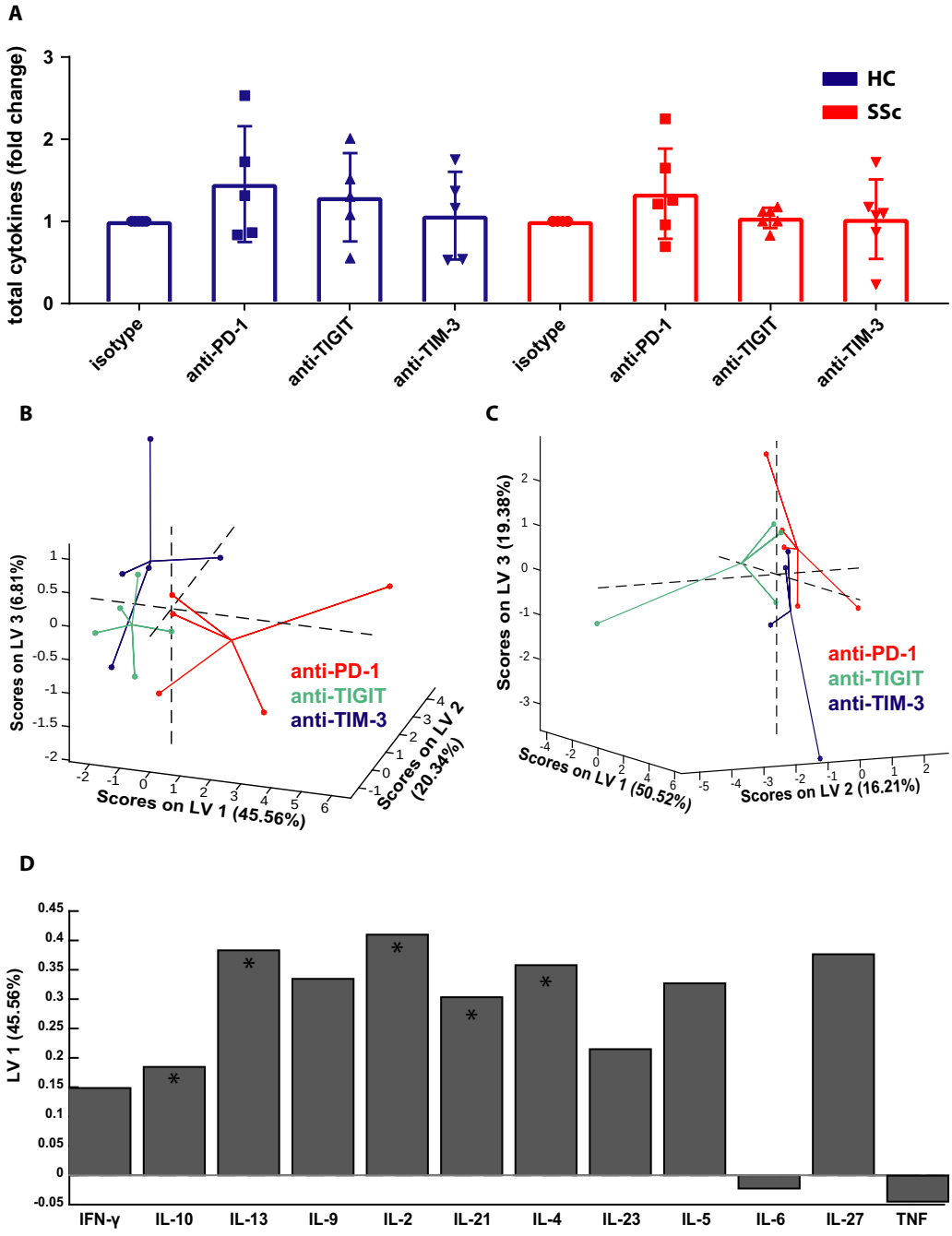

Figure 4. Cytokine production is modulated by coinhibitory receptor (co-IR)–blocking antibodies against PD-1, but not those against TIGIT or TIM-3, in SSc PBMCs. **A,** Fold changes in the levels of total cytokines (relative to values in isotype controls) after co-IR blockade are shown. Each symbol represents an individual healthy control or SSc patient; bars show the mean ± SEM. **B–D,** Multiplex cytokine data were subjected to partial least squares discriminant analysis to identify variations in patterns of cytokine production (normalized to isotype control values) after blockade with co-IR–blocking antibodies. Graphs show data points from each co-IR–blocking antibody culture condition with cells from SSc patients **(B)** and healthy controls **(C)**, mapped onto 3-dimensional latent variable (LV) space and connected with lines that meet at their centroid. **D,** The contribution of each cytokine from the SSc mixed lymphocyte reaction cultures to LV1 is shown, with asterisks denoting cytokines with a variable importance in projection score >1, indicating greater than average contribution. IFNγ = interferon-γ; IL-10 = interleukin-10; TNF = tumor necrosis factor (see Figure 1 for other definitions). Color figure can be viewed in the online issue, which is available at http://onlinelibrary.wiley.com/doi/10.1002/art.40399/abstract.

Cytokine levels in each treatment group were normalized relative to those in isotype-treated controls, to account for the large differences in total cytokine produced between subjects. The samples were then mapped onto 3-dimensional LV space and connected with lines that meet at their centroid. In SSc patients, our analysis showed that profiles of cytokine secretion differed between anti–PD-1–treated cells and anti–TIM-3–treated and anti-TIGIT–treated cells (Figure 4B), with a model confidence of 88%; this distinction was not found in samples from healthy controls (Figure 4C). The PLSDA model was unable to show any differences in anti-TIGIT or anti–TIM-3 effects on cytokine production between healthy controls and SSc patients.

Multiple cytokines contributed to LV1, which separated the effects of anti–PD-1 treatment from those of anti-TIGIT and anti–TIM-3 treatment in SSc patients (Figure 4D). Increased overall production of IL-10, IL-13, IL-2, IL-21, and IL-4 in the anti–PD-1–treated SSc samples contributed most significantly to the distinction, as determined by VIP score. This analysis thus strengthens the conclusion that in SSc patients, PD-1 continued to exert its normal function of actively inhibiting T cell cytokine production, but the TIGIT and TIM-3 pathways, while actively controlling cytokine secretion in healthy controls, became defective or refractory to reversal in SSc. Such a separation between the functionality of PD-1 on the one hand, and TIGIT/TIM-3 on the other hand, has not been previously demonstrated in a human autoimmune disease.

Modulation of SSc fibroblast activation following the alteration of T cell cytokine production by co-IR blockade. Much of the pathogenesis of SSc is driven by fibrosis in target organs. It is thought that pathogenic fibroblasts produce large amounts of collagen, leading to loss of cellularity and elasticity in the skin and internal organs (26). To explore whether antibody blockade of co-IRs on T cells could have a potential effect on this cell type, we cultured SSc primary fibroblasts for 24 hours with the supernatants collected from MLR cultures (the same cultures as shown in Figure 3). Fibroblasts were washed and RNA was isolated for NanoString analysis of genes previously described to be important in SSc disease pathogenesis (16). Interestingly, hierarchical clustering revealed that the 2 main clusters are largely driven by the 2 distinct cytokine signatures identified in Figure 3: the "proinflammatory" group and the "diverse/Th2" group (further details available upon request from the corresponding author). Within these 2 groups, donor-specific patterns of gene expression appeared to be the most similar. Since our data demonstrated that treatment with co-IR–blocking antibodies mostly resulted in quantitative, rather than qualitative, changes in cytokine production, it is perhaps not surprising that supernatants from treated cultures did not lead to uniformly clustered changes in the patterns of basic fibroblast gene expression.

We next examined whether multivariate mathematical modeling was capable of distinguishing the effects of anti–co-IR treatment on fibroblast gene expression

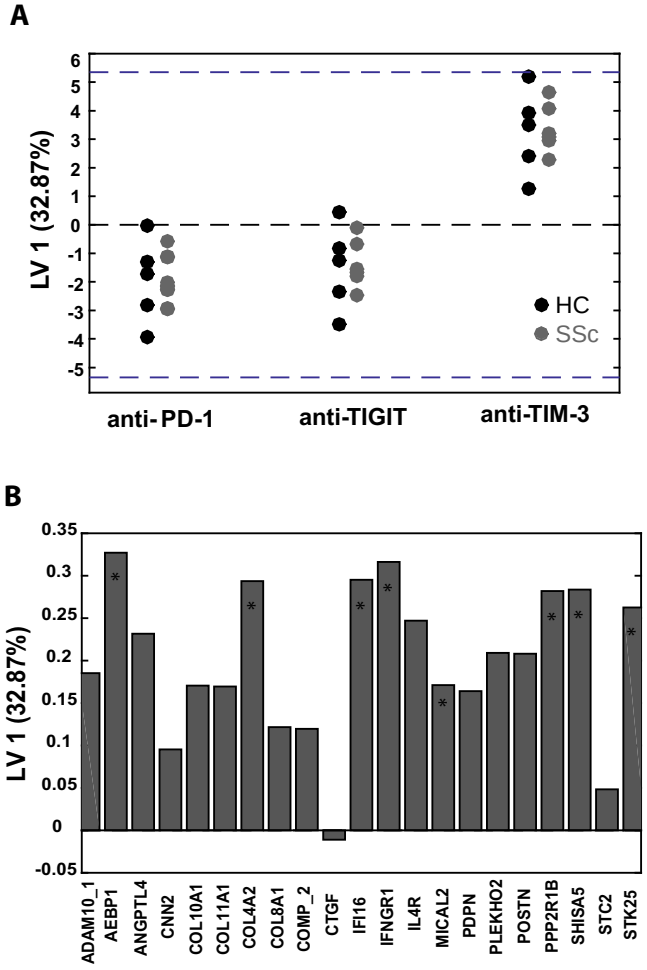

Figure 5. Blocking of TIM-3 in mixed lymphocyte reaction (MLR) cultures promotes the production of soluble factors that alter SSc fibroblast gene expression. SSc fibroblasts were cultured for 24 hours with supernatants from MLR cultures. Fibroblast RNA was prepared, and the expression of selected genes was measured with NanoString technology. **A,** Partial least squares discriminant analysis was applied to the NanoString data. The plots show the fibroblast gene expression data contributing to latent variable 1 (LV1) obtained from fibroblasts exposed to supernatants from each coinhibitory receptor antibody–treated MLR. Symbols represent data from individual healthy control subjects and SSc patients. Broken horizontal lines indicate the zero value and the boundaries of the 95% confidence interval. **B,** The contribution of each individual gene to LV1 is shown, with asterisks denoting genes with a variable importance of projection score >1, indicating greater than average contribution. See Figure 1 for other definitions.

after exposure to culture supernatants. Feature selection using the LASSO algorithm was performed, resulting in narrowing of our gene set from 53 genes to 21 genes. Subsequently, PLSDA was applied to identify patterns of fibroblast gene expression that differentiated the treatment groups. Surprisingly, we found that fibroblasts treated with supernatants from anti–TIM-3–treated MLRs, both those derived from SSc samples and those derived from healthy control samples, had a distinctly modified gene expression profile as compared to the anti–PD-1 and anti-TIGIT treatment groups (Figure 5A).

This distinct gene expression profile from the anti–TIM-3 group showed separation based on LV1 (Figure 5B). Since we observed that TIM-3 did not strongly regulate the 12 cytokines measured in SSc lymphocytes (as shown in Figure 3 and Figures 4A and B), it is likely that an unknown factor, induced after TIM-3 blockade, is an important regulator of SSc fibroblast gene expression. Importantly, the main drivers of LV1 were profibrotic genes, suggesting that TIM-3 might play a protective role in SSc fibrosis. Contrary to that seen with anti–TIM-3 treatment, anti–PD-1 treatment did not appear to drive gene expression changes in fibroblasts, suggesting that PD-1 mostly controls the amount of cytokines produced, without significantly changing the composition of the supernatants.

DISCUSSION

In this study, we analyzed the expression and function of the co-IRs PD-1, TIM-3, TIGIT, and LAG-3 in SSc PBMCs. PD-1 and TIGIT are increased and coexpressed on multiple T cell subsets from SSc patients, while TIM-3 is increased on the cytotoxic CD16+CD56^{medium} subset of NK cells. Co-IRs play distinct roles in regulating the production of cytokines, and their functionality differed significantly between individual donors. Importantly, TIGIT and TIM-3, but not PD-1, showed reduced activity in SSc patients compared to healthy controls. Our observations thus support a cell-specific altered expression pattern of co-IRs in SSc immune cells, rather than a broad up-regulation of these receptors. Moreover, co-IRs play complex and patient-specific roles in the regulation of cytokine production, a finding with potential implications for achieving a better understanding of this heterogeneous disease.

SSc is a poorly understood autoimmune disorder that produces extreme reduction in quality of life, and the 10-year survival rate in patients with SSc currently averages 50% (27). Patients have few treatment options, and a greater understanding of the underlying immunologic mechanisms of the disease is needed to assess the feasibility of developing immunotherapies. While many studies have focused on understanding aberrant fibroblast differentiation in SSc, there is also evidence that immune cells and the cytokines they produce play a critical role in fibrosis. In many fibrotic diseases, it is well-established that Th2-type immune responses, producing IL-4 and IL-13, promote fibrosis (28). T cell–derived TGFβ may contribute as well (29). In SSc, however, robust evidence of a critical role of bona fide Th2 cells remains limited (30). CD8+ T cells may also be a source of IL-13, as was demonstrated by Fuschiotti et al in SSc peripheral blood (4) and skin (31). One intriguing study demonstrated that skin Treg cells can produce IL-4 and IL-13, possibly contributing to a fibrotic phenotype (5). This finding, combined with studies indicating that the numbers of bona fide FoxP3+ Treg cells are reduced in the skin of SSc patients (32,33), suggests that Treg cell deficiencies play a role in SSc. It would be of interest to determine whether the specific reduction in CD45RO+ effector/memory Treg cells that we observed in SSc blood would correlate with the reported decrease in tissue-resident Treg cells. A number of recent studies have indicated that Th17 cells are present in SSc and may contribute to the disease process (34,35). Taken together, the findings in these studies underscore the need for a better understanding of the regulatory mechanisms underlying the potential profibrotic and proinflammatory functions of various T cell subsets in SSc.

Co-IRs such as PD-1, TIM-3, LAG-3, and TIGIT are an important class of molecules controlling T cell effector responses. Our finding that these receptors are aberrantly expressed in SSc patients is consistent with the general trend of increased levels of these receptors in other rheumatic diseases. However, the co-IR expression patterns on various lymphocyte subsets show considerable disease-dependent variation. For example, the levels of PD-1 were found to be increased in CD4+ and CD8+ T and NK cells from lupus patients (36,37) and in CD3+ T cells from patients with psoriatic arthritis (38), whereas in the present study, in patients with SSc, PD-1 was only significantly enhanced in Treg cells and γδ T cells (Figure 1C). In addition, serum levels of soluble forms of PD-1, and its ligand PD-L2, were recently shown to be elevated in SSc (14).

Li et al observed increased levels of TIM-3 on CD4+ and CD8+ T cells in the peripheral blood of patients with rheumatoid arthritis (39), whereas our study showed no changes in TIM-3 in SSc T cell subsets, but did show an increase in NK cells (Figure 1E). In lupus patients, the levels of TIGIT were found to be up-regulated on CD4+ T cells but reduced in CD8+ T cells, NK cells, and Treg cells (40), an expression

pattern that does not match with our observations in patients with SSc (Figure 1D). Deciphering the origin and functional consequences of these differences constitutes an important future research direction.

Co-IRs have been demonstrated to play critical functional roles in in vivo models of autoimmune disorders (7) and in chronic viral infections and cancer (9). In HIV and cancer, increased expression of PD-1 and the coexpression of multiple co-IRs is linked with a corresponding decrease in the effector function of T cells (9), a state described as T cell exhaustion. Blocking co-IRs can restore effector function, as has been shown in successful immunotherapy for cancer (41,42). However, epigenetic mechanisms dictating exhaustion can provide a barrier to lymphocyte rejuvenation (43). Our findings showing that anti-TIGIT and anti–TIM-3 antibody blockade were largely ineffective in enhancing cytokine production in PBMCs from SSc patients, and that SSc patients had increased numbers of PD-1+TIGIT+ double-positive T cells, suggest that a more robust state of T cell exhaustion, perhaps epigenetically controlled, is present in SSc patients compared to healthy controls.

Our antibody blocking experiments revealed that PD-1 played the most dominant role in modulating cytokine secretion. PD-1 has been extensively characterized as a co-IR that limits the production of cytokines in immune cells. It is therefore feasible that increased PD-1 expression in SSc patients represents a regulatory mechanism that attempts to limit tissue damage. However, absence of the ligands engaging PD-1 in the tissue microenvironment may preclude successful engagement of this pathway.

Alternatively, PD-1, TIM-3, and TIGIT may suppress some T cell cytokines, but not others, leading to subtle skewing of cytokine profiles. Such changes in cytokine signatures due to aberrant expression of combinations of co-IRs and, perhaps, their ligands in fibrotic tissues may impinge on disease processes. In support of this hypothesis, our data show that co-IR blockade during an in vitro immune response provokes changes in soluble factors that can have an impact on fibroblast gene expression. In some cases, these changes may be attributed to the presence of specific cytokines that have known activities in fibroblasts. IL-13, for example, is a potent inducer of collagen production (44). However, one intriguing possibility, revealed by mathematical modeling, was that TIM-3 modulated the production of unidentified soluble factors that had a distinct effect on SSc fibroblast gene expression. One obvious candidate to initiate these changes would be the profibrotic cytokine TGFβ, but recombinant TGFβ alone was not able to recapitulate the gene expression profile induced by any of the co-IR blocking antibodies (results not shown).

In summary, our study documents the fact that SSc patients express co-IR signatures reminiscent of immune cell exhaustion. Our findings from functional analysis and mathematical modeling of the impact of these co-IRs on disease-relevant cytokine production and fibroblast gene expression suggest that these co-IR pathways play a role in the pathophysiology of SSc and may be amenable targets for therapy.

ACKNOWLEDGMENTS

We thank Nina Kishore and Eric Stratton for help with patient enrollment, and Ashna Gupta for assistance with clinical data analysis. We acknowledge the technical support provided by Matthew Au at the Boston University Analytical Core, and by staff at the Flow Cytometry Core Facility. We also thank the patients for their participation in the study.

AUTHOR CONTRIBUTIONS

All authors were involved in drafting the article or revising it critically for important intellectual content, and all authors approved the final version to be published. Dr. Dooms had full access to all of the data in the study and takes responsibility for the integrity of the data and the accuracy of the data analysis.

Study conception and design. Fleury, Snyder-Cappione, Lafyatis, Dooms.

Acquisition of data. Fleury, Belkina, Zammitti, Simms.

Analysis and interpretation of data. Fleury, Belkina, Proctor, Zammitti, Lauffenburger, Snyder-Cappione, Lafyatis, Dooms.

REFERENCES

1. Van den Hoogen F, Khanna D, Fransen J, Johnson SR, Baron M, Tyndall A, et al. 2013 classification criteria for systemic sclerosis: an American College of Rheumatology/European League Against Rheumatism collaborative initiative. Arthritis Rheum 2013;65:2737–47.
2. Allanore Y, Simms R, Distler O, Trojanowska M, Pope J, Denton CP, et al. Systemic sclerosis. Nat Rev Dis Primers 2015;1:15002.
3. Almeida I, Silva SV, Fonseca AR, Silva I, Vasconcelos C, Lima M. T and NK cell phenotypic abnormalities in systemic sclerosis: a cohort study and a comprehensive literature review. Clin Rev Allergy Immunol 2015;49:347–69.
4. Li P, Medsger TA Jr, Morel PA. Effector CD8+ T cells in systemic sclerosis patients produce abnormally high levels of interleukin-13 associated with increased skin fibrosis. Arthritis Rheum 2009;60:1119–28.
5. Macdonald KG, Dawson NA, Huang Q, Dunne JV, Levings MK, Broady R. Regulatory T cells produce profibrotic cytokines in the skin of patients with systemic sclerosis. J Allergy Clin Immunol 2015;135:946–55.e9.
6. Baraut J, Michel L, Verrecchia F, Farge D. Relationship between cytokine profiles and clinical outcomes in patients with systemic sclerosis. Autoimmun Rev 2010;10:65–73.
7. Anderson AC, Joller N, Kuchroo VK. Lag-3, Tim-3, and TIGIT: co-inhibitory receptors with specialized functions in immune regulation. Immunity 2016;44:989–1004.
8. Ferris RL, Lu B, Kane LP. Too much of a good thing? Tim-3 and TCR signaling in T cell exhaustion. J Immunol 2014;193:1525–30.

9. Wherry EJ. T cell exhaustion. Nat Immunol 2011;12:492–9.
10. McKinney EF, Lee JC, Jayne DR, Lyons PA, Smith KG. T-cell exhaustion, co-stimulation and clinical outcome in autoimmunity and infection. Nature 2015;523:612–6.
11. Day CL, Kaufmann DE, Kiepiela P, Brown JA, Moodley ES, Reddy S, et al. PD-1 expression on HIV-specific T cells is associated with T-cell exhaustion and disease progression. Nature 2006;443:350–4.
12. June CH, Warshauer JT, Bluestone JA. Is autoimmunity the Achilles' heel of cancer immunotherapy? Nat Med 2017;23:540–7.
13. Saresella M, Piancone F, Marventano I, La Rosa F, Tortorella P, Caputo D, et al. A role for the TIM-3/GAL-9/BAT3 pathway in determining the clinical phenotype of multiple sclerosis. FASEB J 2014;28:5000–9.
14. Fukasawa T, Yoshizaki A, Ebata S, Nakamura K, Saigusa R, Miura S, et al. Contribution of soluble forms of programmed death 1 and programmed death ligand 2 to disease severity and progression in systemic sclerosis. Arthritis Rheumatol 2017;69: 1879–90.
15. Belkina AC, Snyder-Cappione JE. OMIP-037: 16-color panel to measure inhibitory receptor signatures from multiple human immune cell subsets. Cytometry A 2017;91:175–9.
16. Rice LM, Ziemek J, Stratton EA, McLaughlin SR, Padilla CM, Mathes AL, et al. A longitudinal biomarker for the extent of skin disease in patients with diffuse cutaneous systemic sclerosis. Arthritis Rheumatol 2015;67:3004–15.
17. Liu W, Putnam AL, Xu-Yu Z, Szot GL, Lee MR, Zhu S, et al. CD127 expression inversely correlates with FoxP3 and suppressive function of human CD4+ T reg cells. J Exp Med 2006;203:1701–11.
18. Seddiki N, Santner-Nanan B, Martinson J, Zaunders J, Sasson S, Landay A, et al. Expression of interleukin (IL)-2 and IL-7 receptors discriminates between human regulatory and activated T cells. J Exp Med 2006;203:1693–700.
19. Rothstein DM, Yamada A, Schlossman SF, Morimoto C. Cyclic regulation of CD45 isoform expression in a long term human CD4+CD45RA+ T cell line. J Immunol 1991;146:1175–83.
20. Stecher C, Battin C, Leitner J, Zettl M, Grabmeier-Pfistershammer K, Höller C, et al. PD-1 blockade promotes emerging checkpoint inhibitors in enhancing T cell responses to allogeneic dendritic cells. Front Immunol 2017;8:1–13.
21. Wang C, Thudium KB, Han M, Wang XT, Huang H, Feingersh D, et al. In vitro characterization of the anti-PD-1 antibody nivolumab, BMS-936558, and in vivo toxicology in non-human primates. Cancer Immunol Res 2014;2:846–56.
22. Stewart R, Morrow M, Hammond SA, Mulgrew K, Marcus D, Poon E, et al. Identification and characterization of MEDI4736, an antagonistic anti-PD-L1 monoclonal antibody. Cancer Immunol Res 2015;3:1052–62.
23. Lázár-Molnár E, Scandiuzzi L, Basu I, Quinn T, Sylvestre E, Palmieri E, et al. Structure-guided development of a high-affinity human programmed cell death-1: implications for tumor immunotherapy. EBioMedicine 2017;17:30–44.
24. Lau KS, Cortez-Retamozo V, Philips SR, Pittet MJ, Lauffenburger DA, Haigis KM. Multi-scale in vivo systems analysis reveals the influence of immune cells on TNF-α-induced apoptosis in the intestinal epithelium. PLoS Biol 2012;10:e1001393.
25. Ip B, Cilfone NA, Belkina AC, DeFuria J, Jagannathan-Bogdan M, Zhu M, et al. Th17 cytokines differentiate obesity from obesity-associated type 2 diabetes and promote TNFα production. Obesity (Silver Spring) 2016;24:102–12.
26. Pattanaik D, Brown M, Postlethwaite BC, Postlethwaite AE. Pathogenesis of systemic sclerosis. Front Immunol 2015;6:272.
27. Elhai M, Meune C, Avouac J, Kahan A, Allanore Y. Trends in mortality in patients with systemic sclerosis over 40 years: a systematic review and meta-analysis of cohort studies. Rheumatology (Oxford) 2012;51:1017–26.
28. Wynn TA. Type 2 cytokines: mechanisms and therapeutic strategies. Nat Rev Immunol 2015;15:271–82.
29. Roberts AB, Sporn MB, Assoian RK, Smith JM, Roche NS, Wakefield LM, et al. Transforming growth factor type β: rapid induction of fibrosis and angiogenesis in vivo and stimulation of collagen formation in vitro. Proc Natl Acad Sci 1986;83:4167–71.
30. O'Reilly S, Hügle T, van Laar JM. T cells in systemic sclerosis: a reappraisal. Rheumatology (Oxford) 2012;51:1540–9.
31. Fuschiotti P, Larregina AT, Ho J, Feghali-Bostwick C, Medsger TA Jr. Interleukin-13–producing CD8+ T cells mediate dermal fibrosis in patients with systemic sclerosis. Arthritis Rheum 2013;65:236–46.
32. Antiga E, Quaglino P, Bellandi S, Volpi W, del Bianco E, Comessatti A, et al. Regulatory T cells in the skin lesions and blood of patients with systemic sclerosis and morphoea. Br J Dermatol 2010;162: 1056–63.
33. Klein S, Kretz CC, Ruland V, Stumpf C, Haust M, Hartschuh W, et al. Reduction of regulatory T cells in skin lesions but not in peripheral blood of patients with systemic scleroderma. Ann Rheum Dis 2011;70:1475–81.
34. Radstake TR, van Bon L, Broen J, Hussiani A, Hesselstrand R, Wuttge DM, et al. The pronounced Th17 profile in systemic sclerosis (SSc) together with intracellular expression of TGFβ and IFNγ distinguishes SSc phenotypes. PLoS One 2009;4:e5903.
35. Fenoglio D, Battaglia F, Parodi A, Stringara S, Negrini S, Panico N, et al. Alteration of Th17 and Treg cell subpopulations co-exist in patients affected with systemic sclerosis. Clin Immunol 2011;139:249–57.
36. Bertsias GK, Nakou M, Choulaki C, Raptopoulou A, Papadimitraki E, Goulielmos G, et al. Genetic, immunologic, and immunohistochemical analysis of the programmed death 1/programmed death ligand 1 pathway in human systemic lupus erythematosus. Arthritis Rheum 2009;60:207–18.
37. Jiao Q, Liu C, Yang Z, Ding Q, Wang M, Li M, et al. Upregulated PD-1 expression is associated with the development of systemic lupus erythematosus, but not the PD-1.1 allele of the PDCD1 gene. Int J Genomics 2014;2014:10–2.
38. Peled M, Strazza M, Azoulay-Alfaguter I, Mor A. Analysis of programmed death-1 in patients with psoriatic arthritis. Inflammation 2015;38:1573–9.
39. Li S, Peng D, He Y, Zhang H, Sun H, Shan S, et al. Expression of TIM-3 on CD4+ and CD8+ T cells in the peripheral blood and synovial fluid of rheumatoid arthritis. APMIS 2014;122:899–904.
40. Mao L, Hou H, Wu S, Zhou Y, Wang J, Yu J, et al. TIGIT signalling pathway negatively regulates CD4+ T-cell responses in systemic lupus erythematosus. Immunology 2017;151:280–90.
41. Topalian SL, Sznol M, McDermott DF, Kluger HM, Carvajal RD, Sharfman WH, et al. Survival, durable tumor remission, and long-term safety in patients with advanced melanoma receiving nivolumab. J Clin Oncol 2014;32:1020–30.
42. Yang Y. Cancer immunotherapy: harnessing the immune system to battle cancer. J Clin Invest 2015;125:3335–7.
43. Ghoneim HE, Fan Y, Moustaki A, Abdelsamed HA, Dash P, Dogra P, et al. De novo epigenetic programs inhibit PD-1 blockade-mediated T cell rejuvenation. Cell 2017;170:142–57.e19.
44. Chiaramonte MG, Donaldson DD, Cheever AW, Wynn TA. An IL-13 inhibitor blocks the development of hepatic fibrosis during a T-helper type 2–dominated inflammatory response. J Clin Invest 1999;104:777–85.

ARTHRITIS & RHEUMATOLOGY
Vol. 70, No. 4, April 2018, pp 578–584
DOI 10.1002/art.40384

Frequency of Chronic Joint Pain Following Chikungunya Virus Infection

A Colombian Cohort Study

Aileen Y. Chang,[1] Liliana Encinales,[2] Alexandra Porras,[3] Nelly Pacheco,[2] St. Patrick Reid,[4] Karen A. O. Martins,[5] Shamila Pacheco,[2] Eyda Bravo,[2] Marianda Navarno,[2] Alejandro Rico Mendoza,[3] Richard Amdur,[1] Priyanka Kamalapathy,[1] Gary S. Firestein,[6] Jeffrey M. Bethony,[1] and Gary L. Simon[1]

Objective. **To estimate the frequency of chronic joint pain after infection with chikungunya virus in a Latin American cohort.**

Methods. **A cross-sectional follow-up of a prospective cohort of 500 patients from the Atlántico Department, Colombia who were clinically diagnosed as having chikungunya virus during the 2014–2015 epidemic was conducted. Baseline symptoms and follow-up symptoms at 20 months were evaluated in serologically confirmed cases.**

Results. **Among the 500 patients enrolled, 485 had serologically confirmed chikungunya virus and reported joint pain status. Patients were predominantly adults (mean ± SD age 49 ± 16 years) and female, had an education level of high school or less, and were of Mestizo ethnicity. The most commonly affected joints were the small joints, including the wrists, ankles, and fingers. The initial virus symptoms lasted a median of 4 days (interquartile range [IQR] 3–8 days). Sixteen percent of the participants reported missing school or work (median 4 days [IQR 2–7 days]). After 20 months, one-fourth of the participants had persistent joint pain. A multivariable analysis indicated that significant predictors of persistent joint pain included college graduate status, initial symptoms of headache or knee pain, missed work, normal activities affected, ≥4 days of initial symptoms, and ≥4 weeks of initial joint pain.**

Conclusion. **This is the first report to describe the frequency of chikungunya virus–related arthritis in the Americas after a 20-month follow-up. The high frequency of chronic disease highlights the need for the development of prevention and treatment methods.**

Chikungunya virus is a mosquito-borne illness that can lead to chronic joint pain and arthritis (1). Patients with acute infection present with fever, headache, muscle pain, rash, and joint pain. Prior outbreaks have been reported in Africa, Asia, Europe, and the Indian and Pacific Ocean islands (2). In 2013, chikungunya virus was seen for the first time in the Caribbean basin, and it has now infected >1.2 million people throughout the Americas (3). Studies conducted prior to the American epidemics showed that 30–70% of chikungunya virus–infected patients have persistent joint pain months or years after their acute illness (1,3–14). Until now there have been no large-scale observational studies of the frequency of chikungunya arthritis in the Americas. It is estimated that ~48% of Latin American patients will develop chronic chikungunya arthritis a median of 20 months after chikungunya virus infection (15).

The views expressed herein are solely the responsibility of the authors and do not necessarily represent the official views of the Rheumatology Research Foundation, the NIH, or the US Army.

Supported by a Pilot award from the Rheumatology Research Foundation and the NIH (National Center for Advancing Translational Sciences grants UL1-TR-001876 and KL2-TR-001877).

[1]Aileen Y. Chang, MD, MSPH, Richard Amdur, PhD, Priyanka Kamalapathy, MD, Jeffrey M. Bethony, PhD, Gary L. Simon, MD, PhD: The George Washington University, Washington, DC; [2]Liliana Encinales, MD, Nelly Pacheco, Shamila Pacheco, Eyda Bravo, Marianda Navarno: Allied Research Society, Barranquilla, Colombia; [3]Alexandra Porras, PhD, Alejandro Rico Mendoza, PhD: Universidad El Bosque, Bogotá, Colombia; [4]St. Patrick Reid, PhD: University of Nebraska Medical Center, Omaha; [5]Karen A. O. Martins, PhD: US Army Medical Research Institute of Infectious Diseases, Fort Detrick, Maryland; [6]Gary S. Firestein, MD: University of California at San Diego.

Drs. Bethony and Simon contributed equally to this work.

Address correspondence to Aileen Y. Chang, MD, MSPH, The George Washington University School of Medicine and Health Sciences, 2150 Pennsylvania Avenue, Suite 5-416, Washington, DC 20037. E-mail: chang@email.gwu.edu.

Submitted for publication June 9, 2017; accepted in revised form November 14, 2017.

With the exception of the Andes Mountains region, most of Colombia has an elevation of less than 1,000 meters and is thus favorable for the proliferation of *Aedes aegypti*, the mosquito vector of chikungunya virus in the Americas. Thus, much of the population is vulnerable to infection with this virus. In the Americas in 2015, 693,489 cases of chikungunya virus were reported, of which Colombia bore the largest burden with 356,079 cases (16).

There has been little description of the frequency of chronic arthritis in the Americas. One study of 39 Colombian patients with chikungunya virus, ranging from 6 to 65 weeks after infection, showed that 90% had persistent polyarthralgias or arthritis at the time of evaluation (17).

The primary objective of the present study was to describe the frequency of persistent joint pain and disability in a Latin American cohort of chikungunya virus patients from Colombia. Our hypothesis was that chronic joint pain will be present in one-third of our Latin American cohort, which is similar to findings reported from other outbreaks of the Asian strain of the virus at 18 months (5,18). Defining the frequency of chronic joint pain and disability after chikungunya virus infection is important to understanding the long-term impact of the American outbreak.

PATIENTS AND METHODS

Study design. Five hundred patients with clinically confirmed chikungunya virus infection were enrolled as part of a prospective cohort in January 2015. Diagnosis of chikungunya virus was serologically confirmed via IgM and IgG antibody capture enzyme-linked immunosorbent assay (ELISA) (described below). A baseline 33-item survey was conducted to ascertain demographic characteristics, exposure history, and symptoms. A subsequent 56-item telephone survey was performed a median of 20 months after infection and included an assessment of the character and duration of persistent chikungunya arthritis symptoms, including swollen joint count, tender joint count, comorbidities, missed work or school, and a global score of pain during the last week (from the Disease Activity Score in 28 joints [DAS28] [19]), as well as therapies received.

Institutional review board (IRB) approval. This study was approved by the ethics committee of the Universidad El Bosque under a protocol entitled "Surveillance of sentinel infectious events prevalent in Colombia" with a non–human subjects determination made by The George Washington University IRB for analysis of deidentified data. Written informed consent was obtained from all participants, and all samples were collected by qualified medical personnel.

Setting. Patients were referred to the study from the Sabanalarga, Barranquilla, Juan de Acosta, Manatí, Luruaco, and Baranoa municipalities in the Atlántico Department, Colombia, which is located on the Caribbean coastal plane (20).

Participants. Primary care providers referred patients with clinically suspected chikungunya virus for enrollment. Clinical chikungunya virus was defined by the Colombian Institute of Health as a fever of >38°C, severe joint pain or arthritis, and acute onset of erythema multiforme, with symptoms not explained by other medical conditions. In addition, patients must reside in or have visited a municipality with evidence of chikungunya virus transmission or traveled within 30 km of confirmed viral transmission (21). Clinically suspected cases of chikungunya virus were confirmed serologically for the purposes of this study.

Variables. Demographic factors obtained included age, sex, ethnicity, education level, and insurance status. Outcomes were assessed at the follow-up survey. The primary outcome measure was the percentage of individuals with self-reported persistent chikungunya virus–related joint pain at follow-up ~20 months after infection. Secondary self-reported outcomes included the duration of initial joint pain since many individuals describe relapsing–remitting symptoms after initial infection, the percentage of individuals who missed work or school, the median days of missed work or school, the percentage of patients whose symptoms impacted their capacity to continue normal activity, and an estimate of disease severity. The latter included elements of the DAS28, including mean swollen joint count, mean tender joint count, and mean global pain score (19). The full DAS28 could not be calculated because this measure includes the C-reactive protein level, and no follow-up blood draw was performed. Potential effect modifiers included medical comorbidities such as chronic arthritis, gout, osteoarthritis, ischemic heart disease, kidney disease, lung disease, diabetes, hypertension, and depression. Finally, analysis included the types of therapies used for chikungunya arthritis, including aspirin, ibuprofen, acetaminophen, prednisone, methotrexate, medicinal plants, or other modalities.

Anti-chikungunya virus IgG and IgM. IgG and IgM levels were assayed using a Euroimmun anti–chikungunya virus ELISA (IgG/IgM) according to the manufacturer's instructions. These assays provide a qualitative evaluation of the presence or absence of anti-chikungunya virus IgG and IgM.

Statistical analysis. All 500 patients were contacted for the follow-up telephone survey. Excluded patients (n = 15) had no serologic confirmation of chikungunya virus or were missing data on current joint pain status. Variable distributions were examined for normality and outliers. Continuous variables were log-transformed if necessary. Univariable associations between patient variables and the presence of persistent joint pain, and between initial symptoms and sex, were tested using chi-square or Fisher's exact test for categorical variables and *t*-test or the Kruskal-Wallis test for continuous variables. A multivariable logistic regression model for persistent joint pain was tested using any baseline variable that was significantly associated with persistent joint pain as a factor. Backward selection was used, dropping predictors that had a *P* value of greater than 0.20. SAS (version 9.3) was used for data analysis. *P* values less than 0.05 were considered significant, except when Bonferroni correction was applied, as indicated in the table footnotes.

RESULTS

Five hundred participants with clinically suspected chikungunya virus infection were enrolled (Figure 1). Four

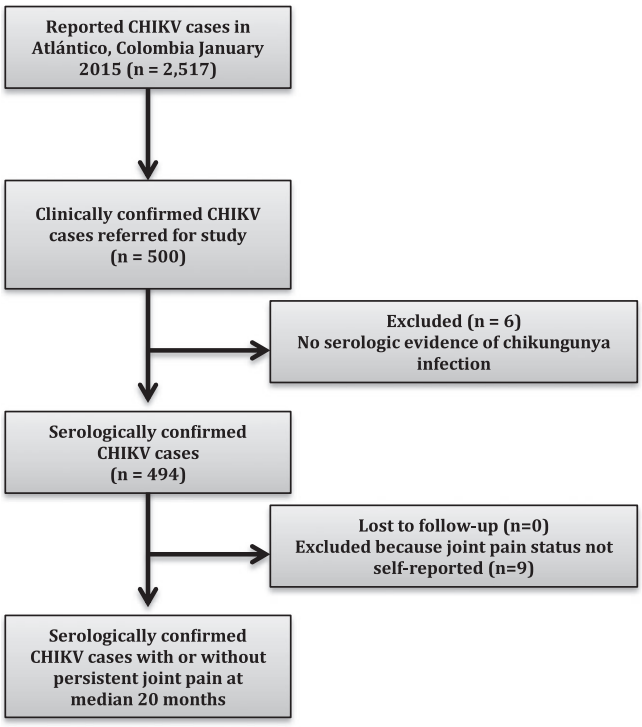

Figure 1. Study flow diagram. A chikungunya virus (CHIKV) epidemic occurred in 2014–2015 in the Atlántico Department of Colombia. At the time of study enrollment, there were 2,517 affected cases. Five hundred clinically confirmed cases were referred for the study, of which 494 were serologically confirmed. There was no attrition. All patients completed the follow-up telephone survey a median of 20 months after infection.

hundred ninety-four cases were confirmed by ELISA. Of these, 483 were acute cases (481 who were positive for both IgM and IgG and 2 who were positive for IgM and negative for IgG) and 11 were convalescent (6 who had equivocal IgM status but were positive for IgG and 5 who were negative for IgM and positive for IgG). Six cases were negative for IgM and IgG antibodies and were excluded from the analysis. All 500 participants were reached for the follow-up telephone survey. However, 9 participants did not report joint pain status and were excluded from the analysis (n = 485).

At baseline (Table 1), the confirmed cases were predominantly adults (mean age 49.1 years) and female and had an education level of high school or less. Almost all were of Mestizo ethnicity (i.e., mixed European, often Iberian, and indigenous Latin American ancestry) and had health insurance. The most common baseline comorbidity was hypertension (12%), and only 17 patients (4%) reported prior arthritis at baseline. The most commonly reported initial symptoms were muscle pain, weakness, joint pain, rash, fever, and headache (Table 2). The most commonly affected joints were the small joints, including the wrists, ankles, and fingers. The most commonly used medication to treat chikungunya virus–related joint pain was acetaminophen, which was taken by every patient. Forty-six patients took ibuprofen, prednisone, or medicinal plants. The initial joint pain during acute infection lasted a median of 4 weeks (interquartile range [IQR] 2–16 weeks), and many patients had intermittent or persistent joint pain after the initial infection. Sixteen percent of the participants reported missing school or work as a result of their chikungunya virus infection, with a median of 4 days (IQR 2–7 days) lost (Table 3). When patients were stratified by sex (Table 4), it was found that women were more likely to have chikungunya virus infection symptoms, including weakness, rash, nausea or vomiting, and elbow pain.

After 20 months, one-fourth of the participants (123 of 485) had persistent joint pain. Among these patients, most had only 1 swollen joint but had tenderness in 3 other joints. They had a mean ± SD global pain score of 47 ± 20 (Table 3). Participants with persistent joint pain were more likely to be female (Table 1) and to have had more severe initial symptoms (Table 2). These patients reported greater joint involvement, including the number of joints involved and the duration of initial joint symptoms. They were also more likely to report having

Table 1. Baseline demographic characteristics of the patients with serologically confirmed chikungunya virus classified according to joint pain status at a median follow-up of 20 months*

	All serologically confirmed cases (n = 485)	Persistent joint pain (n =123)	No persistent joint pain (n = 362)
Age at baseline, mean ± SD years	49.1 ± 16.1	49.1 ± 17.1	49.2 ± 15.8
Female	388 (80)	109 (89)	279 (77)†
Ethnicity‡			
Mestizo	451 (94)	115 (96)	336 (93)
African Colombian	4 (1)	0 (0)	4 (1)
White Colombian	26 (5)	5 (4)	21 (6)
Mean education level			
High school or less	377 (78)	96 (78)	281 (78)
Some college	98 (20)	23 (19)	75 (21)
College graduate	10 (2)	4 (3)	6 (2)
Health insurance‡	461 (97)	117 (98)	344 (97)
Prior comorbidity			
Hypertension	57 (12)	16 (13)	41 (11)
Diabetes	34 (7)	9 (7)	25 (7)
Any type of arthritis	17 (4)	7 (6)	10 (3)
Lung disease	19 (4)	5 (4)	14 (4)
Depression	21 (4)	6 (5)	15 (4)
Chronic foot pain	14 (3)	5 (4)	9 (2)
Gout	12 (2)	5 (4)	7 (2)
Osteoarthritis	13 (3)	4 (3)	9 (2)
Ischemic heart disease	13 (3)	4 (3)	9 (2)
Kidney disease	12 (2)	3 (2)	9 (2)

* Except where indicated otherwise, values are the number (%).
† $P = 0.004$ versus persistent joint pain.
‡ Data were not available for all patients.

Table 2. Initial symptoms and treatment of patients with serologically confirmed chikungunya virus classified according to joint pain status at a median follow-up of 20 months*

	All serologically confirmed cases (n = 485)	Persistent joint pain (n = 123)	No persistent joint pain (n = 362)	*P*
Initial symptoms				
Muscle pain	471 (98)	119 (98)	352 (98)	0.99
Weakness	427 (88)	114 (93)	313 (86)	0.09
Joint pain and/or inflammation	476 (98)	120 (98)	356 (98)	0.70
Rash	409 (85)	104 (85)	305 (84)	0.99
Fever	376 (79)	99 (83)	277 (78)	0.28
Headache	354 (73)	101 (82)	253 (70)	0.009
Lymphadenopathy	343 (71)	90 (73)	253 (70)	0.52
Cool extremities	257 (53)	68 (55)	189 (52)	0.57
Nausea or vomiting	178 (37)	54 (44)	125 (35)	0.16
Bruising	76 (16)	22 (18)	54 (15)	0.42
Hemorrhage	11 (2)	1 (1)	10 (3)	0.21
Nose bleed	5 (1)	1 (1)	4 (1)	0.99
Oral bleeding	6 (1)	2 (2)	4 (1)	0.65
Initial rheumatic symptoms during acute chikungunya infection				
Wrist pain	426 (90)	110 (92)	316 (89)	0.37
Ankle pain	412 (87)	113 (94)	299 (84)	0.0047
Finger pain	403 (84)	103 (86)	300 (84)	0.64
Elbow pain	395 (83)	111 (93)	284 (80)	0.0013†
Toe pain	387 (81)	109 (92)	278 (78)	0.001†
Knee pain	383 (80)	113 (94)	270 (76)	<0.0001†
Hip pain	342 (72)	106 (89)	236 (66)	<0.0001†
Initial chikungunya virus symptom duration, days				<0.0001†‡
Mean ± SD	12.9 ± 30.6	14.2 ± 22.8	12.3 ± 33.3	–
Median (IQR)	4 (3–8)	5 (4–10)	4 (3–7)	–
Range	1–365	1–90	1–365	–
Duration of initial joint pain, weeks				<0.0001†‡
Mean ± SD	18.4 ± 32.4	45.3 ± 39.5	10.5 ± 25.1	–
Median (IQR)	4 (2–16)	40 (6–92)	3 (2–8)	–
Range	0–365	0.6–104	0–365	–
Treatment				
Acetaminophen	478 (100)	122 (100)	356 (100)	–
Ibuprofen	36 (8)	11 (9)	25 (7)	0.47
Prednisone	5 (1)	2 (2)	3 (1)	0.61
Medicinal plants	5 (1)	1 (1)	4 (1)	0.99
Aspirin	0 (0)	0 (0)	0 (0)	–
Methotrexate	0 (0)	0 (0)	0 (0)	–

* Except where indicated otherwise, value are the number (%). Data were not available for all patients. IQR = interquartile range.
† Significant ($P < 0.002$) after Bonferroni adjustment.
‡ By Kruskal-Wallis nonparametric test.

missed work or school and to report that their normal activities were affected by the infection (Table 3).

In a model to examine factors that had independent associations with persistent joint pain, the area under the receiver operating characteristic curve was 0.84, indicating good discrimination. Significant factors included being a college graduate, headache, knee pain, missed work, normal activities affected, ≥4 days of initial symptoms, and ≥4 weeks of initial joint pain (Table 5).

DISCUSSION

We found the frequency of chronic joint pain after infection with chikungunya virus in a large Latin American cohort to be 25% a median of 20 months after infection. Significant predictors of persistent joint pain included being a college graduate, headache, knee pain, missed work, normal activities affected, ≥4 days of initial symptoms, and ≥4 weeks of initial joint pain.

This is the first large-scale observational study of chikungunya virus–associated arthritis in the Americas. The finding of chronic joint pain ~2 years after initial infection in one-fourth of the patients infected with chikungunya virus has important implications for the prediction of the magnitude of disability and health system costs after the Latin American epidemic. Prior predictions had overestimated the expected frequency of chikungunya virus–related joint pain in Latin America, indicating that 48% of chikungunya virus–infected patients were predicted to have chronic chikungunya arthritis 20 months

Table 3. Symptoms and disability in patients with serologically confirmed chikungunya virus classified according to joint pain status at a median follow-up of 20 months

	All serologically confirmed cases (n = 485)	Persistent joint pain (n = 123)	No persistent joint pain (n = 362)	*P*
Time since onset, months				0.017
Mean ± SD	20.0 ± 1.3	20.2 ± 0. 8	19.9 ± 1.4	–
Median (IQR)*	19.7 (19.4–20.8)	19.8 (19.4–20.9)	19.6 (19.4–20.6)	–
Range	8.9–31.4	19.2–22.9	8.9–31.4	–
No. (%) who missed work or school during initial infection	79 (16)	49 (40)	30 (8)	<0.0001†
Days of missed work/school				0.83‡
Mean ± SD	5.5 ± 5.3	6.0 ± 6.3	4.7 ± 3.0	–
Median (IQR)	4 (2–7)	4 (2–7)	3.5 (2–7)	–
Range	0–30	2–30	0–14	–
No. (%) with symptoms impacting capacity to continue normal activity	46 (9)	33 (27)	13 (4)	<0.0001†
Swollen joint count, mean ± SD	0.2 ± 0.6	0.5 ± 1.0	0.06 ± 0.3	<0.0001†‡
Tender joint count, mean ± SD	0.9 ± 1.8	2.9 ± 2.3	0.2 ± 0.8	<0.0001†‡
Global pain score in the last week, mean ± SD (range 0–100)	45.8 ± 19.6	46.7 ± 20.2	41.5 ± 16.3	0.39

* IQR = interquartile range.
† Significant ($P < 0.0017$) after Bonferroni adjustment.
‡ By Kruskal-Wallis nonparametric test.

Table 4. Initial chikungunya virus symptoms and baseline comorbidities by sex*

	Women (n = 388)	Men (n = 95)	*P*
Initial symptoms			
Muscle pain	377 (97)	93 (98)	0.99
Weakness	353 (91)	73 (77)	<0.0001†
Joint pain and/or inflammation	383 (99)	92 (97)	0.19
Rash/itch	339 (87)	69 (73)	0.0004†
Fever	304 (80)	71 (76)	0.49
Headache	291 (75)	62 (65)	0.06
Lymphadenopathy	287 (74)	55 (58)	0.002
Cool extremities	216 (56)	40 (42)	0.018
Nausea or vomiting	157 (41)	21 (22)	0.0004†
Bruising	69 (18)	7 (7)	0.012
Hemorrhage	8 (2)	3 (3)	0.46
Nose bleed	3 (1)	2 (2)	0.25
Oral bleeding	4 (1)	2 (2)	0.34
Initial rheumatic symptoms			
Wrist pain	347 (91)	78 (85)	0.10
Ankle pain	331 (86)	80 (87)	0.89
Finger pain	325 (85)	77 (83)	0.62
Elbow pain	329 (86)	65 (71)	0.0005†
Toe pain	312 (82)	74 (80)	0.78
Knee pain	306 (80)	76 (82)	0.72
Hip pain	286 (75)	55 (59)	0.0022
Prior comorbidities			
Arthritis	9 (2)	8 (9)	0.009
Chronic foot pain	8 (2)	6 (6)	0.04
Gout	7 (2)	5 (5)	0.07
Osteoarthritis	10 (3)	3 (3)	0.73
Heart disease	10 (3)	3 (3)	0.73
Kidney disease	10 (3)	2 (2)	0.99
Lung disease	17 (4)	2 (2)	0.39
Diabetes	31 (8)	3 (3)	0.10
Hypertension	47 (12)	10 (11)	0.66
Depression	15 (4)	5 (5)	0.58

* Values are the number (%). Data on sex were missing for 2 patients; data on symptoms were not available for all patients.
† Significant ($P < 0.00167$) after Bonferroni adjustment.

after acute infection (15). Our findings are consistent with findings reported from other outbreaks of the Asian strain of the virus at 18 months, showing that approximately one-third of the patients had persistent joint pain (5,18), and lower than the findings of a 15–18-month follow-up of patients affected by the East Central African strain on Réunion Island from 2005–2006, in which persistent joint pain was reported in 43–75% of chikungunya virus–infected patients (9,12,13).

Significant predictors of persistent joint pain included factors that may indicate a more severe or prolonged initial infection, such as missed work, normal activities affected, ≥4 days of initial symptoms, and ≥4 weeks of initial joint pain. Determination of the risk factors for persistent arthritis during initial infection enables early

Table 5. Multivariable logistic regression model of persistent joint pain in patients with chikungunya virus*

Baseline factor	Adjusted OR (95% Wald confidence limit)	*P*
College graduate	5.53 (1.13–27.17)	0.0353
Headache	2.17 (1.16–4.07)	0.0157
Knee pain	4.69 (1.91–11.51)	0.0007
Missed work	5.23 (2.87–9.52)	<0.0001
Normal activities affected	8.80 (3.89–19.89)	<0.0001
≥4 days of initial symptoms	2.69 (1.57–4.60)	0.0003
≥4 weeks of initial joint pain	2.39 (1.40–4.08)	0.0014

* C = 0.84. Backward selection was used, dropping predictors that had a *P* value of less than 0.20. SAS (version 9.3) was used for data analysis, with *P* values less than 0.05 considered significant, except for values where Bonferroni correction was applied. (*P* values less than 0.002 were considered significant in Table 2 and *P* values less than 0.0017 were considered significant in Table 3.) OR = odds ratio.

identification of patients who may require follow-up care. This finding is consistent with the findings of Hoarau et al (22) and Sissoko et al (9) on Réunion Island (East Central African chikungunya virus strain outbreak) that showed that increased initial chikungunya viral load (22) and severe initial joint pain (9) were predictors of persistent arthritis. However, in contrast to the findings of Hoarau et al and Sissoko et al, we did not find that older age was associated with an increased frequency of persistent chikungunya virus–related arthritis. This difference may be due to differences in the chikungunya virus strains involved in the epidemics on Réunion Island as opposed to the Americas and the significantly smaller cohort sizes, older mean age, and higher prevalence of underlying osteoarthritis comorbidity in the Réunion Island studies (26% in the study by Sissoko et al [9] versus 3% in our cohort).

A limitation of this study is the lack of a control group. It is possible that, over the course of 20 months, a few of the study participants might have developed joint symptoms and pain due to another etiology that they attributed to chikungunya virus infection. Furthermore, patients were not tested for other arboviral infections that may contribute to joint pain. While dengue and Zika are flaviviruses known to cause acute joint pain, Mayaro virus is an alphavirus, like chikungunya virus, known to cause similar chronic joint pain with known cross-reactivity between anti-Mayaro and anti-chikungunya virus antibodies (23). Both patients with chikungunya virus and those with Mayaro virus viral arthritis almost universally report morning stiffness, which is a symptom of true inflammatory arthritis, even in the chronic phase of the disease. In comparison, dengue and Zika infections most commonly cause arthralgias rather than inflammatory arthritis, which is an important distinction, since the alphaviruses preferentially invade and replicate within the synovium, whereas flaviviruses do not. During the chikungunya virus epidemic there was no known Mayaro virus circulation in the Atlántico Department. However, Mayaro virus is known to sporadically affect the Colombian Amazon region (24), so it is possible that a few of these cases could have been Mayaro virus infections. Other limitations include the fact that self-reported joint pain was the primary outcome without serologic markers of inflammation, and the lack of formal assessment of validated quality of life measures.

This study represents the largest Latin American cohort of chikungunya patients to be followed up a median of 20 months after infection. The study sample was Colombian and consisted predominantly of Mestizo women. Nevertheless, our findings have important implications for future planning as this outbreak spreads.

ACKNOWLEDGMENTS

This publication was made possible by the support of multiple institutions, including the Allied Research Society, Universidad El Bosque, The George Washington University, and the Medical Faculty Associates (Washington, DC). Specifically, the authors would like to thank Martha Utrera, Ariel Gonzalez, April Barbour, Alan Wasserman, Donna Embersit, and Andreas Suhrbier for their support in this project.

AUTHOR CONTRIBUTIONS

All authors were involved in drafting the article or revising it critically for important intellectual content, and all authors approved the final version to be published. Dr. Chang had full access to all of the data in the study and takes responsibility for the integrity of the data and the accuracy of the data analysis.

Study conception and design. Chang, Encinales, Porras, N. Pacheco, Rico Mendoza, Bethony, Simon.

Acquisition of data. Chang, Encinales, Porras, N. Pacheco, S. Pacheco, Bravo, Navarno, Rico Mendoza, Kamalapathy.

Analysis and interpretation of data. Chang, Encinales, Reid, Martins, Amdur, Firestein, Bethony, Simon.

REFERENCES

1. Manimunda SP, Vijayachari P, Uppoor R, Sugunan AP, Singh SS, Rai SK, et al. Clinical progression of chikungunya fever during acute and chronic arthritic stages and the changes in joint morphology as revealed by imaging. Trans R Soc Trop Med Hyg 2010;104:392–9.
2. Powers AM. Risks to the Americas associated with the continued expansion of chikungunya virus. J Gen Virol 2015;96:1–5.
3. Centers for Disease Control and Prevention. Chikungunya virus: resources for healthcare providers. URL: https://www.cdc.gov/chikungunya/hc/resources.html.
4. Kularatne SA, Gihan MC, Weerasinghe SC, Gunasena S. Concurrent outbreaks of chikungunya and dengue fever in Kandy, Sri Lanka, 2006–07: a comparative analysis of clinical and laboratory features. Postgrad Med J 2009;85:342–6.
5. Rahim AA, Thekkekara RJ, Bina T, Paul BJ. Disability with persistent pain following an epidemic of chikungunya in rural South India. J Rheumatol 2016;43:440–4.
6. Gauri L, Thaned A, Fatima Q, Yadav H, Singh A, Jaipal H, et al. Clinical spectrum of chikungunya in Bikaner (North Western India) in 2006 and follow up of patients for five years. J Assoc Physicians India 2016;64:22.
7. Suhrbier A, Jaffar-Bandjee M, Gasque P. Arthritogenic alphaviruses: an overview. Nat Rev Rheumatol 2012;8:420–9.
8. Brighton S, Prozesky O, de la Harpe A. Chikungunya virus infection: a retrospective study of 107 cases. S Afr Med J 1983;63:313–5.
9. Sissoko D, Malvy D, Ezzedine K, Renault P, Moscetti F, Ledrans M, et al. Post-epidemic Chikungunya disease on Reunion Island: course of rheumatic manifestations and associated factors over a 15-month period. PLoS Negl Trop Dis 2009;3:e389.
10. Ganu MA, Ganu A. Post-chikungunya chronic arthritis: our experience with DMARDs over two year follow up. J Assoc Physicians India 2011;59:83–6.
11. Chopra A, Anuradha V, Ghorpade R, Saluja M. Acute chikungunya and persistent musculoskeletal pain following the 2006 Indian epidemic: a 2-year prospective rural community study. Epidemiol Infect 2012;140:842–50.
12. Gérardin P, Fianu A, Malvy D, Mussard C, Boussaïd K, Rollot O, et al. Perceived morbidity and community burden after a chikungunya outbreak: the TELECHIK survey, a population-based cohort study. BMC Med 2011;9:5.
13. Borgherini G, Poubeau P, Staikowsky F, Lory M, le Moullec N, Becquart JP, et al. Outbreak of chikungunya on Reunion Island:

early clinical and laboratory features in 157 adult patients. Clin Infect Dis 2007;44:1401–7.
14. Borgherini G, Poubeau P, Jossaume A, Gouix A, Cotte L, Michault A, et al. Persistent arthralgia associated with chikungunya virus: a study of 88 adult patients on Reunion Island. Clin Infect Dis 2008;47:469–75.
15. Rodriguez-Morales A, Cardona-Ospina J, Villamil-Gómez W, Paniz-Mondolfi A. How many patients with post-chikungunya chronic inflammatory rheumatism can we expect in the new endemic areas of Latin America? Rheumatol Int 2015;35:2091–4.
16. World Health Organization. Chikungunya. 2017. URL: http://www.who.int/mediacentre/factsheets/fs327/en/.
17. Rodriguez-Morales AJ, Villamil-Gomez W, Merlano-Espinosa M, Simone-Kleber L. Post-chikungunya chronic arthralgia: a first retrospective follow-up study of 39 cases in Colombia. Clin Rheumatol 2016;35:831–2.
18. Lanciotti RS, Lambert AJ. Phylogenetic analysis of chikungunya virus strains circulating in the Western Hemisphere. Am J Trop Med Hyg 2016;94:800–3.
19. Prevoo ML, van't Hof MA, Kuper H, van Leeuwen MA, van de Putte LB, van Riel PL. Modified disease activity scores that include twenty-eight–joint counts: development and validation in a prospective longitudinal study of patients with rheumatoid arthritis. Arthritis Rheum 1995;38:44–8.
20. The Editors of Encyclopedia Britannica. Atlántico Department, Colombia. Encyclopedia Britannica. 2017. URL: https://www.britannica.com/place/Atlantico.
21. Ospina ML, Martínez Duran ME, Pacheco García OE, Quijada Bonilla H. Protocolo de Vigilancia en Salud Pública: Chikunguña. Instituto Nacional de Salud Vigilancia y Analysis del Riesgo en Salud Pública 2016;2:1–33.
22. Hoarau JJ, Jaffar Bandjee MC, Krejbich Trotot P, Das T, Li-Pat-Yuen G, Dassa B, et al. Persistent chronic inflammation and infection by chikungunya arthritogenic alphavirus in spite of a robust host immune response. J Immunol 2010;184:5914–27.
23. Fox JM, Long F, Edeling MA, Lin H, van Duijl-Richter MK, Fong RH, et al. Broadly neutralizing alphavirus antibodies bind an epitope on E2 and inhibit entry and egress. Cell 2015;163:1095–7.
24. Rodriguez-Morales AJ, Paniz-Mondolfi AE, Villamil-Gomez WE, Navarro JC. Mayaro, Oropouche and Venezuelan equine encephalitis viruses: following in the footsteps of Zika? Travel Med Infect Dis 2017;15:72–3.

ARTHRITIS & RHEUMATOLOGY
Vol. 70, No. 4, April 2018, pp 585–593
DOI 10.1002/art.40383

Chikungunya Arthritis Mechanisms in the Americas

A Cross-Sectional Analysis of Chikungunya Arthritis Patients Twenty-Two Months After Infection Demonstrating No Detectable Viral Persistence in Synovial Fluid

Aileen Y. Chang,[1] Karen A. O. Martins,[2] Liliana Encinales,[3] St. Patrick Reid,[4] Marlon Acuña,[3] Carlos Encinales,[3] Christian B. Matranga,[5] Nelly Pacheco,[3] Carlos Cure,[6] Bhavarth Shukla,[7] Teofilo Ruiz Arteta,[3] Richard Amdur,[1] Lisa H. Cazares,[2] Melissa Gregory,[2] Michael D. Ward,[2] Alexandra Porras,[8] Alejandro Rico Mendoza,[8] Lian Dong,[2] Tara Kenny,[2] Ernie Brueggemann,[2] Lydia G. Downey,[2] Priyanka Kamalapathy,[1] Paola Lichtenberger,[7] Orlando Falls,[3] Gary L. Simon,[1] Jeffrey M. Bethony,[1] and Gary S. Firestein[9]

Objective. **To determine if chikungunya virus persists in synovial fluid after infection, potentially acting as a causative mechanism of persistent arthritis.**

Methods. **We conducted a cross-sectional study of 38 Colombian participants with clinical chikungunya virus infection during the 2014–2015 epidemic who reported chronic arthritis and 10 location-matched controls without chikungunya virus or arthritis. Prior chikungunya virus infection status was serologically confirmed, and the presence of synovial fluid chikungunya virus, viral RNA, and viral proteins was determined by viral culture, quantitative reverse transcription–polymerase chain reaction (qRT-PCR), and mass spectrometry, respectively. Biomarkers were assessed by multiplex analysis.**

Results. **Patients with serologically confirmed chikungunya arthritis (33 of 38 [87%]) were predominantly female (82%) and African Colombian (55%) or white Colombian (33%), with moderate disease activity (mean ± SD Disease Activity Score in 28 joints 4.52 ± 0.77) a median of 22 months after infection (interquartile range 21–23 months). Initial symptoms of chikungunya virus infection included joint pain (97%), swelling (97%), stiffness (91%), and fever (91%). The most commonly affected joints were the knees (87%), elbows (76%), wrists (75%), ankles (56%), fingers (56%), and toes (56%). Synovial fluid samples from all patients with chikungunya arthritis were negative for chikungunya virus on qRT-PCR, showed no viral proteins on mass spectrometry, and cultures were negative. Case and control plasma cytokine and chemokine concentrations did not differ significantly.**

Conclusion. **This is one of the largest observational studies involving analysis of the synovial fluid of chikungunya arthritis patients. Synovial fluid analysis revealed no detectable chikungunya virus. This finding suggests that chikungunya virus may cause arthritis through induction of potential host autoimmunity, suggesting a role for immunomodulating agents in the treatment of chikungunya**

ClinicalTrials.gov identifier: NCT02463968.

The views expressed herein are solely the responsibility of the authors and do not necessarily represent the official views of the Rheumatology Research Foundation, the NIH, or the US Army.

Supported by a Pilot award from the Rheumatology Research Foundation and the NIH (National Center for Advancing Translational Sciences grants UL1-TR-001876 and KL2-TR-001877).

[1]Aileen Y. Chang, MD, MSPH, Richard Amdur, PhD, Priyanka Kamalapathy, MD, Gary L. Simon, MD, PhD, Jeffrey M. Bethony, PhD: The George Washington University, Washington, DC; [2]Karen A. O. Martins, PhD, Lisa H. Cazares, PhD, Melissa Gregory, PhD, Michael D. Ward, PhD, Lian Dong, PhD, Tara Kenny, PhD, Ernie Brueggemann, PhD, Lydia G. Downey, PhD: US Army Medical Research Institute of Infectious Diseases, Fort Detrick, Maryland; [3]Liliana Encinales, MD, Marlon Acuña, MD, Carlos Encinales, MD, Nelly Pacheco, Teofilo Ruiz Arteta, MD, Orlando Falls, MD: Allied Research Society, Barranquilla, Colombia; [4]St. Patrick Reid, PhD: University of Nebraska Medical Center, Omaha; [5]Christian B. Matranga, PhD: Broad Institute, Boston, Massachusetts; [6]Carlos Cure, MD: Biomelab, Barranquilla, Colombia; [7]Bhavarth Shukla, MD, MPH, Paola Lichtenberger, MD: University of Miami, Miami, Florida; [8]Alexandra Porras, PhD, Alejandro Rico Mendoza, PhD: Universidad El Bosque, Bogotá, Colombia; [9]Gary S. Firestein, MD: University of California at San Diego.

Drs. Chang and Martins contributed equally to this work.

Address correspondence to Aileen Y. Chang, MD, MSPH, The George Washington University School of Medicine and Health Sciences, 2150 Pennsylvania Avenue, Suite 5-416, Washington, DC 20037. E-mail: chang@email.gwu.edu.

Submitted for publication July 14, 2017; accepted in revised form November 14, 2017.

arthritis, or that low-level viral persistence exists in synovial tissue only and is undetectable in synovial fluid.

Patients infected with chikungunya virus present with fever, headache, muscle pain, rash, and joint pain. Following resolution of acute chikungunya virus infection, chronic arthritis may develop, often lasting months to years (1,2). Chikungunya virus had previously been restricted to Africa, Asia, Europe, and the Indian and Pacific Ocean regions (3), but, in 2013, chikungunya virus was first described in the Americas and has now infected >1.5 million people in this region (1). Outbreaks of the Asian strain of chikungunya virus leave approximately one-third of patients with persistent joint pain 18 months after infection (4,5).

After transmission by an *Aedes aegypti* or *Aedes albopictus* mosquito bite, chikungunya virus undergoes local replication and then dissemination to lymphoid tissue (6). While viremia lasts only 5–12 days (7,8), a study in non-human primates demonstrated that chikungunya virus persists in the lymphoid organs, liver, joints, muscle, and macrophages for up to 3 months and that chikungunya virus RNA remains in the spleen, liver, and muscle for extended periods (9). In another study, chikungunya virus RNA was detected in the synovial tissue of a patient 18 months after infection (10). Similar findings of inflammatory macrophage infiltrates (11,12) and synovial viral RNA persistence (13) have been seen in polyarthritis caused by another alphavirus, Ross River virus. These findings have led to the hypothesis that chikungunya virus might persist in the joint in cases of chronic arthritis.

Chikungunya virus is known to evade neutralizing antibodies by residing within apoptotic blebs (14). While in the blebs, chikungunya virus can infect neighboring cells in vitro (15). Furthermore, in vitro chikungunya virus inhibits RNA kinase needed to make antiviral messenger RNA transcripts, thereby freezing host antiviral protein synthesis (16). Interleukin-6 (IL-6), monocyte chemotactic protein 1 (MCP-1), and interferon-α (IFNα) have been detected during the acute phase of infection, and elevated levels of analytes, including IL-6, MCP-1, IFNγ-inducible 10-kd protein (IP-10), IL-1 receptor α, eotaxin, IL-17, and granulocyte–macrophage colony-stimulating factor (GM-CSF), have further been associated with disease severity, chronic arthralgia, and/or viral load (17–19).

There is currently no standard treatment for chikungunya virus–associated arthritis (20). However, several small studies have demonstrated clinical benefit from treatment with antivirals such as ribavirin (21) and immunosuppressants such as methotrexate (22–24), hydroxychloroquine (22), etanercept (23), adalimumab (23), and sulfasalazine (24). Further characterization of chikungunya virus disease pathophysiology is needed to provide a rationale for large-scale randomized clinical trials to evaluate the effectiveness of these potential therapies. If persistent chikungunya virus infection is responsible for ongoing arthritis, immunocompromising disease-modifying agents may be improper and potentially dangerous treatments. Alternatively, if chikungunya virus does not persist in the joint, then evaluation of immunomodulating agents could be useful. The objective of the Chikungunya Arthritis Mechanisms in the Americas (CAMA) study was to determine if there was evidence of chikungunya virus in the synovial fluid of patients with chikungunya arthritis in order to understand disease pathogenesis and, perhaps, guide chikungunya arthritis therapy.

PATIENTS AND METHODS

Setting. Patients were recruited from the Atlántico and Bolívar Departments of Colombia. In September 2014, the first locally acquired chikungunya virus case was reported in the Bolívar Department. During the height of the epidemic, from 2014 to 2015, many suspected chikungunya virus cases were reported in the Departments of Atlántico (2,480 cases) and Bolívar (5,997 cases).

Inclusion criteria. Participants were Spanish-speaking adults ≥18 years old. Chronic chikungunya arthritis was defined as clinically or laboratory-confirmed diagnosis of chikungunya virus infection, with persistent arthritis or arthralgias. Arthritis and arthralgias included knee pain and swelling for at least 3 months after diagnosis of chikungunya virus infection as well as joint pain at the time of follow-up. As per the Colombian Institute of Health, a clinically confirmed case of chikungunya virus infection is defined as a fever of >38°C, severe joint pain or arthritis, and the acute onset of erythema multiforme with symptoms not explained by other medical conditions. In addition, these individuals must reside in or have visited a municipality where evidence of chikungunya virus transmission is present or have traveled within 30 km of confirmed viral circulation. No patients were excluded for prior arthritis; prior arthritis status was included in the analysis. All suspected chikungunya virus cases were laboratory confirmed for the purposes of this study. Healthy controls were defined as participants from the same region who reported no history of chikungunya virus infection and did not present with arthritis.

Exclusion criteria. Subjects were excluded if they reported a known bleeding disorder or were receiving anticoagulant medications. The study also excluded children, adults unable to give consent, prisoners, and pregnant women.

Recruitment. In 2014–2015, as part of a chikungunya virus surveillance study across the Atlántico and Bolívar Departments, 907 patients with clinically confirmed (n = 424) or laboratory-confirmed (n = 483) chikungunya virus infection were referred by their primary care providers from clinics located in Barranquilla, Atlántico; Sabanalarga, Atlántico; and San Juan Nepomuceno, Bolívar. Of these patients, 65 were randomly selected for eligibility screening, of whom 38 were eligible for study participation in the chronic arthritis group with current knee joint pain. Patients were not eligible if they did not have persistent

knee pain after chikungunya virus infection. Ten healthy controls were also recruited from among volunteers at the clinic in Barranquilla, Atlántico. Synovial fluid was not collected from healthy controls since it was not clinically indicated.

Ethics statement. The study protocol was approved by The George Washington University Institutional Review Board (IRB; protocol 041612), the Universidad El Bosque (UB 387-2015), and the US Army Medical Research Institute of Infectious Diseases Human Research Protections Office (FY15-32). Research on human subjects was conducted in compliance with Department of Defense, Federal, and State statutes and regulations relating to the protection of human subjects, and adheres to principles identified in the Belmont Report (1979). All data collection and research on human subjects for this publication were conducted under an IRB-approved protocol. All participants were adults and provided written informed consent during an in-person interview.

Primary outcome measure. We hypothesized that persistent active viral replication is responsible for chronic arthritis and joint pain. Therefore, the primary outcome measure of the present study protocol was the identification of the presence of chikungunya virus in synovial fluid. Attempts to find evidence of chikungunya virus in synovial fluid included viral culture, quantitative reverse transcription–polymerase chain reaction (qRT-PCR) for chikungunya virus RNA, and mass spectrometry analysis for viral proteins.

Secondary outcome measures. As part of this study, we evaluated clinical outcomes, such as the effect on daily living and arthritis severity as measured by the Disease Activity Score in 28 joints (DAS28) (25), a validated rheumatoid arthritis (RA) assessment tool that is a composite score of the number of tender joints, number of swollen joints, global disease activity during the most recent week measured on a scale of 0–100, and C-reactive protein (CRP) level. This clinical outcomes questionnaire was administered to all of the participants in a face-to-face interview. Laboratory studies in these patients included testing for plasma CRP level, serum IgM rheumatoid factor (IgM-RF) antibody, IgG-RF antibody, anti–cyclic citrullinated peptide (anti-CCP) antibody, and selected cytokines and chemokines.

Sample collection. After obtaining of informed consent and administration of a questionnaire concerning the participant's demographic characteristics and symptom history, blood was obtained by venipuncture. An orthopedic surgeon performed an arthrocentesis for primary evaluation of the swollen knee joint with needle lavage, where 0–20 ml of saline was injected at the discretion of the clinician. Samples collected in this manner are referred to as "synovial fluid." Blood samples were collected into 8-ml CPT cell preparation tubes with sodium citrate (catalog no. 362761; Becton Dickinson), and synovial fluid was transferred to cell preparation tubes in an effort to isolate cells from the fluid.

Sample preparation. The blood samples were centrifuged at room temperature (18–25°C) in a horizontal rotor for 20 minutes at 1,500 relative centrifugal force. Plasma was removed from the blood collection tubes and frozen at −80°C until analyzed. Synovial fluid samples were similarly centrifuged and frozen for subsequent analysis. There was no visible cell pellet after centrifugation of the synovial fluid; therefore, supernatant and any present cells were stored as one specimen at −80°C.

Data management. All patients were assigned a unique patient identification number, which was used in the database and for labeling of patient samples. All patient data were free of personal identifiers and were stored in the REDCap database at The George Washington University.

Anti-chikungunya virus IgG and IgM. IgG and IgM levels in plasma were assayed using InBios CHIKjj Detect enzyme-linked immunosorbent assays (ELISAs) (CHKG-R and CHKM-R). These assays provide a qualitative evaluation of the presence or absence of anti-chikungunya virus IgG and IgM and include controls to calculate an immune status ratio. Plasma was diluted 1:100 in kit dilution buffer and tested in duplicate, according to the manufacturer's instructions.

RNA isolation and qRT-PCR. RNA isolation was attempted from 140 μl of plasma or synovial fluid using a Qiagen QIAamp Viral RNA Mini kit (catalog no. 52904). Control samples contained spiked RNA, which was isolated in parallel to ensure recovery and detection by qRT-PCR. Samples were run on an ABI 7500 HT system under the conditions listed below.

Both plasma and synovial fluid samples were evaluated using an RNA UltraSense One-Step Quantitative RT-PCR System. A standard curve was run in parallel with the samples, with duplicate evaluation of samples ranging from 1×10^7 to 1×10^2 copies/ml. The assay limit of detection is ~80 copies/ml. The primer and probe sequences were as follows: 5′-GGGCTATTCTCTAAACCGTTGGT-3′ (forward), 5′-CTCCCGGCCTATTATCCCAAT-3′ (reverse), and 5′-FAM-TCTGTGTATTACGCGGATAA-3′ MGB NFQ (probe). These primer and probe sequences (located in the peptidase C9 domain of the nonstructural polyprotein) were designed against chikungunya virus of Asian lineage, since the strains currently circulating in South America are of the Asian lineage. The cycling program was as follows: 50°C for 15 minutes, 95°C for 2 minutes, and 40 cycles of 95°C for 15 seconds and 60°C for 30 seconds.

To confirm the results of the first assay, a second qRT-PCR assay was used to retest the synovial fluid samples with different primers that were specifically designed against isolates emerging from Colombia (GenBank accession nos. KX496989.1 and KT192707.1) and also target sequences in the peptidase C9 region of the nonstructural polyprotein. Samples were tested using a Power SYBR Green RNA-to-CT 1-Step Kit (catalog no. 4389986; ABI). The assay limit of detection is ~100 copies/ml. The primer sequences were 5′-GGCAGTGGTCCCAGATAATTCAAG-3′ (forward) and 5′-GCTGTCTAGATCCACCCCATACATG-3′ (reverse). The cycling program was as follows: 48°C for 30 minutes, 95°C for 10 minutes, and 40 cycles of 95°C for 15 seconds and 60°C for 1 minute.

Synovial fluid culture. Vero cells were cultured in 12-well plates to 90% confluency. The culture media consisted of RPMI 1640, 10% fetal bovine serum, 1% penicillin/streptomycin, and 1% HEPES. Media were removed, and 500 μl of synovial fluid was added to each well and incubated for 1 hour. Where > 500 μl of synovial fluid was available, multiple cultures were established. As a positive control, chikungunya virus (strain 15661) was added to 2 wells, at ~10 plaque-forming units (PFU)/well and 1 PFU/well, with the aim of confirming detection of low levels of viremia in the samples. After 1 hour, 2.5 ml of complete media was added to each well, and the cells were incubated for 4 days (passage 1). On the fourth day, the supernatant was transferred to fresh Vero cells (90% confluency) in a 6-well plate (passage 2). An additional 3 ml of media was added, and the cells were cultured an additional 3 days. On the third day, a 140-μl aliquot of supernatant was collected for analysis. Then 3 ml of the supernatant was transferred again to fresh Vero cells (90% confluency) in a 6-well plate (passage 3). An additional 3 ml of media was

added, and the cells were cultured an additional 3 days. On the final day, a 140-μl aliquot of supernatant was collected for analysis. Remaining supernatant was then removed, and the cells were lysed in Buffer AVL (Qiagen). Buffer AVL was also added to the supernatant samples according to the manufacturer's instructions. The samples were heated at 56°C for 1 hour and removed from the biosafety level 3 laboratory, and the presence of viral nucleic acid was measured using PCR as described above.

Biomarker analysis. Levels of IgG-RF and IgM-RF were measured using an Inova Diagnostics Quanta Lite kit according to the manufacturer's instructions, using plasma samples instead of serum samples. Anti-CCP antibody levels were measured using an Inova Diagnostics Quanta Lite CCP3.1 IgG/IgA ELISA (catalog no. 704550) according to the manufacturer's instructions. Plasma samples were diluted 1:100 and quantified based on the assay standard curve. Multiplex assessment of a panel of cytokines and chemokines was conducted using a custom Meso Scale Discovery assay kit. Analytes included IFNα2a, CRP, IFNγ, IL-1β, IL-2, IL-4, IL-6, IL-8, IL-10, IL-12p70, GM-CSF, IL-1α, IL-12/23p40, IL-15, IL-17A, eotaxin, macrophage inflammatory protein 1β (MIP-1β), IP-10, MIP-1α, and MCP-1. Samples were diluted according to the manufacturer's instructions for each analyte.

Mass spectrometry analysis. *Sample preparation.* Twenty-five microliters of each synovial fluid sample was added to 200 μl of Solution UT8 (8*M* urea) and processed by filter-assisted sample preparation (FASP) per the manufacturer's protocol. Briefly, proteins are bound to the FASP filter (catalog no. MRCF0R030; Millipore) in UT8 and alkylated in 55 m*M* iodoacetamide followed by digestion with 40 ng/μl trypsin/Lys-C (Promega) overnight at 37°C. Peptides were eluted in 50 m*M* NaCl and subsequently desalted using C18 spin columns (catalog no. 89870; Pierce) per the manufacturer's instructions. Eluted peptides were dried to completion. Digests were stored at −20°C until analyzed by liquid chromatography mass spectrometry/mass spectrometry (LC-MS/MS).

LC-MS/MS analysis and protein search. Sample digests were resuspended in 20 μl of 0.1% formic acid and mixed briefly. Using a Dionex 3000 RSLCnano system (Thermo Scientific), 2.5 μl of each digest was injected onto a precolumn (a PepMap100 C18 column with a particle size of 5 μm, length of 5 mm, and internal diameter of 0.3 mm) housed in a 10-port Nano switching valve using a flow rate of 10 μl/minute. The loading solvent was 0.1% formic acid in high-performance liquid chromatography–grade water. The precolumn eluent was directed to waste. After 5 minutes, the switching valve changed to backflush the trapped peptides from the precolumn onto an EASY-Spray analytical column (15 cm × 75 μm) packed with PepMap C18 (with a particle size of 3 μm and a pore size of 100Å; Thermo Scientific). A 2–42% B gradient elution in 95 minutes was formed using pump A (0.1% formic acid) and pump B (85% acetonitrile in 0.1% formic acid) at a flow rate of 300 nl/minute. The column eluent was connected to an EASY-Spray nanospray source (Thermo Scientific) with an electrospray ionization voltage of 2.2 kV. An Orbitrap Elite mass spectrometer (Thermo Scientific) with an ion transfer tube temperature of 300°C and an S-lens setting of 50% was used to focus the peptides. Low-resolution rapid collision-induced dissociation (CID) MS/MS spectra were acquired with an automatic gain control of 1×10^4 ions and a maximum injection time of 50 msec. The isolation width for ms/ms CID fragmentation was set to 2 daltons. The normalized collision energy was 35% with a q value of 0.250. The dynamic exclusion duration was 30 seconds.

Searches were performed with Proteome Discoverer software version 2.1 (Thermo Scientific) using a human and chikungunya virus subset of the Swiss-Prot_2016_10_05 database. Variable modifications used were methyl (DE), acetyl (K), deamidated (NQ), oxidation (M), and carbamyl (K). Cysteine carbamidomethylation was specified as a constant modification. The false discovery rate was set at 0.1%. Mass tolerances were 10 parts per million for the MS1 scan and 200 ppm for all MS/MS scans. Search results were filtered such that only high-confidence/unambiguous peptide spectral matches were used.

Table 1. Baseline characteristics of the CAMA study participants*

	Serologically confirmed chikungunya arthritis cases			
	No history of arthritis (n = 25)	History of arthritis (n = 8)	Controls (n = 10)	*P* for trend
Age, mean ± SD	56.0 ± 10.0	59.6 ± 12.2	31.7 ± 7.8	<0.0001
Body mass index, mean ± SD	30.0 ± 4.5	27.1 ± 5.8	24.7 ± 5.3	0.03
Women	20 (80.0)	7 (87.5)	7 (70.0)	0.99
African Colombian ethnicity	13 (52.0)	5 (62.5)	5 (50.0)	0.90
White Colombian ethnicity	8 (32.0)	3 (37.5)	4 (40.0)	–
Education level of high school or less	23 (92.0)	8 (100.0)	0 (0.0)	<0.0001
Presence of comorbidities	9 (36.0)	6 (75.0)	0 (0.0)	0.0025
>3 comorbidities	0 (0.0)	1 (12.5)	0 (0.0)	0.19
Comorbidities				
Rheumatoid arthritis	0 (0.0)	1 (12.5)	0 (0.0)	0.19
Osteoarthritis	0 (0.0)	3 (37.5)	0 (0.0)	0.0045
Ischemic heart disease	0 (0.0)	0 (0.0)	0 (0.0)	NA
Chronic kidney disease	0 (0.0)	0 (0.0)	0 (0.0)	NA
Chronic pulmonary disease	0 (0.0)	0 (0.0)	0 (0.0)	NA
Diabetes	1 (4.0)	1 (12.5)	0 (0.0)	0.39
Hypertension	7 (28.0)	4 (50.0)	0 (0.0)	0.05
Depression	1 (4.0)	0 (0.0)	0 (0.0)	0.99

* Except where indicated otherwise, values are the number (%). CAMA = Chikungunya Arthritis Mechanisms in the Americas; NA = not applicable.

Table 2. Chikungunya infection–related symptoms in serologically confirmed chikungunya arthritis cases at initial presentation*

	All cases (n = 33)	No history of arthritis (n = 25)	History of arthritis (n = 8)
Chikungunya virus–related symptoms			
Joint tenderness	32 (97)	25 (100)	7 (88)
Joint swelling	32 (97)	25 (100)	7 (88)
Joint stiffness	30 (91)	22 (88)	8 (100)
Fever	30 (91)	23 (92)	7 (88)
Rash	29 (88)	22 (88)	7 (88)
Commonly initially affected joints†			
Knees	27 (87)	19 (83)	8 (100)
Elbow	25 (76)	19 (76)	6 (75)
Wrist	24 (75)	18 (75)	6 (75)
Fingers	18 (56)	14 (58)	4 (50)
Ankles	18 (56)	13 (57)	5 (63)
Toes	18 (56)	15 (63)	3 (38)
Hips	8 (26)	6 (26)	2 (25)

* Values are the number (%).
† Data were not available for all cases.

Statistical analysis. For univariate tests across diagnostic groups, the chi-square test or Fisher's exact test was used to compare categorical variables, analysis of variance was used for normally distributed continuous variables, and the Kruskal-Wallis test was used for skewed continuous variables. SAS (version 9.3) was used for data analysis. *P* values less than 0.05 were considered significant.

Given the sample size, there was suboptimal statistical power for some comparisons of secondary outcomes. For example, when comparing confirmed chikungunya virus cases with and those without prior arthritis (n = 33) to controls without chikungunya virus or arthritis (n = 10) with regard to categorical variables, using a 2-tailed chi-square test with an alpha of 0.05, power was >0.80 only for an effect size where the proportions that were positive were on the order of 40% versus 1%. However, the study had more robust power for detecting differences in continuous variables. For example, power was >0.80 for detecting a difference of mean ± SD 39 ± 10 versus 30 ± 10 (Cohen's $d = 0.9$) between patients with chikungunya virus and controls using a 2-tailed *t*-test.

RESULTS

Baseline characteristics of the subjects. Prior chikungunya infection was serologically confirmed in 33 (87%) of the 38 cases by IgM ELISA (in 1 [3%] of 33) and IgG ELISA (in 33 [100%]). Patients with confirmed chikungunya arthritis were predominantly female (27 [82%] of 33) and African Colombian (18 [55%] of 33) or white Colombian (11 [33%] of 33), with an education level of high school or less (31 [94%] of 33). Compared to healthy controls, the patients with chikungunya arthritis tended to be older, have less education, and have at least 1 comorbidity (Table 1). Participants with chikungunya arthritis with a history of prior arthritis were comparable to those with no history of arthritis in terms of age, sex, ethnicity, and education level. One patient with confirmed chikungunya virus exposure self-reported preexisting RA but was found to be negative for RF and anti-CCP antibody.

Chikungunya infection–related symptoms. Chikungunya arthritis patients were assessed a median of 22 months (interquartile range 21–23 months) after chikungunya virus infection. Initial symptoms of chikungunya virus infection included joint pain (97%), joint swelling (97%), joint stiffness (91%), fever (91%), and rash (88%) (Table 2); these symptoms were reported at the time of initial infection. The joints most commonly affected initially were knees (87%), elbows (76%), wrists (75%), fingers (56%), ankles (56%), and toes (56%). At follow-up, most participants reported that their arthritis had an effect on their activities of daily living (82%) (Table 3). However, patients were not necessarily experiencing a disease flare at the time of sample collection. Thirty-eight percent of the participants reported missing school or work during their initial infection. At the time of sample collection, participants had a mean ± SD of 5.5 ± 5.4 tender joints and 3.0 ± 2.8 swollen joints. The mean ± SD patient-reported global disease activity measure (on a

Table 3. Chikungunya infection–related effects assessed in serologically confirmed chikungunya arthritis cases at follow-up a median of 22 months after infection*

	All cases (n = 33)	No history of arthritis (n = 25)	History of arthritis (n = 8)	*P*
Effect on activities of daily living, no. (%)	27 (82)	19 (76)	8 (100)	0.30
Missed work/school, no. (%)†	12 (38)	7 (29)	5 (63)	0.12
Tender joint count	5.5 ± 5.4	5.4 ± 5.5	6.0 ± 5.2	0.0002‡
Swollen joint count	3.0 ± 2.8	2.8 ± 2.4	3.9 ± 4.0	<0.0001‡
Patient's global assessment of disease activity	93.4 ± 14.3	91.3 ± 15.9	100.0 ± 0	0.14
DAS28-CRP	4.52 ± 0.77	4.44 ± 0.73	4.78 ± 0.87	0.29

* Except where indicated otherwise, values are the mean ± SD. DAS28-CRP = Disease Activity Score in 28 joints using the C-reactive protein level.
† Data were not available for all cases.
‡ Using nonparametric Kruskal-Wallis test.

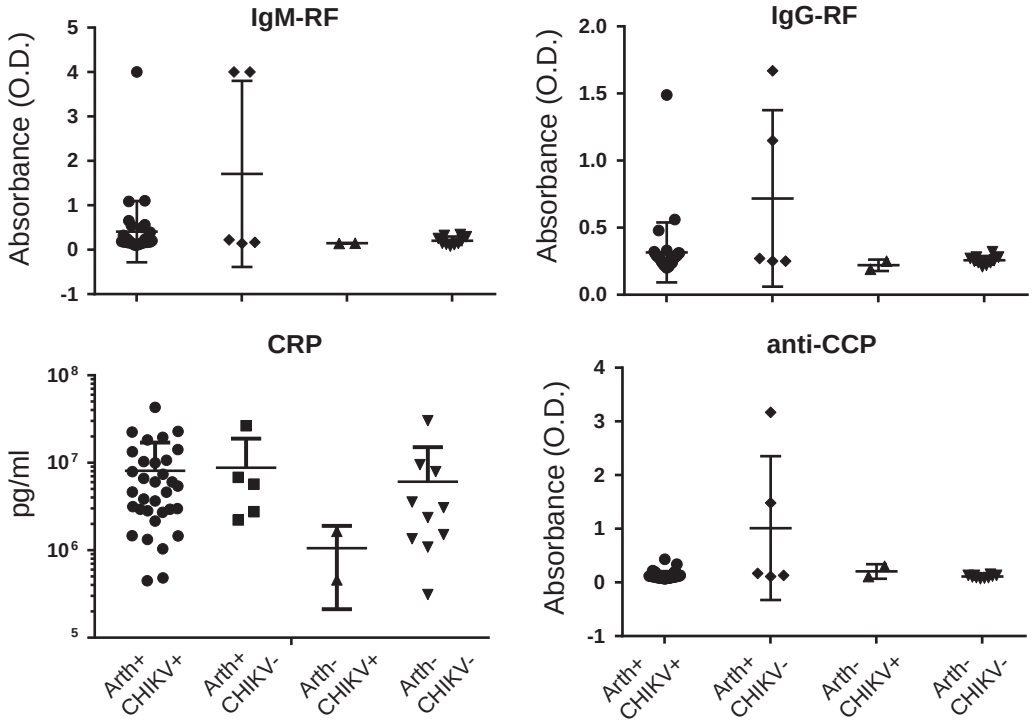

Figure 1. Levels of IgM rheumatoid factor (IgM-RF), IgG-RF, C-reactive protein (CRP), and anti–cyclic citrullinated peptide (anti-CCP) antibodies in patients with chikungunya virus (CHIKV) and arthraglia (Arth), patients with arthralgia without chikungunya virus, patients with chikungunya virus without arthralgia, and those without arthralgia or chikungunya virus. There was no significant increase in rheumatoid arthritis–associated markers or CRP level in patients with chikungunya virus–associated arthritis. Symbols represent individual subjects; horizontal lines and error bars show the mean ± SD.

scale of 0–100 with 100 being the most active) in the last week was 93 ± 14. The disease severity was moderate, as indicated by a mean ± SD DAS28 using the CRP level of 4.52 ± 0.77. There were no significant differences between chikungunya arthritis patients with a prior history of arthritis and those without a prior history of arthritis, with the exception of ~1 additional joint being tender and swollen in the participants with prior arthritis.

Virologic and serologic outcomes. All samples tested for persistent viral RNA (both plasma and synovial fluid) were negative for chikungunya virus on 2 separate qRT-PCR assays. To more rigorously evaluate if low-level viremia might be present in the samples, synovial fluid samples were added to cell cultures in an attempt to expand out any replication-competent virus. Cultures of synovial fluid from chikungunya arthritis patients also showed no viral growth after 3 passages and 10 days of culture; in contrast, controls with low quantities of virus (~1 PFU/well) yielded growth and allowed detection of the virus.

Plasma markers for RA were present in only a fraction of the participants with chikungunya virus–associated arthritis. IgM-RF antibody was present in 9% of the patients, and IgG-RF antibody was present in 12%. Anti-CCP antibody was not detected in any of the patients.

Table 4. Plasma cytokine and chemokine concentrations a median of 22 months after chikungunya infection*

Analyte	Chikungunya virus arthritis cases (n = 33)	Controls (n = 10)
Cytokine		
IL-1α	1.29 (0.58–3.82)	1.42 (0–4.93)
IL-1β	0.27 (0.17–0.69)	0.20 (0.10–0.28)
IL-2	1.70 (1.25–2.89)	2.06 (1.70–2.89)
IL-4	1.08 (0.76–2.80)	1.31 (0.61–2.51)
IL-6	1.69 (1.01–3.18)	1.32 (0.73–1.69)
IL-10	1.80 (1.29–2.56)	1.92 (1.29–2.08)
IL-12/p40	111 (92.0–137)	116 (87.4–161)
IL-12/p70	1.91 (1.37–6.20)	1.78 (1.05–6.79)
IL-15	2.55 (2.01–2.97)	2.64 (1.89–3.32)
IL-17α	7.81 (6.35–9.19)	7.2 (4.95–8.44)
IFNγ	7.44 (3.92–16.1)	6.7 (3.92–13.0)
GM-CSF	0.93 (0.60–1.30)	0.80 (0.32–1.15)
Chemokine		
Eotaxin	101 (68.0–136)	104 (65.0–134)
MIP-1α	23.9 (18.2–36.3)	27.6 (23.8–37.9)
IP-10	162 (123–227)	153 (133–197)
MCP-1	123 (88.3–140)	106 (87.5–144)
MIP-1β	46.6 (33.8–56.5)	38.13 (32.7–54.0)
IL-8	7.91 (6.15–16.9)	6.7 (5.44–11.4)

* Values are the median (interquartile range) pg/ml. IL-1α = interleukin-1α; IFNγ = interferon-γ; GM-CSF = granulocyte–macrophage colony-stimulating factor; MIP-1α = macrophage inflammatory protein 1α; IP-10 = interferon-γ–inducible 10-kd protein; MCP-1 = monocyte chemotactic protein 1.

Subjects with chikungunya virus–associated arthritis had no significant increase in RA-associated markers or CRP level (Figure 1). Interestingly, 2 of the 5 individuals who were enrolled in the study as having clinical chikungunya virus–associated arthralgia, but who were found to be seronegative for chikungunya virus, were positive for RF and/or anti-CCP antibody, suggesting they may have actually had RA or another related disease unlinked to chikungunya virus infection.

Plasma cytokine and chemokine data demonstrated trends that suggested differences between the patients with chikungunya virus with arthralgia and the controls, but which failed to reach statistical significance (Table 4). As observed in other studies (10,26,27), IL-6, IL-12p70, MCP-1, MIP-1β, and IL-8 were modestly elevated in patients compared to controls.

Proteomic analysis of synovial fluid. Mass spectrometry was used to identify proteins present in the synovial fluid of patients with arthralgia associated with chikungunya virus. The primary aim of the analysis was to determine if mass spectrometry could detect the presence of viral proteins, since this would suggest the persistence of antigen. However, mass spectrometry did not identify any chikungunya virus viral proteins in the fluid.

DISCUSSION

The CAMA study is the largest observational study involving synovial fluid analysis of patients with chikungunya arthritis in the Americas to date. We hypothesized that persistent active chikungunya virus is responsible for chronic arthritis and joint pain and that chikungunya virus viral RNA would be present in the synovial fluid. However, this study did not demonstrate viable virus after culture of synovial fluid in any of the participants who were studied, a median of 22 months after infection. Similarly, PCR analysis did not reveal viral RNA in the plasma or in the synovial fluid. Furthermore, proteomic analysis showed no evidence of viral proteins in the synovial fluid. These results have important implications for determining the mechanisms of persistent arthritis in patients with chikungunya virus and suggest that either there is no chikungunya virus in synovial fluid or that chikungunya virus does not replicate to high enough levels for detection in the synovial fluid 2 years after infection.

This study was inspired by the work of Hoarau et al (10), who found chikungunya virus antigen in macrophages and chikungunya virus RNA in synovial biopsy tissue 18 months after chikungunya virus infection in a single subject. In contrast, in our analysis of 33 patients (many with relapsing–remitting disease) 22 months after acute infection, we did not identify viral RNA or proteins, suggesting that viral persistence may not be a requirement for persistent joint pain. Another consideration is that synovial tissue analysis, as opposed to synovial fluid analysis, may permit improved viral recovery. Furthermore, this study may suggest that the pathophysiology behind human relapsing–remitting chikungunya virus–associated arthritis may differ from the pathophysiology of continuous erosive arthropathy seen in some patients.

In the context of animal studies, studies of nonhuman primates (9) and mice (28) have demonstrated viral persistence up to 44 and 100 days, respectively. Given our evaluation at significantly longer times after infection (22 month), it is conceivable that any virus present was eliminated by this later end point. Furthermore, murine models have yet to reproduce the relapsing–remitting nature of human chikungunya arthritis, suggesting that differing pathophysiology may be at play.

From a clinical perspective, patients with chikungunya virus–associated arthritis described substantial clinical disease burden. Eighty-two percent reported arthritis affecting their activities of daily living and moderate disease severity, as measured by the DAS28. This is consistent with other studies following up patients after chikungunya virus infection that have demonstrated symptoms of persistent arthralgia that may be relapsing or unremitting, often affect multiple joints, and are associated with functional loss impairing activities of daily living and reduced quality of life (29,30).

Multiple studies have shown elevated levels of inflammatory analytes during acute chikungunya virus infection, with IL-8, MCP-1, IL-6, MIP-1α, IL-1α, and MIP-1β reportedly elevated in some chronic chikungunya virus–associated arthralgia cohorts (10,26,27). We measured the levels of these cytokines and chemokines as well as several relevant RA-associated biomarkers. Consistent with the literature, RA-associated factors such as RF and anti-CCP were not elevated in our chikungunya virus–associated arthralgia cohort (2,23,31). Of interest, there were no significant differences in cytokine and chemokine levels within our cohort compared to location-matched controls at a median of 22 months. This might be the result of the very late stage of disease that we studied or the size of our control cohort. There was a trend toward elevation of proinflammatory markers (most notably IL-6) in our cohort, but whether a greater number of subjects would yield statistical significance can only be speculated.

It is possible that the apparent lack of a consistent pattern of markers of inflammation in patients with reported joint pain may be related to the relapsing–remitting nature of the joint pain described by patients with chikungunya arthritis. Patients describe periods of relative relief and "flare" periods of worsened joint symptoms in

response to physical stress or infection. Such relapse was also described by Borgherini et al in their study of the Réunion Island outbreak (32). In our study, while all patients reported joint pain, the relative intensity varied.

Given these results, additional potential mechanisms of the persistence of arthritis symptoms in the absence of chikungunya virus persistence in synovial fluid should be considered. First, it is possible that chikungunya virus or viral antigens persist at low levels in synovial tissue that cannot be detected in synovial fluid. Other potential mechanisms include chikungunya virus–induced epigenetic modifications of host DNA resulting in persistent alterations of host gene transcription, as has been seen in other viruses such as Epstein-Barr virus (33). Alternatively, macrophages could be modified through epigenetic imprinting, much like fibroblast-like synoviocytes are in RA, leading to more aggressive cell behavior even in the absence of replicating virus (34). Molecular mimicry may also play a role in chikungunya virus–induced arthritis, where the continued production of a chikungunya virus–specific antibody that cross-reacts with antigen in the synovium could account for chikungunya virus–associated inflammation. Finally, although unlikely, patients could have seronegative RA, or alternatively, seronegative RA could reflect prior infection with chikungunya virus or other arthritogenic viruses.

There are several limitations to this study that need to be addressed. First, during sample collection, 0–20 ml of saline was used to flush the joints, and this could affect our ability to detect virus in the synovial fluid samples. To mitigate this problem, we cultured 0.5–1.5 ml (as available) of the collected synovial fluid from each patient to attempt to expand any replication-competent virus in the samples. We also used 2 complementary PCR assays to detect nucleic acid as well as a proteomic approach to look for viral proteins. Proving the absence of a target is difficult, and we recognize that it is possible that our approach failed to detect low-level viral antigen; however, our orthogonal approach clearly demonstrates that if viral antigen exists in the synovial fluid, it is at extremely low levels. Though it is a more invasive procedure, future studies may benefit from using synovial biopsy rather than examining fluid. The advent of new ultrasound-guided biopsy techniques may permit this approach in the future. A second limitation of this study is the lack of control subjects who had a history of chikungunya virus infection without chronic arthritis, as well as the lack of age- and sex-matched healthy controls. Furthermore, our healthy controls were on average younger than the chikungunya virus–affected patients, and age is known to be associated with increased production of inflammatory cytokines, most notably IL-6 (35,36).

These study findings may have important clinical relevance for chikungunya virus in the Americas. Since there is no current standard of care guidance for treatment of chikungunya arthritis, some patients are currently being treated with immunosuppressive agents such as methotrexate (22–24), hydroxychloroquine (22), etanercept (23), adalimumab (23), sulfasalazine (24), fingolimod (37), abatacept, and tofacitinib (38). This practice could be potentially harmful in the setting of replicating virus in the synovium since it could permit re-emergence of a systemic viral infection. To date, no such resurgence has been reported. The failure to detect viral persistence in the synovial fluid in the present study may provide some reassurance that treatment with antirheumatic immunosuppressants 2 years after infection is a viable option.

ACKNOWLEDGMENTS

This study was made possible by the support of the following institutions and individuals: Allied Research Society, Falab Laboratory, La Universidad Metropolitiano, La Universidad El Bosque, The George Washington University, La Fundación Santa Fe, El Laboratorio Fals Borda, Lorena Encinales, Walberto Mariaga, Slyvana Insignares, Cesly Arteta, Martha Castillo Jimenez, Jaime Cantillo, April Barbour, Alan Wasserman, Donna Embersit, Sofia Tang, Armando Gonzalez Brunal, Olga Lucia Barran, Margarita Arroyave-Wessel, Fabiola Pomgrico, Julio Cesar Padilla, Jose Ziade, Beda Brichacek, Michael Bukrinksy, Pierre Roques, David Boyle, and Andreas Suhrbier.

ADDITIONAL DISCLOSURES

Author Cure is an employee of Biomelab.

AUTHOR CONTRIBUTIONS

All authors were involved in drafting the article or revising it critically for important intellectual content, and all authors approved the final version to be published. Dr. Chang had full access to all of the data in the study and takes responsibility for the integrity of the data and the accuracy of the data analysis.

Study conception and design. Chang, Martins, L. Encinales, Reid, Acuña, C. Encinales, Matranga, Pacheco, Cure, Shukla, Ruiz Arteta, Amdur, Porras, Rico Mendoza, Lichtenberger, Simon, Bethony, Firestein.

Acquisition of data. Chang, Martins, L. Encinales, Reid, Acuña, C. Encinales, Matranga, Pacheco, Cure, Shukla, Ruiz Arteta, Porras, Rico Mendoza, Falls, Simon, Bethony, Firestein.

Analysis and interpretation of data. Chang, Martins, L. Encinales, Reid, Matranga, Shukla, Amdur, Cazares, Gregory, Ward, Dong, Kenny, Brueggemann, Downey, Kamalapathy, Simon, Bethony, Firestein.

REFERENCES

1. Centers for Disease Control and Prevention. Chikungunya virus: resources for healthcare providers. URL: https://www.cdc.gov/chikungunya/hc/resources.html.
2. Manimunda SP, Vijayachari P, Uppoor R, Sugunan AP, Singh SS, Rai SK, et al. Clinical progression of chikungunya fever during acute

and chronic arthritic stages and the changes in joint morphology as revealed by imaging. Trans R Soc Trop Med Hyg 2010;104:392–9.
3. Powers AM. Risks to the Americas associated with the continued expansion of chikungunya virus. J Gen Virol 2015;96:1–5.
4. Rahim AA, Thekkekara RJ, Bina T, Paul BJ. Disability with persistent pain following an epidemic of chikungunya in rural South India. J Rheumatol 2016;43:440–4.
5. Lanciotti RS, Lambert AJ. Phylogenetic analysis of chikungunya virus strains circulating in the Western Hemisphere. Am J Trop Med Hyg 2016;94:800–3.
6. Schwartz O, Albert ML. Biology and pathogenesis of chikungunya virus. Nat Rev Microbiol 2010;8:491–500.
7. Laurent P, le Roux K, Grivard P, Bertil G, Naze F, Picard M, et al. Development of a sensitive real-time reverse transcriptase PCR assay with an internal control to detect and quantify chikungunya virus. Clin Chem 2007;53:1408–14.
8. Parola P, de Lamballerie X, Jourdan J, Rovery C, Vaillant V, Minodier P, et al. Novel chikungunya virus variant in travelers returning from Indian Ocean islands. Emerg Infect Dis 2006;12:1493–9.
9. Labadie K, Larcher T, Joubert C, Mannioui A, Delache B, Brochard P, et al. Chikungunya disease in nonhuman primates involves long-term viral persistence in macrophages. J Clin Invest 2010;120:894–906.
10. Hoarau JJ, Jaffar Bandjee MC, Krejbich Trotot P, Das T, Li-Pat-Yuen G, Dassa B, et al. Persistent chronic inflammation and infection by Chikungunya arthritogenic alphavirus in spite of a robust host immune response. J Immunol 2010;184:5914–27.
11. Morrison TE, Whitmore AC, Shabman RS, Lidbury BA, Mahalingam S, Heise MT. Characterization of Ross River virus tropism and virus-induced inflammation in a mouse model of viral arthritis and myositis. J Virol 2006;80:737–49.
12. Herrero LJ, Nelson M, Srikiatkhachorn A, Gu R, Anantapreecha S, Fingerle-Rowson G, et al. Critical role for macrophage migration inhibitory factor (MIF) in Ross River virus-induced arthritis and myositis. Proc Natl Acad Sci U S A 2011;108:12048–53.
13. Soden M, Vasudevan H, Roberts B, Coelen R, Hamlin G, Vasudevan S, et al. Detection of viral ribonucleic acid and histologic analysis of inflamed synovium in Ross River virus infection. Arthritis Rheum 2000;43:365–9.
14. Suhrbier A, la Linn M. Clinical and pathologic aspects of arthritis due to Ross River virus and other alphaviruses. Curr Opin Rheumatol 2004;16:374–9.
15. Krejbich-Trotot P, Denizot M, Hoarau JJ, Jaffar-Bandjee MC, Das T, Gasque P. Chikungunya virus mobilizes the apoptotic machinery to invade host cell defenses. FASEB J 2011;25:314–25.
16. White LK, Sali T, Alvarado D, Gatti E, Pierre P, Streblow D, et al. Chikungunya virus induces IPS-1-dependent innate immune activation and protein kinase R-independent translational shutoff. J Virol 2011;85:606–20.
17. Teng T, Kam Y, Lee B, Hapuarachchi HC, Wimal A, Ng L, et al. A systematic meta-analysis of immune signatures in patients with acute chikungunya virus infection. J Infect Dis 2015;211:1925–35.
18. Chow A, Her Z, Ong EK, Chen JM, Dimatatac F, Kwek DJ, et al. Persistent arthralgia induced by chikungunya virus infection is associated with interleukin-6 and granulocyte macrophage colony-stimulating factor. J Infect Dis 2011;203:149–57.
19. Reddy V, Mani RS, Desai A, Ravi V. Correlation of plasma viral loads and presence of chikungunya IgM antibodies with cytokine/chemokine levels during acute chikungunya virus infection. J Med Virol 2014;86:1393–401.
20. Caglioti C, Lalle E, Castilletti C, Carletti F, Capobianchi MR, Bordi L. Chikungunya virus infection: an overview. New Microbiol 2013;36:211–27.
21. Ravichandran R, Manian M. Ribavirin therapy for chikungunya arthritis. J Infect Dev Ctries 2008;2:140–2.
22. Pandya S. Methotrexate and hydroxychloroquine combination therapy in chronic chikungunya arthritis: a 16-week study. Indian J Rheumatol 2008;3:93–7.
23. Bouquillard É, Combe B. A report of 21 cases of rheumatoid arthritis following chikungunya fever: a mean follow-up of two years. Joint Bone Spine 2009;76:654–7.
24. Ganu MA, Ganu A. Post-chikungunya chronic arthritis: our experience with DMARDs over two year follow up. J Assoc Physicians India 2011;59:83–6.
25. Prevoo ML, van't Hof MA, Kuper H, van Leeuwen MA, van de Putte LB, van Riel PL. Modified disease activity scores that include twenty-eight–joint counts: development and validation in a prospective longitudinal study of patients with rheumatoid arthritis. Arthritis Rheum 1995;38:44–8.
26. Chaaithanya IK, Muruganandam N, Sundaram SG, Kawalekar O, Sugunan AP, Manimunda SP, et al. Role of proinflammatory cytokines and chemokines in chronic arthropathy in CHIKV infection. Viral Immunol 2011;24:265–71.
27. Schilte C, Staikovsky F, Couderc T, Madec Y, Carpentier F, Kassab S, et al. Chikungunya virus-associated long-term arthralgia: a 36-month prospective longitudinal study. PLoS Negl Trop Dis 2013;7:e2137.
28. Poo YS, Rudd PA, Gardner J, Wilson JA, Larcher T, Colle M, et al. Multiple immune factors are involved in controlling acute and chronic chikungunya virus infection. PLoS Negl Trop Dis 2014;8:e3354.
29. Couturier E, Guillemin F, Mura M, Leon L, Virion JM, Letort MJ, et al. Impaired quality of life after chikungunya virus infection: a 2-year follow-up study. Rheumatology (Oxford) 2012;51:1315–22.
30. Marimoutou C, Vivier E, Oliver M, Boutin JP, Simon F. Morbidity and impaired quality of life 30 months after chikungunya infection: comparative cohort of infected and uninfected French military policemen in Reunion Island. Medicine (Baltimore) 2012;91:212–9.
31. Gasque P, Couderc T, Lecuit M, Roques P, Ng LF. Chikungunya virus pathogenesis and immunity. Vector Borne Zoonotic Dis 2015;15:241–9.
32. Borgherini G, Poubeau P, Jossaume A, Gouix A, Cotte L, Michault A, et al. Persistent arthralgia associated with chikungunya virus: a study of 88 adult patients on Reunion Island. Clin Infect Dis 2008;47:469–75.
33. Asgari S. Epigenetic modifications underlying symbiont-host interactions. Adv Genet 2014;86:253–76.
34. Bottini N, Firestein GS. Duality of fibroblast-like synoviocytes in RA: passive responders and imprinted aggressors. Nat Rev Rheumatol 2013;9:24–33.
35. Ershler WB, Keller ET. Age-associated increased interleukin-6 gene expression, late-life diseases, and frailty. Annu Rev Med 2000;51:245–70.
36. Ershler WB, Sun WH, Binkley N, Gravenstein S, Volk MJ, Kamoske G, et al. Interleukin-6 and aging: blood levels and mononuclear cell production increase with advancing age and in vitro production is modifiable by dietary restriction. Lymphokine Cytokine Res 1993;12:225–30.
37. Teo TH, Chan YH, Lee WW, Lum FM, Amrun SN, Her Z, et al. Fingolimod treatment abrogates chikungunya virus-induced arthralgia. Sci Transl Med 2017;9:eaal1333.
38. Miner JJ, Cook LE, Hong JP, Smith AM, Richner JM, Shimak RM, et al. Therapy with CTLA4-Ig and an antiviral monoclonal antibody controls chikungunya virus arthritis. Sci Transl Med 2017;9:eaah3438.

ARTHRITIS & RHEUMATOLOGY
Vol. 70, No. 4, April 2018, pp 594–605
DOI 10.1002/art.40404

High Levels of DEK Autoantibodies in Sera of Patients With Polyarticular Juvenile Idiopathic Arthritis and With Early Disease Flares Following Cessation of Anti–Tumor Necrosis Factor Therapy

Nirit Mor-Vaknin,[1] Miguel Rivas,[1] Maureen Legendre,[1] Smriti Mohan,[1] Ye Yuanfan,[1] Theresa Mau,[1] Anne Johnson,[2] Bin Huang,[3] Lili Zhao,[1] Yukiko Kimura,[4] Steven J. Spalding,[5] Paula W. Morris,[6] Beth S. Gottlieb,[7] Karen Onel,[4] Judyann C. Olson,[8] Barbara S. Edelheit,[9] Michael Shishov,[10] Lawrence K. Jung,[11] Elaine A. Cassidy,[12] Sampath Prahalad,[13] Murray H. Passo,[14] Timothy Beukelman,[15] Jay Mehta,[16] Edward H. Giannini,[2] Barbara S. Adams,[1] Daniel J. Lovell,[2] and David M. Markovitz[1]

Objective. **The nuclear oncoprotein DEK is an autoantigen associated with juvenile idiopathic arthritis (JIA), especially the oligoarticular subtype. DEK is a secreted chemotactic factor. Abundant levels of DEK and DEK autoantibodies are found in inflamed synovium in JIA. We undertook this study to further characterize the nature of DEK autoantibodies in screening serum samples from 2 different cohorts that consisted mostly of patients with JIA.**

Methods. **DEK autoantibody levels were analyzed in sera from 33 JIA patients, 13 patients with other inflammatory conditions, and 11 healthy controls, as well as in 89 serum samples from JIA patients receiving anti–tumor necrosis factor (anti-TNF) therapy. Recombinant His-tagged full-length DEK protein (1–375 amino acids [aa]) and the 187–375-aa and 1–350-aa His-tagged DEK fragments made in a baculovirus system were used for enzyme-linked immunosorbent assay (ELISA) and immunoblotting. The C-terminal 25-aa fragment of DEK was expressed in a glutathione S-transferase–tagged vector. ELISA results were calculated as area under the curve by the trapezoidal rule.**

Results. **DEK autoantibody levels were significantly higher in patients with polyarticular JIA than in those with oligoarticular JIA, and were higher in patients with polyarticular JIA who had more active disease after cessation of anti-TNF therapy. Immunoblotting against the C-terminal 25-aa fragment of DEK confirmed that this section of the DEK molecule is the most immunogenic domain.**

Supported by the NIH (Center for Scientific Review grants R03-AR-056748-01 and K01-AR-055620 to Dr. Mor-Vaknin, grant 2P60AR047784-06A2 to Drs. Huang and Lovell, grant R01-AI-087128 to Drs. Huang, Lovell, and Markovitz, and grants R01-AI-062248 and R01-DK-109188 to Dr. Markovitz), the Burroughs Wellcome Fund (Clinical Scientist Award in Translational Research), and the Rheumatology Research Foundation.

[1]Nirit Mor-Vaknin, PhD, Miguel Rivas, MS, Maureen Legendre, BS, Smriti Mohan, MD, Ye Yuanfan, MPH, Theresa Mau, BS, Lili Zhao, PhD, Barbara S. Adams, MD, David M. Markovitz, MD: University of Michigan, Ann Arbor; [2]Anne Johnson, CCRP, Edward H. Giannini, DrPH, MSc, Daniel J. Lovell, MD, MPH: Cincinnati Children's Hospital Medical Center, Cincinnati, Ohio; [3]Bin Huang, PhD: Cincinnati Children's Hospital Medical Center and University of Cincinnati School of Medicine, Cincinnati, Ohio; [4]Yukiko Kimura, MD, Karen Onel, MD: Joseph M. Sanzari Children's Hospital, Hackensack University Medical Center, Hackensack, New Jersey; [5]Steven J. Spalding, MD: The Cleveland Clinic, Cleveland, Ohio; [6]Paula W. Morris, MD: University of Arkansas for Medical Science, Little Rock; [7]Beth S. Gottlieb, MD, MS: Cohen Children's Medical Center, Northwell Health, Hofstra Norwell School of Medicine, Hempstead, New York; [8]Judyann C. Olson, MD: Medical College of Wisconsin, Milwaukee; [9]Barbara S. Edelheit, MD: Connecticut Children's Medical Center, Hartford; [10]Michael Shishov, MD, MPH: Phoenix Children's Hospital, Phoenix, Arizona; [11]Lawrence K. Jung, MD: Children's National Medical Center, Washington, DC; [12]Elaine A. Cassidy, MD: Children's Hospital of Pittsburgh, Pittsburgh, Pennsylvania; [13]Sampath Prahalad, MD: Emory University School of Medicine, Atlanta, Georgia; [14]Murray H. Passo, MD: Medical University of South Carolina, Charleston; [15]Timothy Beukelman, MD, MSCE: University of Alabama at Birmingham; [16]Jay Mehta, MD: Children's Hospital at Montefiore/Albert Einstein College of Medicine, Bronx, New York.

Address correspondence to Nirit Mor-Vaknin, PhD, University of Michigan, 5240 MSRB III, 1150 West Medical Center Drive, Ann Arbor, MI 48109-5640 (e-mail: morvak@umich.edu); or to David M. Markovitz, MD, University of Michigan, 5220C MSRB III, 1150 West Medical Center Drive, Ann Arbor, MI 48109-5640 (e-mail: dmarkov@umich.edu).

Submitted for publication June 5, 2017; accepted in revised form December 18, 2017.

Conclusion. **DEK autoantibody levels are higher in patients with polyarticular JIA than in those with oligoarticular JIA, and higher in patients who have disease flares after cessation of anti-TNF therapy. The C-terminal 25-aa fragment is the most immunogenic portion of DEK. These findings are significant with respect to the nature of DEK autoantibodies, their contribution to JIA pathogenesis, and their implications for JIA management.**

Juvenile idiopathic arthritis (JIA) is a chronic inflammatory condition that includes a group of heterogeneous autoimmune diseases affecting children under the age of 16 years. It is the most common rheumatic condition in children and may lead to short- or long-term disability. Subtypes of JIA include oligoarticular arthritis (involving ≤4 joints), polyarticular arthritis (involving ≥5 joints, rheumatoid factor [RF] positivity or negativity), systemic-onset arthritis, enthesitis-related arthritis, psoriatic arthritis, and undifferentiated arthritis (1,2). While the pathogenesis of JIA is unknown, discovery of DEK autoantibodies in serum of JIA patients as well as DEK protein and DEK autoantibodies in synovial fluid of JIA patients has sparked investigation of DEK's potential contribution to the pathogenesis of JIA (3–6).

DEK is a nuclear phosphoprotein that was initially characterized as part of the *dek-can* fusion oncogene resulting from a (6;9) translocation in a subset of patients with acute myelogenous leukemia (7,8). DEK is involved in various pathways, including transcriptional regulation, modulation of chromatin architecture, DNA replication, and messenger RNA processing (9–11). DEK can also be secreted and may play a role as an extracellular inflammatory cytokine (12,13).

Autoantibodies to DEK are detectable not only in the serum of patients with JIA, but also in serum of patients with granulomatous diseases (e.g., sarcoidosis, tuberculosis) and several autoimmune diseases, including systemic lupus erythematosus (SLE), scleroderma, and idiopathic uveitis. Thus, DEK autoantibodies are associated with clinical conditions characterized by abnormal immune activation (4,6,14). In view of the limited understanding of JIA, the mechanism by which DEK autoantibodies develop, their specificity, and their contribution to the pathogenesis of JIA are of great interest.

Because nonspecific autoantibodies are not generally characteristic of JIA, the presence of DEK autoantibodies in JIA is particularly intriguing. DEK and DEK autoantibodies contribute directly to joint inflammation via the generation of immune complexes, and acetylation of the DEK protein enhances its immunogenicity (3). In addition, DEK protein can be secreted by monocytes and released by apoptotic T cells acting as an extracellular chemoattractant, which suggests that DEK is a proinflammatory factor recruiting inflammatory cells to the synovium (12,13). We recently found that DEK also contributes directly to the formation of neutrophil extracellular traps (NETs) (15). NETs are chromatin structures that are released by activated neutrophils in response to inflammation in order to clear bacteria or fungal infection (16,17). An excess of NETs can contribute to chronic inflammatory conditions such as rheumatoid arthritis or SLE (18). Indeed, synovial neutrophils from JIA patients spontaneously generate NETs containing DEK that is recognized by DEK autoantibodies purified from the synovial fluid of JIA patients (15). DEK autoantibodies from the synovial fluid of JIA patients have been found to predominantly recognize the C-terminus of DEK (3).

Thus, we hypothesized that anti-DEK antibodies and DEK protein form immune complexes by recognition of the C-terminal portion of the DEK protein, further augmenting the inflammatory process in the joint. In this study we also show that anti-DEK antibodies are found at a particularly high level in patients with polyarticular JIA. These levels are higher than those in patients with oligoarticular JIA, in whom anti-DEK antibody levels were previously thought to be highest.

The treatment of JIA has recently been improved by biologic response modifiers such as anti–tumor necrosis factor (anti-TNF) therapy (19–21). However, anti-TNF therapy is associated with significant adverse events, including infections (22–24) and a possible increased risk of cancer (25). Its long-term effects on children are uncertain, and biologic agents are very expensive. Thus, it is important to ascertain when one can safely discontinue anti-TNF therapy in children with disease in clinical remission without significant risk of relapse. Having ascertained that patients with polyarticular JIA have high titers of anti-DEK antibodies, we measured anti-DEK autoantibody levels in serum samples from patients with polyarticular JIA who participated in a multicenter trial designed to enable better understanding of when anti-TNF therapy could be safely stopped. We found significantly higher levels of DEK autoantibodies upon flare after cessation of anti-TNF therapy. Further, we determined that the C-terminal 25–amino acid (25-aa) sequence is the most immunogenic portion of DEK in a significant percentage of JIA patient sera.

PATIENTS AND METHODS

Patients. Forty-six children (mean age 11.7 years, mean disease duration 6.2 years) were enrolled by the Pediatric Rheumatology clinic at the University of Michigan.

These patients had oligoarticular, polyarticular (RF-positive and RF-negative), systemic-onset, spondyloarthritis, and psoriatic subtypes. Control subjects without JIA included children with chronic pain, fatigue, low-titer antinuclear antibody (ANA) positivity, scleroderma, SLE, and juvenile dermatomyositis, but without joint involvement (no arthritis). Patient recruitment was performed under a protocol approved by the University of Michigan Institutional Review Board (IRB) (HUM00014692).

In a second patient cohort for a multicenter study aiming to identify biomarkers to indicate when it is safe to stop anti-TNF therapy, 137 patients with polyarticular JIA were enrolled (mean age 11.3 years, mean disease duration 5.0 years). Parent's/patient's consent (assent, if appropriate) was obtained and screening for eligibility was performed at the participating site at which the patient was recruited. Each patient's eligibility was validated via eligibility case report forms sent immediately to the Pediatric Rheumatology Collaborative Study Group Coordinating Center at Cincinnati Children's Hospital Medical Center (see Supplementary Table 1, available on the *Arthritis & Rheumatology* web site at http://onlinelibrary.wiley.com/doi/10.1002/art.40404/abstract). The Coordinating Center served as the clinical research organization for this study and oversaw all matters related to regulatory, financial, and clinical affairs, as well as data management, quality assurance, and analysis. The multicenter study was approved by the IRB at each participating site and was conducted in compliance with the Declaration of Helsinki Principles for Human Experimentation.

Study design. The first patient cohort included randomly enrolled patients treated at the Pediatric Rheumatology clinic at the University of Michigan. Most JIA patients were treated with methotrexate and nonsteroidal antiinflammatory drugs (NSAIDs), and several were also treated with TNF inhibitors and other biologic agents. Sera were collected at the time of enrollment.

In the second group, patients were enrolled at 16 pediatric rheumatology centers, and serum samples were collected from 137 children with polyarticular JIA who were receiving anti-TNF therapy, as approved by IRBs (HUM00033009). Therapy was stopped after a minimum of 6 months for patients with persistent clinically inactive disease. Clinically inactive disease was defined using the American College of Rheumatology (ACR) provisional criteria (26). Disease activity was then monitored prospectively for an additional 8 months or until disease flare. The primary outcome for this study was disease flare using a variation of the validated criteria, defined as 30% worsening in ≥3 of any of the 6 juvenile rheumatoid arthritis ACR core set variables (27), with no more than 1 improving by >30% (28). The 6 core set variables include the physician's global assessment of disease activity on a 10-cm visual analog scale (VAS), the parent's/patient's assessment of overall well-being on a 10-cm VAS, functional ability measured by the Childhood Health Assessment Questionnaire (C-HAQ) (29), the number of joints with active arthritis, the number of joints with limited range of motion, and an acute-phase reactant (the erythrocyte sedimentation rate [ESR]).

Because enrolled subjects began the second phase with clinically inactive disease, a 30% worsening could represent a less than clinically important change. Thus, for this study the patient was considered to have had a disease flare if their disease worsened by 30% and by at least the following amounts: increases of at least 2 units on a 21-numbered circle VAS (30) for the physician's assessment and parent's/patient's assessment, increases of at least 2 joints with active arthritis and at least 2 joints with limited range of motion, a minimum increase of 0.125 on the C-HAQ score, and an increase in the ESR from normal to abnormal.

Laboratory assessment. Whole blood samples were obtained from patients seen in the Pediatric Rheumatology clinic at the University of Michigan under a protocol approved by the IRB. Serum in a standard vacutainer blood collection tube was prepared by allowing the blood sample to clot at room temperature for 15–30 minutes followed by centrifugation at 1,000–2,000*g* for 10 minutes. For patients in the anti-TNF study, an additional 8.5-cc P100 tube to collect plasma was used for anti-DEK antibody analysis of all subjects weighing >20 kg at visits 1, 2, and 3 and at disease flare/end of the study. Samples were processed as described above, stored, and shipped to the University of Michigan.

Enzyme-linked immunosorbent assay (ELISA). Microtiter plates were coated with full-length (1–375-aa) or 1–350-aa recombinant DEK (50 μl of 125 ng/well) and incubated overnight at 21°C. Plates were blocked with phosphate buffered saline plus 0.25% bovine serum albumin and 0.05% Tween 20 for 30 minutes at room temperature, followed by 3 washes with double-distilled water, 10 minutes of blocking, and 3 additional washes. Serum samples from JIA patients and controls (dilutions of 1:200, 1:400, 1:800, 1:1,600, and 1:3,200 in blocking buffer) were added to the plates for 2 hours at room temperature, followed by 3 washes, 10 minutes of blocking, and 3 additional washes. Biotinylated goat anti-human secondary antibody (Jackson ImmunoResearch) at a concentration of 1:200,000 in dilution buffer (50 μl/well) was added for 2 hours of incubation at room temperature, followed by 3 washes and 10 minutes of blocking and washing. Streptavidin (1:300 in dilution buffer; 50 μl/well) was added for 1 hour of incubation at room temperature, followed by 5 washes. We added 3,3′,5,5′-tetramethylbenzidine substrate (50 μl/well) to develop the plate for 5–15 minutes prior to stopping the reaction with 1*N* H_2SO_4 (50 μl/well). The optical density (OD) at 450 nm was read within 20 minutes.

Statistical analysis of ELISA results. Anti-DEK antibody levels in sera from JIA patients, measured at 5 different dilutions (1:200, 1:400, 1:800, 1:1,600, and 1:3,200), were compared to those in sera from non-JIA patients and healthy controls and expressed as fold change over those in healthy controls in each individual experiment. Fold changes were calculated by OD. Results were also plotted as the area under the dilution curve (AUDC) of each sample, calculated using the trapezoidal rule. Analysis of variance models were used to compare AUDC between groups of patients. Statistical significance was defined as a 2-sided *P* value of less than 0.05. Receiver operating characteristic (ROC) curve analysis was used to assess the ability of the AUDC to discriminate among groups. Area under the ROC curve (AUC) was calculated, as was its 95% confidence interval (95% CI). The marker showed good discrimination ability if the interval's lower limit was >0.5.

To analyze samples from patients participating in the TNF inhibition study at different time points, we took additional steps to normalize across the different assays using anti-DEK monoclonal antibody (BD Biosciences) as a reference. The anti-DEK AUC values in JIA patients were standardized against those in healthy controls. We analyzed the difference in the AUDC values. Student's *t*-test was used to compare patients

who had disease flares and those who did not by the 8-month follow-up visit after discontinuation of anti-TNF therapy.

Cloning and expression of the C-terminal 25-aa domain of DEK. Expression and purification of His-tagged full-length DEK and of the 187–375-aa and 1–350-aa His-tagged DEK fragments was performed as described previously (31,32). The C-terminal 25-aa portion of the human DEK protein was amplified from the His-tagged full-length DEK vector via polymerase chain reaction (PCR) using primers containing 5′ *Eco* RI and 3′ *Xho* I restriction sites. The PCR product was identified and eluted from an agarose gel prior to digestion with *Eco* RI and *Xho* I. The pGEX-4T1 vector containing glutathione S-transferase (GST) was also digested with *Eco* RI and *Xho* I, and the 25-aa DEK fragment was ligated into the pGEX vector. DNA from clones containing the correct sequence was used to express the protein in the GST-tagged vector.

Immunoblotting. DEK-specific polyclonal antibodies were purified as described (32). Protein aliquots (3.5 μg) were separated by 4–20% sodium dodecyl sulfate–polyacrylamide gel electrophoresis and transferred to a nitrocellulose membrane. The membrane was probed with a 1:400 dilution of patient sera or a 1:1,000 dilution of rabbit anti-DEK antibody followed by a horseradish peroxidase–conjugated secondary goat anti-human antibody or goat anti-rabbit antibody and detected by enhanced chemiluminescence (Amersham Pharmacia Biotech).

RESULTS

Association of high levels of DEK autoantibodies with JIA. Previous studies had shown elevated titers of anti-DEK antibodies in JIA patients, especially those with oligoarticular disease (4,14). We collected 57 serum samples from 11 healthy control individuals (the basis

Table 1. Demographic information on the pediatric patients recruited into both studies*

	University of Michigan cohort		TNF study†	
	JIA patients (n = 33)	Non-JIA patients (n = 13)	Patients with flares (n = 39)	Patients without flares (n = 67)
Age, mean ± SD years	11.7 ± 3.7	14.0 ± 4.0	11.13 ± 5.05	11.18 ± 4.22
Male:female ratio	9:24	5:8	10:29	21:46
Duration of disease, mean ± SD years	6.2 ± 4.2	2.6 ± 1.7	6.37 ± 4.55	4.48 ± 3.14
Diagnosis				
Oligoarticular JIA	8	–	–	–
Extended oligoarticular JIA	1	–	8	9
RF-positive polyarticular JIA (RA)	2	–	2	7
RF-negative polyarticular JIA	12	–	36	59
Systemic-onset JIA	3	–	–	–
Psoriatic arthritis	3	–	–	–
Spondyloarthritis	1	–	–	–
Undifferentiated arthritis	3	–	–	–
UCTD	–	1	–	–
SLE	–	2	–	–
Juvenile DM	–	2	–	–
MCTD	–	2	–	–
Localized scleroderma	–	2	–	–
Other (Kawasaki disease and pericarditis, all ANA positive)	–	3	–	–
Uveitis	4 (12)	1 (8)	–	–
ANA positive	13 (39)	8 (62)	22 (20)	31 (29)
Active arthritis	16 (48)	1 (8)	–	–
Current medications				
Methotrexate	17 (52)	4 (31)	13 (12)	28 (26)
Glucocorticoids	2 (6)	4 (31)	–	–
Hydroxychloroquine	9 (27)	5 (36)	–	–
NSAIDs	24 (73)	2 (15)	–	–
Mycophenolate mofetil	1 (3)	4 (31)	–	–
Leflunomide	3 (9)	0 (0)	–	–
Sulfasalazine	6 (18)	0 (0)	–	–
TNF inhibitors	5 (15)	1 (8)	39 (37)	67 (63)
Infliximab	3	1	3	2
Adalimumab	0	0	4	10
Etanercept	2	0	32	55
Other biologic agents (anakinra)	2 (6)	0 (0)	–	–
Cyclosporine	2 (6)	1 (8)	–	–
IVIG	1 (3)	1 (8)	–	–

* Except where indicated otherwise, values are the number or number (%). JIA = juvenile idiopathic arthritis; TNF = tumor necrosis factor; RF = rheumatoid factor; RA = rheumatoid arthritis; UCTD = undifferentiated connective tissue disease; SLE = systemic lupus erythematosus; DM = dermatomyositis; MCTD = mixed connective tissue disease; ANA = antinuclear antibody; NSAIDs = nonsteroidal antiinflammatory drugs; IVIG = intravenous immunoglobulin.

† Percentages were calculated based on the total number of patients (those with and those without disease flares).

for statistical calculations), 13 non-JIA control patients, and 33 JIA patients who were enrolled in our study at the Pediatric Rheumatology Clinic at the University of Michigan. The mean ± SD age of the JIA patients was 11.7 ± 3.7 years, and their mean ± SD disease duration was 6.2 ± 4.2 years. The majority of JIA patients were female (24 female, 9 male) (Table 1), and among all 12 healthy controls recruited for the study, 5 were female and 7 were male (see Supplementary Table 2, http://onlinelibrary.wiley.com/doi/10.1002/art.40404/abstract). The distribution of JIA subtypes included 24% with oligoarticular arthritis, 36% with RF-negative polyarticular arthritis, 9% with psoriatic arthritis, 9% with systemic-onset JIA, 6% with RF-positive polyarticular arthritis, and 3% with spondyloarthritis. ANA positivity was noted in 39% of patients. Twelve percent of patients had uveitis.

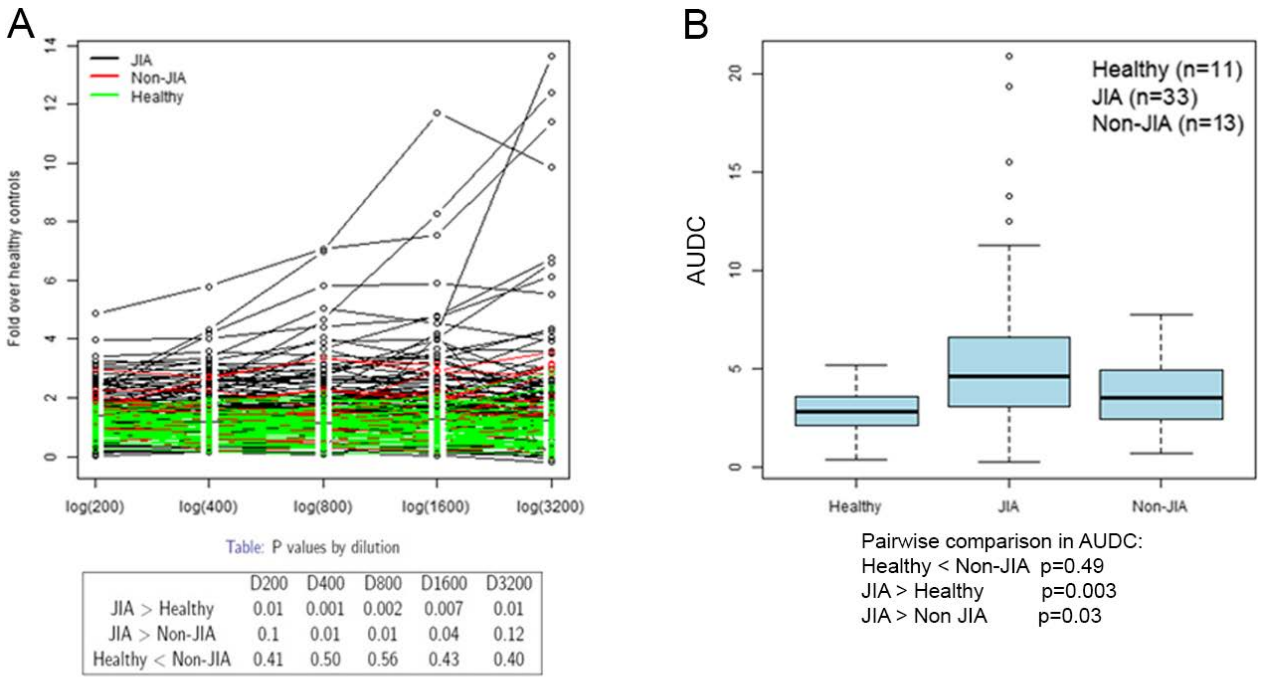

Table: P values by dilution

	D200	D400	D800	D1600	D3200
JIA > Healthy	0.01	0.001	0.002	0.007	0.01
JIA > Non-JIA	0.1	0.01	0.01	0.04	0.12
Healthy < Non-JIA	0.41	0.50	0.56	0.43	0.40

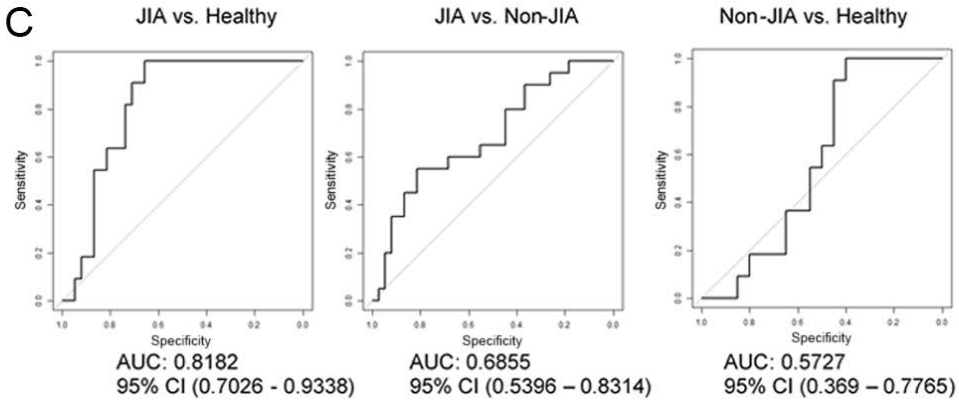

Figure 1. High levels of DEK autoantibodies in patients with juvenile idiopathic arthritis (JIA). **A,** Serum samples from patients with JIA (n = 33), patients with other rheumatic diseases (n = 13), or healthy controls (n = 11) were serially diluted as indicated and tested for anti-DEK antibody levels by enzyme-linked immunosorbent assay (ELISA). Lines represent individual samples. Samples were compared to those from 5 normal healthy controls. Results shown are the average of 2–8 independent ELISAs. **B,** Shown are pairwise comparisons, based on area under the dilution curve (AUDC), among healthy subjects, JIA patients, and non-JIA patients. Data are shown as box plots. Each box represents the 25th to 75th percentiles. Lines inside the boxes represent the median. Lines outside the boxes represent the 10th and 90th percentiles. Circles indicate outliers. **C,** The area under the receiver operating characteristic curve (AUC) was calculated along with its 95% confidence interval (95% CI) to assess the performance of the AUDC measurements in distinguishing between different groups of patients.

With regard to medications used by patients at the time of study enrollment and blood sampling, 52% of patients were being treated with methotrexate, 27% with hydroxychloroquine, 73% with NSAIDs, 6% with glucocorticoids, 9% with leflunomide, 18% with sulfasalazine, 15% with TNF inhibitors, and 6% with anakinra (primarily for systemic-onset JIA). Of these JIA patients, 53% had active disease at the time of blood collection.

The mean ± SD age of the non-JIA patients with rheumatic disease at the time of serum collection was 14.0 ± 4.0 years, and their mean ± SD disease duration was 2.6 ± 1.7 years. There was a fairly equal distribution of other autoimmune diseases in this group, including relatively equal numbers of patients with SLE, juvenile dermatomyositis, mixed connective tissue disease, and localized scleroderma. One patient with idiopathic uveitis who was receiving steroid-sparing agents was also in this group. The healthy control group was made up of healthy college student volunteers with a mean ± SD age of 20 ± 5 years.

Sera were analyzed by ELISA for anti-DEK antibody levels using recombinant DEK protein. Serum samples were serially diluted and were tested for anti-DEK antibody levels as described in Patients and Methods. Figure 1A depicts the average results of 2–8 independent ELISAs. Samples were compared to those from 5 normal healthy controls. As shown in Figure 1A and Supplementary Figure 1 (http://onlinelibrary.wiley.com/doi/10.1002/art.40404/abstract), JIA patients had significantly higher levels of anti-DEK antibodies than did non-JIA patients and healthy controls. Although there appeared to be slightly higher levels of anti-DEK antibodies detected by ELISA among non-JIA patients than among healthy controls, the difference was not statistically significant. Figure 1B demonstrates ELISA antibody titers as pairwise comparisons based on the AUDC values among healthy

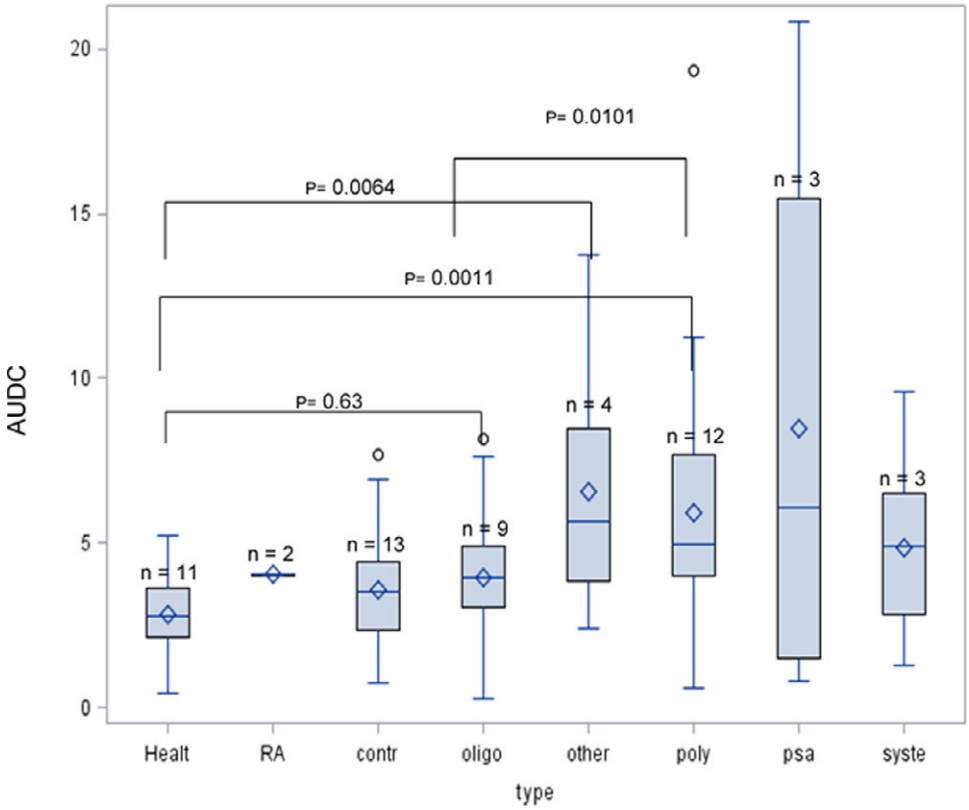

Figure 2. DEK autoantibody levels are significantly higher in patients with polyarticular arthritis (poly) than in those with oligoarticular arthritis (oligo) or in healthy controls (Healt). DEK autoantibody levels in the sera of patients with different juvenile idiopathic arthritis (JIA) subtypes, as analyzed by anti-DEK antibody enzyme-linked immunosorbent assay, were compared to those in healthy controls. All levels of antibodies to DEK were compared to those in sera from healthy individuals based on area under the dilution curve (AUDC). Data are shown as box plots. Each box represents the 25th to 75th percentiles. Lines inside the boxes represent the median. Diamonds represent the mean. Lines outside the boxes represent the 10th and 90th percentiles. Circles indicate outliers. RA = patients with rheumatoid arthritis; contr = patients seen in the rheumatology clinic who did not in fact have arthritis; other = patients with no definitive JIA subtype at the time of diagnosis; PsA = patients with psoriatic arthritis; syste = patients with systemic-onset arthritis. Color figure can be viewed in the online issue, which is available at http://onlinelibrary.wiley.com/doi/10.1002/art.40404/abstract.

subjects, JIA patients, and non-JIA patients. JIA patients had a significantly higher AUDC than did either non-JIA patients ($P = 0.03$) or healthy controls ($P = 0.003$). To test the specificity of our assay, we used the ROC test as shown in Figure 1C. DEK autoantibody levels showed good discrimination among JIA patients, non-JIA patients, and healthy subjects, confirming the presence of increased levels of anti-DEK antibodies in patients with JIA.

Significantly higher DEK autoantibody levels in patients with polyarticular arthritis than in patients with oligoarticular arthritis or in healthy individuals. Previous reports have suggested that anti-DEK antibodies are especially found in JIA patients with the oligoarticular form of the disease. Therefore, DEK autoantibody levels in sera from patients with different JIA subtypes were compared to levels in sera from healthy controls and analyzed by anti-DEK antibody ELISA (Figure 2). All anti-DEK antibody levels were compared to levels in sera from healthy individuals and were assessed as AUDC. As shown in Figure 2, there was a statistically significant difference in AUDC between healthy controls and patients with polyarticular JIA ($P = 0.0011$) and between healthy controls and patients with other forms of JIA ($P = 0.0064$). No significant differences were found between patients with oligoarticular JIA and healthy individuals ($P = 0.63$), but a significant difference was noted between patients with oligoarticular JIA and those with polyarticular JIA ($P = 0.0101$), with the latter group being statistically more likely to have higher levels of DEK autoantibodies. High levels of DEK autoantibodies were also detected in 2 patients with spondyloarthritis and 2 patients with arthritis as a manifestation of their undifferentiated connective tissue disease (categorized as "other").

DEK autoantibody levels in patients receiving anti-TNF therapy. Anti-TNF therapy has proven to be a very valuable modality in the treatment of JIA (19–21). However, it is expensive, and its immunosuppressive effects can lead to opportunistic infections, skin disorders, colitis, and malignancies (33,34). Further, the long-term effects of anti-TNF therapy on children remain unclear (35). Therefore,

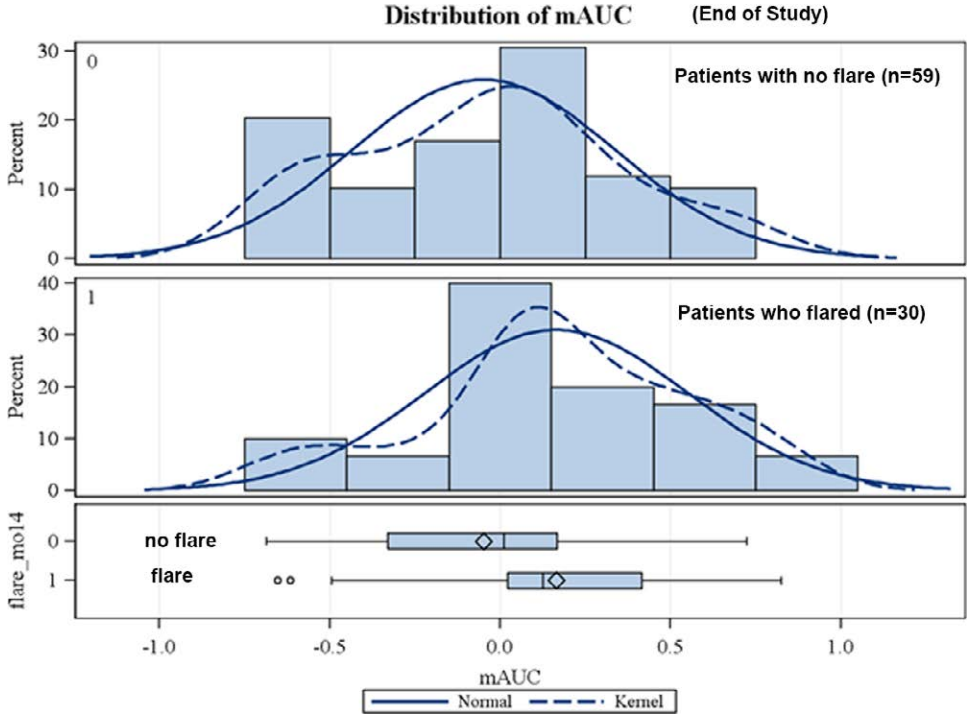

Figure 3. Increase in anti-DEK antibodies is evident in patients with juvenile idiopathic arthritis who have disease flares within 8 months of stopping anti–tumor necrosis factor therapy. Top and middle, Shown are data on sera from 89 of 106 patients who were analyzed for anti-DEK antibody levels. High levels of anti-DEK antibodies (mean ± SD difference in area under the dilution curve [AUDC] values [mAUC] 0.164 ± 0.39 [95% confidence interval {95% CI} 0.02, 0.31]) were detected in the 30 patients who had disease flares within 8 months (middle), while lower levels of anti-DEK antibodies (mean ± SD difference in AUDC values –0.05 ± 0.39 [95% CI –0.15, 0.05]) were detected in the 59 patients who had no disease flares for at least 8 months and up to 14 months (flare_mo14) (top) ($P = 0.016$ by Student's *t*-test). The difference between the 2 populations is demonstrated by a normal distribution, and the same trend is shown by a kernel density distribution to demonstrate the distribution of the data based on the actual spread/density of the results. Bottom, Data are shown as box plots. Each box represents the 25th to 75th percentiles. Lines inside the boxes represent the median. Diamonds represent the mean. Lines outside the boxes represent the 10th and 90th percentiles. Circles indicate outliers. Color figure can be viewed in the online issue, which is available at http://onlinelibrary.wiley.com/doi/10.1002/art.40404/abstract.

strategies are much needed for deciding when to stop treatment after it is initiated. Accordingly, we measured DEK autoantibodies in a larger cohort of JIA patients who received anti-TNF therapy (Table 1; also see Supplementary Table 1, http://onlinelibrary.wiley.com/doi/10.1002/art.40404/abstract). We enrolled 103 female patients and 34 male patients with polyarticular JIA (mean age 11.3 years, mean disease duration 5.0 years). Seventy-seven percent were receiving etanercept, 18% were receiving adalimumab, 5% were receiving infliximab, and 40% were receiving concomitant methotrexate. Thirty-one patients discontinued the study for various reasons, including reactivation of disease during therapy.

Within 8 months of stopping therapy, 39 patients had disease flares but 67 patients did not. Anti-DEK antibody levels at the time of stopping anti-TNF therapy did not differ significantly between these 2 groups of patients (see Supplementary Figure 2, http://onlinelibrary.wiley.com/doi/10.1002/art.40404/abstract). However, at the end of the study, either after 8 months of no disease flare without therapy or at the time of disease flare without therapy, high levels of anti-DEK antibodies (mean ± SD difference in AUDC values 0.164 ± 0.39 [95% CI 0.02, 0.31]) were detected in 30 of the patients who had disease flares, while lower levels of anti-DEK antibodies (mean ± SD difference in AUDC values –0.05 ± 0.39 [95% CI –0.15, 0.05]) were measured in 59 of the patients with no disease flares ($P = 0.016$ by Student's t-test) (Figure 3). Thus, retrospectively, patients who experienced disease flares within 8 months of stopping anti-TNF therapy had significantly higher levels of anti-DEK antibodies than did patients with clinically inactive disease until the end of the study.

Requirement of the C-terminal portion of the DEK protein for autoantibody recognition. Previous studies with a very limited number of sera and synovial fluid samples suggested that anti-DEK antibodies target the last 25

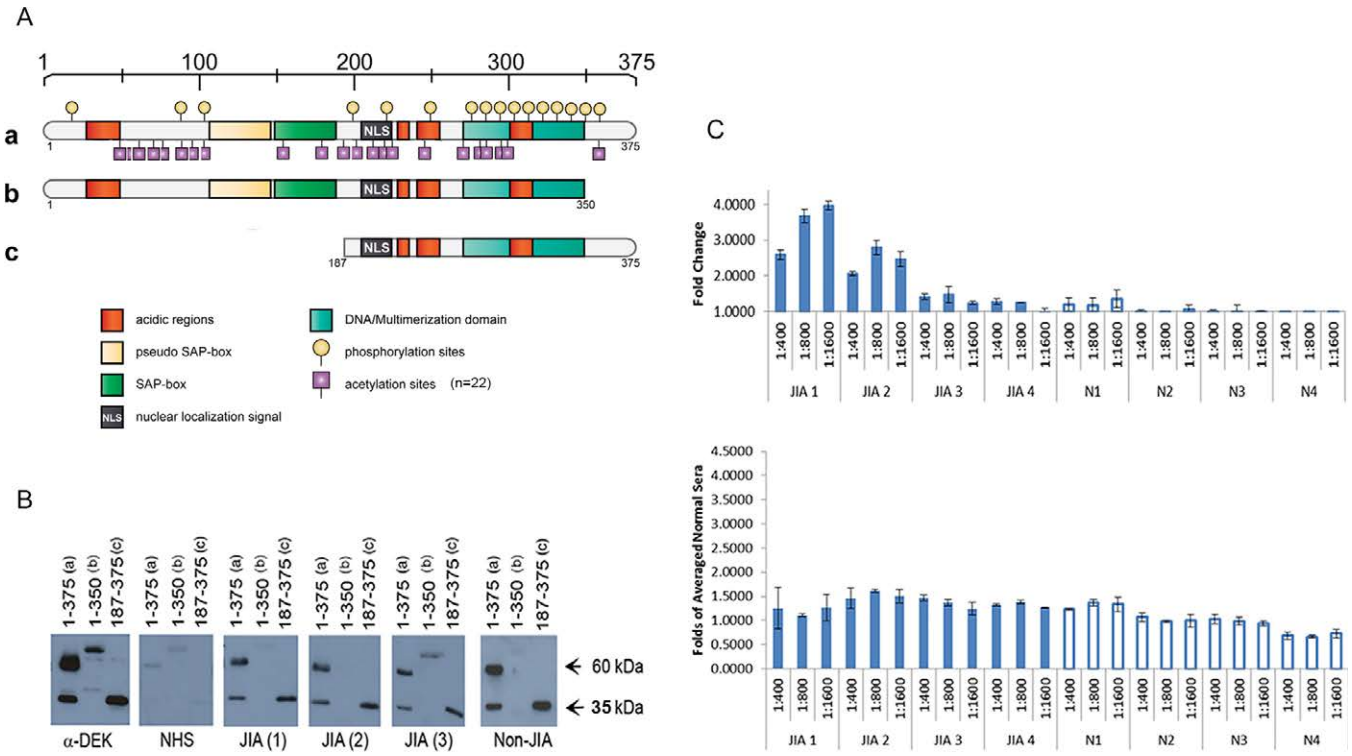

Figure 4. Antibodies in sera from patients with juvenile idiopathic arthritis (JIA) recognize the C-terminal domain of the DEK protein. **A,** Illustration of the different fragments and domains of recombinant histidine-tagged DEK with posttranslational modifications previously identified in primary human macrophages and HeLa cells (3). **B,** Results of Western blot analysis of DEK fragments (1 μg protein per lane) expressed in Sf9 cells. DEK protein was probed with serum samples from a normal healthy control subject (NHS), from 3 JIA patients, or from a rheumatology patient without JIA, or with DEK-specific antibody as a positive control. **C,** Levels of anti-DEK antibodies. Sera from 4 JIA patients and either sera or plasma from 4 healthy controls (N1–N4) were serially diluted and tested for antibodies to full-length (1–375–amino-acid) recombinant DEK (top) or the 1–350–amino-acid DEK fragment (bottom) by enzyme-linked immunosorbent assay (ELISA). Values are the mean ± SD fold change compared to another set of sera from 4 different healthy controls. $P = 0.0337$ by Student's t-test for recognition of full-length DEK by sera from JIA patients versus sera from healthy controls (top). $P = 0.009$ by Student's t-test for recognition of full-length DEK by sera from JIA patients (top) versus recognition of the 1–350–amino-acid DEK fragment by sera from JIA patients (bottom). Color figure can be viewed in the online issue, which is available at http://onlinelibrary.wiley.com/doi/10.1002/art.40404/abstract.

amino acids of the molecule (3). To address this question further, full-length, 1–350-aa, and 187–375-aa fragments of recombinant His-tagged DEK were first expressed in Sf9 insect cells. The overlapping fragments were designed to investigate the immunogenic importance of the C-terminal portion of DEK, specifically the C-terminal 25 amino acids, as shown in Figure 4A. DEK protein fragments were then purified and analyzed by immunoblotting (Figure 4B). DEK protein was probed with serum samples from a normal healthy control subject, from 3 JIA patients, or from a rheumatology patient without JIA, or with DEK-specific antibody as a positive control.

As shown in Figure 4B, the DEK-specific antibody strongly detected all DEK fragments. The full-length DEK protein was detected as expected primarily at 55 kd; a previously identified breakdown form was also detected at 35 kd (12). (The 1–350-aa DEK runs slightly higher than the full-length DEK, perhaps due to changes in its 3-dimensional structure.) Serum from the normal healthy control did not notably detect DEK or its fragments. Sera from all 3 JIA patients readily detected full-length DEK protein as well as the 187–375-aa fragment, which contains the C-terminal 25 amino acids, consistent with our previous findings using autoantibodies found in synovial fluid samples from patients (3). The non-JIA patient sera detected the full-length and 187–375-aa DEK fragments, consistent with the observation that patients with other autoimmune diseases can also have antibodies to DEK. In contrast, the 1–350-aa DEK fragment lacking only the last 25 amino acids could not be recognized by most patient sera (3 of 4 serum samples did not recognize the truncated fragment). These results are consistent with our previous findings that 5 of 8 JIA patients' synovial fluid antibodies that recognized DEK (>50%) failed to recognize DEK when the C-terminal 25 amino acids were deleted as in the 1–350-aa DEK mutant (3).

ELISAs were performed to determine further if autoantibodies in patient sera indeed primarily recognize

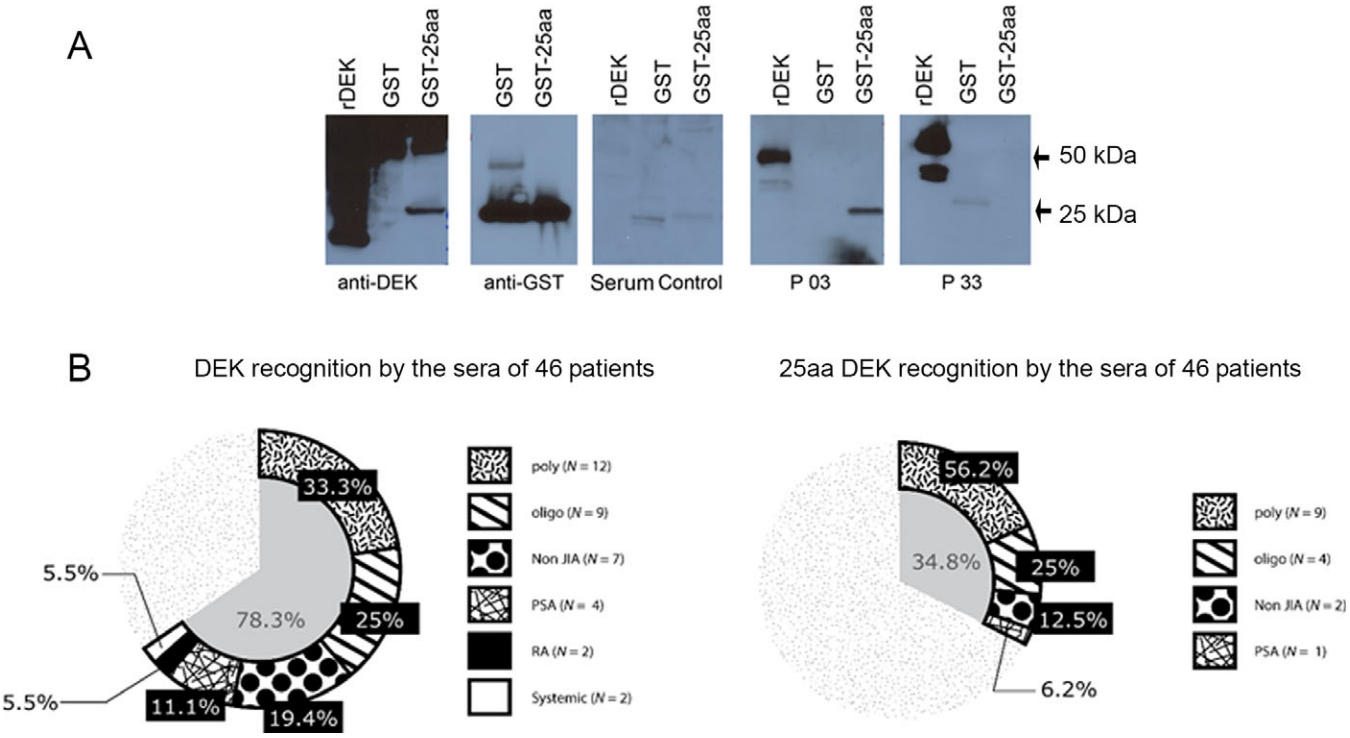

Figure 5. The last 25 amino acids (aa) of DEK are sufficient for recognition by the autoantibodies of a substantial percentage of patients with juvenile idiopathic arthritis (JIA) who have autoantibodies to full-length DEK. **A,** Recombinant full-length DEK (rDEK), glutathione S-transferase (GST) control protein, and the C-terminal GST-tagged 25 amino acids of DEK (GST-25aa) were purified and analyzed by Western blotting and densitometry. Results from 2 different representative JIA patient sera (P03 and P33) are shown in addition to a representative control serum from a healthy individual. **B,** Pie chart demonstrates the percentage of patients who had autoantibodies to full-length DEK as detected in sera from patients with polyarticular JIA (poly), oligoarticular JIA (oligo), psoriatic arthritis (PsA), rheumatoid arthritis (RA), systemic-onset JIA, and non-JIA rheumatic diseases (control) (left). From the 46 patients screened, we also calculated the percentage of patients whose sera recognized the last 25 amino acids of DEK alone, also divided into the different JIA subtypes and non-JIA rheumatic diseases (right). Note that overall, approximately half of the patients' sera that recognized full-length DEK also recognized the isolated C-terminal 25 amino acids of the protein. Color figure can be viewed in the online issue, which is available at http://onlinelibrary.wiley.com/doi/10.1002/art.40404/abstract.

the last 25 amino acids of DEK. Sera from 4 patients with JIA and either sera or plasma from 4 healthy controls were serially diluted and tested for antibodies to full-length (1–375-aa) recombinant DEK or to DEK containing amino acids 1–350 (the entire DEK protein except for the C-terminal 25 amino acids). DEK was not recognized by sera from healthy controls, while sera from JIA patients were able to recognize wild-type DEK (Figure 4C). Although levels of DEK recognition varied among JIA patients, all levels of DEK recognition among JIA patients were significantly greater than among healthy controls. This difference disappeared, however, when ELISA was performed using the 1–350-aa DEK fragment, which was not recognized by sera from JIA patients or controls (Figure 4C).

Antibodies in sera from JIA patients recognize the last 25 amino acids of the DEK protein. To determine if DEK's autoantigenicity truly resides in its terminal 25 amino acids, we produced the last 25 amino acids of DEK with a GST tag. Recombinant full-length DEK, GST control protein, and the C-terminal GST-tagged 25 amino acids of DEK were purified and analyzed using a DEK-specific polyclonal antibody, an antibody to GST, serum from a representative healthy control, and sera from 3 different JIA patients (Figure 5A).

The serum from the healthy control did not detect DEK protein, while sera from all of the JIA patients detected full-length DEK. Sera from 2 representative JIA patients also detected the GST-tagged 25-aa fragment, indicating recognition of the C-terminal portion of the DEK protein but not of the GST control protein. We next screened all 46 patient samples for recognition of full-length DEK and the GST-tagged 25-aa DEK fragment (Figure 5B). Approximately four-fifths (78.3%) of the sera from JIA patients recognized full-length DEK, but only half of those sera (one-third of the sera from the total patient cohort) recognized the C-terminal portion of DEK. Stated another way, of the patients with antibodies to full-length DEK, 50% had antibodies that recognized the C-terminal 25-aa fragment alone. Most of the patients with autoantibodies recognizing the C-terminus of DEK had the polyarticular subtype. Therefore, in some but not all cases, the C-terminal 25-aa DEK fragment can be sufficient to generate DEK autoantibodies. Taken together, these findings demonstrate that the C-terminal 25 amino acids are usually necessary, but only sometimes sufficient, to generate autoantibodies to DEK.

DISCUSSION

DEK, originally identified as a nuclear protein, is a key factor in the modulation of global chromatin structure (10). In addition to that significant function, the DEK protein plays a role in immunity and is also recognized as an autoantigen in JIA and other autoimmune diseases. Our research group found that DEK binds to a specific sequence in the Y box of the HLA–DQA1 promoter (36), an allele that predisposes children in northern European populations to the development of oligoarticular-onset JIA (37,38). We also previously demonstrated that DEK is actively secreted by human macrophages and passively released by apoptotic T cells, attracting leukocytes into the inflamed area (12,13). DEK and DEK autoantibodies are abundant in synovial fluid of patients with JIA, leading to the development of immune complexes in the affected joints (3). Autoantibodies to DEK also show increased affinity for acetylated and poly(ADP-ribosyl)ated DEK (13). We have also recently shown that DEK is not only secreted by activated macrophages but is also released by activated neutrophils, and it was found to be an important component of NETs. Indeed, DEK-knockout mice develop much less joint inflammation after zymosan injection due to decreased formation of NETs, and inflammation in the joints can be reduced by neutralizing DEK with specific anti-DEK aptamers (15). Thus, DEK and DEK autoantibodies appear to contribute to joint inflammation by attracting inflammatory cells, generating immune complexes, and supporting NET formation.

The DEK protein was initially described as an autoantigen in 1991 by Szer et al (4,5). With the exception of ANAs, autoantibodies are commonly absent in children with JIA (14). The discovery of antibodies to the DEK nuclear antigen in JIA therefore holds promise for improving our understanding of the pathogenesis and management of JIA. Reactivity to anti-DEK antibodies was found to be most strongly associated with onset of any JIA subtype before the sixth birthday, particularly early-onset oligoarticular JIA and iridocyclitis. However, DEK autoantibody levels were previously not found to have a correlation with disease severity (14). Using recombinant full-length DEK, we have screened multiple sera from JIA patients from 2 different cohorts, 46 patients from the Pediatric Rheumatology clinic at the University of Michigan and 89 patients with polyarticular JIA receiving anti-TNF therapy from a study coordinated by the Cincinnati Children's Hospital Medical Center. In both patient cohorts, high levels of DEK autoantibodies were significantly correlated with polyarticular arthritis (surprisingly, greater than in oligoarticular arthritis) (Figure 2), and higher levels of DEK autoantibodies were found to be correlated with disease flare within the 8 months after cessation of anti-TNF therapy ($P = 0.016$) (Figure 3). These findings show that DEK autoantibody levels correlate with disease activity and might contribute

to disease pathogenesis. However, while at this point we have shown that anti-DEK antibody levels correlate with active disease, they cannot yet be used to predict whether it is safe to discontinue anti-TNF therapy.

We have now also demonstrated in a large group of patients that the C-terminal 25-aa sequence of DEK is a major autoantigenic region and is sometimes sufficient to generate an autoimmune response. These findings suggest that more refined ELISAs using the C-terminal 25-aa sequence of DEK might prove to be of future use. Taken together, it appears that by understanding the action of DEK and anti-DEK antibodies, improvements can be made in the management of JIA.

AUTHOR CONTRIBUTIONS

All authors were involved in drafting the article or revising it critically for important intellectual content, and all authors approved the final version to be published. Drs. Mor-Vaknin and Markovitz had full access to all of the data in the study and take responsibility for the integrity of the data and the accuracy of the data analysis.

Study conception and design. Mor-Vaknin, Rivas, Johnson, Huang, Zhao, Spalding, Jung, Mehta, Giannini, Adams, Lovell, Markovitz.

Acquisition of data. Mor-Vaknin, Rivas, Legendre, Yuanfan, Mau, Johnson, Zhao, Kimura, Spalding, Morris, Gottlieb, Onel, Olson, Edelheit, Shishov, Jung, Cassidy, Prahalad, Passo, Beukelman, Mehta, Giannini, Adams, Lovell, Markovitz.

Analysis and interpretation of data. Mor-Vaknin, Rivas, Legendre, Mohan, Mau, Huang, Zhao, Mehta, Adams, Lovell, Markovitz.

REFERENCES

1. Prakken B, Albani S, Martini A. Juvenile idiopathic arthritis. Lancet 2011;377:2138–49.
2. Ravelli A, Martini A. Juvenile idiopathic arthritis. Lancet 2007; 369:767–78.
3. Mor-Vaknin N, Kappes F, Dick AE, Legendre M, Damoc C, Teitz-Tennenbaum S, et al. DEK in the synovium of patients with juvenile idiopathic arthritis: characterization of DEK antibodies and posttranslational modification of the DEK autoantigen. Arthritis Rheum 2011;63:556–67.
4. Szer IS, Sierakowska H, Szer W. A novel autoantibody to the putative oncoprotein DEK in pauciarticular onset juvenile rheumatoid arthritis. J Rheumatol 1994;21:2136–42.
5. Szer W, Sierakowska H, Szer IS. Antinuclear antibody profile in juvenile rheumatoid arthritis. J Rheumatol 1991;18:401–8.
6. Dong X, Wang J, Kabir FN, Shaw M, Reed AM, Stein L, et al. Autoantibodies to DEK oncoprotein in human inflammatory disease. Arthritis Rheum 2000;43:85–93.
7. Boer J, Mahmoud H, Raimondi S, Grosveld G, Krance R. Loss of the DEK-CAN fusion transcript in a child with t(6;9) acute myeloid leukemia following chemotherapy and allogeneic bone marrow transplantation. Leukemia 1997;11:299–300.
8. Fornerod M, Boer J, van Baal S, Jaegle M, von Lindern M, Murti KG, et al. Relocation of the carboxyterminal part of CAN from the nuclear envelope to the nucleus as a result of leukemia-specific chromosome rearrangements. Oncogene 1995;10: 1739–48.
9. Fu GK, Grosveld G, Markovitz DM. DEK, an autoantigen involved in a chromosomal translocation in acute myelogenous leukemia, binds to the HIV-2 enhancer. Proc Natl Acad Sci U S A 1997;94:1811–5.
10. Kappes F, Waldmann T, Mathew V, Yu J, Zhang L, Khodadoust MS, et al. The DEK oncoprotein is a Su(var) that is essential to heterochromatin integrity. Genes Dev 2011;25:673–8.
11. Soares LM, Zanier K, Mackereth C, Sattler M, Valcarcel J. Intron removal requires proofreading of U2AF/3′ splice site recognition by DEK. Science 2006;312:1961–5.
12. Mor-Vaknin N, Punturieri A, Sitwala K, Faulkner N, Legendre M, Khodadoust MS, et al. The DEK nuclear autoantigen is a secreted chemotactic factor. Mol Cell Biol 2006;26:9484–96.
13. Kappes F, Fahrer J, Khodadoust MS, Tabbert A, Strasser C, Mor-Vaknin N, et al. DEK is a poly(ADP-ribose) acceptor in apoptosis and mediates resistance to genotoxic stress. Mol Cell Biol 2008;28:3245–57.
14. Murray KJ, Szer W, Grom AA, Donnelly P, Levinson JE, Giannini EH, et al. Antibodies to the 45 kDa DEK nuclear antigen in pauciarticular onset juvenile rheumatoid arthritis and iridocyclitis: selective association with MHC gene. J Rheumatol 1997;24:560–7.
15. Mor-Vaknin N, Saha A, Legendre M, Carmona-Rivera C, Amin MA, Rabquer BJ, et al. DEK-targeting DNA aptamers as therapeutics for inflammatory arthritis. Nat Commun 2017;8:14252.
16. Brinkmann V, Reichard U, Goosmann C, Fauler B, Uhlemann Y, Weiss DS, et al. Neutrophil extracellular traps kill bacteria. Science 2004;303:1532–5.
17. Brinkmann V, Zychlinsky A. Neutrophil extracellular traps: is immunity the second function of chromatin? J Cell Biol 2012; 198:773–83.
18. Kaplan MJ, Radic M. Neutrophil extracellular traps: double-edged swords of innate immunity. J Immunol 2012;189:2689–95.
19. Heiligenhaus A, Horneff G, Greiner K, Mackensen F, Zierhut M, Foeldvari I, et al. Inhibitors of tumour necrosis factor-α for the treatment of arthritis and uveitis in childhood. In German. Klin Monbl Augenheilkd 2007;224:526–31.
20. Foeldvari I, Nielsen S, Kummerle-Deschner J, Espada G, Horneff G, Bica B, et al. Tumor necrosis factor-α blocker in treatment of juvenile idiopathic arthritis-associated uveitis refractory to second-line agents: results of a multinational survey. J Rheumatol 2007;34:1146–50.
21. Gimenez-Roca C, Iglesias E, Torrente-Segarra V, Bou R, Sanchez-Manubens J, Calzada-Hernandez J, et al. Efficacy and safety of TNF-α antagonists in children with juvenile idiopathic arthritis who started treatment under 4 years of age. Rheumatol Int 2015;35:323–6.
22. Beukelman T, Xie F, Baddley JW, Chen L, Mannion ML, Saag KG, et al. The risk of hospitalized infection following initiation of biologic agents versus methotrexate in the treatment of juvenile idiopathic arthritis. Arthritis Res Ther 2016;18:210.
23. Davies R, Southwood TR, Kearsley-Fleet L, Lunt M, Hyrich KL, on behalf of the British Society for Paediatric and Adolescent Rheumatology Etanercept Cohort Study. Medically significant infections are increased in patients with juvenile idiopathic arthritis treated with etanercept: results from the British Society for Paediatric and Adolescent Rheumatology Etanercept Cohort Study. Arthritis Rheumatol 2015;67:2487–94.
24. Klotsche J, Niewerth M, Haas JP, Huppertz HI, Zink A, Horneff G, et al. Long-term safety of etanercept and adalimumab compared to methotrexate in patients with juvenile idiopathic arthritis (JIA). Ann Rheum Dis 2016;75:855–61.
25. Beukelman T, Haynes K, Curtis JR, Xie F, Chen L, Bemrich-Stolz CJ, et al. Rates of malignancy associated with juvenile idiopathic arthritis and its treatment. Arthritis Rheum 2012;64:1263–71.
26. Wallace CA, Giannini EH, Huang B, Itert L, Ruperto N, for the Childhood Arthritis Rheumatology Research Alliance (CARRA), the Pediatric Rheumatology Collaborative Study Group (PRCSG), and the Paediatric Rheumatology International Trials Organisation (PRINTO). American College of Rheumatology provisional criteria for defining clinical inactive disease in select categories of juvenile idiopathic arthritis. Arthritis Care Res (Hoboken) 2011;63: 929–36.

27. Giannini EH, Lovell DJ, Felson DT, Goldsmith CH. Preliminary core set of outcome variables for use in JRA clinical trials [abstract]. Arthritis Rheum 1994;37 Suppl:S428.
28. Brunner HI, Lovell DJ, Finck BK, Giannini EH. Preliminary definition of disease flare in juvenile rheumatoid arthritis. J Rheumatol 2002;29:1058–64.
29. Singh G, Athreya BH, Fries JF, Goldsmith DP. Measurement of health status in children with juvenile rheumatoid arthritis. Arthritis Rheum 1994;37:1761–9.
30. Filocamo G, Davi S, Pistorio A, Bertamino M, Ruperto N, Lattanzi B, et al. Evaluation of 21-numbered circle and 10-centimeter horizontal line visual analog scales for physician and parent subjective ratings in juvenile idiopathic arthritis. J Rheumatol 2010;37:1534–41.
31. Bohm F, Kappes F, Scholten I, Richter N, Matsuo H, Knippers R, et al. The SAF-box domain of chromatin protein DEK. Nucleic Acids Res 2005;33:1101–10.
32. Kappes F, Damoc C, Knippers R, Przybylski M, Pinna LA, Gruss C. Phosphorylation by protein kinase CK2 changes the DNA binding properties of the human chromatin protein DEK. Mol Cell Biol 2004;24:6011–20.
33. Pontikaki I, Gerloni V, Gattinara M, Luriati A, Salmaso A, De Marco G, et al. Side effects of anti-TNFα therapy in juvenile idiopathic arthritis. In Italian. Reumatismo 2006;58:31–8.
34. Pontikaki I, Shahi E, Frasin LA, Gianotti R, Gelmetti C, Gerloni V, et al. Skin manifestations induced by TNF-α inhibitors in juvenile idiopathic arthritis. Clin Rev Allergy Immunol 2012;42:131–4.
35. Tynjala P, Lahdenne P, Vahasalo P, Kautiainen H, Honkanen V. Impact of anti-TNF treatment on growth in severe juvenile idiopathic arthritis. Ann Rheum Dis 2006;65:1044–9.
36. Adams BS, Cha HC, Cleary J, Haiying T, Wang H, Sitwala K, et al. DEK binding to class II MHC Y-box sequences is gene- and allele-specific. Arthritis Res Ther 2003;5:R226–33.
37. Haas JP, Kimura A, Truckenbrodt H, Suschke J, Sasazuki T, Volgger A, et al. Early-onset pauciarticular juvenile chronic arthritis is associated with a mutation in the Y-box of the HLA-DQA1 promoter. Tissue Antigens 1995;45:317–21.
38. Haas JP, Nevinny-Stickel C, Schoenwald U, Truckenbrodt H, Suschke J, Albert ED. Susceptible and protective major histocompatibility complex class II alleles in early-onset pauciarticular juvenile chronic arthritis. Hum Immunol 1994;41:225–33.

ARTHRITIS & RHEUMATOLOGY
Vol. 70, No. 4, April 2018, pp 606–615
DOI 10.1002/art.40410

Switched Memory B Cells Are Increased in Oligoarticular and Polyarticular Juvenile Idiopathic Arthritis and Their Change Over Time Is Related to Response to Tumor Necrosis Factor Inhibitors

Emiliano Marasco, Angela Aquilani, Simona Cascioli, Gian Marco Moneta, Ivan Caiello, Chiara Farroni, Ezio Giorda, Valentina D'Oria, Denise Pires Marafon, Silvia Magni-Manzoni, Rita Carsetti, and Fabrizio De Benedetti

Objective. **To investigate whether abnormalities in B cell subsets in patients with juvenile idiopathic arthritis (JIA) correlate with clinical features and response to treatment.**

Methods. **A total of 109 patients diagnosed as having oligoarticular JIA or polyarticular JIA were enrolled in the study. B cell subsets in peripheral blood and synovial fluid were analyzed by flow cytometry.**

Results. **Switched memory B cells were significantly increased in patients compared to age-matched healthy controls ($P < 0.0001$). When patients were divided according to age at onset of JIA, in patients with early-onset disease (presenting before age 6 years) the expansion in switched memory B cells was more pronounced than that in patients with late-onset disease and persisted throughout the disease course. In longitudinal studies, during methotrexate (MTX) treatment, regardless of the presence or absence of active disease, the number of switched memory B cells increased significantly (median change from baseline 36% [interquartile range {IQR} 15, 66]). During treatment with MTX plus tumor necrosis factor inhibitors (TNFi), in patients maintaining disease remission, the increase in switched memory B cells was significantly lower than that in patients who experienced active disease (median change from baseline 4% [IQR −6, 32] versus 41% [IQR 11, 73]; $P = 0.004$). The yearly rate of increases in switched memory B cells was 1.5% in healthy controls, 1.2% in patients who maintained remission during treatment with MTX plus TNFi, 4.7% in patients who experienced active disease during treatment with MTX plus TNFi, and ~4% in patients treated with MTX alone.**

Conclusion. **Switched memory B cells expand during the disease course at a faster rate in JIA patients than in healthy children. This increase is more evident in patients with early-onset JIA. TNFi treatment inhibits this increase in patients who achieve and maintain remission, but not in those with active disease.**

Juvenile idiopathic arthritis (JIA) is the most common chronic rheumatic disease in children. The 2001 update of the International League of Associations for Rheumatology (ILAR) criteria for JIA identifies 8 different categories based on the number of joints involved, laboratory findings, and extraarticular manifestations (1). The goal of this classification is to group JIA patients into relatively homogeneous categories; however, it is still debated whether these categories group together patients with diseases having common pathogenic mechanisms. In fact, several problems with the present classification are emerging (2,3). For example, it has been proposed that early-onset JIA (presenting before age 6 years) is a distinct clinical entity, regardless of the number of joints involved. Indeed, genetic studies of associations with HLA alleles (4), immunologic studies involving B lymphocytes (5), and the presence of specific clinical features (6) support this proposal.

Supported by Ricerca Corrente, Ministero della Salute.

Emiliano Marasco, MD, Angela Aquilani, MD, Simona Cascioli, PhD, Gian Marco Moneta, MSc, Ivan Caiello, MSc, Chiara Farroni, PhD, Ezio Giorda, PhD, Valentina D'Oria, MSc, Denise Pires Marafon, MD, Silvia Magni-Manzoni, MD, Rita Carsetti, MD, Fabrizio De Benedetti, MD, PhD: Ospedale Pediatrico Bambino Gesù, IRCCS, Rome, Italy.

Drs. Marasco and Aquilani contributed equally to this work.

Dr. De Benedetti has received grants from Novartis, Roche, Pfizer, SOBI, AbbVie, NovImmune, Bristol-Myers Squibb, and Sanofi.

Address correspondence to Emiliano Marasco, MD, or Fabrizio De Benedetti, MD, PhD, Division of Rheumatology, Ospedale Pediatrico Bambino Gesù, IRCCS, Viale di San Paolo, 15, 00146 Rome, Italy. E-mail: em.marasco@yahoo.com or fabrizio.debenedetti@opbg.net.

Submitted for publication June 24, 2017; accepted in revised form January 3, 2018.

Methotrexate (MTX) is used as first-line treatment in patients with JIA, and tumor necrosis factor inhibitors (TNFi) have been shown to be effective in patients with an unsatisfactory response to MTX. Some studies have investigated alterations in circulating B cell subsets in JIA patients, but no major abnormalities have been found (7,8). Given the well-known role of TNF in B cell development and germinal center (GC) reactions and the possible relationship between these effects and therapeutic efficacy (9,10), our aim was to study the distribution of B cell subsets in the peripheral blood of a large cohort of patients with JIA and the correlation of these subsets with disease activity and response to MTX and TNFi.

PATIENTS AND METHODS

Patients and study design. We enrolled 109 patients diagnosed as having oligoarticular JIA or polyarticular JIA according to the ILAR criteria (1). The characteristics of the patients are shown in Table 1. For each patient, we recorded clinical data and laboratory parameters. Antinuclear antibody (ANA) positivity was defined as the presence of a high titer of ANAs (≥1:160) on at least 2 occasions, 3 months apart. Approximately 66% of patients with oligoarticular JIA or polyarticular JIA were ANA positive. Age-matched children were used as healthy controls (n = 304).

Of these 109 patients, 50 patients receiving either MTX alone (n = 17) or MTX plus TNFi (n = 33) were followed up for a median of 11.2 months (range 6.9–21.2 months); their B cell subsets were measured at the first (time 0) and last (time 1) follow-up visits. Active disease was defined as the presence of tender or swollen joints, a high erythrocyte sedimentation rate and/or C-reactive protein (CRP) level, and/or active uveitis. Remission was defined according to the criteria described by Wallace et al (11).

Table 1. Baseline characteristics of the patients according to International League of Associations for Rheumatology subtype*

	Oligoarticular JIA (n = 94)	Polyarticular JIA (n = 15)
ANA positive	62 (66)	10 (66.7)
Female	75 (79.8)	13 (86.7)
Age, median (IQR) years	9.1 (5.8, 12.7)	9.4 (7.2, 12.6)
Age at onset, median (IQR) years	3.1 (2, 6.2)	3.8 (2.1, 6.6)
Disease duration, median (IQR) months	42.0 (10.2, 103.4)	45.6 (8.6, 67.6)
Disease activity		
Active disease	40 (42)	6 (40)
Clinically inactive disease	26 (27.7)	3 (20)
Clinical remission with medication	23 (24.5)	6 (40)
Clinical remission without medication	5 (5.3)	0 (0)
Therapy		
NSAIDs	26 (27.7)	0 (0)
MTX	32 (34)	5 (33.3)
MTX plus TNFi	36 (38.3)	10 (66.7)

* Except where indicated otherwise, values are the number (%). JIA = juvenile idiopathic arthritis; ANA = antinuclear antibody; IQR = interquartile range; NSAIDs = nonsteroidal antiinflammatory drugs; MTX = methotrexate; TNFi = tumor necrosis factor inhibitors.

B cell phenotyping. Peripheral blood mononuclear cells from 109 patients and 304 healthy controls or synovial fluid mononuclear cells (SFMCs) from 18 patients were isolated by Ficoll density-gradient centrifugation and frozen. Mononuclear cells were thawed, counted, assessed for viability, and stained with the following antibodies: phycoerythrin (PE)–Cy5–conjugated anti-CD19 (HIB19), PE–Cy7–conjugated anti-CD38 (HB7), PE-conjugated anti-CD27 (M-T271), Pacific Blue (PB)–conjugated anti-CD14 (M5E2), PB-conjugated anti-CD3 (UCHT1), BV711-conjugated anti-CD24 (ML5), fluorescein isothiocyanate (FITC)–conjugated mouse anti-human IgD (IA6-2) (all from Becton Dickinson), and Alexa Fluor 647–conjugated goat anti-human IgM (no. 109-606-129; Jackson ImmunoResearch). Samples were run on a BD LSRFortessa X-20 instrument (BD Biosciences). Data were analyzed with FlowJo software, version 8.3 (Tree Star). The gating strategy is shown in Supplementary Figure 1, available on the *Arthritis & Rheumatology* web site at http://onlinelibrary.wiley.com/doi/10.1002/art.40410/abstract.

SFMC culture conditions and ANA assay. In order to have a sufficient number of SF B cells for cell culture, CD19+ cells from 13 JIA patients (~85% with oligoarticular JIA) were sorted and cultured together with non–B cells as the feeder layer and stimulated with CpG, as previously described (12). After 8 days of culture, supernatants were collected, and cells were stained to analyze the expression of surface markers. The concentration of total IgG in supernatants was assessed with an in-house enzyme-linked immunosorbent assay (12). The presence of ANAs secreted by memory B cells in undiluted or diluted supernatants was assayed by a commercial ANA kit (ANA Hep2; Eurospital) and detected with FITC-conjugated anti-human IgG. Samples with the highest concentration of IgG were diluted in order to adjust for differences in the amount of total IgG produced in vitro; ANA reactivity remained positive with a concordant nuclear pattern in diluted samples.

Statistical analysis. A nonparametric *t*-test or analysis of variance (ANOVA) followed by Bonferroni post hoc test was used to analyze data. *P* values less than 0.05 were considered significant.

RESULTS

Increased switched memory B cells in patients with oligoarticular JIA or polyarticular JIA. The relative frequency and absolute number of CD19+ B cells were significantly increased in JIA patients in comparison to age-matched healthy controls (Figure 1A; also see Supplementary Table 1, http://onlinelibrary.wiley.com/doi/10.1002/art.40410/abstract). The percentages of transitional and naive B cells did not differ between JIA patients and healthy controls (Figure 1A). We found a significant difference in the B cell memory pool. Switched memory B cells were significantly increased in JIA patients, while IgM memory B cells were significantly reduced (Figure 1A). When we calculated the absolute numbers, we

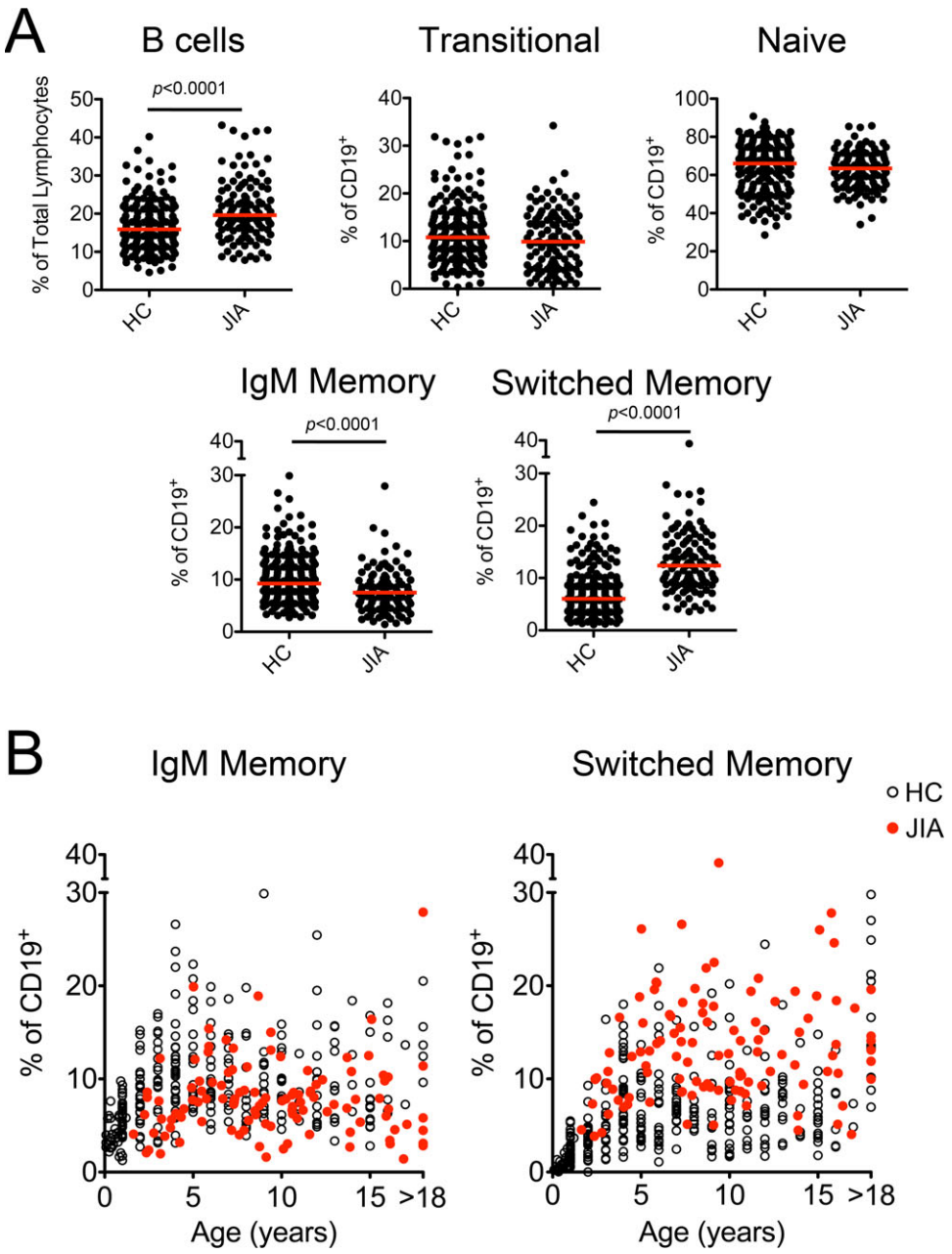

Figure 1. **A,** Percentage of CD19+, transitional, naive, IgM memory, and switched memory B cells in patients with juvenile idiopathic arthritis (JIA) (n = 109) and age-matched healthy controls (HC) (n = 304). Symbols represent individual subjects; horizontal lines indicate the median. **B,** Percentage of IgM memory and switched memory B cells in patients with JIA and healthy controls plotted as a function of age at the time of sampling. Symbols represent individual subjects.

found that all B cell populations were increased in JIA patients (as expected based on the expansion of total CD19+ cells that we and other investigators observed [13]) except for transitional B cells, numbers of which were within the normal range (Supplementary Table 1).

The frequency of IgM memory and switched memory B cells increases throughout childhood upon encounters with antigens (12). However, the absolute number of circulating memory B cells decreases over time due to the reduction in the total number of circulating B cells observed after age 4 years (14,15). In order to study the dynamic changes of the memory B cell compartment in children, we determined the relative frequency of IgM memory and switched memory B cells as a function of

age (16) (Figure 1B; also see Supplementary Figure 2, http://onlinelibrary.wiley.com/doi/10.1002/art.40410/abstract). Switched memory B cells were expanded in JIA patients until age 16 years, while no statistically significant differences were observed between adult JIA patients and adult healthy controls (Supplementary Figure 2). IgM memory B cells appeared to be significantly reduced only in very young children with JIA (Figure 1B; also see Supplementary Figure 2).

In expression profile studies, Barnes et al (5) observed that a B cell signature characterizes patients with oligoarticular JIA or polyarticular JIA with disease beginning before age 6 years (referred to as early-onset JIA) and distinguishes patients with early-onset JIA from those with late-onset JIA and systemic-onset JIA. We divided our JIA patients according to age at the time of disease onset and, to correct for age-related differences in memory B cells, took into account the age at which the blood sample was drawn. In patients with early-onset disease and age <6 years at sampling, switched memory B cells were expanded and IgM memory B cells were reduced compared to age-matched healthy controls (Figures 2A and B). In patients age >6 years at the time of sampling with either early-onset JIA (age <6 years) or late-onset JIA (age >6 years), the frequency of switched memory B cells was significantly increased compared to the frequency in age-matched healthy controls, while the frequency of IgM memory B cells was comparable to that in age-matched healthy controls (Figures 2A and B). Of note, among patients in whom blood samples were obtained at age >6 years, the frequency of switched memory B cells was higher in those with onset at age <6 years than in those with onset at age >6 years. These results are consistent with the conclusion that switched memory B cells are significantly expanded in JIA patients, and that this expansion is more pronounced in patients with early-onset JIA and persists throughout the disease course.

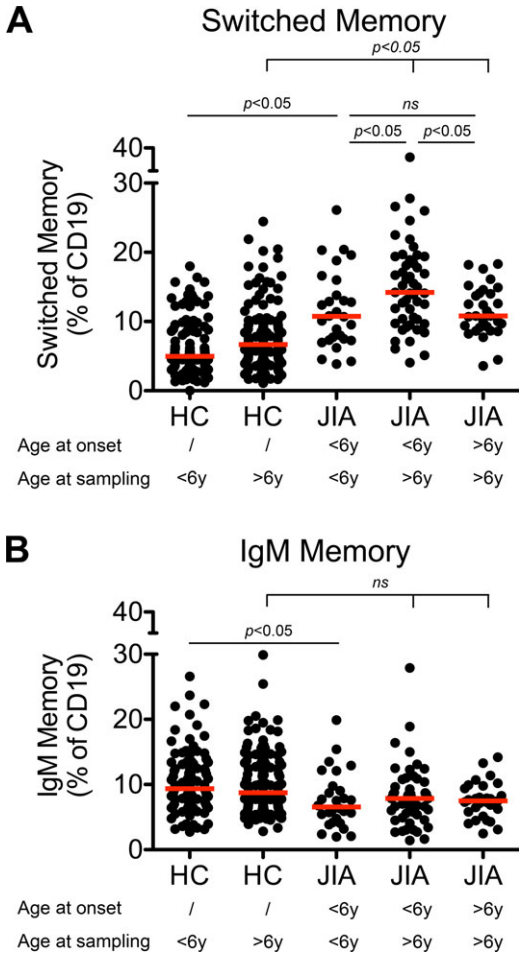

Figure 2. Percentage of switched memory B cells (**A**) and IgM memory B cells (**B**) in patients with juvenile idiopathic arthritis (JIA) and healthy controls (HC) divided according to age at onset of JIA for patients and age at sampling for JIA patients and healthy controls. Symbols represent individual subjects; horizontal lines indicate the median. NS = not significant.

Switched memory B cells are present in inflamed joints and are a source of ANAs. The target organ in JIA is the synovium. Therefore, we sought to analyze the B cell subsets found in SF obtained from JIA patients. As described in a previous report (7), the total number of B cells was lower than that in peripheral blood, accounting for ~1% of SFMCs. Of note, >60% of these B cells were switched memory B cells (Figure 3A), consistent with previous observations (7,17).

Memory B cells are the main B cells responding to CpG (a Toll-like receptor 9 agonist) by proliferating and differentiating into immunoglobulin-secreting plasmablasts (18). After stimulation with CpG, SF memory B cells from 13 JIA patients expanded, acquired a plasmablast phenotype ($CD19^{low}CD27{+}{+}CD38{+}{+}$), and secreted IgG in the supernatants (Figure 3B). We previously showed that after stimulation with CpG, switched memory B cells are responsible for almost all of the IgG secreted in culture (12). Therefore, we tested whether the IgG produced by switched memory B cells in the supernatants contained ANAs. In 6 of 7 ANA-positive patients, IgG secreted by SF switched memory B cells contained ANAs; in contrast, ANAs were undetectable in 6 ANA-negative patients (P = 0.0047 by Fisher's exact test) (Figure 3C). We also tested the reactivity of supernatants of unstimulated culture of SFMCs, and no ANAs were detected (data not shown), indicating that there was no basal production of ANAs and that these autoantibodies were secreted by memory B cells only after stimulation with CpG. Taken together, these data show that switched memory B cells are

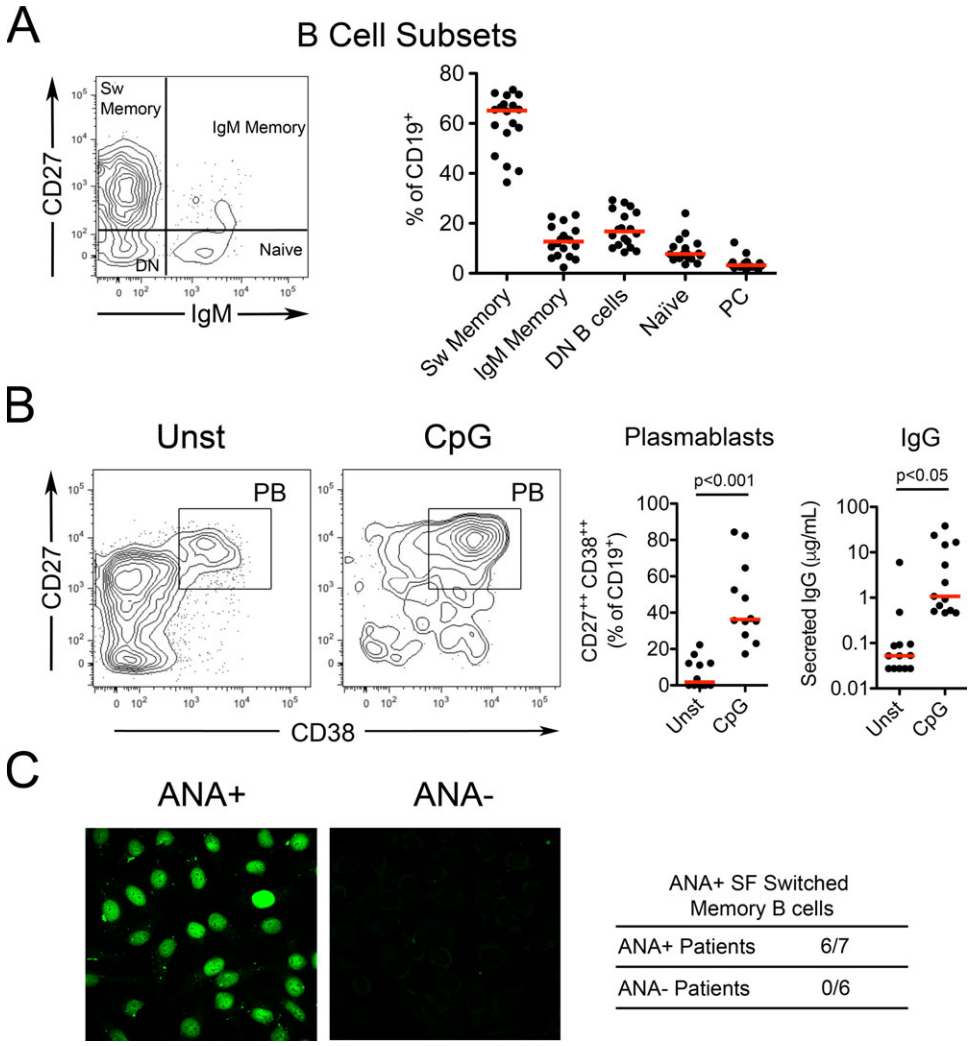

Figure 3. **A,** Representative plot (left) and percentages of B cell subsets in synovial fluid (SF) samples from patients with juvenile idiopathic arthritis (n = 18) (right). Sw = switched; DN = double negative; PC = plasma cells. **B,** Representative plots showing SF B cells differentiating into plasmablasts (PB) ($CD19^{low}$CD27++CD38++) in response to CpG (left), and percentages of plasmablasts (n = 12 individual patients) and amount of IgG secreted in the supernatant (n = 13 individual patients) in response to CpG (right). Unst = unstimulated. **C,** Representative images of antinuclear antibody (ANA) staining with supernatants produced by CpG-stimulated SF switched memory B cells (n = 13 individual patients). Original magnification × 60. In **A** and **B**, symbols represent individual subjects; horizontal lines indicate the median.

markedly expanded in SF, are functionally active (as shown by the maturational response to CpG), and, more important, produce ANAs in ANA-positive JIA patients.

TNFi limit the expansion of switched memory B cells in JIA patients. We found no differences in the number of switched memory B cells between patients with persistent oligoarticular JIA, those with extended oligoarticular JIA, and those with polyarticular JIA (see Supplementary Figure 3A, http://onlinelibrary.wiley.com/doi/10.1002/art.40410/abstract). The expansion of switched memory B cells was not associated with ANA positivity, the presence of uveitis, or the level of disease activity as estimated by the number of joints with active disease or by CRP levels (Supplementary Figures 3B–F).

The frequency of switched memory B cells in patients receiving MTX plus TNFi (14.6% [interquartile range {IQR}10.5, 18.5]) tended to be higher than that in patients treated with MTX alone (12.4% [IQR 8.7, 16.8]) or in patients treated with nonsteroidal antiinflammatory drugs alone (10% [IQR 7.8, 13.7]); however, this did not reach statistical significance (P = 0.0581 by one-way ANOVA) (see Supplementary Figure 3D, http://onlinelibrary.wiley.com/doi/10.1002/art.40410/abstract). These data are in apparent contrast to a previous report (10) that in

adults with rheumatoid arthritis (RA), TNFi caused a reduction in GCs and in circulating memory B cells. Since duration of treatment may be an important variable to consider, we assessed changes in switched memory B cells during treatment with MTX alone and during treatment with MTX plus TNFi.

In patients treated with MTX alone, there was a progressive increase in switched memory B cells over time, and this correlated significantly with treatment duration (r = 0.39, $P = 0.03$) (Figure 4). This increase is consistent with previous observations in MTX-treated patients with RA (10) and in MTX-treated patients with JIA (19) as well as with the known increase in switched memory B cells with age in children (12). In contrast, in patients treated with MTX plus TNFi, the percentage of switched memory B cells did not change (Figure 4). Since MTX is known to have no effect on the development of switched memory B cells (19), their increase in patients treated with MTX alone may simply reflect a physiologic increase with age. The absence of a physiologic increase in switched memory B cells in patients treated with MTX plus TNFi can be explained by the above-mentioned inhibitory effect of TNFi on GCs and on generation and maintenance of switched memory B cells.

TNFi reduce the rate of increase in switched memory B cells only in patients who achieve disease remission. To confirm the effect of TNFi on switched memory B cells mentioned above, we analyzed changes in the percentage of switched memory B cells over time and correlated them with the therapeutic response to TNFi. Fifty JIA patients were followed up during treatment with either MTX alone (n = 17) or MTX plus TNFi (n = 33) for ~1 year. Figure 5A shows the percentage of switched memory B cells at the first (time 0) and second (time 1) sampling (median interval 11.2 months). As expected based on the known increase with age and the data shown previously, in patients treated with MTX alone the percentage of switched memory B cells increased significantly during the follow-up period (median increase from baseline 36% [IQR 15, 66]). There were no differences between patients who achieved and maintained remission during treatment with MTX alone (31% increase from baseline [IQR 9, 57]) and those who did not (47% increase from baseline [IQR 6, 73]) ($P = 0.5$). For this reason, and to simplify the analysis, we included both groups of patients in a single MTX treatment group. In patients treated with MTX plus TNFi who experienced active arthritis or uveitis during treatment (group A), switched memory B cells increased significantly (median increase of 41% from baseline [IQR 11, 73]) to an extent comparable to that in patients treated with MTX alone. In contrast, in patients treated with MTX plus TNFi who achieved and maintained remission during the follow-up period (group R), switched memory B cells did not increase significantly (median increase of 4% from baseline [IQR −6, 32]) (Figures 5A and B).

To correct for variability in the duration of follow-up, we calculated, for each patient, the yearly rate at which switched memory B cells increased over time, determining the slope of the line passing through the 2 points. The slope of the line for MTX plus TNFi–treated patients who experienced active arthritis or uveitis was significantly higher than the slope of the line for MTX plus TNFi–treated patients who achieved and maintained remission

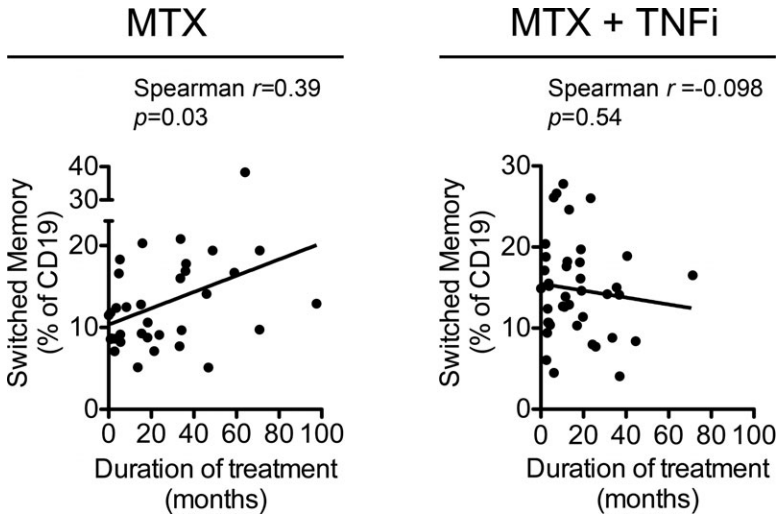

Figure 4. Correlation between the percentage of switched memory B cells and duration of treatment in patients treated with methotrexate (MTX) alone (n = 34) or with MTX plus tumor necrosis factor inhibitors (TNFi) (n = 40).

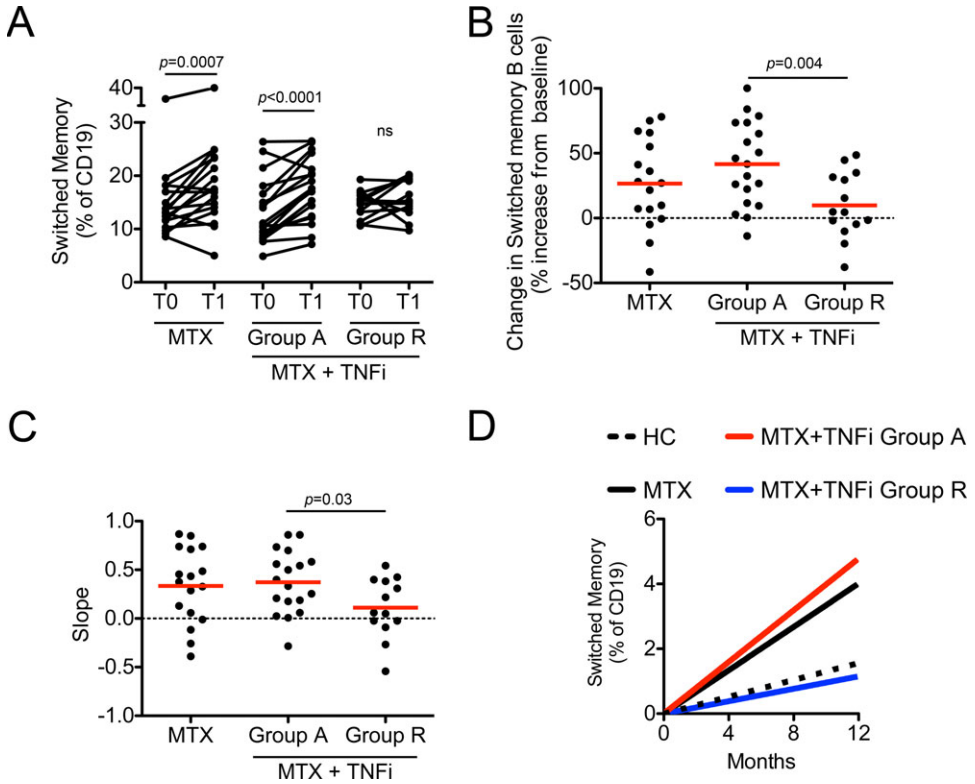

Figure 5. **A,** Percentage of switched memory B cells at baseline (T0) and after 12 months (T1) in patients treated with methotrexate (MTX) alone (n = 17) or with MTX plus tumor necrosis factor inhibitors (TNFi) (n = 33). Those treated with MTX plus TNFi were divided into those who achieved and maintained remission (group R) (n = 14) and those who experienced disease flares (group A) (n = 19). **B,** Percentage increase from baseline (dashed line) of switched memory B cells in the 3 groups of patients described in **A**. **C,** Slopes expressing the steepness of the line conjoining the percentages of switched memory B cells at baseline (dashed line) and at the second blood drawing. **D,** Illustration of the rate at which switched memory B cells increased over time. Using the average slope for patients treated with MTX alone, those treated with MTX plus TNFi who achieved remission, and those treated with MTX plus TNFi who had disease flares, we modeled the functions expressing the yearly increase in switched memory B cells in the 3 groups of patients. In **B** and **C**, symbols represent individual subjects; solid horizontal lines indicate the median. NS = not significant; HC = healthy controls.

(Figure 5C). Knowing the average slope for the different groups of patients, we modeled the equation defining the rate at which switched memory B cells increased over time. It is evident that during a period of 12 months, switched memory B cells increased by ~4% per year in patients receiving MTX alone and 4.7% per year in patients receiving MTX plus TNFi who experienced active arthritis or uveitis (group A). On the other hand, in patients receiving MTX plus TNFi who achieved and maintained remission (group R), the rate was significantly lower (1.2% per year) and comparable to the increase calculated in our cohort of healthy children (1.5% per year) (Figure 5D).

DISCUSSION

We showed that the numbers of circulating switched memory B cells were increased in patients with oligoarticular JIA and patients with polyarticular JIA, especially in those with disease onset before age 6 years. We also showed that switched memory B cells were the most represented B cell subset in SF, and that SF switched memory B cells produced ANAs. Importantly, we found that changes in the frequency of peripheral blood switched memory B cells were associated with a therapeutic response to TNFi.

Previous studies have analyzed B cell subsets in the blood of JIA patients. In one study, switched memory B cells were found to accumulate in the SF of JIA patients; however, the numbers of switched memory B cells in the blood of JIA patients were found not to be different from the numbers in blood from healthy controls (7). The apparent discrepancy with our findings might be explained by differences in disease severity (only 1 patient was receiving TNFi [7]) and by differences in the controls. That study had a small group of controls (n = 20) with a mean age comparable to that of patients. However, no

information was provided about the distribution of B cell subsets across the different ages, and patients and controls of different ages were not compared. More recently, a study of B cell subsets in JIA patients (19) demonstrated that different treatments, including TNFi, did not directly affect circulating memory B cells. That study did not include a longitudinal evaluation; moreover, a comparison with our data is not possible because various subsets of patients with JIA were included, and no comparison with age-matched healthy controls was available.

In our study we evaluated a large number of patients; we focused on 2 relatively homogeneous subsets of patients with JIA, excluding those with rheumatoid factor, enthesitis-related arthritis, psoriatic arthritis, or systemic-onset arthritis. We also used as a control group a large series of healthy children across all ages. The expansion of switched memory B cells was associated with age at onset, being significantly more pronounced in patients with early-onset JIA (presenting before age 6 years). Interestingly, age at onset has been reported to distinguish patients with different pathophysiologic mechanisms (5). A study of HLA association in JIA showed that HLA–DR5 increases the risk of developing JIA early in life (ages 0–8 years) but not at later ages (4). A B cell signature has been shown to characterize patients with disease onset before age 6 years (5); interestingly, this B cell signature was able to distinguish patients with early-onset JIA from those with late-onset JIA, regardless of the number of affected joints at presentation, and from patients with systemic-onset JIA.

We speculate that 2 main mechanisms, not necessarily mutually exclusive, may explain the expansion of switched memory B cells in JIA. First, B cells from patients with JIA may bear an intrinsic lower threshold for activation, as reported for other autoimmune diseases (20), favoring IgG switching and differentiation into memory B cells. Second, since switched memory B cells develop in GCs, the expansion of switched memory B cells may be the consequence of enhanced GC formation. Two pieces of evidence support the latter hypothesis. A genome-wide association study found that a coding single-nucleotide polymorphism in the lymphotoxin β receptor gene was associated with the development of oligoarticular JIA and polyarticular JIA (21). Indeed, the lymphotoxin axis plays a crucial role in GC development (22). Moreover, in the synovial membrane of patients with oligoarticular JIA or polyarticular JIA, the presence of organized B and T cell follicles and the presence of GCs within these structures correlated with the presence of ANAs (23).

As mentioned previously, switched memory B cells are the main subset of B cells found in SF from patients with oligoarticular JIA and those with polyarticular JIA. Our finding that switched memory B cells from SF produce ANAs suggests a direct link between this cell subset and the typical autoimmune feature of the disease. Further pointing to their potential pathogenic role, switched memory B cells in SF from JIA patients were shown to be efficient antigen-presenting cells and to favor Th1 polarization of T cells (17).

We did not find any association between circulating levels of switched memory B cells and disease activity, as measured by the number of joints with active disease and CRP levels (see Supplementary Figure 3, http://onlinelibrary.wiley.com/doi/10.1002/art.40410/abstract). Circulating memory B cells reflect the overall immune responses of the host; for example, switched memory B cells significantly and quickly expand in response to the environmental pathogen milieu, with vaccination being a well-known example (24). These responses may dilute the contribution of switched memory B cells leaking from the inflamed joints, making it difficult to observe a direct correlation with disease activity or other features of JIA. Another factor that may influence the frequency of switched memory B cells is disease duration, especially in children with early-onset JIA; in patients with longer disease duration, switched memory B cells may accumulate due to the ongoing autoimmune response. However, no significant correlation was observed between frequency of switched memory B cells and disease duration, even when the patients were grouped according to age at disease onset and age at sampling as discussed above (data not shown). Finally, assessing disease activity only through CRP levels and number of joints involved may not be ideal, especially in patients with oligoarticular JIA, who represent a significant proportion of patients in our cohort. Longitudinal studies closely assessing disease activity, disease damage, and long-term outcomes will be needed to investigate whether these parameters correlate with switched memory B cells and their change over time.

The TNF pathway plays a pivotal role in GC development. As predicted from the results of animal studies (9), in RA patients administration of TNFi led to disruption of GC structures in lymphoid tissues by affecting the supporting network of follicular dendritic cells, and, subsequently, to the reduction in the frequency of circulating memory B cells (10). We report that treatment with TNFi affects the expansion of switched memory B cells in patients with JIA, as reflected by the reduction in the rate of accumulation in the periphery. In healthy children, switched memory B cells increase progressively during childhood (12), and indeed we show that switched memory B cells increase constantly at a rate of ~1.5–2% per year until age 18 years (Figures 1 and 5). In JIA patients

studied longitudinally, switched memory B cells increase in the periphery at a much faster rate than that in healthy control children. As predicted by the above-mentioned observations in animals and RA patients, treatment with TNFi affects the rate of switched memory B cell expansion. Interestingly, treatment with TNFi reduces the rate of switched memory B cell expansion to a level comparable to that in healthy controls only in patients achieving and maintaining remission during treatment. In sharp contrast, in patients who either did not achieve remission or had disease flares during treatment with TNFi, the yearly rate of switched memory B cell increase was much higher and comparable to that in patients receiving MTX alone.

The therapeutic benefit of TNFi in arthritis may be secondary to a number of mechanisms, including, for example, rapid effects on proinflammatory cytokine production, as anticipated by the original observation on synoviocytes (25). Interestingly, several studies have shown that in RA patients, switched memory B cells are the target of many biologic drugs (TNFi, rituximab, tocilizumab, and abatacept), and a reduction in this subpopulation is associated with more favorable outcomes (10,26–28). Based on our results and on the above-mentioned observations in lymphoid tissues in humans, it is tempting to speculate that inhibition of GCs and of the generation of switched memory B cells may contribute to the ability of TNFi to induce and maintain disease remission in JIA. In TNFi-treated patients who do not achieve remission or have a disease flare, TNFi are not able to control the disease either because they cannot completely neutralize tissue TNF or because the GC reactions, and possibly the switched memory B cells themselves, do not play a crucial role in this subset of patients.

In conclusion, we show that switched memory B cells are expanded in JIA patients, particularly in those with early onset of disease, further pointing to a peculiar subset of JIA patients with early-onset disease. TNFi limit the expansion of switched memory B cells in patients who respond to treatment and achieve remission. Further studies are necessary to elucidate in greater detail the role of memory B cells in JIA pathogenesis and their correlation with the disease course, and to validate their usefulness as biomarkers of disease classification and response to treatment.

AUTHOR CONTRIBUTIONS

All authors were involved in drafting the article or revising it critically for important intellectual content, and all authors approved the final version to be published. Drs. Marasco and De Benedetti had full access to all of the data in the study and take responsibility for the integrity of the data and the accuracy of the data analysis.

Study conception and design. Marasco, Aquilani, Carsetti, De Benedetti.
Acquisition of data. Marasco, Aquilani, Cascioli, Moneta, Caiello, Farroni, Giorda, D'Oria, Magni-Manzoni.
Analysis and interpretation of data. Marasco, Aquilani, Cascioli, Pires Marafon, Magni-Manzoni.

REFERENCES

1. Petty RE, Southwood TR, Manners P, Baum J, Glass DN, Goldenberg J, et al. International League of Associations for Rheumatology classification of juvenile idiopathic arthritis: second revision, Edmonton, 2001. J Rheumatol 2004;31:390–2.
2. Martini A. JIA in 2011: new takes on categorization and treatment. Nat Rev Rheumatol 2012;8:67–8.
3. Martini A, Lovell DJ. Juvenile idiopathic arthritis: state of the art and future perspectives. Ann Rheum Dis 2010;69:1260–3.
4. Murray KJ, Moroldo MB, Donnelly P, Prahalad S, Passo MH, Giannini EH, et al. Age-specific effects of juvenile rheumatoid arthritis–associated HLA alleles. Arthritis Rheum 1999;42:1843–53.
5. Barnes MG, Grom AA, Thompson SD, Griffin TA, Luyrink LK, Colbert RA, et al. Biologic similarities based on age at onset in oligoarticular and polyarticular subtypes of juvenile idiopathic arthritis. Arthritis Rheum 2010;62:3249–58.
6. Ravelli A, Varnier GC, Oliveira S, Castell E, Arguedas O, Magnani A, et al. Antinuclear antibody–positive patients should be grouped as a separate category in the classification of juvenile idiopathic arthritis. Arthritis Rheum 2011;63:267–75.
7. Corcione A, Ferlito F, Gattorno M, Gregorio A, Pistorio A, Gastaldi R, et al. Phenotypic and functional characterization of switch memory B cells from patients with oligoarticular juvenile idiopathic arthritis. Arthritis Res Ther 2009;11:R150.
8. Wiegering V, Girschick HJ, Morbach H. B-cell pathology in juvenile idiopathic arthritis. Arthritis 2010;2010:759868.
9. Pasparakis M, Alexopoulou L, Episkopou V, Kollias G. Immune and inflammatory responses in TNF α-deficient mice: a critical requirement for TNF α in the formation of primary B cell follicles, follicular dendritic cell networks and germinal centers, and in the maturation of the humoral immune response. J Exp Med 1996;184:1397–411.
10. Anolik JH, Ravikumar R, Barnard J, Owen T, Almudevar A, Milner EC, et al. Cutting edge: anti-tumor necrosis factor therapy in rheumatoid arthritis inhibits memory B lymphocytes via effects on lymphoid germinal centers and follicular dendritic cell networks. J Immunol 2008;180:688–92.
11. Wallace CA, Ruperto N, Giannini E. Preliminary criteria for clinical remission for select categories of juvenile idiopathic arthritis. J Rheumatol 2004;31:2290–4.
12. Marasco E, Farroni C, Cascioli S, Marcellini V, Scarsella M, Giorda E, et al. B-cell activation with CD40L or CpG measures the function of B-cell subsets and identifies specific defects in immunodeficient patients. Eur J Immunol 2017;47:131–43.
13. Wouters CH, Ceuppens JL, Stevens EA. Different circulating lymphocyte profiles in patients with different subtypes of juvenile idiopathic arthritis. Clin Exp Rheumatol 2002;20:239–48.
14. Duchamp M, Sterlin D, Diabate A, Uring-Lambert B, Guerin-El Khourouj V, Le Mauff B, et al. B-cell subpopulations in children: national reference values. Immun Inflamm Dis 2014;2:131–40.
15. Piatosa B, Wolska-Kusnierz B, Pac M, Siewiera K, Galkowska E, Bernatowska E. B cell subsets in healthy children: reference values for evaluation of B cell maturation process in peripheral blood. Cytometry B Clin Cytom 2010;78:372–81.
16. Aranburu A, Piano Mortari E, Baban A, Giorda E, Cascioli S, Marcellini V, et al. Human B-cell memory is shaped by age- and tissue-specific T-independent and GC-dependent events. Eur J Immunol 2017;47:327–44.
17. Morbach H, Wiegering V, Richl P, Schwarz T, Suffa N, Eichhorn EM, et al. Activated memory B cells may function as antigen-presenting

cells in the joints of children with juvenile idiopathic arthritis. Arthritis Rheum 2011;63:3458–66.
18. Capolunghi F, Cascioli S, Giorda E, Rosado MM, Plebani A, Auriti C, et al. CpG drives human transitional B cells to terminal differentiation and production of natural antibodies. J Immunol 2008;180:800–8.
19. Glaesener S, Quách TD, Onken N, Weller-Heinemann F, Dressler F, Huppertz HI, et al. Distinct effects of methotrexate and etanercept on the B cell compartment in patients with juvenile idiopathic arthritis. Arthritis Rheumatol 2014;66:2590–600.
20. Manjarrez-Orduno N, Marasco E, Chung SA, Katz MS, Kiridly JF, Simpfendorfer KR, et al. CSK regulatory polymorphism is associated with systemic lupus erythematosus and influences B-cell signaling and activation. Nat Genet 2012;44:1227–30.
21. Hinks A, Cobb J, Marion MC, Prahalad S, Sudman M, Bowes J, et al. Dense genotyping of immune-related disease regions identifies 14 new susceptibility loci for juvenile idiopathic arthritis. Nat Genet 2013;45:664–9.
22. Endres R, Alimzhanov MB, Plitz T, Futterer A, Kosco-Vilbois MH, Nedospasov SA, et al. Mature follicular dendritic cell networks depend on expression of lymphotoxin β receptor by radioresistant stromal cells and of lymphotoxin β and tumor necrosis factor by B cells. J Exp Med 1999;189:159–68.
23. Gregorio A, Gambini C, Gerloni V, Parafioriti A, Sormani MP, Gregorio S, et al. Lymphoid neogenesis in juvenile idiopathic arthritis correlates with ANA positivity and plasma cells infiltration. Rheumatology (Oxford) 2007;46:308–13.
24. Tsang JS, Schwartzberg PL, Kotliarov Y, Biancotto A, Xie Z, Germain RN, et al. Global analyses of human immune variation reveal baseline predictors of postvaccination responses. Cell 2014;157:499–513.
25. Brennan FM, Chantry D, Jackson A, Maini R, Feldmann M. Inhibitory effect of TNF α antibodies on synovial cell interleukin-1 production in rheumatoid arthritis. Lancet 1989;2:244–7.
26. Roll P, Dörner T, Tony HP. Anti-CD20 therapy in patients with rheumatoid arthritis: predictors of response and B cell subset regeneration after repeated treatment. Arthritis Rheum 2008;58:1566–75.
27. Muhammad K, Roll P, Seibold T, Kleinert S, Einsele H, Dorner T, et al. Impact of IL-6 receptor inhibition on human memory B cells in vivo: impaired somatic hypermutation in preswitch memory B cells and modulation of mutational targeting in memory B cells. Ann Rheum Dis 2011;70:1507–10.
28. Scarsi M, Paolini L, Ricotta D, Pedrini A, Piantoni S, Caimi L, et al. Abatacept reduces levels of switched memory B cells, autoantibodies, and immunoglobulins in patients with rheumatoid arthritis. J Rheumatol 2014;41:666–72.

ARTHRITIS & RHEUMATOLOGY
Vol. 70, No. 4, April 2018, pp 616–624
DOI 10.1002/art.40417

Features, Treatment, and Outcomes of Macrophage Activation Syndrome in Childhood-Onset Systemic Lupus Erythematosus

R. Ezequiel Borgia, Maya Gerstein, Deborah M. Levy, Earl D. Silverman, and Linda T. Hiraki

Objective. **To describe the features and treatment of macrophage activation syndrome (MAS) in a single-center cohort of patients with childhood-onset systemic lupus erythematosus (SLE), and to compare childhood-onset SLE manifestations and outcomes between those with and those without MAS.**

Methods. **We included all patients with childhood-onset SLE followed up at The Hospital for Sick Children from 2002 to 2012, and identified those also diagnosed as having MAS. Demographic, clinical, and laboratory features of MAS and SLE, medication use, hospital and pediatric intensive care unit (PICU) admissions, as well as damage indices and mortality data were extracted from the Lupus database. Student's *t*-tests and Fisher's exact tests were used to compare continuous and categorical variables, respectively. We calculated incidence rate ratios of hospital and PICU admissions comparing patients with and those without MAS, using Poisson models. Kaplan-Meier survival analysis was used to examine the time to disease damage accrual.**

Results. **Of the 403 patients with childhood-onset SLE, 38 (9%) had MAS. The majority (68%) had concomitant MAS and SLE diagnoses. Fever was the most common MAS clinical feature. The frequency of renal and central nervous system disease, hospital admissions, the average daily dose of steroids, and time to disease damage were similar between those with and those without MAS. We observed a higher mortality rate among those with MAS (5%) than those without MAS (0.2%) ($P = 0.02$).**

Conclusion. **MAS was most likely to develop concomitantly with childhood-onset SLE diagnosis. The majority of the MAS patients were successfully treated with corticosteroids with no MAS relapses. Although the numbers were small, there was a higher risk of death associated with MAS compared to SLE without MAS.**

Macrophage activation syndrome (MAS) is a potentially life-threatening complication of systemic lupus erythematosus (SLE) characterized by excessive activation and proliferation of T lymphocytes and macrophages and a consequent massive production of cytokines, or "cytokine storm" (1–4). MAS is considered a secondary or acquired form of hemophagocytic lymphohistiocytosis (HLH) and is usually associated with infection, rheumatic disease, or malignancy (5). Primary or familial HLH is caused by mutations in genes involved in the granule-dependent cytolytic secretory pathway. Despite the different inciting causes, primary and secondary HLH share similar clinical and biochemical features (5).

MAS was initially described in association with systemic juvenile idiopathic arthritis (JIA) (6); however, it has been increasingly recognized as a complication of SLE (3,5,7). There are only a few studies examining the clinical and laboratory features of MAS in childhood-onset SLE, and most of the available data are based on cross-sectional studies and case reports (3,8–12). As a result, the true prevalence of MAS in childhood-onset SLE is unknown. MAS is life-threatening, with mortality rates ranging from 8% to 22% in pediatric autoimmune diseases generally (11,13) and 10–22% in MAS complicating childhood-onset SLE specifically (3,8,14). Yet there are limited available data on long-term outcomes, including rates of recurrence of MAS in childhood-onset SLE (3,8,14). Moreover, it remains unclear whether childhood-onset SLE complicated by MAS has a distinctive

Supported by the Canadian Institute of Health Research (Fellowship award to Dr. Hiraki).

R. Ezequiel Borgia, MD, Maya Gerstein, MD, Deborah M. Levy, MD, MS, FRCPC, Earl D. Silverman, MD, FRCPC, Linda T. Hiraki, MD, FRCPC, MS, ScD: The Hospital for Sick Children and University of Toronto, Toronto, Ontario, Canada.

Drs. Silverman and Hiraki contributed equally to this work.

Address correspondence to Linda T. Hiraki, MD, FRCPC, MS, ScD, Division of Rheumatology, Research Institute, The Hospital for Sick Children, PGCRL, 686 Bay Street, Toronto, Ontario M5G 0A4, Canada. E-mail: linda.hiraki@sickkids.ca.

Submitted for publication May 31, 2017; accepted in revised form January 9, 2018.

disease course in terms of organ involvement and damage accrual in long-term follow-up when compared to childhood-onset SLE without MAS.

The aims of this study were to 1) describe the clinical and laboratory characteristics, outcomes, and treatment of MAS in a large childhood-onset SLE cohort from a single pediatric tertiary care center; and 2) compare clinical and laboratory SLE features and disease-associated outcomes between childhood-onset SLE patients with MAS and those without MAS.

PATIENTS AND METHODS

Study population. We included all patients diagnosed as having and followed up for childhood-onset SLE at The Hospital for Sick Children (SickKids) between January 2002 and December 2012 (n = 403). All patients met the American College of Rheumatology (ACR) and/or Systemic Lupus International Collaborating Clinics (SLICC) classification criteria for SLE (15,16). Since there are no validated or universally accepted diagnostic criteria for MAS in SLE, the diagnosis of MAS was based on the treating pediatric rheumatologist's expert opinion at the time of the initial presentation. The treating pediatric rheumatologists had 35 years (EDS) and >15 years (DML) of experience in caring for children with SLE. These diagnoses were independently reviewed by one investigator (MG), and any questionable diagnoses were brought to the attention of all authors. There were 4 cases in which the diagnosis of MAS was disputed. After individual case review, 2 were excluded as MAS cases. The final decision regarding MAS diagnosis and subsequent inclusion of the MAS patients in the study was made by agreement among all authors. Institutional Research Ethics Board (REB) approval was obtained prior to initiation of the study (REB #1000035186).

Variables. Prospectively collected demographic, clinical, and laboratory data on SLE and MAS features were extracted from the SickKids Lupus database and supplemented by data from hospital medical records. The diagnoses of MAS and childhood-onset SLE were considered "concomitant" if MAS was diagnosed within 7 days of childhood-onset SLE.

Demographic features included age at diagnosis of childhood-onset SLE, age at diagnosis of MAS, and sex. The following clinical MAS features (3,17) were extracted: fever, hepatosplenomegaly, lymphadenopathy, clinical bleeding episodes (hemorrhages), and central nervous system (CNS) involvement. CNS involvement secondary to MAS was defined as any evidence of altered level of consciousness or seizures at the time of MAS presentation, excluding those associated with infections, drugs, or metabolic causes. Since MAS with CNS involvement may overlap with the clinical spectrum of neuropsychiatric SLE (NPSLE) (18), the definition of CNS disease secondary to MAS was based on a multidisciplinary team approach including pediatric neurologists, neuroradiologists, oncologists, and rheumatologists.

Laboratory MAS features extracted included platelet count, hemoglobin, white blood cell differential count, alanine aminotransferase, aspartate aminotransferase (AST), lactate dehydrogenase (LDH), ferritin, fibrinogen, triglyceride level, D-dimers, partial thromboplastin time, serum sodium level, C-reactive protein level, and erythrocyte sedimentation rate. Additional laboratory features such as natural killer (NK) cell cytotoxic activity, soluble interleukin-2 receptor (sIL-2R) levels, bone marrow aspirate/biopsy findings, and evaluations for infection were also included when available. We also reviewed the results of Sanger sequencing of exons 2 and 3 in the perforin gene (*PRF1*) (19) and of exome sequencing of known HLH-associated variants in genes (*AP3B1*, *BLOC1S6*, *CD27*, *ITK*, *LYST*, *NLRC4*, *PRF1*, *RAB27A*, *SH2D1A*, *SLC7A7*, *STX11*, *STXBP2*, *UNC13D*, and *XIAP*) (20) when available. We applied the preliminary diagnostic criteria for MAS proposed by Parodi et al (3) in our MAS cohort. Medications prescribed for MAS treatment were reviewed and reported. Calcineurin inhibitor therapy was attributed to childhood-onset SLE in those with concomitant membranous lupus nephritis and MAS. Otherwise, calcineurin inhibitor use was attributed to MAS.

All clinical and laboratory SLE features (15,16) available during complete follow-up were extracted. Patients with

Table 1. Demographic, clinical, and laboratory features of patients with childhood-onset SLE with MAS and those without MAS*

	Patients with MAS (n = 38)	Patients without MAS (n = 365)	*P*
Female	30 (79)	302 (83)	0.51
Mean ± SD age at SLE diagnosis, years	13.7 ± 2.8	13.2 ± 3.2	0.35
Mean ± SD duration of follow-up, years	3.5 ± 1.6	4 ± 2.4	0.21
SLE clinical features			
Malar rash	25 (66)	288 (79)	0.10
Oral or nasal ulcers	15 (39)	131 (36)	0.72
Arthritis	22 (58)	258 (71)	0.14
Serositis†	9 (24)	48 (13)	0.09
Myositis	1 (3)	17 (5)	1.00
Headaches	9 (24)	81 (22)	0.52
Lupus nephritis	18 (47)	115 (32)	0.07
Mesangial	3 (17)	6 (5)	0.04‡
Proliferative	11 (61)	66 (57)	0.80
Membranous	3 (17)	25 (22)	0.76
Mixed proliferative/ membranous	1 (6)	18 (16)	0.47
CNS involvement	10 (26)	85 (23)	0.68
Psychosis	4 (40)	43 (51)	0.74
Cognitive dysfunction	4 (40)	32 (38)	1.00
Acute confusional state	2 (20)	10 (12)	0.60
SLE laboratory features			
Hematologic involvement	34 (89)	282 (77)	0.09
Thrombocytopenia	19 (56)	95 (34)	0.004‡
Lymphopenia	29 (85)	173 (61)	0.001‡
Coombs-positive hemolytic anemia	17 (50)	96 (34)	0.02‡
Specific autoantibodies			
Anti-dsDNA	33 (87)	202 (55)	0.0001‡
Anti-Sm	17 (45)	99 (27)	0.04‡
Anti-RNP	17 (45)	137 (38)	0.39
Anti-Ro	18 (47)	138 (38)	0.29
Anti-La	6 (16)	54 (15)	0.81
Lupus anticoagulant	3 (8)	43 (12)	0.60
Anticardiolipin	17 (45)	127 (35)	0.29

* Except where indicated otherwise, values are the number (%). MAS = macrophage activation syndrome; CNS = central nervous system; anti-dsDNA = anti–double-stranded DNA.
† Pericarditis and/or pleuritis.
‡ Significant Bonferroni-corrected *P* value: $P < 0.005$ (corrected for number of American College of Rheumatology criteria for systemic lupus erythematosus [SLE]) and $P < 0.007$ (corrected for specific autoantibodies).

clinical evidence of lupus nephritis underwent kidney biopsy unless contraindicated. Lupus nephritis was classified according to the International Society of Nephrology/Renal Pathology Society 2003 revised criteria (21). The definition of CNS disease secondary to SLE was based on ACR 1999 nomenclature and case definitions for NPSLE syndromes (18).

In order to assess SLE disease severity and long-term SLE outcomes in patients with MAS and patients without MAS, the following variables were recorded: immunosuppressive drug use, average daily dose of corticosteroids, and number of pediatric intensive care unit (PICU) admissions during follow-up. Hospital admissions with a length of stay of ≥72 hours were considered clinically relevant in order to assess and compare lupus disease severity between patients with MAS and patients without MAS over the follow-up period. However, hospital admissions that were entirely for medical procedures (e.g., for kidney biopsy) were excluded since they were not considered an accurate indicator of disease severity. All deaths during follow-up at SickKids were documented in both groups. The SLICC/ACR Damage Index (SDI), previously validated in childhood-onset SLE, was used to assess damage 6 months after diagnosis of childhood-onset SLE and at each subsequent visit in both groups (22,23). All variables were collected until the last lupus clinic visit at SickKids.

Statistical analysis. Demographic data, clinical features, and laboratory features were analyzed using descriptive statistics. Continuous and categorical variables were compared between patients with and those without MAS, using Student's *t*-test and Fisher's exact test, respectively. Incidence rate ratios (IRRs) were calculated using Poisson models to compare the rates of hospital and PICU admissions between those with and those without MAS. Kaplan-Meier survival analyses were used to examine the rate of disease damage accrual over time in both cohorts. *P* values less than 0.05 were considered statistically significant, and a Bonferroni correction for multiple testing was used when testing multiple independent associations. All statistical analyses were performed using Stata release 14 (StataCorp).

RESULTS

Demographic data. Of the 403 patients in our childhood-onset SLE cohort who were diagnosed and followed up at SickKids Hospital, 38 (9%) had MAS. The majority of the MAS patients were female (79%), the mean ± SD age at SLE diagnosis was 13.7 ± 2.8 years, and the mean ± SD length of follow-up was 3.5 ± 1.6 years. We did not observe a difference in age at SLE diagnosis or in the duration of follow-up between the patients with MAS and the patients without MAS (Table 1 and Figure 1). MAS was diagnosed concomitantly with childhood-onset SLE in the majority of the patients (68%), and 18% were diagnosed with MAS within 180 days of childhood-onset SLE diagnosis. Only 11% developed MAS >180 days after diagnosis of childhood-onset SLE. In 1 patient, the diagnosis of MAS secondary to Kikuchi-Fujimoto disease preceded the diagnosis of childhood-onset SLE by 3 years. There was no statistically significant change in annual incidence of MAS over the study period in our childhood-onset SLE cohort (data not shown).

Clinical and laboratory MAS features at presentation and initial treatment in the MAS cohort. *Clinical and laboratory features of MAS.* All MAS patients had fever at presentation. The second most common manifestation was generalized lymphadenopathy (24%)

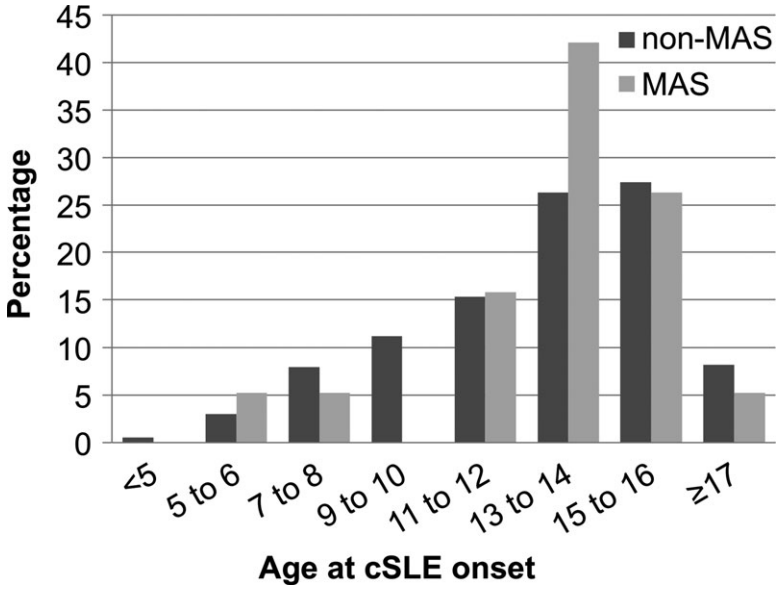

Figure 1. Age at diagnosis of childhood-onset systemic lupus erythematosus (cSLE) in patients with macrophage activation syndrome (MAS; n = 38) and patients without MAS (n = 365). The x-axis shows the age in years at diagnosis of childhood-onset SLE, and the y-axis shows the percentage of patients with MAS and those without MAS diagnosed in each age category.

Table 2. Frequency of clinical and laboratory MAS features and treatment*

	Number (%)	Median (IQR)	Abnormal SickKids reference values
Clinical features (n = 38)†			
Fever‡	38 (100)	–	–
Generalized lymphadenopathy	9 (24)	–	–
CNS dysfunction§	7 (18)	–	–
Hepatomegaly	7 (18)	–	–
Hemorrhage¶	5 (13)	–	–
Splenomegaly	4 (11)	–	–
Laboratory features#			
Hemoglobin, gm/liter (n = 38)**	37 (97)	94 (84–107)	Female <120; male <140
White blood cell count, $\times 10^9$/liter (n = 38)**	34 (89)	2.15 (1.6–2.9)	<4
Neutrophil count, $\times 10^9$/liter (n = 38)	32 (84)	1.1 (0.7–1.7)	<2
Platelet count, $\times 10^9$/liter (n = 38)**	23 (61)	140 (107–166)	<150
AST, units/liter (n = 38)**	37 (97)	123 (73–247)	>31
LDH, IU/liter (n = 36)**	35 (97)	2,186 (1,189–3,092)	>580
ALT, units/liter (n = 38)	33 (87)	83 (50–137)	>40
PTT, seconds (n = 33)	18 (55)	35 (31–45)	>36
D-dimer, ng/ml (n = 35)	17 (49)	240 (4.7–1,346)	>0.51
Fibrinogen, gm/liter (n = 35)**	6 (17)	2.8 (2.1–3.4)	<1.9
ESR, mm/hour (n = 38)	37 (97)	64 (32–103)	>10
CRP, mg/liter (n = 24)	21 (88)	18.4 (1.9–48.5)	>1.0
Ferritin, μg/liter (n = 36)**	36 (100)	2,453 (1,072–5,516)	>78.8
Triglycerides, mmoles/liter (n = 35)**	19 (54)	2.4 (1.9–3.4)	>1.3
Sodium, mmoles/liter (n = 37)	15 (41)	135 (134–139)	<135
Bone marrow aspirate/biopsy findings (n = 25)			
Hemophagocytosis	8 (32)	–	–
MAS treatment (n = 38)			
IV methylprednisolone	26 (68)	–	–
IVIG	22 (58)	–	–
Calcineurin inhibitor††	13 (34)	–	–
Prednisone (oral) alone	7 (18)	–	–
Dexamethasone (oral or intravenous) alone or in combination with other medications	6 (16)	–	–
Etoposide	5 (13)	–	–
Anakinra	2 (5)	–	–
Intrathecal methotrexate	1 (3)	–	–
Alemtuzumab	1 (3)	–	–

* ALT = alanine aminotransferase; PTT = partial thromboplastin time; ESR = erythrocyte sedimentation rate; CRP = C-reactive protein; IV = intravenous; IVIG = IV immunoglobulin.

† Clinical macrophage activation syndrome (MAS) features at the time of diagnosis. Fever, central nervous system (CNS) dysfunction, hepatomegaly, hemorrhage, and splenomegaly were also proposed by Parodi et al (3) as clinical features of MAS.

‡ Fever was defined as a temperature of >38°C (rectal), >37.7°C (oral), or >37.5°C (axillary or otic).

§ CNS dysfunction is defined as irritability, disorientation, lethargy, headache, seizures, or coma (excluding those related to infection, drugs, or metabolic causes).

¶ Hemorrhage is defined as at least one of the following: pulmonary hemorrhage, cerebral hemorrhage, hematochezia, epistaxis, or gum bleeding with heavy menstruation.

Percentages are the proportion of MAS patients with abnormal Hospital for Sick Children (SickKids) laboratory reference values prior to the initiation of MAS treatment. The median (interquartile range [IQR]) values are for the most abnormal laboratory value at MAS presentation and prior to MAS treatment.

** The number (%) of MAS patients who met the MAS laboratory criteria proposed by Parodi et al (3) at the time of MAS diagnosis and prior to MAS treatment was as follows: for hemoglobin ≤9 gm/liter, 14 (37%); for white blood cell count ≤4.0 $\times 10^9$/liter, 34 (89%); for platelet count ≤150 cells $\times 10^9$/liter, 23 (61%); for aspartate aminotransferase (AST) >40 units/liter, 37 (97%); for lactate dehydrogenase (LDH) >567 IU/liter, 35 (97%); for fibrinogen ≤1.5 gm/liter, 3 (9%); for ferritin >500 μg/liter, 32 (89%); and for triglycerides >2 mmoles/liter (or >178 mg/dl), 25 (71%).

†† Tacrolimus (for 2 patients) or cyclosporine (for 11 patients).

followed by CNS involvement secondary to MAS (18%) (Table 2). Attribution of CNS manifestations to either MAS or childhood-onset SLE was difficult in some cases, but upon review, attribution was agreed upon by all authors. An example of MAS CNS involvement included focal seizures with residual hemiparesis and subsequent coma with biochemical evidence of MAS. Another patient had onset of CNS lupus manifestations, including visual hallucinations and cognitive slowing, 1 week after treatment for MAS. Due to the nature and timing of her symptoms, and since other MAS manifestations such as pancytopenia and diffuse lymphadenopathy improved, her CNS manifestations were attributed to childhood-onset SLE.

All MAS patients had ferritin levels above the laboratory reference range. Elevated LDH and AST levels were each present in 97% of the patients (Table 2). NK cell cytotoxic activity was found to be normal in all 3 patients tested, and sIL-2R levels were elevated in all 4 patients tested (median concentration 3,239 units/ml [range 1,047–7,012]; normal range 460–1,580 units/ml). Seven patients had *PRF1* sequencing, and 6 had exome sequencing of HLH-associated genes. The majority (11 of 13) did not carry variants associated with HLH, with the remainder of those tested being heterozygous carriers of variants of uncertain significance in *LYST* or *RAB27A* (minor allele frequencies of 0.001–0.015 depending on the ancestral population).

There was evidence of hemophagocytosis in 32% of the patients who underwent bone marrow aspirate/biopsy (Table 2). A minority of patients (16%) had documented concomitant infections at the time of MAS presentation (1 group A streptococcal bacteremia, 1 herpes simplex virus type 1 cutaneous infection, 1 acute Epstein-Barr virus infection, 1 *Escherichia coli* urinary tract infection [UTI], 1 *Candida* UTI, and 1 disseminated tuberculosis infection), and 1 patient received the meningococcal vaccination 2 weeks prior to MAS diagnosis. All patients with childhood-onset SLE clinically diagnosed as having MAS met the preliminary diagnostic criteria for MAS proposed by Parodi et al (3) (Table 2).

MAS treatment. All MAS patients were treated with corticosteroids (Table 2). The majority (68%) received intravenous (IV) high-dose methylprednisolone followed by either oral prednisone or lower-dose IV methylprednisolone. Twenty-two patients (58%) received IV immunoglobulin. One-third of the patients received an oral calcineurin inhibitor, and 13% received etoposide. Two patients died during the acute phase of MAS. Both required anakinra and plasmapheresis, while one also received alemtuzumab and intrathecal methotrexate due to severe, refractory CNS disease secondary to MAS (Table 2).

MAS outcome. The mean ± SD duration of follow-up from the time of SLE diagnosis to the last visit was 3.5 ± 1.6 years for MAS patients. All patients required hospital admission at MAS diagnosis, and 21% also required PICU admission. Of the 2 MAS patients who died during the acute episode, one had CNS disease and disseminated tuberculosis, and the other had CNS involvement (brain biopsy showing CD163+ macrophage, erythrophagocyte, and lymphophagocyte infiltrate).

Three of the 5 patients with seizures had no further seizure recurrence after the MAS episode resolved. The 2 patients who initially presented with isolated altered levels of consciousness had normal brain magnetic resonance imaging scans at presentation and completely recovered without further CNS involvement. None of the MAS patients experienced a MAS recurrence during follow-up at SickKids.

Comparison of SLE clinical and laboratory features and treatment between patients with MAS and those without MAS. The mean ± SD duration of follow-up among patients with childhood-onset SLE without MAS was 4 ± 2.4 years. Over the follow-up period, a higher proportion of those with MAS had lymphopenia, thrombocytopenia, and anti–double-stranded DNA (anti-dsDNA) antibodies compared to the group without MAS ($P < 0.01$) (Table 1). The average daily dose of prednisone or prednisone equivalent over the course of follow-up (including use for MAS treatment) was similar between the cohort with MAS and the cohort without MAS (mean ± SD 18.3 ± 7.3 mg/day versus 18.6 ± 18.7 mg/day, respectively; $P = 0.94$), as was the proportion of patients who received immunosuppressive agents during the follow-up period (Table 3). There was a trend toward more frequent azathioprine use in the group without MAS than in the group with MAS, but this was not statistically significant after Bonferroni correction for multiple comparisons (Table 3).

SLE outcomes in the patients with MAS and those without MAS. There were no differences in the rate of hospital or PICU admissions per year between the patients with MAS and those without MAS during the follow-up period (IRR 1.11 [95% confidence interval 0.83–1.48] for hospital admissions and IRR 1.60 [95% confidence interval 0.74–3.18] for PICU admissions in the group with MAS compared to the group without MAS).

Table 3. Immunosuppressive agents used to treat childhood-onset SLE during disease follow-up*

	Patients with MAS (n = 38)	Patients without MAS (n = 297)
Mycophenolate mofetil or mycophenolate sodium	19 (50)	117 (39)
Azathioprine	11 (29)	148 (50)†
IV cyclophosphamide	11 (29)	65 (22)
Methotrexate	3 (8)	49 (16)
Calcineurin inhibitors‡	3 (8)	21 (7)
IVIG§	1 (3)	25 (8)
Rituximab	0	28 (9)

* Values are the number (%). All patients with macrophage activation syndrome (MAS) received either corticosteroids or other immunosuppressive drugs during follow-up. Of the 365 patients without MAS, 68 (18%) did not receive any immunosuppressive agents (including corticosteroids) during follow-up. IV = intravenous; IVIG = IV immunoglobulin.

† $P = 0.01$ ($P < 0.007$ following Bonferroni correction for multiple treatments) versus patients with MAS.

‡ Tacrolimus or cyclosporine used to treat childhood-onset systemic lupus erythematosus (SLE) only (excluding use for treatment of MAS).

§ Excluding use for treatment of MAS only.

There was a trend toward a higher proportion of patients with PICU admissions within the first year after diagnosis of childhood-onset SLE in the MAS group (all related to acute MAS presentation) compared to patients without MAS; however, the difference was not statistically significant (23% of the patients with MAS versus 10% of the patients without MAS [$P = 0.05$]).

There was no difference between groups in the proportion of patients who sustained damage (SDI ≥1) during follow-up ($P = 0.3$) (Figure 2). Cataracts were the most common manifestation of damage at the last clinic visit in both groups, followed by avascular necrosis, cognitive impairment, and osteoporosis with fracture or vertebral collapse. Although numbers were small, there was a higher mortality rate in the group with MAS (2 patients [5%]) than in the group without MAS (1 patient [0.3%]) ($P = 0.02$). Both deaths in the MAS cohort occurred in the acute period of MAS presentation, and the death of the patient without MAS occurred 9 years after SLE diagnosis due to a malignancy (Table 4).

DISCUSSION

MAS is an increasingly recognized, life-threatening complication of SLE. However, the natural history of MAS among patients with childhood-onset SLE is unknown. In our population of >400 patients with childhood-onset SLE, those who developed MAS were most likely to be diagnosed as having MAS concomitantly with childhood-onset SLE and did not experience relapses of MAS during the follow-up period. We observed higher rates of lymphopenia, thrombocytopenia, and anti-dsDNA antibody positivity among those with MAS compared to those without MAS. There were no differences in the frequency of other SLE clinical features or in rates of disease damage at last follow-up. Although our mortality numbers were small, we observed a higher mortality rate among those with MAS compared to those without MAS, where deaths in the MAS group occurred in the acute period of MAS disease.

Although the first case of MAS secondary to SLE was reported in 1984, it was not until a 1991 report of 6 cases that MAS was recognized as a complication of SLE (24,25). A 2014 systematic review found 133 cases of MAS secondary to adult SLE reported in the literature, making it the most common cause of MAS in adults with rheumatic diseases (5). There has not been a similar review of MAS in pediatric rheumatology; however, most large series report that MAS is more common in patients with systemic JIA than in those with childhood-onset SLE (8,26). The prevalence of MAS in our childhood-onset SLE cohort of 9% is approximately double the prevalence (4%) reported in reviews and large series examining MAS prevalence in adult SLE (5,26,27). This difference in prevalence may reflect diagnostic bias or a true difference in the risk of MAS between childhood-onset SLE and adult SLE.

Findings in the initial case series suggested that MAS usually occurred at the time of diagnosis of adult SLE (24); however, subsequent studies of adult SLE found that MAS frequently occurred at the time of disease flare as well (28,29). We found that MAS was most likely to develop concomitantly or within 1 month of SLE diagnosis, which is consistent with the findings of other childhood-onset SLE series that examined the timing of MAS relative to SLE diagnosis (3,14). Of note, 1 patient in our cohort developed MAS 3 years prior to childhood-onset SLE diagnosis, and 1 patient who died had SLE

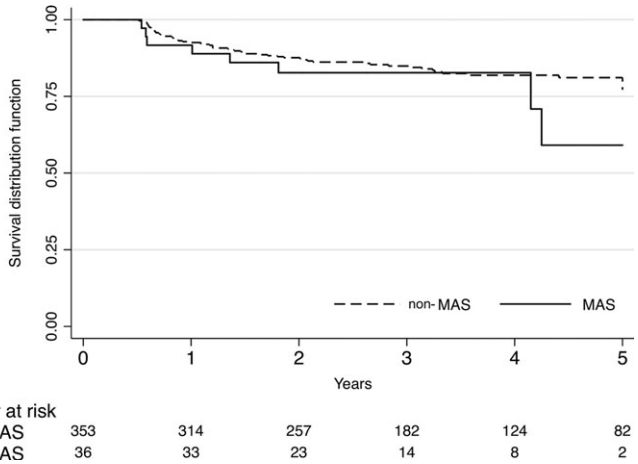

Figure 2. Kaplan-Meier analysis of damage-free survival in patients with childhood-onset systemic lupus erythematosus with macrophage activation syndrome (MAS) and those without MAS. The x-axis shows the time in years, and the y-axis shows the probability of damage-free survival in patients without MAS versus patients with MAS ($P = 0.3$). Values are the number of patients at risk each year.

Table 4. Childhood-onset SLE–related outcomes in patients with MAS and patients without MAS*

	Patients with MAS (n = 38)	Patients without MAS (n = 365)
Deaths	2 (5)†	1 (0.3)‡§
SDI ≥1 at last visit	7 (18)	58 (16)¶
Cataract	6 (16)	27 (7)
Avascular necrosis	2 (5)	15 (4)
Cognitive impairment	1 (3)	10 (3)
Osteoporosis#	0 (0)	10 (3)
Malignancy	0 (0)	1 (0.3)‡

* Values are the number (%).
† Both deaths occurred during the acute phase of macrophage activation syndrome (MAS).
‡ In 1 patient, death occurred 9 years after systemic lupus erythematosus (SLE), diagnosis due to T cell lymphoblastic leukemia following glioblastoma.
§ $P = 0.02$ versus patients with MAS.
¶ Systemic Lupus International Collaborating Clinics/American College of Rheumatology Damage Index (SDI) data were available for 353 of the 365 patients without MAS.
# Defined as a bone density Z score of −2 SD or less, adjusted for age, sex, and bone age, as appropriate, in combination with a fracture or vertebral collapse.

recognized only after death. SLE should be considered in the differential diagnosis of all patients who present with features of MAS even in the absence of clinical findings suggestive of SLE.

Fever was the only clinical MAS feature present in all MAS patients in our cohort, as observed in prior studies of both adult SLE patients and childhood-onset SLE patients (3,7,9). Other clinical features were much less frequently found in our MAS cohort, with generalized lymphadenopathy found in 24% and CNS dysfunction and hepatomegaly each found in 18% of the patients. In contrast, others have reported higher frequencies of lymphadenopathy, hepatomegaly, and CNS dysfunction, in the range of 40–50% (3,7,9). The most common laboratory features in our MAS cohort were elevated AST, LDH, and ferritin levels as well as leukopenia, with rates similar to those in previous studies (3,7).

We observed that only one-third of the MAS patients who underwent a bone marrow aspirate/biopsy had evidence of hemophagocytosis. This rate is lower than rates in other series of adult patients; however, many of those adult series required the presence of hemophagocytosis on bone marrow aspirate/biopsy or lymph node/liver biopsy to make the diagnosis of MAS (1,27,30). We also compared the MAS clinical and laboratory features between those with and those without hemophagocytosis among those who underwent bone marrow aspiration/biopsy (n = 25), and found no significant differences between the groups (data not shown). We suggest that the absence of increased hemophagocytosis on bone marrow examination should not delay the diagnosis of MAS and initiation of therapy. However, bone marrow examination may be required to rule out other processes such as malignancy or infections (e.g., leishmaniasis).

Although MAS has been reported to recur in patients with systemic JIA, recurrence rates are rarely reported in childhood-onset SLE. None of the patients in our cohort experienced a recurrence of MAS during a mean follow-up of 3.5 years. Similarly, other studies of childhood-onset SLE did not observe recurrence of MAS (follow-up times not specified) (1,14). In contrast, 2 studies of adult SLE have shown MAS recurrence in 3 of 12 patients after a mean of 7.1 years of follow-up, and in 4 of 14 adult SLE patients (follow-up time not specified) (1,30). Therefore, although the numbers are small, recurrence of MAS has not been reported in childhood-onset SLE but may occur in up to 25% of cases in adult SLE (1,14,30,31).

We observed a mortality rate of 5% among those with MAS, which is lower than the mortality rate reported in most MAS studies in childhood-onset SLE and adult SLE (up to 22%) (1,3,7,8,14,27,29). In our cohort, 7 MAS patients had CNS manifestations attributed to MAS. Of those, 2 (29%) died with severe CNS involvement and multiple organ failure. (One patient also had concomitant disseminated tuberculosis infection.) Consistent with our findings, a previous study of 19 patients with childhood-onset SLE with MAS suggested that CNS involvement was also associated with a higher mortality rate with multiple organ failure or sepsis frequently as the terminal event (8).

We did not find any significant differences in SLE manifestations between the patients with MAS and those without MAS at presentation or within the first year after diagnosis of SLE (data not shown). An earlier study of 38 patients with childhood-onset SLE and MAS found that these patients had a higher frequency of major organ involvement (lupus nephritis and CNS involvement), hematologic involvement, arthritis, serositis, and oral/nasal ulcers at the time of SLE diagnosis than patients without MAS (n = 387) (3). These differences between studies may reflect differences in the childhood-onset SLE cohorts or applied MAS definitions. However, both our study and the study by Parodi et al (3) showed higher rates of hematologic involvement in the group with MAS than in the group without MAS, which may be the result of cytopenias secondary to MAS itself.

Following the acute illness that was associated with 2 deaths secondary to MAS, we did not find any significant differences in the number of deaths or damage accrual between the cohorts, including overall SDI or any specific damage feature within the score. MAS is a life-threatening complication of childhood-onset SLE and it should be considered an important cause of mortality in childhood-onset SLE. However, if the initial presentation

did not result in death, the long-term outcome seemed to be comparable to that for patients without MAS, and treatment-related damage was not increased in our MAS cohort.

We acknowledge that our study has some limitations. There is currently a lack of validated criteria for MAS in SLE. Hence, we identified patients with MAS based on pediatric rheumatologist expert opinion. However, the diagnosis of MAS was validated by consensus of all the contributing authors. It is therefore possible, but unlikely, that we missed cases. Although all clinical and laboratory data were prospectively collected and entered into our database, we retrospectively reviewed the completeness of data collection with respect to MAS features. Hence, some laboratory data were missing at the time of MAS diagnosis. Although our follow-up extended a mean of 3.5 years, we were unable to obtain data on most patients beyond 18 years of age, into adulthood.

MAS is a potentially fatal complication of pediatric rheumatic diseases. We observed that, unlike in adult SLE, in our childhood-onset SLE cohort MAS was most frequently seen at the time of diagnosis of SLE and did not recur during follow-up. We have demonstrated for the first time that the SLE disease course and outcome did not differ between patients with childhood-onset SLE complicated with MAS and those without MAS. Although a bone marrow examination is frequently warranted in the setting of MAS presentation, in particular to rule out other disease processes, absence of significant hemophagocytosis on bone marrow examination is frequent. The clinical presentation of persistent fever, leukopenia (usually associated with a decrease in a second lineage), and elevated ferritin levels and liver enzymes should raise the suspicion of MAS in patients with childhood-onset SLE.

AUTHOR CONTRIBUTIONS

All authors were involved in drafting the article or revising it critically for important intellectual content, and all authors approved the final version to be published. Dr. Hiraki had full access to all of the data in the study and takes responsibility for the integrity of the data and the accuracy of the data analysis.

Study conception and design. Borgia, Silverman, Hiraki.
Acquisition of data. Borgia, Gerstein, Levy, Silverman, Hiraki.
Analysis and interpretation of data. Borgia, Levy, Silverman, Hiraki.

REFERENCES

1. Lambotte O, Khellaf M, Harmouche H, Bader-Meunier B, Manceron V, Goujard C, et al. Characteristics and long-term outcome of 15 episodes of systemic lupus erythematosus-associated hemophagocytic syndrome. Medicine (Baltimore) 2006;85:169–82.
2. Larroche C, Mouthon L. Pathogenesis of hemophagocytic syndrome (HPS). Autoimmun Rev 2004;3:69–75.
3. Parodi A, Davì S, Pringe AB, Pistorio A, Ruperto N, Magni-Manzoni S, et al. Macrophage activation syndrome in juvenile systemic lupus erythematosus: a multinational multicenter study of thirty-eight patients. Arthritis Rheum 2009;60:3388–99.
4. Grom AA, Mellins ED. Macrophage activation syndrome: advances towards understanding pathogenesis. Curr Opin Rheumatol 2010;22:561–6.
5. Ramos-Casals M, Brito-Zeron P, Lopez-Guillermo A, Khamashta MA, Bosch X. Adult haemophagocytic syndrome. Lancet 2014;383:1503–16.
6. Silverman ED, Miller JJ III, Bernstein B, Shafai T. Consumption coagulopathy associated with systemic juvenile rheumatoid arthritis. J Pediatr 1983;103:872–6.
7. Kumakura S, Murakawa Y. Clinical characteristics and treatment outcomes of autoimmune-associated hemophagocytic syndrome in adults. Arthritis Rheumatol 2014;66:2297–307.
8. Bennett TD, Fluchel M, Hersh AO, Hayward KN, Hersh AL, Brogan TV, et al. Macrophage activation syndrome in children with systemic lupus erythematosus and children with juvenile idiopathic arthritis. Arthritis Rheum 2012;64:4135–42.
9. Gormezano NW, Otsuzi CI, Barros DL, da Silva MA, Pereira RM, Campos LM, et al. Macrophage activation syndrome: a severe and frequent manifestation of acute pancreatitis in 362 childhood-onset compared to 1830 adult-onset systemic lupus erythematosus patients. Semin Arthritis Rheum 2016;45:706–10.
10. Lin CI, Yu HH, Lee JH, Wang LC, Lin YT, Yang YH, et al. Clinical analysis of macrophage activation syndrome in pediatric patients with autoimmune diseases. Clin Rheumatol 2012;31:1223–30.
11. Stephan JL, Kone-Paut I, Galambrun C, Mouy R, Bader-Meunier B, Prieur AM. Reactive haemophagocytic syndrome in children with inflammatory disorders: a retrospective study of 24 patients. Rheumatology (Oxford) 2001;40:1285–92.
12. Stabile A, Bertoni B, Ansuini V, La Torraca I, Salli A, Rigante D. The clinical spectrum and treatment options of macrophage activation syndrome in the pediatric age. Eur Rev Med Pharmacol Sci 2006;10:53–9.
13. Sawhney S, Woo P, Murray KJ. Macrophage activation syndrome: a potentially fatal complication of rheumatic disorders. Arch Dis Child 2001;85:421–6.
14. Pringe A, Trail L, Ruperto N, Buoncompagni A, Loy A, Breda L, et al. Macrophage activation syndrome in juvenile systemic lupus erythematosus: an under-recognized complication? Lupus 2007;16:587–92.
15. Petri M, Orbai AM, Alarcón GS, Gordon C, Merrill JT, Fortin PR, et al. Derivation and validation of the Systemic Lupus International Collaborating Clinics classification criteria for systemic lupus erythematosus. Arthritis Rheum 2012;64:2677–86.
16. Tan EM, Cohen AS, Fries JF, Masi AT, McShane DJ, Rothfield NF, et al. The 1982 revised criteria for the classification of systemic lupus erythematosus. Arthritis Rheum 1982;25:1271–7.
17. Henter JI, Horne A, Aricó M, Egeler RM, Filipovich AH, Imashuku S, et al. HLH-2004: diagnostic and therapeutic guidelines for hemophagocytic lymphohistiocytosis. Pediatr Blood Cancer 2007;48:124–31.
18. ACR Ad Hoc Committee on Neuropsychiatric Lupus Nomenclature. The American College of Rheumatology nomenclature and case definitions for neuropsychiatric lupus syndromes. Arthritis Rheum 1999;42:599–608.
19. Stepp SE, Dufourcq-Lagelouse R, Le Deist F, Bhawan S, Certain S, Mathew PA, et al. Perforin gene defects in familial hemophagocytic lymphohistiocytosis. Science 1999;286:1957–9.
20. Zhang K, Filipovich AH, Johnson J, Marsh RA, Villanueva J. Hemophagocytic lymphohistiocytosis, familial. In: Adam MP, Ardinger HH, Pagon RA, Wallace SE, Bean LJ, Stephens K, et al, editors. GeneReviews. Seattle (WA): University of Washington, Seattle; 1993–2018.
21. Weening JJ, D'Agati VD, Schwartz MM, Seshan SV, Alpers CE, Appel GB, et al, on behalf of the International Society of Nephrology and Renal Pathology Society Working Group on the Classification of Lupus Nephritis. The classification of glomerulonephritis in systemic lupus erythematosus revisited [published

erratum appears in J Am Soc Nephrol 2004;15:835–6]. J Am Soc Nephrol 2004;15:241–50.
22. Brunner HI, Silverman ED, To T, Bombardier C, Feldman BM. Risk factors for damage in childhood-onset systemic lupus erythematosus: cumulative disease activity and medication use predict disease damage. Arthritis Rheum 2002;46:436–44.
23. Gladman D, Ginzler E, Goldsmith C, Fortin P, Liang M, Urowitz M, et al. The development and initial validation of the Systemic Lupus International Collaborating Clinics/American College of Rheumatology damage index for systemic lupus erythematosus. Arthritis Rheum 1996;39:363–9.
24. Wong KF, Hui PK, Chan JK, Chan YW, Ha SY. The acute lupus hemophagocytic syndrome. Ann Intern Med 1991;114: 387–90.
25. Sakurai T, Kono I, Kabashima T, Yamane K, Nagasawa T, Kashiwagi H. Amegakaryocytic thrombocytopenia associated with systemic lupus erythematosus successfully treated by a high-dose prednisolone therapy. Jpn J Med 1984;23:135–8.
26. Atteritano M, David A, Bagnato G, Beninati C, Frisina A, Iaria C, et al. Haemophagocytic syndrome in rheumatic patients: a systematic review. Eur Rev Med Pharmacol Sci 2012;16: 1414–24.
27. Fukaya S, Yasuda S, Hashimoto T, Oku K, Kataoka H, Horita T, et al. Clinical features of haemophagocytic syndrome in patients with systemic autoimmune diseases: analysis of 30 cases. Rheumatology (Oxford) 2008;47:1686–91.
28. Papo T, Andre MH, Amoura Z, Lortholary O, Tribout B, Guillevin L, et al. The spectrum of reactive hemophagocytic syndrome in systemic lupus erythematosus. J Rheumatol 1999;26:927–30.
29. Kim JM, Kwok SK, Ju JH, Kim HY, Park SH. Reactive hemophagocytic syndrome in adult Korean patients with systemic lupus erythematosus: a case-control study and literature review. J Rheumatol 2012;39:86–93.
30. Dhote R, Simon J, Papo T, Detournay B, Sailler L, Andre MH, et al. Reactive hemophagocytic syndrome in adult systemic disease: report of twenty-six cases and literature review. Arthritis Rheum 2003;49:633–9.
31. Arnez MA, de Azevedo MN, Bica BE. Reactive haemophagocytic syndrome in a systemic lupus erythematosus patient: case report. Rev Bras Reumatol 2012;52:790–5.

ARTHRITIS & RHEUMATOLOGY
Vol. 70, No. 4, April 2018, pp 625–628

LETTERS

DOI 10.1002/art.40411

Involvement of X chromosome short arm in autoimmune diseases: comment on the article by Sharma et al

To the Editor:

In a recent report, Sharma et al described associations of X chromosome abnormalities in systemic lupus erythematosus (SLE) and Sjögren's syndrome (SS) (1), proposing that genes located on the short arm of the X chromosome (Xp) mediate the sex bias for SLE and/or SS. Our group had been thinking along these lines too and have found that, in X chromosome–linked chronic granulomatous disease in which chromatin is duplicated from Xp21.2 to the Xp terminus, some mothers who are carriers for X chromosome–linked chronic granulomatous disease have exhibited lupus-like symptoms (2).

We have had an interest in epigenetic involvement in autoimmune diseases, including in the reactivation of genes on the inactive X chromosome (Xi) (3). Previously, we identified 4 factors in Xp22 and the pseudoautosomal region 1 (PAR1) that appear to be most pertinent. Based on this, we presented the "X chromosome–nucleolus nexus" hypothesis, defining a mechanism for autoimmune diseases (2,4,5). The items we identified are as follows: 1) 2 polyamine genes at chromosome Xp22.1; 2) a fragile site, FRAXB in Xp22, that could contain latent viral genes; 3) a "hot," long interspersed nuclear element 1 (LINE1) in chromosome Xp22; and 4) a high content of Alu elements in PAR1.

Polyamines (spermidine and spermine) are important in autoimmune diseases since they can impact epigenetic control. Spermine can stabilize Z-DNA, an autoantigen in SLE and rheumatoid arthritis (RA) (6). Additionally, polyamines can compete with histones in binding DNA, potentially disrupting chromatin. Polyamine synthesis competes with cellular methylation for the methyl donor *S*-adenosyl methionine (SAM). A decrease in SAM could lead to DNA hypomethylation with loss of epigenetic silencing. And polyamines are involved in other important functions such as RNP assembly in the nucleolus.

Spermine synthase and spermidine/spermine N1–acetyltransferase are both at Xp22.1 and epigenetically silenced on the Xi (7). We were curious about consequences that could occur if these gene alleles were reactivated on the Xi. Spermine synthase is involved in polyamine synthesis and requires SAM. Spermidine/spermine N1–acetyltransferase is involved in polyamine recycling. Thus, with Xi disruption, additional expression of spermine synthase and/or spermidine/spermine N1–acetyltransferase could disrupt polyamine levels and waste SAM, leading to DNA hypomethylation. Since spermine synthase depends on SAM, increased polyamine recycling by spermidine/spermine N1–acetyltransferase could reduce levels of free polyamines, hampering their normal functions (8). This was later reported for RA (9).

Publication of the X chromosome sequence (10) revealed FRAXB in Xp22, which could contain latent viruses that could activate with Xi chromosome disruption. A "hot" LINE1 (i.e., with reverse transcriptase functionality) was found in Xp22. A few LINE1s still retain functionality and are suspected to be expressed in vivo. Li and Steinman have reported that Alu sequences constituted up to 55% of free DNA in lupus sera, whereas it constitutes only 10.8% of the human genome (11). They suggested reverse transcription as a possible explanation. Also of interest is the high content of Alu (28.8%) in PAR1 (10), which we calculated to be >2,500 copies. Alu elements have an internal RNA polymerase III (RNAP III) transcription start site but are silenced by positioned nucleosomes. Disruption of PAR1 could create a flood of Alu RNA and then possible reverse transcription. Unlike RNAP II, RNAP III does not require energy (ATP). In addition, Alu RNAs could interfere with signal recognition particle assembly in the nucleolus (8) and nucleolar integrity (12).

Most Xq genes are silenced by X inactivation (initiated from Xq13), so Xq makes up most of the heterochromatic Xi core, with Xp making up much of the Xi surface, rendering Xp22 through PAR1 more vulnerable to reactivation. Consideration of how the Xi could be disrupted led to our proposal of the "X chromosome–nucleolus nexus" hypothesis (2,4,5). Normally the Xi chromosome is located at the nuclear membrane. In one-third of cells throughout the cell cycle and 90% of cells in the S phase, the Xi is also next to a nucleolus (13). Thus, one of the most active, dynamic, and multifunctional cell components, the nucleolus, is next to one of the most inactive components, the Xi, which is sandwiched between the nucleolus and nuclear membrane.

Cellular stress, particularly viral activity, can cause nucleolar expansion, which is directly correlated with increased polyamines (14). Polyamines are critical in the folding and assembly of RNPs in the nucleolus. Many autoantigens, such as nucleolin, SSB/La, SSA/Ro, and spliceosome subunits are, at least transiently, components of the nucleolus (2). Nucleolar expansion could disrupt the neighboring Xi. Altered polyamine levels caused by spermidine/spermine N1–acetyltransferase overexpression could hamper future nucleolar stress response. Alu RNAs from PAR1 could disrupt nucleolar integrity by competing with intronic Alu elements in RNAP II transcripts that, along with nucleolin, provide structure to nucleoli (12). This can lead to nucleolar fragmentation, inefficient nucleolar functioning, and trapping of nucleolar components in misfolded and/or misassembled RNPs that provoke an autoimmune reaction when exposed extracellularly.

The "X chromosome–nucleolus nexus" hypothesis is, thus, cellular stress from different causes can result in disruption of the Xi, especially Xp22 and PAR1, which can then disrupt the nucleolus, leading to formation of autoantigens. The latest version of our hypothesis has just been published (15). I look forward to future reports from Sharma and colleagues in this interesting area of research.

Wesley H. Brooks, PhD, MBA
University of South Florida
Tampa, FL

1. Sharma R, Harris VM, Cavett J, Kurien BT, Liu K, Koelsch KA, et al. Rare X chromosome abnormalities in systemic lupus erythematosus and Sjögren's syndrome. Arthritis Rheumatol 2017;69:2187–92.
2. Brooks WH, Renaudineau Y. Epigenetics and autoimmune diseases: the X chromosome-nucleolus nexus. Front Genet 2015;6:22.
3. Brooks WH. X chromosome inactivation and autoimmunity. Clin Rev Allergy Immun 2010;39:20–9.
4. Brooks WH, Renaudineau Y. The "nucleolus" hypothesis of autoimmune diseases and its implications. Eur Med J 2017;2:82–89.
5. Brooks WH. A review of autoimmune disease hypotheses with introduction of the "nucleolus" hypothesis. Clin Rev Allergy Immunol 2017;52:333–50.

6. Sibley JT, Lee JS, Decoteau WE. Left-handed "Z" DNA antibodies in rheumatoid arthritis and systemic lupus erythematosus. J Rheumatol 1984;11:633–7.
7. Carrel L, Willard HF. X-inactivation profile reveals extensive variability in X-linked gene expression in females. Nature 2005;434:400–4.
8. Brooks W. Autoimmune diseases and polyamines. Clinic Rev Allerg Immun 2012;42:58–70.
9. Karouzakis E, Gay RE, Gay S, Neidhart M. Increased recycling of polyamines is associated with global DNA hypomethylation in rheumatoid arthritis synovial fibroblasts. Arthritis Rheum 2012;64:1809–17.
10. Ross MT, Graham DV, Coffey AJ, Scherer S, McLay K, Muzny D, et al. The DNA sequence of the human X chromosome. Nature 2005;434:325–37.
11. Li JZ, Steinman CR. Plasma DNA in systemic lupus erythematosus. Arthritis Rheum 1989;32:726–33.
12. Caudron-Herger M, Pankert T, Seiler J, Nemeth A, Voit R, Grummt I, et al. Alu element-containing RNAs maintain nucleolar structure and function. EMBO J 2015;34:2758–74.
13. Zhang LF, Huynh KD, Lee JT. Perinucleolar targeting of the inactive X during S phase: evidence for a role in the maintenance of silencing. Cell 2007;129:693–706.
14. Whelly SM. Role of polyamine in the regulation of RNA synthesis in uterine nucleoli. J Steroid Biochem Mol Biol 1991;39:161–7.
15. Brooks WH. Viral impact in autoimmune diseases: expanding the "X chromosome-nucleolus nexus" hypothesis. Front Immunol 2017;8:1657.

DOI 10.1002/art.40409

Reply

To the Editor:

After studying Klinefelter's syndrome (male 47,XXY) and triple X chromosomes (female 47,XXX), we proposed that the number of X chromosomes mediates the female bias for SLE and SS. In our recent report, we described SLE and SS patients with extremely rare X chromosome aneuploidies in which distal Xp was triplicated, implicating genes lying on the short arm of the X chromosome.

In his letter, Dr. Brooks states that X chromosome–linked chronic granulomatosus disease can also have gene duplication from Xp21.2 to Xp terminus, and some female carriers of X chromosome–linked chronic granulomatosus disease have a cutaneous lupus-like illness. Additionally, male patients with X chromosome–linked chronic granulomatosus disease with discoid lupus have also been described (1), but we have not found any reports describing the association of SLE with X chromosome–linked chronic granulomatosus disease or carrier state, except for a single case report (2). Several other primary immune deficiencies are associated with SLE (3).

Brooks also proposes that distal Xp genes may be involved in autoimmunity (4). A central point is that many genes on distal Xp escape X chromosome inactivation. This is clearly the case but varies according to tissue type and stage of development (5). However, escape of X chromosome inactivation by some genes in the X-linked regions of the X chromosome, especially Xp, is a part of normal human physiology (5). Thus, there may be no reason to evoke a disruption of X chromosome inactivation as a cause of autoimmune disease. There are several competing hypotheses for how an X chromosome dose effect might operate, e.g., skewed X chromosome inactivation, acquired chromosome X monosomy, fetal chimerism with female X chromosome mosaicism, and X chromosome reactivation. We have reviewed the evidence for and against these hypotheses (6). Brooks and Renaudineau propose the X chromosome–nucleolus nexus, which predicts abnormal X chromosome inactivation (4).

We found excess 47,XXX and 47,XXY in patients with SLE or SS, but not in those with primary biliary cirrhosis or RA (6–8). Thus, we conclude that there is more than one path to sex bias in autoimmunity. Data for Turner's syndrome support this notion in that these patients have excess type 1 diabetes, autoimmune thyroid disease (AITD), and celiac disease (9), while neither RA nor SLE is overrepresented (9,10). AITD is in highest excess among Turner's syndrome patients with an Xq isochrome (11,12). These patients have 1 copy of Xp, but 3 copies of Xq, which is in contrast to our findings in SLE and SS and to what Brooks hypothesizes for autoimmune disease. These examples again suggest the involvement of multiple pathways.

As noted by Brooks, there are a number of candidate genes at distal Xp, but only 2 have shown genetic association with SLE. These are *TLR7* and *CXorf21* (13), both of which escape X chromosome inactivation in various immune cells (5). The associations and this physiology certainly make enticing possibilities for mediating an X chromosome dose effect in SLE and SS.

R. Hal Scofield, MD
Oklahoma Medical Research Foundation
University of Oklahoma College of Medicine and Oklahoma City Department of Veterans Affairs Medical Center
Oklahoma City, OK
Rohan Sharma, MBBS
University of Arkansas for Medical Sciences
Little Rock, AR
Valerie M. Harris, MS
Oklahoma Medical Research Foundation
University of Oklahoma College of Medicine and Oklahoma City Department of Veterans Affairs Medical Center
Oklahoma City, OK

1. Xie C, Cole T, McLean C, Su JC. Association between discoid lupus erythematosus and chronic granulomatous disease—report of two cases and review of the literature. Pediatr Dermatol 2016;33:e114–20.
2. Manzi S, Urbach AH, McCune AB, Altman HA, Kaplan SS, Medsger TA Jr, et al. Systemic lupus erythematosus in a boy with chronic granulomatous disease: case report and review of the literature. Arthritis Rheum 1991;34:101–5.
3. Carneiro-Sampaio M, Liphaus BL, Jesus AA, Silva CA, Oliveira JB, Kiss MH. Understanding systemic lupus erythematosus physiopathology in the light of primary immunodeficiencies. J Clin Immunol 2008;28 Suppl 1:S34–41.
4. Brooks WH, Renaudineau Y. Epigenetics and autoimmune diseases: the X chromosome-nucleolus nexus. Front Genet 2015;6:22.
5. Tukiainen T, Villani AC, Yen A, Rivas MA, Marshall JL, Satija R, et al. Landscape of X chromosome inactivation across human tissues. Nature 2017;550:244–8.
6. Liu K, Kaufman KM, James JA, Jonsson R, Kurien BT, Mariette X, et al. Sex bias in autoimmune diseases: increased risk of 47, XXX in systemic lupus erythematosus (SLE) and Sjögren's Syndrome (SS) supports the gene dose hypothesis [abstract]. Arthritis Rheum 2013;65 Suppl:S379.
7. Harris VM, Sharma R, Cavett J, Kurien BT, Liu K, Koelsch KA, et al. Klinefelter's syndrome (47,XXY) is in excess among men with Sjogren's syndrome. Clin Immunol 2016;168:25–9.
8. Scofield RH, Bruner GR, Namjou B, Kimberly RP, Ramsey-Goldman R, Petri M, et al. Klinefelter's syndrome (47,XXY) in male systemic lupus erythematosus patients: support for the notion of a gene-dose effect from the X chromosome. Arthritis Rheum 2008;58:2511–7.

6. Sibley JT, Lee JS, Decoteau WE. Left-handed "Z" DNA antibodies in rheumatoid arthritis and systemic lupus erythematosus. J Rheumatol 1984;11:633–7.
7. Carrel L, Willard HF. X-inactivation profile reveals extensive variability in X-linked gene expression in females. Nature 2005;434:400–4.
8. Brooks W. Autoimmune diseases and polyamines. Clinic Rev Allerg Immun 2012;42:58–70.
9. Karouzakis E, Gay RE, Gay S, Neidhart M. Increased recycling of polyamines is associated with global DNA hypomethylation in rheumatoid arthritis synovial fibroblasts. Arthritis Rheum 2012;64:1809–17.
10. Ross MT, Graham DV, Coffey AJ, Scherer S, McLay K, Muzny D, et al. The DNA sequence of the human X chromosome. Nature 2005;434:325–37.
11. Li JZ, Steinman CR. Plasma DNA in systemic lupus erythematosus. Arthritis Rheum 1989;32:726–33.
12. Caudron-Herger M, Pankert T, Seiler J, Nemeth A, Voit R, Grummt I, et al. Alu element-containing RNAs maintain nucleolar structure and function. EMBO J 2015;34:2758–74.
13. Zhang LF, Huynh KD, Lee JT. Perinucleolar targeting of the inactive X during S phase: evidence for a role in the maintenance of silencing. Cell 2007;129:693–706.
14. Whelly SM. Role of polyamine in the regulation of RNA synthesis in uterine nucleoli. J Steroid Biochem Mol Biol 1991;39:161–7.
15. Brooks WH. Viral impact in autoimmune diseases: expanding the "X chromosome-nucleolus nexus" hypothesis. Front Immunol 2017;8:1657.

DOI 10.1002/art.40409

Reply

To the Editor:

After studying Klinefelter's syndrome (male 47,XXY) and triple X chromosomes (female 47,XXX), we proposed that the number of X chromosomes mediates the female bias for SLE and SS. In our recent report, we described SLE and SS patients with extremely rare X chromosome aneuploidies in which distal Xp was triplicated, implicating genes lying on the short arm of the X chromosome.

In his letter, Dr. Brooks states that X chromosome–linked chronic granulomatosus disease can also have gene duplication from Xp21.2 to Xp terminus, and some female carriers of X chromosome–linked chronic granulomatosus disease have a cutaneous lupus-like illness. Additionally, male patients with X chromosome–linked chronic granulomatosus disease with discoid lupus have also been described (1), but we have not found any reports describing the association of SLE with X chromosome–linked chronic granulomatosus disease or carrier state, except for a single case report (2). Several other primary immune deficiencies are associated with SLE (3).

Brooks also proposes that distal Xp genes may be involved in autoimmunity (4). A central point is that many genes on distal Xp escape X chromosome inactivation. This is clearly the case but varies according to tissue type and stage of development (5). However, escape of X chromosome inactivation by some genes in the X-linked regions of the X chromosome, especially Xp, is a part of normal human physiology (5). Thus, there may be no reason to evoke a disruption of X chromosome inactivation as a cause of autoimmune disease. There are several competing hypotheses for how an X chromosome dose effect might operate, e.g., skewed X chromosome inactivation, acquired chromosome X monosomy, fetal chimerism with female X chromosome mosaicism, and X chromosome reactivation. We have reviewed the evidence for and against these hypotheses (6). Brooks and Renaudineau propose the X chromosome–nucleolus nexus, which predicts abnormal X chromosome inactivation (4).

We found excess 47,XXX and 47,XXY in patients with SLE or SS, but not in those with primary biliary cirrhosis or RA (6–8). Thus, we conclude that there is more than one path to sex bias in autoimmunity. Data for Turner's syndrome support this notion in that these patients have excess type 1 diabetes, autoimmune thyroid disease (AITD), and celiac disease (9), while neither RA nor SLE is overrepresented (9,10). AITD is in highest excess among Turner's syndrome patients with an Xq isochrome (11,12). These patients have 1 copy of Xp, but 3 copies of Xq, which is in contrast to our findings in SLE and SS and to what Brooks hypothesizes for autoimmune disease. These examples again suggest the involvement of multiple pathways.

As noted by Brooks, there are a number of candidate genes at distal Xp, but only 2 have shown genetic association with SLE. These are *TLR7* and *CXorf21* (13), both of which escape X chromosome inactivation in various immune cells (5). The associations and this physiology certainly make enticing possibilities for mediating an X chromosome dose effect in SLE and SS.

R. Hal Scofield, MD
Oklahoma Medical Research Foundation
University of Oklahoma College of Medicine and Oklahoma City Department of Veterans Affairs Medical Center
Oklahoma City, OK
Rohan Sharma, MBBS
University of Arkansas for Medical Sciences
Little Rock, AR
Valerie M. Harris, MS
Oklahoma Medical Research Foundation
University of Oklahoma College of Medicine and Oklahoma City Department of Veterans Affairs Medical Center
Oklahoma City, OK

1. Xie C, Cole T, McLean C, Su JC. Association between discoid lupus erythematosus and chronic granulomatous disease—report of two cases and review of the literature. Pediatr Dermatol 2016;33:e114–20.
2. Manzi S, Urbach AH, McCune AB, Altman HA, Kaplan SS, Medsger TA Jr, et al. Systemic lupus erythematosus in a boy with chronic granulomatous disease: case report and review of the literature. Arthritis Rheum 1991;34:101–5.
3. Carneiro-Sampaio M, Liphaus BL, Jesus AA, Silva CA, Oliveira JB, Kiss MH. Understanding systemic lupus erythematosus physiopathology in the light of primary immunodeficiencies. J Clin Immunol 2008;28 Suppl 1:S34–41.
4. Brooks WH, Renaudineau Y. Epigenetics and autoimmune diseases: the X chromosome-nucleolus nexus. Front Genet 2015;6:22.
5. Tukiainen T, Villani AC, Yen A, Rivas MA, Marshall JL, Satija R, et al. Landscape of X chromosome inactivation across human tissues. Nature 2017;550:244–8.
6. Liu K, Kaufman KM, James JA, Jonsson R, Kurien BT, Mariette X, et al. Sex bias in autoimmune diseases: increased risk of 47, XXX in systemic lupus erythematosus (SLE) and Sjögren's Syndrome (SS) supports the gene dose hypothesis [abstract]. Arthritis Rheum 2013;65 Suppl:S379.
7. Harris VM, Sharma R, Cavett J, Kurien BT, Liu K, Koelsch KA, et al. Klinefelter's syndrome (47,XXY) is in excess among men with Sjogren's syndrome. Clin Immunol 2016;168:25–9.
8. Scofield RH, Bruner GR, Namjou B, Kimberly RP, Ramsey-Goldman R, Petri M, et al. Klinefelter's syndrome (47,XXY) in male systemic lupus erythematosus patients: support for the notion of a gene-dose effect from the X chromosome. Arthritis Rheum 2008;58:2511–7.

9. Jorgensen KT, Rostgaard K, Bache I, Biggar RJ, Nielsen NM, Tommerup N, et al. Autoimmune diseases in women with Turner's syndrome. Arthritis Rheum 2010;62:658–66.
10. Cooney CM, Bruner GR, Aberle T, Namjou-Khales B, Myers LK, Feo L, et al. 46,X,del(X)(q13) Turner's syndrome women with systemic lupus erythematosus in a pedigree multiplex for SLE. Genes Immun 2009;10:478–81.
11. Elsheikh M, Wass JA, Conway GS. Autoimmune thyroid syndrome in women with Turner's syndrome: the association with karyotype. Clin Endocrinol (Oxf) 2001;55:223–6.
12. Hamza RT, Raof NA, Abdallah KO. Prevalence of multiple forms of autoimmunity in Egyptian patients with Turner syndrome: relation to karyotype. J Pediatr Endocrinol Metab 2013;26:545–50.
13. Bentham J, Morris DL, Graham DS, Pinder CL, Tombleson P, Behrens TW, et al. Genetic association analyses implicate aberrant regulation of innate and adaptive immunity genes in the pathogenesis of systemic lupus erythematosus. Nat Genet 2015;47:1457–64.

DOI 10.1002/art.40412

Does rheumatoid arthritis cause an obesity paradox? Comment on the article by Sparks et al

To the Editor:

We read with interest the article by Sparks et al describing their study of the association between weight changes in the peri-diagnosis period and mortality among patients with rheumatoid arthritis (RA) (1). The investigators clearly show that weight loss is an important predictor of early mortality in both RA and non-RA patients. Indeed, and perhaps not surprisingly, unintentional weight loss is likely to be a poor prognostic sign regardless of its cause. As a result, the obesity paradox is indeed not an RA-specific phenomenon, but one that has been described in the elderly and in many chronic illnesses in addition to RA (2–4).

Although Sparks and colleagues convincingly demonstrate that weight loss is equally predictive of death regardless of whether it is observed in an RA or a non-RA population, it is important to note that weight loss was far more common among RA patients than among age-matched controls. For example, patients with RA were more likely to lose weight (15.8% versus 10.6%; $P < 0.0001$) and nearly twice as likely to experience severe weight loss (3% versus 1.6%; $P = 0.002$). Because weight loss is more common in RA, we should expect that the obesity paradox would be exacerbated in this group compared to non-RA controls. Thus, the current study importantly validates the prior research in this area.

While we can all agree that relationships between weight loss and mortality are not RA-specific, epidemiologic studies in RA are more likely to encounter bias related to the obesity paradox, due to a greater frequency of important weight loss in this disease group compared to that observed with normal aging.

Joshua F. Baker, MD, MSCE
Philadelphia VA Medical Center and Perelman School of Medicine University of Pennsylvania
Philadelphia, PA
Gail Kerr, MD, FRCP(Edin)
Washington DC VA Medical Center and Georgetown and Howard University Hospitals
Washington, DC
Ted R. Mikuls, MD, MSPH
VA Nebraska–Western Iowa Health Care System and University of Nebraska Medical Center
Omaha, NE

1. Sparks JA, Chang SC, Nguyen US, Barbhaiya M, Tedeschi SK, Lu B, et al. Weight change in the early rheumatoid arthritis period and risk of subsequent mortality among women with rheumatoid arthritis and matched comparators. Arthritis Rheumatol 2018;70:18–29.
2. Lee KS, Moser DK, Lennie TA, Pelter MM, Nesbitt T, Southard JA, et al. Obesity paradox: comparison of heart failure patients with and without comorbid diabetes. Am J Crit Care 2017;26:140–8.
3. Costanzo P, Cleland JG, Pellicori P, Clark AL, Hepburn D, Kilpatrick ES, et al. The obesity paradox in type 2 diabetes mellitus: relationship of body mass index to prognosis: a cohort study. Ann Intern Med 2015;162:610–8.
4. Flegal KM, Kit BK, Orpana H, Graubard BI. Association of all-cause mortality with overweight and obesity using standard body mass index categories: a systematic review and meta-analysis. JAMA 2013;309:71–82.

DOI 10.1002/art.40415

Reply

To the Editor:

We are grateful to Dr. Baker and colleagues for their interest in our recent work and agree with their interpretation of the findings of our investigation of weight change in the early RA period among women with RA versus matched comparators. As they point out, both any weight loss and severe weight loss in the early RA or matched index period were more common among those with RA than among matched comparators. Baker et al suggest that this increased frequency of weight loss may exacerbate the obesity paradox for mortality among patients with RA.

The design of our study was anchored around the date of RA diagnosis (the index date for matched comparators) and included lengthy follow-up for mortality after the end of the early RA/index period. Therefore, we maximized the opportunity to detect a difference between RA patients and non-RA subjects for weight change and mortality risk. Prior studies used RA-only cohorts, mostly with longstanding disease, so weight change was not necessarily related to RA and may have immediately preceded death (1–4). In our study, we found a similar magnitude of effect for the relative risk of weight change on mortality in both RA patients and comparators, so we believe the obesity paradox occurs similarly in these populations. We agree that the scenario of pathologic weight loss may occur in a greater proportion of patients with RA or other chronic diseases compared with the general population, sometimes related to RA itself or due to frailty or other multimorbidities. In our investigation, women with RA with severe weight loss had a mortality rate of 6,909 per 100,000 person-years, compared to 2,070 per 100,000 person-years among those with stable weight. This absolute risk was higher than in matched comparators (3,717 per 100,000 person-years for severe weight loss and 1,461 per 100,000 person-years for stable weight loss). While the absolute mortality risk was higher among RA patients compared with comparators across all weight change categories, the relative risk for mortality among those experiencing severe, pathologic weight loss compared to those with stable weight was similar and therefore unlikely to differ by population.

Our study also differs from others in that we investigated weight gain in addition to weight loss. Perhaps surprisingly, we found that similar proportions of subjects with RA and comparators gained weight during the early RA or index period (for any gain, 19.9% versus 20.5% [$P = 0.74$]; for severe gain, 2.4% versus 2.3% [$P = 0.77$]). Importantly, weight gain did not offer a mortality benefit for patients with RA or

comparators. We believe these findings further emphasize that pathologic weight loss preceding death, rather than a biologic protective effect of excess weight on mortality, is most likely responsible for the apparent obesity paradox for mortality in RA. Healthy strategies for weight loss should continue to be encouraged for patients with RA and the general population.

Jeffrey A. Sparks, MD, MMSc
Elizabeth W. Karlson, MD, MS
Brigham and Women's Hospital and Harvard Medical School
Boston, MA

1. Escalante A, Haas RW, del Rincón I. Paradoxical effect of body mass index on survival in rheumatoid arthritis: role of comorbidity and systemic inflammation. Arch Intern Med 2005;165:1624–9.
2. Wolfe F, Michaud K. Effect of body mass index on mortality and clinical status in rheumatoid arthritis. Arthritis Care Res (Hoboken) 2012;64:1471–9.
3. Baker JF, Billig E, Michaud K, Ibrahim S, Caplan L, Cannon GW, et al. Weight loss, the obesity paradox, and the risk of death in rheumatoid arthritis. Arthritis Rheumatol 2015;67:1711–7.
4. England BR, Baker JF, Sayles H, Michaud K, Caplan L, Davis LA, et al. Body mass index, weight loss, and cause-specific mortality in rheumatoid arthritis. Arthritis Care Res (Hoboken) 2018;70:11–8.

DOI: 10.1002/art.40368

Clinical Images: Arthritis in melorheostosis—an uncommon feature in a rare disease

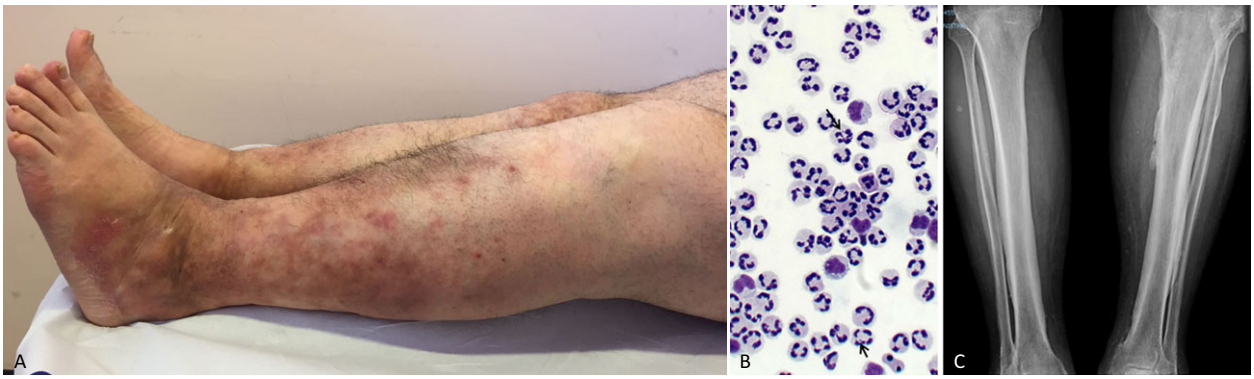

The patient, a 53-year-old man, presented with left knee and left ankle arthritis associated with marked induration of the skin and soft tissue distal to the knees. His left knee was swollen and tender, with a nonreducible contracture, and his left ankle and subtalar joint were stiff and moderately swollen. In addition, diffuse, bluish, small vascular ectasia, hypertrichosis, and melanoderma of the affected sites were evident (**A**). These symptoms had begun 20 years earlier, and the patient had been diagnosed as having eosinophilic fasciitis and was treated with daily prednisone, leading to partial improvement of the symptoms, but not of the knee deformity and soft tissue induration. Blood tests showed an elevated C-reactive protein level and erythrocyte sedimentation rate, with negative results for antinuclear antibodies, rheumatoid factor, and anti–citrullinated protein antibodies. Knee aspiration yielded 20 ml of synovial fluid with 7,500 cells/mm^3 (75% hypersegmented neutrophils) (**B**), often characterized by the presence of nuclear Barr-like bodies (**arrows**). Polarizing microscopy did not reveal urate and pyrophosphate crystals. Radiography of the legs showed a cortical flowing hyperostosis with a "melting candle wax" appearance of the tibiae and peroneum, suggestive of melorheostosis (**C**). No relevant joint deformity was observed. ^{99m}Tc imaging of the bone demonstrated active inflammation in the left knee and both ankles. The patient was treated with an injection of triamcinolone into the joint. Rapid improvement of the arthritis followed. He was discharged, and alendronate (70 mg/week) and physical therapy were prescribed. Melorheostosis is a very rare, nonhereditary disease affecting mesodermal-derived tissues, primarily bone and overlying soft tissues, including muscles, blood vessels, and skin. Its etiology is uncertain, but it has been attributed to mutation of the LEMD3 gene. Diagnosis is primarily based on the typical flowing appearance of the cortical bone and induration of the soft tissues. Arthritis is an uncommon feature, present in <5% of patients, and primarily involves the larger joints. There is no approved treatment for melorheostosis, but options include analgesics and bisphosphonates in patients with increased bone turnover. Physical therapy may help to preserve joint mobility. Severe bone involvement might require orthopedic surgery (1).

1. Smith GC, Pingree MJ, Freeman LA, Matsumoto JM, Howe BM, Kannas SN, et al. Melorheostosis: a retrospective clinical analysis of 24 patients at the Mayo Clinic. PM R 2017;9:283–8.

Enrico Selvi, MD
Marco Bardelli, MD
University of Siena
Siena, Italy
Giacomo Maria Guidelli, MD
Humanitas Research Hospital
Milan, Italy